

A GLOBAL REVIEW OF HUMAN-INDUCED EARTHQUAKES

Gillian R. Foulger¹, Miles Wilson¹, Jon Gluyas¹, Bruce R. Julian¹ & Richard Davies²

¹Department of Earth Sciences, Durham University, Durham, DH1 3LE, U.K.

²School of Civil Engineering and Geosciences, Newcastle University, Newcastle upon Tyne
NE1 7RU, UK

16	1	Introduction.....	6
17	1.1	Intraplate earthquakes.....	7
18	1.2	Induced vs. triggered earthquakes.....	7
19	1.3	Factors involved in the nucleation of earthquakes.....	9
20	1.4	Earthquake locations.....	10
21	1.5	Earthquake magnitudes.....	11
22	1.6	Earthquake counts.....	11
23	1.7	The database.....	12
24	1.8	Earthquakes and belief systems.....	12
25	2	Surface operations.....	13
26	2.1	Adding mass.....	13
27	2.1.1	Water impoundment behind dams.....	13
28	2.1.2	Erecting tall buildings.....	15
29	2.1.3	Coastal land gain.....	16
30	2.2	Surface operations: Removing mass.....	16
31	2.3	Surface operations: Summary.....	16
32	3	Extraction from the subsurface.....	17
33	3.1	Groundwater extraction.....	17
34	3.2	Mining.....	18
35	3.2.1	Traditional mining.....	19
36	3.2.2	Solution mining.....	21
37	3.2.3	Tunnel excavation.....	22
38	3.3	Hydrocarbons.....	23
39	3.3.1	Gas.....	23
40	3.3.2	Oil.....	25
41	3.4	Geothermal production (heat/fluids).....	27
42	3.5	Extraction from the subsurface: Summary.....	29
43	4	Injection into the subsurface.....	29
44	4.1	Liquid.....	30
45	4.1.1	Military waste.....	30
46	4.1.2	Wastewater disposal.....	31
47	4.1.3	Water injected for enhanced oil recovery.....	35
48	4.1.4	Enhanced Geothermal Systems (EGS).....	36
49	4.1.5	Geothermal reinjection.....	39
50	4.1.6	Shale-gas hydrofracturing.....	42
51	4.1.7	Allowing mines to flood.....	44
52	4.1.8	Research projects.....	45
53	4.2	Gas.....	47
54	4.2.1	Natural gas storage.....	47
55	4.2.2	CO ₂ for oil recovery.....	48
56	4.2.3	Carbon Capture and Storage (CCS).....	49
57	4.2.4	Injection into the subsurface: Summary.....	51
58	5	Explosions.....	51
59	6	Summary.....	53

60	7	Discussion and conclusions	56
61	7.1	How common are induced earthquakes?	56
62	7.2	Hydraulics	57
63	7.3	How much stress loading is required to induce earthquakes?	58
64	7.3.1	Earth tides	59
65	7.3.2	Static stress changes resulting from large earthquakes.....	59
66	7.3.3	Remote triggering	60
67	7.3.4	Weather	60
68	7.4	How large are induced earthquakes?	60
69	7.5	Natural or induced?.....	61
70	7.6	Why are earthquakes induced by some industrial projects and not others?	62
71	7.7	Future trends	63
72	7.8	Earthquake prediction	63
73	7.9	Earthquake management.....	64
74			
75		Online supporting material	
76			
77	A	Method used to construct the database.	231
78	B	Description of the database	231
79	C	Explanations of database column headings.....	234
80	D	List of the 705 entries in the database.....	236
81	E	Bibliography	261
82			

83 *Abstract*

84

85 The Durham *iQuake* Database, which currently contains over 700 cases spanning the period
86 1868 - 2016, was constructed as part of a comprehensive global review of human-induced
87 earthquake sequences. A surprisingly broad range of industrial activity has been proposed to
88 induce earthquakes including the impoundment of water reservoirs behind dams, erecting tall
89 buildings, coastal engineering, quarrying, extraction of groundwater, coal and minerals,
90 excavation of tunnels, and extraction of gas, oil and geothermal fluids. The addition of
91 material to the subsurface is also potentially seismogenic and this includes allowing
92 underground cavities to flood after cessation of mining, injecting fluid for waste disposal,
93 enhanced oil recovery, hydrofracturing, gas storage, and carbon sequestration. Nuclear
94 explosions induce earthquakes in abundance but evidence for chemical explosions doing so is
95 weak. We describe illustrative cases of particular interest in all these categories. Challenges
96 to constructing the database include major under-reporting which we estimate to be 30% of
97 $M \sim 4$ events, 60% of $M \sim 3$ events and $\sim 90\%$ of $M \sim 2$ events. Imperfect understanding of
98 the phenomenon of induced seismicity likely results in cases going unrecognized and lack of
99 seismic monitoring likely results in cases going unobserved. An additional problem is the
100 fundamental impossibility of attributing unique causes to earthquakes that occur in response
101 to multiple ongoing anthropogenic and natural stress-loading processes that include tectonic-
102 and isostatic motions, surface deformation and changes in fault-zone hydrology and
103 mineralization. The amount of stress released in an induced earthquake is not necessarily the
104 same as the anthropogenic stress added and earthquakes that seem disproportionately large
105 compared with the industrial activity may be induced. Stress is released by aseismic
106 deformation and when an earthquake occurs stress from natural processes may be released
107 also. In addition, large earthquakes commonly comprise a sequence of sub-events, each of
108 which is triggered by the previous sub-event, so large earthquakes may result from the
109 induction of a much smaller initial event. Anthropological stress loading may discourage as
110 well as encourage earthquakes, depending on the relative orientations of faults and the
111 induced stress tensor. Knowledge of the magnitude of the largest expected induced
112 earthquake in a sequence, M_{MAX} , is important for hazard reduction. For projects in planning,
113 the largest M_{MAX} that has occurred in the past in association with projects of the same type is
114 of interest. The upper-bound of M_{MAX} for induced earthquake sequences correlates with the
115 scale of industrial projects in terms of both the diameter of the area exploited and the mass
116 and volume of material added or removed. We also find positive correlations between
117 maximum M_{MAX} and fluid injection pressure and rate, and the yield of nuclear devices.
118 Counter-intuitively, we find a negative correlation with calculated values of inducing stress
119 change. This is probably because induced stresses tend to correlate inversely with project
120 scale. The largest earthquake reported to date to be induced by fluid injection is M 5.7 (the
121 1993 Prague, Oklahoma earthquake), by water-reservoir impoundment $M \sim 8$ (the 2008
122 Wenchuan, China, earthquake), and by mass removal M 7.3 (the 1976 Gazli, Uzbekistan
123 earthquake). The minimum amount of anthropogenic stress needed to induce an earthquake is
124 an unsound concept since earthquakes occur in the absence of industrial activity. However, it
125 is possible to estimate the minimum amount of stress that modulates earthquake activity to an
126 observable degree by studying atmospheric pressure changes, solid Earth tides and the
127 phenomenon of remote triggering. Modulations in earthquake activity correlating with those
128 processes have been reliably detected in the presence of stress changes as small as a few
129 hundredths of a megapascal, and possibly detected at the level of a few thousandths of a
130 megapascal. Such stress levels are equivalent to changes in the depth to the water table of a
131 few tens of centimeters. Faults near to failure are pervasive in the continental crust and
132 induced earthquakes may thus occur essentially anywhere. In intraplate regions neither

133 infrastructure nor populations may be prepared for earthquakes. As the scale of
134 industrialization has increased over the last century or so, the largest reported human-induced
135 earthquake has increased from M 6.3 in 1933 to M ~ 8 in 2008. Relative to the number of
136 industrial projects in progress, human-induced earthquakes that cause nuisance are rare.
137 However, in some cases they have become a significant problem, *e.g.*, in the hydrocarbon-
138 producing areas of Oklahoma, USA, and in the gas fields of The Netherlands. As the size of
139 projects and density of populations increase, the problem of induced earthquakes also
140 increases and effective management strategies are needed.

141

142 **1 Introduction**

143 Many natural processes modulate the spatial and temporal occurrence of earthquakes. These
144 include tectonic stress changes, the migration of fluids in the crust, Earth tides, surface ice
145 and snow loading, heavy precipitation, atmospheric pressure changes, sediment unloading
146 and groundwater loss [e.g., Kundu *et al.*, 2015]. Such processes perturb stress on faults by
147 only small amounts, but since rock failure in earthquakes is a critical process, nucleation of
148 each event is ultimately brought about by a final, small change in stress. Thus, it is
149 unsurprising that anthropogenic activity that perturbs stress in the crust, even if by just a
150 small amount, from time to time modulates seismicity. In most cases such effects probably go
151 unnoticed (Section 7.1), but as industrial projects become larger in scale and more numerous,
152 the number of cases where a link is obvious is increasing.

153 The issues of mining- and dam-induced earthquakes have been known for several decades.
154 Now, concern is growing about earthquakes induced, for example, by hydraulic fracturing for
155 shale-gas extraction and waste-water disposal by injection into boreholes. As hydrocarbon
156 reservoirs enter their tertiary phases of production, seismicity may also increase there.

157 The full extent of human activities that may induce earthquakes is, however, wider than
158 generally appreciated. We have conducted an extensive and thorough search to build as near
159 complete a catalog as possible of cases of induced seismicity that have been reported to date.
160 Our work greatly expands previous reviews of the subject. McGarr [2002] provides a general
161 overview. Nicol *et al.* [2011] assembled a list of 75 cases. Suckale [2009] listed 70 cases
162 related to hydrocarbon fields alone, and most recently Davies *et al.* [2013] listed 198 cases.

163 The new database we report here, the Durham *iQuake* Database, contains over 700 cases of
164 anthropogenic projects postulated to induce earthquake activity. This is, to our knowledge,
165 the largest compilation made to date. It is publically available on our website
166 www.inducedearthquakes.org which includes a form for additional community contributions.

167 We constructed the database by searching published papers, conference abstracts, books,
168 reports, and web-based material and personal communications we judged to have merit. It
169 was not within the remit of this project to review or develop theories for anthropogenic
170 earthquake induction nor to judge whether claims of anthropogenesis are correct or not. We
171 included all cases where a clear scientific case had been made, whilst recognizing that some
172 proposals of anthropogenic induction are tentative or have been challenged, e.g., the 1983
173 M_w 6.2 Coalinga, California, event (Section 3.3.2). The *iQuake* database thus comes with the
174 *caveat emptor* that judgment regarding the strength of the arguments for anthropogenic
175 induction of individual cases is left to the user. For this purpose, information regarding our
176 information sources are also included.

177 In this paper we present an introduction and lay out the basics of some relevant, fundamental,
178 but sometimes-misunderstood background issues. We then give examples of seismicity
179 postulated to be related to:

- 180 a) Surface operations,
- 181 b) Extraction of mass from the subsurface,
- 182 c) Introduction of mass into the subsurface, and
- 183 d) Explosions.

184 We divide each of these categories into sub-categories. In some cases, categorization is
 185 tentative because more than one anthropogenic process may have preceded or been ongoing
 186 at the time of the relevant earthquakes. For example, fluid extraction and injection are often
 187 conducted simultaneously in hydrocarbon reservoirs. Finally, we summarize features of the
 188 database and comment on some related issues with which scientists are currently grappling.

189 *1.1 Intraplate earthquakes*

190 Plate tectonic theory in its simplest form considers plates to be relatively rigid and expects
 191 most large earthquakes to occur in plate boundary zones. The fact that intraplate earthquakes
 192 occur, and may be large, is *prima facie* evidence that the plates are not rigid but simply
 193 deform more slowly in their interiors than at their boundaries. Plate interiors are structurally
 194 heterogeneous. Stress within them changes cyclically as elastic- and viscoelastic stress
 195 diffuses through them following the great earthquakes and volcanic events that sum to bring
 196 about what geologists model as plate movements [Foulger *et al.*, 1992; Heki *et al.*, 1993].
 197 The configuration of plate boundaries is furthermore geometrically unstable and evolving.
 198 For example, in Europe the formation of extensional features such as the Rhine Graben
 199 (Germany) and the Bresse Graben (France and Switzerland), and the emplacement of
 200 volcanics such as the Vogelsberg and the Eifel volcanic fields (both in Germany), are likely
 201 ultimately related to southerly migration (“slab roll-back”) of the Mediterranean collision
 202 zone between Africa and Europe. Intraplate European seismicity is probably ultimately
 203 related to the same process (Figure 1) [Nielsen *et al.*, 2007].

204 Intraplate seismicity is commonly expected to be relatively stable spatially, so that future
 205 earthquakes will occur in places where they have occurred in the past. This assumption has
 206 been re-visited in recent years, in particular as a result of geodetic work done in the New
 207 Madrid Seismic Zone, USA [*e.g.*, Newman *et al.*, 1999; Stein *et al.*, 2009]. There, it is widely
 208 expected that future large earthquakes will follow the damaging 1811-1812 sequence of four
 209 $M \geq 7$ earthquakes [*e.g.*, Johnston & Schweig, 1996]. As a result, significant resources have
 210 been invested in earthquake hazard mitigation. Recent GPS surveying has, however, failed to
 211 detect any ongoing strain build-up. This observation has led to the proposal that the spatial
 212 distribution of intraplate earthquakes in general is not stationary and that the locations of past,
 213 large earthquakes are not a good predictors of future earthquakes. Wrong forecasts of the
 214 likely location of future damaging earthquakes may lead to inefficient deployment of hazard-
 215 reduction resources. This theory thus has significant implications for public safety.

216 A non-stationary spatial pattern of seismicity accords with observations that the crust is
 217 critically stressed in most intraplate regions. Stress measurements made in boreholes
 218 commonly show that stress is close to the depth-dependent strength of the crust as estimated
 219 by laboratory experiments [*e.g.*, Brudy *et al.*, 1997; Zoback & Healy, 1984]. Furthermore, the
 220 ambient pore pressure is generally close to hydrostatic. The crust is, in general, pervasively
 221 faulted and these faults are, in general, close to failure. This conclusion is consistent with
 222 observations that anthropogenically induced seismicity may occur, and even be seemingly
 223 disproportionately large, in regions that have been historically aseismic.

224 *1.2 Induced vs. triggered earthquakes*

225 The fact that many if not all earthquakes related to human activity release more stress than
 226 artificially added to the crust was highlighted by McGarr [2002]. He suggested using the
 227 terms “induced” for earthquakes resulting from an activity that causes a stress change
 228 comparable in magnitude to the ambient shear stress acting on a fault to cause slip. He further

229 proposed using the term “triggered” where the anthropogenic stress change is much smaller,
 230 and “stimulated” where there are insufficient data to make the distinction.

231 It is beyond dispute that in many cases seismic strain energy released in earthquakes is many
 232 orders of magnitude larger than that introduced into the crust by the industrial activity. In this
 233 paper, however, we use the term “induced” for all earthquakes postulated to be related to
 234 human activity. The reasons for this are:

235 a) All earthquakes probably release some pre-existing strain energy and are thus likely
 236 to be technically “triggered”. Indeed, only in cases where rock is entirely unstressed
 237 in its initial state could this not be the case. This is not possible in a heterogeneous,
 238 gravitating half-space. Even nuclear tests, which are purely explosive sources, trigger
 239 the release of some regional tectonic stress as is shown by the significant shear
 240 components in their focal mechanisms [e.g., Toksöz & Kehrler, 1972].

241 b) The amount of tectonic strain energy loaded into the crust that is relieved seismically,
 242 on what time-scale, and the amount released aseismically are poorly understood. In
 243 rapidly deforming regions, e.g., plate boundary zones, aseismic deformation can be
 244 measured geodetically [e.g., Heki *et al.*, 1997] and surface subsidence is commonly
 245 observed above producing reservoirs [e.g., the Wilmington Oilfield, California;
 246 Kovach, 1974; Nagel, 2001]. Observations suggest that only a fraction of the total
 247 strain energy is relieved seismically but it is difficult to determine what this fraction
 248 is. Surface geodetic data have low sensitivity to fault motion at depth. Estimates of
 249 the percentage of strain energy that is dissipated aseismically varies from ~20% to
 250 1000% of that released seismically [Villegas-Lanza *et al.*, 2016]. The recent under-
 251 prediction of the magnitude of the 2011 M_w 9 Tohoku-oki, Japan, earthquake which
 252 killed > 18,000 people and did as-yet-unassessable economic damage, brought into
 253 sharp focus the fact that our assumptions regarding the length of the “seismic cycle”
 254 may be incorrect. Even moderate and large earthquakes may not relieve all the stress
 255 on a particular fault so our ability to estimate long-term stress buildup in the crust is
 256 incomplete.

257
 258 The same considerations hold true for industrial projects. If the timescale of energy
 259 release is underestimated, and with it the size of the largest expected earthquake
 260 (which dominates the energy budget because of the fractal nature of earthquake
 261 magnitudes), the maximum expected future earthquake magnitude (M_{MAX}) may be
 262 underestimated.

263 c) It is at best impractical and at worst fundamentally impossible to determine how much
 264 of the strain energy released in a seismic event pre-existed. Even in cases where the
 265 energy released is comparable to the amount anthropogenically added [e.g., McGarr,
 266 1991], much of the latter may have been relieved by aseismic deformation such as
 267 ground subsidence, or inflow of water at depth. These processes may themselves
 268 trigger earthquakes or load adjacent regions to seismic failure [e.g., Guglielmi *et al.*,
 269 2015].

270 Our use of the term “induced” as neutral and without implications for the origin of the
 271 causative stress change is in accord with the usage of the Committee on Induced Seismicity
 272 Potential [Hitzman, 2013]. That committee uses the term “induced” to mean “earthquakes

273 related to human activities”¹.

274 1.3 Factors involved in the nucleation of earthquakes

275 Shear slip on fault planes, with or without crack-opening or closing components, is the most
276 common earthquake source process. Factors involved in nucleation, i.e. the onset of motion,
277 include:

- 278 • the coefficient of friction on the fault plane;
- 279 • compressive normal stress on the fault plane;
- 280 • pore pressure in the fault zone; and
- 281 • shear stress on the fault.

282 According to the widely used Coulomb Theory, the shear stress required for failure τ is

$$283 \quad \tau = \tau_0 + \mu(\sigma_n - p) \quad \text{Eq. 1}$$

284 where τ_0 is the cohesion, μ is the coefficient of friction, σ_n is the normal stress across the
285 fault, and p is the pore pressure in the fault zone [e.g., McGarr *et al.*, 2002]. The onset of an
286 earthquake may thus result from reduction of the cohesion or normal stress on the fault plane,
287 or increase in the shear stress or pore pressure.

288 The loss or gain of overlying mass, introduction of fluid into a fault zone, or the imposition of
289 vertical and/or horizontal stress by other means e.g., stress transfer from nearby earthquakes,
290 can bring a fault closer to failure. Where there are rapid temperature changes, e.g., where
291 cold water is injected into geothermal areas, thermal effects may also be a significant.

292 Both the anthropological addition and removal of material is associated with earthquake
293 occurrence. The removal of water from aquifers (Section 3.1) and rock from mines (Section
294 3.2) may reduce the confining stress on fault planes. The introduction of water via reservoir
295 impoundment (Section 2.1.1) or injection (Section 4.1) may alter the fluid pressure in fault
296 zones. The cessation of groundwater pumping, e.g., in mines, may result in an influx of
297 groundwater and increase in pore pressure (Section 4.1.7). The addition of solid mass to the
298 surface may also alter hydrogeological conditions (Section 2.1.2).

299 Theories for the mechanism of induced earthquakes include the asperity model of Pennington
300 *et al.* [1986] which suggests that fluid extraction results in differential compaction or
301 aseismic fault motion, which in turn increases stress on locked portions of faults. This stress
302 is eventually relieved when asperities break. The poroelastic model of Segall [1985; 1992]
303 suggests that declining pore pressures resulting from fluid extraction cause contraction of the
304 reservoir rocks and stress build-up. *Ad hoc* theories for induced earthquakes at individual
305 localities may provide plausible explanations *a posteriori*. However, developing a method
306 that can reliably predict *a priori* which industrial projects will induce earthquakes and which

¹ “Some researchers (e.g., McGarr *et al.*, 2002) draw a distinction between “induced” seismicity and “triggered” seismicity. Under this distinction, induced seismicity results from human-caused stress changes in the Earth’s crust that are on the same order as the ambient stress on a fault that causes slip. Triggered seismicity results from stress changes that are a small fraction of the ambient stress on a fault that causes slip. Anthropogenic processes cannot “induce” large and potentially damaging earthquakes, but anthropogenic processes could potentially “trigger” such events. In this report we do not distinguish between the two and use the term “induced seismicity” to cover both categories.” Hitzman, M. W. (Ed.) (2013), Induced Seismicity Potential in Energy Technologies x+248 pp., National Academies Press, Washington, D.C..

307 not is still a work in progress.

308 1.4 Earthquake locations

309 Earthquakes in the *iQuake* database date from 1868 to 2016. Seismological technology has
310 improved vastly during this period, but even today the standard of monitoring is non-uniform.
311 Many projects may not be monitored at all until nuisance seismicity has already begun. In
312 contrast, others may be monitored by dense seismic networks installed well before the onset
313 of operations, in order to obtain a pre-operational baseline [*e.g.*, Cladouhos *et al.*, 2013]. As a
314 result, the event locations, magnitudes and other information such as focal mechanisms in the
315 *iQuake* database vary in quality.

316 Inaccurate hypocentral locations hamper efforts to associate earthquakes with operations on
317 the basis of spatial correlations, especially if the errors are larger than the separation between
318 boreholes or producing horizons. An example is the case of the Crooked Lake, Alberta,
319 earthquake sequences, thought to have been induced by shale-gas hydrofracturing (Section
320 4.1.6) [Schultz *et al.*, 2015]. A pre-operational seismic baseline was not available for small-
321 and medium-magnitude earthquakes, there was little information on the local crustal
322 structure, and most of the seismic data were from stations more than 100 km away. As a
323 result, it is unclear whether the lack of spatial correlation of some events with operations is
324 real or merely a consequence of inaccurate locations.

325 By far the largest source of hypocentral uncertainty is imperfect knowledge of crustal
326 structure. This factor is not included in the error estimates computed by many commonly
327 used hypocenter-location computer programs. Those programs typically base uncertainty
328 estimates on root-mean-square arrival-time residuals, a technique which implies that the
329 crustal model is perfect. Such residuals may be reduced to quite small values by
330 systematically mislocating hypocenters, giving a highly misleading idea of the quality of the
331 results. Advanced earthquake location methods such as master-event techniques, relative
332 locations [“double-differencing”; Waldhauser & Ellsworth, 2000] or using waveform cross-
333 correlation [Got *et al.*, 1994] can improve the accuracy of locations *relative to one another*
334 but do not reduce systematic errors in the absolute accuracy of entire clusters of events.
335 Accurate depths in particular are out of reach if geometrically strong data are not available
336 because errors in hypocentral depth are typically 2-3 times the error in horizontal (epicentral)
337 location. Insufficient numbers of stations, and too large distances between them and the
338 earthquakes, are also hindrances to obtaining accurate locations (Section 4.2.1).

339 For the purpose of accurately locating earthquakes associated with relatively small-scale
340 industrial projects, obtaining accurate local velocity models may be challenging. Available
341 information may be limited to well-logs, global or national crustal models, or models from
342 analogous geological areas [*e.g.*, Schultz *et al.*, 2015]. Such models are not adequate for
343 reducing location uncertainties to sub-hectometer (100 m) levels. Ideally, high-quality crustal
344 models based on active-source seismic surveying and/or one- and three-dimensional
345 inversions of local earthquake data will be available. Projects will be monitored by dense
346 networks of seismic stations with at least one station every 1-2 km². Experimental designs of
347 this kind can return locations accurate to about a hectometer. Reducing errors still further
348 requires calibration shots. This subject was recently discussed in detail by Foulger and Julian
349 [2014] for the case of earthquakes induced by Enhanced Geothermal Systems (EGS)
350 operations (Section 4.1.4).

351 In order to inform discussions regarding whether earthquakes are induced or natural, a pre-

352 operation baseline is required. For this purpose, seismic networks must be deployed prior to
 353 commencement of operations. An effort to establish such a baseline for the entire UK prior to
 354 possible expansion of shale-gas hydrofracturing was recently made by Wilson *et al.* [2015].

355 1.5 Earthquake magnitudes

356 Because of the definitions of earthquake magnitudes, values quoted for a single event often
 357 differ by up to a whole magnitude unit, even if calculated correctly. This is because:

358 • Traditional scales such as local magnitude (M_L) use measurements of the amplitudes
 359 of certain seismic phases recorded on seismic stations. Amplitudes are a poor measure
 360 of the size of an earthquake because they are influenced by factors such as the
 361 orientation of the fault that slipped and source-to-station crustal structure. Because of
 362 these and other factors, different recordings of the same earthquake at different
 363 stations may yield different magnitudes even using the same scale.

364 • Different magnitude scales such as M_L and surface-wave magnitude (M_S) use different
 365 types of seismic waves. There are both systematic and random differences in the
 366 magnitudes calculated using them. For example, shallow earthquakes excite stronger
 367 surface waves than deep earthquakes, so M_S , which relies on measurements of the
 368 amplitudes of surface waves, underestimates the sizes of deeper earthquakes.

369 • Seismological practice is notoriously non-standard in respect of magnitudes, and local
 370 magnitude scales and practices often depart considerably from those originally
 371 defined. For example, many local seismic stations and networks use their own
 372 customized magnitude scales, often constructed by calibrating them using a few
 373 earthquakes measured in common with the nearest permanent or calibrated station.
 374 That station may in turn have been calibrated in the same way. Local magnitude M_L
 375 technically refers to recordings made on Wood-Anderson seismographs, but such
 376 instruments are now rare. As a result, magnitudes reported from one seismic network
 377 may not be comparable to those reported from another, even if the same magnitude
 378 scale has, in theory, been used.

379 In view of these factors, and because the information published is often limited, especially for
 380 older cases, it is beyond the scope of this paper to render all magnitudes to a single scale. In
 381 this paper we thus do not discriminate between magnitude types reported. We record the
 382 information where available herein and in the *iQuake* database, *e.g.*, M_L (local magnitude),
 383 m_b (body-wave magnitude), M_S (surface-wave magnitude), M_d (duration magnitude) and M_W
 384 (moment magnitude). Where magnitude type is not specified we use the notation M . Where
 385 several different estimates are published, we preferentially cite M_W . If M_W is not available,
 386 and more than one other magnitude has been published, we cite the largest. Rationalizing the
 387 magnitude data is a significant task for the future.

388 1.6 Earthquake counts

389 The total number of earthquakes reported in a sequence depends strongly on the density of
 390 seismic monitoring. This may change with time, for example if additional seismic stations are
 391 installed after nuisance seismicity has begun. Earthquakes are a fractal phenomenon, and
 392 their numbers increase by about an order of magnitude for each reduction in magnitude unit.
 393 Where earthquake counts are compared, they must thus be related to a common low-
 394 magnitude cut-off threshold.

395 The numbers of earthquakes induced may be of interest where monitoring networks are stable
 396 since this parameter may serve as a sensitive strainmeter. As a result, earthquake counts have
 397 been particularly useful for monitoring active volcanoes. The availability of many
 398 earthquakes is also an advantage for research purposes such as tracking injected fluids. In
 399 such cases, hypocentral distributions can be defined better if data are plentiful. From the
 400 point of view of potential damage from large earthquakes, however, the ones of most
 401 relevance are the relatively few large-magnitude events and possibly only the largest one.

402 1.7 The database

403 The approach we used to construct the database is described in the online material.
 404 Challenges intrinsic to the task included:

- 405 • Incomplete reporting. This is without doubt severe and is quantified and discussed in
 406 Section 7.1;
- 407 • Ambiguous reporting, *e.g.*, “Seismicity is not reported”;
- 408 • Lack of reported data, *e.g.*, operational parameters not given;
- 409 • Uncertainty regarding whether earthquakes were induced, *e.g.*, some postulated
 410 associations are based simply on short-term temporal correlations or weak spatial
 411 correlations that cannot be supported statistically and may be coincidences. Our
 412 approach was to include all proposals published in peer-reviewed journals, and other
 413 reasonable proposals in the *iQuake* database. Responsibility for judging the strength
 414 of the evidence for human induction for particular cases is the responsibility of the
 415 user;
- 416 • Multiple possible induction processes ongoing simultaneously, *e.g.*, hydrocarbon
 417 extraction and wastewater injection;
- 418 • Non-uniformity of magnitude reporting. Many magnitude scales are used, instruments
 419 are often locally calibrated, magnitude type may not be reported, or several different
 420 magnitudes may be reported for the same earthquake in different publications
 421 (Section 1.5). Our approach was to report M_w if available, and if not the largest other
 422 magnitude;
- 423 • Lack of suitable networks to detect earthquakes. This hampers studies where
 424 earthquakes were not expected and suitable instruments were installed only after
 425 seismicity onset (Section 1.4);
- 426 • Poor accuracy of some earthquake locations (Section 1.4).

428 A list of the column headings in the database is given in Table 1. Additionally, in the online
 429 material, we provide more details of the method used to construct the *iQuake* database, a full
 430 description, explanations of the column headings, an abbreviated version and a bibliography
 431 of publications on induced earthquakes. We also provide the full database electronically in
 432 the form of an Excel spreadsheet, and an electronic database of related published references
 433 as an EndNote library. Continually updated versions of the latter two items are obtainable
 434 from the *iQuake* Database website at <http://www.inducedearthquakes.org>.

435 1.8 Earthquakes and belief systems

436 Public attitudes to induced earthquakes may have major implications for industrial projects.
 437 Human reactions to earthquakes may not be based on a full understanding of seismology, or
 438 even on scientific evidence of any kind. Because of their apparently random and spontaneous
 439 nature, and lack of obvious causes, earthquakes have for millennia been explained in terms of

440 folklore, religion, and other belief systems [e.g., Harris, 2012]. This includes Chinese,
 441 Russian and Japanese folklore and the religions of the ancient Greeks and Polynesians. All
 442 three mainstream Abrahamic religions—Christianity, Islam and Judaism—are based on ancient
 443 texts that attribute earthquakes to perceived shortfalls in human moral behavior.

444 Recent cases where explanations for earthquakes in terms of belief systems have had
 445 significant societal impacts include:

- 446 • In 2015, the Malaysian government attributed a M_w 6.0 earthquake that killed 18
 447 people to tourists posing nude on Mt. Kinabalu, one of the country's sacred
 448 mountains.
- 449 • In 2014 local people in the Altai Mountains, Siberia, attributed earthquakes to the
 450 removal of the mummified remains of a 5th-century BC noblewoman for
 451 archaeological research.
- 452 • In 2010, the American evangelist Pat Robertson allegedly attributed the devastating
 453 M_w 7.0 Haiti earthquake to the successful 1791-1804 anti-slavery insurrection on the
 454 island.

455 These examples serve to emphasize that public information and outreach is an important
 456 element of preparation to any industrial project that might induce earthquakes.

457 **2 Surface operations**

458 *2.1 Adding mass*

459 Earthquakes have been postulated to have been induced in association with three styles of
 460 surface mass addition. These are water impoundment behind dams (168 cases), erecting
 461 heavy buildings (1 case), and engineering accumulation of coastal sediments (1 case).

462 Seismic events in mines were known even before scientists understood the cause of
 463 earthquakes. The earliest report of earthquakes induced by water reservoir impoundment is
 464 from Lake Mead, Nevada and Arizona, USA (Figure 2) [Carder, 1945]. It was followed by
 465 numerous additional reports in the 1960s and later. At the time of writing several probable
 466 water-reservoir-induced earthquakes have resulted in fatalities and extensive property
 467 damage. The largest earthquake claimed to have been induced in this way is the 2008 $M \sim 8$
 468 Wenchuan, China, earthquake, which has been associated with impoundment of the reservoir
 469 behind the Zipingpu dam. In contrast, reports of earthquakes induced by erecting heavy
 470 buildings and engineering coastal land gain are, to date, rare and speculative.

471 2.1.1 Water impoundment behind dams

472 A well-studied example is that of the Koyna Dam, India (Figure 3). A detailed overview of
 473 this case, along with a review of dam-induced earthquakes, is given by Gupta [2002]. The
 474 103-m-high Koyna Dam was raised in 1962 and contains a reservoir up to 75 m deep and 52
 475 km long. Five years after it was completed, a sequence of earthquakes with magnitudes up to
 476 M_S 6.3 occurred causing ~ 200 deaths and slightly damaging the dam. The largest earthquake
 477 nucleated at shallow depth, probably < 5 km, and its epicenter was ~ 10 km from the dam.
 478 Earthquake activity has continued subsequently, correlating to some extent with water level
 479 in the reservoir (Figure 4) [Talwani, 1995]. A $M > 5$ event occurs there about every four
 480 years.

481 A second notable example is the Nurek dam, Tadjikistan (Figure 5) [Keith *et al.*, 1982; Leith
482 *et al.*, 1981; Simpson & Soboleva, 1977; Simpson & Negmatullaev, 1981]. Building of this
483 dam began in 1961 and, at 317 m, it is currently the highest in the world. It contains a
484 reservoir $\sim 10 \text{ km}^3$ in volume (Figure 6). The largest earthquake to have occurred there to date
485 is the 1972 M_S 4.6 event (Figure 7) [Simpson & Negmatullaev, 1981]. Seismicity is ongoing
486 and there is evidence for correlation with periods of increase in water depth (Figure 8).

487 The largest volume reservoir in the world is $1.64 \times 10^{11} \text{ m}^3$ and is contained by the 111-m-
488 high Aswan dam, Egypt. Earthquakes induced there are thought to occur in two depth
489 intervals at ~ 0 -10 km and ~ 15 -25 km (Figure 9 and Figure 10). This vertical separation is
490 postulated to indicate two different processes/environments of induction [Awad & Mizoue,
491 1995]. The largest earthquake observed to date, a M 5.7 earthquake that occurred in 1981, is
492 thought to have nucleated in the deeper zone.

493 A rare case where induced seismicity damaged the dam itself is that of the 105-m-high
494 Xinfengjian Reservoir, China. Impoundment of the $1.39 \times 10^{10} \text{ m}^3$ volume reservoir began in
495 1959 and seismic activity onset just one month later. A M_S 6.1 earthquake occurred in 1962
496 which caused minor cracking of the dam.

497 A case of particular interest is that of the May 2008 M_W ~ 8 Wenchuan, China, earthquake
498 (Figure 11). This earthquake was so large relative to the height of the nearby Zipingpu dam
499 (156 m) and the volume of the reservoir ($\sim 10^9 \text{ m}^3$) that it is controversial whether it was
500 induced or not. It nevertheless occurred ~ 20 km from the dam within months of full
501 impoundment of the reservoir. The earthquake was responsible for $\sim 90,000$ deaths and
502 serious damage to more than 100 towns, including collapsing houses, roads and bridges.

503 The area lies at the transition between the low-strain-rate ($< 10^{-10}$ per year), stable Sichuan
504 Basin continental region and the tectonically active Tibet plateau where strain rates are $> 10^{-8}$
505 /year. This transition is marked by the multi-stranded Longmenshan fault zone which
506 accommodates both thrust and strike-slip motion. Paleoseismic work suggests an earthquake
507 recurrence time of $\sim 7,000$ years for M 7-8 earthquakes [Klose, 2012].

508 Prior to impoundment of the reservoir, earthquake activity had been ongoing at a low level in
509 the vicinity of the dam at a rate of ~ 40 recorded events per month. This rate increased at the
510 beginning of the impoundment period, in October 2005, when the water level rose rapidly by
511 ~ 80 m. The level peaked in October 2006 at ~ 120 m above pre-impoundment levels. At this
512 point, earthquake activity surged to ~ 90 events per month but reduced thereafter (Figure 12).

513 The 2008 M_W ~ 8 mainshock nucleated at ~ 16 km depth and thrust motion propagated up
514 toward the surface beneath the reservoir. Rupture then transitioned to strike-slip motion and
515 propagated laterally along the fault in both directions, rupturing a > 300 km length of the
516 Longmenshan thrust belt with an average slip of 2.4 m, peaking at 7.3 m. The source time
517 function, which lasted 90 s, indicated that failure occurred in five sub-events that sequentially
518 released 14%, 60%, 8%, 17% and 6% of the total moment (Figure 13) [Zhang *et al.*, 2008].
519 The average stress drop during the earthquake was 18 MPa, peaking at 53 MPa. Similar to
520 other great earthquakes, this event thus owes its large size to chain-reaction of progressive
521 activation of adjacent fault segments in a series of sub-events.

522 The increase in shear and normal stresses, caused by impoundment of the water reservoir,
523 that were orientated to encourage slip on the fault were calculated to be no more than a few
524 kPa [Klose, 2012]. This is small, even compared with the stress changes associated with

525 Earth tides (Section 7.3). Klose [2012] suggests that this stress modulated the timescale on
526 which the great earthquake occurred, advancing it in time by ~60 years.

527 It has been much disputed whether or not the very small stress perturbation caused by this
528 water-reservoir impoundment was sufficient to trigger such a large earthquake. It is, however,
529 of the same order as stress loading suggested to encourage failure in other cases (*e.g.*, Section
530 3.1). A more relevant question is perhaps whether impoundment of the reservoir could have
531 induced the initial $M_W \sim 7.5$ sub-event, since it is that sub-event which triggered the
532 subsequent cascade of segment failures that grew the earthquake to a magnitude of $M_W \sim 8$.

533 In 2007 an unusual dam-related seismic sequence occurred in association with the Beni
534 Haroun hydraulic complex in the Mila region, 30 km west of the city of Constantine, Algeria
535 [Semmane *et al.*, 2012]. In that year, a sequence of earthquakes with magnitudes up to $M_d 3.9$
536 occurred. It is thought to have been induced by the leakage into the ground of $\sim 400,000 \text{ m}^3$ of
537 pressurized water as it was being pumped between two reservoirs. More than 7,200
538 earthquakes were recorded over a ~ 2 -month period.

539 The Beni Haroun hydraulic complex comprises a main dam 120 m high and a reservoir with
540 a capacity of $\sim 10^9 \text{ m}^3$ of water. This is connected by pipelines to a secondary reservoir, the
541 Oued Athmania reservoir, about 15 km south of the main dam (Figure 14). A 6-km stretch of
542 this pipeline system passes through a mountain at a depth of up to ~ 400 m below surface as a
543 lined tunnel 1.4–3.6 m in diameter. The pumping system, which raises the water by ~ 600 m,
544 has a capacity of $600,000 \text{ m}^3/\text{day}$.

545 In 2007 a large amount of water leaked from this tunnel via defective joints and penetrated
546 deep into the ground via fractures, faults and karst cavities. Earthquakes onset within days of
547 the leakage (Figure 15). The area had no prior record of swarm activity on a similar scale,
548 and installation of the infrastructure in 2000 had not been associated with an increase in
549 seismicity. The events did not cause damage but they alarmed local people unaccustomed to
550 earthquakes. It is reported that the earthquakes were heard loudly [Semmane *et al.*, 2012].

551 The Colorado River, USA, is dammed with numerous dams. The two largest are the 220-m-
552 high Glen Canyon dam, a concrete arch that impounds Lake Powell in Arizona, and the
553 Hoover dam, some 600 km further downstream to the southwest. This has a similar height
554 and impounds Lake Mead which is mostly in Nevada. Glen Canyon dam is built in Mesozoic
555 sedimentary rocks whereas the Hoover dam is built in Tertiary volcanics, part of the
556 tectonically active basin-range province. Somewhat unusually the intuitive expectation, that
557 the latter might be seismogenic and the former not, is in this case borne out (Figure 16).

558 Currently, attention is focused on the 181-m-high Three Gorges dam, China (Figure 17). The
559 40 km^3 water reservoir was fully impounded in 2010 and power generated came online in
560 2012. The total generation capacity is 22,500 MW. The area lies within a seismogenic region
561 that includes two major fault lines. The reservoir is not the largest in the world, but
562 earthquakes are already being reported with a $M_L 4.6$ event occurring in 2014.²

563 2.1.2 Erecting tall buildings

564 Lin [2005] suggested that erection of the ~ 500 -m high Taipei 101 building, Taiwan,

² <https://journal.probeinternational.org/2014/04/07/three-gorges-dam-triggers-frequent-seismic-activities/>

565 influenced the pattern of seismicity in the immediate neighborhood of the building. This $7 \times$
 566 10^8 kg building increased stress on the ground at its base by ~ 0.47 MPa. In the eight-year
 567 period prior to building, nine earthquakes with $M_L \leq 2.0$ occurred whereas during the eight-
 568 year period that spanned construction and followed it, 20 earthquakes up to $M 3.8$ occurred.
 569 Earthquakes were unusually frequent during the construction period (Figure 18).

570 This unusual case is the only published report to date of earthquakes being induced by raising
 571 a heavy building. Taiwan lies in the convergent plate boundary zone where the Philippine Sea
 572 plate is subducting beneath the Eurasian plate at the Manila trench. As a consequence it is
 573 seismically active.

574 This case raises the question of whether other such examples exist, *e.g.*, in Japan. The
 575 building that is currently the tallest in the world, the 825-m-high Burj Khalifa, Dubai, weighs
 576 less than the Taipei 101 building, at only 4.5×10^8 kg. There are no known reports of changes
 577 in earthquake activity from the New York or Tokyo regions where large buildings are
 578 common, though to our knowledge the issue has not been studied in detail.

579 2.1.3 Coastal land gain

580 It has been suggested that the 2007 $M_L 4.2$ Folkestone, Kent, UK, earthquake was triggered
 581 by geo-engineering of shingle accumulation in the harbor since 1806. There is substantial
 582 coastal land loss as a result of erosion to the southwest and northeast of Folkestone, but land
 583 gain by anthropogenic shingle accumulation in Folkestone harbor has been ongoing for ~ 200
 584 years. An estimated total of $\sim 2.8 \times 10^9$ kg had accumulated by 2007, four times the mass of
 585 the Taipei 101 building. This altered the stress by an estimated 0.001-0.03 MPa at 2 km depth
 586 [Klose, 2007a]. The earthquake epicenter was located ~ 1 km (epicentral error ~ 5 km) from
 587 the shingle, and nucleated at shallow depth.

588 2.2 *Surface operations: Removing mass*

589 Surface operations that remove mass from the surface and are reported to induce earthquakes
 590 are limited to quarrying. The *iQuake* database contains 16 such cases.

591 The largest earthquake that has been associated with quarrying is the 2013 $M 6.1$ Kuzbass,
 592 Siberia, event [Emanov *et al.*, 2014; Yakovlev *et al.*, 2013]. It occurred in the Bachatsky
 593 open-cast coal mine. This mine is 10×2.2 km in horizontal dimensions, excavated up to 320
 594 m deep, and produces $> 9 \times 10^6$ tonnes of coal per year. The earthquake was strong enough to
 595 collapse buildings in local communities and to be felt in neighboring provinces.

596 Moderate earthquake activity had been detected in the mine in early 2012 when a $M_L 4.3$
 597 event and associated aftershocks occurred. A dense local seismic network was installed, and a
 598 low level of small earthquakes with magnitudes up to $\sim M_L 2$ was found to be occurring. The
 599 magnitude of events increased with time, and 15 months later a $M_L 3.9$ event occurred
 600 followed a month later by the $M 6.1$ mainshock.

601 2.3 *Surface operations: Summary*

602 The impoundment of water in reservoirs behind dams is one of the best-known
 603 anthropological activities that induces earthquakes. It does so in abundance and accounts for
 604 168 (24%) of all the cases in the *iQuake* database. Ignoring natural lakes where dams have
 605 made minor changes to the water level, reservoirs are up to $8,502 \text{ km}^2$ in area (Lake Volta,

606 behind the Akosombo Dam, Ghana). Earthquakes may thus be induced throughout relatively
607 large regions.

608 In eight cases, earthquakes with $M > 6$ have been induced, associated with the dams at
609 Zipingpu (China), Lake Hebgen (USA), Polyphyto (Greece), Koyna (India), Kariba
610 (Zambia/Zimbabwe), Kremasta (Greece), Hsingfengkiang (China) and Killari (India). In
611 China there are 348 reservoirs with volumes exceeding 0.1 km^3 . Of these, 22 (6.3%) are
612 reported to be seismogenic.

613 Much has been published on the mechanism of triggering [see Gupta, 2002 for a summary].
614 Stresses induced by reservoirs at the depths at which earthquakes occur are small, perhaps of
615 the order of 0.1 MPa. This is much smaller than typical stress drops in earthquakes which are
616 commonly in the range 1-10 MPa. They are, nevertheless, larger than Earth tidal stresses. It is
617 speculated that the mechanism of induction may be that the surface load alters hydraulic
618 conditions at depth, causing fluid to migrate into fault zones and increase pore pressure. This
619 process may also explain the seismicity postulated to have been induced by erecting the
620 Taipei 101 building, Taiwan (Section 2.1.2) and engineered shingle accumulation at
621 Folkstone, UK (Section 2.1.3).

622 **3 Extraction from the subsurface**

623 *3.1 Groundwater extraction*

624 We have identified five reported cases of earthquakes postulated to be associated with
625 anthropogenic removal of groundwater. A particularly remarkable case is that of the 2011
626 M_w 5.1 Lorca, Spain, event that is suggested to have been induced by groundwater extraction
627 (Figure 19) [Gonzalez *et al.*, 2012]. This earthquake caused extensive damage to the town of
628 Lorca, seriously damaging both modern and historic buildings, killing nine people and
629 injuring several hundred others (Figure 20).

630 The region lies in a transpressive shear zone, comprising thrust- and strike-slip faults, that
631 forms part of the Nubia-Eurasia plate boundary. The M_w 5.1 mainshock nucleated on the
632 Alhama de Murcia fault at unusually shallow depth ($\sim 3 \text{ km}$). This fault has generated several
633 large earthquakes over the past few centuries. Considerable geodetic data were available,
634 from radar interferometry and GPS surveying, constraining co-seismic deformation.
635 Numerical modeling of this deformation was consistent with slip of up to $\sim 15 \text{ cm}$ on a $\sim 10 \times$
636 10 km section of the fault in the depth interval $\sim 1\text{-}4 \text{ km}$ (Figure 21).

637 Geodetic data also constrained regional surface deformation over the several decades
638 preceding the earthquake. To the southeast of the Alhama de Murcia fault, long-term
639 groundwater pumping had lowered the water table by $> 250 \text{ m}$ in the period 1960-2010. This
640 had been accompanied by surface subsidence at rates of $> 10 \text{ cm/year}$, totaling $> 2 \text{ m}$ over the
641 preceding 20 years. Significant environmental effects had occurred as a result (Figure 22).

642 González *et al.* [2012] calculated the subsurface stress change resulting from water-mass
643 removal to investigate the effect of groundwater pumping on the Alhama de Murcia fault.
644 The Coulomb stress changes would have encouraged faulting of the type that occurred. A slip
645 deficit of up to $\sim 12 \text{ cm}$ had probably accumulated in the Alhama de Murcia fault since the
646 last large earthquake on the fault segment ~ 200 years earlier. Numerical modeling results
647 were consistent with a groundwater crustal unloading process that enabled tectonically
648 accumulated stress to have been released in the 2011 M 5.1 earthquake. González *et al.*

649 [2012] concluded that the cumulative long-term hydraulic unloading, coupled with the
 650 relative position and type of the fault with respect to the depleting aquifer, contributed to the
 651 stress conditions that resulted in the earthquake.

652 Several other cases of induced seismicity of this kind have been proposed. The 2015 M_w 7.8
 653 Gorkha, Nepal, earthquake has been linked to removal of groundwater from the Gangetic
 654 plains to the south [Kundu *et al.*, 2015]. This thrust earthquake caused ~8000 deaths and
 655 ~\$10 billion of economic loss, ~50% of the Gross Domestic Product of Nepal.

656 The Gangetic plains, which cover $\sim 2.5 \times 10^6$ km², are home to ~0.5 billion people. Extraction
 657 of groundwater amounts to the removal of $\sim 23 \times 10^{12}$ m³/year, equivalent to a drop in the
 658 water table of ~ 1 m/year (Figure 23). This load is being removed from the footwall of the
 659 Main Himalayan Thrust, thus encouraging slip on the fault zone in the same way as
 660 groundwater removal near Lorca, Spain (Figure 24). The Gangetic plains form the most
 661 intensely irrigated region in southeast Asia and have the highest population density. Kundu *et*
 662 *al.* [2015] suggest that anthropogenic crustal unloading causes a significant component of
 663 horizontal compression that adds to the secular compressional stress buildup along the Main
 664 Himalayan Thrust.

665 Kundu *et al.* [2015] calculated the Coulomb failure stress change to have been ~ 0.003 - 0.008
 666 MPa since 1960. Such a stress change is at the lower limit of those induced by Earth tides
 667 (Section 7.3). It is comparable, however, to the calculated natural rate of stress accumulation
 668 on the Main Himalayan Thrust, which is ~ 0.001 - 0.002 MPa/year. The dewatering of the
 669 Gangetic plains is thus accelerating stress accumulation on the Main Himalayan Thrust by
 670 4.5-20%.

671 In the San Joaquin Valley, California, the groundwater has been depleted by some 1.6×10^{11}
 672 m³ over the past ~150 years [Amos *et al.*, 2014; McGarr, 1991]. Depletion and recharge from
 673 precipitation is seasonal, with the most rapid depletion during the summer agricultural
 674 growing months and the most rapid recharge during the winter and spring. Annual fault-
 675 normal seasonal stress variations on the San Andreas fault zone from this source are
 676 calculated to be ~ 0.001 MPa, encouraging earthquakes during the summer and autumn
 677 months. The expected seasonality in seismicity is seen in earthquakes with $M > 1.25$. The
 678 stress rate estimated is similar to that calculated for the Main Himalayan Thrust from
 679 dewatering the Gangetic plains [Kundu *et al.*, 2015].

680 A similar process was suggested to modulate seismicity in the Gran Sasso chain in the central
 681 Apennines, Italy [Bella *et al.*, 1998]. There, tunneling for construction of a highway in the
 682 period 1970-1986 was observed to significantly change the hydrology of natural springs.
 683 Changes in the spatial pattern of local seismicity, an increase in seismic rate, and the
 684 occurrence of three $M > 3$ events were postulated to be linked to the hydraulic changes. In
 685 addition, Klose [2007b] attributes the 1989 M_L 5.6 Newcastle, New South Wales, Australia,
 686 event to the dewatering of deep coal mines bringing a local fault closer to failure.

687 3.2 Mining

688 Deep mine excavations strongly perturb the stresses in surrounding rocks and may reduce
 689 some components from values initially of the order of 100 MPa to atmospheric (0.1 MPa).
 690 The resulting stress differences can exceed the strength of competent rocks and cause
 691 earthquakes. These are traditionally known as “rock bursts” or “coal bumps”.

692 In modern times excellent seismic data have been recorded on dense, multicomponent arrays
 693 installed for hazard mitigation purposes. Propagation paths are often short, pass through
 694 homogeneous rock, and are free from the effects of the weathered surface layer that degrade
 695 surface observations. Significant advances in understanding the source physics of
 696 earthquakes have been achieved using these data. In particular, it has been shown that many
 697 mining-induced earthquakes have net implosive source mechanisms, consistent with partial
 698 closure of the artificial voids created by the removal of mass [e.g., Feignier & Young, 1992;
 699 Kuznir *et al.*, 1982; Rudajev & Sileny, 1985; Wong & McGarr, 1990; Wong *et al.*, 1989]. A
 700 detailed review of this aspect of mining seismicity is given by Miller *et al.* [1998b, Section
 701 3.4].

702 3.2.1 Traditional mining

703 In recent years mining has delved progressively deeper and removed progressively larger
 704 masses from the subsurface. The increasing demand for coal and other minerals requires, in
 705 the absence of other solutions, that this trend continues. The problem of mining-induced
 706 earthquakes is thus likely to grow unless management solutions are found.

707 Seismicity of this sort may be disproportionately serious because of the large loss of life and
 708 economic resources caused. This includes environmental damage such as surface subsidence
 709 which may render buildings beyond repair. Dealing with, and mitigating, mining-induced
 710 seismicity is likely to be a major technical challenge, and even a limiting factor, to the
 711 industry in future [e.g., Tang *et al.*, 2010].

712 During the ~50-year period 1949-1997, over 2000 coal bursts occurred in 33 mines in China,
 713 killing several hundred people and costing > 1300 days in lost production [Tang *et al.*, 2010].
 714 Figure 25 shows the distribution of state-owned coal mines and mining-induced seismicity in
 715 China. In 2007 some 102 coal mines and 20 other mines reported seismicity.

716 Li *et al.* [2007] report that seven of these were associated with events of $M > 4.0$ and 27 with
 717 events of $M \geq 3.0$. Earthquakes are shallow, occurring in the depth range 0-7 km. The largest
 718 coal mining event that has occurred in China is the 1977 M_L 4.3 event at Taiji mine, Beipiao,
 719 Liaoning [Li *et al.*, 2007]. Coal mining in China is increasing in depth of extraction and
 720 volume removed, and the problem of mining-induced seismicity is increasing also (Figure 26
 721 and Figure 27).

722 One of the most spectacular cases of mining-induced seismicity occurred in 1989 in the
 723 Volkershausen Ernst Thaelmann/Merkers potash mine, Germany. An event with M_L 5.6
 724 [Bennett *et al.*, 1994; Knoll, 1990] was associated with the collapse of ~3,200 pillars
 725 throughout an area of ~6 km² in the depth range 850-900 m. A large part of the local town of
 726 Düren was devastated, including several hundred buildings damaged and 19 totally
 727 destroyed. Three people are reported to have been killed and several injured. Seismic records
 728 suggest a multiple event involving three main sub-events with magnitudes of M_L 4.4, 5.1 and
 729 5.5. The M_L 5.5 event was attributed in part to the injection of fluid waste which had
 730 increased pore pressure by ~0.3-1.1 MPa. The event was classified as a fluid-induced
 731 rockburst involving an earthquake in the overlying rock which induced collapse of the pillars
 732 [Knoll, 1990].

733 An unusual case that involved litigation over the cause of a fatal mine-related earthquake is
 734 that of the 2007 M_w 4.1 Crandall Coal Mine, Utah, event. Nine miners and rescuers were
 735 killed as a result of a gallery collapse. The cause of the collapse was variously attributed to

736 triggering by a natural earthquake or unsafe back-stripping mining practices. Calculation of
 737 the seismic moment tensor of the event using recordings from regional seismic stations
 738 contributed to resolving the controversy. The study showed that the focal mechanism was not
 739 consistent with shear slip on a fault, as would be expected for a natural earthquake, but with a
 740 rapidly closing crack, as would be expected for a gallery collapse (Figure 28) [Dreger et al.,
 741 2008]. The following year, the US Mine Safety and Health Administration levied fines
 742 totaling \$1.85 million for unsafe mining practices at Crandall Coal Mine.

743 The UK has a long history of mining dating from the Neolithic period that includes flint,
 744 lead, copper, coal, tin mining in Cornwall and gold mining in Wales (Figure 29). During the
 745 19th and 20th centuries coal mining became a major industry. At the height of this industry, in
 746 1913, 292 million tonnes of coal were extracted from 3024 mines, some of which were
 747 excavated to a depth of ~1200 m and even extended several kilometers offshore beneath the
 748 North Sea^{3,4}. The *iQuake* database includes the largest-magnitude earthquake recorded in
 749 each major UK coalfield.

750 Wilson *et al.* [2015] reviewed earthquakes in the UK with the objective of determining a
 751 national baseline for seismic activity in advance of possible future shale-gas hydrofracturing.
 752 They used the earthquake database of the British Geological Survey. Of the ~8000 onshore
 753 British earthquakes in that catalog for the period 1970-2012 they estimated ~21% to have
 754 been anthropogenic, the majority caused by coal mining (Figure 30). The correlation between
 755 coal production and earthquakes is shown in Figure 31 [Wilson *et al.*, 2015]. This is an
 756 interesting case history because it shows the large reduction in seismicity that accompanied a
 757 major reduction in coal production during the 1984-85 miners' strike. The economic cost of
 758 that strike is estimated to have been several billion pounds, from which can be calculated that
 759 the mitigation of each earthquake cost ~ £10 million. The earthquake rate returned to a level
 760 corresponding to coal production following the end of the strike in the spring of 1985.

761 The region that is perhaps the most renowned for large mining-induced earthquakes is South
 762 Africa. There, two of the world's richest ore bodies are mined—the gold-bearing
 763 conglomerates of the Witwatersrand Basin and the platinum-bearing pyroxenites of the
 764 Bushveld Complex. Both bodies extend to depths of several kilometers, and mining depths
 765 exceed 3.5 kilometers [Durrheim, 2010]. The current regional stress field is extensional but
 766 tectonically inactive. Mining-induced earthquakes are thought to result from collapses of up
 767 to ~1 m in the vertical. These collapses contract galleries in the form of horizontal tabular
 768 voids for up to several kilometers of their lengths. Earthquakes with magnitudes up to m_b 5.6
 769 have occurred (President Brand mine, Welkom, in 1994).

770 The problem of induced seismicity in South Africa became apparent early in the 20th century
 771 when large-scale mining penetrated to depths of several hundred meters. It is now a major
 772 issue and in recent decades great efforts have been made to mitigate the risk. These include
 773 development of the safest possible mining techniques, optimal design of equipment, and
 774 seismological monitoring. As a result, fatality rates have been reduced though they still run to
 775 several tens of deaths per year. A large body of literature has been published on the subject
 776 [e.g., Amidzic *et al.*, 1999; Boettcher *et al.*, 2015; deBruyn & Bell, 1997; Durrheim, 2010;

³ <https://www.gov.uk/government/statistical-data-sets/historical-coal-data-coal-production-availability-and-consumption-1853-to-2011>

⁴ <http://www.dmm.org.uk/mindex.htm>

777 Durrheim *et al.*, 2013; Durrheim *et al.*, 2006; Heesakkers *et al.*, 2005; Jaku *et al.*, 2001; Julià
778 *et al.*, 2009; Kozłowska *et al.*, 2015; Lippmann-Pipke *et al.*, 2011; Milev & Spottiswoode,
779 2002; Richardson & Jordan, 2002; Wright *et al.*, 2003; Yabe *et al.*, 2015; Ziegler *et al.*,
780 2015].

781 An example of a serious earthquake is a M_L 4.0 event that occurred in Western Deep Levels
782 East gold mine in 1996. It nucleated in complex geology ahead of actual mining, and
783 extensively damaged the area. Work at the time involved removing a large pillar formed by
784 earlier, smaller-scale mining. This damaging earthquake had a significant impact on mining
785 techniques and adherence to safe practice, and resulted in improved seismicity management
786 strategies [Amidzic *et al.*, 1999].

787 An even larger event, with M_L 5.3, occurred in the Klerksdorp district of South Africa in
788 2005. This earthquake caused serious damage to the nearby town of Stilfontein, injuring 58
789 people. Two mineworkers in a nearby gold mine were killed and thousands of others were
790 evacuated. This large earthquake was attributed to stress loading by past mining, rather than
791 the mining then ongoing [Durrheim *et al.*, 2006]. The case highlighted the issue of
792 insufficiently well-documented past mining activities, a problem for all nations with long
793 traditions of mining. It also raised the question of whether earthquakes induced by one
794 industrial project could present hazard to others nearby. Furthermore, its delayed occurrence
795 suggested that seismic hazard may remain a problem not only during deep mining but beyond
796 mine closure.

797 Because of the problem that induced seismicity poses in deep South African gold mines,
798 state-of-the-art monitoring networks have been installed. These networks have gathered
799 unusually high-quality data which have enabled some remarkable advances in seismological
800 techniques and knowledge. McGarr [1992a] derived full moment tensors for 10
801 Witwatersrand mining-induced earthquakes with magnitudes of M 1.9-3.3. The earthquakes
802 formed two distinct types. Seven involved substantial coseismic volumetric reduction
803 combined with normal faulting and three had no significant volumetric component. McGarr
804 [1992a] concluded that those with volumetric components involved interaction between a
805 mine stope and a shear fault.

806 These conclusions were confirmed by later workers. Julià *et al.* [2009] obtained focal
807 mechanisms for 76 mine tremors with M 0.5-2.6 that occurred at the deep AngloGold
808 Ashanti Savuka gold mine. These events were recorded on 20 high-frequency geophones in
809 the mine. The largest principal stress was vertical and was relieved by a combination of
810 volumetric closure and normal faulting, consistent with the vertical closure of galleries.
811 Richardson and Jordan [2002] studied seismicity associated with five deep mines in the Far
812 West Rand district using data recorded in the period 1994-2000 by in-mine arrays of three-
813 component sensors. Seismic rates exceeded 1,000 events per day. Some earthquakes occurred
814 within 100 m of active mining faces or development tunnels, and generally had $M < 1$. They
815 attributed those events to the response to blasting, stress perturbations from the excavation,
816 and closure of individual stopes. Other events were distributed throughout the active mining
817 region. Some had magnitudes of $M > 3$, and appeared to be similar to regional tectonic
818 earthquakes.

819 3.2.2 Solution mining

820 Solution mining, or “in-situ leaching” recovers minerals via boreholes drilled into the
821 deposit. A lixiviant—a liquid used to dissolve the target mineral—is pumped into the resource

822 via an injection borehole. It circulates through the rock dissolving the mineral and is
 823 extracted via a production well. The lixiviant may be water (*e.g.*, to extract salt), or acid or
 824 sodium bicarbonate to extract metals, *e.g.*, uranium, copper, gold or lithium. Roughly half
 825 the world's uranium is produced by solution mining.

826 Our database contains eight cases of seismicity postulated to be associated with solution
 827 mining. The best-documented is from the Vauvert Field, France. There, brine is produced
 828 from a layer comprising ~50% salt at 1900-3000 m depth (Figure 32). Water is circulated
 829 through fractured zones via a well doublet. Some, but not all, of the cavities created dissipate
 830 by salt creep. Earthquakes occur where this process cannot keep up with mass removal.
 831 Additional seismicity results from hydraulic fracturing used to create porosity. Over 125,000
 832 earthquakes with $M -3$ to -0.5 that occurred in the period 1992-2007 have been located
 833 [Godano *et al.*, 2010].

834 Larger earthquakes are reported for solution mines in the USA. There, three cases are
 835 documented from Attica (New York), Cleveland (Ohio), and Dale (New York). Of three M_L
 836 ~5 events that occurred near Attica, in 1929, 1966 and 1967, two had estimated hypocentral
 837 depths as shallow as 2-3 km [Herrmann, 1978]. They are postulated to have been induced by
 838 local salt solution mining, though this was not recognized at the time [Nicholson & Wesson,
 839 1992].

840 In China, a M_L 4.6 earthquake is reported to have occurred in 1985 in association with
 841 solution mining of salt from depths of 800–1800 m at the Zigong salt mine, Sichuan Province
 842 [Li *et al.*, 2007]. This earthquake is reported to have induced the highest intensity of ground
 843 shaking observed for any mining-induced earthquake in China. It is the largest-magnitude
 844 mining-related event of any kind that is known from China.

845 At Mishraq, Iraq, earthquakes occurred in association with the mining of sulfur by injecting
 846 hot (~150°C) water at pressures of 0.6-0.8 MPa into layers up to 190 m deep [Terashima,
 847 1981]. Rapid surface subsidence occurred—up to several mm/day—and resulted in surface
 848 cracking. Felt earthquakes occurred 1973-1975 and were most numerous at times of high
 849 injection rate.

850 3.2.3 Tunnel excavation

851 We have identified 20 case histories of earthquakes accompanying the excavation of tunnels
 852 and cavities. These have been excavated for purposes that include power-station housing
 853 (*e.g.*, the underground powerhouse of the Pubugou, China hydroelectric station), water
 854 transport at hydro-electric and nuclear power stations (*e.g.*, the Yuzixi hydro-electric station,
 855 China, and the Forsmark nuclear plant, Sweden), road and railway transport (*e.g.*, the Ritsem
 856 tunnel, Sweden, and the Qinling railway tunnel, China) [Tang *et al.*, 2010].

857 A particularly well-documented example is the case of the Gotthard Base Tunnel,
 858 Switzerland, part of the New Alpine Traverse through the Swiss Alps [Husen *et al.*, 2012].
 859 This 57-km-long tunnel was excavated for freight and passenger rail transport in the period
 860 2002-2006 using drilling and blasting. It includes three “Multi-Function Stations” (MFSs)
 861 which divide the tunnel into five sections.

862 A series of 112 earthquakes with M_L -1.0 to 2.4 occurred 2005-2007 in association with
 863 excavation of the southernmost station, MFS Faido. The largest event was shallow (0.5-1.0
 864 km below the surface) and felt strongly at the surface. No surface damage was reported. The

865 station cavity was, however, damaged significantly including flaking of the reinforced walls
 866 and upwarping of the floor by ~ 0.5 m. The seismicity correlated spatially and temporally
 867 with excavation of the station (Figure 33 and Figure 34). Highly accurate locations obtained
 868 using a dense, temporary seismic network showed that, on average, the earthquakes occurred
 869 at the same depth as the tunnel. Some correlated with large rockbursts observed in the tunnel
 870 shortly after blasting.

871 The focal mechanism of the largest earthquake indicated normal faulting on a steep fault
 872 plane belonging to the fault system mapped locally. An estimate of the source dimensions
 873 suggested a failure region 50-170 m long. The tunnel traverses mostly igneous and
 874 metamorphic rocks, but it also crosses a complex of structures with different rheological
 875 properties, including faulted and heavily fractured sections. Two-dimensional discontinuum
 876 modeling suggested that the earthquake activity resulted from an unfavorable juxtaposition of
 877 rocks with different rheologies combined with a fault zone. The horizontal stresses imposed
 878 by the excavations were relieved by shrinking of the tunnel which reactivated the fault zone.

879 3.3 *Hydrocarbons*

880 Reviews of induced seismicity associated with hydrocarbon production are provided by
 881 Suckale [2009; 2010]. There are $\sim 67,000$ hydrocarbon fields worldwide [Li, 2011] including
 882 ~ 1500 giant and major fields, and of the order of a million producing oil and gas wells. The
 883 seismic response to hydrocarbon production varies from field to field and no seismicity is
 884 reported for the vast majority. Reporting is, however, incomplete. Many fields are not
 885 instrumented and it is thus inevitable that cases of seismogenesis go unpublished and even
 886 unnoticed (Section 7.1). Earthquakes account for only a small percentage of the deformation
 887 associated with reservoir compaction with the majority being taken up by ground subsidence
 888 or counteracted by fluid recharge from the sides. In many cases the earthquakes reported
 889 occurred on faults that were either not known before or considered to be tectonically inactive.

890 3.3.1 Gas

891 We have identified 36 cases of seismicity postulated to have been induced by extraction of
 892 natural gas from reservoirs. These are from Canada (1 case), China (1 case), France (2 cases)
 893 Germany (7 cases), Italy (1 case), the Netherlands (18 cases), Oman (1 case), the USA (4
 894 cases) and Uzbekistan (1 case). By far the most numerous are from The Netherlands, which
 895 accounts for 50% of all cases we found.

896 Worldwide, the most extreme case of earthquakes induced by gas production is that of the
 897 Gazli reservoir, Uzbekistan. In 1976 and 1984, three $M_S \sim 7$ earthquakes occurred, seriously
 898 damaging the local town of Gazli, reportedly causing one death and ~ 100 injuries [Simpson
 899 & Leith, 1985]. An additional $M_S 5.7$ event occurred in 1978. A timeline of events is as
 900 follows:

- 901 • 1956 the Gazli field was discovered;
- 902 • 1963 pipelines to the Urals industrial region were completed;
- 903 • 1966 production of ~ 20 billion m^3 /year of gas began. Reservoir pressure was
 904 initially ~ 7 MPa;
- 905 • 1968-71 production peaked;
- 906 • 1976 pressure had declined to 3-3.5 MPa; two $M_S \sim 7$ earthquakes occurred;
- 907 • 1978 a $M_S 5.7$ earthquake occurred;

- 908 • 1984 a third $M_S \sim 7$ earthquake occurred;
- 909 • 1985 pressure had declined to 1.5 MPa.

910

911 During the period when gas was produced it was drawn from a reservoir at a depth of ~ 2 km,
 912 hosted in an open anticline of tight Paleogene sandstones. This structure is cut by several
 913 blind faults and the $M_S \sim 7$ earthquakes are thought to have occurred on one of these (top
 914 panel, Figure 35). The epicenters of the events formed an arcuate array north of the field.
 915 Fault-plane solutions suggest that they occurred on a north-dipping, approximately east-west
 916 striking thrust fault, consistent with the tectonics of the region. Extrapolation of this fault to
 917 shallow depth suggests that it intersects with the gas reservoir (bottom panel, Figure 35).

918 In addition to this geometric correspondence, Simpson and Leith [1985] cite four indications
 919 that these events, although exceptionally large, were induced:

- 920 • previous seismic quiescence;
- 921 • the anomalous magnitude distribution of events which involved three $M_S \sim 7$ events
 922 rather than a clear mainshock-aftershock sequence;
- 923 • the large decrease in pressure in the gas reservoir; and
- 924 • source modeling that indicated that, unusually, rupture propagated downwards on the
 925 fault plane.

926

927 The proposal that these earthquakes were induced has nevertheless been challenged, *e.g.*, by
 928 Bossu *et al.* [1996], on the grounds that the stress perturbation on the fault was too small to
 929 have triggered such large earthquakes.

930 Possible analyses of this case are limited because details available about the recovery
 931 procedure are sparse. However, the case of Gazli is important because of its serious
 932 implications for the possible maximum magnitude of earthquakes that could conceivably be
 933 induced by gas extraction.

934 The largest earthquake postulated to have been induced by gas extraction in Europe is the
 935 1951 $M 5.5$ event that occurred in the Caviaga Gasfield, Po Valley, Italy. There, large-scale
 936 extraction of methane at pressures > 10 MPa had been underway. The earthquake cannot be
 937 well studied because of the limited instrumentation in place at the time. Simple analysis of
 938 paper recordings of the largest, $M_L 5.5$, event suggested that it nucleated at ~ 5 km depth and
 939 had a thrust mechanism. The region where it occurred had previously been aseismic [Caloi *et*
 940 *al.*, 1956].

941 The case of Caviaga is the only $M \geq 5$ gas-extraction-induced earthquake reported for
 942 Europe. Several other European gas-extraction projects are associated with $M \geq 4$ seismicity.
 943 A case of abundant seismicity is the Lacq Gasfield, France, which has generated earthquakes
 944 with magnitudes up to $M_L 4.2$ (Figure 36). A full review of the > 2000 earthquakes located
 945 there in the period 1974-1997 is given by Bardainne *et al.* [2008].

946 Production at Lacq started in 1957 with extraction of gas from a reservoir at a depth of 3.2-5
 947 km, beneath a 600-m-deep oilfield. The reservoir occupies a 20-km-long, densely fractured
 948 anticline in Mesozoic limestones sealed by a Cretaceous marl (Figure 37). Reservoir pressure
 949 decreased from 66 MPa to 2.3 MPa in the period 1957-2008 and surface subsidence of ~ 6 cm
 950 occurred.

951 The first earthquake noticed, which had an estimated magnitude of M 3-4, was felt in 1969
952 after the gas pressure had declined to 36 MPa. This, and the seismicity that followed, is
953 unlikely to be natural because of its concentration in the gasfield and because Lacq is 30 km
954 north of the nearest major seismically active structure, the Pyrenean Frontal Thrust (Figure
955 36). About 70% of the earthquakes located above the gas reservoir. They nucleated
956 preferentially on faults optimally-oriented with respect to the poroelastic stress perturbation
957 caused by gas removal. Poorly oriented faults tended to be aseismic. There is poor correlation
958 between the surface subsidence and the seismicity with both seismic and aseismic regions
959 subsiding. During the observation period, seismicity migrated from the centre to the
960 periphery of the reservoir (Figure 38). Comparison of the spatial distribution of hypocenters
961 with theoretical deformation models favored the model of Odonne et al. [1999] rather than
962 that of Segall [1989] (Figure 39).

963 Seismicity induced by gas extraction is particularly abundant in The Netherlands. There,
964 ~300 gasfields are produced. Of these, just a few percent are reported to be seismically active
965 but on a global scale this is an exceptionally high rate of reported seismogenesis. The
966 induction mechanism is thought to be differential compaction [Gee *et al.*, 2016].

967 One of the largest earthquakes to be attributed to induction in The Netherlands to date is the
968 2012 Groningen M_L 3.4 event. In addition to this a further 8 events with M > 3.0 have
969 occurred in that field (Figure 40). Seismicity was first recorded in December 1991 when the
970 reservoir reached ~28% depletion, some 28 years after the start of gas extraction in 1962
971 (Figure 41).

972 Historically, The Netherlands had a low rate of natural seismicity compared with neighboring
973 countries where much higher rates are associated with the Upper Rhine Graben (Figure 42
974 and Figure 43) [van Eck *et al.*, 2006]. Today, the vast majority of seismicity in the northern
975 Netherlands is associated with gas extraction. Several hundred earthquakes have been
976 recorded in the Groningen Field alone. This reservoir, the largest natural gasfield in Europe
977 and the tenth-largest in the world, originally contained some $3 \times 10^9 \text{ m}^3$ of gas in a porous
978 sandstone formation up to 300 m thick and 45 x 25 km in area. Both the seismic rate and the
979 magnitudes of the largest earthquakes have increased on a time scale of a few years (Figure
980 41 and Figure 44). An apparent increase in the slope of the Gutenberg-Richter distribution
981 (the “*b*-value”) with time is consistent, however. This means there is a progressive reduction
982 in the proportion of large to small earthquakes (Figure 45 and Figure 46) [van Eck *et al.*,
983 2006; Van Wees *et al.*, 2014]. Reservoir compaction is greatest in two northwesterly trending
984 zones of the reservoir and the earthquakes correlate well with the southernmost of these
985 (Figure 47).

986 A renowned case of seismicity induced by gas extraction in the USA is that of the Fashing
987 Gasfield, Texas (Figure 48). Production there started in 1958 from a depth of 3.2 km. By
988 1983 the pressure had decreased by ~7 MPa and a M 3.4 earthquake occurred (Figure 49).
989 The reservoir was replenished by water recharge as it became depleted and injection was
990 undertaken for disposal of produced water. In 1992 a M 4.3 earthquake occurred and in 2011
991 the largest event, with M_w 4.8. This case is usually discussed jointly with the nearby Imogene
992 Oilfield (Section 3.3.2).

993 3.3.2 Oil

994 In many oilfields multiple processes are underway simultaneously including oil and gas
995 extraction, waste-water disposal, water injection to aid oil recovery and hydrofracturing or

996 thermal fracturing. It is thus often difficult to attribute unambiguously any seismicity to oil
 997 extraction alone (Section 1.7). Nevertheless, we have identified eight cases where
 998 earthquakes have been postulated to be associated with oil extraction. These are from the
 999 USA, Iran, Russia and Norway. The total is extraordinarily few compared with the large
 1000 number of producing oilfields worldwide (Section 3.3).

1001 One of the earliest reports of earthquakes accompanying oil production is from Goose Creek,
 1002 Texas, where a series of small earthquakes was reported in the 1920s (Figure 50). This field
 1003 is remarkable for the major surface subsidence that occurred there. Following the extraction
 1004 of several million barrels of oil an area $\sim 10 \text{ km}^2$ in size subsided by up to 1 m over an ~ 8 -
 1005 year period [Nicholson & Wesson, 1992; Pratt & Johnson, 1926]. Goose Creek is a coastal
 1006 region and a substantial area sank below sea level requiring industrial infrastructure to be
 1007 adapted to the flooded conditions.

1008 The largest earthquake in our database attributed to oil extraction is the M_W 6.2 1983
 1009 Coalinga, California, event. This event, along with the 1985 M_W 6.1 Kettleman North Dome
 1010 earthquake and the 1987 M_L 5.9 Montebello Fields (Whittier Narrows) earthquake, both also
 1011 in California, were attributed by McGarr [1991] to the removal of oil from fields in uplifting
 1012 anticlines. The Coalinga and Whittier Narrows events were felt throughout much of
 1013 California and caused multiple deaths and injuries (Figure 51).

1014 All three events nucleated at $\sim 10 \text{ km}$ depth. McGarr [1991] suggested that net extraction of
 1015 oil and water reduced the average density of the upper crust, and that the seismic deformation
 1016 was approximately equal to that required to restore isostatic equilibrium (Figure 52). This
 1017 suggestion was challenged by other workers. Segall [1989] calculated stress loading and
 1018 concluded that depletion of the reservoir would have only loaded the nucleation region by
 1019 $\sim 0.01\text{-}0.03 \text{ MPa}$. Nicholson and Wesson [1992] suggested an alternative explanation, that the
 1020 earthquake might have occurred in response to larger stresses imposed by fluids migrating
 1021 into the mid-to-lower crust. They suggested that changes in pressure resulting from
 1022 withdrawal of oil might have induced such fluid migration and brought the fault closer to
 1023 failure. It has also been suggested that the Coalinga earthquake was induced by extraction of
 1024 groundwater for irrigation purposes from the nearby San Joaquin valley (Section 3.1) [Amos
 1025 *et al.*, 2014]. A further suggestion is that the Coalinga earthquake contributed to stress
 1026 buildup that was released six years later in the 1989 M_W 6.9 Loma Prieta earthquake. This
 1027 event ruptured a section of the San Andreas fault system 96 km south of San Francisco and
 1028 caused 63 deaths, 3,757 injuries and \$5.6–6 billion of damage [Reasenber & Simpson,
 1029 1992].

1030 Another major damaging earthquake proposed to be associated with oil extraction in
 1031 California is the 1933 M_L 6.3 Long Beach, California, earthquake which killed > 100 people
 1032 and did \$40 million of damage. This earthquake may have resulted from oil production in the
 1033 nearby Wilmington and Huntington Beach Oilfields (Section 4.1.3) [Nicholson & Wesson,
 1034 1992].

1035 An example where there is little dispute that earthquakes were primarily induced by oil
 1036 extraction is from the Imogene Oilfield, Texas [Pennington *et al.*, 1986]. This field lies just
 1037 $\sim 25 \text{ km}$ from the seismogenic Fashing Gasfield (Section 3.3.1; Figure 48). In 1984 a M_L 3.9
 1038 earthquake occurred in the Imogene Oilfield, followed by aftershocks located at 2-3 km depth
 1039 at or near the reservoir bounding fault.

1040 The Imogene Oilfield is contained in Cretaceous limestone and bounded by high-angle faults

1041 that splay at shallow depth. Production of oil began in 1944 from a 33-m-thick horizon at 2.4
 1042 km depth. By 1973 reservoir pressure had dropped from an initial 25 MPa to ~10 MPa. In the
 1043 period 1972-1978 it was flooded with 55,000 m³ of water via injection wells in an effort to
 1044 mitigate this pressure reduction. This is, however, a much smaller volume than the ~ 1
 1045 million m³ of oil and gas that had been produced, and flooding ceased several years before
 1046 the 1984 earthquake. As a consequence, the seismicity has been attributed to depressurization
 1047 of the field as a result of oil depletion.

1048 The most spectacular example of subsidence and induced earthquakes associated with a
 1049 producing oilfield is that of the Wilmington Field, California, one of the largest oilfields in
 1050 the USA (Figure 53 and Figure 50). Oil production began in 1936 and over the following 30
 1051 years up to 9 m of subsidence and 3.6 m of horizontal contraction occurred. Strain rates were
 1052 > 1000 times greater than those along locked sections of the San Andreas fault [Kovach,
 1053 1974; Segall, 1989].

1054 Seismicity onset above and below the reservoir when the reduction in pressure reached ~10
 1055 MPa. Eight earthquakes with magnitudes of M_L 2.4-5.1 occurred on shallow, low-angle
 1056 bedding planes in the field. The largest, which occurred in 1949, sheared off hundreds of
 1057 production wells causing > \$9 million of damage. An area of ~ 5.7 km² was affected and
 1058 ground deformation of up to 20 cm occurred. Because the event was so shallow, surface
 1059 waves were generated [Nicholson & Wesson, 1992; Segall, 1989].

1060 Seven of the eight earthquakes occurred during the oil production period and one occurred
 1061 after significant water flooding began in 1958 to mitigate the subsidence. No further
 1062 earthquakes occurred in the field after 1961 and subsidence had been arrested by 1966. This
 1063 is a case where seismicity may have been stopped by the introduction of fluids rather than
 1064 induced.

1065 Despite the large quantities of oil produced from the Middle East, we have found only two
 1066 accounts of earthquakes postulated to have been induced by oil extraction there. One reports
 1067 hundreds of earthquakes with magnitudes up to M_L 4.24 in the Uthmaniyah-Hawaiyah and
 1068 Haradh production divisions of the Ghawar oil/gas field, Saudi Arabia. These earthquakes
 1069 occurred below the production divisions and are attributed to hydrocarbon fluid extraction.
 1070 Focal mechanism solutions and structural cross-sections suggest the active elements are
 1071 crust-penetrative basement faults [Mogren & Mukhopadhyay, 2013].

1072 The other example is from Kuwait, where 465 M 0.3-4.3 earthquakes are reported to have
 1073 occurred in the period 1997-2007. A large percentage locate in the oilfields, including the
 1074 Sabiriyah, Raudhatain, Bahra, Minagish, Umm Gudair, Wafra, Abduliyah and Dharif Fields
 1075 (Figure 54). It is considered likely that at least some of this seismic activity is associated with
 1076 oil extraction [Al-Enezi *et al.*, 2008]. The largest event proposed to be related to Middle
 1077 Eastern oilfields is the 1993 M 4.7 event in Kuwait. It was suggested that it was induced by
 1078 the 1990 gushing and burning of oil wells by Iraqi armed forces leading to rapid pore
 1079 pressure reduction and changes in subsurface stress [Bou-Rabee & Nur, 2002].

1080 3.4 Geothermal production (heat/fluids)

1081 Small, natural earthquakes are common in wet, high-temperature geothermal areas, and were
 1082 known in Iceland as “hverakippur” (trans: “hot-spring bump”) long before they were studied
 1083 scientifically. They are likely caused in part by active tectonics in plate-boundary zones and
 1084 volcanoes, and in part by natural geothermal heat loss. This causes cooling and contraction of

1085 the geothermal heat source and stress is relieved by rock fracturing with a component of
 1086 tensile failure. Both the opening and closing of voids have been identified seismically
 1087 [Foulger, 1988a; b; Foulger & Long, 1984; Foulger *et al.*, 1989; Miller *et al.*, 1998a; Miller *et*
 1088 *al.*, 1998b; Ross *et al.*, 1999]. It is to be expected that production from geothermal fields by
 1089 the extraction of hot fluids will enhance the natural fluid- and heat-loss process and increase
 1090 seismic rates.

1091 It is, however, often difficult to attribute confidently earthquakes in an exploited geothermal
 1092 areas to a particular process because they could result from production, re-injection or natural
 1093 tectonic loading and heat loss. It is also possible that they are induced by natural recharge,
 1094 either by shallow, cold groundwater or deep, hot water. Our database contains only six cases
 1095 where earthquakes are postulated to have been associated with geothermal production. These
 1096 cases are the Cerro Prieto Field, Mexico [Glowacka & Nava, 1996], the Reykjanes and
 1097 Svartsengi Fields, Iceland [Keiding *et al.*, 2010], Larderello, Italy [Batini *et al.*, 1985], The
 1098 Geysers, USA [Eberhart-Phillips & Oppenheimer, 1984] and Olkaria, Kenya [Simiyu &
 1099 Keller, 2000].

1100 The largest earthquakes proposed to have been induced by geothermal production are the
 1101 strike-slip events in the Imperial Valley (1979, M_L 6.6), Victoria (~30 km southeast of the
 1102 Cerro Prieto field; 1980, M 6.1), and at Cerro Prieto (1987, M 5.4) (Figure 55). Glowacka
 1103 and Nava [1996] base this proposal on qualitative correlations between increases in sustained
 1104 fluid extraction and periods of increased seismic moment release, with delays of ~1 year
 1105 (Figure 56).

1106 Electrical power production at Cerro Prieto began in 1973. A mixture of steam and water
 1107 with temperatures of 250-350°C is produced from depths of 1500-3000 m. In the period
 1108 1973-1996 > 1 km³ of fluid was extracted. The region is part of the plate boundary between
 1109 the Pacific and North American plates and the tectonics are dominated by the strike-slip
 1110 Imperial fault which has a history of $M > 6$ earthquakes. Glowacka and Nava [1996] found
 1111 that the numerical data are insufficient to support statistically a correlation between
 1112 production and the large earthquakes but argue that pore pressure decreases in the geothermal
 1113 field, which amounted to a few MPa, were sufficient to have triggered them. Earlier, Majer
 1114 and McEvelly [1981; 1982] suggested, on the basis of data from local, temporary seismic
 1115 network deployments, that earlier increases in production at Cerro Prieto correlated with
 1116 increases in the rate of small earthquakes.

1117 Examples from Iceland where correlation between geothermal production and earthquakes
 1118 has been proposed are the Reykjanes and Svartsengi geothermal areas on the Reykjanes
 1119 Peninsula [Keiding *et al.*, 2010]. These areas, which lie on the spreading plate boundary
 1120 where it first comes on land in southwest Iceland, were studied intensively using
 1121 Interferometric Synthetic Aperture Radar (InSAR) and GPS data from 1992-2009.
 1122 Deformation detected was concluded to be associated with extension along the plate
 1123 boundary and ~5 cm/a of subsidence resulting from geothermal fluid extraction. Swarms of
 1124 earthquakes with magnitudes up to M_L 4.1 occurred on the flanks of the rifts within which the
 1125 geothermal areas lie. The events were postulated to have been induced by stress changes
 1126 brought about by geothermal fluid extraction (Figure 57). This area is naturally seismically
 1127 active since it comprises part of the spreading plate boundary, so it is not possible to rule out
 1128 a tectonic origin for many of these earthquakes.

1129 The case of The Geysers geothermal field, California, is complex. It is a vapor-dominated

1130 field and has been exploited for over 150 years, including generating electricity. It is
 1131 intensely seismically active (Figure 58) and seismicity was recorded even before large-scale
 1132 fluid injections began (Figure 59). Very likely the pre-injection seismicity, and some current
 1133 seismicity, is production-related [Eberhart-Phillips & Oppenheimer, 1984]. It is problematic
 1134 to distinguish production- from injection-related seismicity there currently, however, because
 1135 both processes are underway simultaneously. In general over the last 50 years or so, the
 1136 seismic rate as a whole appears to correlate grossly with injection. Seismicity at The Geysers
 1137 is discussed in more detail in Section 4.1.5.

1138 3.5 Extraction from the subsurface: Summary

1139 Mining is by far the commonest cause of extraction-related induced earthquakes and
 1140 contributes 267 cases to our database (Figure 60). The second most common postulated
 1141 causative process is water reservoir impoundment, which contributes 168 entries. Five cases
 1142 relate to groundwater and six to geothermal resources. The largest earthquakes postulated to
 1143 be induced by subsurface extraction are the M_W 7.8 Gorkha, Nepal, earthquake, the M_L 6.1
 1144 Bachatsky, Russia, earthquake, the M_S 7.3 Gazli, Uzbekistan earthquake and the M_L 6.6
 1145 Cerro Prieto, Imperial Valley, Mexico, earthquake.

1146 In the case of groundwater-withdrawal cases, some extraordinarily small stress changes have
 1147 been postulated to induce events—as small as 0.001 MPa [*e.g.*, for the 2015 M_W 7.8 Gorkha,
 1148 Nepal, earthquake; Kundu *et al.*, 2015]. This is small even compared with Earth tides
 1149 (Section 7.3). The ability of such small stresses to induce earthquakes is theoretically in
 1150 keeping with the self-similar, critical earthquake nucleation process. However, such small
 1151 effects may be comparable to many other natural and anthropogenic processes such as
 1152 weather and the expansion of cities.

1153 We summarize postulated gas-extraction induced earthquakes in Figure 61 which shows
 1154 M_{MAX} for the 35 cases of where this parameter is reported. There is a continuous spectrum of
 1155 sizes with the exception of the M_S 7.3 Gazli, Uzbekistan, event, which is 1.8 magnitude units
 1156 larger than the second largest case.

1157 Although oil extraction removes extremely large masses from the crust, we found
 1158 surprisingly few cases of earthquakes proposed to be induced by this process. Possible
 1159 reasons for this are:

- 1160 • the process is only weakly seismogenic, perhaps because natural aquifer influx
- 1161 (peripheral or bottom water) partially replaces mass extracted;
- 1162 • under-reporting; and
- 1163 • ambiguity of induction process, since fluid injection often accompanies production.

1164
 1165 For geothermal fields, Figure 62 shows a histogram of numbers of seismogenic power-
 1166 producing fields ranked by size [data from Bertani, 2010]. It is clear that the larger the
 1167 geothermal operation the more likely it is to induce earthquakes.

1168 4 Injection into the subsurface

1169 The burgeoning issue of injection-related earthquakes was highlighted by Ellsworth [2013]
 1170 who pointed out the recent dramatic increase in earthquake rate for $M \geq 3$ events in the
 1171 central and eastern USA. More than 100 such earthquakes occurred annually, on average, in
 1172 the period 2010-2012 compared with just 21 events/year on average for the period 1967-

1173 2000. Despite the problem of incomplete reporting, our database shows that the trend toward
 1174 increasing incidence of injection-related earthquakes is a broad international one and not
 1175 confined to the USA.

1176 Fluids are injected into the ground for diverse reasons that include (Table 2):

- 1177 • solution mining (Section 3.2.2);
- 1178 • disposal of unwanted by-products;
- 1179 • enhancing oil recovery;
- 1180 • fracturing rock (i.e. the very process that causes earthquakes);
- 1181 • research into the earthquake nucleation process;
- 1182 • underground heat storage by way of injection of hot water from waste heat processes;
- 1183 • underground storage of natural gas, hydrogen and compressed air; and
- 1184 • CO₂ geostorage to reduce emissions.

1185

1186 In addition, passive groundwater inflow may occur when reservoirs are produced or pumping
 1187 to suppress groundwater levels is abandoned in mines.

1188 Our database contains 180 projects where injections have been postulated to induce
 1189 seismicity and includes examples of most of the above processes. Whereas in general, the
 1190 removal of mass from the crust is expected to reduce the normal stress that prevents slip on
 1191 faults, the introduction of fluids into faulted rock is expected to increase the pore pressure
 1192 that encourages failure. Both these changes thus, capriciously, are predicted to induce
 1193 earthquakes. In the case of injections, in addition to the hazard induced earthquakes pose to
 1194 people and infrastructure there is the added risk that if the target formation or its caprock are
 1195 ruptured by the direct or indirect effects of earthquakes, the injected fluid might escape. This
 1196 could add to hazard, for example, where the injectate is polluted water, natural gas or CO₂.

1197 4.1 *Liquid*

1198 4.1.1 Military waste

1199 Our database contains only one case where seismicity is postulated with a high degree of
 1200 confidence to result from the injection of military waste. This is the legendary case of the so-
 1201 called Denver earthquakes. Although not the first earthquakes to have been recognized as
 1202 induced by human activity, they did result in widespread awareness both in the seismological
 1203 community and the general public that human activity can induce earthquakes.

1204 The incident began in 1961 when the Army Corps of Engineers drilled a 3.7-km deep well
 1205 into highly fractured crystalline Precambrian basement at the Rocky Mountain Arsenal,
 1206 northeast of Denver, Colorado [Evans, 1966; Hsieh & Bredehoeft, 1981]. The purpose of the
 1207 well was disposal of contaminated wastewater which was done by injection into the bottom,
 1208 unlined, 21 m. Disposal began in March 1962 at pressures ranging from atmospheric to ~ 7.2
 1209 MPa above formation pressure. In the four-year period up to 1966 a total of 625,000 m³ of
 1210 fluid were injected.

1211 Minor earthquakes onset in the Denver area shortly after injection started and by 1967 over
 1212 1500 earthquakes, some of which were of M 3-4, had been recorded (Figure 63). The
 1213 correlation between volume injected and frequency of earthquakes, along with epicenters
 1214 located within 8 km of the well, prompted Evans [1966] to suggest they had been induced.

1215 Although waste disposal ceased in 1966, earthquake activity continued and in 1967 three
 1216 earthquakes with $M_L > 5$ occurred, causing damage to infrastructure in Denver. Seismicity
 1217 declined after 1967 and by the early 1980s had essentially ceased. It was interestingly pointed
 1218 out that the large earthquakes that occurred after the end of injection weakened the temporal
 1219 correlation between earthquakes and injection and thus the case argued for induction. It was
 1220 immediately countered, however, that diffusion of the fluid would have continued after
 1221 injection stopped and could account for the ongoing seismicity [Healy *et al.*, 1968]. This
 1222 early case significantly increased understanding of the earthquake induction process.

1223 4.1.2 Wastewater disposal

1224 Large quantities of connate brine and/or connate brine mixed with injection water are
 1225 typically co-produced with oil, especially as fields age. Water-to-oil ratios may exceed 20
 1226 [Gluyas & Peters, 2010]. Such produced water is commonly re-injected into depleted
 1227 oilfields both for disposal and to maintain reservoir pressure and promote sweep thus aiding
 1228 oil recovery. The cold water injected commonly leads to thermal fracturing, especially in
 1229 low-permeability reservoirs. Indeed, thermal fracturing is a desirable outcome as it allows
 1230 lower injection pressures (and thus lower pump power requirements and costs) to be used. In
 1231 California alone there are currently ~2,300 wastewater injection wells.

1232 We have identified 33 cases of induced seismicity specifically attributed to waste fluid
 1233 injection. Of these, three are in Canada, two from China, one from Italy and 27 from the
 1234 USA. A case of particular renown is that of wastewater disposal in Paradox Valley, Colorado,
 1235 so-named because the Dolores River runs transversely across the valley. This case is
 1236 noteworthy in particular because of the apparently large distances from the injecting well at
 1237 which some of the postulated induced earthquakes nucleated [Ake *et al.*, 2005; Block *et al.*,
 1238 2015; King *et al.*, 2014; Yeck *et al.*, 2015].

1239 At Paradox Valley, brine is injected into a sub-horizontal layer of Mississippian-age
 1240 limestone at the bottom of a 4800-m-deep well. The objective is to reduce the salinity of
 1241 Dolores River water and, as a consequence, the Colorado River into which it flows. Salt
 1242 enters the Dolores River via groundwater inflow of brine ~ 8 times more saline than sea
 1243 water. To reduce this, the shallow brine is extracted from the ground via nine production
 1244 wells and re-injected at greater depth into a single disposal well at surface pressures up to 35
 1245 MPa [Yeck *et al.*, 2015]. Continuous injection has been underway since 1996. In the
 1246 following two decades > 5,700 earthquakes surmised to have been induced were located,
 1247 including a M 4.3 event in 2000 (Figure 64). Some epicenters lie > 10 km from the disposal
 1248 well, and a few up to ~25 km distant.

1249 A cautionary case where a large earthquake occurred close to critical infrastructure is that of
 1250 the 1986 M_W 4.9 Painesville, Ohio, earthquake [Ahmad & Smith, 1988; McGarr, 2014;
 1251 Nicholson *et al.*, 1988]. This event, which was felt in 11 states and parts of Canada, occurred
 1252 in Precambrian basement within 17 km of the Perry Nuclear Power Plant on the edge of Lake
 1253 Erie. There, ground acceleration was as high as 0.23 g.

1254 The injection of $1.2 \times 10^6 \text{ m}^3$ of liquid agricultural waste into three wells ~12 km away was
 1255 implicated. These injections began in 1976 and thus the mainshock and its associated $M < 2.5$
 1256 aftershocks did not onset until a decade after the suspected induction operations began. By
 1257 then, a pressure increase of 11.8 MPa had built up at the injection location.

1258 Whether or not the earthquake sequence was induced is controversial. Similar earthquakes

1259 occurred in 1906, 1928, 1943 and 1958 (i.e. about every ~20 years) in a zone that includes
1260 the 1986 sequence, though most of those older locations are not instrumentally based. It is
1261 thus possible the 1986 earthquakes could have been natural. The long delay of seismicity
1262 after the start of injection also erodes confidence that the two processes were linked
1263 [Hitzman, 2013]. However, the many cases of postulated delayed earthquake induction that
1264 have occurred subsequently now render it more plausible that the 1986 Painesville
1265 earthquakes were induced.

1266 A European case of earthquakes postulated to have been induced by wastewater disposal is
1267 that of the 2012 M_L 5.9 Emilia-Romagna, Italy, earthquake sequence which resulted in 27
1268 fatalities [Cartlidge, 2014]. It was postulated that hydrocarbon exploitation at the Mirandola
1269 Field and geothermal exploitation at Casaglia both contributed to the stress changes that
1270 caused this earthquake sequence to occur. Because of the serious impact to people and
1271 infrastructure a commission was established to investigate the possibility it was induced
1272 [Styles *et al.*, 2014].

1273 The commission found that there were statistical correlations between the increase of
1274 production parameters in the weeks before the earthquakes but that stress changes resulting
1275 from reservoir depletion would not have contributed. They concluded that, while it could not
1276 be ruled out that the anthropogenic extraction and injection of fluids contributed to activation
1277 of the pre-stressed fault system that failed, it was “highly unlikely” that the earthquake
1278 sequence had been induced.

1279 A link between injection pressure and induced earthquakes is reported for the Huangjiachang
1280 Gasfield, Sichuan Basin, China [Lei *et al.*, 2013]. Few earthquakes occurred there until
1281 injection wellhead pressure rose above 2 MPa. After that, more than 5000 $M > 1.0$
1282 earthquakes occurred close to reservoir depth, the largest with a magnitude of M_L 4.4.

1283 The Sichuan Basin is relatively tectonically stable with only sparse historic seismicity. Gas is
1284 contained in shallow, high-porosity limestone/dolomite anticlines of Paleozoic and Mesozoic
1285 age. Local faults cross both reservoirs and basement. The Huangjiachang Gasfield itself is
1286 small and hosted in a fractured, jointed, karstified Permian limestone formation at a depth of
1287 2500 m. Injection of wastewater began there in 2007 when a production well was converted
1288 to an injector. For the first two years, water was introduced under atmospheric pressure and
1289 seismic rates were low. In 2009 injection pressures were increased, ultimately reached 2.1 -
1290 2.9 MPa, and seismicity onset.

1291 Particularly vigorous induced seismicity is reported to have been induced by wastewater
1292 disposal in the Rongchang Field, also in the Sichuan Basin [Lei *et al.*, 2008]. Earthquakes
1293 onset there in 1989, only two months after water injection began. More than 32,000
1294 earthquakes were observed, the largest with M_L 5.2. That event reactivated a thrust fault in
1295 the basement. Earthquake locations suggested that seismic failure occurred in both the
1296 reservoir and the basement.

1297 In recent years the issue of induced earthquakes in Oklahoma has become particularly
1298 prominent because of an unprecedented surge in seismic rate there that onset in 2009 (Figure
1299 65) [Ellsworth, 2013]. This rendered Oklahoma the most seismically active state in the USA
1300 for earthquakes with $M > 3$ in the period 2008-2013. Rates exceeded even those of California
1301 which hosts the San Andreas fault zone and several seismogenic volcanic and geothermal

1302 areas [D. Oppenheimer, personal communication]⁵. The seismic rate of Oklahoma also
 1303 exceeds that of the New Madrid Seismic Zone in Missouri and neighboring states, formerly
 1304 considered to be the most hazardous intraplate seismic zone in the USA. The largest event
 1305 since 1950 in the New Madrid Seismic Zone has been M 4.9 whereas in Oklahoma it has
 1306 been M_W 5.7.

1307 Although faulting in Oklahoma is widespread, only one fault is known to have been active
 1308 historically. This is the Meers fault, which is thought to have generated M 6.5-7 earthquakes
 1309 over the last 3,500 years [McNamara *et al.*, 2015]. It was suspected early that Oklahoma
 1310 might be experiencing earthquakes induced by hydrocarbon-related activities. The injection
 1311 of water for enhanced oil recovery has been practiced since the 1930s and it has been
 1312 suggested that the 1952 M ~5.6 event (the El Reno earthquake) was related to the extraction
 1313 of oil and gas [Nicholson & Wesson, 1992]. Hough and Page [2015] studied the historic rate
 1314 of earthquake occurrence in Oklahoma by looking at population statistics to see if the
 1315 population had been sufficiently stable historically for comparable earthquake activity to
 1316 have been noted in the past. Oklahoma has had a large and well-distributed population from
 1317 early in the 20th century, suggesting that that knowledge of M ≥4 earthquakes is nearly
 1318 complete (Figure 66). Industrially induced earthquakes in Oklahoma are thus now essentially
 1319 beyond doubt.

1320 As is the case elsewhere, multiple industrial processes are underway simultaneously in the
 1321 hydrocarbon fields of Oklahoma so it is generally difficult to be certain which may have
 1322 induced any particular earthquake. In addition to hydrocarbon production there are ~7,000
 1323 injection wells that are used for:

- 1324 • the disposal of produced brine (the dominant use);
- 1325 • enhanced oil recovery;
- 1326 • hydrofracturing to increase permeability in shale; and
- 1327 • the disposal of hydrofracture fluid.

1328 Most of the fluid is injected into the Arbuckle Group, a sequence of carbonates and
 1329 sandstones closely overlying Precambrian crystalline basement (Figure 67).

1330 The largest and most damaging earthquake ever to have occurred in Oklahoma, the 2011 M_W
 1331 5.7 Prague earthquake, along with its associated sequence, is relatively unambiguously
 1332 associated with wastewater disposal into a depleted oilfield [*e.g.*, Keranen *et al.*, 2013]. The
 1333 Prague earthquake was felt in at least 17 states and in Chicago at a distance of 1,000 km. It
 1334 caused considerable damage to local infrastructure, destroying 14 houses, and injuring two
 1335 people. It is, to date, the largest earthquake in the world associated with waste-water disposal
 1336 and led to a re-assessment of both the potential size of injection-induced earthquakes and the
 1337 delay time following the onset of operations.

1338 Earthquake activity in the Prague area began in February 2010 with a M_W 4.1 earthquake in
 1339 the Wilzetta Oilfield. This lies within the ~200-km-long Pennsylvanian Wilzetta fault zone
 1340 (Figure 68). In 2011 this activity culminated in the Prague sequence that included three
 1341 earthquakes with M_W 5.0, 5.7, and 5.0 (Figure 69) on 5, 6, and 8 November, along with
 1342 prolific aftershocks. Analysis of hypocentral locations and focal mechanisms using data from

⁵ *e.g.*, http://www.nytimes.com/2016/03/29/us/earthquake-risk-in-oklahoma-and-kansas-comparable-to-california.html?_r=0

1343 1,183 aftershocks recorded on a dense temporary seismic network clarified the geometry of
1344 the hypocentral zone (Figure 70) [Keranen *et al.*, 2013]. Failure comprised strike-slip motion
1345 on planes that dip steeply and intersect both the sedimentary layers and the basement. The tip
1346 of the initial rupture plane lay within ~200 m of active injection wells at a depth of ~1 km.

1347 In the Wilzetta zone, oil is contained in fault-bounded structural traps that are barriers to fluid
1348 migration through the porous limestone host formation. Where the Prague sequence occurred,
1349 production had been ongoing since the 1950s but is now at a low level. Three active waste-
1350 disposal injection wells which came online in 1993 are in the vicinity (Figure 70). They inject
1351 water into sealed rock compartments at ~1.3 - 2.1 km depth.

1352 Over the 17-year period 1993-2011 injection pressure progressively increased from
1353 atmospheric to 3.6 MPa in 2006. Seismicity is thought to have onset when the injected
1354 volume exceeded that extracted from the fault-bounded compartment. Once the compartment
1355 had been refilled ongoing injection is thought to have reduced the confining stress on the
1356 reservoir-bounding faults which failed as a consequence. More stress was released than
1357 corresponds to the total volume injected, so tectonic stress was likely also released. Both
1358 injection and $M > 3$ earthquakes continue in the Wilzetta Field at the time of writing.

1359 Figure 71 shows seismicity and oil production in Oklahoma for the last century. Between
1360 2009 and 2014, 26 $M \geq 4$ events occurred in the state. Over 100 $M \geq 3.5$ events occurred in
1361 2014 alone. Monthly statewide wastewater injectate volume has doubled since 1997 [Walsh
1362 & Zoback, 2015]. Correlations between earthquakes and injection or production are rare.
1363 Figure 69 and Figure 72 show earthquakes and fluid injections for the entire state and for
1364 individual study areas. Earthquakes do not correlate with faults and most earthquakes occur
1365 in the least faulted part of Oklahoma.

1366 It is thought that faults that fail in general in Oklahoma are those favorably oriented relative
1367 to the regional stress direction. Most events occur at depths of 5-6 km in the crystalline
1368 basement, on faults of the order of kilometers or tens of kilometers in length. Such faults can
1369 maximally sustain M 5-6 earthquakes. Some earthquakes occur on well-known faults that
1370 have large seismic potentials and the length of fault activated can be determined from
1371 aftershock distributions.

1372 The earthquake activity of Oklahoma exhibits both similarities and differences compared
1373 with other examples of induced seismicity. No short-term monthly correlation with injection
1374 is apparent and seismicity surged many years after the start of injections, 17 years in the case
1375 of the Prague sequence. In this it resembles the behavior of the Wilmington Oilfield,
1376 California, where induced seismicity onset years after water injection began for enhanced oil
1377 recovery (Section 4.1.3). However, it is unlike that of the Rocky Mountain Arsenal, Colorado
1378 (the “Denver earthquakes”; Section 4.1.1) where earthquakes onset almost immediately after
1379 injections began. Induced earthquake sequences do not necessarily start with the largest
1380 event, and stress from one induced earthquake may trigger larger subsequent events.

1381 In addition to earthquakes in Oklahoma being induced by hydrocarbon-related operations,
1382 they may also be triggered by natural regional earthquakes. Van der Elst *et al.* [2013] studied
1383 earthquakes there for time periods following several large, distant earthquakes. A surge in
1384 earthquake activity, including a M_w 4.1 event near Prague, occurred following the 27
1385 February 2010 M_w 8.8 Maule, Chile, earthquake (Figure 73). Earthquakes in Oklahoma are
1386 thus induced both by anthropogenic and natural processes.

1387 4.1.3 Water injected for enhanced oil recovery

1388 Enhanced oil recovery includes low salinity water injection, water alternating gas injection,
 1389 injection of water viscosifiers and thermal and chemical methods all of which aim to modify
 1390 either the viscosity of one or more of the fluids or the surface properties of the host reservoir.
 1391 Distinguishing earthquakes induced by these processes from events induced by oil extraction
 1392 may not be straightforward if both processes are underway simultaneously. Temporal
 1393 associations are persuasive, *e.g.*, cases where seismicity rates surge shortly after water
 1394 injection commences in producing oilfields that were previously aseismic.

1395 We have found 38 cases of seismicity proposed to have been induced by enhanced oil
 1396 recovery. Of these, 24 are from the USA and the rest from Canada, China, Denmark, France,
 1397 Kuwait, Norway, Romania, Russia and Turkmenistan.

1398 The classic example is the case of the Rangely Oilfield, Colorado, where induced earthquakes
 1399 could be controlled (see also Section 4.1.8) [Raleigh *et al.*, 1976]. There, water injection for
 1400 oil recovery was conducted in wells up to 2 km deep where the formation pressure was ~17
 1401 MPa. The seismic rate could be increased or decreased by varying the pore pressure around
 1402 26 MPa (Figure 74). This experimental case led to hopes that earthquakes might be
 1403 controlled, including damaging events on the San Andreas fault system. However, it was
 1404 quickly realized that the fractal nature of earthquakes is such that the stress released by a few
 1405 moderate earthquakes cannot substitute for a single large earthquake. Thus, hopes that
 1406 damaging earthquakes might be averted by using engineering means were not realized.

1407 The largest earthquakes postulated to have been induced by water flooding or reinjection for
 1408 enhanced oil recovery are the M 6.2 1983 Coalinga event, the 1985 M_w 6.1 Kettleman North
 1409 Dome event, and the 1987 M_L 5.9 Montebello Fields (Whittier Narrows) event, all in
 1410 California. The primary cause for these earthquakes is, however, most likely oil extraction
 1411 (Section 3.3.2) [McGarr, 1991].

1412 More clear-cut examples come from the Newport-Inglewood fault zone, Los Angeles Basin,
 1413 California. Of the three billion barrels of original reserves in the giant Wilmington Oilfield,
 1414 2.7 billion (~440,000,000 m³) have been removed. Early production from this field may have
 1415 contributed to the damaging 1933 M_L 6.3 Long Beach, California, earthquake, and the events
 1416 of 1947, 1949, 1951, 1954, 1955, and 1961 (Section 3.3.2) [Kovach, 1974].

1417 Water flooding for enhanced oil recovery and to counteract massive subsidence started there
 1418 in 1954. Despite significant ambiguity regarding causation, earthquakes with magnitudes up
 1419 to M 3.0 that occurred during 1971 are thought to have correlated with injection volumes.
 1420 Following these small events, injection was continued at approximately the same volumetric
 1421 rate as production and the suspected induced seismicity did not continue [Nicholson &
 1422 Wesson, 1992].

1423 A more persuasive case of water-flooding-induced seismicity which caused significant
 1424 damage and loss of life is that of the Inglewood Field, some 20 km further north along the
 1425 Newport-Inglewood fault zone. In December 1963 the earth dam containing the nearby
 1426 Baldwin Hills Reservoir failed, releasing 11×10^6 m³ of water into a residential area. This
 1427 flood damaged over 1,000 homes, killed five people and caused \$12 million of damage.
 1428 Failure of the dam was attributed to cumulative fault displacements that resulted from water
 1429 flooding of the Inglewood Oilfield for enhanced oil recovery [Castle & Yerkes, 1976;
 1430 Hamilton & Meehan, 1971].

1431 Discovered in 1924, the Inglewood Oilfield occupies an anticline within a zone of faults and
 1432 folds. Reserves were initially 430 million barrels but the field is now ~93% depleted. For the
 1433 first three decades production occurred under only exsolution-gas (pressure depletion) drive
 1434 and peripheral-water drive. Some $83 \times 10^6 \text{ m}^3$ of oil, water and sand were extracted.
 1435 Pressures declined from 3.9 to 0.34 MPa from the start of production up to the 1950s. A well-
 1436 defined subsidence bowl centered on the oilfield developed and surface deformation was
 1437 monitored from 1939. Subsidence was up to 1.75 m in the period 1911-1963. Horizontal
 1438 displacements were up to 0.68 m in the period 1934-1961 with radially oriented extension.
 1439 The Baldwin Hills reservoir lay on the edge of this subsidence bowl.

1440 In 1954 a water-flood program for enhanced oil recovery began which was expanded to a
 1441 full-scale program in 1957. Acceleration of deformation in the form of surface cracks, creep
 1442 and small jumps in fault displacement onset immediately on minor faults and joints
 1443 concentric to the center of subsidence. There had been close correlation between subsidence
 1444 and liquid production, and a sharp reduction in subsidence occurred in the eastern part of the
 1445 field when major water-flooding began. The orientation of the horizontal displacements and
 1446 strain were consistent with the operations and a cause for the deformation of tectonic origin
 1447 could be rejected to a high degree of certainty.

1448 Increased shallow seismicity onset in 1962 and the following year the Baldwin Hills dam
 1449 ruptured. It was deduced that movement on one of the faults allowed water to flow into the
 1450 soil under the dam, resulting in failure. This case, and that of the Wilmington Oilfield,
 1451 highlight the risk of conducting major hydrocarbon operations near to dense populations,
 1452 particularly where prior tectonic activity is known.

1453 4.1.4 Enhanced Geothermal Systems (EGS)

1454 The extraction of geothermal heat from bodies of rock that contain insufficient water
 1455 naturally was pioneered in the 1970s by the “hot dry rock” projects of Fenton Hill, New
 1456 Mexico, and Cornwall, UK. These projects did not lead directly to economic development
 1457 and were abandoned. The technology was resurrected early in the 21st century as “Enhanced
 1458 Geothermal Systems” (EGS). An important milestone in this process was the landmark report
 1459 “*The Future of Geothermal Energy*”, prepared by the Massachusetts Institute of Technology
 1460 for the U.S. Department of Energy [Tester & al., 2006]⁶.

1461 The fundamental concept of EGS is to pump high-pressure fluid into a well to hydrofracture
 1462 and thermofracture hot rock, enhancing permeability and creating an underground heat
 1463 exchanger. If one or more production wells do not already exist, they are drilled into the
 1464 fractured rock mass. Cold water is pumped down the injection well, it circulates through the
 1465 hot rock, and hot water and steam are extracted via production wells.

1466 The objective of injection is to produce a network of fractures in the otherwise low-
 1467 permeability target formation. As is the case for shale-gas hydrofracturing, earthquakes are
 1468 an inevitable consequence of a successful EGS project. Dense seismometer networks are
 1469 installed prior to hydrofracturing in order to obtain the best possible earthquake hypocentral
 1470 locations, magnitudes and source mechanisms since these results can assist in targeting the
 1471 production well. Such projects are currently providing superb data and advancing basic
 1472 seismology.

⁶ <http://geothermal.inel.gov> and http://www1.eere.energy.gov/geothermal/egs_technology.html

1473 Notable EGS projects have been conducted at:

- 1474 • Fenton Hill, New Mexico [*e.g.*, Ferrazzini *et al.*, 1990];
- 1475 • Cornwall, UK [*e.g.*, Turbitt *et al.*, 1983];
- 1476 • Soultz-sous-Forêts, France [*e.g.*, Baisch *et al.*, 2010; Calo *et al.*, 2014];
- 1477 • Basel, Switzerland [*e.g.*, Zang *et al.*, 2014a];
- 1478 • Newberry volcano, Oregon [Cladouhos *et al.*, 2013];
- 1479 • the Coso geothermal area, California (see Section 4.1.5) [Julian *et al.*, 2010];
- 1480 • Desert Peak, Nevada [Chabora *et al.*, 2012]; and
- 1481 • Cooper Basin, Australia [*e.g.*, Asanuma *et al.*, 2005].

1482

1483 The Fenton Hill, New Mexico, hot dry rock project was the first of its kind. It was completed
 1484 in 1977 in rock at a depth of ~2.6 km and temperatures of 185°C. Work at Fenton Hill
 1485 continued into the 1990s, achieving a production of ~10 MW thermal, but was terminated
 1486 because of lack of funding.

1487 An early modern EGS project commenced at Soultz-sous-Forêts, in the central Upper Rhine
 1488 Graben, France in 1987 (Figure 75) [Baisch *et al.*, 2010; Calo *et al.*, 2014]. The site lies in
 1489 highly fractured granite overlain by ~1,400 m of sediments. It contains three ~5,000 m deep
 1490 injection wells and several shallower wells. Massive hydraulic stimulations were performed
 1491 in the injectors at depths > 4,000 m. In 2000, well GPK2 was stimulated with ~23,000 m³ of
 1492 water at flow rates of 30–50 l/s and overpressures of up to 13 MPa. Well GPK3 was
 1493 stimulated in 2003 with ~37,000 m³ of water at similar flow rates and overpressures. Well
 1494 GPK4 was stimulated twice with a total of ~22,000 m³ of fluid. In 2010 the project began to
 1495 deliver 1.5 MW to the grid, a world first.

1496 The hydraulic injections were monitored using a sparse local seismic network of multi-
 1497 component, down-hole sensors at depths of 1500-3500 m. More than 114,000 seismic events
 1498 were detected at rates of up to 8000 events per day (Figure 76). The activity migrated away
 1499 from the injection well with time and, as has been observed elsewhere, the largest events
 1500 occurred after injection had stopped. Such behavior causes problems for “traffic light”
 1501 systems designed to adjust injection strategies to avoid large earthquakes on the basis of the
 1502 ongoing seismicity. Earthquake magnitudes eventually reached M_L 2.9 and, although modest
 1503 in size, caused public concern. After the largest event in 2003 the flow rates and volumes of
 1504 stimulations were scaled back.

1505 The larger events are thought to have occurred on a sub-vertical structure that might be a
 1506 component of the Rhine Graben complex. The project demonstrated that a better
 1507 understanding of the induced seismicity associated with such projects is needed if the
 1508 problem is not to jeopardize commercial implementation of EGS technology.

1509 Perhaps the most infamous case example of nuisance seismicity induced by EGS operations
 1510 is that of the Basel, Switzerland project. The city of Basel is located where the Upper Rhine
 1511 Graben intersects the Jura Mountains fold/thrust belt (Figure 1). Basel has a history of large-
 1512 magnitude seismicity, including the largest historical event in NW Europe, the $M \sim 6.5$
 1513 earthquake of 1356, which destroyed the city. There may have been additional $M \sim 7$ events
 1514 in the post-Pleistocene period.

1515 Details of this disappointing project are published in many papers, including a concise
 1516 summary by Häring *et al.* [2008] and a collection published as a Special Issue of

1517 Geothermics in 2014 [Zang *et al.*, 2014a]. In brief, the project was designed to provide power
 1518 to the city of Basel. A seismic network was installed in 2006 and the Basel-1 well was drilled
 1519 the same year to a depth of 5 km. The wellbore intersects 2.4 km of sedimentary rocks and
 1520 2.6 km of granitic basement.

1521 The granite in the open hole below 4629 m was hydraulically stimulated with a total of
 1522 11,570 m³ of fluid. The initial plan was to inject over a period of 21 days. However,
 1523 seismicity became intense during the first 6 days, with events up to M_L 2.6 occurring in the
 1524 depth range ~4.6-5.0 km (Figure 77). These events precipitated cessation of injection in
 1525 response to a pre-approved procedure. Five hours after the well was shut in an earthquake
 1526 with M_L 3.4 occurred and a further three $M > 3$ events followed over the next 56 days (Figure
 1527 78). There was considerable citizen anxiety and the project is now abandoned.

1528 EGS has been extensively conducted in Cooper Basin, Australia, where the largest
 1529 earthquake induced to date has a magnitude of M_W 3.7. Cooper Basin is ideal for
 1530 development of EGS. It lies in the interior of Australia in southwest Queensland, remote from
 1531 large population centers. It contains significant oil and gas resources which have been
 1532 explored and exploited since the 1960s so industrial infrastructure was already in place in
 1533 2002 when geothermal exploration started. The target heat source is granitic rocks with
 1534 temperatures up to 240°C at 3.5 km depth. These are the hottest known granitic rocks in the
 1535 world at economic drilling depths that are not in the vicinity of active volcanoes.

1536 Six deep wells were drilled into the granite to depths of 3629-4852 m. Four of these are in the
 1537 Habanero Field and the other two are 9 and 18 km away in the Jolokia and Savina Fields.
 1538 EGS fluid injection experiments were conducted 2003-2012 and documented in detail in
 1539 several published papers [e.g., Asanuma *et al.*, 2005; Baisch *et al.*, 2009a; Baisch *et al.*,
 1540 2009b; Baisch *et al.*, 2006a; Baisch *et al.*, 2006b; Baisch *et al.*, 2015; Kaieda *et al.*, 2010].
 1541 Some of the injections induced over 20,000 earthquakes which were well-recorded by dense,
 1542 modern seismic networks.

1543 Despite the fact that all the stimulations were conducted in the same granite formation, they
 1544 induced variable seismic responses (Figure 79). These are exemplified by two that were
 1545 carried out in 2010 and 2012 [Baisch *et al.*, 2015]. The 2010 stimulation injected fluid into
 1546 the Jolokia well at a depth of > 4000 m. It induced only minor seismic activity, even at
 1547 extremely high fluid pressures (~120 MPa), and the injection rate achieved was only ~1.0 l/s,
 1548 one to two orders of magnitude less than typical. Only 73 earthquakes with M_L -1.4 to 1.0
 1549 were recorded over an eight-day stimulation period and an additional 139 over the next six
 1550 months. The largest of these was M 1.6 which occurred 127 days after the end of the
 1551 injection. This is another case where the largest induced earthquake occurred after injection
 1552 had terminated. Hypocenters clustered around the injection well at distances of a few tens or
 1553 hundreds of meters, suggesting that the events occurred on steeply dipping fractures poorly
 1554 oriented for shearing in the regional stress field.

1555 The 2012 stimulation was carried out in well Habanero 4. Approximately 34,000 m³ of water
 1556 were injected at depths of 4100-4400 m, flow rates of > 60 l/s, and wellhead pressures of ~50
 1557 MPa. This induced > 29,000 earthquakes with M_L -1.6 to 3.0 which were recorded on a local
 1558 24-station network. Of these, 21,720 could be located and focal mechanisms determined for
 1559 525. This is probably the most prolific EGS-induced earthquake dataset ever collected. In
 1560 contrast to the well-hugging, sub-vertical fracture activated by stimulation of well Jolokia 1,
 1561 the Habanero 4 stimulation activated a single, sub-horizontal fault zone thought to have a

1562 vertical thickness of only a few meters and extending to > 1.5 km from the well. Failure was
1563 consistent with the regional stress field.

1564 These two very different styles of seismic response characterized injections in different wells
1565 penetrating the same granite formation. This case history exemplifies the challenge of
1566 predicting the behavior of formations under stimulation, even when excellent geological
1567 knowledge is available. Despite the major technological advances achieved in the Cooper
1568 Basin project, due to low oil prices and changing government priorities, the project was
1569 decommissioned in 2016.

1570 Despite the challenges that currently face the development of EGS, much has been learned in
1571 recent years that will underpin the future of the industry. Because it is known beforehand that
1572 projects induce seismicity, exemplary seismic monitoring and public outreach practices have
1573 been developed. These include installing custom-designed networks of three-component
1574 borehole instruments well in advance of operations in order to obtain a pre-operational
1575 baseline for seismic activity. Data are streamed to public websites and outreach includes
1576 town-hall meetings, installing seismometers in public buildings in nearby communities,
1577 distributing information to the public orally, in printed form and on the internet, and
1578 involving local communities in the commercial activity.

1579 4.1.5 Geothermal reinjection

1580 Water is re-injected into exploited geothermal fields in order to maintain pressure. Although
1581 classified technically as renewable resources, geothermal fields are, in reality, not so. If large
1582 quantities of hot fluid are removed at high rates for many years, exceeding natural recharge,
1583 the resource will become depleted. This is typically manifest as a progressive reduction in
1584 reservoir pressure leading to reduced production. To maintain pressure, water is re-injected.
1585 The aim is to re-inject in a way that does not compromise production wells by reducing the
1586 temperature of produced fluids.

1587 Perhaps the most remarkable case of seismicity that can be attributed with confidence to
1588 geothermal reinjection is that of The Geysers geothermal field, California (Figure 58). The
1589 Geysers is a steam-dominated geothermal reservoir that lies in the strike-slip stress regime of
1590 the San Andreas fault system in California. Exploitation there began in the 1860s. Steam was
1591 first used to generate electricity in 1922 when one kilowatt was produced. Production peaked
1592 in 1987 at about $3.5 \times 10^3 \text{ kg s}^{-1}$ of steam from which 1800 MW of electricity were generated
1593 (Figure 59).

1594 Power production decreased thereafter because the modest amount of reinjection done could
1595 not maintain the falling steam pressure. At that time, condensate was the main re-injectate
1596 and less was available than the amount of water produced. Reservoir pressure is sub-
1597 hydrostatic and thus the water could be reintroduced at atmospheric pressure, i.e. simply
1598 poured into boreholes to drain back into the formation under gravity.

1599 The US Geological Survey routinely locates > 10,000 earthquakes in The Geysers reservoir
1600 each year. The annual seismic rate is currently 200-300 M 2 earthquakes and 1-2 M 4
1601 earthquakes. The Geysers earthquake dataset is without doubt the richest set of induced
1602 earthquake data available in the world with > 250,000 located events in the catalog of the

1603 Northern California Earthquake Data Center⁷.

1604 For many years it was not acknowledged that the industrial activity induced the earthquakes.
1605 However, as data accumulated the link could not be denied. It was initially assumed that
1606 production caused the earthquakes as a result of the contracting reservoir collapsing in on
1607 itself. Surface deformation is indeed large, and subsidence rates of up to 5 cm/year have been
1608 reported [Lofgren, 1978; Mossop & Segall, 1999; Vasco *et al.*, 2013].

1609 In recent years, however, it has become clear that seismicity correlates better with reinjection
1610 than with production [*e.g.*, Majer & Peterson, 2007; Stark, 1990]. It has been possible to
1611 make this link in particular since 1998 when the first of two major water-acquisition and
1612 reinjection projects began. The South East Geysers Effluent Project (SEGEP) began to re-
1613 inject water via a 46-km-long pipeline from Lake County that delivers up to 22×10^6 l/day. In
1614 2003 the second project came online, the Santa Rosa Geysers Recharge Project (SGRP),
1615 which delivers up to 41×10^6 l/day via a 64-km-long pipeline from Santa Rosa (Figure 59)
1616 [Majer & Peterson, 2007]. Surges in earthquake rate correlate with the increases in water
1617 injection that accompanied the onset of those projects.

1618 In addition to the correlation between the seismicity in general and injection, surges of
1619 earthquakes correlate with both individual injections and injection wells [Majer & Peterson,
1620 2007; Stark, 1990]. In the high-temperature northwest Geysers, for example, a sharp increase
1621 in injection in late 2004 correlated with surges of earthquakes that cluster around the bottom
1622 of a well (Figure 80).

1623 Ground shaking from earthquakes with Modified Mercalli intensities of II – VI are felt daily
1624 in settlements near The Geysers. The largest earthquake that has occurred there is the 2014
1625 M_w 4.5 event. On the basis of historical seismicity, the absence of continuous, long faults in
1626 the reservoir, and the lack of alignment of epicenters, Majer *et al.* [2007] tentatively
1627 suggested that the largest earthquake that could occur was $M \sim 5.0$.

1628 An extensive review of The Geysers seismicity is provided by Majer and Peterson [2007].
1629 They conclude that the seismicity results from a diverse set of processes that may work
1630 independently or together and either enhance or possibly reduce seismicity. To the processes
1631 listed in Section 1.3, thermal contraction from cooling the rock matrix can be added.

1632 A second example of particularly rich geothermal-induced seismicity is that of the Coso
1633 geothermal field. This field lies in the southwestern corner of the Basin and Range province
1634 in eastern California, at a right releasing step-over in the southern Owens Valley fault zone
1635 [Monastero *et al.*, 2005]. It lies on a US Navy weapons test site, and is thus uninhabited and
1636 not generally accessible to the public. Electricity has been generated there since the 1980s,
1637 producing about 250 MW. Because there is a shortage of water locally, only about half the
1638 volume produced can be replaced by reinjection and a major lowering of the local water table
1639 has resulted.

1640 There is a high level of tectonic seismicity in the region, but even in this context the
1641 geothermal field is anomalously seismogenic. Several thousand locatable earthquakes per
1642 year occur within the $\sim 5 \times 5$ km production field, the majority of which must be induced by
1643 operations. These earthquakes have been subject to detailed research by numerous

⁷ <http://www.ncedc.org>

1644 institutions for many years [e.g., Julian *et al.*, 2004; Julian *et al.*, 2007; Kaven *et al.*, 2014;
 1645 Monastero *et al.*, 2005]. Most production and reinjection data are proprietary, so published
 1646 detailed correlations between operations and seismicity are rare.

1647 One of these rare cases is described by Julian *et al.* [2007]. In 2005 an existing well at Coso
 1648 was used in an experimental Enhanced Geothermal Systems operation. Fluid was injected at
 1649 rates of up to 20 l/s into well 34-9RD2 on the east flank of the reservoir. The objective was to
 1650 increase permeability and enhance production in a cluster of nearby producing wells. The
 1651 well was re-worked in advance of the project including deepening it and replacing the
 1652 existing slotted liner with an un-slotted one.

1653 During the work, major unexpected circulation-loss zones were encountered resulting in a
 1654 total loss of up to 20 l/s of drilling mud at a depth of about 2672 m. The planned EGS project
 1655 thus instantly metamorphosed into an unplanned reinjection operation. A vigorous earthquake
 1656 swarm onset immediately. High-resolution locations, relative locations, and full moment
 1657 tensors were determined using data from the high-quality seismic network operated by the
 1658 Geothermal Program Office of the US Navy, which had been densified with an array of
 1659 temporary stations for the purpose of monitoring the EGS experiment. As a result, an
 1660 exceptionally high-quality dataset was available from a total of 36 digital, three-component
 1661 stations.

1662 The results showed that the swarm activated several hundred meters of a preexisting fault
 1663 immediately adjacent to the well that opened in tensile mode. The existence of the structure
 1664 deduced from the seismic evidence was confirmed by surface geological mapping and by
 1665 data from a borehole televiewer log. This experiment was an early demonstration of the
 1666 potential of earthquake techniques to yield information on the detailed subsurface fracture
 1667 network in a geothermal reservoir.

1668 In Europe, three geothermal projects have been associated with $M > 3$ induced earthquakes,
 1669 all of them in Italy:

- 1670 • Larderello-Travale (M_{MAX} 3.2);
- 1671 • the Monte Amiata geothermal field (M_{MAX} 3.5); and
- 1672 • the Torre Alfina Field (M_{MAX} 3.0).

1673 Of these, the most notable case is that of the Larderello-Travale, Tuscany, vapor-dominated
 1674 system. Tuscany is an active tectonic region with a transcurrent/transensional/strike-slip
 1675 deformation style, high thermal gradients and temperatures up to 400°C. Within it there are
 1676 several geothermal fields of economic interest. The shallower Larderello-Travale reservoirs
 1677 are contained in Triassic carbonate and evaporite rocks. The deeper reservoirs are in
 1678 fractured, metamorphic basement.

1679 Larderello-Travale has generated electricity almost continuously since 1904, and the
 1680 reservoir is thought to have a long history of seismicity. In the early 1970s, injection of cold
 1681 condensate from the power plants was initiated in order to recharge the upper reservoir. A
 1682 seismic monitoring network was installed, in part to monitor the impact of the injection. It is
 1683 only since this network was installed that the seismicity could be studied in detail [Batini *et al.*,
 1684 1985; Batini *et al.*, 1980].

1685 The activity is variable regarding both event rate and b -values. The events are mostly
 1686 shallower than 8 km, with 75% located in the depth range 3.0-5.5 km. The largest event

1687 reported is a M 3.2 event that occurred in 1977. Events studied in detail were found to have
 1688 significant non-shear components in their focal mechanisms, indicating a tensile component
 1689 [Kravania *et al.*, 2000]. As would be expected, seismicity is reported to have enhanced the
 1690 permeability.

1691 Because of the long history of seismic activity many of the events are thought to be natural.
 1692 Nevertheless, a clear correlation between volume of injected water and number of events is
 1693 reported for small-magnitude earthquakes. It has been suggested that events with $M \geq 2.0$ do
 1694 not occur in response to injection [Batini *et al.*, 1985; Evans *et al.*, 2012].

1695 4.1.6 Shale-gas hydrofracturing

1696 Gas-bearing shale formations are hydrofractured (“fracked”) in order to increase permeability
 1697 so the gas can be extracted. It is typically done by drilling horizontal wells at relatively
 1698 shallow depths (up to ~2 km deep) into the target formation. Fluids are injected containing
 1699 chemicals and solids designed to propagate fractures and prop them open. The method has
 1700 been extensively applied in the USA where it has brought about a major reduction in the cost
 1701 of natural gas (Figure 81). As a result of this success there is widespread interest in other
 1702 countries in implementing the technology. However, in shale-gas regions where population
 1703 density is high there may be public concern about potential environmental effects, including
 1704 ground-water pollution, industrialization and induced earthquakes.

1705 Although over 2.5 million shale-gas hydrofracturing jobs have been completed worldwide, to
 1706 date maximum magnitudes of only 21 cases of induced seismicity have been reported (Figure
 1707 82). Of these cases, eight are from the USA, 12 are from Canada, and one is from the UK
 1708 [Baisch & Vörös, 2011; de Pater & Baisch, 2011]. This amounts to only 0.001% of all shale-
 1709 gas hydrofracturing jobs (Section 7.1). Of those cases, significantly large earthquakes are
 1710 reported from British Columbia (M 4.4, 4.4 and 3.8 events) and Alberta (M_L 4.4), both in
 1711 Canada [Kao *et al.*, 2015; Schultz *et al.*, 2015]. In the USA the largest shale-gas
 1712 hydrofracturing-related earthquakes reported have been four M > 3 events in Oklahoma and
 1713 Ohio [Darold *et al.*, 2014; Skoumal *et al.*, 2015].

1714 These statistics are misleading because the fundamental purpose of hydrofracturing in gas-
 1715 bearing shale is to crack the rock, i.e. to induce the very process that causes earthquakes.
 1716 Thus, all successful hydrofracturing jobs induce earthquakes. The desire is, of course, that the
 1717 earthquakes are small and do not cause nuisance by endangering health and safety, damaging
 1718 infrastructure or the environment, or annoying citizens. Meeting this objective is helped in
 1719 the USA and Canada by operating in regions of low population density. Seismic monitoring
 1720 is commonly done because the earthquake locations can provide information of use to
 1721 operations, *e.g.*, the location and volume of the fractured network created. However, if
 1722 nuisance seismicity is not induced there is little reason to report it. Seismic analyses focus on
 1723 investigating the spatial distribution and mode of fracturing achieved, the results are not of
 1724 public interest, and they are likely to remain proprietary.

1725 One of the most remarkable of these cases is a sequence associated with injection operations
 1726 in 2013 near Crooked Lake, Alberta. This sequence induced the highest-magnitude shale-gas
 1727 hydrofracturing-related earthquakes on record to date. The target formation is the Devonian
 1728 Duvemay organic-rich shale. Hydraulic fracturing operations there involve multi-stage, high-
 1729 pressure operations using proppant-weight-in-well of typically 60 MPa and volumes typically
 1730 of a few thousand cubic meters. Of ~3000 hydrofracturing operations in Alberta in 2013,
 1731 only three (0.1%) are reported to have been accompanied by noteworthy seismicity, with 160

1732 events up to M_L 4.4 being observed over a ~2-year period [Schultz *et al.*, 2015].

1733 The quality of information about the sequences is limited because local seismic stations were
1734 not available and detailed information on local crustal structure was absent. Data from distant
1735 stations therefore had to be subject to sophisticated processing. A close spatial and temporal
1736 correlation was reported between the earthquakes and the shale-gas hydrofracturing (Figure
1737 83 and Figure 84). Correlation was also observed between injection stages, a “screen-out”
1738 (i.e. an interruption in the flow of slurry that caused shutdown of injection) and seismicity.
1739 Associations between screen-outs and seismicity have been reported from elsewhere [Clarke
1740 *et al.*, 2014b; Skoumal *et al.*, 2015]. The seismicity may have interfered with operations at
1741 Crooked Lake.

1742 A classic case history is that of the Horn River Basin, a major shale gas production area in
1743 British Columbia. Fracking commenced there in 2006 and shale gas production peaked in
1744 2010 and 2011 [Farahbod *et al.*, 2015]. Prior to shale-gas hydrofracturing, seismicity rates
1745 were low and only 24 earthquakes with M 1.8-2.9 were located in a ~2-year period in the
1746 area. When shale-gas hydrofracturing started, the seismic rate increased to over 100
1747 earthquakes per year and correlated with days when hydrofracturing was conducted (Figure
1748 85). A logarithmic correlation between seismic moment, maximum magnitude and volume
1749 injected was observed (Figure 86).

1750 For the entire Horn River Basin, injected volume was more closely related to induced
1751 seismicity than injection pressure. Increases in injected volume are reported to increase
1752 earthquake frequency but not magnitude, and large earthquakes (seismic moment release
1753 $>10^{14}$ N m, i.e., $M \sim 3.5$) occurred only when ~150,000 m³ of fluid were injected per month.
1754 Time lags between injections and seismicity ranged from days to several months.

1755 The embryonic UK shale-gas industry began with the unfortunate case of the 2011 Preese
1756 Hall, Lancashire, earthquake sequence. There, the first UK dedicated multi-stage shale-gas
1757 hydrofracturing operation was conducted in a 1000-m section of the Carboniferous gas-
1758 bearing Bowland Shale. Following the injection of 2245 m³ of fluid and 117 tonnes of
1759 proppant, a nearby M_L 2.3 earthquake was reported by the British Geological Survey. The
1760 earthquake was felt, and was unusual in this location. The nearest monitoring station was 80
1761 km away. Additional seismic stations were deployed rapidly but no aftershocks were
1762 recorded. UK shale-gas hydrofracturing thus started life with a very rare phenomenon—the
1763 suspected induction of a nuisance earthquake.

1764 Operations continued, but about six weeks later a second felt event of M_L 1.5 occurred ~1.0
1765 km from the well. Citizen disquiet followed and operations were suspended. A total of 52
1766 earthquakes in the magnitude range M_L -2.0 to 2.3 were detected with similar waveforms to
1767 the two largest events. A government enquiry and 18-month suspension of operations ensued
1768 while the problem was investigated. The close relationship between operational parameters
1769 and seismicity left little doubt that the earthquakes had been induced by the hydrofracturing
1770 (Figure 87).

1771 The UK Department of Energy and Climate Change (DECC) commissioned a review and
1772 recommendations for the mitigation of seismic risk associated with future shale-gas
1773 hydrofracturing operations in the UK. Recommendations included the monitoring of test
1774 injections prior to the main injections, monitoring fracture growth during injections, near-
1775 real-time seismic monitoring of injections, and halting or changing injection strategy at the
1776 occurrence of seismicity with a threshold magnitude of M_L 0.5 [Green *et al.*, 2012].

1777 Detailed studies of the locations and fault mechanisms of the poorly recorded seismicity,
 1778 combined with seismic reflection data, showed that the earthquakes likely occurred a few
 1779 hundred meters below the well perforations on a fault that was not known to exist at the time
 1780 [Clarke *et al.*, 2014a; Green *et al.*, 2012]. The fault does not intersect the borehole but was
 1781 close enough that hydrofracture fluid may have leaked into it, reducing the normal stress and
 1782 permitting strike-slip motion to occur. The fault that slipped is an ancient transpressional
 1783 fault that formed at the end of a Carboniferous basin inversion and which had been inactive
 1784 for the last 260 Ma. This case history showed that even long-inactive faults, which are
 1785 common in most continental crust, are close to failure and may be induced to slip if injections
 1786 occur nearby.

1787 4.1.7 Allowing mines to flood

1788 Removal of mined material reduces confining stress on nearby faults and brings them closer
 1789 to failure. The simultaneous pumping out of water during mining lowers the pore pressure
 1790 and thus increases the strength of faults, counteracting the effect of rock removal. These two
 1791 process may roughly balance until a mine is abandoned and pumping stopped. After this,
 1792 natural groundwater recharge may encourage seismicity.

1793 A classic case where this is thought to have occurred is that of the 1994 Cacoosing Valley,
 1794 Pennsylvania, earthquake sequence (Figure 88) [Seeber *et al.*, 1998]. Groundwater recharge
 1795 is thought to be responsible for a M_L 4.4 earthquake that occurred beneath an 800-m-wide
 1796 carbonate quarry from which $\sim 4 \times 10^6 \text{ m}^3$ had been removed. The earthquake caused \sim \$2
 1797 million of damage to nearby homes. The quarry had been excavated to an average depth of 50
 1798 m over the 58-year time period 1934-1992. Groundwater pumping had been done during the
 1799 mining period to prevent the quarry from flooding. After mining stopped this pumping ceased
 1800 and the water table rose by \sim 10 m over a period of a few months. The rock is highly
 1801 permeable karstic carbonate, and depletion of groundwater, along with subsequent recharge,
 1802 likely extended over a wider area than the footprint of the quarry.

1803 Earthquake activity commenced approximately five months after cessation of pumping. A
 1804 sequence of 67 aftershocks was recorded on a rapidly deployed temporary seismometer
 1805 network. The aftershock sequence occurred in the upper 2.5 km and formed a planar pattern
 1806 that was interpreted as the fault plane that slipped. Focal mechanism studies suggested that
 1807 the mainshock had a thrust mechanism and that the earthquakes were situated in the hanging
 1808 wall block such that unloading by rock removal would have encouraged slip (Figure 89).
 1809 Surprisingly, the seismic sequence did not activate any of the plentiful, known, large-
 1810 displacement faults in the region. Instead, stress was released on a fracture set of small,
 1811 unmapped faults which probably had a more suitable orientation. The mining had reduced
 1812 confining stress by \sim 0.13 MPa, which may be compared with a calculated stress drop of 1-4
 1813 MPa for the M_L 4.4 mainshock.

1814 The Cacoosing Valley event is thought to be similar to one that occurred two decades earlier
 1815 beneath a large quarry at Wappinger Falls, New York [Pomeroy *et al.*, 1976]. There, a m_b 3.3
 1816 earthquake occurred in 1974. Again, the mainshock and associated aftershocks nucleated at
 1817 exceptionally shallow depth with some aftershocks as shallow as 0.5 km. Slip occurred on a
 1818 reverse fault immediately below a large quarry and had source mechanisms consistent with
 1819 the regional stress field. Over the preceding \sim 75 years $\sim 30 \times 10^6 \text{ m}^3$ of rock had been
 1820 removed by open-casting down to a depth of \sim 50 m. This changed the stress by \sim 1.5 MPa at
 1821 the surface and reduced the normal stress on faults below.

1822 4.1.8 Research projects

1823 In the wake of the Denver, Colorado earthquakes (Section 4.1.1) there was speculation that
 1824 earthquakes might be controllable. Partly as a result of this idea, a series of earthquake-
 1825 induction experiments have been conducted for research purposes. These have investigated
 1826 the physical properties of natural fault zones and the processes that accompany earthquake
 1827 occurrence. We have identified 13 cases of earthquakes induced by research projects.

1828 The first such project was conducted in 1969 at the Rangely Oilfield, Colorado [Raleigh *et*
 1829 *al.*, 1976]. This oilfield occupies Mesozoic and Paleozoic sedimentary rocks at a depth of
 1830 ~1700 m and is underlain by crystalline basement at ~3000 m. There is little significant local
 1831 faulting, but earthquake activity was known to occur associated with water flooding for
 1832 enhanced recovery (Section 4.1.3). As a result, a seismograph array and prior earthquake
 1833 record were already available. The fluid pressure in wells in the vicinity of the earthquakes
 1834 was experimentally cycled to investigate the effect on the seismicity. A close correlation
 1835 between seismicity and high pore pressure was observed, and events up to M_L 3.1 were
 1836 induced (Figure 90).

1837 In 1970, shortly after the Rangely experiment, another experiment was conducted at
 1838 Matsushiro, Japan. A volume of 2883 m³ of water at wellhead pressures of 1.4-5.0 MPa was
 1839 pumped into an 1800-m-deep well to test whether earthquakes were induced by increasing
 1840 pore pressure in a fault zone. After several days of injection earthquake activity onset within
 1841 a few kilometers of the well [Ohtake, 1974].

1842 After a hiatus in experimenting of 16 years, in 1990, perhaps the best known research
 1843 experiment to study fluid-induced seismicity was begun—the Kontinentales
 1844 Tiefbohrprogramm der Bundesrepublik Deutschland (KTB)—the German Continental Deep
 1845 Drilling Program. The literature documenting this project is extensive and includes a 1997
 1846 special section of *Journal of Geophysical Research* (No. 102) [*e.g.*, Baisch & Harjes, 2003;
 1847 Baisch *et al.*, 2002; Bohnhoff *et al.*, 2004; Erzinger & Stober, 2005; Fielitz & Wegler, 2015;
 1848 Grasle *et al.*, 2006; Jahr *et al.*, 2005; Jahr *et al.*, 2007; Jahr *et al.*, 2008; Jost *et al.*, 1998;
 1849 Shapiro *et al.*, 2006; Zoback & Harjes, 1997].

1850 The main borehole was drilled 1990-1994 to a depth of 9.1 km. The first hydraulic
 1851 stimulation was conducted in 1994 at depths and pressures close to the brittle-ductile
 1852 transition. About 400 earthquakes up to M_L 1.2 were induced at about 8.8 km depth (Figure
 1853 91). Focal mechanisms were consistent with stress measured in the borehole. Seismicity
 1854 onset within a few hours of pumping and a few tens of meters from the borehole. Modeling
 1855 suggested that the earthquakes occurred in response to pressure perturbations of < 1 MPa, *i.e.*
 1856 less than 1% of the ambient, hydrostatic pore pressure at the nucleation depth.

1857 An important conclusion of this experiment was that differential stress in the crust is limited
 1858 by the frictional strength of well-oriented, pre-existing faults (“Byerlee’s Law”), and that the
 1859 crust is in brittle failure equilibrium even at great depth in relatively stable intraplate areas.
 1860 Hydraulic experiments at the site have continued up to recent years [*e.g.*, Jahr *et al.*, 2008].

1861 A later project conducted in the Phillipines in 1997 injected 36,000 m³ of water into a well
 1862 intersecting a creeping portion of the Philippine Fault at the Tongonan geothermal field. The
 1863 water entered the formation at depths of 1308-2177 m below the surface [Prioul *et al.*, 2000].
 1864 Several hundred earthquakes were observed but all occurred away from the fault and within
 1865 the geothermal reservoir. Prioul *et al.* [2000] concluded that tectonic stress on the fault is

- 1866 relieved aseismically and as a consequence there was no differential shear stress to release by
1867 the water injection.
- 1868 In the same year, a water-injection experiment was conducted in the Nojima fault zone,
1869 Japan, shortly after it ruptured in the 1995 M 6.9 Kobe earthquake [Tadokoro *et al.*, 2000].
1870 This experiment offered the opportunity to gather information on the physical properties of a
1871 fault plane in the immediate post-rupture period. Over periods of a few days, 258 m³ of water
1872 were injected into an 1800-m-deep borehole at a pressure of ~4 MPa at the surface, entering
1873 the fault zone at 1480-1670 m depth. An increase in seismicity in the magnitude range M -2
1874 to 1 occurred a few days after each injection. It was concluded that the fault zone was highly
1875 permeable and could slip with pore-fluid pressure increases of less than 10%.
- 1876 Two additional experiments have been conducted in recent years, the first in 2013 as part of
1877 the Wenchuan Earthquake Fault Science Drilling (WFSD) project [Ma *et al.*, 2015]. This
1878 project studied the fault healing process. Over the four-month period November 2013 -
1879 March 2014, 47,520 m³ of water at pressures of 10-15 MPa were injected at rates of up to 1.7
1880 l/s into a 552-m-deep well that intersected a fault zone at 430 m depth. The fault was
1881 activated and over 20,000 earthquakes up to M ~1 were detected using downhole
1882 observations. The hypocentral zone suggested failure in the same sense as the regional stress.
- 1883 A similar phenomenon was reported by Guglielmi *et al.* [2015] in an experiment that
1884 stimulated an inactive fault in a carbonate formation. The experiment injected 0.95 m³ of
1885 water into a 518-m-deep underground experimental facility in southeastern France where a
1886 vertical well intersected a fault at a depth of 282 m. Aseismic shear slip started at a pressure
1887 of ~1.5 MPa, and ~80 earthquakes occurred a few meters from the injection point. These
1888 accounted for only a small fraction of the slip on the fault, however. The accumulated
1889 moment at the end of the experiment was $M_0 = 65 \times 10^9$ Nm, (equivalent to an event with M_W
1890 1.17). This was far larger than the moment released by the seismicity, which was $M_0 < -2$
1891 N m. Aseismic slip dominated deformation in the fault zone and the earthquakes occurred in
1892 the rock mass outside the pressurized zone. Other experiments have been performed in a salt
1893 solution mine at Cerville-Buissoncourt in Lorraine, France [Kinscher *et al.*, 2015; Mercerat
1894 *et al.*, 2010] and the Wairakei geothermal field, New Zealand [Allis *et al.*, 1985; Davis &
1895 Frohlich, 1993].
- 1896 This multi-decade, multi-national research subject has yielded a vast amount of data and
1897 answered some critical questions, not always the ones originally posed and not always with
1898 the preferred answer. Relieving in a controlled way the stress naturally released in large
1899 earthquakes is likely to be scientifically and politically difficult. The continental crust is near
1900 to failure, even to great depths and where large faults are not known. Earthquakes can be
1901 induced by relatively small stress perturbations, but in some cases stress on a targeted fault is
1902 relieved aseismically. In these cases, motion on that fault may induce secondary earthquakes
1903 in the surrounding rock mass. Fluid injection may thus induce primarily aseismic slip, and
1904 seismicity may be a secondary effect, with imperfect spatial correlation with the injection
1905 activities. In many cases of induced seismicity more stress is released than is loaded on faults
1906 by the anthropogenic process, since pre-existing tectonic stress is also released. However, the
1907 Wenchuan and southeastern France experiments illustrate that the reverse sometimes occurs—
1908 that some of the anthropogenically loaded stress may be released aseismically.

1909 4.2 Gas

1910 4.2.1 Natural gas storage

1911 In order to stabilize supply, and for energy security, nations store natural gas reserves often
 1912 underground. As of May 2015, 268 underground gas storage facilities existed or were
 1913 planned in Europe (Figure 92), and there were over 400 in the USA.

1914 Depleted hydrocarbon reservoirs, aquifers, and salt cavern formations are obvious
 1915 repositories because they are usually well understood geologically. Furthermore, in the case
 1916 of hydrocarbon reservoirs, engineering infrastructure including wells and pipelines may
 1917 already be in place. In addition, they may be conveniently close to consumption centers.

1918 We have identified seven cases of induced seismicity reported to have been associated with
 1919 underground gas storage:

- 1920 • Gazli, Uzbekistan [Simpson & Leith, 1985];
- 1921 • the Castor project (in the old Amposta Field), Spain [Cesca *et al.*, 2014; Gaité *et al.*,
 1922 2016];
- 1923 • Bergermeer, Norg and Grijpskerk, Netherlands [Anonymous, 2014];
- 1924 • Hájé, Czech Republic [Benetatos *et al.*, 2013; Zedník *et al.*, 2001]; and
- 1925 • Hutubi, China [Tang *et al.*, 2015].

1926
 1927 A few small earthquakes up to M 0.7 were recorded in 2013 in association with the injection
 1928 of cushion gas in the Bergermeer Gasfield. Up to 15 earthquakes per month up to M 1.5,
 1929 several of which were felt, were reported for the Hájé storage facility. Larger earthquakes
 1930 were reported in association with gas storage at Hutubi, with over 700 earthquakes up to M
 1931 3.6 in the period 2009-2015.

1932 The case of the Gazli Gasfield, Uzbekistan, is primarily renowned for the three damaging M_S
 1933 ~ 7 earthquakes that caused death and destruction in the local town of Gazli in 1976 and 1984
 1934 (Section 3.3.1). When this field had been largely depleted, it was used for storage. Gas was
 1935 cycled in and out as required. Plotnikova *et al.* [1996] report seismicity induced by this
 1936 process that correlates with the amount of gas stored (Figure 93). Earthquakes with
 1937 magnitudes up to M 5 are reported.

1938 By far the best-documented case is, however, that of the Castor project, Spain. This project
 1939 aimed to use a depleted oilfield in the Gulf of Valencia, the old Amposta Field, ~ 20 km from
 1940 the coast of northeast Spain (Figure 94). It was planned to store 1.3×10^9 m³ of natural gas in
 1941 this reservoir, sufficient to meet 25% of Spain's storage requirements. Earthquake activity
 1942 onset shortly after the commencement of gas injection, however. Ultimately, on 1 October,
 1943 2013, the largest earthquake, with M_W 4.3, occurred. Public reaction to the earthquakes was
 1944 negative, perhaps not least because the population had been sensitized by the 2011 M_W 5.1
 1945 Lorca earthquake which occurred only two years before and 250 km further south along the
 1946 coast (Section 3.1). We understand that, as a result, the project has been discontinued.

1947 The old Amposta oil reservoir occupies fractured and brecciated Lower Cretaceous dolomitic
 1948 limestone and is one of several in the region (Figure 95). It produced 56 million barrels ($\sim 9 \times$
 1949 10^6 m³) of an estimated total in-place volume of 140 million barrels of oil (22×10^6 m³) in the
 1950 period 1973-1989. Secondary injection for enhanced recovery was not needed because of

- 1951 strong natural water drive. After 1989 the field was largely depleted and lay dormant.
- 1952 Installation of the necessary infrastructure for conversion of the reservoir into a gas storage
 1953 facility commenced in March 2009 and included a platform and a gas pipeline. Injection of
 1954 an initial $\sim 10^8$ m³ (at 25°C and 0.1 MPa pressure) of cushion gas (i.e. gas intended as
 1955 permanent inventory in the reservoir) was conducted 2-16 September, 2013 at 1.75 km below
 1956 sea level.
- 1957 Three days after injection began, seismicity onset (Figure 96). Earthquakes with magnitudes
 1958 up to M 2.6 occurred (Figure 97). Injection was stopped 16 September but earthquakes
 1959 continued to occur. The largest, a M_w 4.3 event, occurred 1 October, two weeks after
 1960 injection stopped. In total, over 1000 earthquakes were detected, more than 420 with M \geq 2
 1961 (Figure 97). Seismicity was still ongoing in 2016 [Gaite *et al.*, 2016].
- 1962 Accurate hypocentral locations were difficult to determine because the project, being
 1963 offshore, was monitored by a seismic network with limited coverage. The closest station was
 1964 26 km from the Castor platform and, since most of the stations were on land, there was
 1965 restricted azimuthal coverage [Gaite *et al.*, 2016]. As a result, different studies of the
 1966 hypocentral locations show different results and even the orientation of the hypocentral
 1967 distribution as a whole (which might contribute to identifying the activated fault structure)
 1968 and the hypocentral depths (which are important to determine whether or not, and how, the
 1969 earthquakes were linked to the gas injection) vary significantly between studies. Both NW
 1970 and NE orientations for the hypocentral zone are reported, along with depths that vary from
 1971 close to the gas injection depth to several kilometers deeper (Figure 96) [*e.g.*, Cesca *et al.*,
 1972 2014; Gaite *et al.*, 2016].
- 1973 The epicentral area forms part of the dominantly ENE-WSW Catalan-Valencian normal-
 1974 faulting extensional region [Perea *et al.*, 2012] and focal mechanism studies of the mainshock
 1975 show motion compatible with slip in this sense [Cesca *et al.*, 2014]. The most significant
 1976 potentially seismogenic feature near the old Amposta Field is the 51-km-long NE-SW
 1977 oriented, Fosa de Amposta fault system [Gaite *et al.*, 2016]. Such a major fault zone, were it
 1978 to rupture in its entirety, is potentially capable of generating a M 5-7 earthquake (Figure 98).
 1979 Combined interpretation of the hypocentral locations and source mechanisms suggests that
 1980 this fault was not activated, however.
- 1981 The activity of September and October 2013 was unusual for the area regards both magnitude
 1982 and seismic rate compared with the preceding two decades (Figure 94). Although earthquake
 1983 activity occurs along the coast of Spain to the north and south, the Pyrenees mountain chain
 1984 in Portugal, and the coast of North Africa, no significant historical seismicity was known to
 1985 have involved the fault system local to the Castor project prior to the gas injection. For this
 1986 reason, and because of the very close spatial and temporal correlation with the gas injection,
 1987 there is little doubt that the earthquakes were induced.
- 1988 4.2.2 CO₂ for oil recovery
- 1989 There are approximately 100 enhanced oil recovery injection sites where CO₂ is used, mostly
 1990 in Texas. We have, however, found only two cases where seismicity is postulated to be
 1991 unambiguously induced by this process. These are the cases of the Cogdell Field, Texas [Gan
 1992 & Frohlich, 2013] and Weyburn Oilfield, Saskatchewan [Maxwell & Fabriol, 2004; Verdon
 1993 *et al.*, 2013]. The latter is a hybrid project and also considered to be a case of Carbon Capture
 1994 and Storage (CCS) so it is described in Section 4.2.3.

1995 The case of the Cogdell Oilfield is described in detail by Gan and Frolich [2013]. Early on in
 1996 its history, this field generated earthquakes surmised to have been induced by water injection.
 1997 Lately, CO₂ has been injected for enhanced oil recovery and this is associated with
 1998 earthquakes up to M_w 4.4 (Figure 99).

1999 The Cogdell Oilfield is a large subsurface limestone reef mound, not a fault-bounded oil trap,
 2000 and there are no geologically mapped faults nearby. Production began in 1949 and in the
 2001 period 1957-1983 oil recovery was enhanced by brine injection. In the period 1975-1982 this
 2002 was associated with earthquakes that were surmised to have been induced. They included a
 2003 M_L 5.3 event in 1978. Despite its size, this earthquake was only poorly located, an indication
 2004 of the rudimentary nature of seismic monitoring in Texas at this time. Davis and Pennington
 2005 [1989] suggested that the seismicity correlated with injection volume at Cogdell and
 2006 concluded that earthquakes occurred where reservoir pressure gradients were high.

2007 Enhanced oil recovery using gas began in 2001 and injection built up to a constant, high level
 2008 of $\sim 40 \times 10^6$ m³/mo from 2004 onwards. Injection was conducted at ~ 2.1 km depth, 20 MPa
 2009 pressure and 75°C, under which conditions CO₂ is supercritical. In 2006, after 23 years of
 2010 seismic quiescence and following a significant increase in gas injection rate, earthquakes
 2011 onset again. Over the following five years 18 earthquakes with M > 3 and occurred and in
 2012 2011 one of M_w 4.4.

2013 The 21-month period March 2009 - December 2010 could be studied in detail because at this
 2014 time USArray, a rolling program to cover the entire country with temporary seismic stations⁸,
 2015 swept across Texas. During this period the network recorded 93 locatable events, many
 2016 within 2 km of wells actively injecting gas into the Cogdell Oilfield. Locations, coupled with
 2017 focal mechanisms, suggested that the events occurred on previously unknown faults.
 2018 Interestingly, although the neighboring Kelly-Snyder and Salt Creek Fields have similar
 2019 operational histories, seismicity does not appear to be induced in them.

2020 4.2.3 Carbon Capture and Storage (CCS)

2021 The issue of induced earthquakes is particularly important in the case of Carbon Capture and
 2022 Storage (CCS). In addition to causing a nuisance, earthquakes could also rupture the
 2023 impermeable containment caprock that contains the CO₂ in the storage reservoir, and release
 2024 it back into the environment. Carbon geostorage is in its infancy, but there are already 20-30
 2025 tests underway globally, including eight operational commercial-scale CCS plants⁹. Of these,
 2026 three are reported to be seismogenic. An illustrative range of seismic responses is provided
 2027 by the Sleipner Field (Norwegian North Sea), the Weyburn Field (Saskatchewan, Canada)
 2028 and In Salah (Algeria) [Verdon *et al.*, 2013].

2029 In the Sleipner Field, since 1996 CO₂ has been removed from the natural gas produced and
 2030 re-injected into a shallow saline aquifer (the Utsira Formation) at a rate of $\sim 10^6$ tonnes/year.
 2031 The aquifer is large and comprises well-connected, little-faulted sandstone with high porosity
 2032 and permeability at ~ 1 km depth beneath North Sea mean sea level. By 2011 the total volume
 2033 of CO₂ injected amounted to only $\sim 0.003\%$ of the available pore space. No pore-pressure
 2034 increase, mechanical deformation or seismicity has been detected for the entire >20 years of

⁸ <http://www.usarray.org>

⁹ <http://www.ccsassociation.org/faqs/ccs-globally/>

2035 injection. The Sleipner Field is, however, not seismically monitored locally so small
 2036 earthquakes would go undetected. The nearest earthquakes to the Sleipner Field listed in the
 2037 British Geological Survey catalogue are a M_L 3.5 event at 1 km distance and a M 2.5
 2038 earthquake at 6 km distance. The uncertainties in these locations may be considerable.

2039 The Weyburn Oilfield, Saskatchewan, Canada, has been exploited for 45 years and is
 2040 somewhat seismogenic. CO_2 injections started in 2000 both for enhanced oil production and
 2041 CO_2 sequestration and now $\sim 3 \times 10^6$ tonnes/year are injected annually. This is accompanied
 2042 by minor earthquake activity. Figure 100 shows the relationships between earthquake
 2043 occurrence, CO_2 injection, and water injection. Some of the earthquakes clustered near
 2044 injection wells, but no clear temporal correlations are apparent. All the earthquakes were
 2045 small.

2046 Vigorous earthquake activity accompanied CO_2 sequestration at the producing In Salah
 2047 Gasfield, Algeria. There, CO_2 was injected into a low-permeability, 13–20% porosity, ~ 20 -
 2048 m-thick fractured sandstone in a non-producing, water-dominated part of field at depth of
 2049 1,850–1,950 m. Hundreds of earthquakes occurred, accompanied by uplift detected using
 2050 InSAR.

2051 CO_2 injection at In Salah started in 2004 and over the following nine years a total of $\sim 3.85 \times$
 2052 10^6 tonnes of CO_2 produced from several nearby gas wells were re-injected via horizontal
 2053 boreholes. There was little apparent pressure communication with the producing part of the
 2054 field. Calculations suggest that pore pressures increased from initial conditions of ~ 18 MPa at
 2055 the injection points to ~ 30 MPa whilst at the same time they reduced in the production parts
 2056 of the reservoir (Figure 101). Deformation measured using InSAR detected surface-blistering
 2057 type uplift of up to ~ 1 cm/year locally around the injection wells.

2058 A three-component borehole seismometer deployed nearby detected over 1000 events in
 2059 2010. The data were consistent with locations in the receiving formation beneath the injection
 2060 well though there was no clear correlation with CO_2 injection (Figure 102). The project has
 2061 since been terminated as a result of seal integrity concerns.

2062 Verdon *et al.* [2013] conclude that at Sleipner, where the target aquifer is large and pressure
 2063 increases during injection minimal, little deformation, either seismic or aseismic, results. At
 2064 Weyburn, deformation and seismicity may be partly mitigated by ongoing oil extraction
 2065 which serves to offset pressure increase resulting from the CO_2 injections. At In Salah,
 2066 however, the formation into which CO_2 is injected had poor pressure communication with the
 2067 producing parts of the reservoir and natural gas extraction did not compensate for the
 2068 injections. Pore pressures increased significantly as a consequence leading to both seismic
 2069 and aseismic deformation.

2070 A CCS demonstration site reported to be seismogenic is at Decatur, Illinois [Kaven *et al.*,
 2071 2015]. There, $\sim 10^6$ tonnes of supercritical CO_2 were injected over a period of three years at a
 2072 depth of 2.1 km into a regionally extensive, 460-m-thick high porosity/permeability
 2073 sandstone. The CO_2 used is a by-product of local ethanol production. Approximately 180
 2074 earthquakes up to M_w 1.26 were reported over a period of about two years within a few
 2075 kilometers of the injection well and at the approximate depth of injection. Kaven *et al.* [2015]
 2076 concluded that earthquakes nucleate on preexisting faults in the basement that are well
 2077 oriented with respect to the regional stress field. They further conclude that little seismic
 2078 hazard is posed to the host formation because the earthquakes are relatively distant and small.

2079 All other CCS projects have, to date, been shorter in duration and typically with total
 2080 volumes no more than 10s or 100s of thousands of tonnes. CCS projects have developed
 2081 recently in China where eleven projects are reported including five as recent as 2014
 2082 [Huaman & Jun, 2014]. Limited information is available on these projects and none regarding
 2083 seismicity induced by subsurface CO₂ injection.

2084 4.2.4 Injection into the subsurface: Summary

2085 Diverse fluids are injected into the ground for diverse reasons and diverse related
 2086 seismogenic behavior results. For a large majority of projects no earthquakes are reported.
 2087 For others, minor, small-magnitude earthquakes occur that are of insufficient public interest
 2088 to result in publication of details. For a small minority seismicity induced is sufficiently
 2089 troublesome to hinder operations or, in rare cases, result in project abandonment.

2090 Spatial, temporal, and magnitude correlations with the postulated causative operations are
 2091 variable. Earthquakes thought to be induced may be co-located with injections at a level of
 2092 10s or 100s of meters or they may occur up to tens of kilometers distant. Earthquakes may
 2093 onset as soon as operations begin or be delayed for decades. Small operations may induce
 2094 large earthquakes and large operations may be aseismic.

2095 An interesting question is why Oklahoma is so highly seismogenic while large-scale injection
 2096 projects are conducted in many states of the USA without nuisance earthquakes. We are not
 2097 aware of any current theories as to why this is.

2098 **5 Explosions**

2099 Since the first test of a nuclear device, the Trinity explosion of July 16, 1945, approximately
 2100 2000 such tests have been conducted by eight nations, 1,352 of them underground. We have
 2101 found reports of seismicity associated with 22 of these, 21 in the USA and one in Russia
 2102 [Boucher *et al.*, 1969; Engdahl, 1972; Hamilton *et al.*, 1972; McKeown, 1975; McKeown &
 2103 Dickey, 1969].

2104 American nuclear tests were conducted at the Nevada Test Site for the 48-year-period 1945-
 2105 1992 (Figure 103). Boucher *et al.* [1969] investigated the possibility of induced seismicity
 2106 associated with 16 nuclear tests by searching the University of Nevada database of
 2107 earthquake locations. They reported that seismicity was induced after all of the 10 tests where
 2108 the explosion itself registered $m_b \geq 5.0$. We have not included the explosions themselves in
 2109 the *iQuake* database. The largest earthquake induced was at least one magnitude unit smaller
 2110 than the inducing explosion. This suggests that earthquakes may have been induced by
 2111 many, if not all of the tests, but some were too small to be clearly recorded.

2112 A test ironically named Faultless (19/01/1968) is infamous for having induced clearly visible
 2113 surface slip on faults up to 40 km from ground zero, even though the test was only one
 2114 megaton in yield. Ground deformation associated with this, and other nuclear tests, has been
 2115 captured on film [McKeown & Dickey, 1969]¹⁰.

2116 Carefully-documented studies of the seismicity induced by large nuclear tests were done for
 2117 the Benham (19/12/1968), Purse (07/05/1969), Jorum (16/09/1969) and Handley
 2118 (26/03/1970) tests (Figure 104) [Hamilton *et al.*, 1972; McKeown, 1975]. The earthquakes

¹⁰ See, for example, <https://www.youtube.com/watch?v=6ETHnsKnKiA>

2119 induced occurred immediately after the tests and clustered on Pahute Mesa, Nevada, where
2120 there is a four-kilometer-thick sequence of volcanic rocks containing both calderas and basin-
2121 range-type normal faults. Most of the induced earthquakes occurred over periods of 10-70
2122 days following the tests, at depths of less than five kilometers and distances smaller than ~15
2123 km from ground zero.

2124 The spatial distribution of the earthquakes was found to be mostly controlled by local
2125 geological structure. The scales and fractal dimensions of the two sets of faults compared
2126 with those of the test-related earthquakes suggested that events occurred on faults in the
2127 buried caldera ring-fracture zones rather than on the regional basin-range faults (Figure 104).
2128 McKeown [1975] concluded that the subsidiary, not the dominant, fault and fracture system
2129 in the region had been activated.

2130 Underground nuclear tests in Amchitka, Alaska, resulted in permanent displacement on
2131 geological faults of as much as 1 m in the vertical and 15 cm in the horizontal for fault
2132 lengths up to 8 km [McKeown & Dickey, 1969]. The seismic effects of tests Milrow (1969)
2133 and Cannikin (1971) there were monitored by local seismic stations. Both tests generated
2134 several hundred small earthquakes with $M < 4$. They were thought to be related to
2135 deterioration of the explosion cavity. The sequences concluded with large, complex events
2136 and simultaneous subsidence of the surface resulting from final collapse of the explosion
2137 cavity. In the case of the Cannikin test, small tectonic events continued up to 13 km from
2138 ground zero for several weeks. The events were shallow, had waveforms characteristic of
2139 normal tectonic earthquakes, and focal mechanisms consistent with existing faults. They are
2140 thought to have represented release of ambient tectonic stresses as a result of the explosions.
2141 The more modest post-test seismic response from tests in Amchitka compared with those
2142 conducted in Nevada is thought to result from the lower level of tectonic stress [Engdahl,
2143 1972].

2144 Most large chemical explosions are associated with rocket launching, military research and
2145 operations, and accidents in the military, space-program and industrial sectors. Such
2146 explosions may be equivalent of several kilotonnes (kt) of TNT. They occur at the surface on
2147 land or on ships and are thus poorly coupled to the ground. Tsunamis, but not earthquakes,
2148 have been reported in association with some of these.

2149 It has been suggested that deep penetrating bombs may modulate earthquake activity.
2150 Balassanian [2005] examined earthquake activity over ~2-year periods spanning bombing
2151 incidents at Kosovo, Yugoslavia (1999), Baghdad, Iraq (1991), Tora Bora, Afghanistan
2152 (2001) and Kirkuk, Iraq (2003). It was suggested that the incidence of $M \geq 5$ earthquakes
2153 increased within 1000 km and one year of the bombings at Kosovo and Tora Bora but not
2154 after those at Baghdad and Kirkuk. Arkhipova *et al.* [2012] suggested that the 23 October,
2155 2011 M 7.8 Van earthquake, eastern Turkey, was encouraged by mass bombing associated
2156 with the Libyan conflict, 1300-1500 km away.

2157 Deep penetrating bombs explode at depths of a few meters in the ground, improving the
2158 coupling by factors of several tens of percent compared with equivalent surface explosions.
2159 Nevertheless, deep penetrating bombs are generally not larger than the equivalent of ~1 kt of
2160 TNT, much smaller than the megatonne- or multi-megatonne scale typical of the nuclear
2161 devices reported to have induced earthquakes. In the case of the nuclear tests, earthquakes
2162 have been induced out to a maximum of ~40 km away and activity has decayed away over
2163 periods of a few days or weeks [Boucher *et al.*, 1969].

2164 Given the relatively small subsurface effects of chemical explosions and the great distances
 2165 and relatively long time delays of the earthquakes postulated to have been induced by them,
 2166 these suggestions must be considered speculative. Without them, there are no credible reports
 2167 of earthquakes induced by chemical explosions. This ignores large landslides which may be
 2168 considered to represent earthquakes at the free surface with focal mechanisms equivalent to a
 2169 net force [Julian *et al.*, 1998].

2170 Only nuclear explosions are known with a high degree of confidence to induce earthquakes.
 2171 Not only do they induce aftershocks that may persist for some time after the blast, but
 2172 tectonic stress is also released simultaneously with the explosions themselves. This is shown
 2173 by the focal mechanisms of the blasts, which often involve both shear and explosive
 2174 components (Figure 28) [Toksöz & Kehrner, 1972; Wallace *et al.*, 1983]. The largest
 2175 earthquake we have found reported to have been induced by a nuclear test had a magnitude of
 2176 m_b 4.9 and was associated with collapse of the cavity of the Cannikin, Amchitka test.

2177 6 Summary

2178 A map of the global distribution of human-induced earthquake sequences is given in Figure
 2179 105. Such earthquakes are reported from every continent except Antarctica. In Figure 106 -
 2180 Figure 111 regional maps are shown for Europe, the Middle East, central- and east Asia,
 2181 India and vicinity, southern Africa, North-, central- and South America, Australia and New
 2182 Zealand. Induced seismicity clearly correlates with industrial activity and a lack of
 2183 correlation with tectonic plate boundaries.

2184 The magnitudes of the largest earthquakes postulated to be associated with projects of
 2185 different types varies greatly (Figure 60). The largest earthquakes have been reported for
 2186 water reservoirs, conventional oil and gas exploitation, and geothermal operations. Median
 2187 magnitudes also vary between project types but the most commonly reported are $3 \leq M < 4$
 2188 which apply to water reservoirs, construction, conventional oil and gas, hydrofracturing,
 2189 mining, and research projects. In some cases, however, the total number of cases reported is
 2190 small. For all project types it is essentially certain that large numbers of smaller induced
 2191 M_{MAX} earthquakes have not been reported.

2192 Relationships between various seismic and operational parameters have been suggested for a
 2193 number of individual projects. For example, there is a clear relationship between the seismic
 2194 moment released and the volume injected in shale gas hydrofracturing operations at the Etsho
 2195 area, Horn River Basin, British Columbia (Figure 86) [Farahbod *et al.*, 2015]. A question of
 2196 interest for future projects is, however, what correlations might exist for all projects of the
 2197 same kind.

2198 From the point of view of nuisance, the magnitudes of the largest earthquakes induced are by
 2199 far the most important. Seismic rate and the total number of earthquakes are of secondary
 2200 importance because the fractal nature of earthquakes means that most are small. Because a
 2201 large and systematic part of the true dataset is missing (i.e. the unreported cases) correlations
 2202 with operational parameters cannot convey any information on average M_{MAX} . Of interest is
 2203 whether *the largest* M_{MAX} correlates with operational parameters.

2204 This is illustrated, for example, by Figure 112, which shows a plot of M_{MAX} vs. water
 2205 reservoir volume for 126 cases. Clearly the magnitude of *the largest* M_{MAX} increases with
 2206 reservoir volume. However, there is no significant correlation between M_{MAX} and reservoir
 2207 volume for the dataset as a whole. If reporting were complete, the region of the plot beneath

2208 the M_{MAX} upper bound would be populated with points. Because the reported data are biased
 2209 in this way we have not calculated correlation coefficients between all values of M_{MAX} and
 2210 other parameters.

2211 Cases where a relationship is observed are:

- 2212 • *Water reservoir volume* (Figure 112): Volumes plotted range from 0.004 km³ to 164
 2213 km³. There is a nearly linear boundary to the upper left of the cloud of points which
 2214 suggests a relationship between reservoir volume and the largest possible M_{MAX} .
 2215 Interestingly, the 2008 $M_w \sim 8$ Wenchuan, China, which is disputed because of its
 2216 seemingly disproportionately large size, also plots on this alignment.
- 2217 • *Water reservoir mass per unit area* (Figure 113): There is a weak tendency for the
 2218 largest M_{MAX} (i.e. the upper bound of M_{MAX}) to increase with reservoir water mass per
 2219 unit area.
- 2220 • *Volume added or removed in surface operations* (Figure 114): We combined as many
 2221 cases of surface operations as possible. There is a clear tendency for the largest M_{MAX}
 2222 to increase with this parameter.
- 2223 • *Volume of material removed from the subsurface* (Figure 115): We combined
 2224 conventional oil and gas, geothermal, and mining-produced volumes. There is a weak
 2225 tendency for the largest reported M_{MAX} to increase with volume produced. The
 2226 relationship for M_{MAX} for injection volumes proposed by McGarr [2014] on the basis
 2227 of theoretical considerations fits these data well (Figure 116).
- 2228 • *Shale-gas hydrofracturing – injection pressure, rate and volume* (Figure 117): We
 2229 observe a tendency for the largest M_{MAX} to increase with all these parameters. This is
 2230 in agreement with the relationship proposed by McGarr [2014].
- 2231 • *Injected volume for all projects* (Figure 118): We found data for 69 cases to study this
 2232 parameter. The largest earthquake reported is the 2011 M_w 5.7 Prague, Oklahoma,
 2233 event. This and a small number of additional earthquakes, mostly postulated to be
 2234 induced by waste fluid injection, exceed the upper-bound magnitude limit proposed
 2235 by McGarr [2014].
- 2236 • *Injection pressure* (Figure 129): We were able to study this relationship for 79 cases.
 2237 Pressures range from atmospheric to 89 MPa. There is a tendency for the largest M_{MAX}
 2238 to reduce with maximum injection pressure.
- 2239 • *Volume or proxy volume removed from or added to the subsurface* (Figure 119): We
 2240 calculated volume or proxy volume (mass converted to volume using an appropriate
 2241 density) for 218 cases. There is a clear, systematic upper bound for M_{MAX} . The
 2242 relationship proposed by McGarr [2014] for injection volumes fits this wider dataset
 2243 well with a few exceptions.
- 2244 • *Mass removed from or added to the subsurface* (Figure 120): As with volume, there is
 2245 a clear linear observed upper bound to M_{MAX} .
- 2246 • *Yield of nuclear devices* (Figure 121): The magnitudes of induced earthquakes
 2247 correlate with explosion size for the seven cases for which data are available. This
 2248 finding is in agreement with the correlation between the activated-fault length and
 2249 explosive yield at Pahute Mesa, Nevada Test Site (Figure 122) [McKeown & Dickey,
 2250 1969].
- 2251 • *Project scale* (Figure 123): We updated the plot of McGarr *et al.* [2002] with 20
 2252 additional cases from our expanded database. The addition of more data generally
 2253 confirmed the earlier observations. Two cases exceed the empirical upper bound of
 2254 McGarr *et al.* [2002]—the 1979 M_L 6.6 Imperial Valley, California, earthquake (linked

2255 to the Cerro Prieto geothermal field; Section 3.4) and the 2008 $M_w \sim 8$ Wenchuan,
2256 China, earthquake (Section 2.1.1).

- 2257 • *Project type* (Figure 124): The largest earthquakes postulated to have been induced, in
2258 order of decreasing magnitude, are associated with water reservoirs, groundwater
2259 extraction and conventional oil and gas operations. These have all been linked to
2260 earthquakes with $M > 7$. To date, only relatively small earthquakes have been
2261 postulated to be associated with CCS, research experiments, construction and
2262 hydrofracturing. The number of projects in each category varies.
- 2263 • *Distance of epicenter from the inducing project* (Figure 125): There is a slight
2264 tendency for the largest reported M_{MAX} to decrease with distance from the project.

2265

2266 Cases where a relationship is not observed are:

- 2267 • *Dam height* (Figure 126): The number of cases for which data are available is 159.
2268 Many are from Brazil, China, and the USA. There is little tendency for the largest
2269 reported M_{MAX} to correlate with dam height.
- 2270 • *Water reservoir area* (Figure 127): Reservoir areas for seismogenic cases range from
2271 1.6 km^2 to $53,600 \text{ km}^2$. No significant tendency is seen for the largest M_{MAX} to
2272 increase with reservoir area. This result is perhaps unsurprising because large parts of
2273 a reservoir may be shallow.
- 2274 • *Pressure change in subsurface reservoirs* (Figure 128): There is no correlation
2275 between the largest reported M_{MAX} and reservoir pressure change for the 55 cases
2276 where data are available.
- 2277 • *Injection rate for all projects* (Figure 130): This is independent of the largest reported
2278 M_{MAX} . Although some individual projects report correlations there is no clear
2279 correlation for projects as a whole.

2280

2281 The largest reported induced earthquake has increased with time from $\sim M 6.3$ in 1933 to \sim
2282 $M 8$ in 2008 (Figure 131). The number of reported cases of induced seismicity has also
2283 increased greatly, probably because of the increasing number of large-scale industrial
2284 projects. The lower magnitude threshold of reporting is reducing, probably partly because of
2285 improved monitoring.

2286 Figure 132 shows the distribution of induced earthquakes by tectonic regime. By far the most
2287 numerous are from intraplate areas (79% of all cases) with the next largest category (13%)
2288 located in convergent plate-boundary zones. Most large industrial projects are conducted on
2289 land and most land is in the interior of plates with plate boundaries usually comprising
2290 relatively (though not absolutely) narrow zones. Most spreading plate boundaries are in the
2291 oceans and currently beyond reach of industrial development. Because induced earthquakes
2292 are mostly in intraplate regions they are likely to affect regions that are not traditionally
2293 associated with seismicity nor accustomed to it.

2294 The seemingly surprising lack of a relationship between M_{MAX} and operational parameters
2295 such as injection rate, coupled with the difficulty of predicting which projects will be
2296 seismogenetic and which will not, suggests that non-operational parameters are important.
2297 The pre-existing stress state is the most obvious such parameter. However, several lines of
2298 research indicate that most faults in the crust are nearly critically stressed, though they may
2299 not be optimally oriented to slip under ambient conditions. The local geology, and in
2300 particular the nature of pre-existing faults and fractures, must be important for understanding
2301 the extreme variations in seismogenesis between apparently similar projects in different

2302 locations. Geological and tectonic factors may thus be more important than engineering
 2303 parameters. In order for significant earthquakes to occur, faults that are suitably orientated
 2304 and stressed must exist.

2305 It is interesting to speculate what the empirical results of the present study might imply for
 2306 particular projects. For example, at The Geysers geothermal field, California, net production
 2307 (i.e. total production minus re-injection) since 1960 has been $\sim 1.7 \times 10^9 \text{ m}^3$. The relationship
 2308 of McGarr [2014] which links fluid-injection volume to the largest M_{MAX} (Figure 118) fits
 2309 well data from all volumetric projects. This relationship predicts that the upper bound to
 2310 induced earthquakes associated with The Geysers volume change is M 7.0. This geothermal
 2311 field has a maximum NW-SE long dimension of $\sim 21 \text{ km}$. The largest induced earthquake
 2312 that has occurred at projects of this scale is $\sim M$ 6.6 (Figure 123).

2313 To date, the largest earthquake that has occurred at The Geysers is the 2014 M_{W} 4.5 event.
 2314 There is no evidence that a fault long enough to sustain a M 6.6 or 7.0 earthquake exists in
 2315 the reservoir. However, The Geysers lies between the regional Mercuryville fault to the
 2316 southwest and the Collayomi fault zone to the northeast, within the active Pacific/North
 2317 America transform plate boundary zone. There is no evidence that the Mercuryville fault
 2318 zone is active, but the Collayomi fault zone contains at least one active fault [Lofgren, 1981].

2319 **7 Discussion and conclusions**

2320 *7.1 How common are induced earthquakes?*

2321 The total number of industrial projects in various categories, along with the number reported
 2322 to be seismogenic are given in Table 3. Without doubt under-reporting is severe. Seismicity
 2323 at projects far from human habitation is likely to escape notice. Known cases may not be
 2324 made publically known unless they are of large-magnitude, a nuisance, or unusual interest.
 2325 For example, ~ 2.5 million shale-gas hydrofracture jobs have now been completed world-
 2326 wide. All successful hydrofracturing projects induce small earthquakes but we found only 21
 2327 cases where seismicity has been reported (Table 3; Section 4.1.6). The absence of reports of
 2328 seismicity thus does not correspond to an absence of seismicity. Furthermore, statements
 2329 such as “no seismicity is reported” does not equate to no induced earthquakes. Some
 2330 earthquakes may also have been reported by national seismic networks without their induced
 2331 nature being recognized.

2332 A histogram showing M_{MAX} for the 562 seismogenic projects where this parameter is
 2333 reported is shown in Figure 133. The same data are shown as a plot of cumulative number of
 2334 cases vs. M_{MAX} in Figure 134. The linearity of the distribution at the high-magnitude end
 2335 suggests that reporting is complete for M_{MAX} 5 and above, and that underreporting becomes
 2336 progressively greater for projects smaller than M_{MAX} 4. Downward extrapolation of the
 2337 linear, M_{MAX} 5 - 7 part of the plot suggests that approximately 30% of $M \sim 4$ induced
 2338 earthquakes have gone unrecognized or unreported, 60% of $M \sim 3$ events and $\sim 90\%$ of those
 2339 with $M \sim 2$ (Table 4).

2340 The hydrocarbon fields around Britain provide a regional example of this problem.
 2341 Comparison of the UK earthquake database of the British Geological Survey with maps of
 2342 hydrocarbon fields in the North Sea suggests correlations between fields and earthquake
 2343 locations (Figure 135). Expanded maps of several fields are shown in Figure 136. There is a
 2344 spatial correlation between seismicity and the Beatrice Oilfield (Moray Firth), the Britannia
 2345 Gasfield, the Southern North Sea Gas Province and the Leman Gasfield.

2346 Most of the recorded earthquakes in the southern North Sea occur in or near fields developed
 2347 in Permian Rotliegend reservoirs. There, gas is produced using simple pressure depletion
 2348 from fields, most of which were near hydrostatic pressure when first discovered. Water is not
 2349 injected to support production. Many of the poorer-quality wells used to explore and appraise
 2350 this gas province were prop-fracked to obtain initial gas flow and a few fields [*e.g.*, Clipper
 2351 South, Gluyas & Swarbrick, in press, 2016; Purvis *et al.*, 2010] used hydrofracturing in
 2352 development wells. The Viking Graben contains mostly oilfields that were developed by
 2353 allowing natural pressure decline to deliver the first oil and then injecting water to support
 2354 continued production. The water used is seawater at typical North Sea temperatures of $\sim 4^{\circ}\text{C}$,
 2355 while the reservoirs are at $90\text{-}140^{\circ}\text{C}$. The central North Sea and Moray Firth contain a
 2356 heterogeneous mix of oil and gas fields produced by a combination of pressure depletion and
 2357 water injection. When discovered a few fields were naturally at very high pressure and close
 2358 to the fracture gradient.

2359 Many of these activities are potentially seismogenic. Nevertheless, there are no reports of
 2360 induced seismicity from these fields. Comparison of seismicity with hydrocarbon production
 2361 information available from DECC for the period 1975-2008 fails to show temporal
 2362 correlations and, because the North Sea was seismogenic before hydrocarbon production
 2363 started, it cannot be ruled out that the seismicity is natural. Detailed work on individual
 2364 events and their possible connection to activity in individual oil and gas fields is required
 2365 before the seismic events can be categorized as natural or induced [Wilson *et al.*, 2015].

2366 7.2 Hydraulics

2367 Groundwater has a major influence on earthquake occurrence. Overwhelming, observational
 2368 data show that pore pressure in fault zones can strongly influence seismicity (Section 1.3).
 2369 The 2011 M_w 5.1 Lorca, Spain, earthquake is a particularly compelling example (Section
 2370 3.1). These facts imply an unfortunate association between earthquakes and human need to
 2371 manage water, both for utilization and for flood control.

2372 The Lorca case and the four other cases we found of earthquakes possibly linked to
 2373 groundwater extraction, raise the question of whether other recent earthquakes that were both
 2374 shallow and located where major local anthropogenic water table changes have occurred
 2375 might have been induced. An example is the 2011 M 7.1 Christchurch, New Zealand,
 2376 earthquake (Figure 137). The city of Christchurch is built on what was once an extensive
 2377 swamp fed by the rivers Avon and Heathcote and numerous smaller streams. Major
 2378 engineering changes have been made there to control water over the last century.

2379 The 1811-1812 $M \sim 7$ New Madrid earthquakes occurred in the central Mississippi river
 2380 valley, and affected the states of Missouri, Illinois, Kentucky, Tennessee, and Arkansas. This
 2381 renowned sequence included three $M \sim 7$ earthquakes and probably seven with $M > \sim 6.5$.
 2382 These earthquakes are remarkable for having been felt at distances of up to 1700 km as a
 2383 result of the efficient transmission of seismic waves in the lithosphere of the eastern USA.
 2384 They are also remarkable in that they occurred in an intraplate area far from the nearest plate
 2385 boundary. They thus serve as a curiosity in the context of the current paradigm that expects
 2386 large earthquakes to occur in plate boundary zones.

2387 The New Madrid earthquakes occurred at and just south of the confluence of the $6,000 \text{ m}^3/\text{s}$
 2388 Middle Mississippi and the $8,000 \text{ m}^3/\text{s}$ Ohio rivers which forms the Lower Mississippi River.
 2389 The possibility that the earthquake activity is linked to local hydraulics has been suggested
 2390 previously but not seriously entertained. In view of the growing evidence that hydraulic

2391 changes can modulate the seismic behavior of faults it may be timely to revisit this possibility
 2392 with geological investigation into the pre-earthquake hydraulic activity and numerical
 2393 modeling.

2394 Hydraulic effects may explain the apparently paradoxical observations that both mass
 2395 addition and mass removal can induce earthquakes. This is illustrated by the fact that the
 2396 commonest anthropogenic earthquake-induction process is mining (i.e. mass removal—38% of
 2397 cases; Figure 138) and the second most common is water reservoir impoundment (i.e. mass
 2398 addition—24%). Hydraulic changes induced by mass redistribution may result in migration of
 2399 fluid into fault zones, increasing pore pressure. This process may thus explain the possible
 2400 induction of earthquakes in the single case reported of erecting a heavy building (the Taipei
 2401 101 building; Section 2.1.2). It may also help to understand some cases of earthquake
 2402 induction by hydrocarbon extraction in the absence of fluid injections, since natural
 2403 groundwater recharge may occur.

2404 Examination of global earthquake databases shows that it is not uncommon for moderate
 2405 earthquakes to occur near large lakes and reservoirs, *e.g.*, in east Africa, even though
 2406 induction has not been proposed. Intraplate earthquakes in the UK are not currently
 2407 understood. At least 21% of UK earthquakes in the British Geological Survey catalog are
 2408 thought to be related to mines, but many others are probably natural. The seismic rate in the
 2409 UK is \sim one M_L 3.6 event per year [Wilson *et al.*, 2015]. A possible link with hydraulics is
 2410 under investigation [Graham *et al.*, 2017].

2411 7.3 *How much stress loading is required to induce earthquakes?*

2412 Earthquakes occur naturally, without any human intervention at all. The minimum amount of
 2413 added anthropogenic stress needed for an earthquake to onset is thus zero.

2414 Many natural processes contribute simultaneously to stress build-up on faults. These include
 2415 tectonic deformation, volcanism, natural heat loss, isostatic uplift following deglaciation or
 2416 oceanic unloading, Earth tides, intraplate deformation resulting from distant plate boundary
 2417 events, remote large earthquakes, erosion, dissolution, the natural migration of groundwater
 2418 and weather. To these are added anthropogenic activities. It is fundamentally an ill-posed
 2419 question to ask the origin of the final stress increment that “broke the camel’s back” and
 2420 precipitated an earthquake. In the cases of large earthquakes this question may be akin to that
 2421 of whether a particular windmill could have been responsible for a hurricane.

2422 It has been suggested that instead of viewing industrial activity as inducing earthquakes, it
 2423 could instead be viewed as modulating the timescale on which inevitable earthquakes occur.
 2424 Unfortunately it cannot be known how events would have occurred had the industrial activity
 2425 not occurred because history cannot be re-run with a change of circumstance. Furthermore,
 2426 had an equivalent earthquake occurred at a different time, it cannot be known if it would have
 2427 affected people and infrastructure to the same extent. Nevertheless, in the cases of many
 2428 industrial projects, the association between earthquakes and the project is undeniable. The
 2429 clear induction of some earthquakes by very small incremental stresses means that some
 2430 published objections to induced status on the grounds that the stress perturbation was too
 2431 small may be moot. In those cases the above arguments may be of academic interest only.

2432 A wide range of stress changes brought about by anthropogenic activities has been postulated
 2433 to have induced earthquakes, from a fraction of a MPa [*e.g.*, Keranen *et al.*, 2014], the
 2434 equivalent of about a meter of rock overburden, to several tens of MPa (Table 5) (Figure

2435 139). For example, the 2007 M_L 4.2 Folkestone, UK, earthquake and the 2008 M_W ~8
 2436 Wenchuan, China, earthquake have been attributed to anthropogenic changes of only a few
 2437 kPa.

2438 The minimum amount of stress loading that might plausibly induce an earthquake is of
 2439 interest. The question “How much stress change is needed to induce earthquakes?” may be
 2440 unanswerable. However, it may be possible to address the question “What is the minimum
 2441 stress change that can be demonstrated to have induced earthquakes?” This could be
 2442 attempted by exploring the natural stress changes known to correlate with earthquakes, as
 2443 follows (Table 6).

2444 7.3.1 Earth tides

2445 The spatial non-uniformity of the gravitational fields of the Sun and Moon (and to a much
 2446 smaller extent, other celestial bodies) produces stresses in the solid body of Earth
 2447 approaching 0.005 MPa. Loading of the solid Earth by the ocean tides produces additional
 2448 stresses that can be about an order of magnitude larger but depend strongly on geographic
 2449 location. The stress drops of most earthquakes are in the range 1 - 10 MPa so tides might
 2450 sometimes have a detectable effect on earthquake occurrence.

2451 Most early studies of earthquakes and tides failed to find any significant correlation. The
 2452 main cause of this failure was probably over-simplification of the problem. Both stresses and
 2453 earthquake mechanisms are tensors, but many studies looked, for example, for correlations
 2454 between seismicity and tidal amplitude ranges, effectively treating both stress and earthquake
 2455 mechanism as scalars. Another difficulty with any such analysis was the difficulty of
 2456 computing ocean tides from the complicated shapes of the ocean basins.

2457 There were, however, two exceptions to this failure. First, deep moonquakes, detected by
 2458 seismometers placed by Apollo astronauts, correlate strongly with tides [Latham *et al.*, 1973].
 2459 Second, earthquakes at volcanic and geothermal areas show a tidal effect that is fairly easily
 2460 detected [*e.g.*, McNutt & Beavan, 1981]. This suggests that interactions between fluid
 2461 pressure and the volumetric components of earthquake mechanisms are important. Most
 2462 recently, studies that account for earthquake focal mechanisms and compute ocean loading
 2463 accurately have found that the occurrence of shallow thrust-faulting earthquakes does
 2464 correlate significantly with tidal stresses [Cochran *et al.*, 2004].

2465 7.3.2 Static stress changes resulting from large earthquakes

2466 The 1989 M_W 6.9 Loma Prieta, California, earthquake modulated seismicity in the region
 2467 around the epicenter out to distances where the coseismic stress changes were no more than
 2468 0.01 MPa (equivalent to ~0.4 m of overburden) [Reasenber & Simpson, 1992]. The 1992
 2469 M_W 7.3 Landers, California, earthquake also modulated the seismicity nearby. Aftershocks
 2470 were abundant up to about two source dimensions from the mainshock (a few tens of km),
 2471 where the Coulomb stress on optimally orientated faults was increased by > 0.05 MPa. They
 2472 were sparse where stress was reduced by this amount (Figure 140). The 1992 M_W 6.5 Big
 2473 Bear aftershock occurred in a region where stress was increased by 0.3 MPa [King *et al.*,
 2474 1994]. The effect of static stress changes on neighboring faults has also been expressed in
 2475 terms of the number of years by which the next large earthquake has been advanced in time
 2476 [*e.g.*, King *et al.*, 1994; Reasenber & Simpson, 1992].

2477 7.3.3 Remote triggering

2478 The 1992 M_w 7.3 Landers, California, earthquake is particularly remarkable because it
 2479 precipitated earthquake activity up to 17 source dimensions distant from the mainshock
 2480 (1,250 km). Most of this activity occurred at volcanic or geothermal areas such as
 2481 Yellowstone. Static stress changes are vanishingly small at such distances. These remote
 2482 earthquakes are thought to have been triggered by dynamic stress changes of a few tenths of a
 2483 MPa in the propagating shear and surface elastic waves interacting with fluids in the
 2484 hydrothermal and magmatic systems [Hill *et al.*, 1993]. The phenomenon of remote
 2485 triggering has subsequently been recognized elsewhere. When first unambiguously
 2486 recognized following the Landers earthquake, it was thought that only volcanic and
 2487 geothermal areas were affected and that the process might reveal the locations of geothermal
 2488 areas previously unknown. However, remote triggering has now been reported in other
 2489 environments, *e.g.*, the hydrocarbon region of Oklahoma (Figure 73) [van der Elst *et al.*,
 2490 2013].

2491 7.3.4 Weather

2492 A number of studies have postulated that earthquakes were induced by heavy rainfall [e.g.,
 2493 Husen *et al.*, 2007; Roth *et al.*, 1992]. In addition, a recent report suggests correlations
 2494 between “slow earthquakes” (accelerated creep on faults) and atmospheric pressure changes
 2495 accompanying typhoons in Taiwan. [Liu *et al.*, 2009]. Such pressure changes alter stress on
 2496 land areas but not beneath the ocean because seawater flow can maintain pressure
 2497 equilibrium offshore. The effect contributes a stress change of ~ 0.003 MPa that encourages
 2498 slip on coast-parallel thrust faults.

2499 7.4 *How large are induced earthquakes?*

2500 The stress change that might induce an earthquake does not correlate positively with the total
 2501 stress reduction brought about by the earthquake or the final magnitude of the earthquake.
 2502 Indeed, counter-intuitively, M_{MAX} reported for induced sequences *decreases* with increasing
 2503 calculated stress perturbation (Figure 139). The final size of an earthquake is determined by
 2504 how much of a fault was in a sufficiently critical state to move, once activation began. If slip
 2505 on a fault reduces to almost zero before the next event on the same fault starts, a series of
 2506 discrete events is recognized. If slip does not stop, the event may grow into a large or great
 2507 earthquake and all the strain release is considered to have occurred in a single event. Great
 2508 earthquakes (events with $M \geq 8$) that rupture much of the lithosphere typically comprise a
 2509 cascading chain of $M > 7$ sub-events, each triggered by the stress changes caused by the
 2510 previous ones. Although likely very rare, it cannot be ruled out that industrial activity could
 2511 contribute to the onset of the first sub-event. It is also not uncommon for foreshocks to occur
 2512 immediately preceding onset of a mainshock several magnitude units higher.

2513 In the case of recent seismicity in Oklahoma, in particular the 2011 Prague sequence (Section
 2514 4.1.2) Keranen *et al.* [2013] concluded that stress from fluid injections may build up for
 2515 decades before the onset of induced earthquakes. They further concluded that the initial M_w 5
 2516 rupture triggered successive earthquakes, including the M_w 5.7 event that occurred the
 2517 following day. In the case of the great 2008 $M_w \sim 8$ Wenchuan earthquake (Section 2.1.1),
 2518 once the first sub-event began, slip on the fault did not stop until several large fault segments
 2519 had failed.

2520 This view is consistent with the findings of McGarr [2014]. He derived a relationship that

2521 related volume injected to the size of fluid-injection-induced earthquakes and showed that it
 2522 fit well observations of 18 of the largest-magnitude earthquakes (Figure 116). However, he
 2523 also pointed out that this upper bound only applies to induced earthquakes whose source
 2524 regions were confined to the volumes directly affected by the injection, and that if fault slip
 2525 propagated outside of this volume then larger earthquakes could occur.

2526 7.5 *Natural or induced?*

2527 For different earthquake sequences, there is great variation in the strength of the evidence for
 2528 anthropogenic induction. In some cases the association with an industrial activity is beyond
 2529 any reasonable doubt. For example, over 250,000 earthquakes have been located in a tight
 2530 cluster in The Geysers geothermal area, California, by the U.S. Geological Survey during the
 2531 last half century. At the other end of the spectrum, induction has been suggested for cases
 2532 where only one earthquake occurred and the calculated stress changes were smaller than
 2533 those induced by Earth tides, *e.g.*, for the 2007 M_L 4.2 Folkestone, UK, earthquake, for which
 2534 an inductive stress change of 0.001-0.03 MPa was proposed [Klose, 2007a]. For those cases,
 2535 mere coincidence cannot be ruled out (Section 2.1.3 and Section 7.3). Induction of
 2536 earthquakes over 1,000 km away and over a year later by bombing of cities with non-nuclear
 2537 weapons is one of the proposed cases in the *iQuake* database most in need of supporting
 2538 evidence (Section 5).

2539 The number of cases postulated to be induced is increasing rapidly and with it the urgency for
 2540 management strategies. It is desirable, not only to know *a posteriori* whether an earthquake
 2541 was natural or induced, but also to forecast which projects may be seismogenic and how great
 2542 the hazard is likely to be. In the past, schemes have been proposed to address the question
 2543 whether earthquakes are natural or induced. For example, Davis and Frohlich [1993] list
 2544 seven questions to profile a seismic sequence and judge whether it was induced or not (Table
 2545 7).

2546 In the light of the large number of case histories now available, some parameters suggested
 2547 earlier to be diagnostic can be re-visited. These include:

- 2548 1. *Whether the region had a previous history of seismicity.* Induced earthquakes have now
 2549 been postulated to occur in both historically seismic and aseismic areas. Evidence from
 2550 research in boreholes suggests that faults everywhere are close to failure, regardless of
 2551 the known history of seismicity.
 2552
- 2553 2. *Close temporal association with the induction activity.* Reported delays in the onset of
 2554 postulated induced seismicity vary from essentially zero to several decades.
- 2555 3. *In the case of injection-related earthquakes, proximity of a few kilometers.* Distances of
 2556 up to 25 km have now been reported (Figure 125; Section 4.1.2).
- 2557 4. *Known geological structures that can channel flow.* Many earthquakes postulated to be
 2558 induced have been attributed to previously unknown faults.
- 2559 5. *Substantial stress changes.* Stress changes as small as a few kPa have now been
 2560 postulated to induce earthquakes (Section 2.1.3).

2561 Simple criteria for deciding whether an earthquake is induced or not are thus elusive. There is
 2562 extreme diversity in the circumstances of cases. Postulated induction activities may take
 2563 place over time periods from a few minutes to decades. The volumes of material added or
 2564 removed vary over many orders of magnitude and the maximum magnitude of events

2565 postulated to be induced vary from $M < 0$ to $M \sim 8$.

2566 Several unusual characteristics are commonly, though not universally, reported for
2567 earthquakes suspected of having been induced. These include:

- 2568 1. Unusually shallow nucleation depths (*e.g.*, the 2011 M_w 5.1 Lorca, Spain, earthquake,
2569 Section 3.1);
- 2570 2. Occurrence on previously unknown faults (“blind faults”; *e.g.*, in the Cogdell oilfield,
2571 Texas, Section 4.2.2);
- 2572 3. Release of stress in the same sense as the regional on suitably orientated structures
2573 (*e.g.*, in Oklahoma, Section 4.1.2);
- 2574 4. The largest earthquake in a sequence occurring after the induction activity has ceased,
2575 suggesting that fluid diffusion is important (*e.g.*, the 1962-1968 Denver earthquakes,
2576 Section 4.1.1);
- 2577 5. Faults in the basement beneath water and hydrocarbon reservoirs being reactivated,
2578 sometimes transecting the sedimentary formations above (*e.g.*, the Coalinga,
2579 California, earthquake; Section 3.3.2).

2580 These observations raise a number of questions. For example, if induced seismicity
2581 commonly occurs on previously unknown faults, could hazard be reduced by extensive
2582 subsurface mapping prior to operations? Since the crust is thought to be pervasively faulted
2583 and near to failure essentially everywhere, it is not clear this would be the case—perhaps
2584 everywhere should be considered potentially seismogenic. Also, if large earthquakes occur
2585 after operations have stopped, for how long should seismic hazard mitigation measures be
2586 continued after the end of a project?

2587 More reliable, but less universally applicable ways of discriminating include:

- 2588 1. Simple spatial and temporal associations, *e.g.*, earthquakes onsetting as soon as injection
2589 starts and close to the injection point;
- 2590 2. Visual observation, *e.g.*, gallery collapses in mines or ground rupture when a nuclear test
2591 is conducted;
- 2592 3. Earthquake focal mechanisms, *e.g.*, discriminating between natural, shear-faulting
2593 earthquakes and volumetric mining collapses, as was done by McGarr [1992a; b] for
2594 well-recorded earthquakes in South African gold mines and Dreger *et al.* [2008] for a
2595 mining collapse in Utah.

2596 Work is currently ongoing to develop additional ways of discriminating induced from natural
2597 earthquakes. These include using statistical features of background earthquakes and clustered
2598 sub-populations. For example, Zaliapin and Ben-Zion [2016] have suggested several
2599 statistical features that may distinguish induced seismicity from natural tectonic activity
2600 including a higher rate of background events and more rapid aftershock decay.

2601 *7.6 Why are earthquakes induced by some industrial projects and not others?*

2602 In addition to needing an explanation for why earthquakes occur at particular projects, any
2603 theory for induced earthquakes must be able to explain why they do not occur at most
2604 projects. This endeavor is hampered by under-reporting (Section 7.1; Table 3). A necessary
2605 pre-requisite to explaining the incidence of induced seismicity as a whole or in different
2606 categories is to know its true extent.

2607 In the context of industrial activity as a whole, reports of induced earthquakes are
 2608 extraordinarily rare (Table 3). Induced nuisance earthquakes are even rarer. Only ~ 2% of
 2609 mines, water reservoirs, and CCS projects are reported to be seismogenic. All other
 2610 categories of project for which we found data were < 2% seismogenic.

2611 Individual cases of induced seismicity are diverse and site-specific and the lack of similarities
 2612 is perhaps a stronger feature than common factors. With the exception of large geothermal
 2613 projects and hydrofracturing (where almost all are probably seismogenic but only 0.001% are
 2614 reported to be so) it is seemingly unpredictable which projects will report induced
 2615 earthquakes. Many if not most induced earthquakes, except at hydrofracturing projects, were
 2616 unexpected. On the other hand, a research experiment that specifically aimed to induce
 2617 seismicity, by injecting water into an active fault zone, surprisingly failed to do so (Section
 2618 4.1.8) [Prioul *et al.*, 2000].

2619 A large majority of induced earthquakes occur in intraplate areas (Figure 132). This does not
 2620 come as a surprise in view of the fact that rocks seem to be close to failure everywhere so the
 2621 potential for inducing earthquakes in intraplate and plate-boundary regions may be similar
 2622 (Section 1.1). This, coupled with the observation that many earthquake sequences were
 2623 unexpected and in areas previously aseismic, means that populations may be unprepared for
 2624 earthquakes. To add to this, pre-industrial seismic risk assessments may be difficult if there is
 2625 no history of seismicity or seismic monitoring. Wilson *et al.* [2015] recently tried to rectify
 2626 this problem for the UK in advance of possible expansion of the shale-gas industry by
 2627 estimating a baseline for UK seismicity.

2628 For most non-research purposes the parameter of importance is not whether seismicity is
 2629 induced but whether nuisance seismicity is induced. M_{MAX} is thus critical. In Section 6
 2630 describe an initial examination of the database for correlations. The currently observed upper
 2631 limit to M_{MAX} correlates with water reservoir volume and mass per unit area, volume added
 2632 or removed at the surface, volume extracted or added to the subsurface, injection pressure
 2633 (negative correlation), rate and volume, the yield of nuclear tests and scale of project. Most of
 2634 these are basically measures of project size. Factors such as reservoir pressure change and
 2635 injection/extraction rate do not correlate with the largest M_{MAX} .

2636 Suggestions have been made regarding what operational parameters might be adjusted in
 2637 order to mitigate induced seismicity. These suggestions include injecting into formations that
 2638 are sealed from the basement, and avoiding known faults. There has, however, yet to be a
 2639 demonstration of an approach that works in general for projects of a particular type. It is also
 2640 not clear how we would we recognize success since there can be no evidence for the
 2641 earthquake that did not occur. More complete reporting would be beneficial.

2642 7.7 *Future trends*

2643 7.8 *Earthquake prediction*

2644 There is presently no reliable method to predict earthquakes. Current approaches to reducing
 2645 hazard comprise general long-term forecasting based on the history of past earthquakes
 2646 including instrumental data, historical documents, and paleoseismology using methods such
 2647 as trenching [*e.g.*, Obermeier, 1996]. This approach assumes that patterns of seismicity
 2648 persist in local areas. It cannot make precise predictions, even in plate boundary zones
 2649 [Lindh, 2005], and may work even more poorly in intraplate areas (Section 1.1) [Stein *et al.*,
 2650 2015]. In regions with little history of seismicity it may not be possible to implement.

2651 Nicol *et al.* [2011] reviewed this issue from the point of view of CCS. They pointed out that
 2652 the focus tends to be on reservoir-scale pressure increases and the effect of crustal loading on
 2653 local faults is not routinely considered. Modeling crustal loading or unloading, and likely
 2654 effects on the dynamics of groundwater, might be fruitful avenues of approach. Another
 2655 useful approach could be to study jointly surface deformation and seismicity. In many of the
 2656 cases in our database pre-seismic deformation ranging from large to small is reported.
 2657 Although the two have been jointly interpreted in the case of several individual projects [*e.g.*,
 2658 Goertz-Allmann *et al.*, 2014; Keiding *et al.*, 2010] we are not aware that systematic
 2659 relationships have been explored for induced earthquakes as a whole.

2660 7.9 Earthquake management

2661 There is a weak tendency for the size of the largest induced earthquake to increase with time
 2662 (Figure 131). There is also a strong tendency for the number of reports of induced seismicity
 2663 to increase with time and for the lower limit of magnitude reporting to reduce. The latter is
 2664 likely partly a result of improved instrumentation. It is not clear if the former reflects
 2665 improved recognition and reporting or simply larger induced earthquakes.

2666 Coal mining in China is an illustrative case. The expanding Chinese economy is founded on
 2667 coal as an energy source but at the same time shallow resources are being rapidly depleted
 2668 (Figure 141). The future trend is thus to go deeper [Li *et al.*, 2007]. In the two decades from
 2669 1980-2000 the average mining depth increased from 288 m to 500 m. Now, over 75% of the
 2670 coal has been removed from the top 1000 m and the recent increase in mine seismicity there
 2671 results largely from increases in mining depth and the size of galleries. Super-deep mines
 2672 (>1200 m in depth), as have induced seismicity in South Africa for decades, are planned in
 2673 China for the future. Fluid injection for waste disposal, enhanced oil recovery,
 2674 hydrofracturing and geothermal energy, are also expanding rapidly and have resulted in some
 2675 of the most significant increases in induced seismicity in recent years [Ellsworth, 2013].
 2676 Other industries such as building dams and CCS may be expected to expand over the coming
 2677 years.

2678 Management of the problem is moving forward rapidly as additional stakeholders become
 2679 involved [*e.g.*, Wang *et al.*, 2016]. For example, the issue of induced earthquakes is now of
 2680 concern to the US Army Corps of Engineers because of the threat to critical federal
 2681 infrastructure, *e.g.*, levees and dams. No societal benefit comes without price—there is no such
 2682 thing as a free lunch—but public policy, engineering, preparation, and outreach can enable
 2683 societally beneficial projects to go ahead under appropriate health-and-safety circumstances
 2684 and in contexts that are understood and acceptable to stakeholders.

2685

2686

2687

2688 *Acknowledgments*

2689 This work benefitted from discussions with Julian Bommer, Bruce Julian, Kosuke Heki,
 2690 Tianhui Ma, Steve Spottiswoode, Michelle Grobbelaar and Deborah Weiser. Ang Li assisted
 2691 with locating Chinese cases. The project was funded by the Nederlandse Aardolie
 2692 Maatschappij BV (NAM), Schepersmaat 2, 9405 TA Assen, The Netherlands. This paper is
 2693 based on a report submitted to Jan van Elk and Dirk Doornhof (NAM).

2694

2695

2696 *References*

- 2697 Ahmad, M. U., and J. A. Smith (1988), Earthquakes, injection wells, and the Perry Nuclear
2698 Power Plant, Cleveland, Ohio, *Geology*, 16, 739-742.
- 2699 Ake, J., K. Mahrer, D. O'Connell, and L. Block (2005), Deep-injection and closely monitored
2700 induced seismicity at Paradox Valley, Colorado, *Bull. seismol. Soc. Am.*, 95, 664-683,
2701 doi:10.1785/0120040072.
- 2702 Al-Enezi, A., L. Petrat, R. Abdel-Fattah, and G. D. M. Technologie (2008), Induced
2703 seismicity and surface deformation within Kuwait's oil fields, *Proceedings of the Proc.*
2704 *Int. Conf. Geol. Seismol.*, pp. 177-183.
- 2705 Allis, R. G., S. A. Currie, J. D. Leaver, and S. Sherburn (1985), Results of injection testing at
2706 Wairakei geothermal field, New Zealand, *Transactions of the Geothermal Resources*
2707 *Council*, 289-294.
- 2708 Amidzic, D., S. K. Murphy, and G. Van Aswegen (1999), Case study of a large seismic event
2709 at a South African gold mine, *Proceedings of the 9th ISRM Congress*.
- 2710 Amos, C. B., P. Audet, W. C. Hammond, R. Bürgmann, I. A. Johanson, and G. Blewitt
2711 (2014), Uplift and seismicity driven by groundwater depletion in central California,
2712 *Nature*, 509, 483-486.
- 2713 Anonymous (2014), Literature review on injection-related induced seismicity and its
2714 relevance to nitrogen injection, pp 46, *Earth, Environmental and Life Sciences*, Utrecht,
2715 Netherlands Report TNO 2014 R11761.
- 2716 Arkhipova, E. V., A. D. Zhigalin, L. I. Morozova, and A. V. Nikolaev (2012), The Van
2717 earthquake on October 23, 2011: Natural and technogenic causes, *Proceedings of the*
2718 *Doklady Earth Sciences Conference*, pp. 1176-1179.
- 2719 Asanuma, H., N. Soma, H. Kaieda, Y. Kumano, T. Izumi, K. Tezuka, H. Niitsuma, and D.
2720 Wyborn (2005), Microseismic monitoring of hydraulic stimulation at the Australian HDR
2721 project in Cooper Basin, *Proceedings of the Proceedings World Geothermal Congress*, pp.
2722 24-29.
- 2723 Avouac, J.-P. (2012), Earthquakes: Human-induced shaking, *Nature Geoscience*, 5, 763-764,
2724 doi:doi:10.1038/ngeo1609.
- 2725 Awad, M., and M. Mizoue (1995), Earthquake activity in the Aswan region, Egypt, *Pure*
2726 *Appl. Geophys.*, 145, 69-86, doi:10.1007/bf00879484.
- 2727 Baisch, S., and H. P. Harjes (2003), A model for fluid-injection-induced seismicity at the
2728 KTB, Germany, *Geophys. J. Int.*, 152, 160-170, doi:10.1046/j.1365-246X.2003.01837.x.
- 2729 Baisch, S., and R. Vörös (2011), Geomechanical study of Blackpool seismicity, pp 58,
2730 Report prepared for Cuadrilla Ltd. by Q-con GmbH.
- 2731 Baisch, S., R. Vörös, R. Weidler, and D. Wyborn (2009a), Investigation of fault mechanisms
2732 during geothermal reservoir stimulation experiments in the Cooper Basin, Australia, *Bull.*
2733 *seismol. Soc. Am.*, 99, 148-158.
- 2734 Baisch, S., R. Voeroes, R. Weidler, and D. Wyborn (2009b), Investigation of Fault
2735 Mechanisms during Geothermal Reservoir Stimulation Experiments in the Cooper Basin,
2736 Australia, *Bull. seismol. Soc. Am.*, 99, 148-158, doi:10.1785/0120080055.
- 2737 Baisch, S., M. Bohnhoff, L. Ceranna, Y. Tu, and H. P. Harjes (2002), Probing the crust to 9-
2738 km depth: Fluid-injection experiments and induced seismicity at the KTB superdeep
2739 drilling hole, Germany, *Bull. seismol. Soc. Am.*, 92, 2369-2380, doi:10.1785/0120010236.
- 2740 Baisch, S., R. Weidler, R. Vörös, D. Wyborn, and L. de Graaf (2006a), Induced seismicity
2741 during the stimulation of a geothermal HFR reservoir in the Cooper Basin, Australia, *Bull.*
2742 *seismol. Soc. Am.*, 96, 2242-2256.

- 2743 Baisch, S., R. Weidler, R. Voros, D. Wyborn, and L. de Graaf (2006b), Induced seismicity
2744 during the stimulation of a geothermal HFR reservoir in the Cooper Basin, Australia, *Bull.*
2745 *seismol. Soc. Am.*, 96, 2242-2256, doi:10.1785/0120050255.
- 2746 Baisch, S., R. Voeroes, E. Rothert, H. Stang, R. Jung, and R. Schellschmidt (2010), A
2747 numerical model for fluid injection induced seismicity at Soultz-sous-Forets, *International*
2748 *Journal of Rock Mechanics and Mining Sciences*, 47, 405-413,
2749 doi:10.1016/j.ijrmms.2009.10.001.
- 2750 Baisch, S., E. Rothert, H. Stang, R. Voeroes, C. Koch, and A. McMahon (2015), Continued
2751 geothermal reservoir stimulation experiments in the Cooper Basin (Australia), *Bull.*
2752 *seismol. Soc. Am.*, 105, 198-209, doi:10.1785/0120140208.
- 2753 Balassanian, S. Y. (2005), Earthquakes induced by deep penetrating bombing?, *Acta*
2754 *Seismologica Sinica*, 18, 741-745.
- 2755 Bardainne, T., N. Dubos-Sallee, G. Senechal, P. Gaillot, and H. Perroud (2008), Analysis of
2756 the induced seismicity of the Lacq gas field (southwestern France) and model of
2757 deformation, *Geophys. J. Int.*, 172, 1151-1162, doi:10.1111/j.1365-246X.2007.03705.x.
- 2758 Batini, F., R. Console, and G. Luongo (1985), Seismological study of Larderello-Travale
2759 geothermal area, *Geothermics*, 14, 255-272.
- 2760 Batini, F., C. Bufe, G. M. Cameli, R. Console, and A. Fiordelisi (1980), Seismic monitoring
2761 in Italian geothermal areas I: seismic activity in the Larderello-Travale region,
2762 *Proceedings of the Second DOE-ENEL Workshop on Cooperative Research in*
2763 *Geothermal Energy*, Lawrence Berkeley Laboratory, Berkeley, CA, USA, October 20-22,
2764 pp. 20-47.
- 2765 Bella, F., P. F. Biagi, M. Caputo, E. Cozzi, G. Della Monica, A. Ermini, W. Plastino, and V.
2766 Sgrigna (1998), Aquifer-induced seismicity in the Central Apennines (Italy), *Pure Appl.*
2767 *Geophys.*, 153, 179-194, doi:10.1007/s000240050191.
- 2768 Benetatos, C., J. Malek, and F. Verga (2013), Moment tensor inversion for two micro-
2769 earthquakes occurring inside the Haje gas storage facilities, Czech Republic, *Journal of*
2770 *Seismology*, 17, 557-577, doi:10.1007/s10950-012-9337-0.
- 2771 Bennett, T. J., M. E. Marshall, B. W. Barker, and J. R. Murphy (1994), Characteristics of
2772 rockbursts for use in seismic discrimination, Maxwell Labs Inc, San Diego, California
2773 SSS-FR-93-14382.
- 2774 Bertani, R. (2010), Geothermal power generation in the world: 2005-2010 update report,
2775 *Proceedings of the World Geothermal Congress 2010*, Bali, Indonesia, 25-29 April 2010.
- 2776 Block, L. V., C. K. Wood, W. L. Yeck, and V. M. King (2015), Induced seismicity
2777 constraints on subsurface geological structure, Paradox Valley, Colorado, *Geophys. J. Int.*,
2778 200, 1170-1193, doi:10.1093/gji/ggu459.
- 2779 Boettcher, M. S., D. L. Kane, A. McGarr, M. J. S. Johnston, and Z. Reches (2015), Moment
2780 tensors and other source parameters of mining-induced earthquakes in TauTona Mine,
2781 South Africa, *Bull. seismol. Soc. Am.*, 105, 1576-1593, doi:10.1785/0120140300.
- 2782 Bohnhoff, M., S. Baisch, and H. P. Harjes (2004), Fault mechanisms of induced seismicity at
2783 the superdeep German Continental Deep Drilling Program (KTB) borehole and their
2784 relation to fault structure and stress field, *J. Geophys. Res.*, 109,
2785 doi:10.1029/2003jb002528.
- 2786 Bossu, R., J. R. Grasso, L. M. Plotnikova, B. Nurtaev, J. Frechet, and M. Moisy (1996),
2787 Complexity of intracontinental seismic faultings: The Gazli, Uzbekistan, sequence, *Bull.*
2788 *seismol. Soc. Am.*, 86, 959-971.
- 2789 Bou-Rabee, F., and A. Nur (2002), The 1993 M 4.7 Kuwait earthquake: Induced by the
2790 burning of the oil fields, *Kuwait J. Sci. Eng.*, 29, 155-163.
- 2791 Boucher, G., A. Ryall, and A. E. Jones (1969), Earthquakes associated with underground
2792 nuclear explosions, *J. Geophys. Res.*, 74, 3808-3820.

- 2793 Bourne, S. J., S. J. Oates, J. J. Bommer, B. Dost, J. van Elk, and D. Doornhof (2015), Monte
 2794 Carlo method for probabilistic hazard assessment of induced seismicity due to
 2795 conventional natural gas production, *Bull. seismol. Soc. Am.*, 105, 1721-1738,
 2796 doi:10.1785/0120140302.
- 2797 Brudy, M., M. D. Zoback, K. Fuchs, F. Rummel, and J. Baumgartner (1997), Estimation of
 2798 the complete stress tensor to 8 km depth in the KTB scientific drill holes: Implications for
 2799 crustal strength, *J. Geophys. Res.*, 102, 18453-18475.
- 2800 Calo, M., C. Dorbath, and M. Frogneux (2014), Injection tests at the EGS reservoir of Soultz-
 2801 sous-Forets. Seismic response of the GPK4 stimulations, *Geothermics*, 52, 50-58,
 2802 doi:10.1016/j.geothermics.2013.10.007.
- 2803 Caloi, P., M. De Panfilis, D. Di Filippo, L. Marcelli, and M. C. Spadea (1956), Terremoti
 2804 della Val Padana del 15-16 maggio 1951, *Annals of Geophysics*, 9, 63-105.
- 2805 Carder, D. S. (1945), Seismic investigations in the Boulder Dam area, 1940-1944, and the
 2806 influence of reservoir loading on local earthquake activity, *Bull. seismol. Soc. Am.*, 35,
 2807 175-192.
- 2808 Cartlidge, E. (2014), Human activity may have triggered fatal Italian earthquakes, panel says,
 2809 *Science*, 344, 141.
- 2810 Castle, R. O., and R. F. Yerkes (1976), Recent surface movements in the Baldwin Hills, Los
 2811 Angeles county, California, U.S. Geological Survey Professional Paper 882, pp viii+125,
 2812 U.S. Geological Survey, Washington, D.C.
- 2813 Cesca, S., F. Grigoli, S. Heimann, A. Gonzalez, E. Buforn, S. Maghsoudi, E. Blanch, and T.
 2814 Dahm (2014), The 2013 September-October seismic sequence offshore Spain: a case of
 2815 seismicity triggered by gas injection?, *Geophys. J. Int.*, 198, 941-953,
 2816 doi:10.1093/gji/ggu172.
- 2817 Chabora, E., E. Zemach, P. Spielman, P. Drakos, S. Hickman, S. Lutz, K. Boyle, A. Falconer,
 2818 A. Robertson-Tait, N. C. Davatzes, P. Rose, E. Majer, and S. Jarpe (2012), Hydraulic
 2819 stimulation of Well 27-15, Desert Peak geothermal field, Nevada, U.S.A., Proceedings of
 2820 the 37th Stanford Geothermal Workshop, Stanford, CA.
- 2821 Cladouhos, T., S. Petty, Y. Nordin, M. Moore, K. Grasso, M. Uddenberg, M. Swyer, B.
 2822 Julian, and G. Foulger (2013), Microseismic monitoring of Newberry Volcano EGS
 2823 Demonstration, Proceedings of the Thirty-Eighth Workshop on Geothermal Reservoir
 2824 Engineering, Stanford University, Stanford, California, February 11-13, 2013.
- 2825 Clarke, H., L. Eisner, P. Styles, and P. Turner (2014a), Felt seismicity associated with shale
 2826 gas hydraulic fracturing: The first documented example in Europe, *Geophys. Res. Lett.*,
 2827 41, 8308-8314.
- 2828 Clarke, H., L. Eisner, P. Styles, and P. Turner (2014b), Felt seismicity associated with shale
 2829 gas hydraulic fracturing: The first documented example in Europe, *Geophys. Res. Lett.*,
 2830 41, 8308-8314, doi:10.1002/2014gl062047.
- 2831 Cochran, E. S., J. Vidale, and S. Tanaka (2004), Earth tides can trigger shallow thrust fault
 2832 earthquakes, *Science*, 306, 1164-1166.
- 2833 Darold, A., A. A. Holland, C. Chen, and A. Youngblood (2014), Preliminary analysis of
 2834 seismicity near Eagleton 1-29, Carter County, July 2014, pp 17, Oklahoma Geological
 2835 Survey Open-File Report OF2-2014.
- 2836 Davies, R., G. Foulger, A. Bindley, and P. Styles (2013), Induced seismicity and hydraulic
 2837 fracturing for the recovery of hydrocarbons, *Marine and Petroleum Geology*, 45, 171-185,
 2838 doi:10.1016/j.marpetgeo.2013.03.016.
- 2839 Davis, S. D., and W. D. Pennington (1989), Induced seismic deformation in the Cogdell oil
 2840 field of west Texas, *Bull. seismol. Soc. Am.*, 79, 1477-1495.
- 2841 Davis, S. D., and C. Frohlich (1993), Did (or will) fluid injection cause earthquakes?-criteria
 2842 for a rational assessment, *Seismol. Res. Lett.*, 64, 207-224.

- 2843 de Pater, C. J., and S. Baisch (2011), Geomechanical study of Bowland Shale seismicity.
 2844 Synthesis report, pp 71.
- 2845 deBruyn, I. A., and F. G. Bell (1997), Mining and induced seismicity in South Africa: A
 2846 survey, Proceedings of the International Symposium on Engineering Geology and the
 2847 Environment, Athens, Greece, 23-27 June, pp. 2321-2326.
- 2848 Deichmann, N., and J. Ernst (2009), Earthquake focal mechanisms of the induced seismicity
 2849 in 2006 and 2007 below Basel (Switzerland), Swiss Journal of Geosciences, 102, 457-466,
 2850 doi:10.1007/s00015-009-1336-y.
- 2851 Deichmann, N., and D. Giardini (2009), Earthquakes induced by the stimulation of an
 2852 Enhanced Geothermal System below Basel (Switzerland), Seismol. Res. Lett., 80, 784–
 2853 798, doi:10.1789/gssrl.80.5.784.
- 2854 Dreger, D., S. R. Ford, and W. R. Walter (2008), Source analysis of the Crandall Canyon,
 2855 Utah mine collapse, Science, 321, 217.
- 2856 Durrheim, R. J. (2010), Mitigating the risk of rockbursts in the deep hard rock mines of South
 2857 Africa: 100 years of research, *in* Extracting the Science: a century of mining research,
 2858 edited by J. Brune, pp. 156-171, Society for Mining, Metallurgy, and Exploration, Inc.
- 2859 Durrheim, R. J., D. Vogt, and M. Manzi (2013), Advances in geophysical technologies for
 2860 the exploration and safe mining of deep gold ore bodies in the Witwatersrand basin, South
 2861 Africa, *in* Mineral Deposit Research for a High-Tech World, edited by E. Jonsson, pp.
 2862 118-121.
- 2863 Durrheim, R. J., R. L. Anderson, A. Cichowicz, R. Ebrahim-Trollope, G. Hubert, A. Kijko,
 2864 A. McGarr, W. Ortlepp, and N. van der Merwe (2006), The risks to miners, mines, and the
 2865 public posed by large seismic events in the gold mining districts of South Africa,
 2866 Proceedings of the Proceedings of the Third International Seminar on Deep and High
 2867 Stress Mining, 2-4 October 2006, Quebec City, Canada.
- 2868 Eberhart-Phillips, D., and D. H. Oppenheimer (1984), Induced seismicity in The Geysers
 2869 geothermal area, California, J. Geophys. Res., 89, 1191-1207.
- 2870 Ellsworth, W. L. (2013), Injection-induced earthquakes, Science, 341, 142-149.
- 2871 Emanov, A. F., A. A. Emanov, A. V. Fateev, E. V. Leskova, E. V. Shevkunova, and V. G.
 2872 Podkorytova (2014), Mining-induced seismicity at open pit mines in Kuzbass (Bachatsky
 2873 earthquake on June 18, 2013), Journal of Mining Science, 50, 224-228,
 2874 doi:10.1134/s1062739114020033.
- 2875 Engdahl, E. R. (1972), Seismic effects of the MILROW and CANNIKIN nuclear explosions,
 2876 Bull. seismol. Soc. Am., 62, 1411-1423.
- 2877 Erzinger, J., and I. Stober (2005), Introduction to special issue: long-term fluid production in
 2878 the KTB pilot hole, Germany, Geofluids, 5, 1-7, doi:10.1111/j.1468-8123.2004.00107.x.
- 2879 Evans, D. M. (1966), The Denver area earthquakes and the Rocky Mountain Arsenal disposal
 2880 well, The Mountain Geologist, 3, 23-36.
- 2881 Evans, K. F., A. Zappone, T. Kraft, N. Deichmann, and F. Moia (2012), A survey of the
 2882 induced seismic responses to fluid injection in geothermal and CO₂ reservoirs in Europe,
 2883 Geothermics, 41, 30-54, doi:10.1016/j.geothermics.2011.08.002.
- 2884 Farahbod, A. M., H. Kao, D. M. Walker, and J. F. Cassidy (2015), Investigation of regional
 2885 seismicity before and after hydraulic fracturing in the Horn River Basin, northeast British
 2886 Columbia, Canadian Journal of Earth Sciences, 52, 112-122, doi:10.1139/cjes-2014-0162.
- 2887 Feignier, B., and R. P. Young (1992), Moment tensor inversion of induced microseismic
 2888 events: Evidence of non-shear failures in the $-4 < M < -2$ moment magnitude range,
 2889 Geophys. Res. Lett., 19, 1503-1506.
- 2890 Ferrazzini, V., B. Chouet, M. Fehler, and K. Aki (1990), Quantitative analysis of long-period
 2891 events recorded during hydrofracture experiments at Fenton Hill, New Mexico, J.
 2892 Geophys. Res., 95, 21871-21884.

- 2893 Fielitz, D., and U. Wegler (2015), Intrinsic and scattering attenuation as derived from fluid
2894 induced microseismicity at the German Continental Deep Drilling site, *Geophys. J. Int.*,
2895 201, 1346-1361, doi:10.1093/gji/ggv064.
- 2896 Foulger, G. R. (1988a), Hengill triple junction, SW Iceland; 1. Tectonic structure and the
2897 spatial and temporal distribution of local earthquakes, *J. Geophys. Res.*, 93, 13493-13506.
- 2898 Foulger, G. R. (1988b), Hengill triple junction, SW Iceland; 2. Anomalous earthquake focal
2899 mechanisms and implications for process within the geothermal reservoir and at
2900 accretionary plate boundaries, *J. Geophys. Res.*, 93, 13,507-513,523.
- 2901 Foulger, G. R., and R. E. Long (1984), Anomalous focal mechanisms; tensile crack formation
2902 on an accreting plate boundary, *Nature*, 310, 43-45.
- 2903 Foulger, G. R., and B. R. Julian (2014), Maximizing EGS earthquake location accuracies,
2904 Proceedings of the Thirty-Ninth Workshop on Geothermal Reservoir Engineering,
2905 Stanford, California, February 24-26, 2014, SGP-TR-202.
- 2906 Foulger, G. R., R. E. Long, P. Einarsson, and A. Björnsson (1989), Implosive earthquakes at
2907 the active accretionary plate boundary in northern Iceland, *Nature*, 337, 640-642.
- 2908 Foulger, G. R., C.-H. Jahn, G. Seeber, P. Einarsson, B. R. Julian, and K. Heki (1992), Post-
2909 rifting stress relaxation at the divergent plate boundary in Iceland, *Nature*, 358, 488-490.
- 2910 Gaite, B., A. Ugalde, A. Villaseñor, and E. Blanch (2016), Improving the location of induced
2911 earthquakes associated with an underground gas storage in the Gulf of Valencia (Spain),
2912 *Phys. Earth Planet. Int.*, 254, 46–59.
- 2913 Gan, W., and C. Frohlich (2013), Gas injection may have triggered earthquakes in the
2914 Cogdell oil field, Texas, *Proc. Nat. Acad. Sci.*, 110, 18786-18791,
2915 doi:10.1073/pnas.1311316110.
- 2916 Gee, D., A. Sowter, S. Marsh, and J. G. Gluyas (2016), Monitoring land subsidence due to
2917 natural gas extraction; validation of the Intermittent SBAS (ISBAS) DInSAR algorithm
2918 over reservoirs of North Holland, Netherlands, *Marine and Petroleum Geology*, submitted.
- 2919 Glowacka, E., and F. A. Nava (1996), Major earthquakes in Mexicali Valley, Mexico, and
2920 fluid extraction at Cerro Prieto geothermal field, *Bull. seismol. Soc. Am.*, 86, 93-105.
- 2921 Gluyas, J., and R. Swarbrick (in press, 2016), *Petroleum Geoscience*, 2nd ed., Wiley-
2922 Blackwell.
- 2923 Gluyas, J. G., and A. Peters (2010), Late field-life for oil reservoirs – a hydrogeological
2924 problem, paper presented at British Hydrological Society Third International Symposium,
2925 Managing Consequences of a Changing Global Environment.
- 2926 Godano, M., E. Gaucher, T. Bardainne, M. Regnier, A. Deschamps, and M. Valette (2010),
2927 Assessment of focal mechanisms of microseismic events computed from two three-
2928 component receivers: application to the Arkema-Vauvert field (France), *Geophysical*
2929 *Prospecting*, 58, 772-787, doi:10.1111/j.1365-2478.2010.00906.x.
- 2930 Goertz-Allmann, B. P., D. Kuhn, V. Oye, B. Bohloli, and E. Aker (2014), Combining
2931 microseismic and geomechanical observations to interpret storage integrity at the In Salah
2932 CCS site, *Geophys. J. Int.*, 198, 447-461, doi:10.1093/gji/ggu010.
- 2933 Gonzalez, P. J., K. F. Tiampo, M. Palano, F. Cannavo, and J. Fernandez (2012), The 2011
2934 Lorca earthquake slip distribution controlled by groundwater crustal unloading, *Nature*
2935 *Geoscience*, 5, 821-825, doi:10.1038/ngeo1610.
- 2936 Got, J.-L., J. Frechet, and F. W. Klein (1994), Deep fault plane geometry inferred from
2937 multiplet relative relocation beneath the south flank of Kilauea, *J. Geophys. Res.*, 99,
2938 15375-15386.
- 2939 Graham, S. P., M. Wilson, G. R. Foulger, and B. R. Julian (2017), Earthquake weather, in
2940 preparation.

- 2941 Grasle, W., W. Kessels, H. J. Kumpel, and X. Li (2006), Hydraulic observations from a 1
 2942 year fluid production test in the 4000 m deep KTB pilot borehole, *Geofluids*, 6, 8-23,
 2943 doi:10.1111/j.1468-8123.2006.00124.x.
- 2944 Green, C. A., P. Styles, and B. J. Baptie (2012), Preese Hall shale gas fracturing review &
 2945 recommendations for induced seismic mitigation: UK Department of Energy and Climate
 2946 Change, *Induced Seismicity Mitigation Report*, pp iv+26 5055.
- 2947 Guglielmi, Y., F. Cappa, J.-P. Avouac, P. Henry, and D. Elsworth (2015), Seismicity
 2948 triggered by fluid injection-induced aseismic slip, *Science*, 348, 1224-1226,
 2949 doi:10.1126/science.aab0476.
- 2950 Gupta, H. K. (2002), A review of recent studies of triggered earthquakes by artificial water
 2951 reservoirs with special emphasis on earthquakes in Koyna, India, *Earth-Science Reviews*,
 2952 58, 279-310, doi:10.1016/s0012-8252(02)00063-6.
- 2953 Hamilton, D. H., and R. L. Meehan (1971), Ground rupture in the Baldwin Hills, *Science*,
 2954 172, 333-344.
- 2955 Hamilton, R. M., B. E. Smith, F. G. Fischer, and P. J. Papanek (1972), Earthquakes caused by
 2956 underground nuclear explosions on Pahute Mesa, Nevada Test Site, *Bull. seismol. Soc.*
 2957 *Am.*, 62, 1319-1341.
- 2958 Hanks, T. C. (1977), Earthquake stress drops, ambient tectonic stresses and stresses that drive
 2959 plate motions, *Pure Appl. Geophys.*, 115, 441-458.
- 2960 Hanks, T. C., and H. Kanamori (1979), A moment magnitude scale, *J. Geophys. Res.*, 84,
 2961 2348-2350.
- 2962 Häring, M. O., U. Schanz, F. Ladner, and B. C. Dyer (2008), Characterisation of the Basel 1
 2963 enhanced geothermal system, *Geothermics*, 37, 469-495.
- 2964 Harris, D. (2012), The impact of cultural and religious influences during natural disasters
 2965 (volcano eruptions), *Earthquake-Report.com*, [http://earthquake-](http://earthquake-report.com/2012/09/27/the-impact-of-cultural-and-religious-influences-during-natural-disasters-volcano-eruptions/)
 2966 [report.com/2012/09/27/the-impact-of-cultural-and-religious-influences-during-natural-](http://earthquake-report.com/2012/09/27/the-impact-of-cultural-and-religious-influences-during-natural-disasters-volcano-eruptions/)
 2967 [disasters-volcano-eruptions/](http://earthquake-report.com/2012/09/27/the-impact-of-cultural-and-religious-influences-during-natural-disasters-volcano-eruptions/), 3:05 pm September 27, 2012.
- 2968 Hartline, C. (2014), *Seismic Monitoring Advisory Committee Review*, pp 44, Calpine
 2969 Corporation.
- 2970 Healy, J. H., W. W. Rubey, D. T. Griggs, and C. B. Raleigh (1968), The Denver earthquakes,
 2971 *Science*, 61, 1301-1310.
- 2972 Heesakkers, V., S. K. Murphy, G. van Aswegen, R. Domoney, S. Addams, T. Dewers, M.
 2973 Zechmeister, and Z. Reches (2005), The rupture zone of the M=2.2 earthquake that
 2974 reactivated the ancient Pretorius Fault in TauTona Mine, South Africa, *Proceedings of the*
 2975 *Fall Meeting of the American Geophysical Union abstract #S31B-04*, San Francisco.
- 2976 Heki, K., S. Miyazaki, and H. Tsuji (1997), Silent fault slip following an interplate thrust
 2977 earthquake at the Japan Trench, *Nature*, 386, 595-598.
- 2978 Heki, K., G. R. Foulger, B. R. Julian, and C.-H. Jahn (1993), Plate dynamics near divergent
 2979 boundaries: Geophysical implications of postdrifting crustal deformation in NE Iceland, *J.*
 2980 *Geophys. Res.*, 98, 14279-14297.
- 2981 Herrmann, R. B. (1978), A seismological study of two Attica, New York earthquakes, *Bull.*
 2982 *seismol. Soc. Am.*, 68, 641-651.
- 2983 Hill, D. P., P. A. Reasenber, A. Michael, W. J. Arabasz, G. Beroza, D. Brumbaugh, J. N.
 2984 Brune, R. Castro, S. Davis, D. dePolo, W. L. Ellsworth, J. Gomberg, S. Harmsen, L.
 2985 House, S. M. Jackson, M. J. S. Johnston, L. Jones, R. Keller, S. Malone, L. Munguia, S.
 2986 Nava, J. C. Pechmann, A. Sanford, R. W. Simpson, R. B. Smith, M. Stark, M. Stickney,
 2987 A. Vidal, S. Walter, V. Wong, and J. Zollweg (1993), Seismicity remotely triggered by the
 2988 magnitude 7.3 Landers, California, earthquake, *Science*, 260, 1617-1623.
- 2989 Hitzman, M. W. (Ed.) (2013), *Induced Seismicity Potential in Energy Technologies* x+248
 2990 pp., National Academies Press, Washington, D.C.

- 2991 Hough, S. E., and M. Page (2015), A Century of Induced Earthquakes in Oklahoma?, *Bull.*
2992 *seismol. Soc. Am.*, 105, 2863-2870, doi:10.1785/0120150109.
- 2993 Hsieh, P. A., and J. D. Bredehoeft (1981), A reservoir analysis of the Denver earthquakes: A
2994 case of induced seismicity, *J. Geophys. Res.*, 86, 903-920.
- 2995 Huaman, R. N. E., and T. X. Jun (2014), Energy related CO₂ emissions and the progress on
2996 CCS projects: a review, *Renewable and Sustainable Energy Reviews*, 31, 368-385.
- 2997 Husen, S., C. Bachmann, and D. Giardini (2007), Locally triggered seismicity in the central
2998 Swiss Alps following the large rainfall event of August 2005, *Geophys. J. Int.*, 171, 1126-
2999 1134, doi:10.1111/j.1365-246X.2007.03561.x.
- 3000 Husen, S., E. Kissling, and A. von Deschanden (2012), Induced seismicity during the
3001 construction of the Gotthard Base Tunnel, Switzerland: hypocenter locations and source
3002 dimensions, *Journal of Seismology*, 16, 195-213, doi:10.1007/s10950-011-9261-8.
- 3003 Jahr, T., G. Jentzsch, H. Letz, and M. Sauter (2005), Fluid injection and surface deformation
3004 at the KTB location: Modelling of expected tilt effects, *Geofluids*, 5, 20-27,
3005 doi:10.1111/j.1468-8123.2004.00103.x.
- 3006 Jahr, T., G. Jentzsch, H. Letz, and A. Gebauer (2007), Tilt observation around the KTB-site
3007 Germany: Monitoring and modelling of fluid induced deformation of the upper crust of
3008 the Earth, *in* *Dynamic Planet: Monitoring and Understanding a Dynamic Planet with*
3009 *Geodetic and Oceanographic Tools*, edited by P. Tregoning and C. Rizos, pp. 467-472.
- 3010 Jahr, T., G. Jentzsch, A. Gebauer, and T. Lau (2008), Deformation, seismicity, and fluids:
3011 Results of the 2004/2005 water injection experiment at the KTB/Germany, *J. Geophys.*
3012 *Res.*, 113, doi:10.1029/2008jb005610.
- 3013 Jaku, E. P., A. J. Jager, and M. K. C. Roberts (2001), A review of rock-related fatality trends
3014 in the South African gold mining industry, *in* *Rock Mechanics in the National Interest*,
3015 edited by D. Elsworth, J. P. Tinucci and K. A. Heasley, pp. 467-471.
- 3016 Johnston, A. C., and E. S. Schweig (1996), The enigma of the New Madrid earthquakes of
3017 1811-1812, *Annual Review of Earth and Planetary Sciences.*, 24, 339-384,
3018 doi:10.1146/annurev.earth.24.1.339.
- 3019 Jost, M. L., T. Busselberg, O. Jost, and H. P. Harjes (1998), Source parameters of injection-
3020 induced microearthquakes at 9 km depth at the KTB deep drilling site, Germany, *Bull.*
3021 *seismol. Soc. Am.*, 88, 815-832.
- 3022 Julià, J., A. A. Nyblade, R. Durrheim, L. Linzer, R. Gök, P. Dirks, and W. Walter (2009),
3023 Source mechanisms of mine-related seismicity, Savuka mine, South Africa, *Bull. seismol.*
3024 *Soc. Am.*, 99, 2801-2814.
- 3025 Julian, B. R., A. D. Miller, and G. R. Foulger (1998), Non-double-couple earthquakes I.
3026 Theory, *Rev. Geophys.*, 36, 525-549.
- 3027 Julian, B. R., G. R. Foulger, and K. Richards-Dinger (2004), The Coso Geothermal Area: A
3028 Laboratory for Advanced MEQ Studies for Geothermal Monitoring, *Proceedings of the*
3029 *Geothermal Resources Council Annual Meeting, Palm Springs, August 2004.*
- 3030 Julian, B. R., G. R. Foulger, and F. Monastero (2007), Microearthquake moment tensors from
3031 the Coso Geothermal area, *Proceedings of the Thirty-Second Workshop on Geothermal*
3032 *Reservoir Engineering, Stanford University, Stanford, California, January 22-24, pp. SGP-*
3033 *TR-183.*
- 3034 Julian, B. R., G. R. Foulger, F. C. Monastero, and S. Bjornstad (2010), Imaging hydraulic
3035 fractures in a geothermal reservoir, *Geophys. Res. Lett.*, 37, doi:10.1029/2009GL040933.
- 3036 Kaieda, H., S. Sasaki, and D. Wyborn (2010), Comparison of characteristics of micro-
3037 earthquakes observed during hydraulic stimulation operations in Ogachi, Hijiori and
3038 Cooper Basin HDR projects, *Proceedings of the World Geothermal Congress, Bali,*
3039 *Indonesia, April 25 - 30.*

- 3040 Kao, H., A. M. Farahbod, J. F. Cassidy, M. Lamontagne, D. Snyder, and D. Lavoie (2015),
 3041 Natural resources Canada's induced seismicity research, Proceedings of the Schatzalp
 3042 Induced Seismicity Workshop, Davos, Switzerland, 10-13 March.
- 3043 Kaven, J. O., S. H. Hickman, and N. C. Davatzes (2014), Micro-seismicity and seismic
 3044 moment release within the Coso Geothermal Field, California, Proceedings of the Thirty-
 3045 Ninth Workshop on Geothermal Reservoir Engineering, Stanford University, Stanford,
 3046 California, February 24-26, 2014, pp. SGP-TR-202.
- 3047 Kaven, J. O., S. H. Hickman, A. F. McGarr, and W. L. Ellsworth (2015), Surface monitoring
 3048 of microseismicity at the Decatur, Illinois, CO₂ sequestration demonstration site, *Seismol.*
 3049 *Res. Lett.*, 86, 1096-1101.
- 3050 Keiding, M., T. Arnadóttir, S. Jonsson, J. Decriem, and A. Hooper (2010), Plate boundary
 3051 deformation and man-made subsidence around geothermal fields on the Reykjanes
 3052 Peninsula, Iceland, *J. Volc. Geotherm. Res.*, 194, 139-149,
 3053 doi:10.1016/j.jvolgeores.2010.04.011.
- 3054 Keith, C. M., D. W. Simpson, and O. V. Soboleva (1982), INDUCED SEISMICITY AND
 3055 STYLE OF DEFORMATION AT NUREK RESERVOIR, TADJIK SSR, *J. Geophys.*
 3056 *Res.*, 87, 4609-4624, doi:10.1029/JB087iB06p04609.
- 3057 Keranen, K. M., H. M. Savage, G. A. Abers, and E. S. Cochran (2013), Potentially induced
 3058 earthquakes in Oklahoma, USA: Links between wastewater injection and the 2011 Mw 5.7
 3059 earthquake sequence, *Geology*, 41, 699-702, doi:10.1130/g34045.1.
- 3060 Keranen, K. M., M. Weingarten, G. A. Abers, B. A. Bekins, and S. Ge (2014), Sharp increase
 3061 in central Oklahoma seismicity since 2008 induced by massive wastewater injection,
 3062 *Science*, 345, 448-451, doi:10.1126/science.1255802.
- 3063 King, G. C. P., R. S. Stein, and J. Lin (1994), Static stress changes and the triggering of
 3064 earthquakes, *Bull. seismol. Soc. Am.*, in press.
- 3065 King, V. M., L. V. Block, W. L. Yeck, C. K. Wood, and S. A. Derouin (2014), Geological
 3066 structure of the Paradox Valley Region, Colorado, and relationship to seismicity induced
 3067 by deep well injection, *J. Geophys. Res.*, 119, 4955-4978, doi:10.1002/2013jb010651.
- 3068 Kinscher, J., P. Bernard, I. Contrucci, A. Mangeney, J. P. Pigué, and P. Bigarre (2015),
 3069 Location of microseismic swarms induced by salt solution mining, *Geophys. J. Int.*, 200,
 3070 337-362, doi:10.1093/gji/ggu396.
- 3071 Klein, F. W., P. Einarsson, and M. Wyss (1977), The Reykjanes Peninsula, Iceland,
 3072 earthquake swarm of September 1972 and its tectonic significance, *J. Geophys. Res.*, 82,
 3073 865-887.
- 3074 Klose, C. D. (2007a), Coastal land loss and gain as potential earthquake trigger mechanism in
 3075 SCRs, Proceedings of the Fall Meeting of the American Geophysical Union abstract
 3076 #T51D-0759, San Francisco, 10-14 December.
- 3077 Klose, C. D. (2007b), Geomechanical modeling of the nucleation process of Australia's 1989
 3078 M5.6 Newcastle earthquake, *Earth planet. Sci. Lett.*, 256, 547-553,
 3079 doi:10.1016/j.epsl.2007.02.009.
- 3080 Klose, C. D. (2012), Evidence for anthropogenic surface loading as trigger mechanism of the
 3081 2008 Wenchuan earthquake, *Environmental Earth Sciences*, 66, 1439-1447,
 3082 doi:10.1007/s12665-011-1355-7.
- 3083 Knoll, P. (1990), The fluid-induced tectonic rock burst of March 13, 1989 in Werra potash
 3084 mining district of the GDR (first results), *Gerlands Beitrage zur Geophysik*, 99, 239-245.
- 3085 Kovach, R. L. (1974), Source mechanisms for Wilmington oil field, California, subsidence
 3086 earthquakes, *Bull. seismol. Soc. Am.*, 64, 699-711.
- 3087 Kozłowska, M., B. Orlecka-Sikora, G. Kwiatek, M. S. Boettcher, and G. Dresen (2015),
 3088 Nanoseismicity and picoseismicity rate changes from static stress triggering caused by a

- 3089 Mw 2.2 earthquake in Mponeng gold mine, South Africa, *J. Geophys. Res.*, 120, 290-307,
 3090 doi:10.1002/2014jb011410.
- 3091 Kravanja, S., F. Batini, A. Fiordelise, and G. F. Panza (2000), Full moment tensor retrieval
 3092 from waveform inversion in the Larderello geothermal area, *Pure Appl. Geophys.*, 157,
 3093 1379-1392.
- 3094 Kundu, B., N. K. Vissa, and V. K. Gahalaut (2015), Influence of anthropogenic groundwater
 3095 unloading in Indo-Gangetic plains on the 25 April 2015 Mw 7.8 Gorkha, Nepal
 3096 earthquake, *Geophys. Res. Lett.*, 42, 10,607–610,613.
- 3097 Kuszniir, N. J., N. H. Al-Saigh, and D. P. Ashwin (1982), Induced seismicity generated by
 3098 longwall coal mining in the North Staffordshire coal-field, U. K., *Proceedings of the*
 3099 *Proceedings of the First International Congress on Rockbursts and Seismicity in Mines,*
 3100 *Johannesburg, South Africa*, pp. 153-160.
- 3101 Latham, G., J. Dorman, F. Duennebier, M. Ewing, D. Lammlein, and Y. Nakamura (1973),
 3102 Moonquakes, meteoroids, and the state of the lunar interior, *Proceedings of the Third*
 3103 *Lunar and Planetary Science Conference abstract, Houston, Texas, January 10-13.*
- 3104 Lei, X., G. Yu, S. Ma, X. Wen, and Q. Wang (2008), Earthquakes induced by water injection
 3105 at~ 3 km depth within the Rongchang gas field, Chongqing, China, *J. Geophys. Res.*, 113,
 3106 doi:10.1029/2008JB005604.
- 3107 Lei, X., S. Ma, W. Chen, C. Pang, J. Zeng, and B. Jiang (2013), A detailed view of the
 3108 injection-induced seismicity in a natural gas reservoir in Zigong, southwestern Sichuan
 3109 Basin, China, *J. Geophys. Res.*, 118, 4296-4311, doi:10.1002/jgrb.50310.
- 3110 Leith, W., D. W. Simpson, and W. Alvarez (1981), STRUCTURE AND PERMEABILITY -
 3111 GEOLOGIC CONTROLS ON INDUCED SEISMICITY AT NUREK RESERVOIR,
 3112 TADJIKISTAN, USSR, *Geology*, 9, 440-444, doi:10.1130/0091-
 3113 7613(1981)9<440:sapgc>2.0.co;2.
- 3114 Li, G. (2011), *World atlas of oil and gas basins*, Wiley-Blackwell, 496 pp.
- 3115 Li, T., M. F. Cai, and M. Cai (2007), A review of mining-induced seismicity in China,
 3116 *International Journal of Rock Mechanics and Mining Sciences*, 44, 1149-1171,
 3117 doi:10.1016/j.ijrmms.2007.06.002.
- 3118 Lin, C. H. (2005), Seismicity increase after the construction of the world's tallest building:
 3119 An active blind fault beneath the Taipei 101, *Geophys. Res. Lett.*, 32,
 3120 doi:10.1029/2005gl024223.
- 3121 Lindh, A. G. (2005), Success and failure at Parkfield, *Seismol. Res. Lett.*, 76, 3-6.
- 3122 Lippmann-Pipke, J., J. Erzinger, M. Zimmer, C. Kujawa, M. Boettcher, E. Van Heerden, A.
 3123 Bester, H. Moller, N. A. Stroncik, and Z. Reches (2011), Geogas transport in fractured
 3124 hard rock - Correlations with mining seismicity at 3.54 km depth, TauTona gold mine,
 3125 South Africa, *Applied Geochemistry*, 26, 2134-2146,
 3126 doi:10.1016/j.apgeochem.2011.07.011.
- 3127 Liu, C., A. T. Linde, and I. S. Sacks (2009), Slow earthquakes triggered by typhoons, *Nature*,
 3128 459, 833-836.
- 3129 Lofgren, B. E. (1978), Monitoring crustal deformation in The Geysers-Clear Lake geothermal
 3130 area, California, Open-File Report 78-597, pp iv+26, 28 maps, U.S. Geological Survey,
 3131 Washington, D.C.
- 3132 Lofgren, B. E. (1981), Monitoring crustal deformation in the Geysers-Clear Lake region, *in*
 3133 *Research in the Geysers-Clear Lake geothermal area, Northern California*, edited by R. J.
 3134 McLaughlin and J. M. Donnelly-Nolan, p. viii+259, U.S. Geological Survey Professional
 3135 Paper 1141, Washington, D.C.

- 3136 Ma, X., Z. Li, P. Hua, J. Jiang, F. Zhao, C. Han, P. Yuan, S. Lu, and L. Peng (2015), Fluid-
3137 injection-induced seismicity experiment of the WFSD-3P borehole, *Acta Geologica Sinica*
3138 (English Edition), 89, 1057-1058.
- 3139 Majer, E. L., and T. V. McEvilly (1981), Detailed microearthquake studies at the Cerro Prieto
3140 Geothermal Field, Proceedings of the Third Symposium on the Cerro Prieto Geothermal
3141 Field, Baja California, Mexico, Lawrence Berkeley Laboratory, Berkeley, California,
3142 March 24-26, pp. 347-352.
- 3143 Majer, E. L., and T. V. McEvilly (1982), Seismological studies at the Cerro Prieto Field:
3144 1978-1982, Proceedings of the Fourth Symposium on the Cerro Prieto Geothermal Field,
3145 Baja California, Mexico, Lawrence Berkeley Laboratory, Berkeley, California, 10-12
3146 August, pp. 145-151.
- 3147 Majer, E. L., and J. E. Peterson (2007), The impact of injection on seismicity at The Geysers,
3148 California Geothermal Field, *International Journal of Rock Mechanics and Mining*
3149 *Sciences*, 44, 1079-1090, doi:10.1016/j.ijrmms.2007.07.023.
- 3150 Majer, E. L., R. Baria, M. Stark, S. Oates, J. Bommer, B. Smith, and H. Asanuma (2007),
3151 Induced seismicity associated with enhanced geothermal systems, *Geothermics*, 36, 185-
3152 222, doi:10.1016/j.geothermics.2007.03.003.
- 3153 Maxwell, S. C., and H. Fabriol (2004), Passive Seismic Imaging of CO₂ Sequestration at
3154 Weyburn, Proceedings of the Society of Engineering Geophysicists International
3155 Exposition and 74th Annual Meeting, Denver, Colorado, 10-15 October.
- 3156 McGarr, A. (1991), On a possible connection between three major earthquakes in California
3157 and oil production, *Bull. seismol. Soc. Am.*, 81, 948-970.
- 3158 McGarr, A. (1992a), Moment tensors of ten Witwatersrand mine tremors, *Pure Appl.*
3159 *Geophys.*, 139, 781-800.
- 3160 McGarr, A. (1992b), An implosive component in the seismic moment tensor of a mining-
3161 induced tremor, *Geophys. Res. Lett.*, 19, 1579-1582.
- 3162 McGarr, A. (2014), Maximum magnitude earthquakes induced by fluid injection, *Journal of*
3163 *Geophysical Research-Solid Earth*, 119, 1008-1019, doi:10.1002/2013jb010597.
- 3164 McGarr, A., D. Simpson, and L. Seeber (2002), Case histories of induced and triggered
3165 seismicity, *in* *International Geophysics Series, International Handbook of Earthquake and*
3166 *Engineering Seismology*, edited by W. H. Lee, P. Jennings, C. Kisslinger and H.
3167 Kanamori, pp. 647-664.
- 3168 McKeown, F. A. (1975), Relation of geological structure to seismicity at Pahute Mesa,
3169 Nevada Test Site, *Bull. seismol. Soc. Am.*, 65, 747-764.
- 3170 McKeown, F. A., and D. D. Dickey (1969), Fault displacements and motion related to
3171 nuclear explosions, *Bull. seismol. Soc. Am.*, 59, 2253-2269.
- 3172 McNamara, D. E., H. M. Benz, R. B. Herrmann, E. A. Bergman, P. Earle, A. Holland, R.
3173 Baldwin, and A. Gassner (2015), Earthquake hypocenters and focal mechanisms in central
3174 Oklahoma reveal a complex system of reactivated subsurface strike-slip faulting,
3175 *Geophys. Res. Lett.*, 42, 2742-2749, doi:10.1002/2014gl062730.
- 3176 McNutt, S. R., and R. J. Beavan (1981), Volcanic earthquakes at Pavlof volcano correlated
3177 with the solid earth tide, *Nature*, 194, 615-618.
- 3178 Mercerat, E. D., L. Driad-Lebeau, and P. Bernard (2010), Induced seismicity monitoring of
3179 an underground salt cavern prone to collapse, *Pure Appl. Geophys.*, 167, 5-25,
3180 doi:10.1007/s00024-009-0008-1.
- 3181 Milev, A. M., and S. M. Spottiswoode (2002), Effect of the rock properties on mining-
3182 induced seismicity around the Ventersdorp Contact Reef, Witwatersrand basin, south
3183 Africa, *Pure Appl. Geophys.*, 159, 165-177, doi:10.1007/pl00001249.

- 3184 Miller, A. D., B. R. Julian, and G. R. Foulger (1998a), Three-dimensional seismic structure
3185 and moment tensors of non-double-couple earthquakes at the Hengill-Grensdalur volcanic
3186 complex, Iceland, *Geophys. J. Int.*, 133, 309-325.
- 3187 Miller, A. D., G. R. Foulger, and B. R. Julian (1998b), Non-double-couple earthquakes II.
3188 Observations, *Rev. Geophys.*, 36, 551-568.
- 3189 Mogren, S. M., and M. Mukhopadhyay (2013), Study of seismogenic crust in the eastern
3190 province of Saudi Arabia and its relation to the seismicity of the Ghawar fields, paper
3191 presented at American Geophysical Union Fall Meeting, 9-13 December.
- 3192 Monastero, F. C., A. M. Katzenstein, J. S. Miller, J. R. Unruh, M. C. Adams, and K.
3193 Richards-Dinger (2005), The Coso geothermal field: A nascent metamorphic core
3194 complex, *Bull. Geol. Soc. Am.*, 117, 1534-1553.
- 3195 Mossop, A., and P. Segall (1999), Volume strain within The Geysers geothermal field, *J.*
3196 *Geophys. Res.*, 104, 29113-29131, doi:10.1029/1999jb900284.
- 3197 Nagel, N. B. (2001), Compaction and subsidence issues within the petroleum industry: From
3198 Wilmington to Ekofisk and beyond, *Physics and Chemistry of the Earth, Part A: Solid*
3199 *Earth and Geodesy*, 26, 3-14.
- 3200 Newman, A., S. Stein, J. Weber, J. Engeln, A. Mao, and T. Dixon (1999), Slow deformation
3201 and low seismic hazard at the New Madrid seismic zone, *Science*, 284, 619-621.
- 3202 Nicholson, C., and R. L. Wesson (1992), Triggered earthquakes and deep well activities, *Pure*
3203 *Appl. Geophys.*, 139, 561-578.
- 3204 Nicholson, C., E. Roeloffs, and R. L. Wesson (1988), The northeastern Ohio earthquake of
3205 31 January 1986: Was it induced?, *Bull. seismol. Soc. Am.*, 78, 188-217.
- 3206 Nicol, A., R. Carne, M. Gerstenberger, and A. Christophersen (2011), Induced seismicity and
3207 its implications for CO₂ storage risk, *in* 10th International Conference on Greenhouse Gas
3208 Control Technologies, edited by J. Gale, C. Hendriks and W. Turkenberg, pp. 3699-3706.
- 3209 Nielsen, S. B., R. Stephenson, and E. Thomsen (2007), Dynamics of Mid-Palaeocene North
3210 Atlantic rifting linked with European intra-plate deformations, *Nature*, 450, 1071-1074.
- 3211 Obermeier, S. F. (1996), Use of liquefaction-induced features for paleoseismic analysis,
3212 *Engineering Geology*, 44, 1-76.
- 3213 Odonne, F., I. Ménéard, G. Massonat, and J.-P. Rolando (1999), Abnormal reverse faulting
3214 above a depleting reservoir, *Geology*, 27, 111-114.
- 3215 Ohtake, M. (1974), Seismic activity induced by water injection at Matsushiro, Japan, *Journal*
3216 *of Physics of the Earth*, 22, 163-176.
- 3217 Pavlovski, O. A. (1998), Radiological consequences of nuclear testing for the population of
3218 the former USSR (Input information, models, dose and risk estimates), *in* Atmospheric
3219 Nuclear Tests (Environmental and human consequences), Proceedings of the NATO
3220 Advanced Research Workshop, edited by C. S. Shapiro, pp. 219-260, Springer, Berlin.
- 3221 Pennington, W. D., S. D. Davis, S. M. Carlson, J. DuPree, and T. E. Ewing (1986), The
3222 evolution of seismic barriers and asperities caused by the depressuring of fault planes in
3223 oil and gas fields of South Texas, *Bull. seismol. Soc. Am.*, 76, 939-948.
- 3224 Perea, H., E. Masana, and P. Santanach (2012), An active zone characterized by slow normal
3225 faults, the northwestern margin of the Valencia trough (NE Iberia): a review, *Journal of*
3226 *Iberian Geology*, 38, 31-52, doi:http://dx.doi.org/10.5209/rev_JIGE.2012.v38.
- 3227 Plotnikova, I. M., B. S. Nurtaev, J. R. Grasso, L. M. Matasova, and R. Bossu (1996), The
3228 character and extent of seismic deformation in the focal zone of Gazli earthquakes of 1976
3229 and 1984, *M>7.0*, *Pure Appl. Geophys.*, 147, 377-387.
- 3230 Pomeroy, P. W., D. W. Simpson, and M. L. Sbar (1976), Earthquakes triggered by surface
3231 quarrying-the Wappingers Falls, New York sequence of June, 1974, *Bull. seismol. Soc.*
3232 *Am.*, 66, 685-700.

- 3233 Pratt, W. E., and D. W. Johnson (1926), Local subsidence of the Goose Creek oil field, *J.*
 3234 *Geol.*, 34, 577-590.
- 3235 Prioul, R., F. H. Cornet, C. Dorbath, L. Dorbath, M. Ogena, and E. Ramos (2000), An
 3236 induced seismicity experiment across a creeping segment of the Philippine Fault, *J.*
 3237 *Geophys. Res.*, 105, 13595-13612, doi:10.1029/2000jb900052.
- 3238 Purvis, K., K. E. Overshott, J. C. Madgett, and T. Niven (2010), The Ensign enigma:
 3239 improving well deliverability in a tight gas reservoir, *Proceedings of the Petroleum*
 3240 *Geology: From Mature Basins to New Frontiers – Proceedings of the 7th Petroleum*
 3241 *Geology Conference, London*, pp. 325-336.
- 3242 Raleigh, C. B., J. H. Healy, and J. D. Bredehoeft (1976), An experiment in earthquake control
 3243 at Rangely, Colorado, *Science*, 191, 1230-1237.
- 3244 Reasenber, P. A., and R. W. Simpson (1992), Response of regional seismicity to the static
 3245 stress change produced by the Loma Prieta earthquake, *Science*, 255, 1687-1690.
- 3246 Richardson, E., and T. H. Jordan (2002), Seismicity in deep gold mines of South Africa:
 3247 Implications for tectonic earthquakes, *Bull. seismol. Soc. Am.*, 92, 1766-1782,
 3248 doi:10.1785/0120000226.
- 3249 Ross, A., G. R. Foulger, and B. R. Julian (1999), Source processes of industrially-induced
 3250 earthquakes at The Geysers geothermal area, California, *Geophysics*, 64, 1877-1889.
- 3251 Roth, P., N. Pavoni, and N. Deichmann (1992), Seismotectonics of the eastern Swiss Alps
 3252 and evidence for precipitation-induced variations of seismic activity, *Tectonophysics*, 207,
 3253 183-197, doi:10.1016/0040-1951(92)90477-n.
- 3254 Rudajev, V., and J. Sileny (1985), Seismic events with non-shear components: II Rockbursts
 3255 with implosive source component, *Pure Appl. Geophys.*, 123, 17-25.
- 3256 Schultz, R., V. Stern, M. Novakovic, G. Atkinson, and Y. J. Gu (2015), Hydraulic fracturing
 3257 and the Crooked Lake Sequences: Insights gleaned from regional seismic networks,
 3258 *Geophys. Res. Lett.*, 42, 2750-2758, doi:10.1002/2015gl063455.
- 3259 Seeber, L., J. G. Armbruster, W.-Y. Kim, and N. Barstow (1998), The 1994 Cacoosing
 3260 Valley earthquakes near Reading, Pennsylvania: A shallow rupture triggered by quarry
 3261 unloading, *J. Geophys. Res.*, 103, 24505-24521.
- 3262 Segall, P. (1985), Stress and subsidence resulting from subsurface fluid withdrawal in the
 3263 epicentral region of the 1983 Coalinga earthquake, *J. Geophys. Res.*, 90, 6801-6816.
- 3264 Segall, P. (1989), Earthquakes triggered by fluid extraction, *Geology*, 17, 942-946.
- 3265 Segall, P. (1992), Induced stresses due to fluid extraction from axisymmetrical reservoirs,
 3266 *Pure Appl. Geophys.*, 139, 535-560, doi:10.1007/bf00879950.
- 3267 Semmane, F., I. Abacha, A. K. Yelles-Chaouche, A. Haned, H. Beldjoudi, and A. Amrani
 3268 (2012), The earthquake swarm of December 2007 in the Mila region of northeastern
 3269 Algeria, *Natural Hazards*, 64, 1855-1871, doi:10.1007/s11069-012-0338-7.
- 3270 Shapiro, S. A., J. Kummerow, C. Dinske, G. Asch, E. Rothert, J. Erzinger, H. J. Kumpel, and
 3271 R. Kind (2006), Fluid induced seismicity guided by a continental fault: Injection
 3272 experiment of 2004/2005 at the German Deep Drilling Site (KTB), *Geophys. Res. Lett.*,
 3273 33, doi:10.1029/2005gl024659.
- 3274 Simiyu, S. M., and G. R. Keller (2000), Seismic monitoring of the Olkaria Geothermal area,
 3275 Kenya Rift valley, *J. Volc. Geotherm. Res.*, 95, 197-208.
- 3276 Simpson, D. W., and O. V. Soboleva (1977), WATER LEVEL VARIATIONS AND
 3277 RESERVOIR-INDUCED SEISMICITY AT NUREK, USSR, *Transactions-American*
 3278 *Geophysical Union*, 58, 1196-1196.
- 3279 Simpson, D. W., and S. K. Negmatullaev (1981), Induced seismicity at Nurek reservoir,
 3280 Tadjikistan, USSR, *Bull. seismol. Soc. Am.*, 71, 1561-1586.
- 3281 Simpson, D. W., and W. Leith (1985), The 1976 and 1984 Gazli, USSR, earthquakes—were
 3282 they induced?, *Bull. seismol. Soc. Am.*, 75, 1465-1468.

- 3283 Skoumal, R. J., M. R. Brudzinski, and B. S. Currie (2015), Earthquakes induced by hydraulic
3284 fracturing in Poland Township, Ohio, *Bull. seismol. Soc. Am.*, 105, 189-197.
- 3285 Stark, M. A. (1990), Imaging injected water in The Geysers reservoir using microearthquake
3286 data, *GRC Transactions*, 17, 1697-1704.
- 3287 Stein, S., M. Liu, E. Calais, and Q. Li (2009), Midcontinent earthquakes as a complex
3288 system, *Seismol. Res. Lett.*, 80, 551-553.
- 3289 Stein, S., M. Liu, T. Camelbeeck, M. Merino, A. Landgraf, E. Hintersberger, and S. Kuebler
3290 (2015), Challenges in assessing seismic hazard in intraplate Europe, *in* *Seismicity, Fault*
3291 *Rupture and Earthquake Hazards in Slowly Deforming Regions*, edited by A. Landgraf, S.
3292 Kuebler, E. Hintersberger and S. Stein, Geological Society, London, Special Publications,
3293 London.
- 3294 Styles, P., P. Gasparini, E. Huenges, P. Scandone, S. Lasocki, and F. Terlizzese (2014),
3295 Report on the hydrocarbon exploration and seismicity in Emilia region, pp 213,
3296 International Commission on Hydrocarbon Exploration and Seismicity in the Emilia
3297 Region.
- 3298 Suckale, J. (2009), Induced seismicity in hydrocarbon fields, *Advances in Geophysics*, 51,
3299 55-106.
- 3300 Suckale, J. (2010), Moderate-to-large seismicity induced by hydrocarbon production, *The*
3301 *Leading Edge*, 29, 310-319, doi:10.1190/1.3353728.
- 3302 Tadokoro, K., M. Ando, and K. Nishigami (2000), Induced earthquakes accompanying the
3303 water injection experiment at the Nojima fault zone, Japan: Seismicity and its migration, *J.*
3304 *Geophys. Res.*, 105, 6089-6104, doi:10.1029/1999jb900416.
- 3305 Talwani, P. (1995), Speculation on the causes of continuing seismicity near Koyna reservoir,
3306 India, *Pure Appl. Geophys.*, 145, 167-174, doi:10.1007/bf00879492.
- 3307 Tang, C., J. W. Wang, and J. Zhang (2010), Preliminary engineering application of
3308 microseismic monitoring technique to rockburst prediction in tunneling of Jinping II
3309 project, *Journal of Rock Mechanics and Geotechnical Engineering*, 3.
- 3310 Tang, L., M. Zhang, L. Sun, and L. Wen (2015), Injection-induced seismicity in a natural gas
3311 reservoir in Hutubi, southern Junggar Basin, northwest China, paper presented at AGU
3312 Fall Meeting.
- 3313 Terashima, T. (1981), Survey on induced seismicity at Mishraq area in Iraq, *Journal of*
3314 *Physics of the Earth*, 29, 371-375.
- 3315 Tester, J. W., and e. al. (2006), *The future of geothermal energy*, pp 372, Massachusetts
3316 Institute of Technology, Cambridge, Massachusetts.
- 3317 Toksöz, M. N., and H. K. Kehrler (1972), Tectonic strain release by underground nuclear
3318 explosions and its effect on seismic discrimination, *Geophys. J. R. astron. Soc.*, 31, 141-
3319 161.
- 3320 Turbitt, T., A. B. Walker, and C. W. A. Browitt (1983), Monitoring of the background and
3321 induced seismicity at the Cornwall geothermal energy site, *Geophys. J. R. astron. Soc.*, 73,
3322 299-299.
- 3323 van der Elst, N. J., H. M. Savage, K. M. Keranen, and G. A. Abers (2013), Enhanced remote
3324 earthquake triggering at fluid-injection sites in the midwestern United States, *Science*,
3325 341, 164-167.
- 3326 van Eck, T., F. Goutbeek, H. Haak, and B. Dost (2006), Seismic hazard due to small-
3327 magnitude, shallow-source, induced earthquakes in The Netherlands, *Engineering*
3328 *Geology*, 87, 105-121.
- 3329 Van Wees, J. D., L. Buijze, K. Van Thienen-Visser, M. Nepveu, B. B. T. Wassing, B. Orlic,
3330 and P. A. Fokker (2014), Geomechanics response and induced seismicity during gas field
3331 depletion in the Netherlands, *Geothermics*, 52, 206-219,
3332 doi:10.1016/j.geothermics.2014.05.004.

- 3333 Vasco, D. W., J. Rutqvist, A. Ferretti, A. Rucci, F. Bellotti, P. Dobson, C. Oldenburg, J.
3334 Garcia, M. Walters, and C. Hartline (2013), Monitoring deformation at The Geysers
3335 Geothermal Field, California using C-band and X-band interferometric synthetic aperture
3336 radar, *Geophys. Res. Lett.*, 40, 2567–2572, doi:10.1002/grl.50314.
- 3337 Verdon, J. P., J.-M. Kendall, A. L. Stork, R. A. Chadwick, D. J. White, and R. C. Bissell
3338 (2013), Comparison of geomechanical deformation induced by megatonne-scale CO₂
3339 storage at Sleipner, Weyburn, and In Salah, *Proceedings of the National Academy of*
3340 *Sciences*, 110, E2762-E2771.
- 3341 Villegas-Lanza, J. C., J.-M. Nocquet, F. Rolandone, M. Vallée, H. Tavera, F. Bondoux, T.
3342 Tran, X. Martin, and M. Chlieh (2016), A mixed seismic–aseismic stress release episode
3343 in the Andean subduction zone, *Nature Geoscience*, 9, 150–154, doi:10.1038/ngeo2620.
- 3344 Waldhauser, F., and W. L. Ellsworth (2000), A double-difference earthquake location
3345 algorithm: Method and application to the northern Hayward Fault, California, *Bull.*
3346 *seismol. Soc. Am.*, 90, 1353-1368.
- 3347 Wallace, T., D. V. Helmberger, and G. R. Engen (1983), Evidence of tectonic release from
3348 underground nuclear explosions in long-period *P* waves, *Bull. seismol. Soc. Am.*, 73, 593-
3349 613.
- 3350 Walsh, F. R., and M. D. Zoback (2015), Oklahoma’s recent earthquakes and saltwater
3351 disposal, *Science Advances*, 1, no. e1500195.
- 3352 Wang, P., M. J. Small, W. Harbert, and M. Pozzi (2016), A bayesian approach for assessing
3353 seismic transitions associated with wastewater injections, *Bull. seismol. Soc. Am.*, 106,
3354 832-845.
- 3355 Wilson, M. P., R. J. Davies, G. R. Foulger, B. R. Julian, P. Styles, J. G. Gluyas, and S.
3356 Almond (2015), Anthropogenic earthquakes in the UK: A national baseline prior to shale
3357 exploitation, *Marine and Petroleum Geology*, 68, 1-17,
3358 doi:10.1016/j.marpetgeo.2015.08.023.
- 3359 Wong, I. G., and A. McGarr (1990), Implosional failure in mining-induced seismicity: A
3360 critical review, *in* *Rockbursts and Seismicity in Mines*, edited by C. Fairhurst, pp. 45-51,
3361 Bakema, Rotterdam.
- 3362 Wong, I. G., J. R. Humphrey, J. A. Adams, and W. J. Silva (1989), Observations of mine
3363 seismicity in the eastern Wasatch Plateau, Utah, U. S. A.: A possible case of implosional
3364 failure, *Pure Appl. Geophys.*, 129, 369-405.
- 3365 Wright, C., E. M. Kgaswane, M. T. O. Kwadiba, R. E. Simon, T. K. Nguuri, and R. McRae-
3366 Samuel (2003), South African seismicity, April 1997 to April 1999, and regional
3367 variations in the crust and uppermost mantle of the Kaapvaal craton, *Lithos*, 71, 369-392,
3368 doi:10.1016/s0024-4937(03)00122-1.
- 3369 Yabe, Y., M. Nakatani, M. Naoi, J. Philipp, C. Janssen, T. Watanabe, T. Katsura, H.
3370 Kawakata, D. Georg, and H. Ogasawara (2015), Nucleation process of an M2 earthquake
3371 in a deep gold mine in South Africa inferred from on-fault foreshock activity, *J. Geophys.*
3372 *Res.*, 120, 5574-5594, doi:10.1002/2014jb011680.
- 3373 Yakovlev, D. V., T. I. Lazarevich, and S. V. Tsirel (2013), Natural and induced seismic
3374 activity in Kuzbass, *Journal of Mining Science*, 49, 862-872.
- 3375 Yeck, W. L., L. V. Block, C. K. Wood, and V. M. King (2015), Maximum magnitude
3376 estimations of induced earthquakes at Paradox Valley, Colorado, from cumulative
3377 injection volume and geometry of seismicity clusters, *Geophys. J. Int.*, 200, 322-336,
3378 doi:10.1093/gji/ggu394.
- 3379 Zaliapin, I., and Y. Ben-Zion (2016), Discriminating characteristics of tectonic and human-
3380 induced seismicity, *Bull. seismol. Soc. Am.*, 106, 846-859.

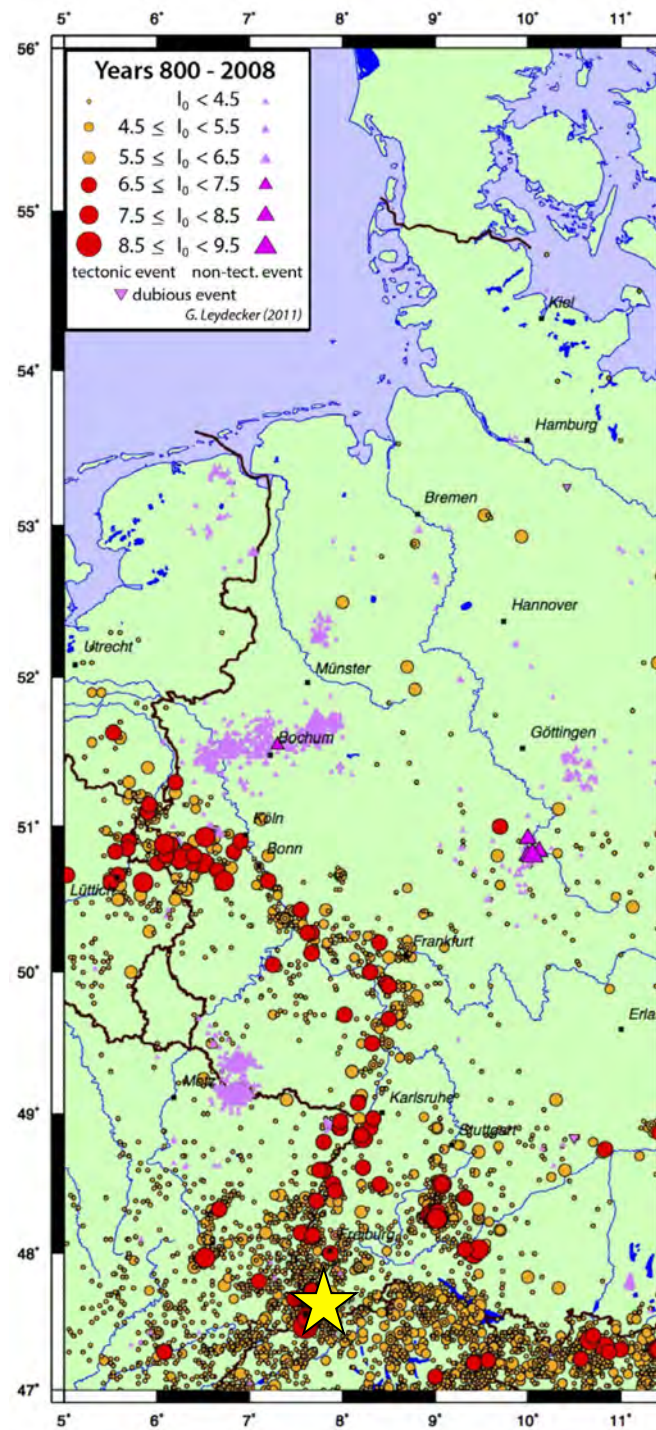
- 3381 Zang, A., E. Majer, and D. Bruhn (2014a), Preface to special issue: Analysis of induced
3382 seismicity in geothermal operations, *Geothermics*, 52, 1-5,
3383 doi:10.1016/j.geothermics.2014.07.006.
- 3384 Zang, A., V. Oye, P. Jousset, N. Deichmann, R. Gritto, A. McGarr, E. Majer, and D. Bruhn
3385 (2014b), Analysis of induced seismicity in geothermal reservoirs - An overview,
3386 *Geothermics*, 52, 6-21, doi:10.1016/j.geothermics.2014.06.005.
- 3387 Zedník, J., J. Pospíšil, B. Růžek, J. Horálek, A. Boušková, P. Jedlička, Z. Skácelová, V.
3388 Nehybka, K. Holub, and J. Rušajová (2001), Earthquakes in the Czech Republic and
3389 surrounding regions in 1995–1999, *Studia Geophysica et Geodaetica*, 45, 267-282.
- 3390 Zhang, Y., W. Feng, L. Xu, C. Zhou, and Y. Chen (2008), Spatio-temporal rupture process of
3391 the 2008 great Wenchuan earthquake, *Science in China Series D: Earth Sciences*, 52, 145-
3392 154, doi:10.1007/s11430-008-0148-7.
- 3393 Ziegler, M., K. Reiter, O. Heidbach, A. Zang, G. Kwiatek, D. Stromeier, T. Dahm, G.
3394 Dresen, and G. Hofmann (2015), Mining-Induced Stress Transfer and Its Relation to a 1.9
3395 Seismic Event in an Ultra-deep South African Gold Mine, *Pure Appl. Geophys.*, 172,
3396 2557-2570, doi:10.1007/s00024-015-1033-x.
- 3397 Zoback, M. D., and J. H. Healy (1984), Friction, faulting, and insitu stress, *Annales*
3398 *Geophysicae*, 2, 689-698.
- 3399 Zoback, M. D., and H. P. Harjes (1997), Injection-induced earthquakes and crustal stress at 9
3400 km depth at the KTB deep drilling site, Germany, *Journal of Geophysical Research-Solid*
3401 *Earth*, 102, 18477-18491, doi:10.1029/96jb02814.

3402

3403

3404

3405



3406

3407

3408 Figure 1: Map of central Europe showing historical earthquakes with different epicentral
 3409 intensities from 800 AD [from Stein *et al.*, 2015]. Yellow star: the city of Basel, Switzerland.

3410

3411

3412



3413

3414

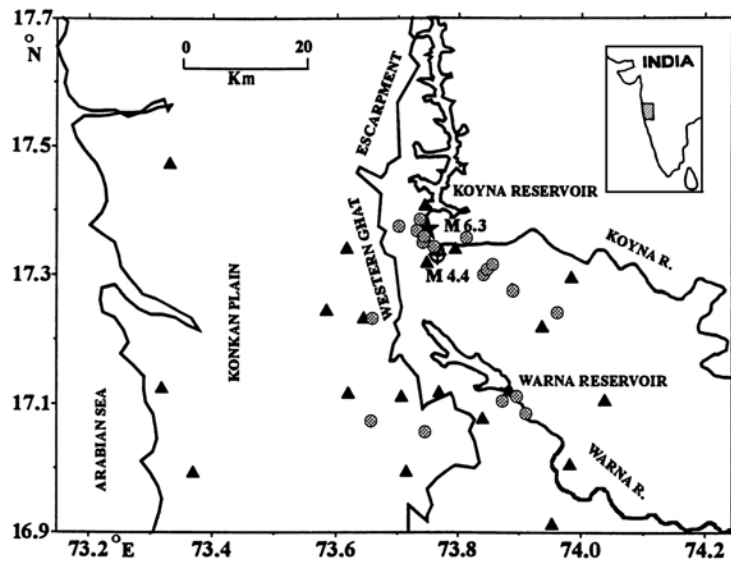
3415 Figure 2: Map of USA showing state names¹¹.

3416

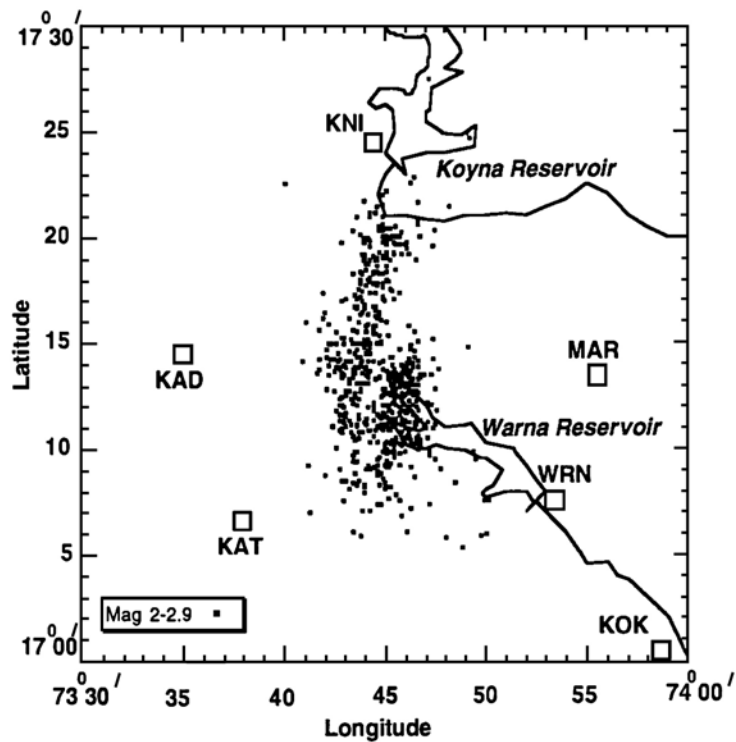
3417

¹¹ From https://commons.wikimedia.org/wiki/File:Map_of_USA_showing_state_names.png

3418



3419



3420

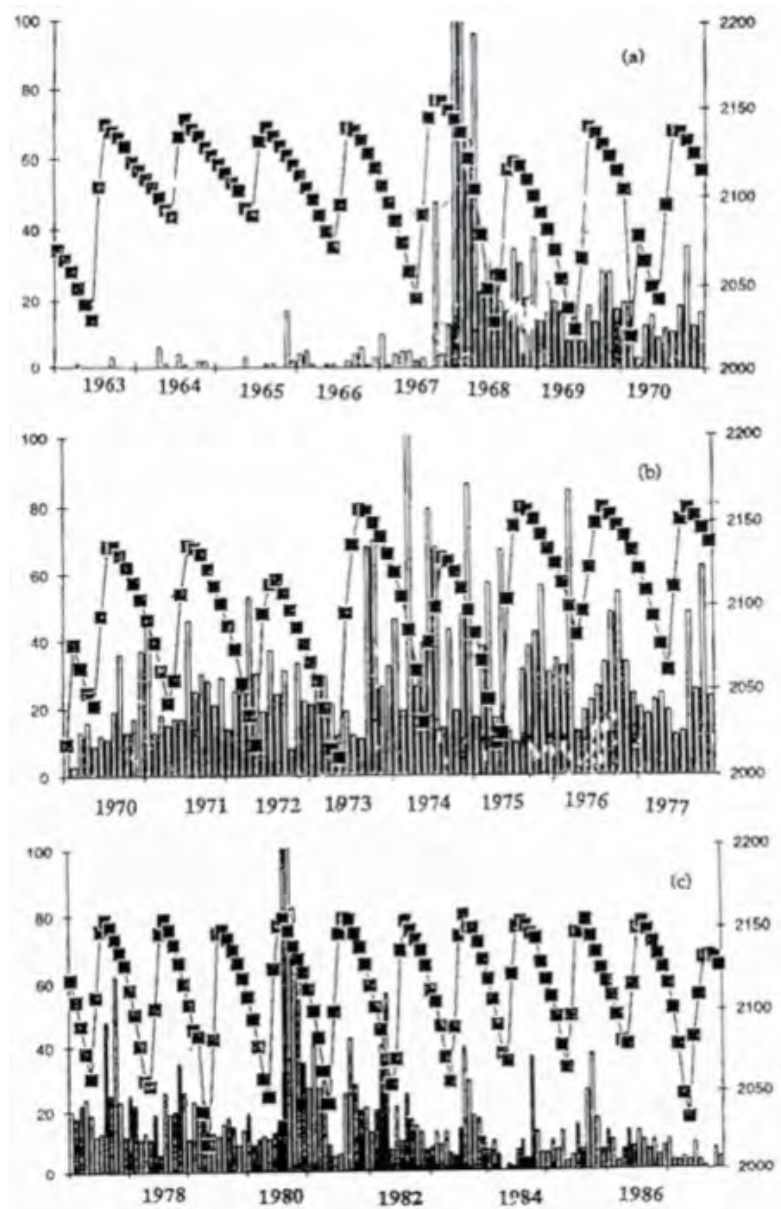
3421

3422 Figure 3: Top: Map of the Koyna, India, area showing the dam, reservoir, seismic stations
 3423 and boreholes. Bottom: Same area showing earthquakes with M 2-2.9 for the period October
 3424 1993 to December 1994 [from Gupta, 2002].

3425

3426

3427



3428

3429

3430 Figure 4: Number of earthquakes in the region of the Koyna dam, India, for the period 1963-
 3431 1986 (left axis), along with reservoir water level (right axis, in m) [from Talwani, 1995].

3432

3433

3434



3435

3436

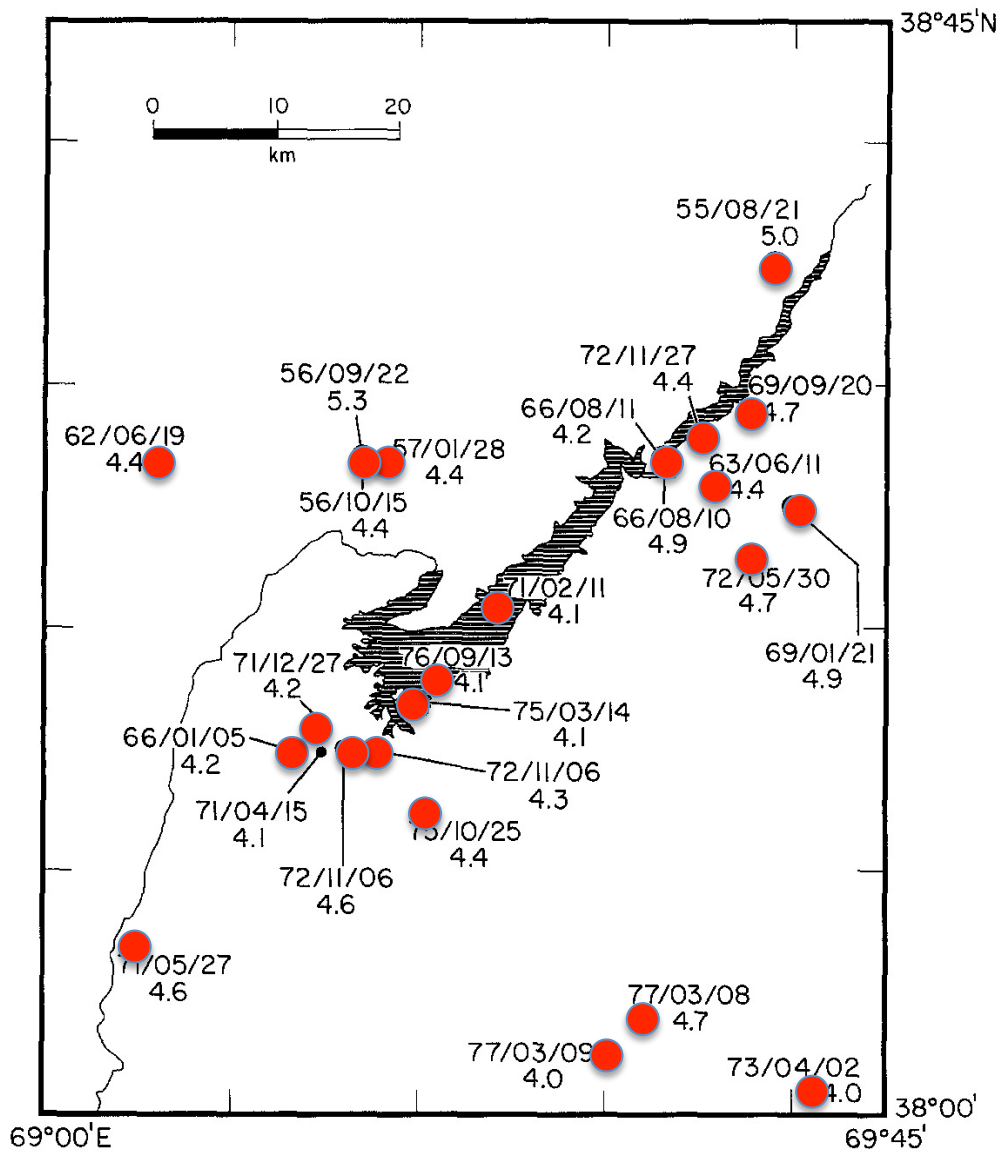
3437 Figure 5: Aerial photograph of Nurek dam, Tadjikistan¹².

3438

3439

¹² <http://www.slideshare.net/wahedullahsabawoon/the-purposes-of-building-a-dam>

3440



3441

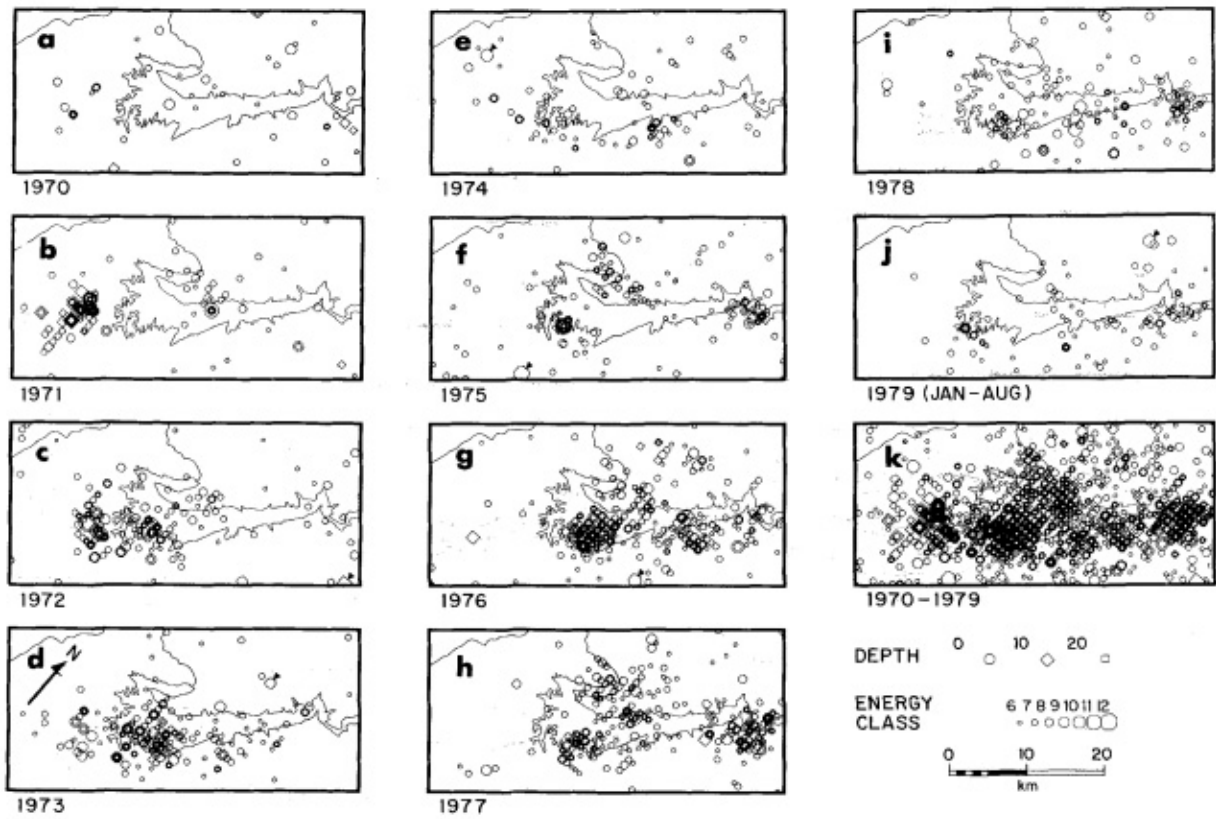
3442

3443 Figure 6: Map of Nurek dam and reservoir, Tajikistan, showing earthquakes with $M \geq 4.0$
 3444 for the period 1955-1979 [from Simpson & Negmatullaev, 1981].

3445

3446

3447



3448

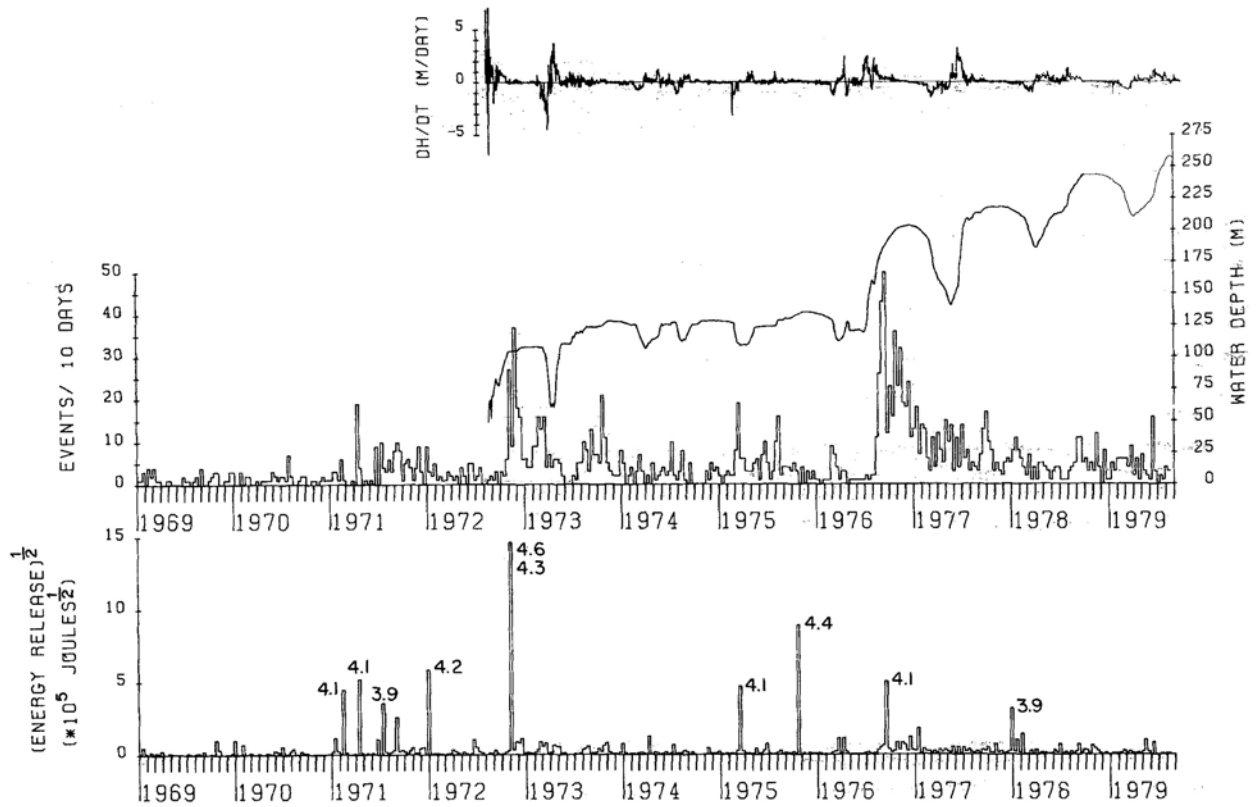
3449

3450 Figure 7: Yearly earthquakes in the vicinity of Nurek dam, Tadjikistan, for the period 1970-
 3451 1979 [from Simpson & Negmatullaev, 1981].

3452

3453

3454



3455

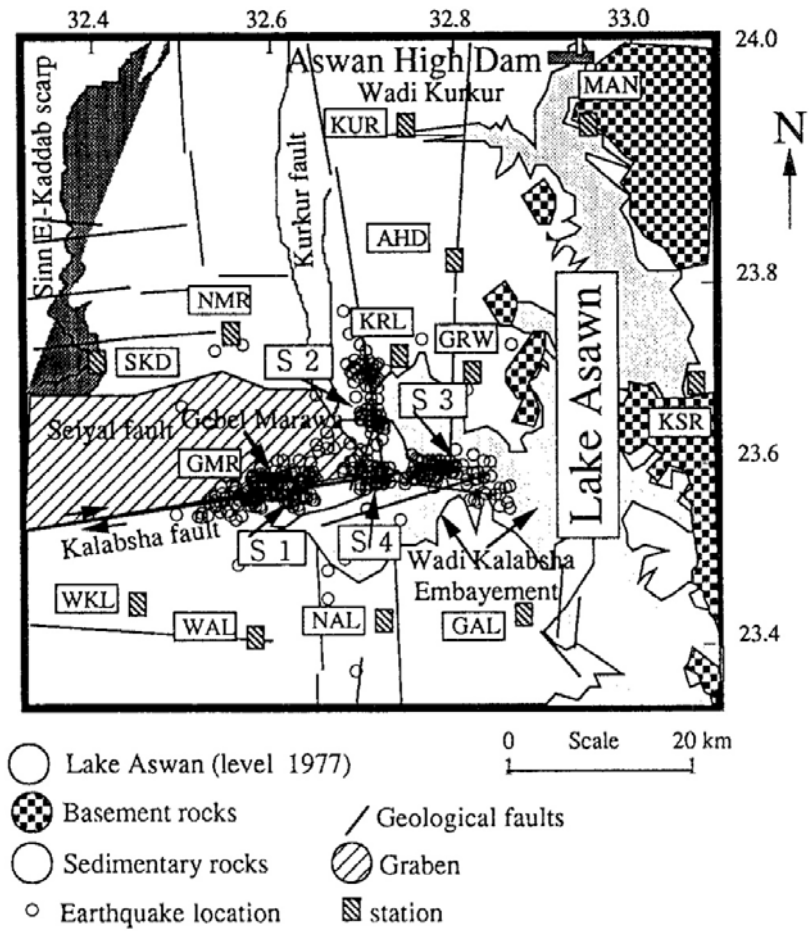
3456

3457 Figure 8: Water depth and seismicity for the period 1969-1979 in the vicinity of Nurek dam,
 3458 Tajikistan [from Simpson & Negmatullaev, 1981].

3459

3460

3461



3462

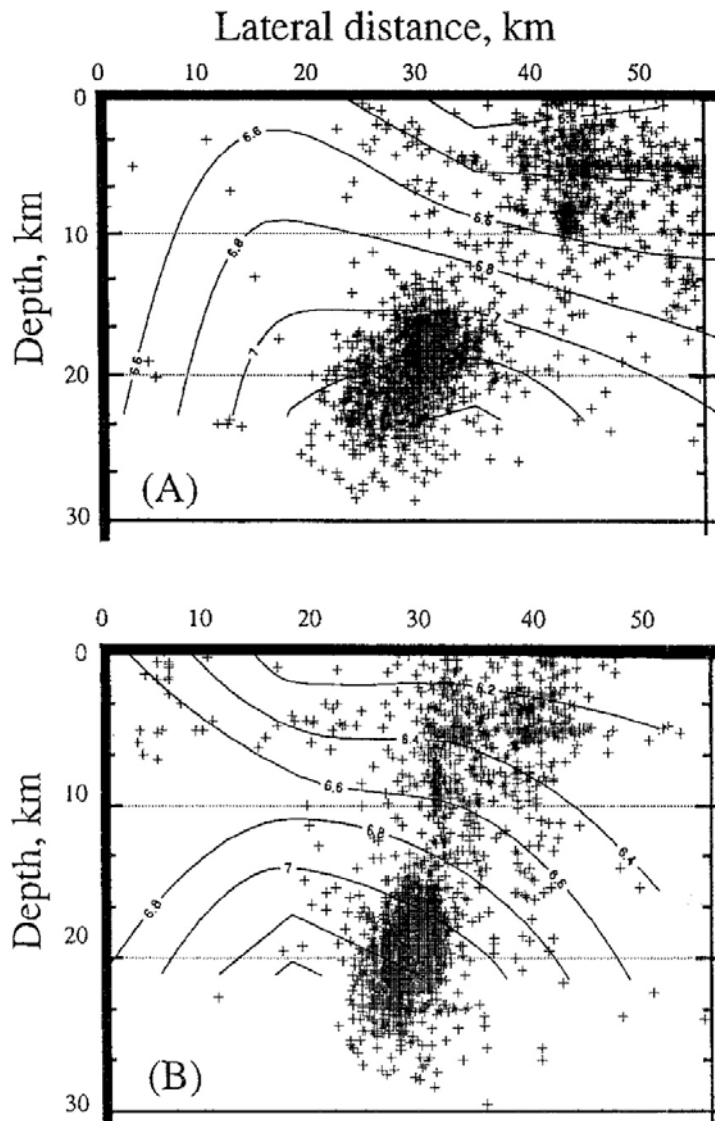
3463

3464 Figure 9: Map showing Lake Aswan, Egypt, and epicenters of induced earthquakes [from
 3465 Awad & Mizoue, 1995].

3466

3467

3468



3469

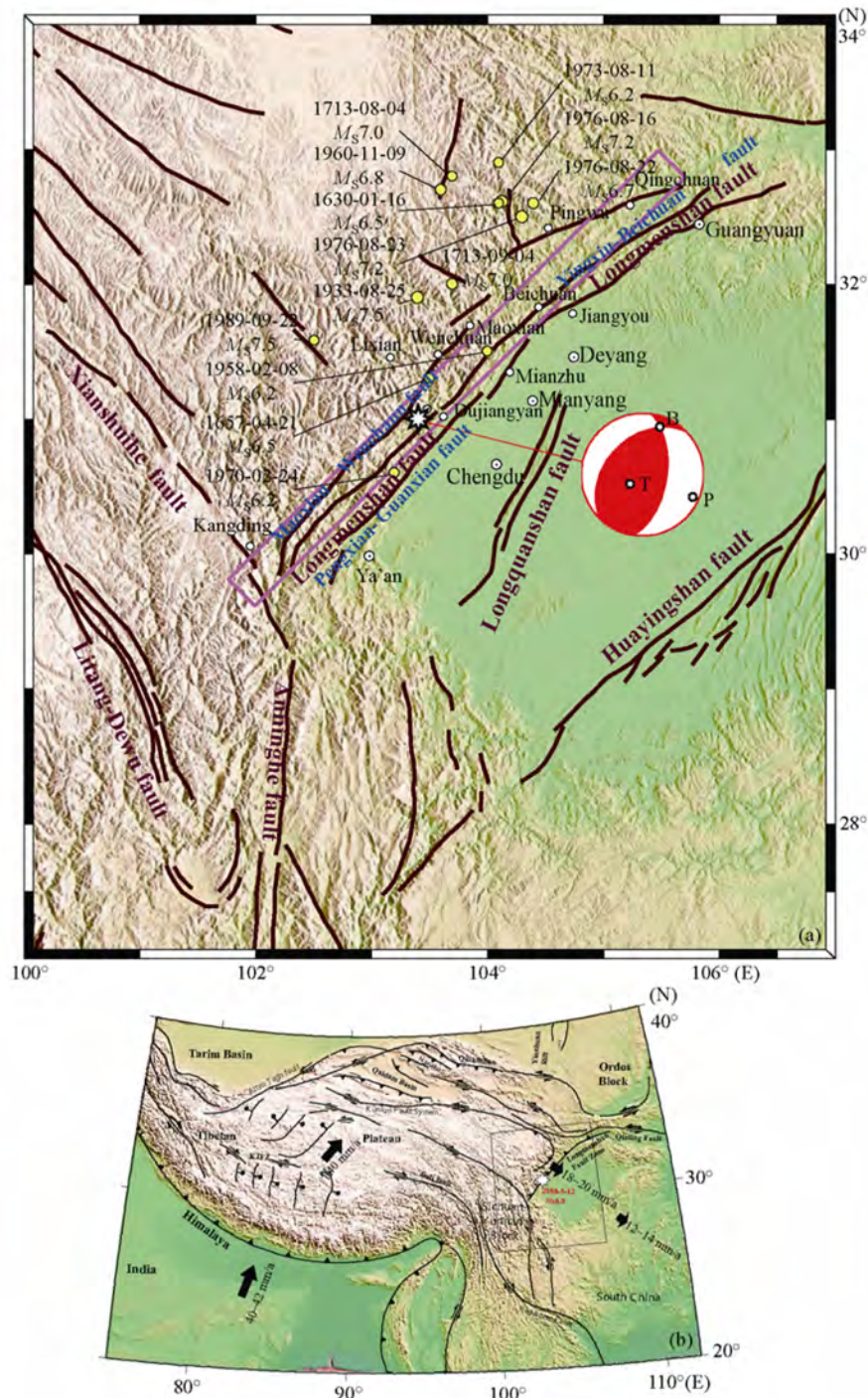
3470

3471 Figure 10: Cross sections showing hypocentral distribution of earthquakes postulated to have
 3472 been induced by impoundment of Lake Aswan [from Awad & Mizoue, 1995].

3473

3474

3475

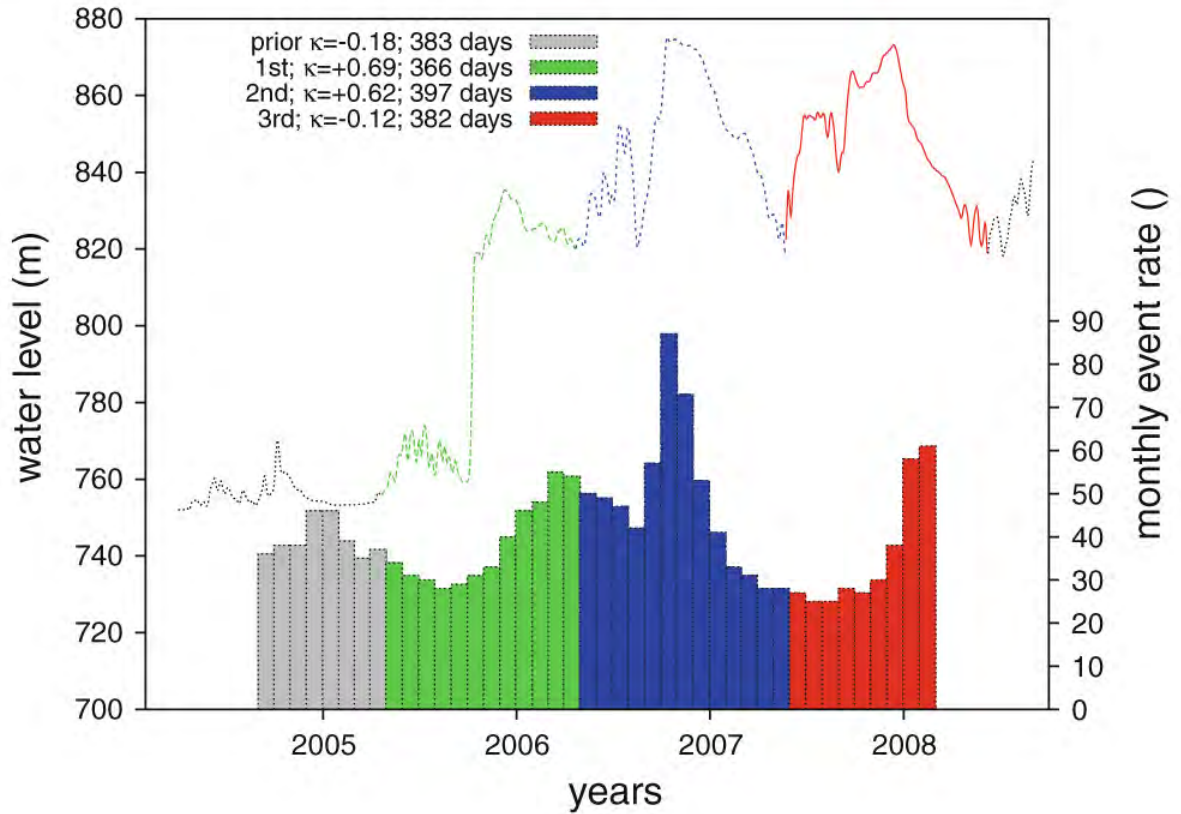


3476
3477

3478 Figure 11: Top: Star: location of the 2008 $M_w \sim 8$ Wenchuan, China, earthquake; lines: main
 3479 faults of the Longmenshan fault zone; yellow circles: historical earthquakes; white circles:
 3480 main cities; lilac rectangle: projection of the fault plane that slipped; beach ball: lower
 3481 hemisphere projection of the focal mechanism of the mainshock. Bottom: regional tectonic
 3482 setting [from Zhang *et al.*, 2008].

3483

3484
3485

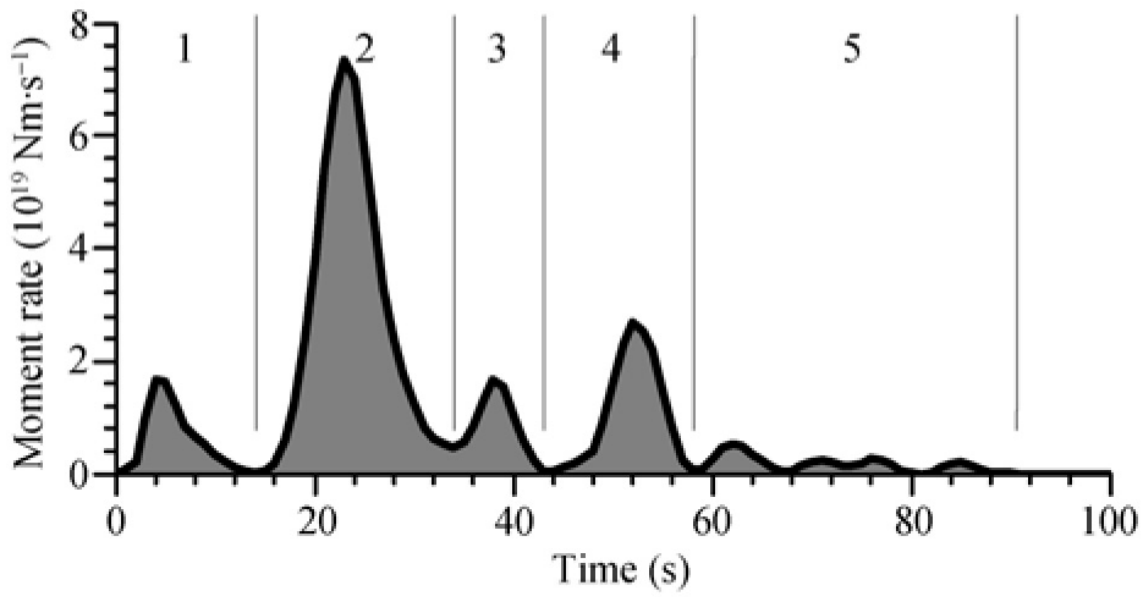


3486
3487

3488 Figure 12: Water level change in the Zipingpu, China, water reservoir and earthquake event
3489 rate in the vicinity for the years prior to the May 2008 $M_w \sim 8$ Wenchuan earthquake [from
3490 Klose, 2012].

3491
3492

3493



3494

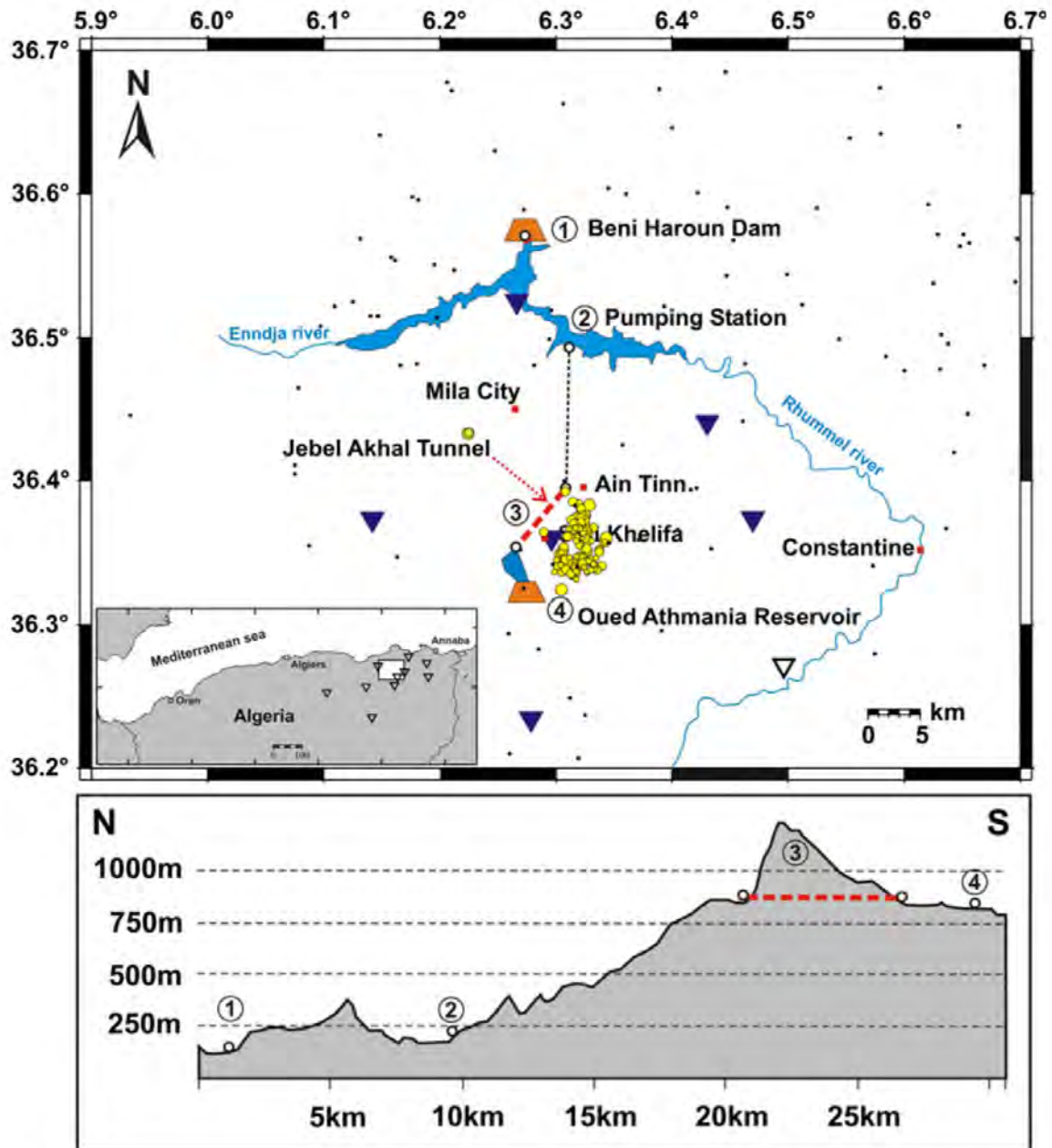
3495

3496 Figure 13: Source time function of the 2008 great Wenchuan, China earthquake [from Zhang
3497 *et al.*, 2008].

3498

3499

3500



3501

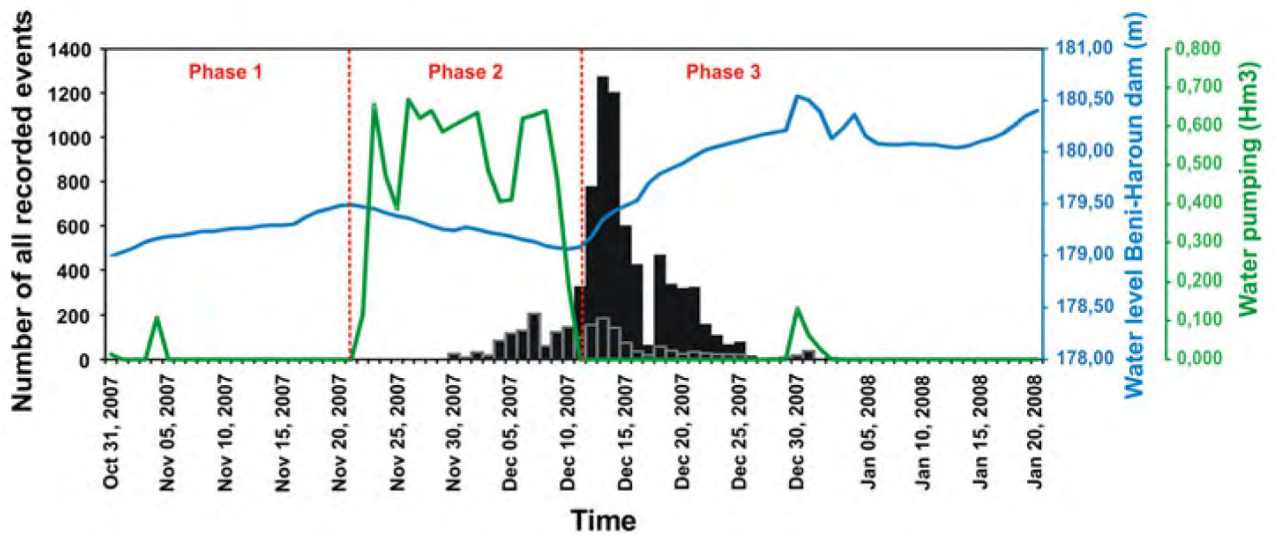
3502

3503 Figure 14: Map of the hydraulic system in the Mila region, Algeria. Top: Water transport
 3504 system (dashed lines) from Beni Haroun dam to Oued Athmania reservoir. Red dashed line:
 3505 tunnel passing through Mt. Jebel Akhal; black dots: seismicity for the two-year period 2006–
 3506 2007; triangles: seismic stations; yellow dots: epicenters of earthquake deduced to be
 3507 triggered by water leakage. Bottom: topographic profile of the hydraulic system [from
 3508 Semmane *et al.*, 2012].

3509

3510

3511



3512

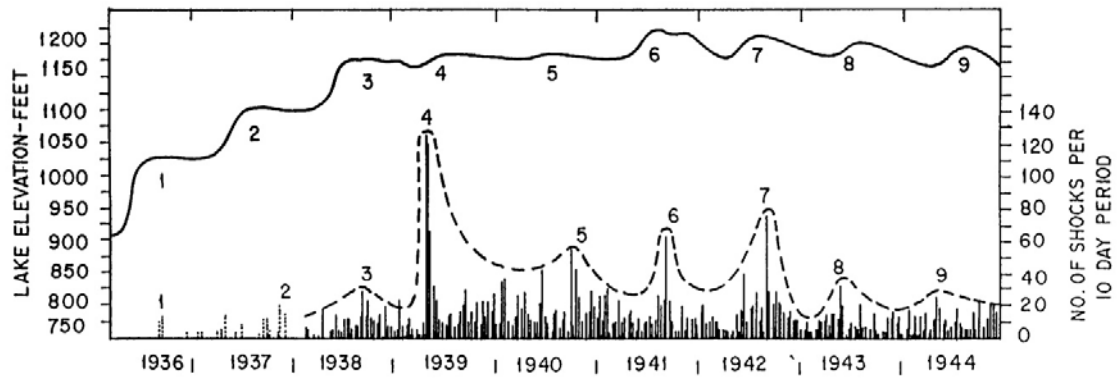
3513

3514 Figure 15: Number of earthquakes recorded, water level in the Beni Haroun dam, and
 3515 volumes of water pumped vs. time around the seismogenic period. Black histogram: events
 3516 recorded; gray histogram: events recorded by the network, discarding a temporary station
 3517 deployed in the epicentral area for 17 days during the swarm [from Semmane *et al.*, 2012].
 3518 This shows an example of the effect of varying the number of seismic stations deployed.

3519

3520

3521



3522

3523

3524 Figure 16: Earthquakes and water level at Lake Mead, Arizona, which is impounded behind
 3525 Hoover dam [from Gupta, 2002].

3526

3527



3528

3529

3530 Figure 17: Aerial photograph of the Three Gorges dam, China¹³.

3531

3532

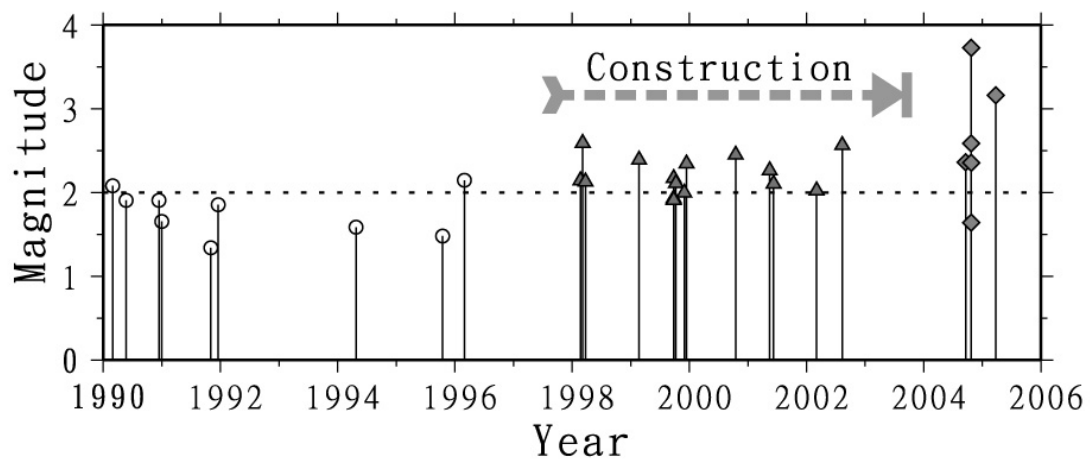
¹³ <http://vizts.com/three-gorges-dam/three-gorges-dam-3/>

3533



3534

3535



3536

3537

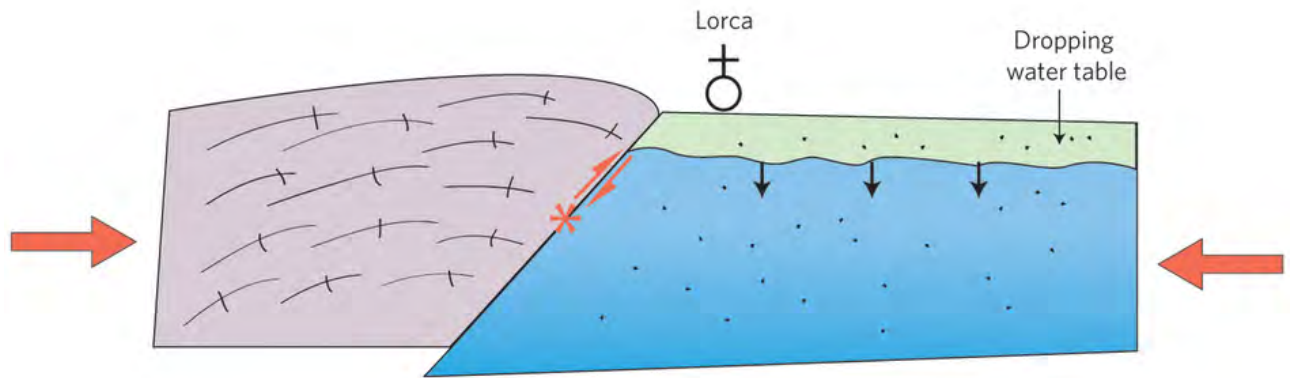
3538 Figure 18: Top: The Taipei 101 building¹⁴. Bottom: Earthquake history for a 16-year period
 3539 spanning the construction of the Taipei 101 building, Taiwan [from Lin, 2005].

3540

3541

¹⁴ <http://inhabitat.com/taipei-101-worlds-tallest-green-building/green-taipei-101-1>

3542



3543

3544

3545 Figure 19: Schematic figure showing the mechanism proposed by Gonzalez *et al.* [2012] for
3546 inducing the 2011 M_w 5.1 Lorca, Spain, earthquake [from Avouac, 2012].

3547

3548

3549



3550

3551

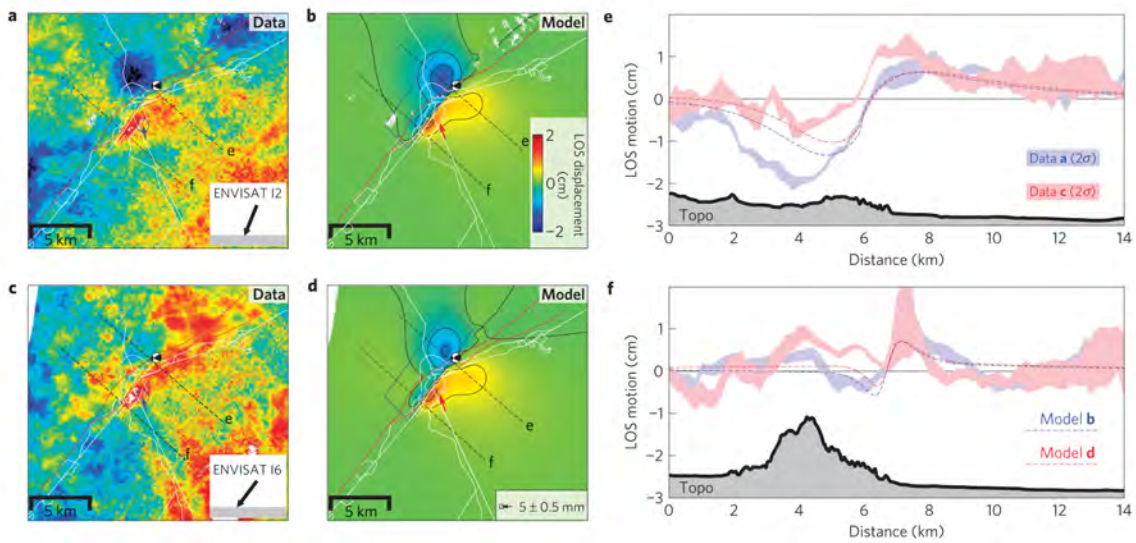
3552 Figure 20: Destruction in the church of Santiago resulting from the 2011 M_w 5.1 Lorca,
3553 Spain, earthquake¹⁵.

3554

3555

¹⁵ https://en.wikipedia.org/wiki/2011_Lorca_earthquake

3556



3557

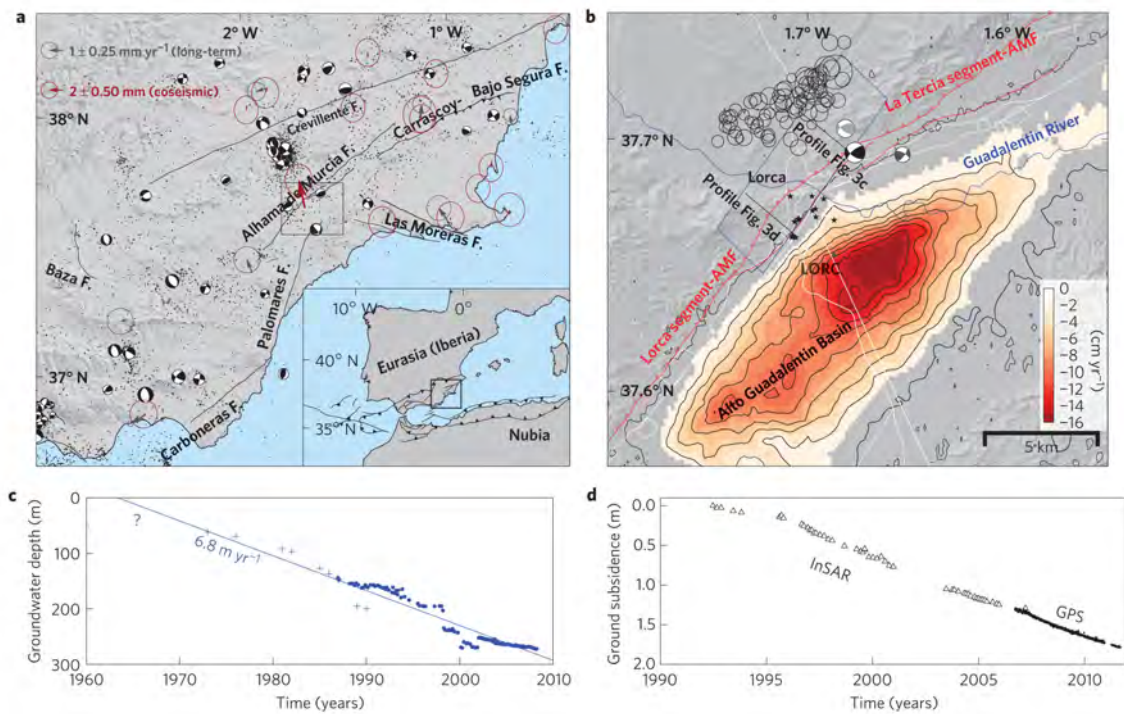
3558

3559 Figure 21: (a–d): ground deformation data and model for the 2011 M_w 5.1 Lorca, Spain,
 3560 earthquake. (a and c): descending line-of-sight (LOS) displacement map and horizontal GPS
 3561 vector; (b and d): distributed slip model predictions. Insets in a and c indicate LOS angle,
 3562 positive values away from the satellite. Blue rectangle: fault surface projection; dashed lines:
 3563 profile locations; (e and f): observed and simulated data along two profiles, and local
 3564 topography [from Gonzalez *et al.*, 2012].

3565

3566

3567



3568

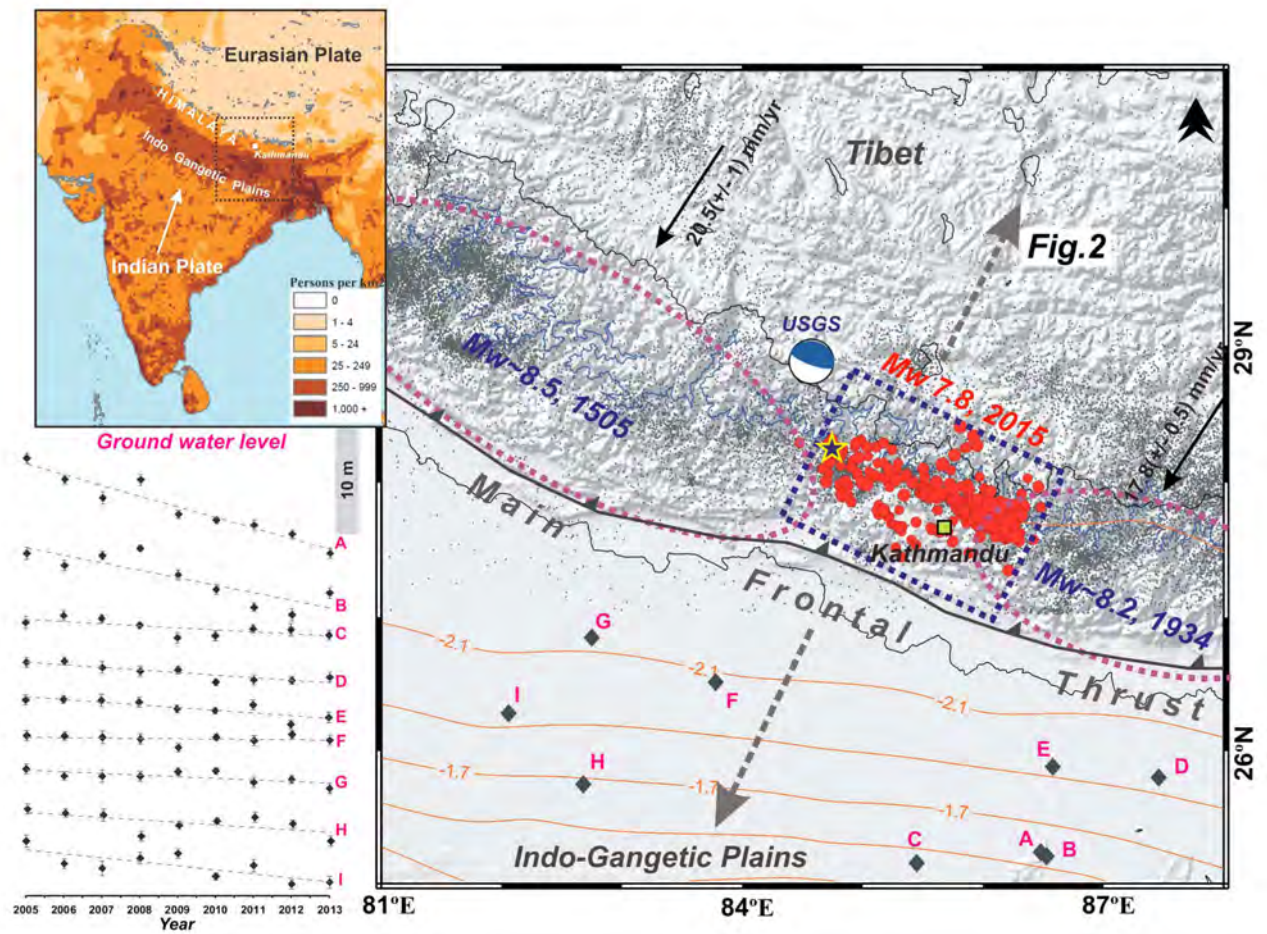
3569

3570 Figure 22: Location and kinematics of the Lorca earthquake. a: southwest Spain seismicity
 3571 (2000–2010), focal mechanisms (1970–2010), long-term GPS velocity (2006–2011, gray)
 3572 and coseismic vectors (red). Major mapped faults are labeled. b: Lorca city and Alto
 3573 Guadalentín Basin. Mainshock focal mechanisms (black), pre-shock (light gray), largest
 3574 aftershock (dark gray), and relocated seismic sequence. Black stars are damage locations, red
 3575 lines are faults. Contour lines indicate 2 cm/a InSAR subsidence due to groundwater
 3576 pumping. Blue rectangle: fault surface projection. AMF, Alhama de Murcia Fault. c,
 3577 Groundwater depth. d, InSAR (triangles) and line-of-sight (LOS)-projected GPS ground-
 3578 surface subsidence at station LORC [from Gonzalez *et al.*, 2012].

3579

3580

3581



3582

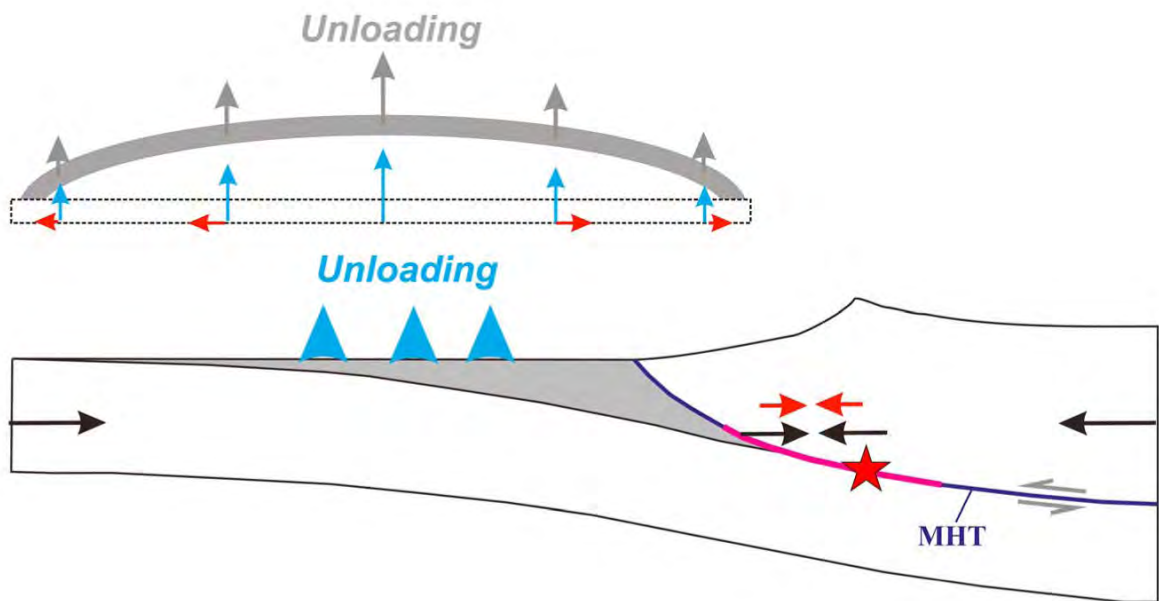
3583

3584 Figure 23: Seismotectonic context of the 2015 M_w 7.8 Gorkha, Nepal earthquake. Black star:
 3585 epicenter of the mainshock; red circles: aftershocks; black arrows: convergence rate; gray
 3586 dots: mid-crustal seismicity 1995-2008; blue contour: 3500-m elevation; ellipses:
 3587 approximate rupture locations of historic events since 1505; orange contours: anthropogenic
 3588 groundwater loss in cm/a water thickness for the period 2002-2008 (multiply by 5 to get drop
 3589 in water table); black diamonds: sampling sites; inset at left: site depletion trends; inset top
 3590 left: population density (people/ km^2) [from Kundu *et al.*, 2015].

3591

3592

3593



3594

3595

3596 Figure 24: Schematic diagram showing the effect of unloading by anthropogenic groundwater
 3597 loss on the Main Himalayan Thrust. Dewatering induces a component of horizontal
 3598 compression (red arrows) that adds to the secular interseismic contraction (black arrows) at
 3599 seismogenic depths. Red star: the 2015 Gorkha, Nepal earthquake; pink line: the associated
 3600 rupture [from Kundu *et al.*, 2015, after].

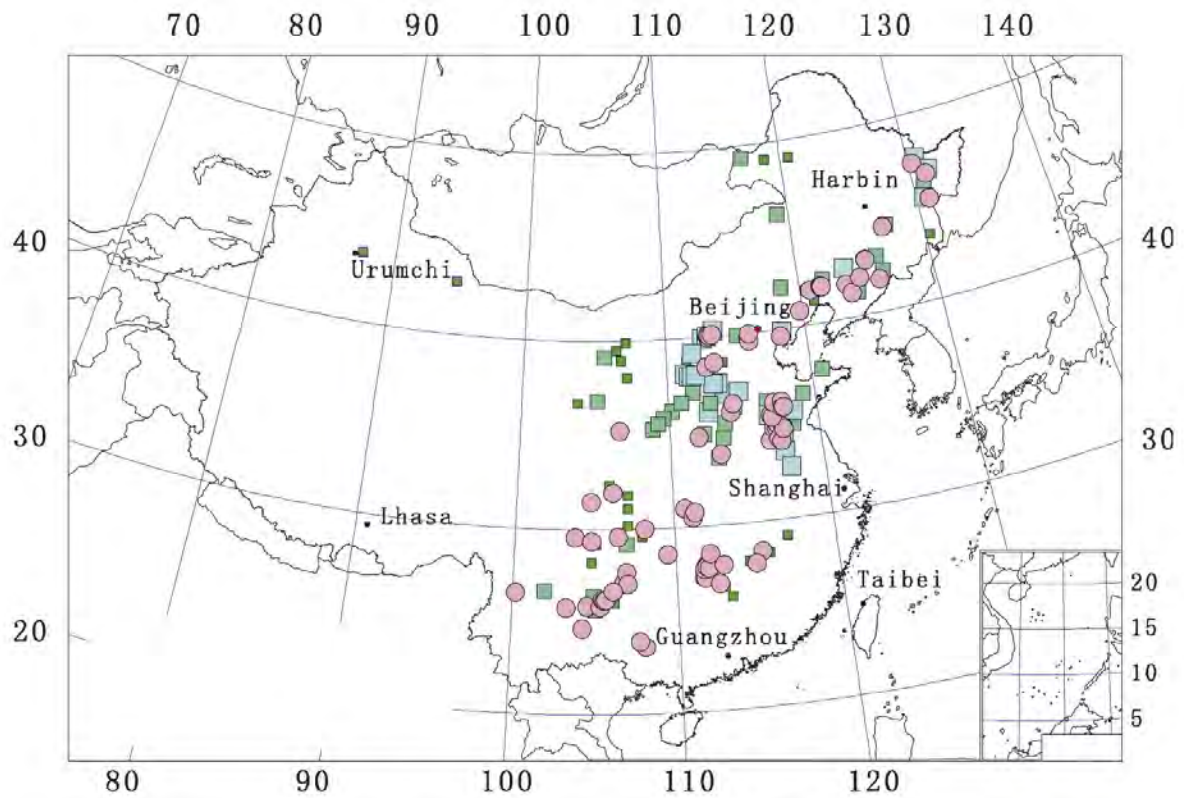
3601

3602

3603

3604

3605



3606

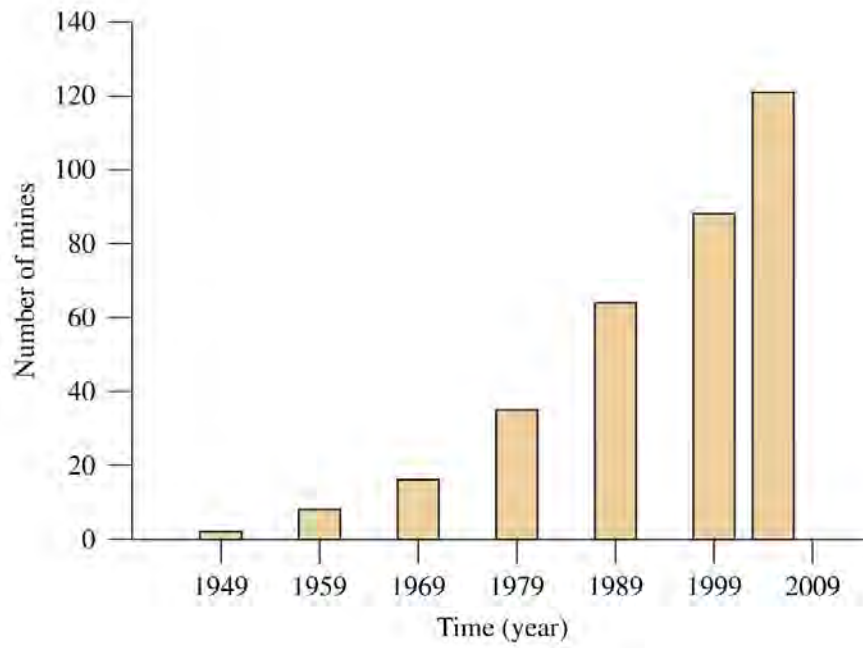
3607

3608 Figure 25: Map of China. Green squares: Small, medium and large state-owned coal mines.
 3609 Pink dots: Coal mines where mining-induced seismicity occurs [from Li *et al.*, 2007].

3610

3611

3612



3613

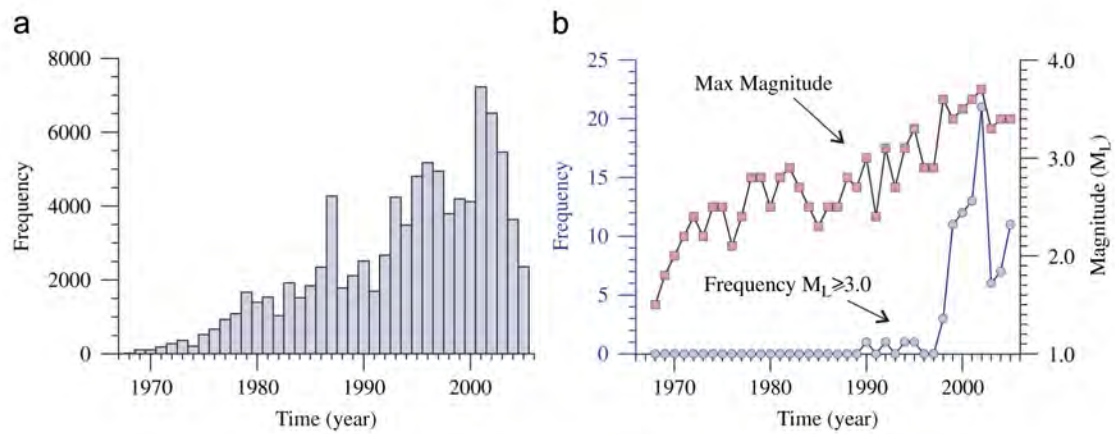
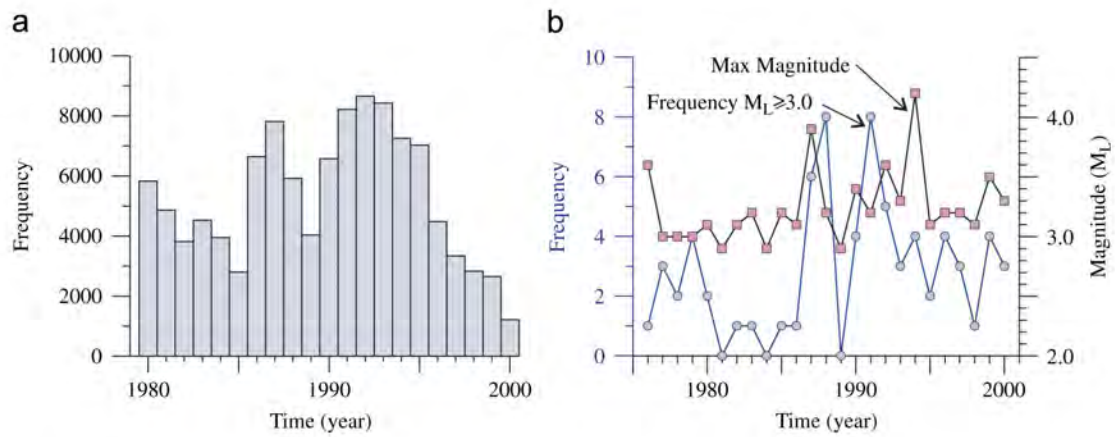
3614

3615 Figure 26: Number of mines in China with rockburst hazard vs. time [from Li *et al.*, 2007].

3616

3617

3618



3619

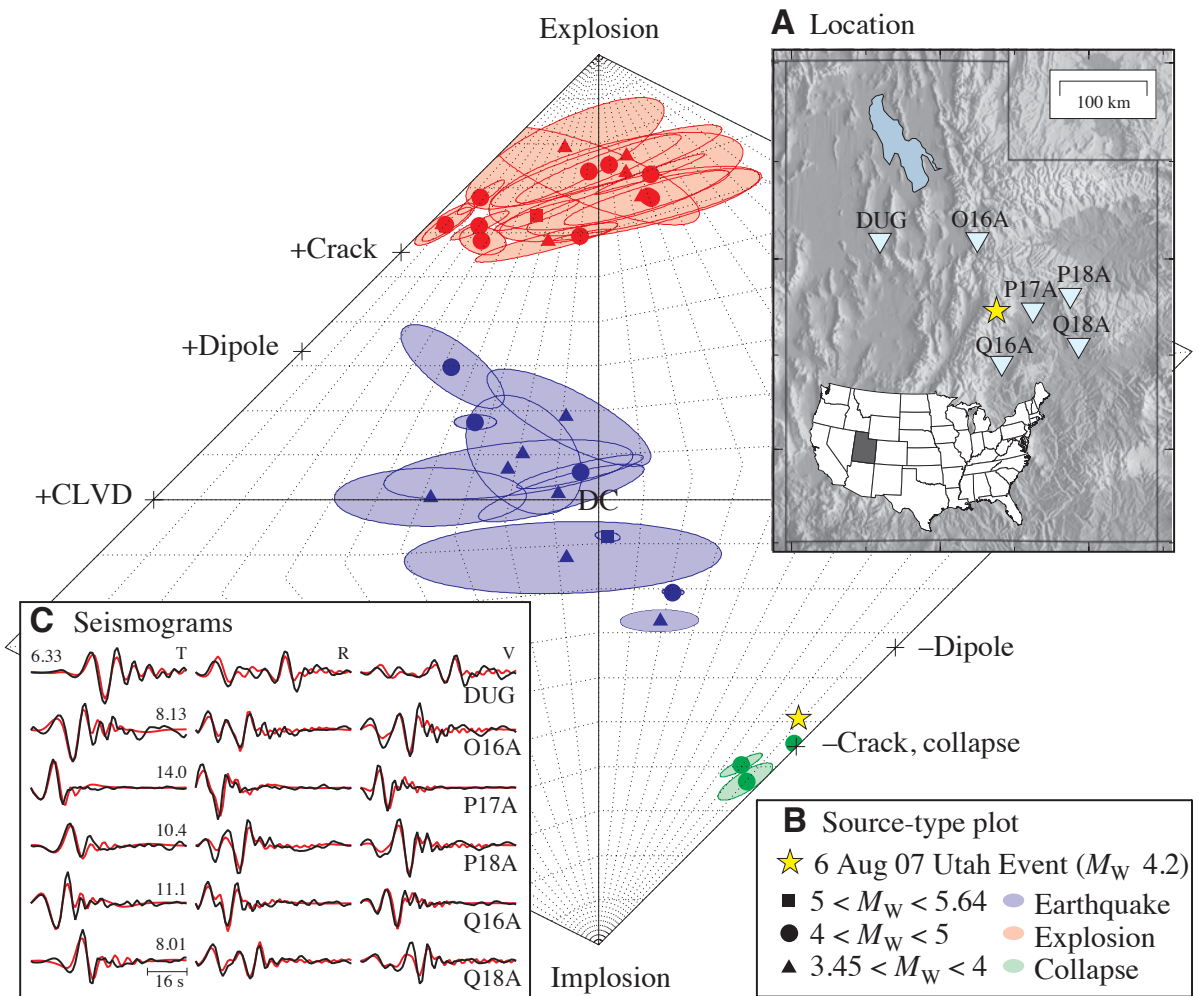
3620

3621 Figure 27: Top panels: Mining-induced earthquakes at Mentougou coal mine, Beijing, (a)
 3622 events $M > 1.0$, (b) events $M > 3.0$ and the maximum event magnitudes. Bottom panels: same
 3623 as top panels except for the Fushun coal mine field in Liaoning Province [from Li *et al.*,
 3624 2007].

3625

3626

3627



3628

3629

3630 Figure 28: (A) Locations of the 6 August 2007 Crandall mine, Utah, earthquake and six of
 3631 the closest USArray and Advanced National Seismic System (ANSS) seismic stations. (B)
 3632 Source-type plot showing separation of populations of earthquakes, explosions, and
 3633 collapses. Yellow star shows the focal mechanisms solution. (C) Observed seismograms
 3634 (black) compared to synthetics (red) for the solution, which is similar to a horizontal closing
 3635 crack (B). The maximum displacement (10^{-7} m) of each set of tangential (T), radial (R), and
 3636 vertical (V) observations is given [from Dreger *et al.*, 2008].

3637

3638

3639

3640
3641

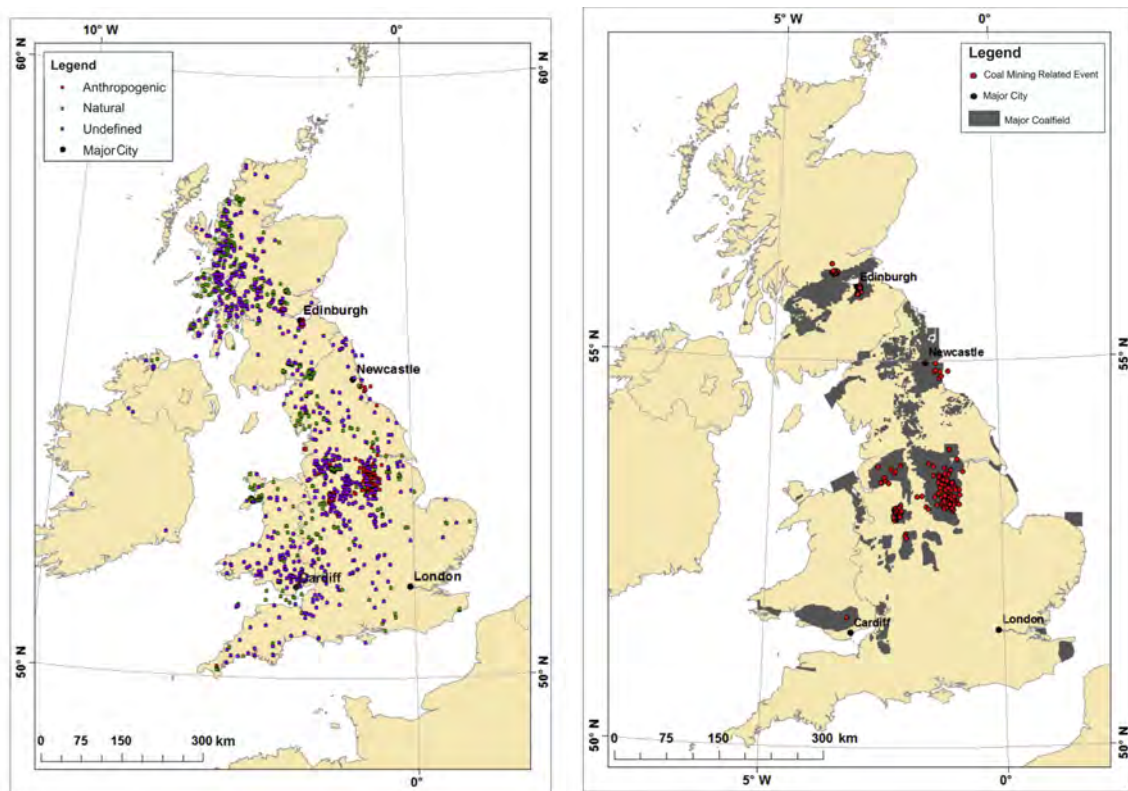
3642 Figure 29: Aerial view of surface imprints of Neolithic flint mining at Grimes Graves,
3643 Suffolk, England¹⁶.

3644

3645

¹⁶ www.english-heritage.org.uk

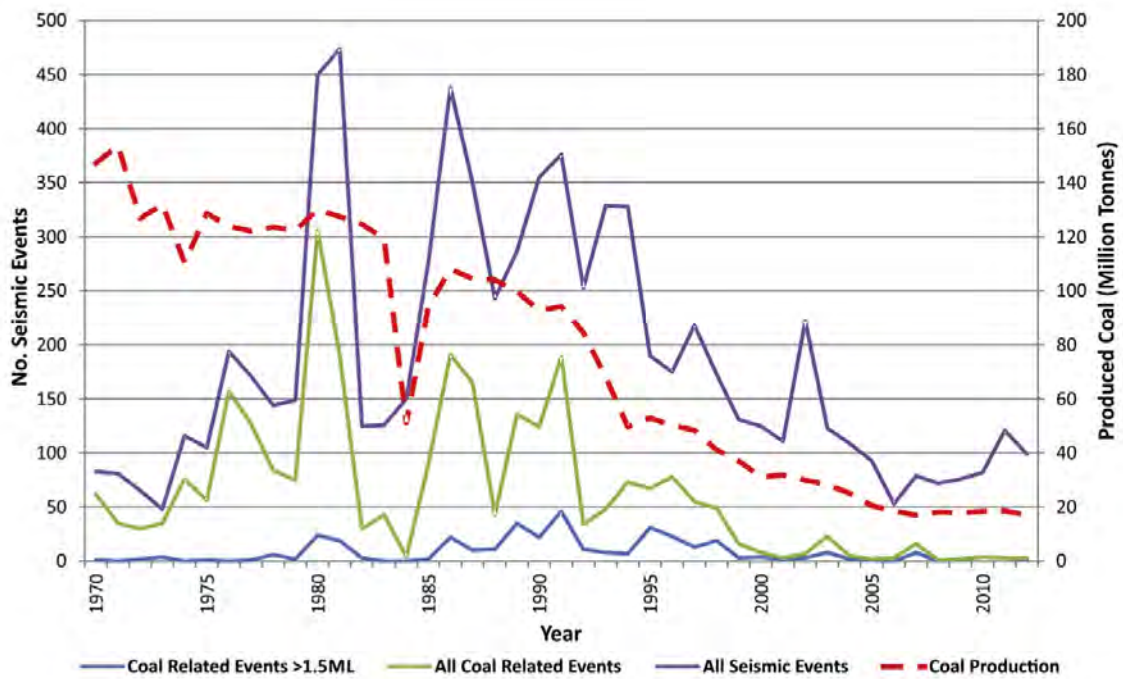
3646

3647
3648

3649 Figure 30: For earthquakes with $M_L \geq 1.5$ for the period 1970-2012, left: map of the UK
 3650 showing 1769 onshore seismic events categorized as anthropogenic (red), natural (green) and
 3651 undefined (purple). Right: 369 events postulated to be induced by coal mining. These
 3652 correlate spatially with major coalfields (dark gray) [from Wilson *et al.*, 2015].

3653
3654

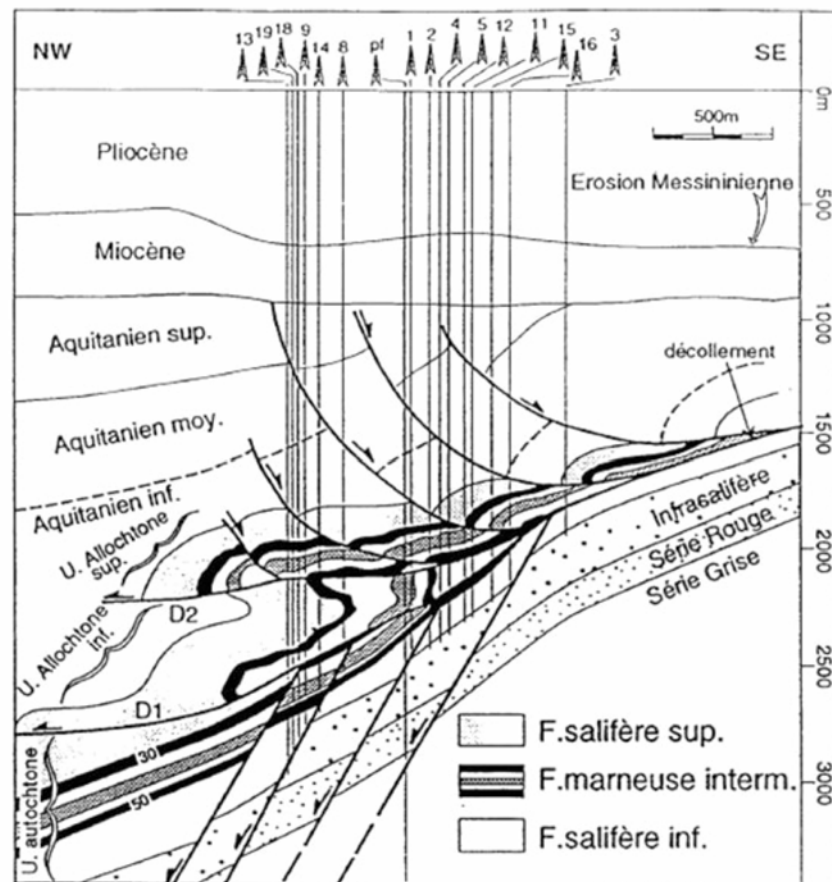
3655

3656
3657

3658 Figure 31: UK coal production (dotted red line) vs. numbers of earthquakes postulated to be
 3659 induced (blue line: $M_L \geq 1.5$, green line: all located earthquakes in the British Geological
 3660 Survey database) for the period 1970-2012. The effect of the miners' strike of 1984 can be
 3661 seen clearly in the drop in production and seismicity [from Wilson *et al.*, 2015].

3662
3663

3664



3665

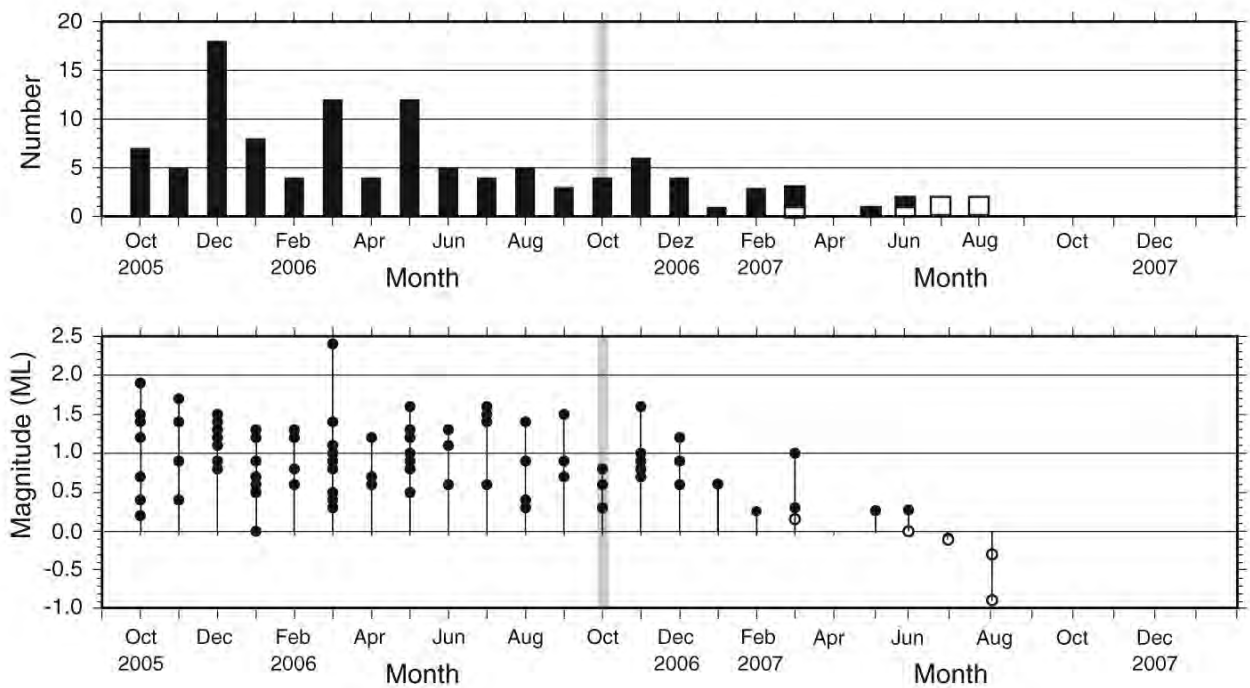
3666

3667 Figure 32: Geological cross-section of the Vauvert, France, solution-mined salt deposit [from
 3668 Godano *et al.*, 2010].

3669

3670

3671



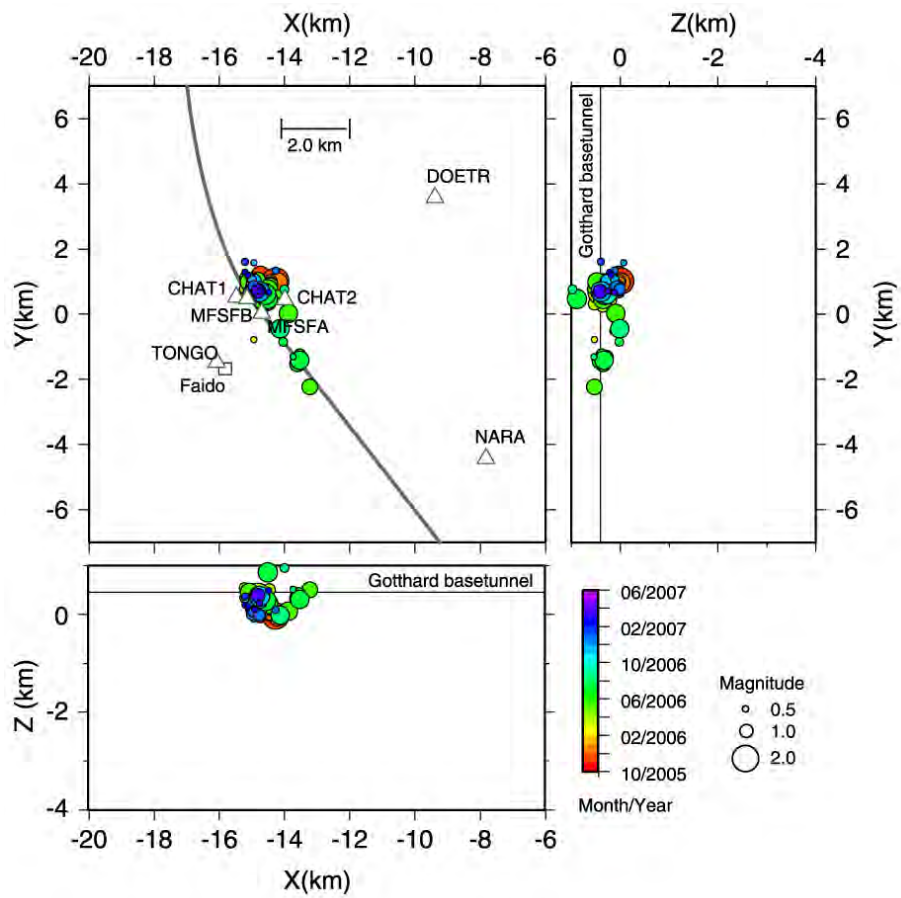
3672

3673

3674 Figure 33: Temporal evolution of the seismicity observed in the vicinity of the multi-function
 3675 station Faido, Switzerland, October 2005 - December 2007. Top: number of events per
 3676 month. Bottom: local magnitudes. Open circles: earthquakes for which magnitude could only
 3677 be computed using data from one station. Gray band marks the end of the excavation work
 3678 [from Husen *et al.*, 2012].

3679

3680



3681

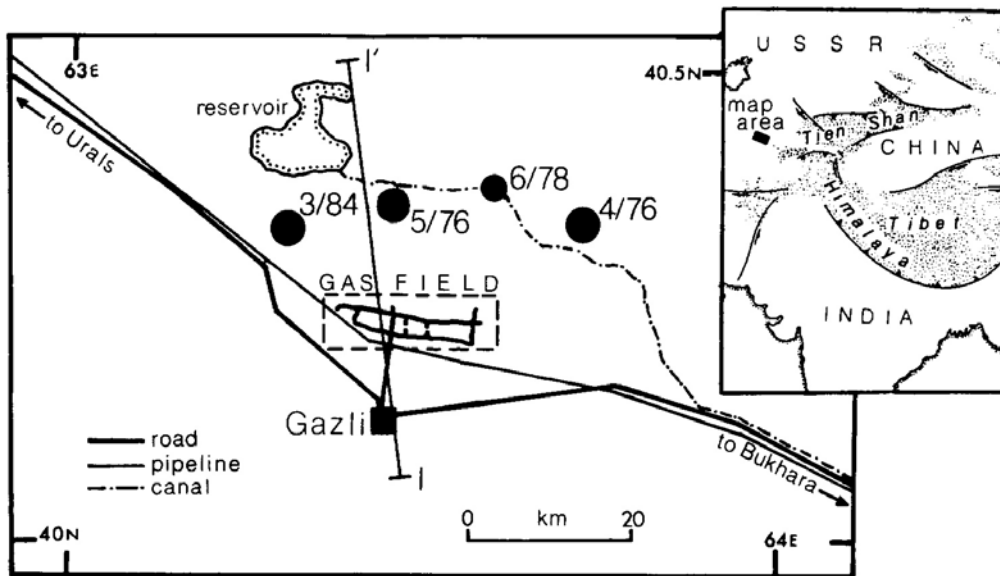
3682

3683 Figure 34: Hypocenter locations of earthquakes in the vicinity of the multi-function station
 3684 Faido, Switzerland, October 2005 - June 2007 [from Husen *et al.*, 2012].

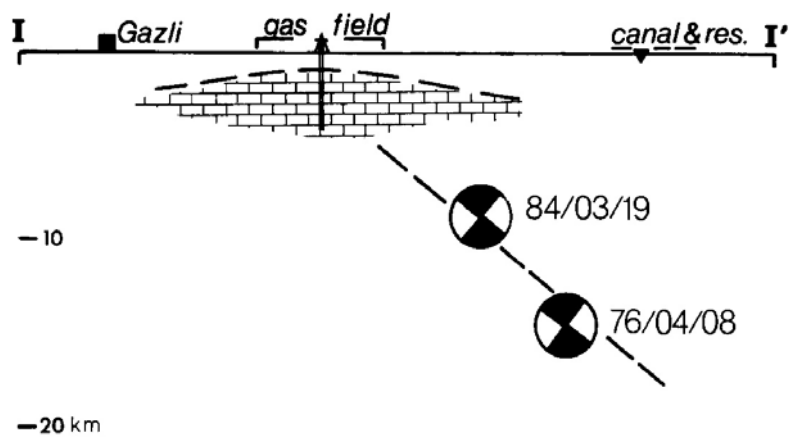
3685

3686

3687



3688



3689

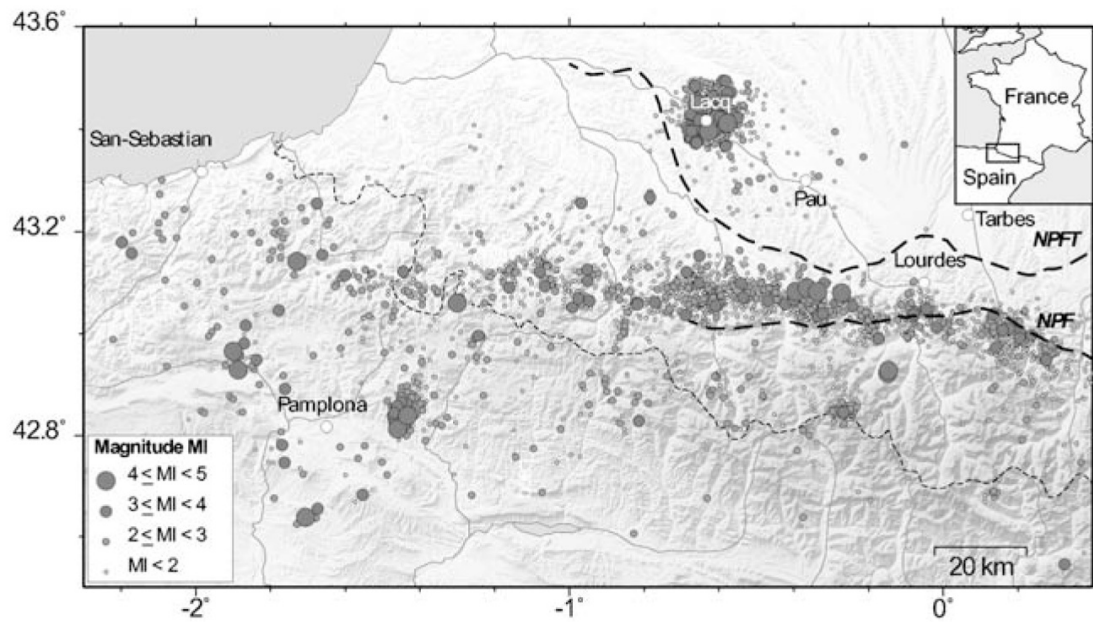
3690

3691 Figure 35: Top: Map of the Gazli, Uzbekistan, area showing epicenters of the three M ~7
 3692 earthquakes in 1976 and 1984, and the M 5.7 earthquake in 1978. Bottom: Cross-section with
 3693 hypocenters projected at their distance from the town of Gazli, with focal mechanisms of the
 3694 M_S 7.0 events of 8 April 1976 and 19 March 1984. The fault plane (dashed line) is deduced
 3695 from geodetic data [from Simpson & Leith, 1985].

3696

3697

3698



3699

3700

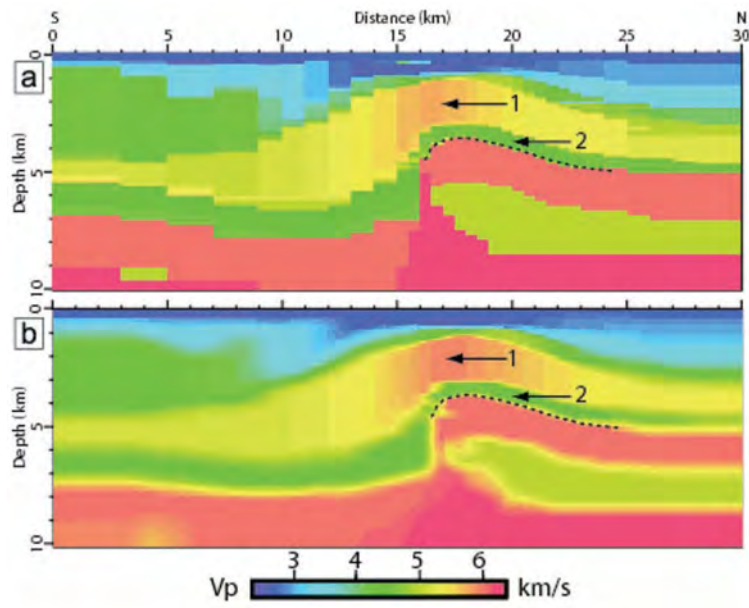
3701 Figure 36: Seismicity of southwest France for 1997–2005¹⁷, along with locally recorded
 3702 earthquakes in the Lacq, France, area. NPF: North Pyrenean Fault. NPFT: North Pyrenean
 3703 Frontal Thrust [from Bardainne *et al.*, 2008].

3704

3705

¹⁷ <http://www.omp.obs-mip.fr/rssp/sismicite`pyrenees/bulletin/bulletin.html>

3706

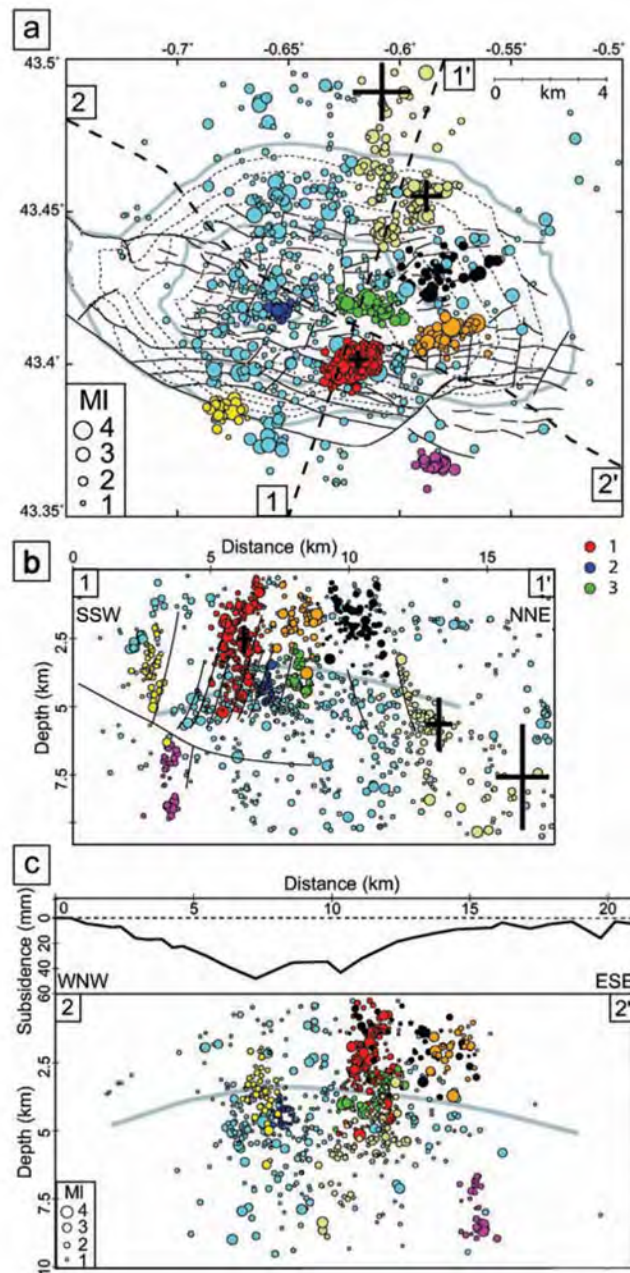
3707
3708

3709 Figure 37: N-S vertical cross-section of the three-dimensional P -wave velocity model for the
 3710 Lacq, France, area from surface seismic and well data. Dotted line: top of gas reservoir; 1:
 3711 upper-Cretaceous reef; 2: ductile Cretaceous marls [from Bardainne *et al.*, 2008].

3712

3713

3714



3715

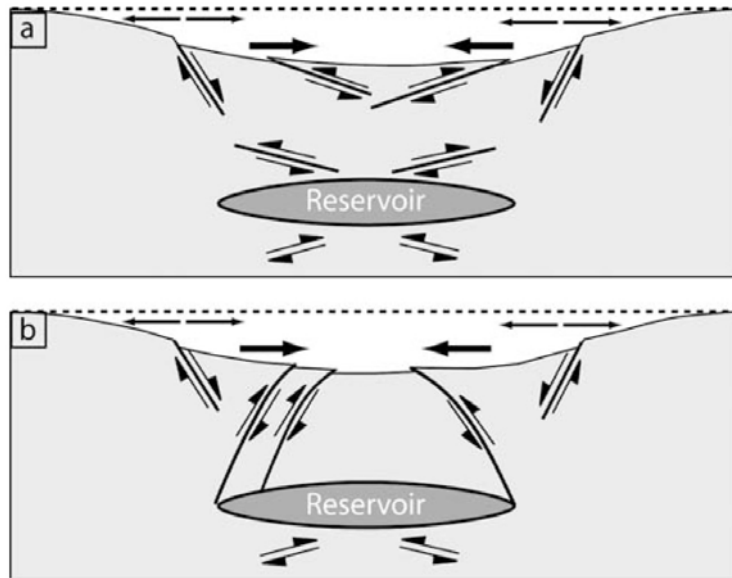
3716

3717 Figure 38: Seismicity in the Lacq Gasfield, France. (a) Map view and location of cross-
 3718 sections. (b) SSW-NNE cross-section and (c) WNW-ESE cross section. Colors: different
 3719 earthquake clusters; dashed and solid gray lines: isobaths of the gasfield; black lines; faults;
 3720 crosses: location uncertainties for three swarms [from Bardainne *et al.*, 2008].

3721

3722

3723



3724

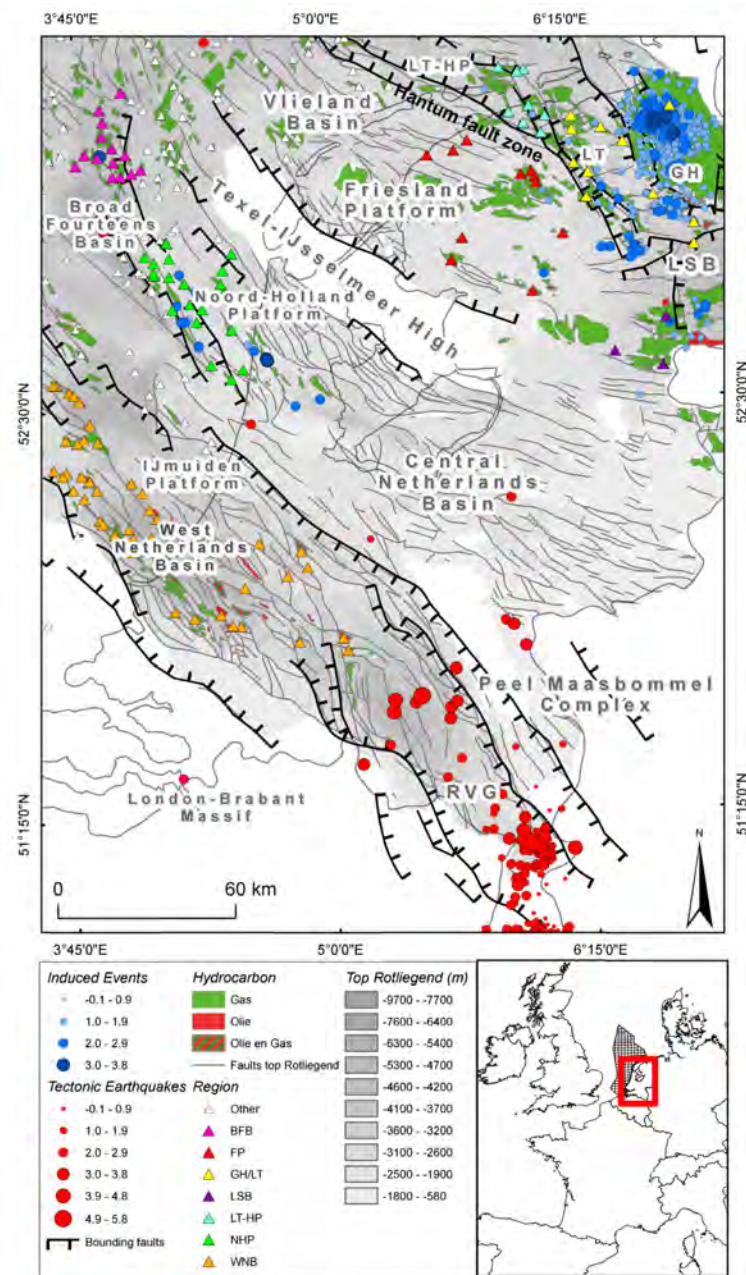
3725

3726 Figure 39: Deformation models of (a) Segall [1989], and (b) Odonne *et al.* [1999] for a
3727 depleting subsurface reservoir. Both models predict extensional deformation on the flanks
3728 and compressional deformation centrally in the field [from Bardainne *et al.*, 2008].

3729

3730

3731



3732

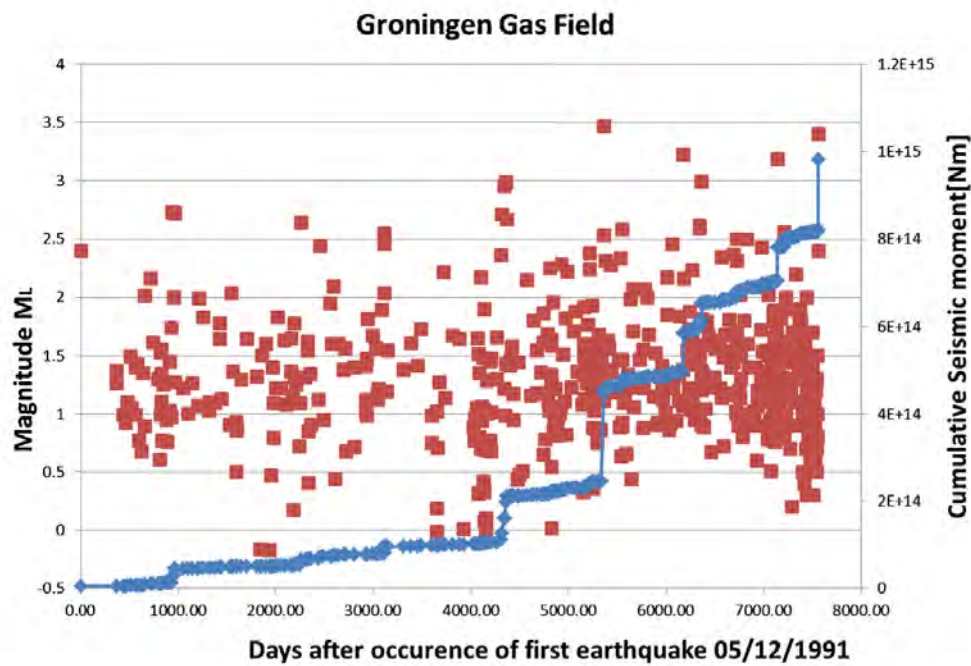
3733

3734 Figure 40: Tectonic map, seismicity, and hydrocarbon reservoirs in the Netherlands. Red
 3735 circles: natural seismicity; blue circles: induced seismicity; green: gas reservoirs; red:
 3736 oil reservoirs; solid lines: major fault zones; triangles: where leak-off tests have been performed.
 3737 BFB=Broad Fourteen Basin, FP=Friesland Platform, GH/LT=Groningen High/Lauwerszee
 3738 Trough, LSB=Lower Saxony Basin, LT-HP=Lauwerszee trough-Hantum Platform,
 3739 NHP=Noord Holland Platform, WNB=West Netherlands Basin, RVG=Roer Valley Graben,
 3740 PB=Peelrand Block, EL=Ems Low [from Van Wees *et al.*, 2014].

3741

3742

3743



3744

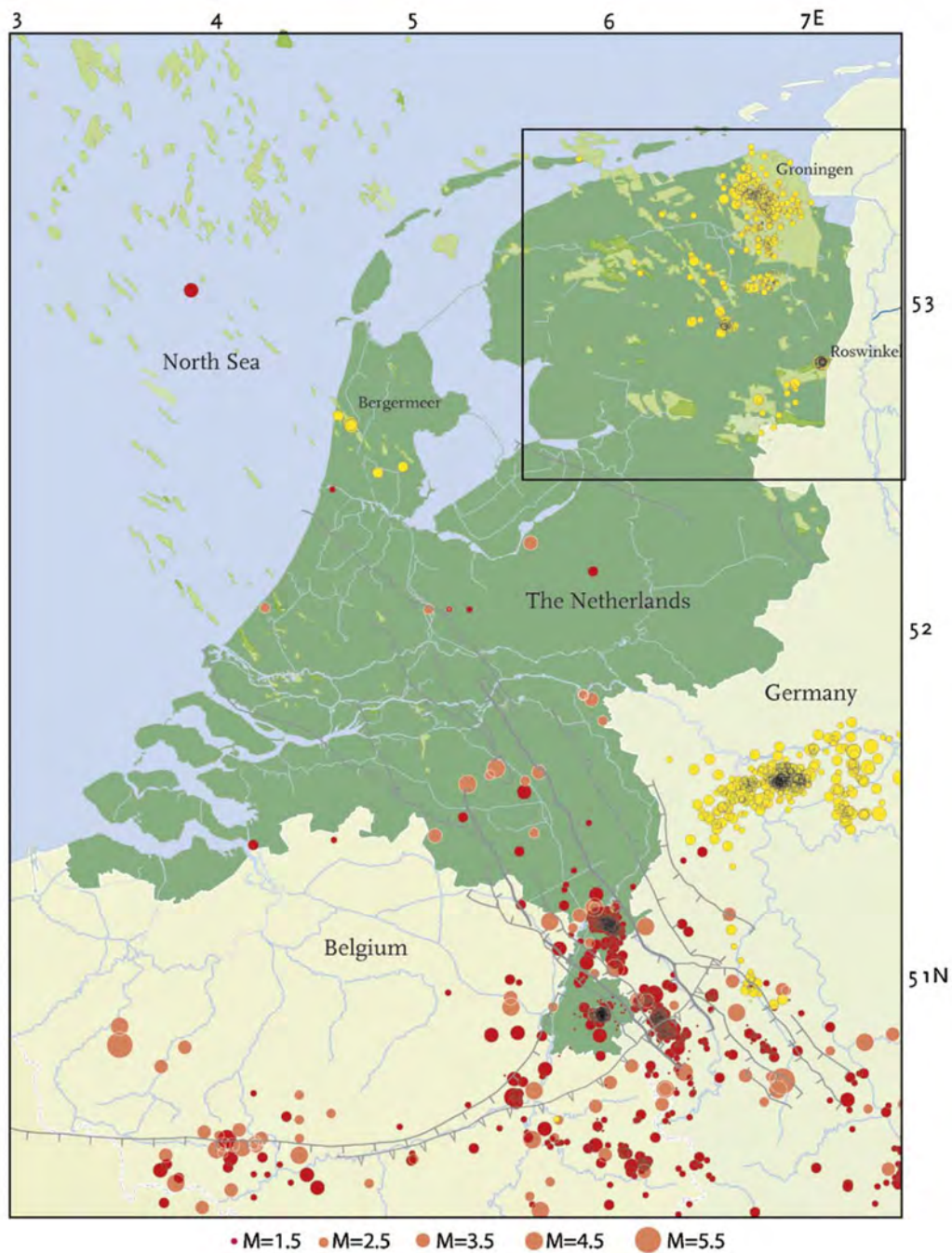
3745

3746 Figure 41: Magnitude of induced events in the Groningen Gasfield, Netherlands, 5
 3747 December, 1991 - 16 August, 2012, and cumulative seismic moment in Nm [from Van Wees
 3748 *et al.*, 2014].

3749

3750

3751



3752

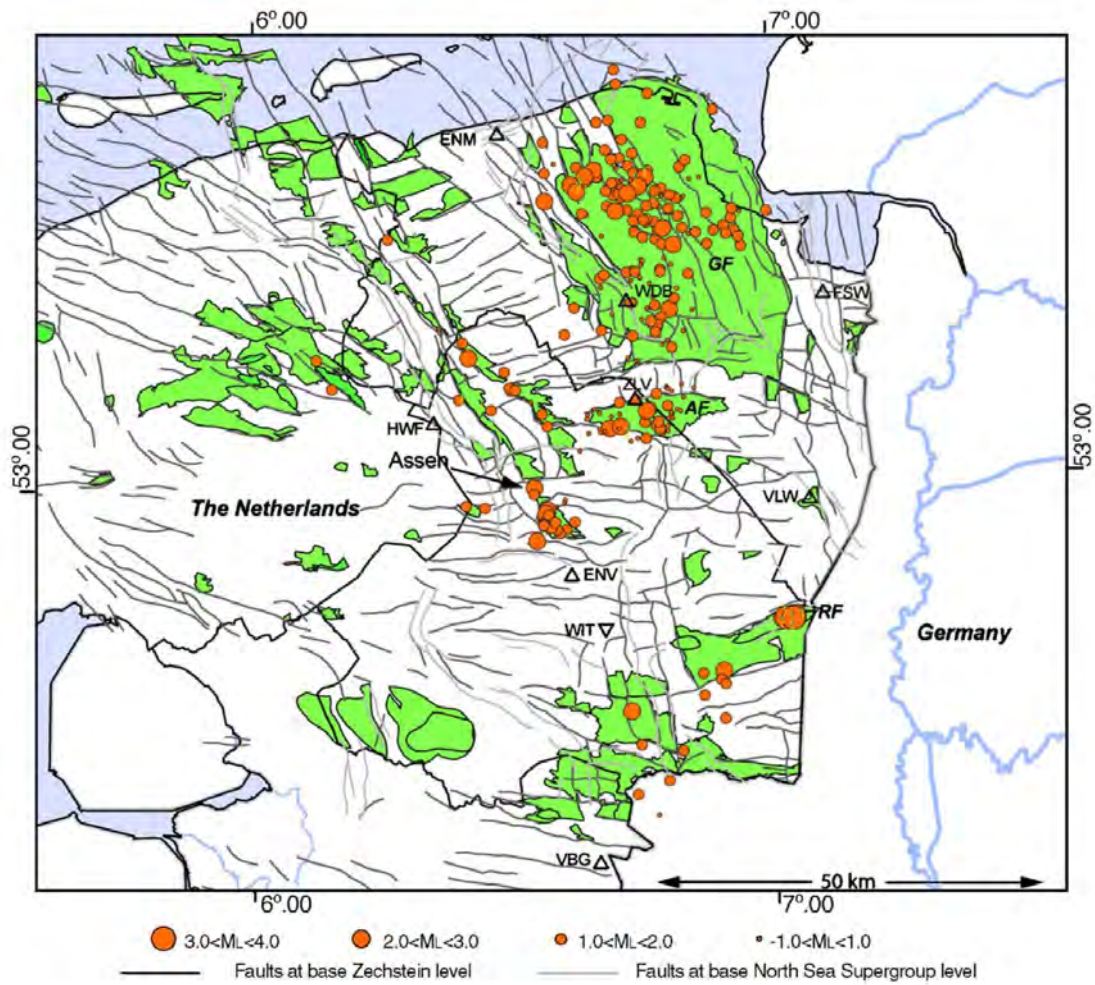
3753

3754 Figure 42: Seismicity in the Netherlands and surrounding region since 1900. Red circles:
 3755 natural tectonic earthquakes; yellow circles: suspected induced earthquakes (usually mining
 3756 or gas exploitation); gray solid lines: mapped faults in the upper-North-Sea formation; light
 3757 green: approximate contours of gasfield. Detail of boxed region shown in Figure 43 [from
 3758 van Eck *et al.*, 2006].

3759

3760

3761



3762

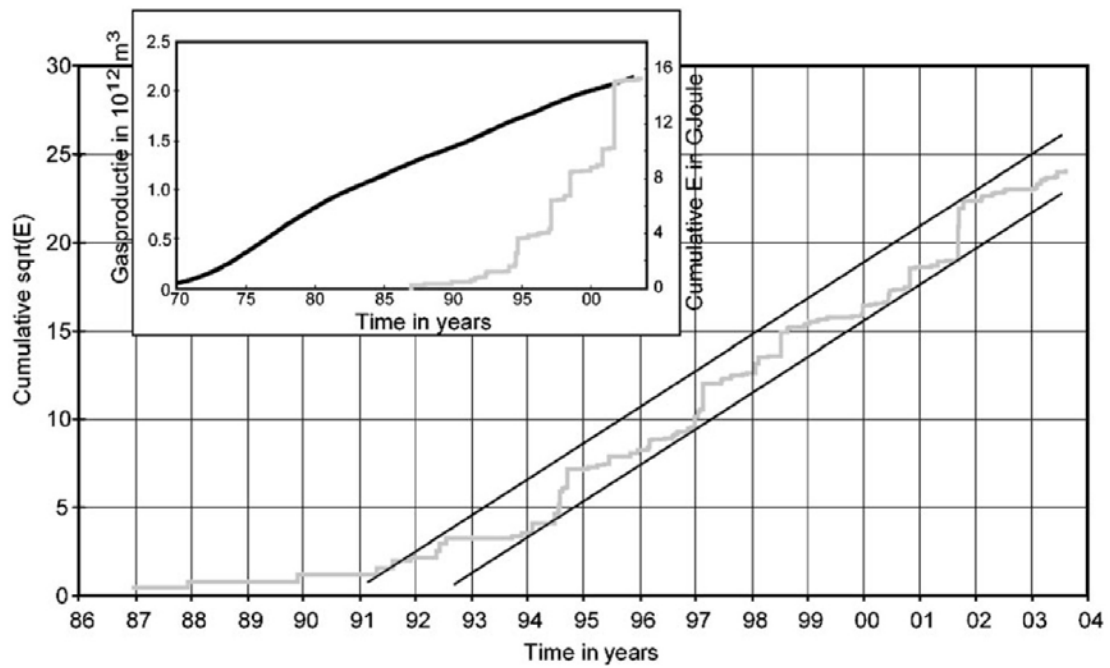
3763

3764 Figure 43: Map showing produced gasfields (green), major fault structures and seismicity
 3765 (orange dots) in the northeast Netherlands (boxed region of Figure 42). RF: Roswinkel Field;
 3766 GF: Groningen Field; EF: Eleveld Field; AF: Annerveen Field [from van Eck *et al.*, 2006].

3767

3768

3769

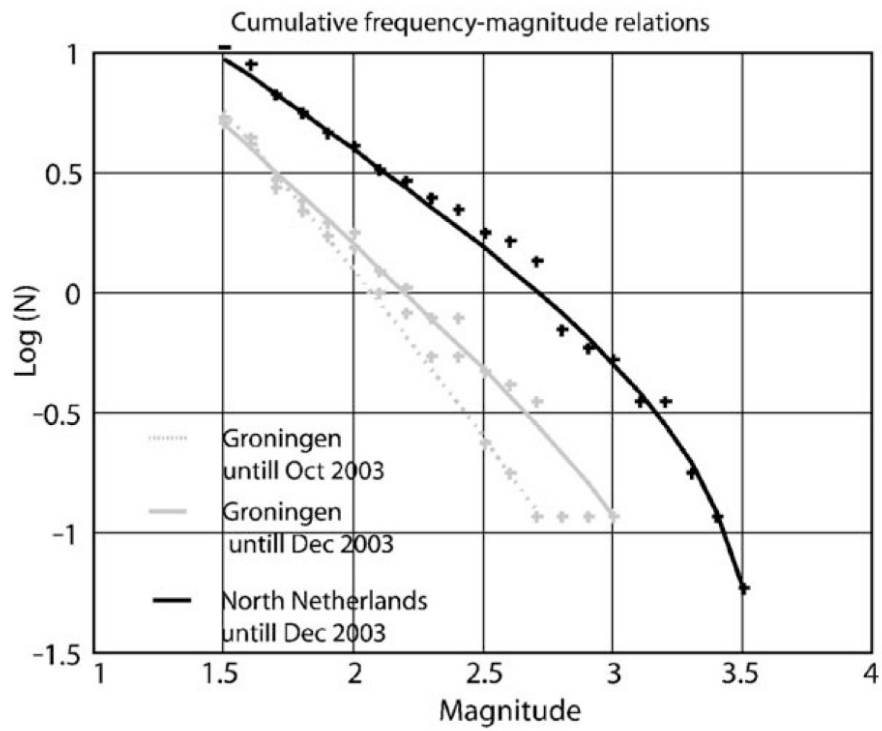
3770
3771

3772 Figure 44: For the Groningen Gasfield, Netherlands, cumulative square root of the seismic
 3773 energy (E) in GJ (light gray curve) of all earthquakes with $M \geq 1.5$ vs. time. Inset shows
 3774 cumulative seismic energy release (light gray) and cumulative gas production on land (black)
 3775 [from van Eck *et al.*, 2006].

3776

3777

3778



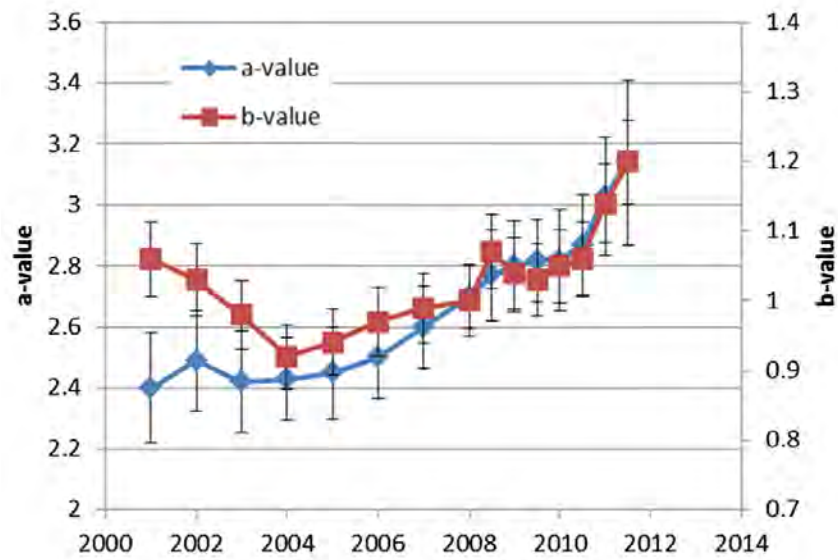
3779

3780 Figure 45: Cumulative annual frequency-magnitude relation for all seismicity thought to be
 3781 induced in the north Netherlands for the period 1986–2003 (black curve). The same
 3782 frequency-magnitude relation for all earthquakes in the Groningen Gasfield (gray curves).
 3783 Gray dashed curve excludes three events with $2.7 < M < 3.0$ that occurred October–
 3784 November 2003. Gray solid curve includes these events [from van Eck *et al.*, 2006].

3785

3786

3787



3788

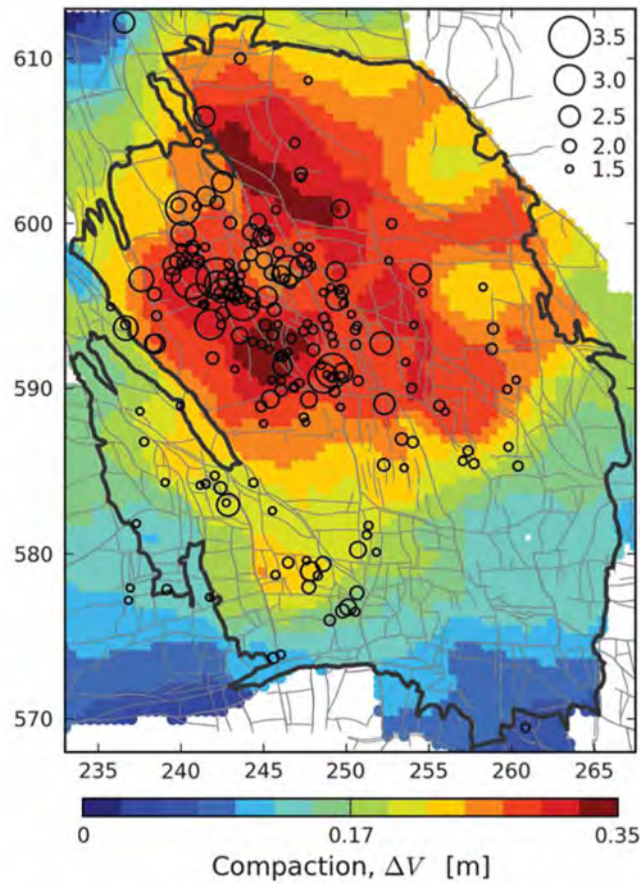
3789

3790 Figure 46: a and b -values of the Gutenberg-Richter relationship for seismicity in the
 3791 Groningen Gasfield, Netherlands, determined using a sliding time-window of three to five
 3792 years, to ensure sufficient events (> 50) in each data bin [from Van Wees *et al.*, 2014].

3793

3794

3795



3796

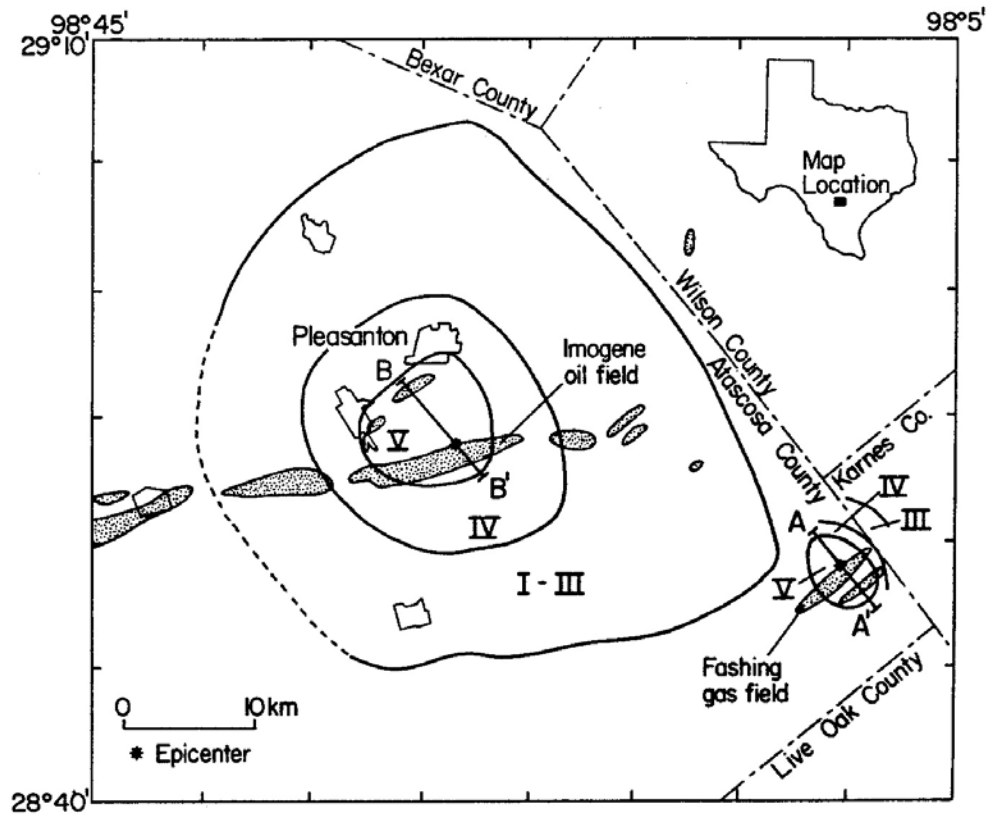
3797

3798 Figure 47: Earthquake epicenters for events with $M \geq 1.5$ for the period 1995-2012,
 3799 superimposed on a model of reservoir compaction for 1960-2012. Black line: perimeter of the
 3800 Groningen Gasfield; thin gray lines: faults close to the reservoir level. Map coordinates are
 3801 kilometers in the Dutch national triangulation coordinate system (Rijksdriehoek) [from
 3802 Bourne *et al.*, 2015].

3803

3804

3805



3806

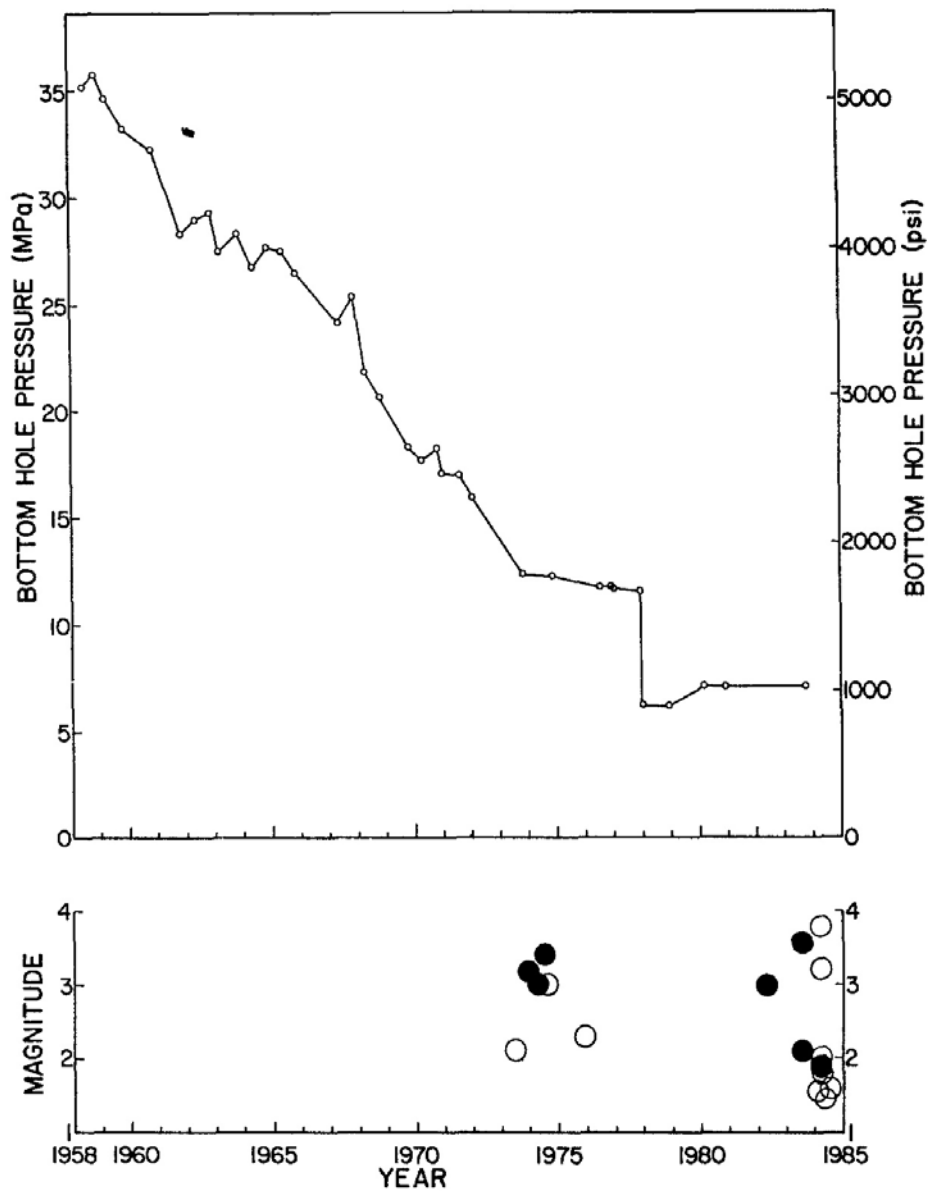
3807

3808 Figure 48: Oilfields and gasfields in the Imogene/Fashing area, south Texas, where
 3809 earthquakes are postulated to have been induced. Shaded regions are more prominent fields.
 3810 Isoseismals for the largest events on the Modified Mercalli intensity scale are shown [from
 3811 Pennington *et al.*, 1986].

3812

3813

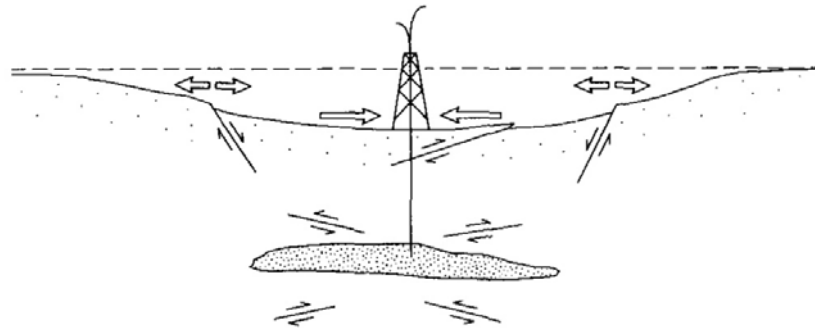
3814

3815
3816

3817 Figure 49: Pressure history of a well near the fault in the Fashing Gasfield along with known
 3818 earthquakes in the Fashing-Pleasanton area. Black dots: earthquakes from the Fashing area;
 3819 open circles: earthquakes from the Pleasanton (Imogene) area [from Pennington *et al.*, 1986].

3820
3821

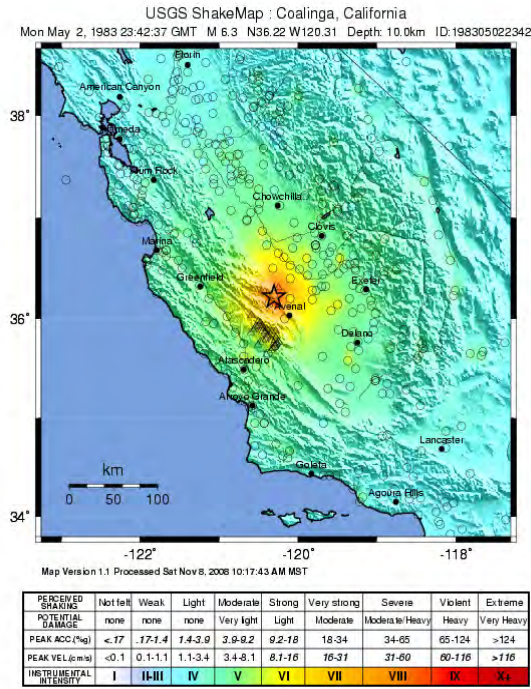
3822

3823
3824

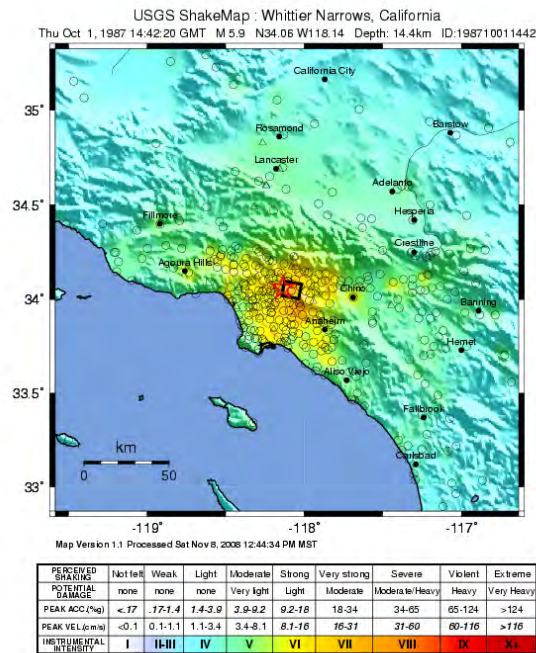
3825 Figure 50: Schematic cross section summarizing surface deformation and faulting associated
3826 with fluid withdrawal. Normal faults develop on the flanks of the field, as observed at the
3827 Goose Creek, Texas, Oilfield. Reverse faults develop above reservoirs as observed at
3828 Wilmington, Buena Vista Hills, the Pau Basin and beneath the Strachan Field [from Segall,
3829 1989].

3830

3831



3832



3833

3834

3835 Figure 51: U.S. Geological Survey shake maps¹⁸. Top: 1983 M_W 6.2 Coalinga, California

3836 earthquake, which injured 94 people and was felt throughout half the state. Bottom: 1987 M_L

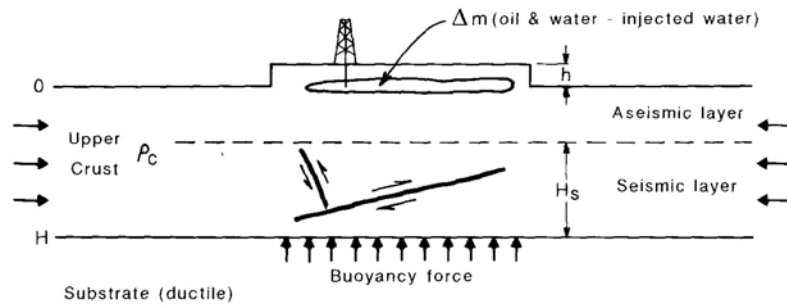
3837 5.9 Whittier Narrows, California earthquake, which killed six people.

3838

3839

¹⁸ <http://earthquake.usgs.gov/earthquakes/shakemap/>

3840



3841

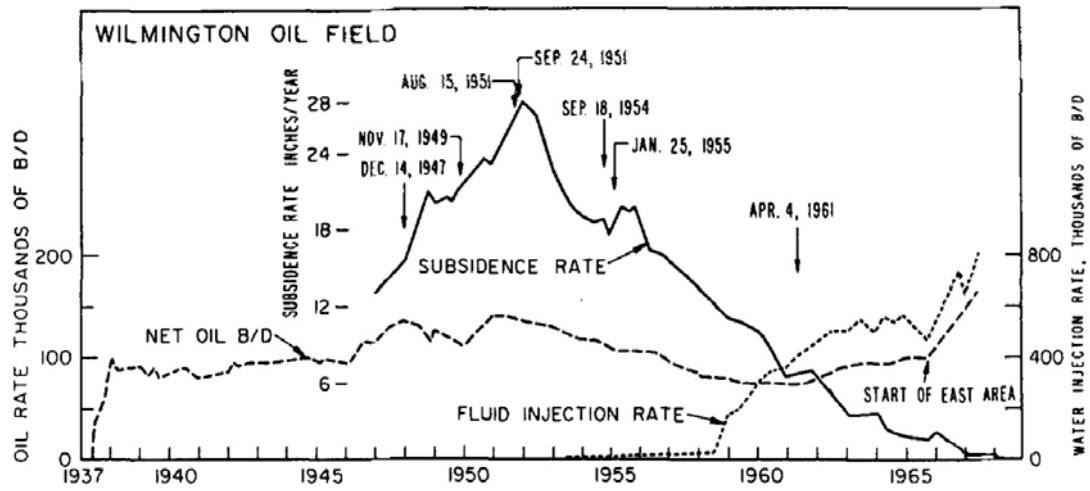
3842

3843 Figure 52: Schematic cross section showing proposed crustal response mechanism to oil
 3844 production. Mass removal results in a vertical force imbalance causing seismic deformation
 3845 in the seismogenic layer. This deformation, together with aseismic deformation in the
 3846 shallow crust, restores isostatic balance [from McGarr, 1991].

3847

3848

3849



3850

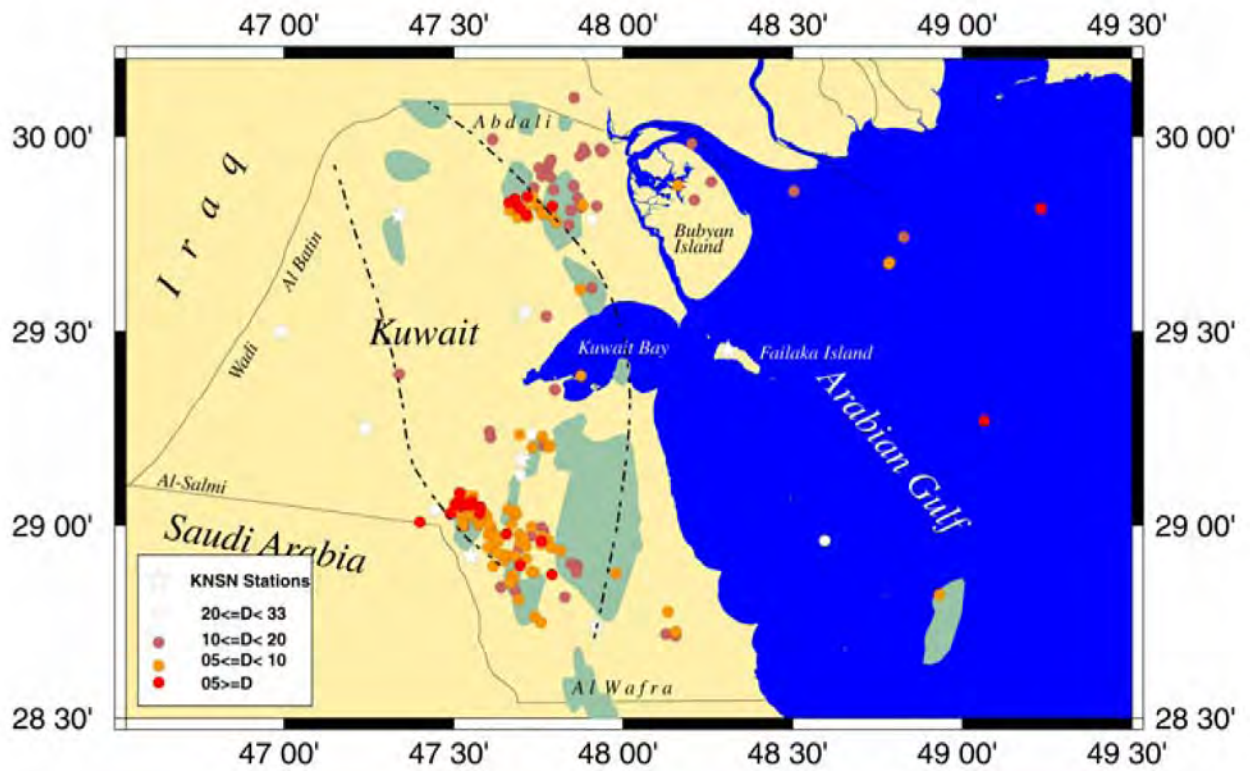
3851

3852 Figure 53: For the Wilmington Oilfield, California, subsidence rate in the center of the field,
 3853 oil production and water injection rates. Arrows show dates of major damaging earthquakes
 3854 [from Kovach, 1974].

3855

3856

3857



3858

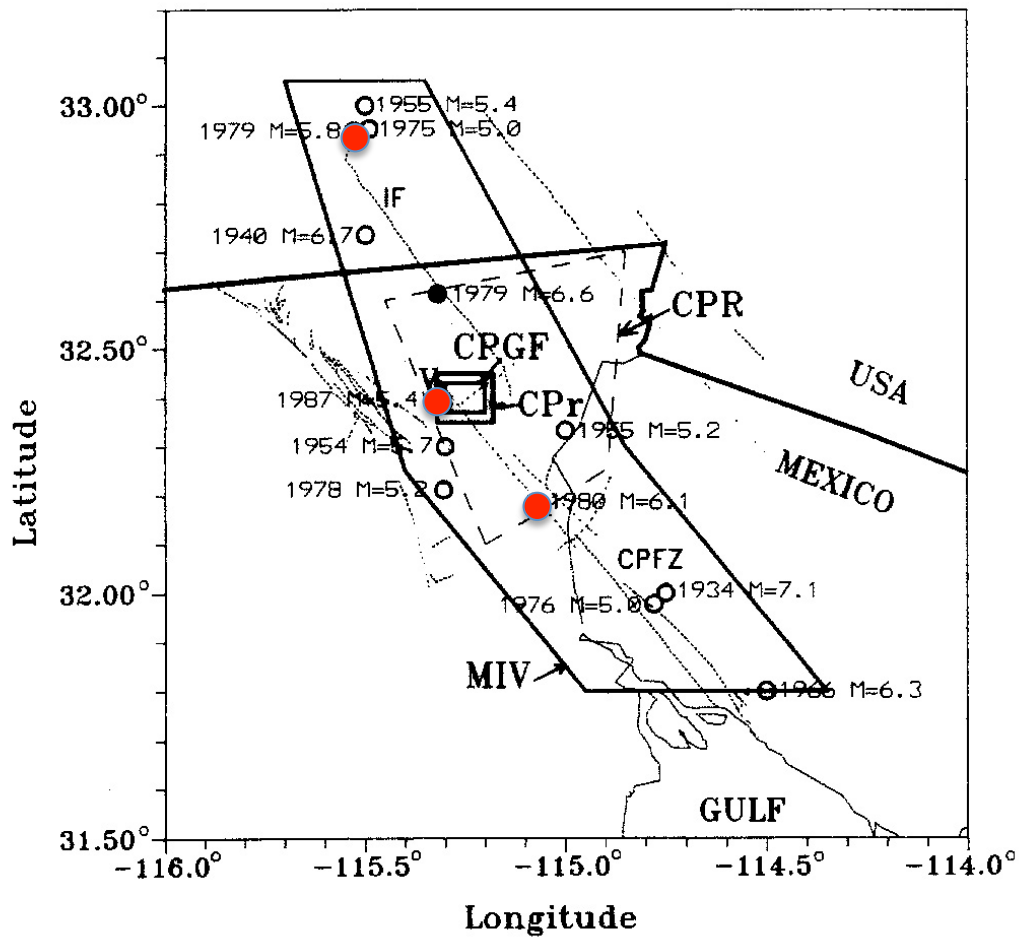
3859

3860 Figure 54: Seismicity of Kuwait for the period March 1997 - October 2007 [from Al-Enezi *et*
 3861 *al.*, 2008].

3862

3863

3864



3865

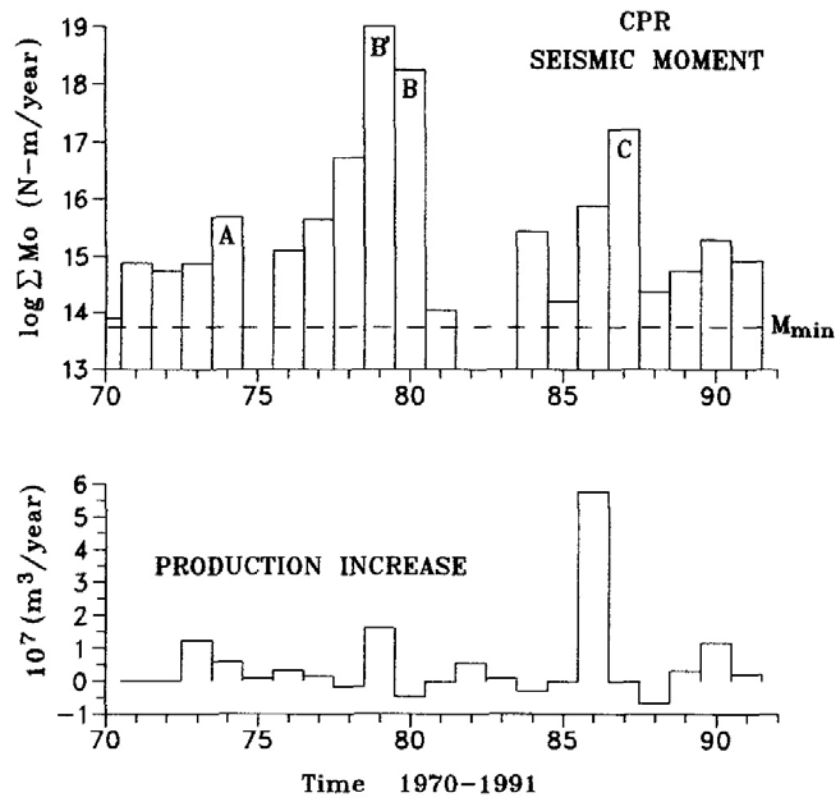
3866

3867 Figure 55: Map showing the Cerro Prieto geothermal field. Circles: earthquakes with $M \geq 5$;
 3868 red dots: earthquakes with $M > 6$; dotted lines: faults; IF: the Imperial fault; CPFZ: Cerro
 3869 Prieto fault zone; V: the Cerro Prieto volcano [from Glowacka & Nava, 1996].

3870

3871

3872



3873

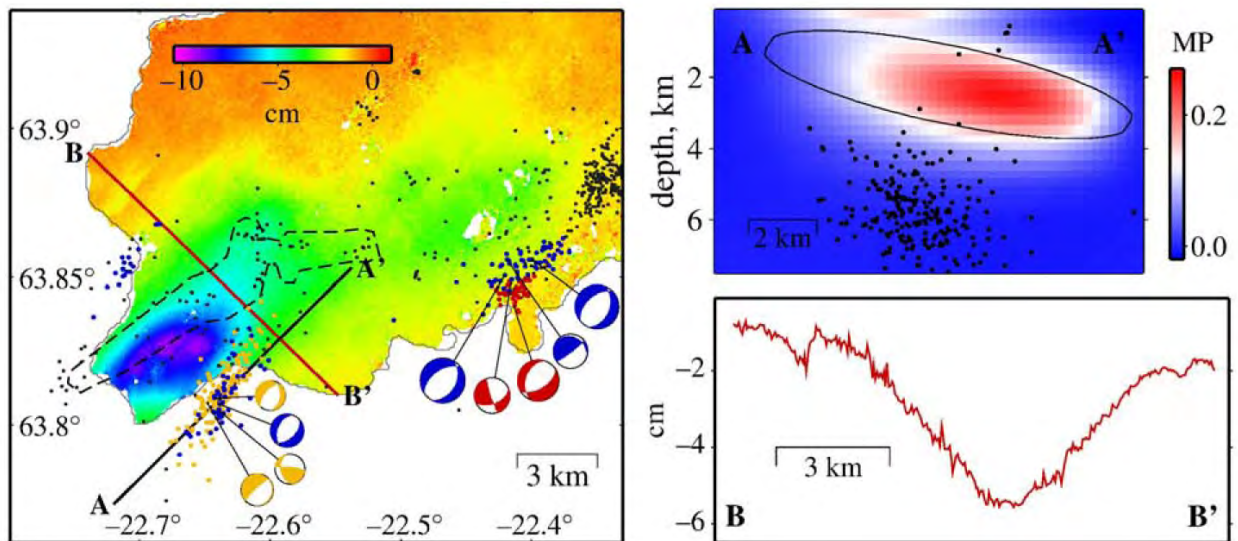
3874

3875 Figure 56: For the Cerro Prieto geothermal field, Mexico, top: annual seismic moment
 3876 release; bottom: production rate [from Glowacka & Nava, 1996].

3877

3878

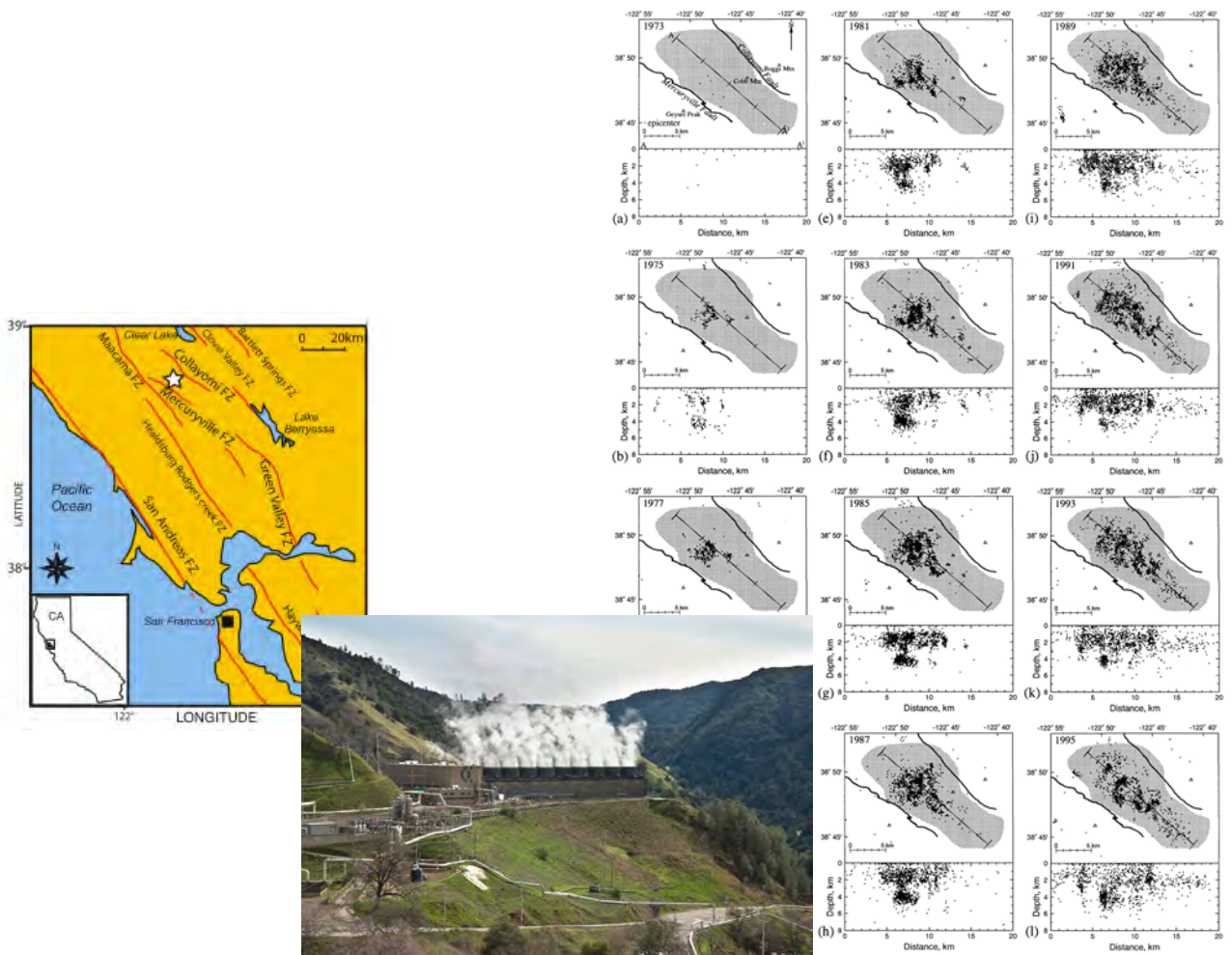
3879

3880
3881

3882 Figure 57: For the Reykjanes and Svartsengi geothermal fields, southwest Iceland, left: the
 3883 near-vertical radar displacement field June 2005 - May 2008, earthquake locations and focal
 3884 mechanisms. Black dots: background events. Distinct swarm events are shown for 2006
 3885 (orange), 2007 (red) and 2008 (blue). Stippled outline: location of the 1972 swarm activity
 3886 from Klein *et al.* [1977]. Top right: profile AA' shows the predicted change in Coulomb
 3887 failure stress for normal slip on NE-SW-trending fault planes, computed using an elastic half-
 3888 space ellipsoidal source model for subsidence around the Reykjanes geothermal field. Bottom
 3889 right: profile BB' shows the observed near-vertical radar displacement across the Reykjanes
 3890 subsidence bowl [from Keiding *et al.*, 2010].

3891
3892

3893



3894

3895

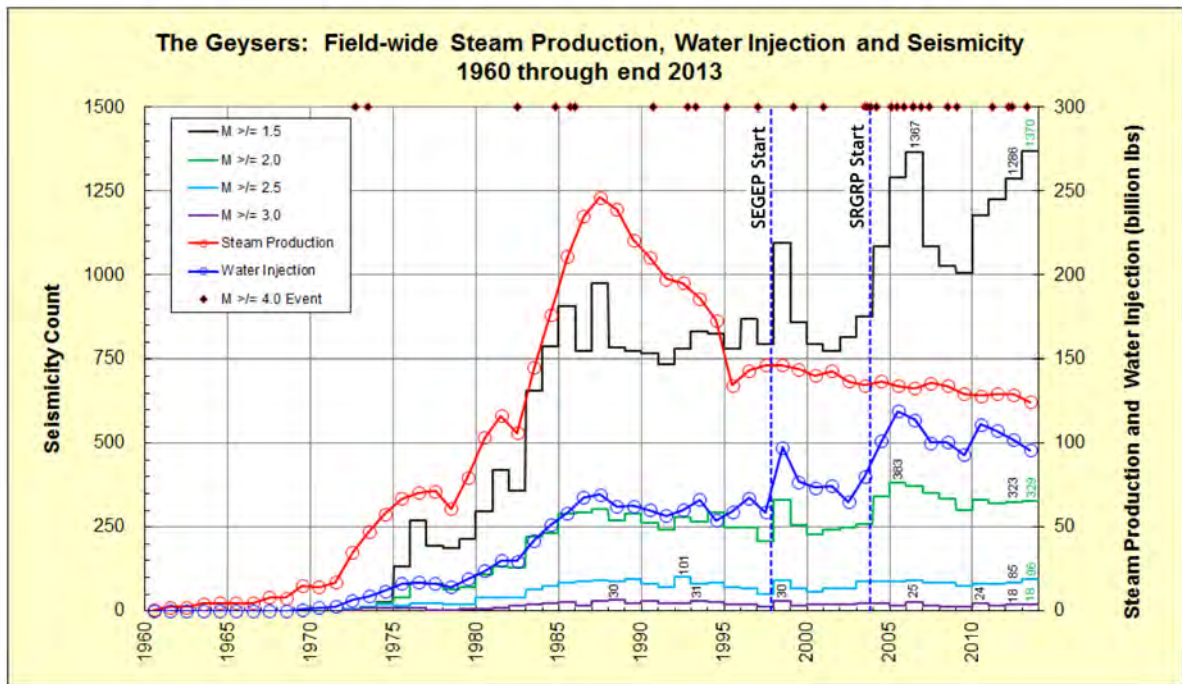
3896 Figure 58: The Geysers geothermal field, California. Left: regional map showing location of
 3897 the field. Middle: McCabe Units 5 and 6 at The Geysers¹⁹. Right: maps of seismicity at The
 3898 Geysers at biannual intervals from 1973 to 1995. Locations are from the Northern California
 3899 Seismic Network catalogue for earthquakes with $M > 1.2$. Gray area: steam field. Line shows
 3900 line-of-section for depth sections below each map [from Ross *et al.*, 1999].

3901

3902

¹⁹ <http://www.energy.ca.gov/tour/geysers/>

3903



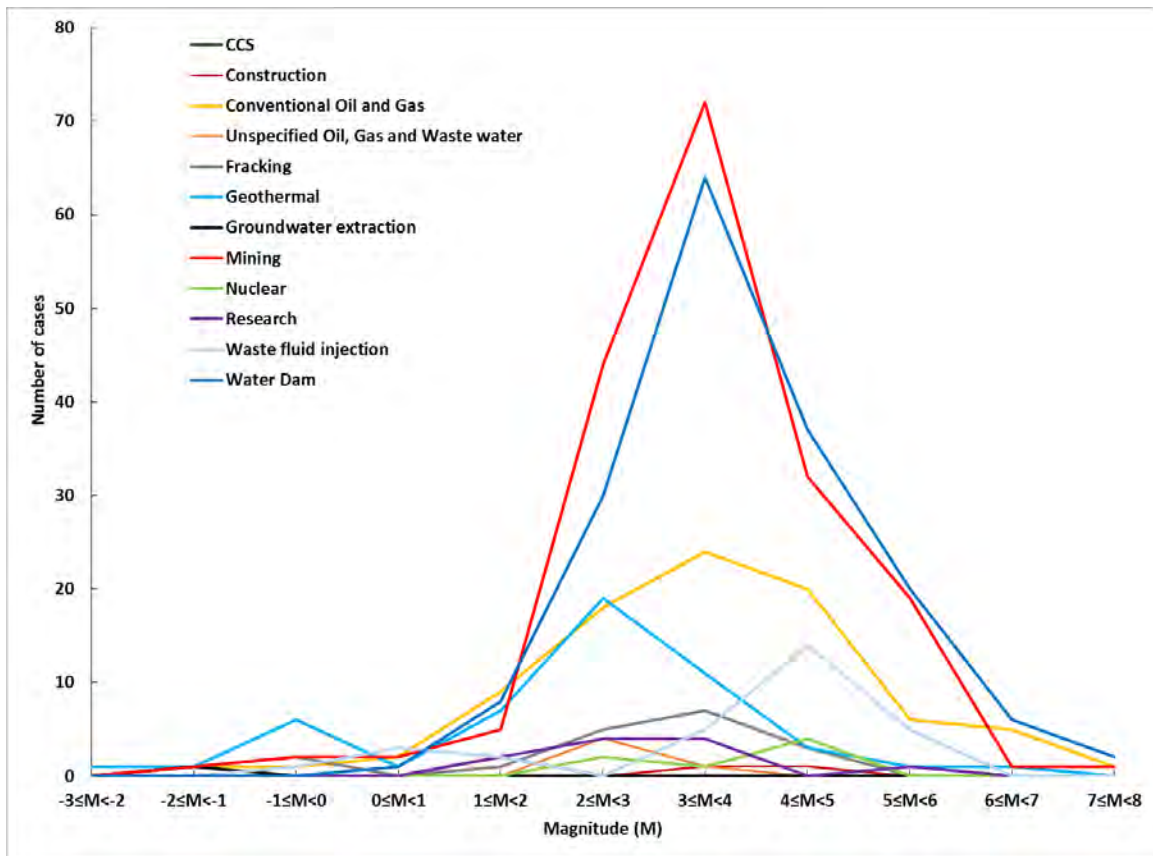
3904
3905

3906 Figure 59: Yearly field-wide steam production, water injection and seismicity 1960-2013.
3907 Earthquakes with $M \geq 4$ are indicated as red diamonds along the top boundary of the graph
3908 [from Hartline, 2014].

3909

3910

3911



3912

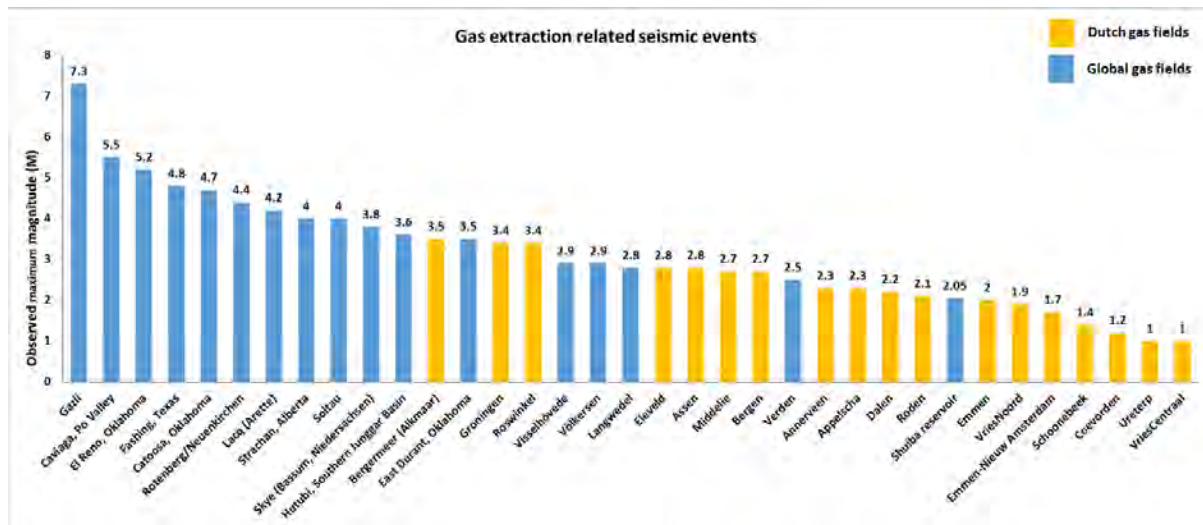
3913

3914 Figure 60: Number of cases reported for projects of various types vs. M_{MAX} for the 562 cases
 3915 for which data are available.

3916

3917

3918



3919

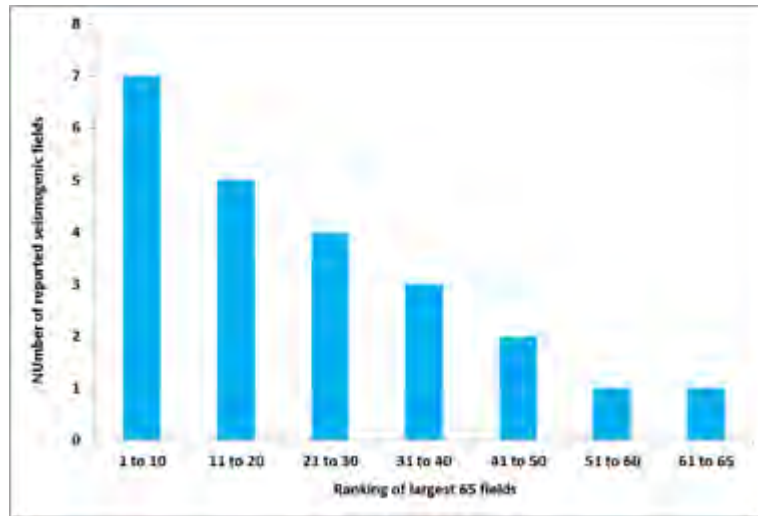
3920

3921 Figure 61: M_{MAX} for seismicity postulated to be induced by the extraction of natural gas at
 3922 the 35 fields where this parameter is reported. The Hutubi, northwest China case is associated
 3923 with both extraction and storage [Tang *et al.*, 2015].

3924

3925

3926



3927

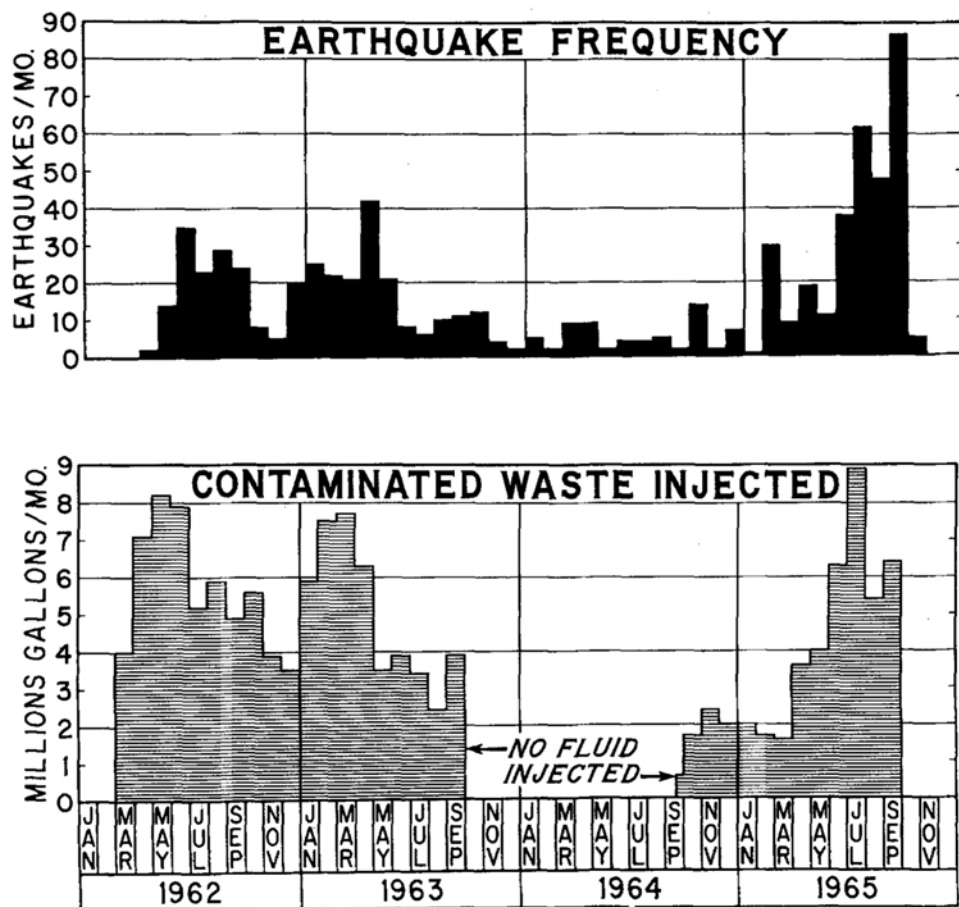
3928

3929 Figure 62: Number of reports of induced seismicity vs. size of field for the 65 largest global
3930 power-producing geothermal fields in groups of 10.

3931

3932

3933



3934

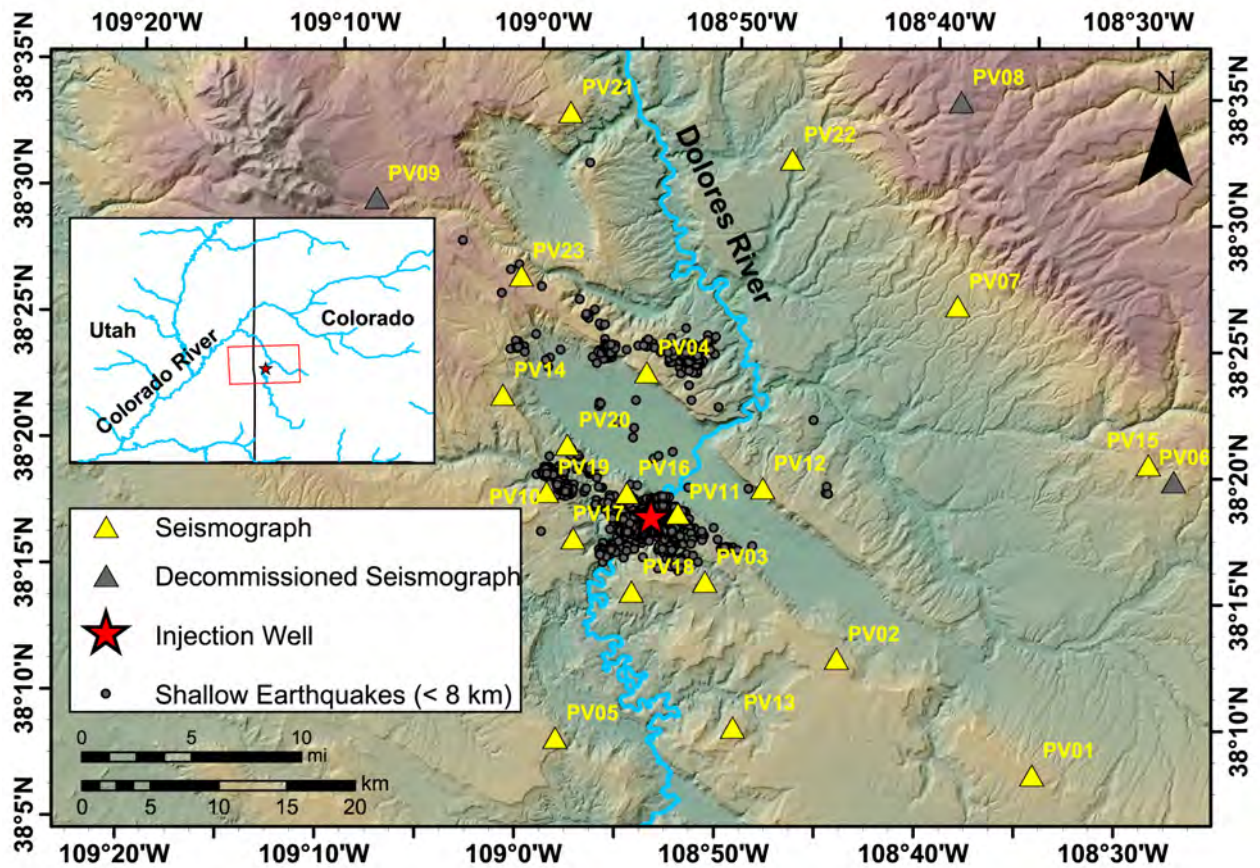
3935

3936 Figure 63: Top: Earthquake frequency. Bottom: injection rate at the Rocky Mountain Arsenal
 3937 well, Colorado [Healy *et al.*, 1968].

3938

3939

3940



3941

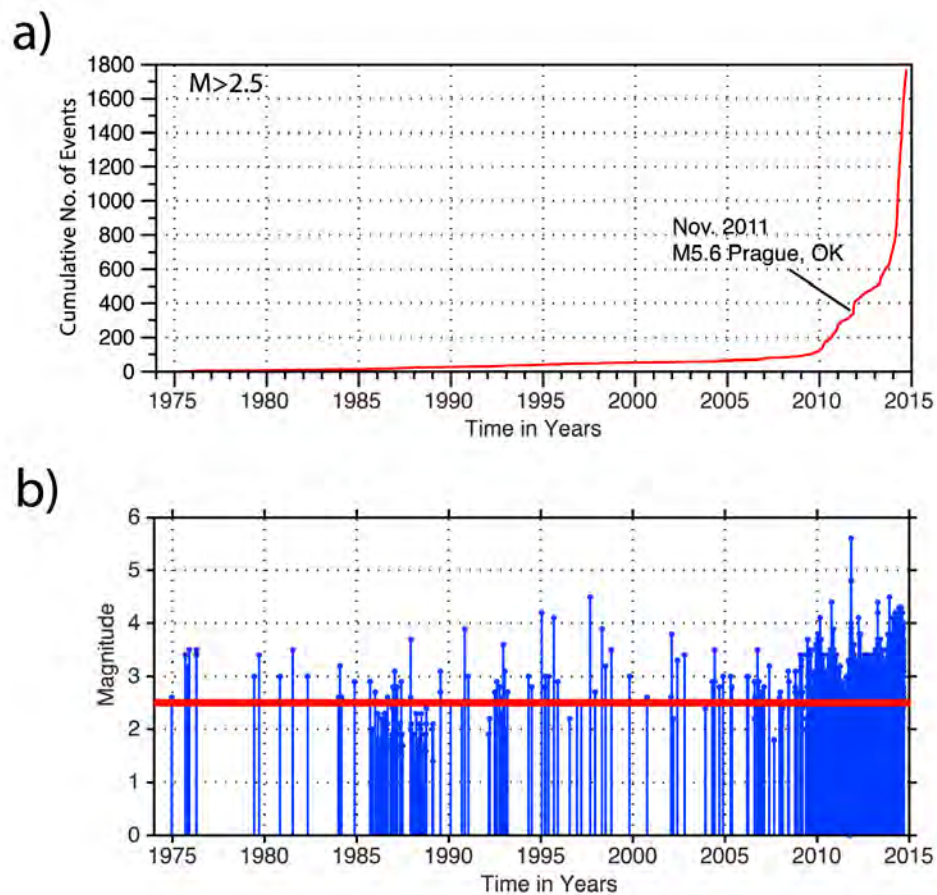
3942

3943 Figure 64: The region around Paradox Valley, Colorado (the northwest-oriented depression).
 3944 Yellow triangles: seismic stations; gray circles: earthquakes thought to be induced by brine
 3945 injections [from Yeck *et al.*, 2015].

3946

3947

3948



3949

3950

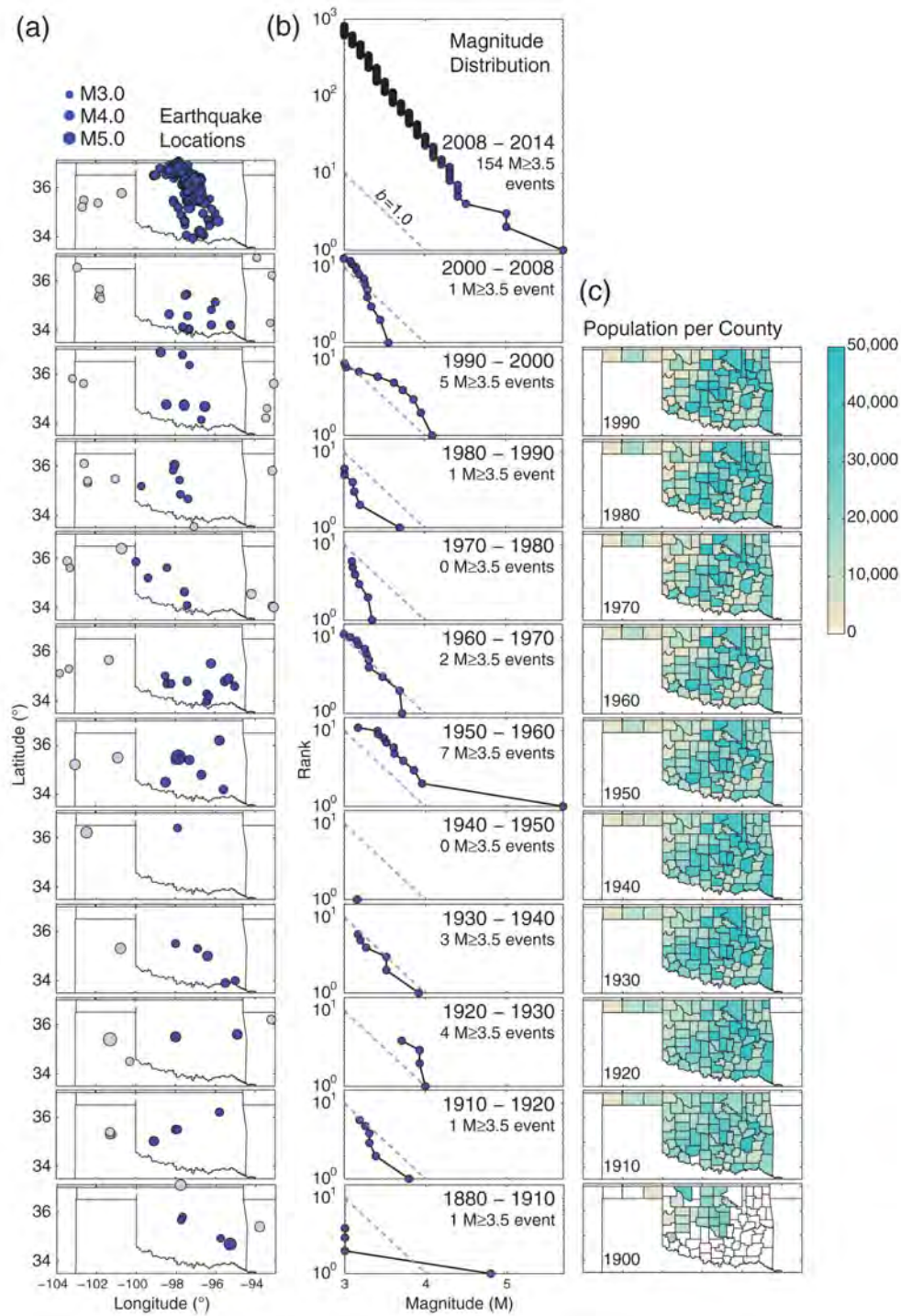
3951 Figure 65: Earthquakes recorded on the National Earthquake Information Center (NEIC)²⁰
 3952 system for the period 1975 through 2014. a) Cumulative seismicity in Oklahoma with $M >$
 3953 2.5. b) Earthquake magnitudes [from McNamara *et al.*, 2015].

3954

3955

²⁰ <http://earthquake.usgs.gov/contactus/golden/neic.php>

3956



3957

3958

3959

3960

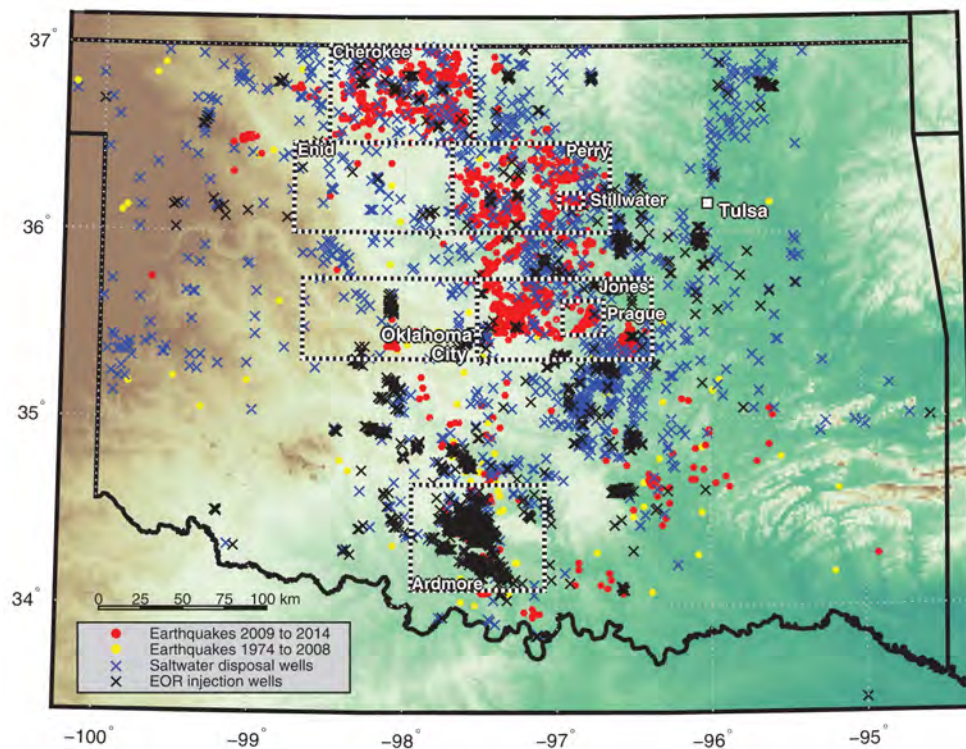
3961

Figure 66: Oklahoma seismicity. Left panels: Earthquake locations: blue—Oklahoma, gray—neighboring states. Centre panels: magnitudes plotted cumulatively 1880 - 2014. Right panels: human population by county [from Hough & Page, 2015].

3962

3963

3964



3965

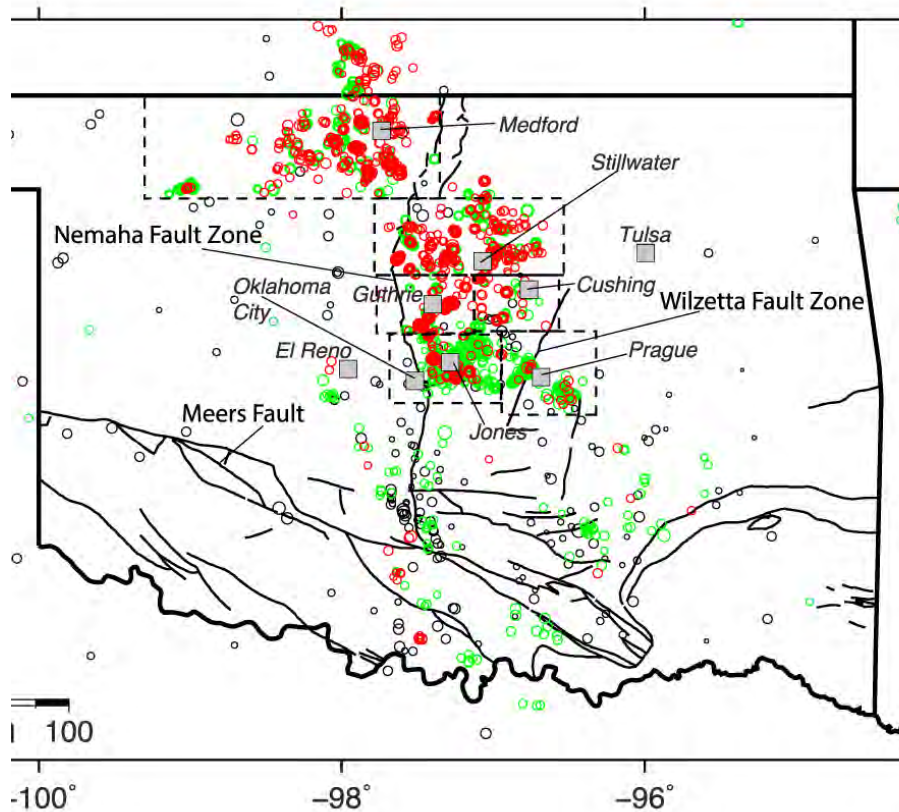
3966

3967 Figure 67: Earthquakes and injection wells in Oklahoma. Red dots: locations of earthquakes
 3968 2009–2014; yellow dots: historical earthquakes 1974–2008; black crosses: enhanced oil
 3969 recovery wells; blue crosses: salt water disposal wells that injected more than 30,000 barrels
 3970 ($\sim 4800 \text{ m}^3$) in any month in the most recent three years of data; boxes: areas of detailed study
 3971 [from Walsh & Zoback, 2015].

3972

3973

3974



3975

3976

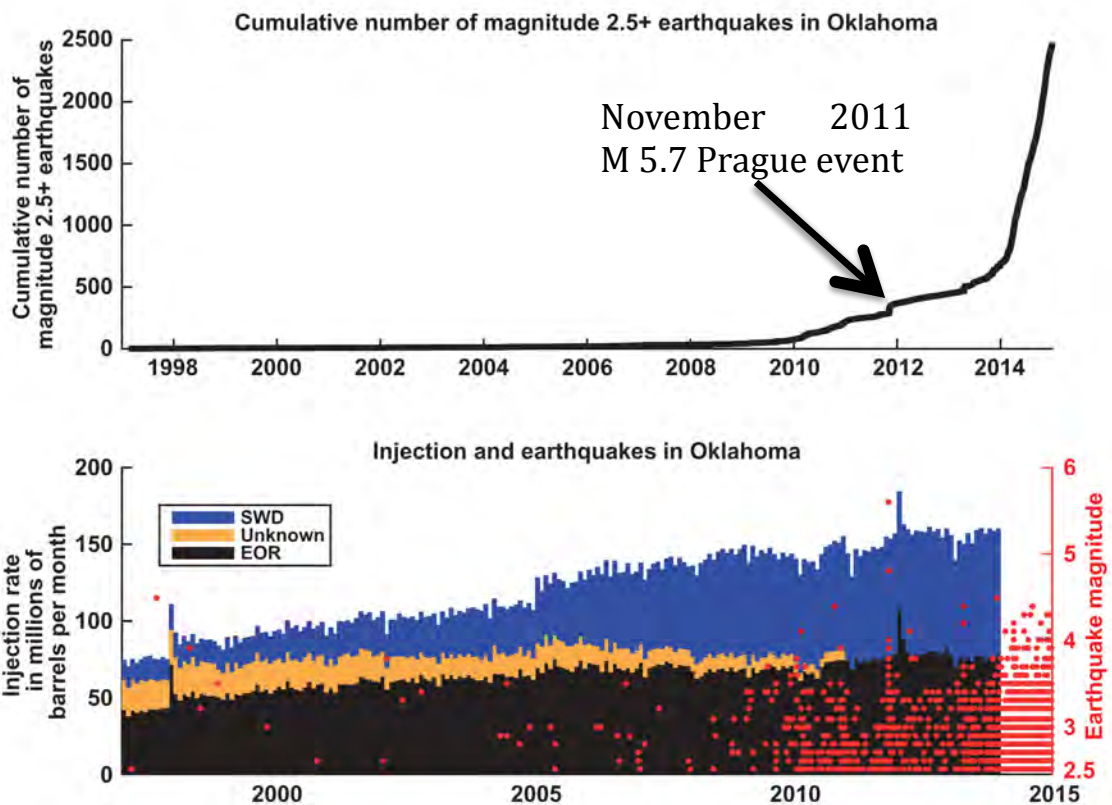
3977 Figure 68: U.S. Geological Survey earthquake epicenters from the National Earthquake
 3978 Information Center (NEIC) database²¹, 1974 - 2014. Black lines: subsurface and surface
 3979 faults; dashed black lines: detailed study regions; Meers fault: the only known active fault in
 3980 Oklahoma prior to the recent increase in seismicity [from McNamara *et al.*, 2015].

3981

3982

²¹ <http://earthquake.usgs.gov/contactus/golden/neic.php>

3983



3984

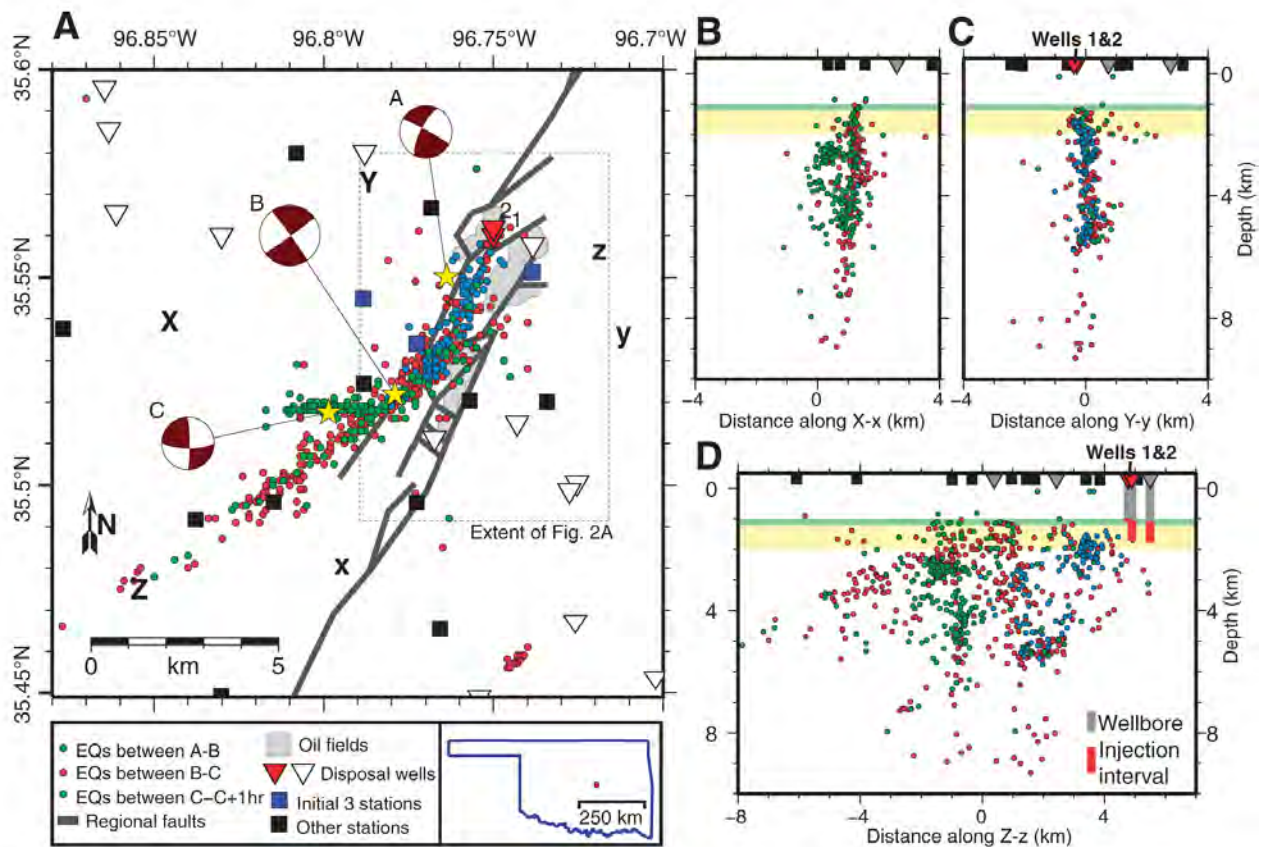
3985

3986 Figure 69: Fluid injection and earthquakes in Oklahoma. Top: Cumulative number of $M \geq 2.5$
 3987 earthquakes for the period 1997-2014. Bottom: left axis shows total combined injection rate
 3988 of all underground injection control wells in Oklahoma, right axis shows all earthquakes in
 3989 Oklahoma by magnitude [from Walsh & Zoback, 2015].

3990

3991

3992



3993

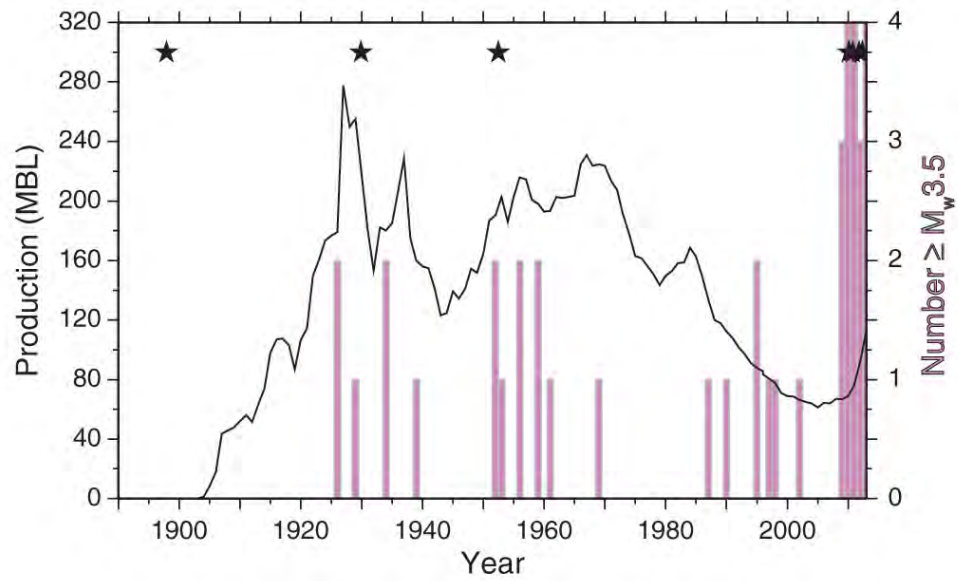
3994

3995 Figure 70: Seismicity, focal mechanisms, seismic stations, active disposal wells, and oilfields
 3996 in the neighborhood of the 2011 Prague, Oklahoma, seismic sequence. Stars: major
 3997 earthquakes in the sequence. B–D: Cross sections showing seismicity projected from up to 4
 3998 km out of plane. Vertical lines: wellbores, red where perforated or open; green bands: the
 3999 Hunton and Simpson Groups; yellow bands: Arbuckle Group which overlies basement. Inset:
 4000 Oklahoma and location of map area [from Keranen *et al.*, 2013].

4001

4002

4003



4004

4005

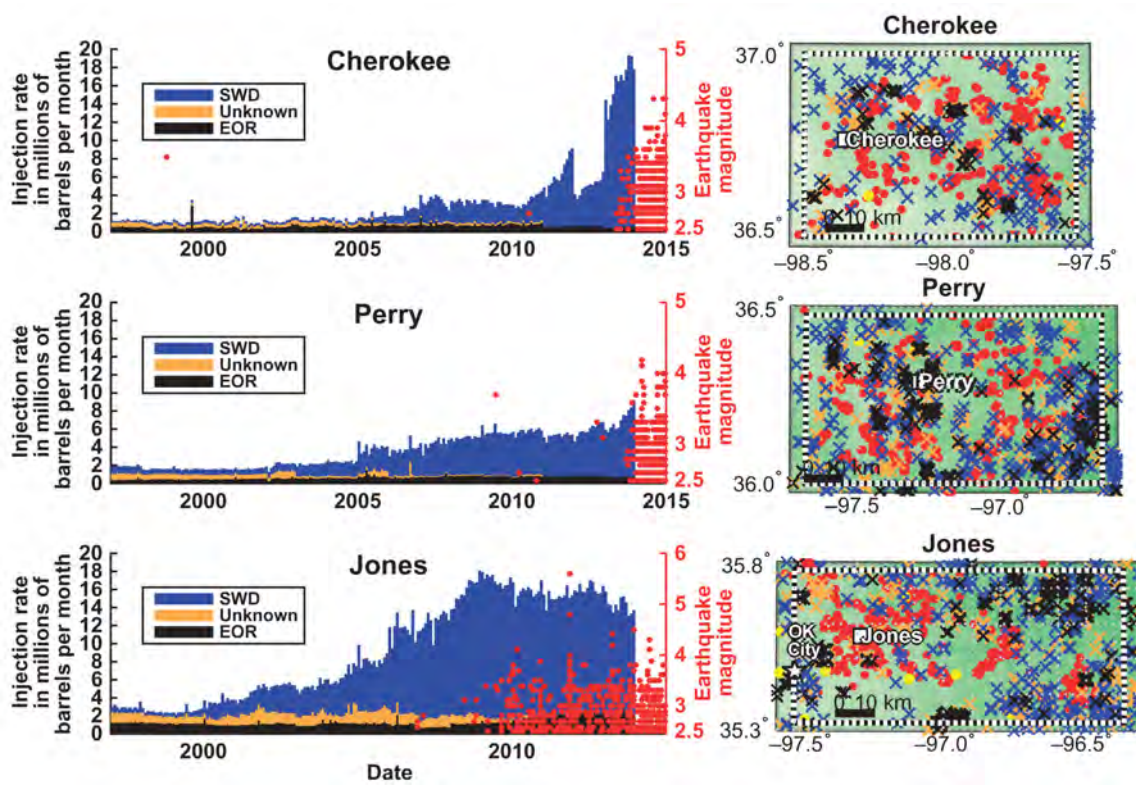
4006 Figure 71: Oklahoma seismicity rates compared with oil production in millions of barrels
 4007 (multiply by 0.159 to convert to m^3). Bars: number of earthquakes with $M \geq 3.5$ in a given
 4008 year; black stars: $M \geq 4$ events [from Hough & Page, 2015].

4009

4010

4011

4012



4013

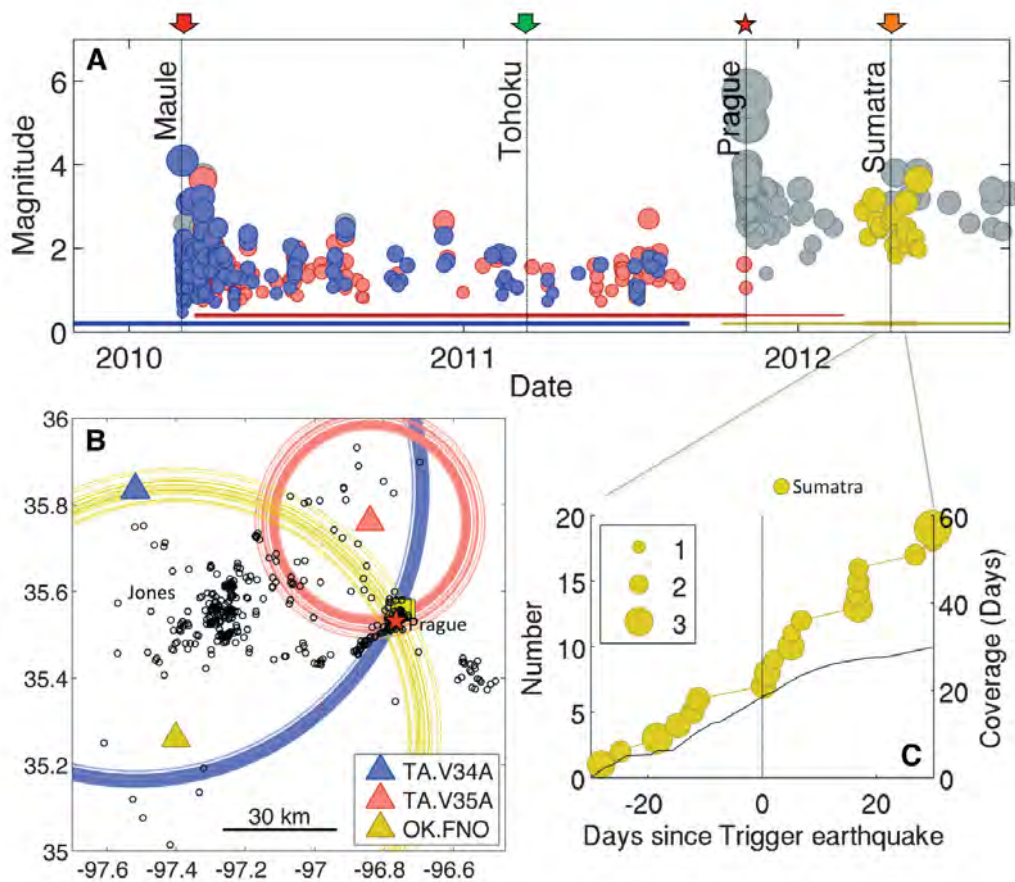
4014

4015 Figure 72: Injection from enhanced oil recovery, brine disposal, and unknown wells, and
 4016 earthquakes in the Cherokee, Perry, and Jones study areas (boxes in Figure 67). Symbols are
 4017 the same as in Figure 67. Each study area is 5000 km² in size [from Walsh & Zoback, 2015].

4018

4019

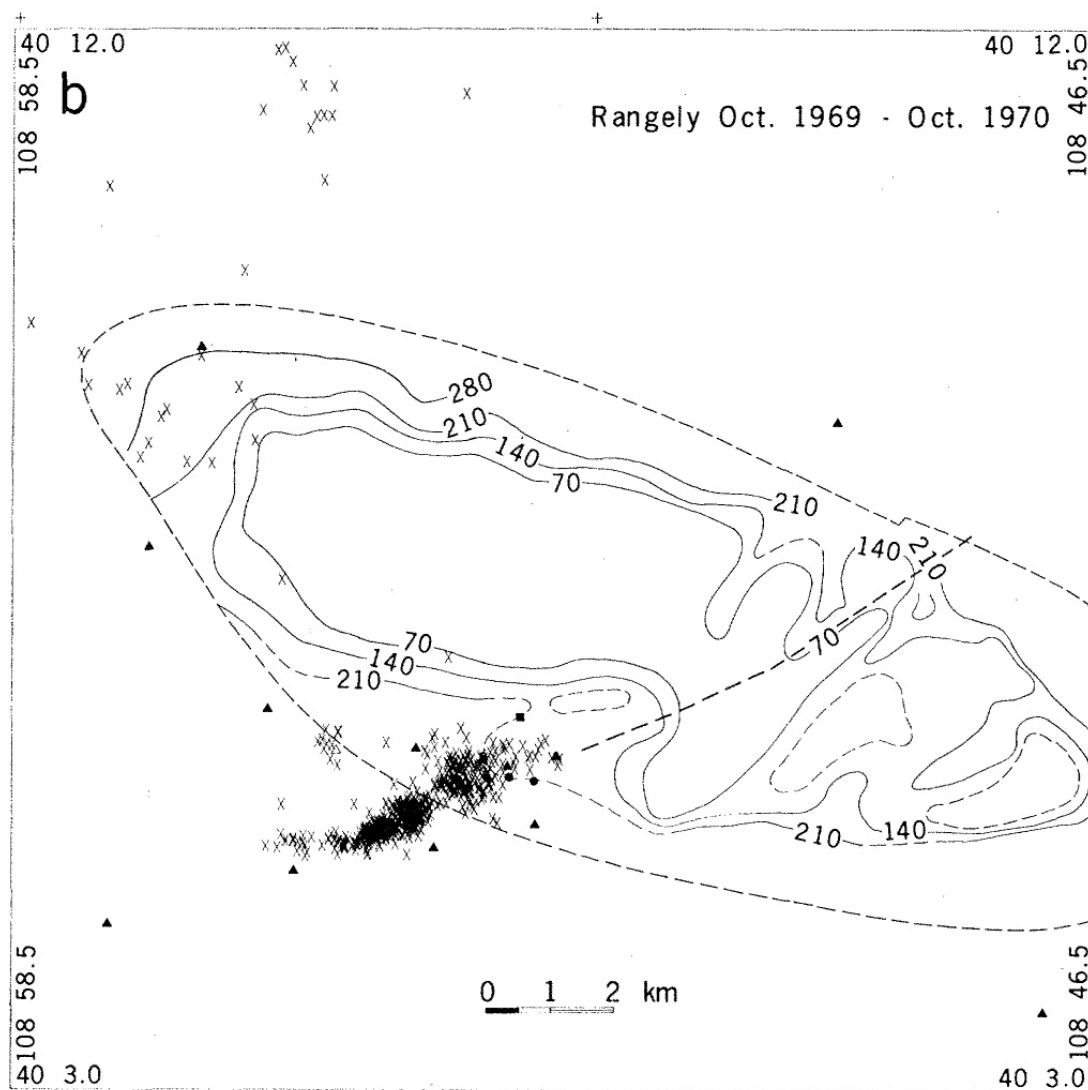
4020

4021
4022

4023 Figure 73: Earthquakes in the Prague, Oklahoma, area. (A) Detected events, showing
 4024 triggering by the 2010 Maule, Chile earthquake. Red star: the 6 November 2011 M_w 5.7
 4025 mainshock. (B) Distances to detected events. (C) Cumulative number of events in the time
 4026 period surrounding the 11 April 2012 M_w 8.6 and 8.2 Sumatra earthquakes [from van der
 4027 Elst *et al.*, 2013].

4028
4029

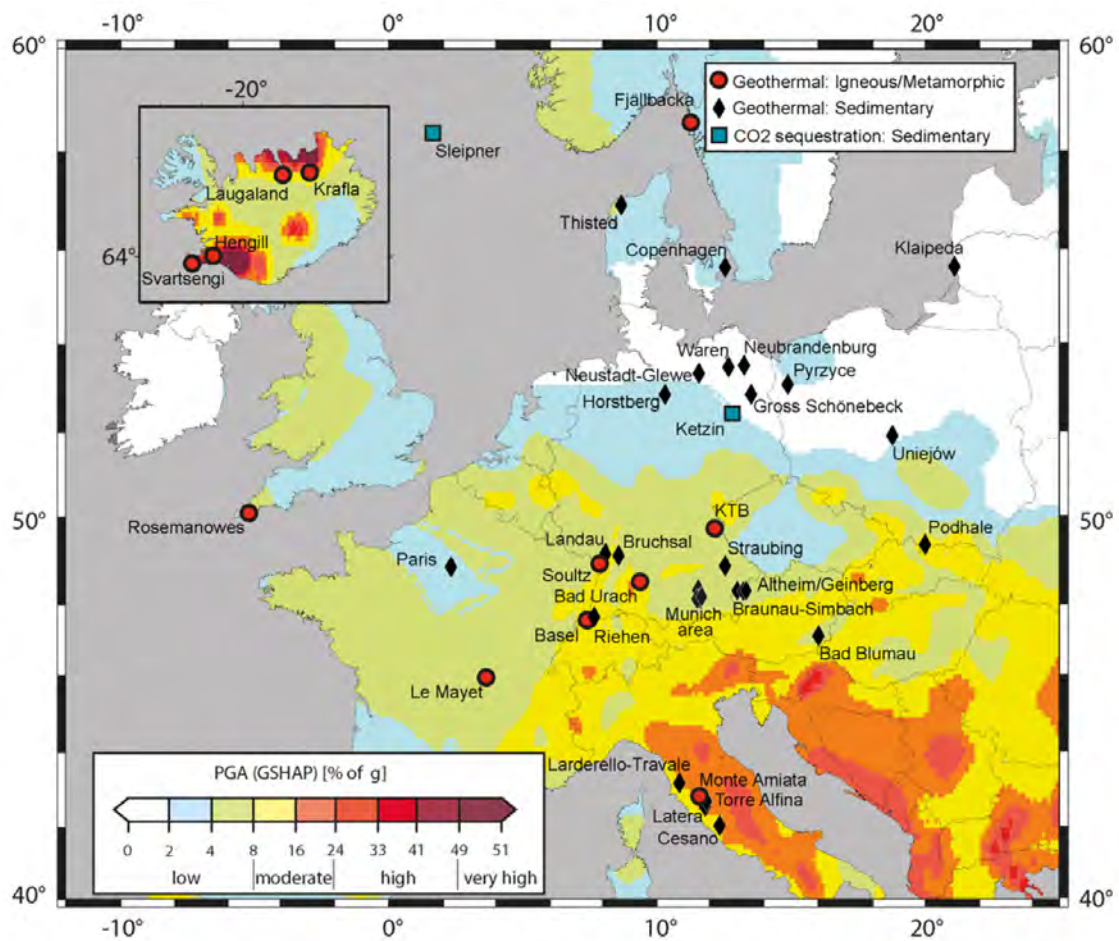
4030

4031
4032

4033 Figure 74: Earthquakes located at Rangely October 1969 - November 1970. The contours are
 4034 bottom-hole, 3-day shut-in pressures as of September 1969. The interval is 7 MPa. Triangles:
 4035 seismic stations; stars: experimental wells; heavy, dashed line: the fault mapped in the
 4036 subsurface [from Raleigh *et al.*, 1976].

4037
4038

4039



4040

4041

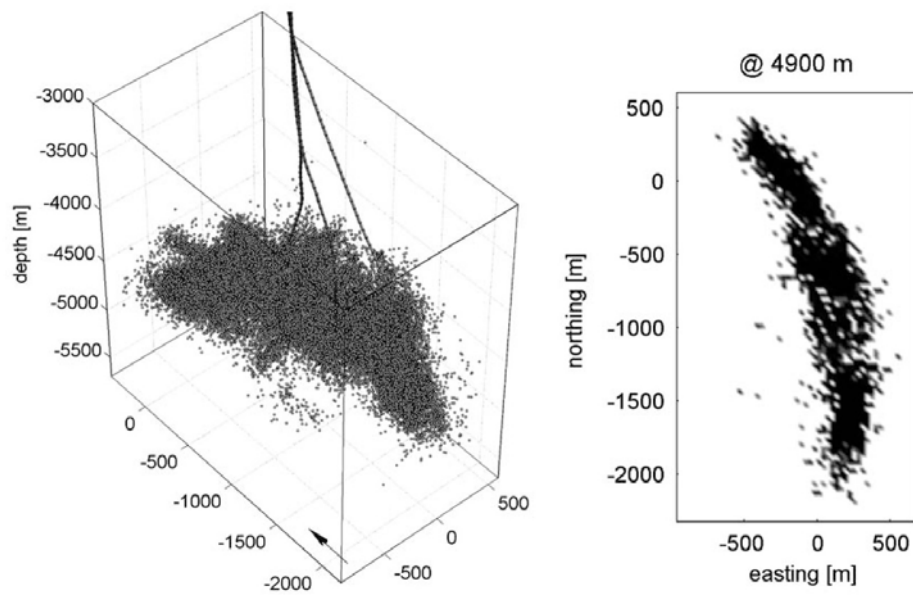
4042 Figure 75: Location of geothermal and CO₂ injection sites in Europe, superimposed on a
 4043 seismic hazard map from the Global Seismic Hazard Assessment Program (GSHAP²²). Color
 4044 scale denotes GSHAP index of local seismic hazard from natural earthquakes defined as peak
 4045 ground acceleration in percent of the acceleration due to gravity (g) on stiff soil that has a
 4046 10% probability of being exceeded in 50 years [equivalent to a recurrence period of 475
 4047 years; from Evans *et al.*, 2012].

4048

4049

²² <http://www.seismo.ethz.ch/static/GSHAP>

4050

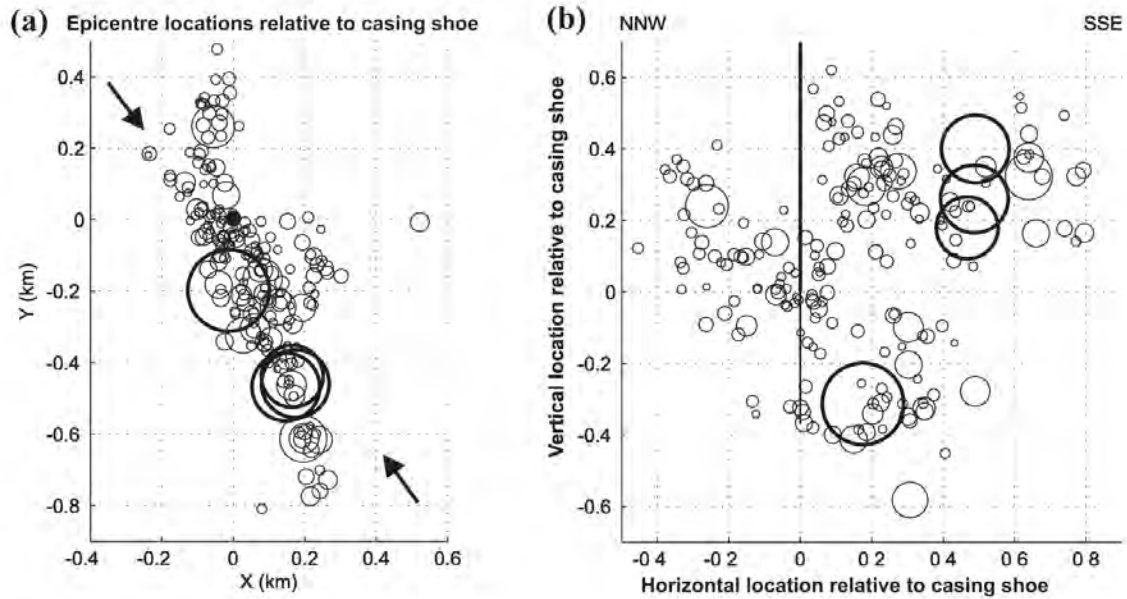
4051
4052

4053 Figure 76: Top left: Distribution of earthquake hypocenters at the Soultz-sous-Forêts EGS
4054 project in perspective view. Solid lines: wells GPK2, GPK3 and GPK4. Top right: Depth
4055 slice of the hypocenter density distribution at 4900 m depth. Dark shading: regions of high
4056 density [from Baisch *et al.*, 2010].

4057

4058

4059



4060

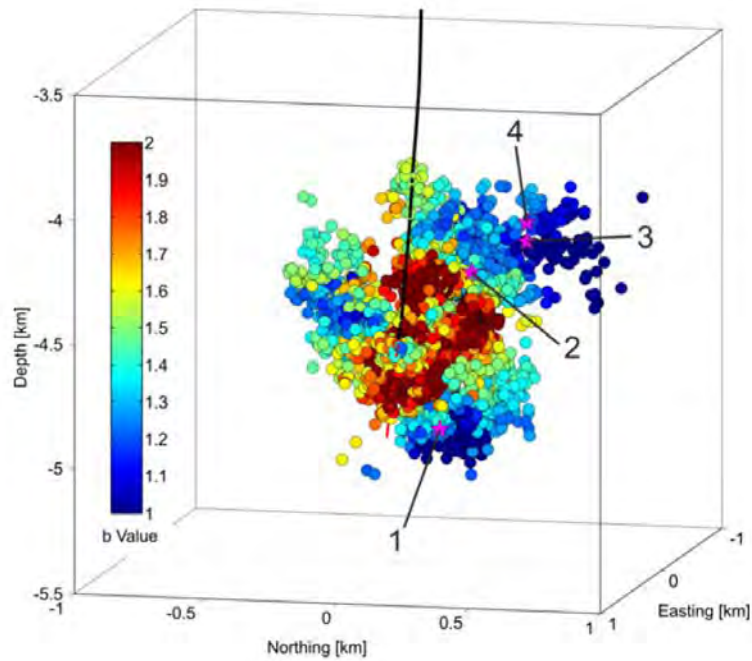
4061

4062 Figure 77: (a) Epicenters, and (b) cross-section showing 195 earthquakes with M 0.7–3.4,
 4063 that occurred December 2, 2006 - November 30, 2007 following EGS stimulation at Basel
 4064 [after Deichmann & Giardini, 2009]. The borehole is indicated by a black dot/vertical line.
 4065 The size of each circle is proportional to the seismic moment of the event. The four events
 4066 with $M_L > 3.0$ are shown as bold circles. The M_L 3.4 event that occurred just after shut-in on
 4067 December 8 is close to the bottom of the well. The other three $M_L > 3$ events occurred 1–2
 4068 months after the well had been vented and wellhead pressures had returned to near-
 4069 hydrostatic levels. The arrows in (a) indicate the mean orientation of the maximum horizontal
 4070 compressive stress in the granite basement [from Evans *et al.*, 2012].

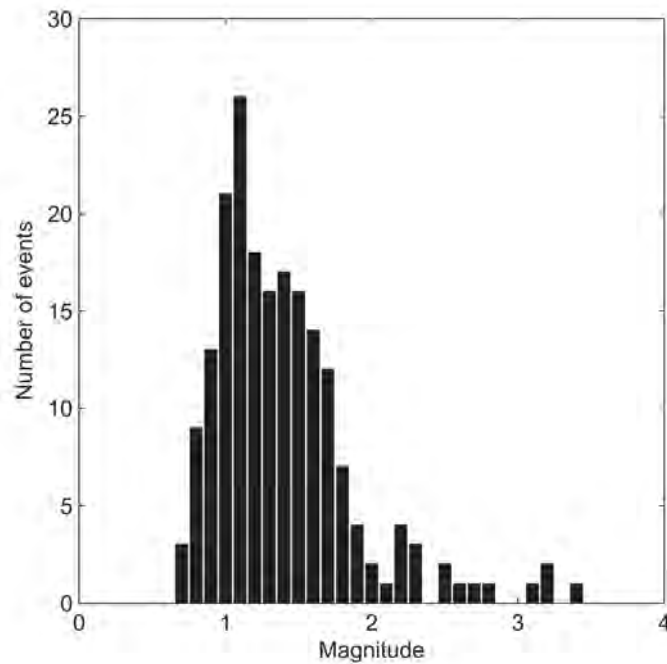
4071

4072

4073



4074



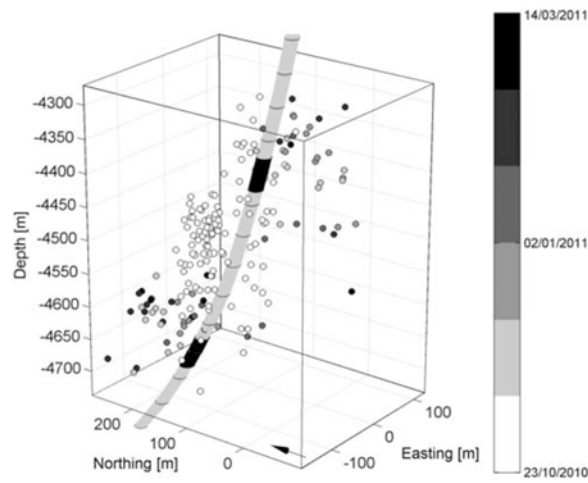
4075

4076

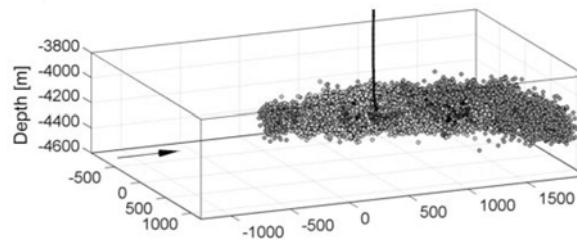
4077 Figure 78: Top: Earthquakes induced by hydraulic stimulation of the Basel, Switzerland,
 4078 EGS injection well in 2006 and 2007. Hypocenters are color coded according to b -values
 4079 calculated for the volume in which they occurred. Stars: large earthquakes [from Zang *et al.*,
 4080 2014b]. Bottom: Magnitude histogram of the induced seismicity recorded by the Swiss
 4081 Seismological Service 3 December, 2006 - 30 November, 2007 [from Deichmann & Ernst,
 4082 2009].

4083

4084



4085



4086

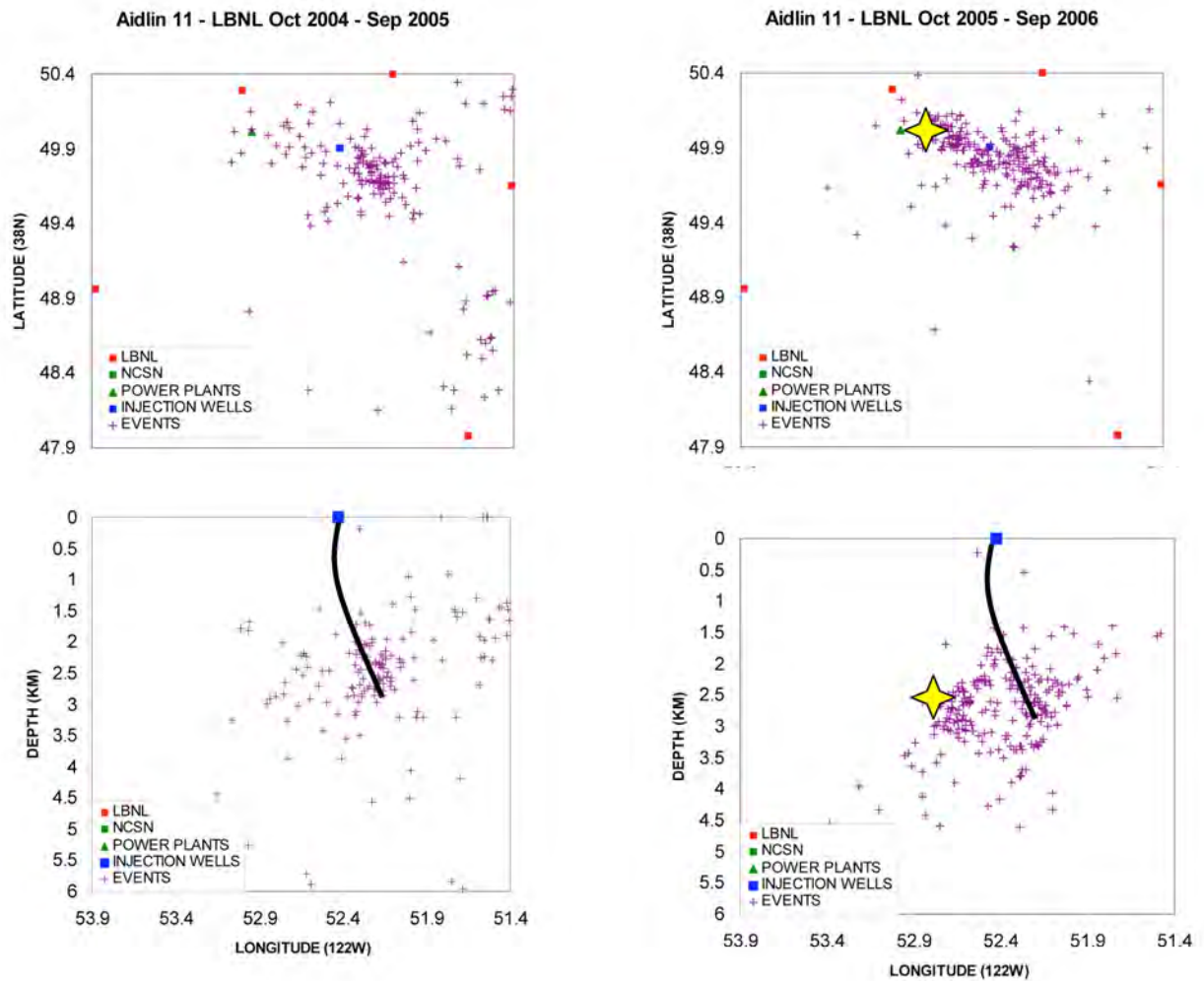
4087

4088 Figure 79: EGS-induced earthquakes at Cooper Basin, Australia. Top: the Jolokia Field–
 4089 hypocenters of earthquakes induced by hydraulic stimulation of well 1 in in 2010. Known
 4090 fracture intersections with the wellbore are shown in black. Bottom: the Habanero field–
 4091 hypocentres of earthquakes induced by stimulation of well 4 (vertical line) in 2012 [from
 4092 Baisch *et al.*, 2015].

4093

4094

4095



4096

4097

4098 Figure 80: Earthquakes surmised to be injection-related at the northwest Geysers geothermal
 4099 area. Maps and east-west cross sections show earthquakes in the Aidlin area. Blue square and
 4100 black line: Injection well; yellow star: a M 4 event that occurred October 2005 [from Majer
 4101 & Peterson, 2007].

4102

4103

4104



4105

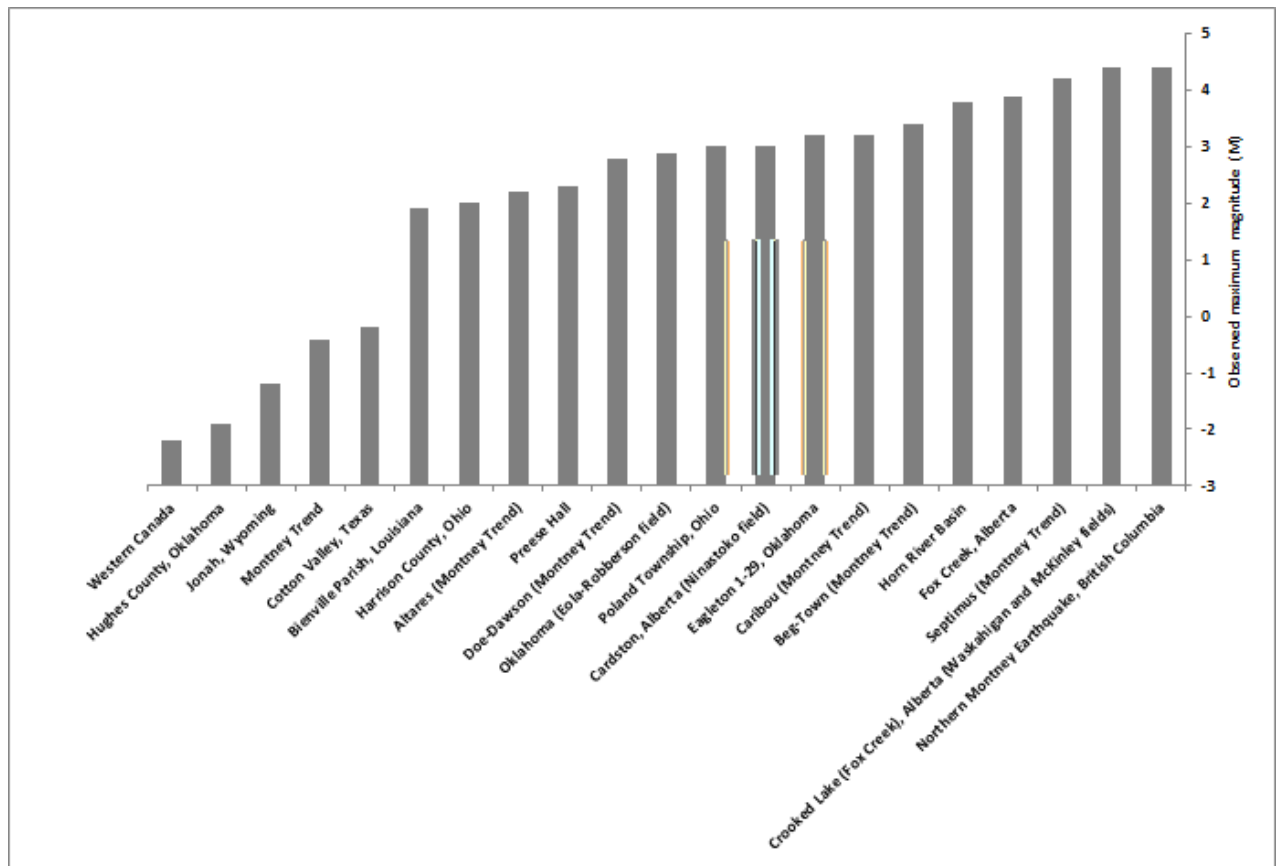
4106

4107 Figure 81: States of the USA where shale-gas hydrofracturing is currently ongoing.

4108

4109

4110



4111

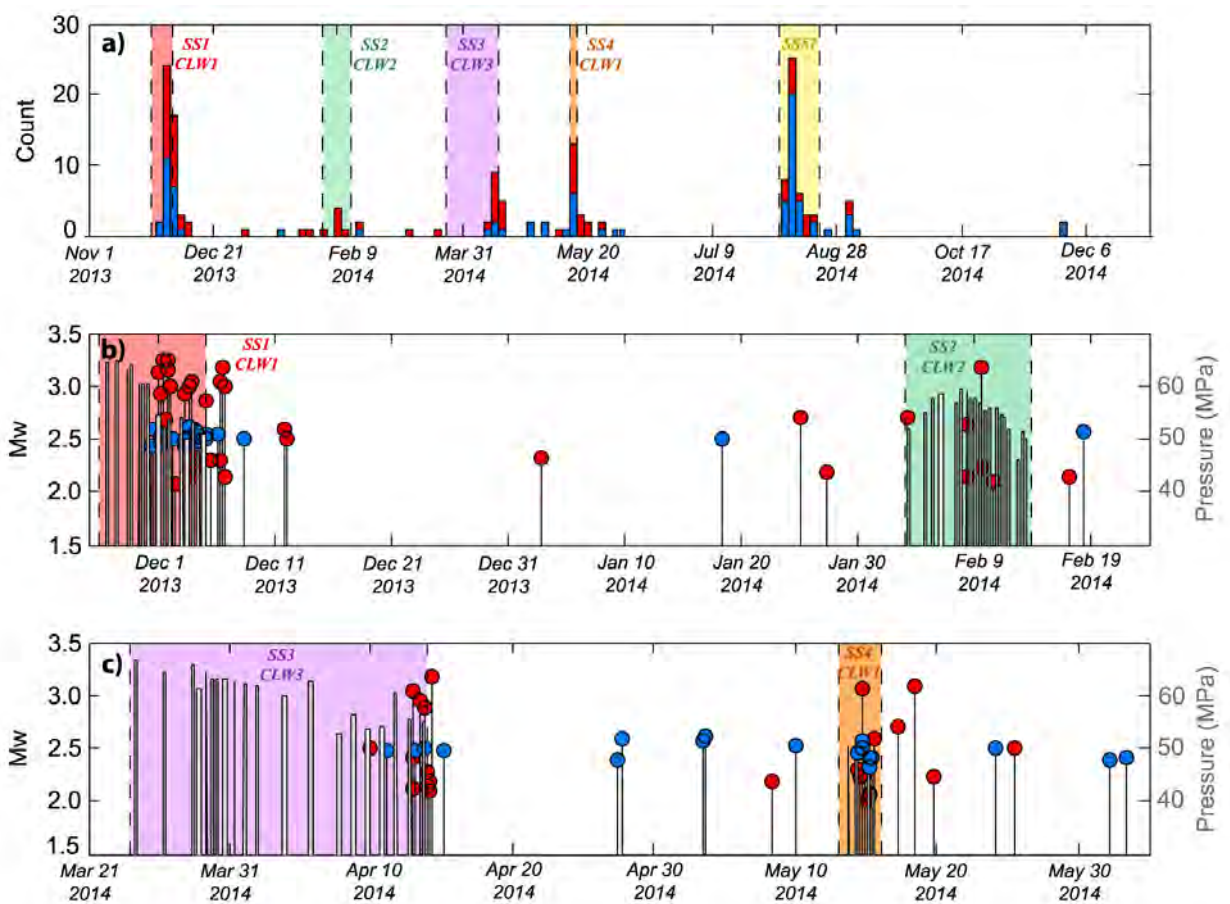
4112

4113 Figure 82: Histogram showing M_{MAX} for the 21 cases of shale-gas hydrofracturing-induced
 4114 earthquakes in the database.

4115

4116

4117



4118

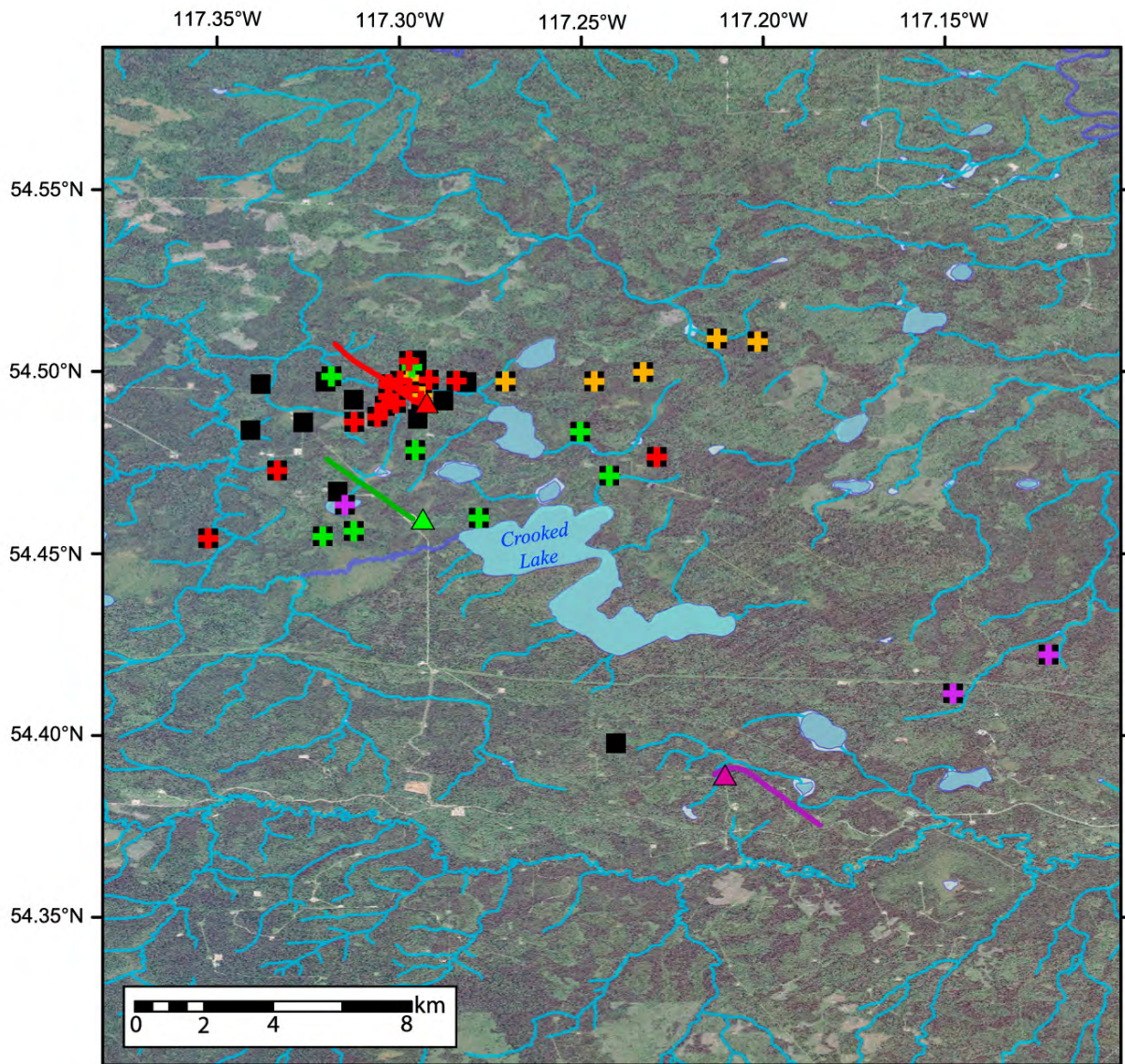
4119

4120 Figure 83: Comparison of earthquakes and hydraulic fracturing completions at Crooked
 4121 Lake, Alberta, Canada. (a) Histogram of located seismicity (red bars), with number of
 4122 earthquakes increased using waveform cross correlation (blue bars). Hydrofracture schedules
 4123 are bounded by colored boxes and labeled with respective sub-sequence and borehole. (b)
 4124 Magnitudes of located (red circles), detected (blue circles) earthquakes and average injection
 4125 pressure during hydrofracture stages (gray bars). (c) Same as (b) for later borehole
 4126 completions [from Schultz *et al.*, 2015].

4127

4128

4129



4130

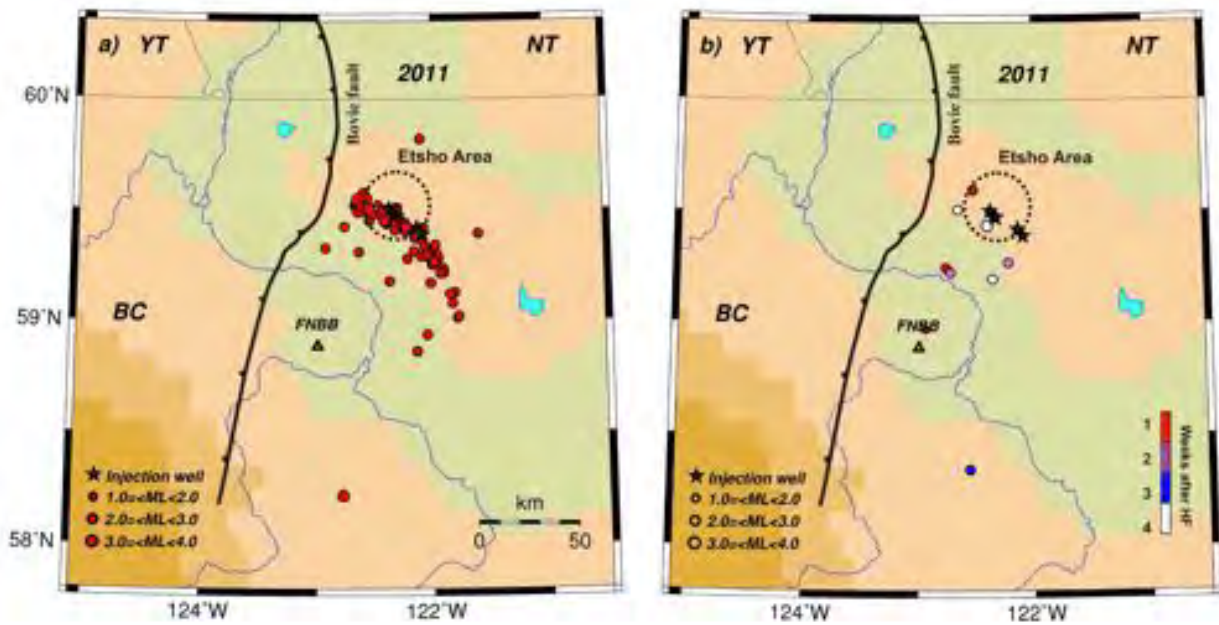
4131

4132 Figure 84: Epicenters (black squares) of earthquakes near Crooked Lake, Alberta, Canada,
 4133 thought to be induced by hydrofracturing. Epicenters are binned according to timing of well
 4134 stimulations SS1 (red crosses), SS2 (green crosses), SS3 (purple crosses), and SS4 (orange
 4135 crosses). Events without crosses occurred during shut-in periods. Triangles: surface locations
 4136 of wells; lines: horizontal well trajectories. Wells are color-coded with their associated
 4137 seismic sequences [from Schultz *et al.*, 2015].

4138

4139

4140



4141

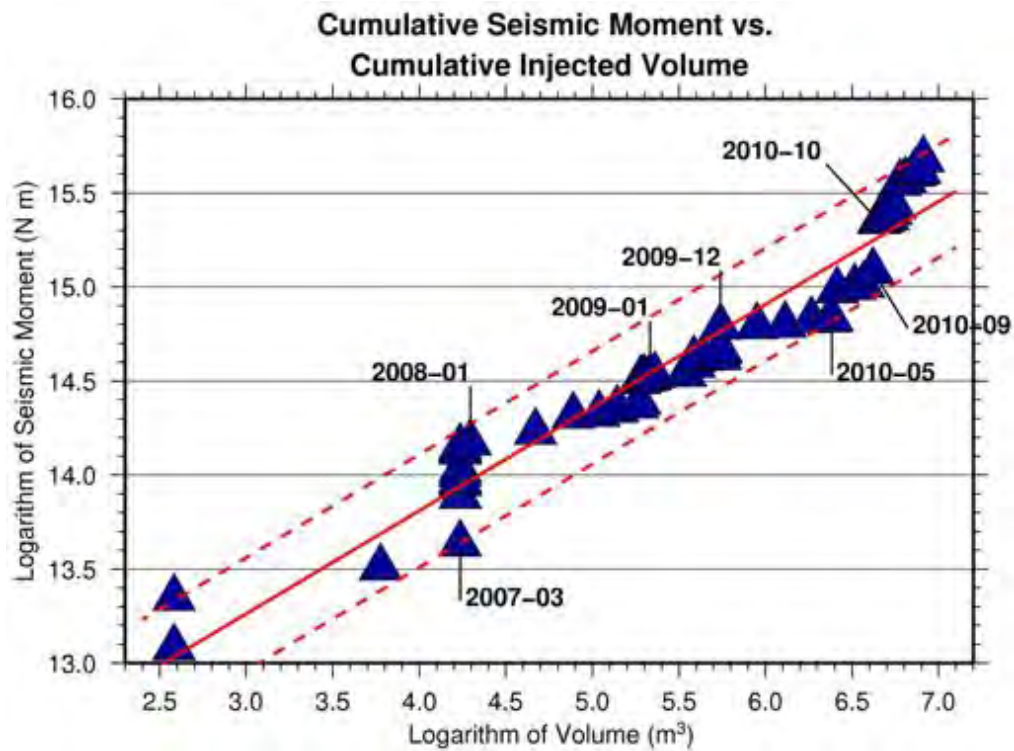
4142

4143 Figure 85: Map of the Horn River Basin, British Columbia, Canada. Left: seismicity on days
 4144 when hydrofracturing took place. Right: days when it did not occur [from Farahbod *et al.*,
 4145 2015].

4146

4147

4148



4149

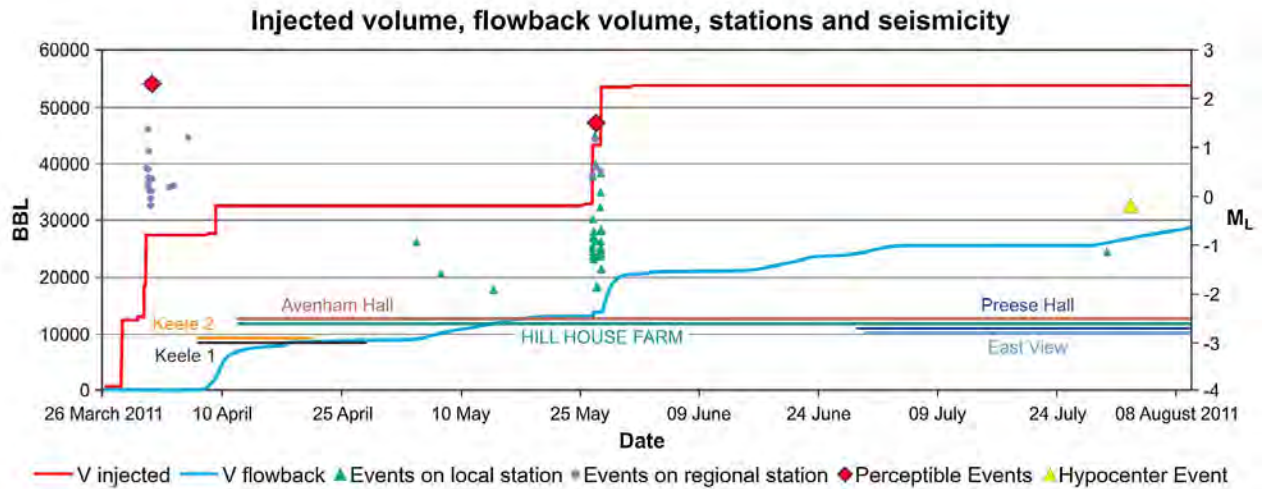
4150

4151 Figure 86: Logarithm of seismic moment vs. logarithm of volume injected in shale gas
 4152 hydrofracturing operations in the Etsho area, Horn River Basin, British Columbia, Canada
 4153 [from Farahbod *et al.*, 2015].

4154

4155

4156



4157

4158

4159 Figure 87: Injection activity and seismicity associated with shale-gas hydrofracturing at
 4160 Preese Hall, Lancashire, UK. Red line: injected volume; blue line: flow-back volume from
 4161 the well-head in US barrels (0.159 m^3); violet dots: earthquakes detected on seismic stations
 4162 at distances of $> 80 \text{ km}$; green triangles: earthquakes detected on two local stations; yellow
 4163 triangle: event for which source mechanism and reliable hypocenter were obtained [from
 4164 Clarke *et al.*, 2014a].

4165

4166

4167



4168

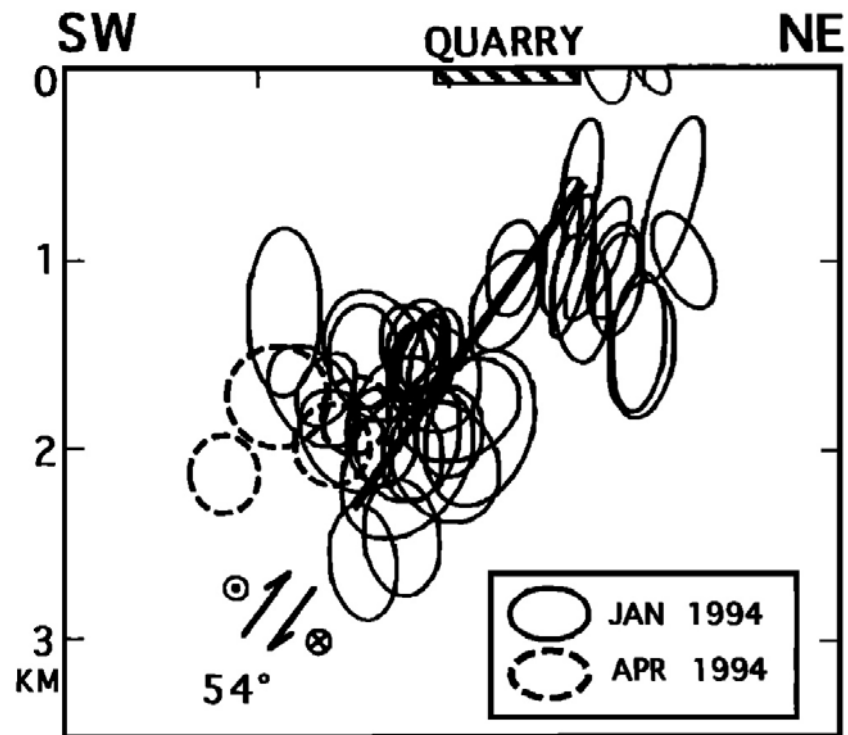
4169

4170 Figure 88: Site of the former Cacoosing Valley, Pennsylvania, quarry. Red oval: approximate
4171 boundary of the old quarry. Satellite image from Google Maps.

4172

4173

4174

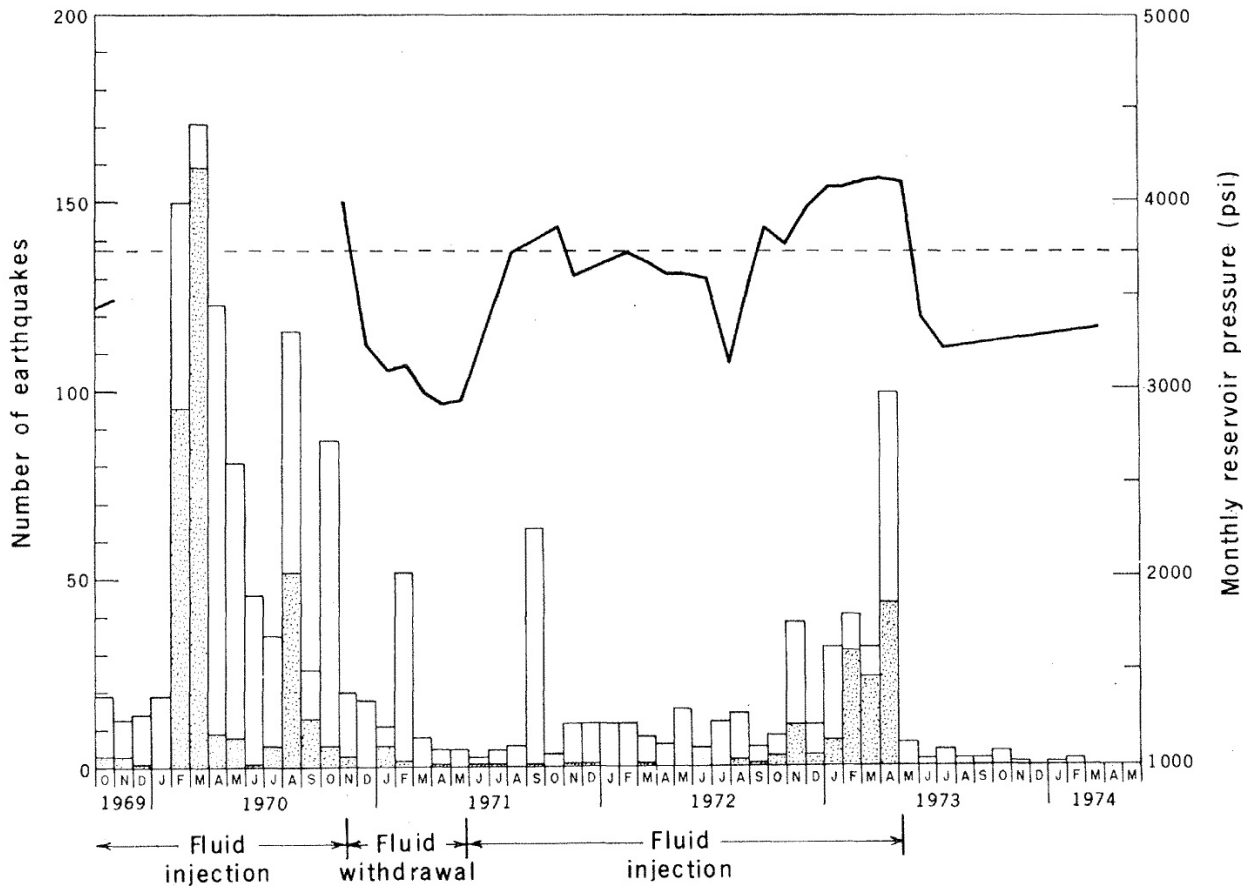
4175
4176

4177 Figure 89: Section perpendicular to the inferred rupture of the 1994 Cacoosing Valley,
 4178 Pennsylvania, earthquake sequence showing hypocenter confidence ellipses, the plane on
 4179 which the main rupture is inferred to have occurred from focal mechanisms studies, and the
 4180 location of the quarry at the surface above the hanging wall block [from Seeber *et al.*, 1998].

4181

4182

4183



4184

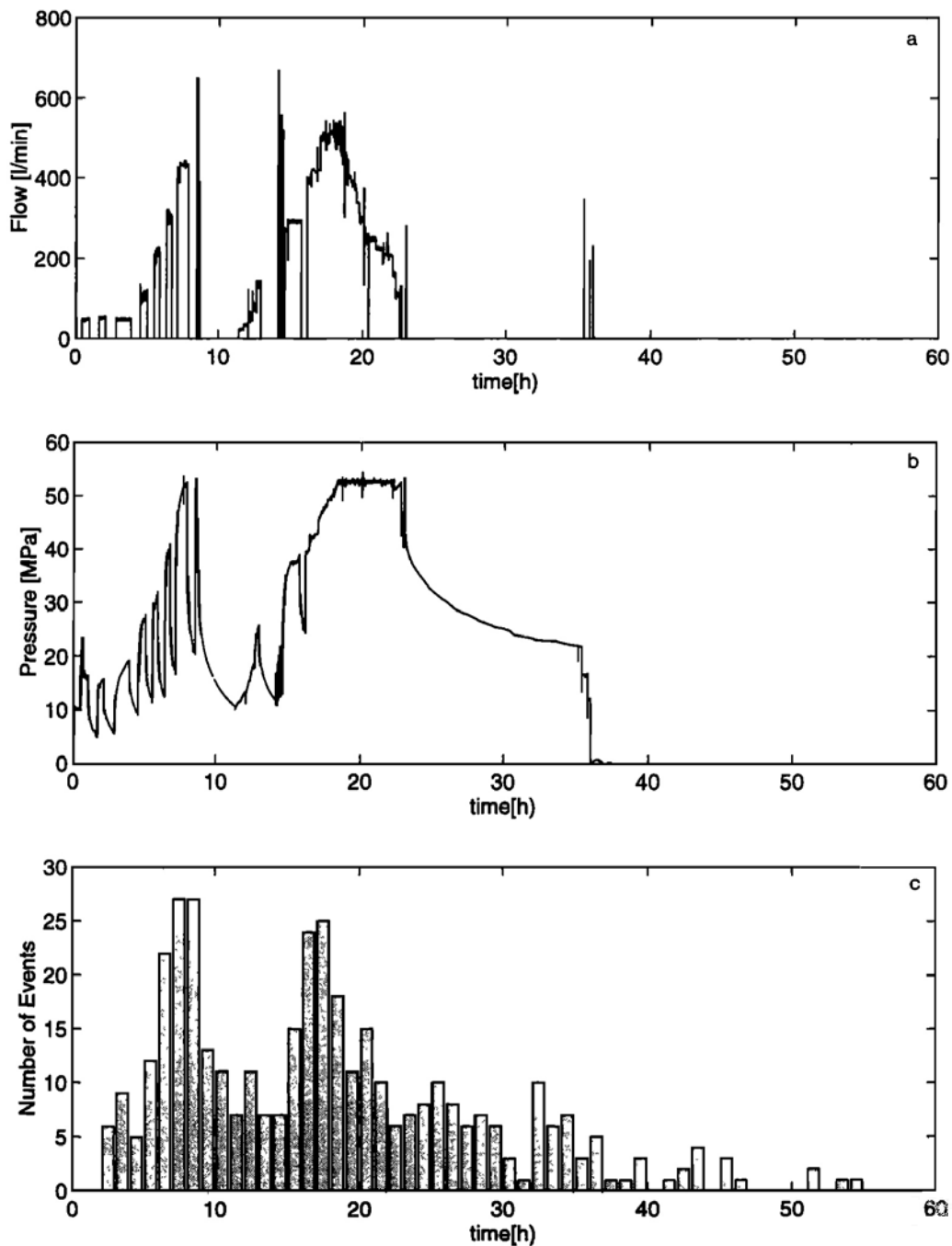
4185

4186 Figure 90: Frequency of earthquakes at the Rangely Oilfield, Colorado, and reservoir
 4187 pressures during fluid injection and fluid withdrawal. Stippled bars: earthquakes within 1 km
 4188 of injection wells; black line: pressure history in injection well Fee 69; dashed line: predicted
 4189 critical reservoir pressure [from Raleigh *et al.*, 1976].

4190

4191

4192



4193

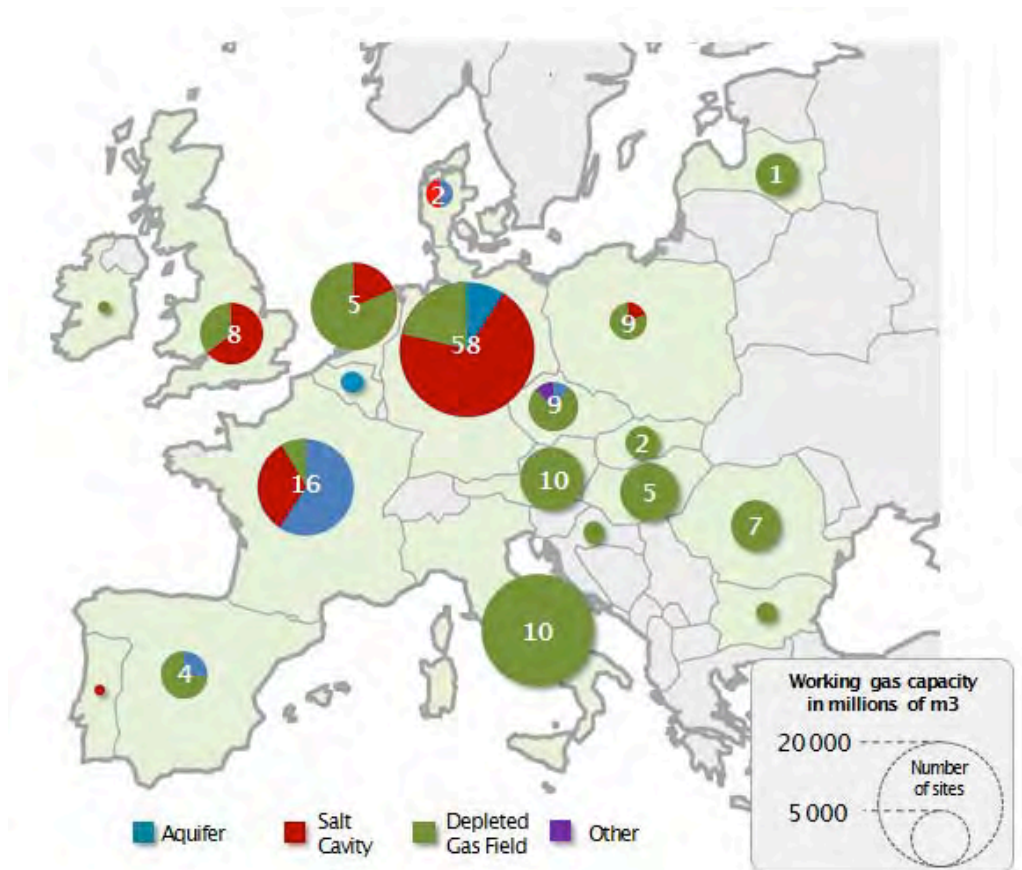
4194

4195 Figure 91: Flow rates, pressure and number of earthquakes induced by brine injection into the
 4196 Kontinentales Tiefbohrprogramm der Bundesrepublik Deutschland (KTB—the German
 4197 Continental Deep Drilling Program) borehole during a 60-hour period [from Zoback &
 4198 Harjes, 1997].

4199

4200

4201

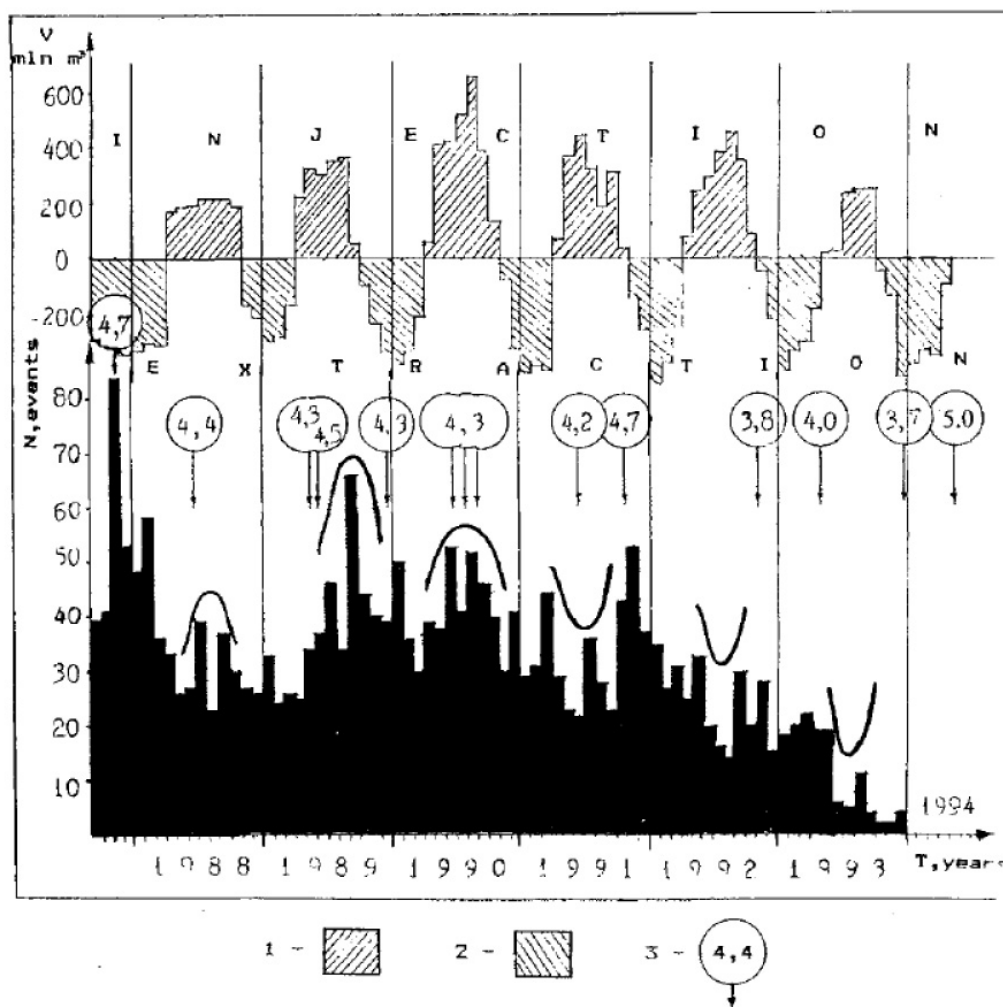
4202
42034204 Figure 92: Working gas capacities of underground storage sites in Europe²³.

4205

4206

²³ <http://www.gasinfocus.com/en/> ; <http://www.gie.eu/index.php/maps-data/gse-storage-map>

4207



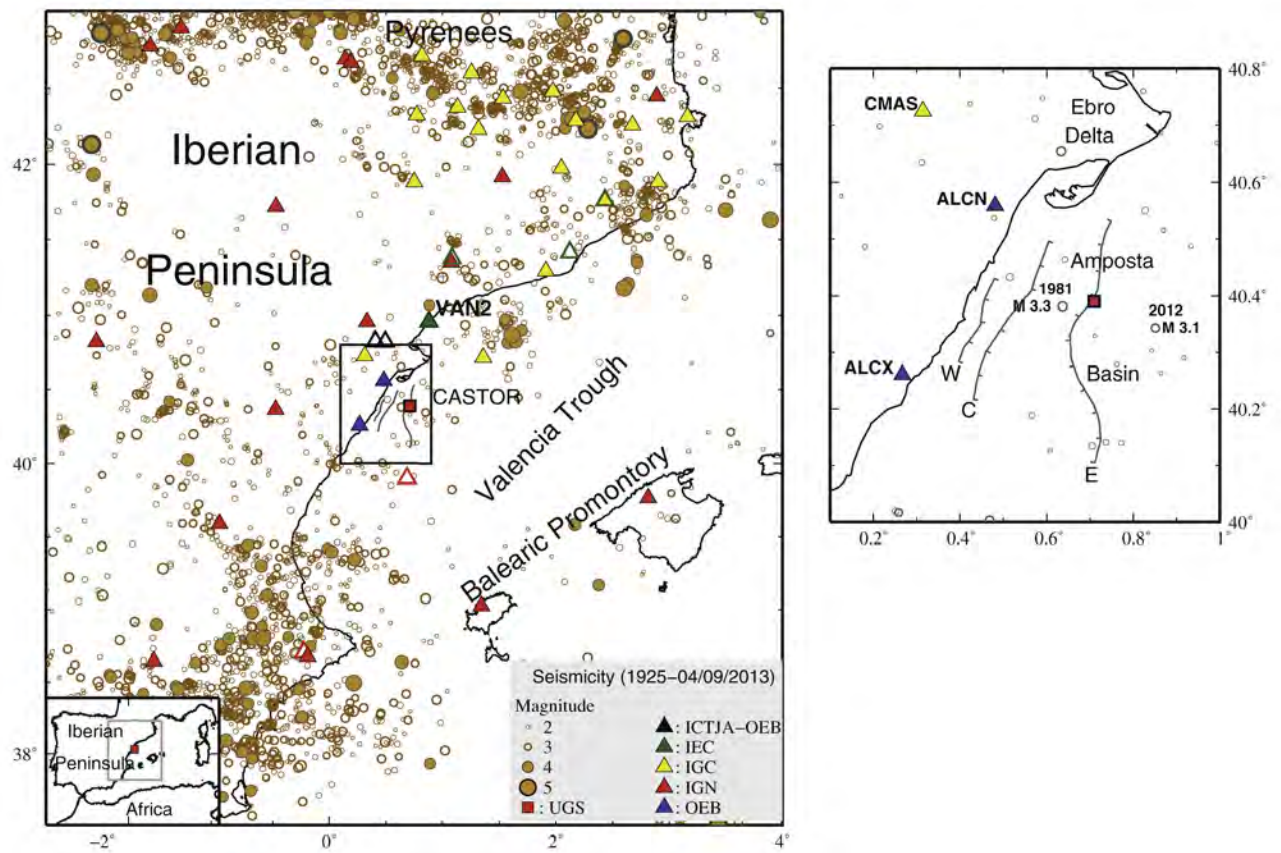
4208

4209

4210 Figure 93: Seismicity in the Gazli region, Uzbekistan, during underground gas storage
 4211 activities. 1: 6-monthly injection; 2: 6-monthly production. Numbers in circles indicate
 4212 earthquake magnitudes [from Plotnikova *et al.*, 1996].

4213

4214



4215

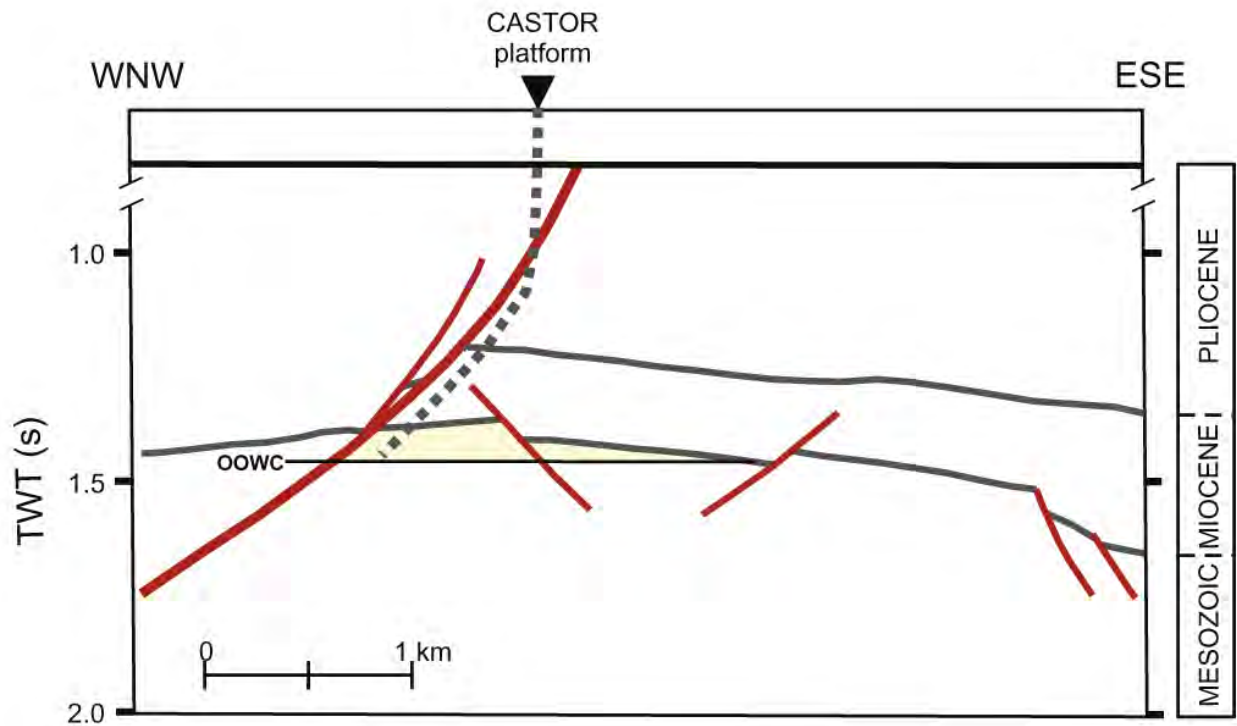
4216

4217 Figure 94: Seismicity of the eastern Iberian Peninsula, Spain. Triangles: seismic stations; red
 4218 square: location of the Castor underground gas storage reservoir. W, C and E denote the
 4219 Western, Central and Eastern Amposta faults [from Gaite *et al.*, 2016].

4220

4221

4222



4223

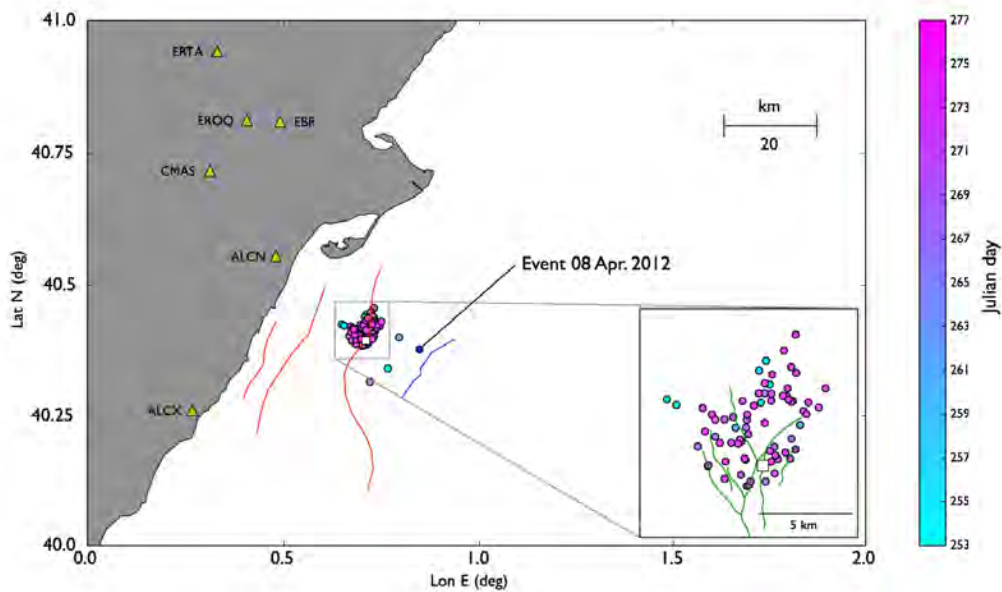
4224

4225 Figure 95: Schematic diagram of the old Amposta Oilfield, Spain, in WNW-ESE section.
 4226 TWT: two-way traveltime; dashed line: approximate location of the Castor injection well:
 4227 OOWC: original oil-water contact at 1940 m depth; yellow area: approximate location of the
 4228 gas reservoir [from Gaite *et al.*, 2016].

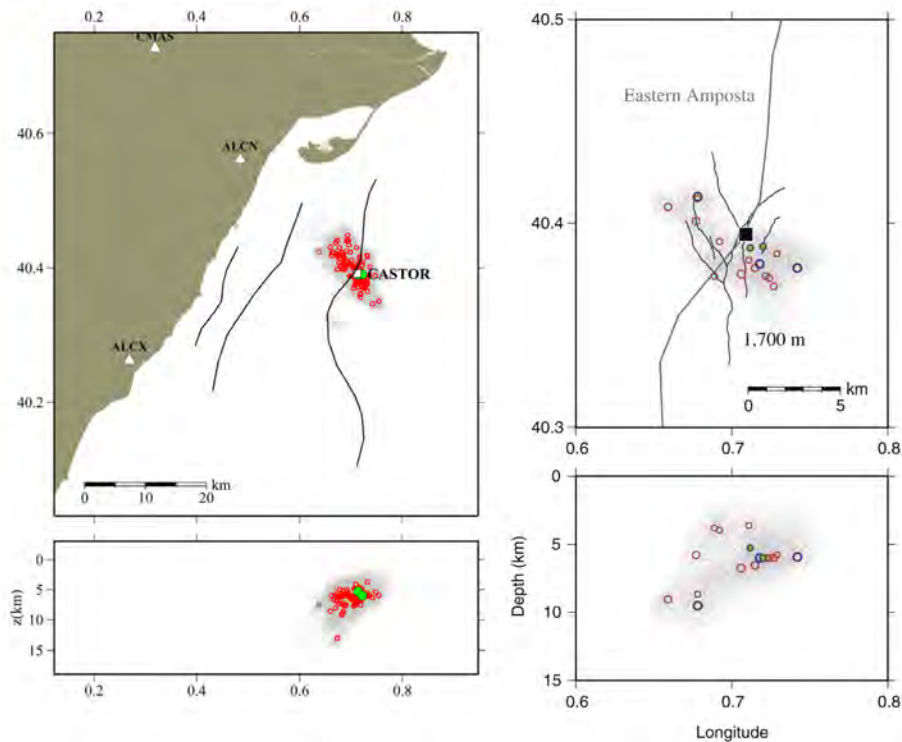
4229

4230

4231



4232



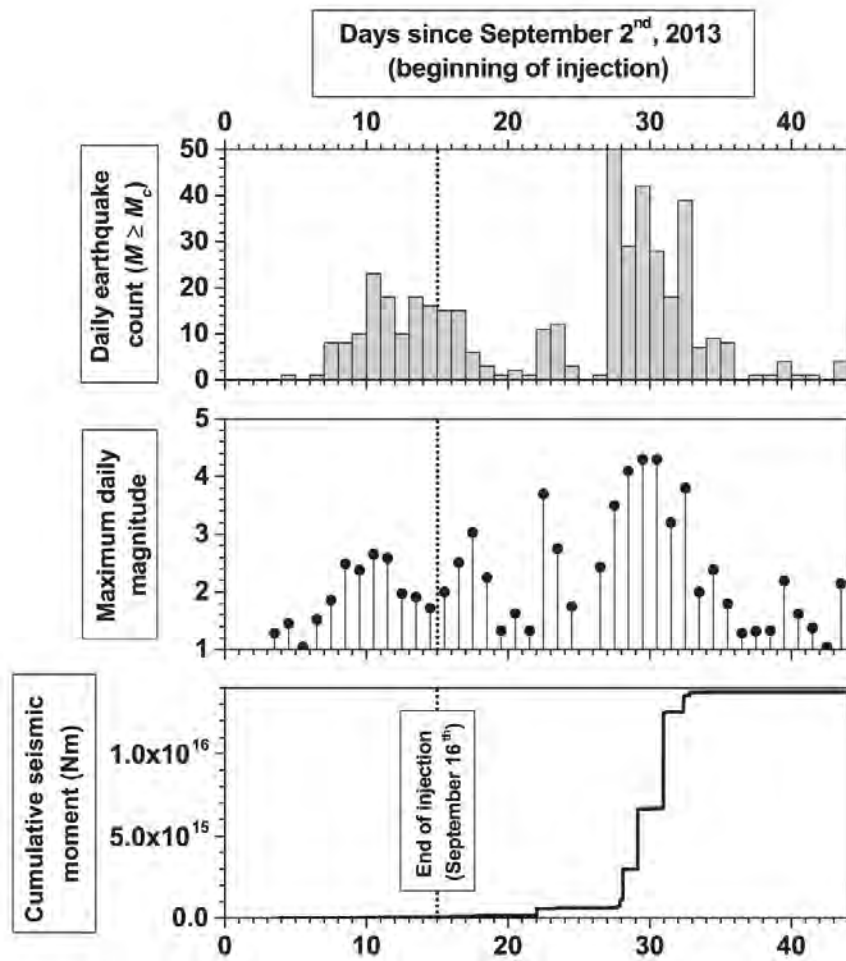
4233

4234

4235 Figure 96: Top: Faults and epicenters for the largest events in the 2013 earthquake sequence
 4236 in the “old Ampostola Field”. White square: Castor platform; colored lines: faults near the
 4237 injection site; red lines: the Ampostola faults; blue and green lines: additional faults [from
 4238 Cesca *et al.*, 2014]. Bottom left: map and cross-section showing 116 earthquakes associated
 4239 as a multiplet; triangles: seismic stations; white square: injection well; green dots: two events
 4240 with M 3.0 and 3.2. Bottom right: map and cross-section of earthquakes with M > 3; black
 4241 square: injection well [from Gaité *et al.*, 2016].

4242

4243
4244



4245

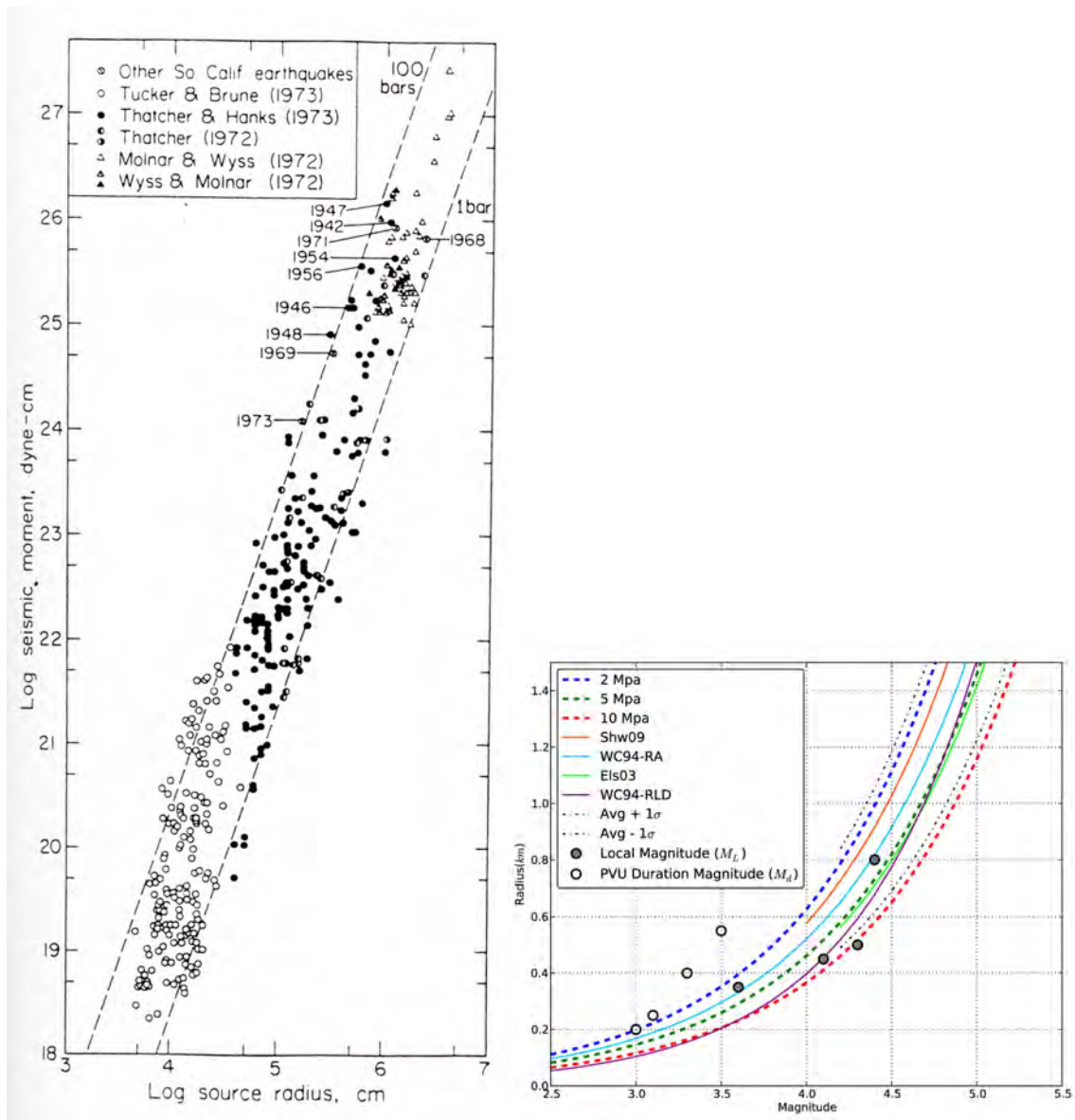
4246

4247 Figure 97: Temporal evolution of seismicity with $M > 2$ associated with the Castor project,
4248 Spain, for 44 days from the beginning of gas injection, 2 September, 2013. Top: daily number
4249 of events. Centre: maximum daily magnitude. Bottom: cumulative seismic moment [from
4250 Cesca *et al.*, 2014].

4251

4252

4253



4254

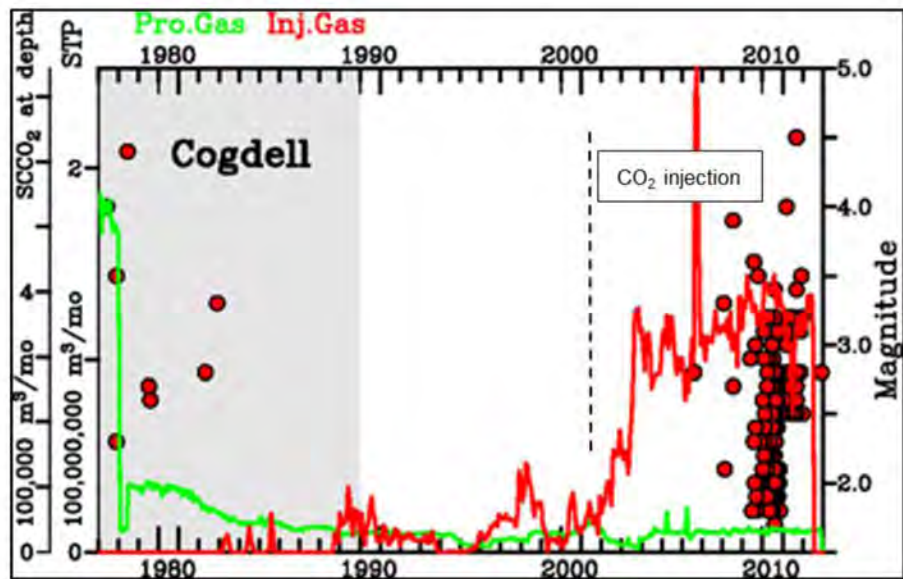
4255

4256 Figure 98: Left: Set of data for small earthquakes showing the relationship between seismic
 4257 moment and source radius. Dashed lines are of constant stress drop [Hanks, 1977]. Right:
 4258 Rupture radius vs. duration earthquake magnitude for several models. Black dotted lines:
 4259 average of these relationships $\pm 1\sigma$; blue, green and red dashed lines: relationships derived
 4260 from the moment-magnitude relation of Hanks and Kanamori [1979] for stress drops of 2, 5
 4261 and 10 MPa respectively, and estimated fault radius using half the rupture-length-at-depth
 4262 parameter; gray and white circles: values for individual earthquakes induced at Paradox
 4263 Valley, Colorado [from Yeck *et al.*, 2015].

4264

4265

4266



4267

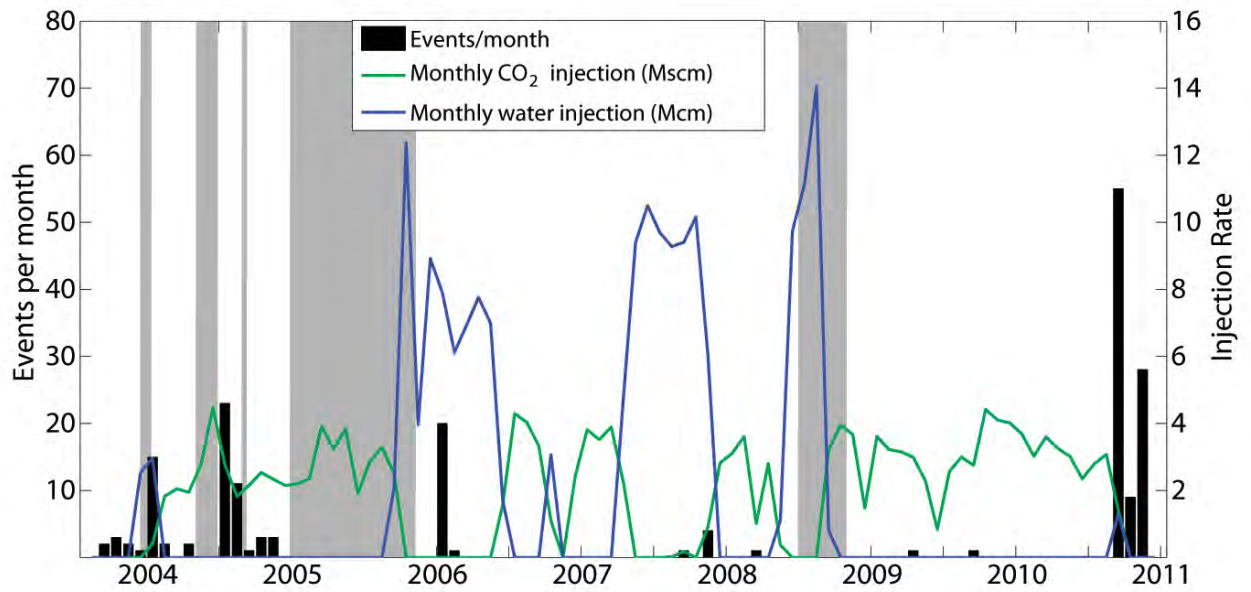
4268

4269 Figure 99: Operations and seismicity at the Cogdell Oilfield, Texas. Green: monthly volumes
 4270 of natural gas produced; red: gas injected; red dots: earthquakes detected 1977-2012. There
 4271 was a clear increase in seismic activity from 2006, five years after the start of CO₂ injection
 4272 [from Gan & Frohlich, 2013].

4273

4274

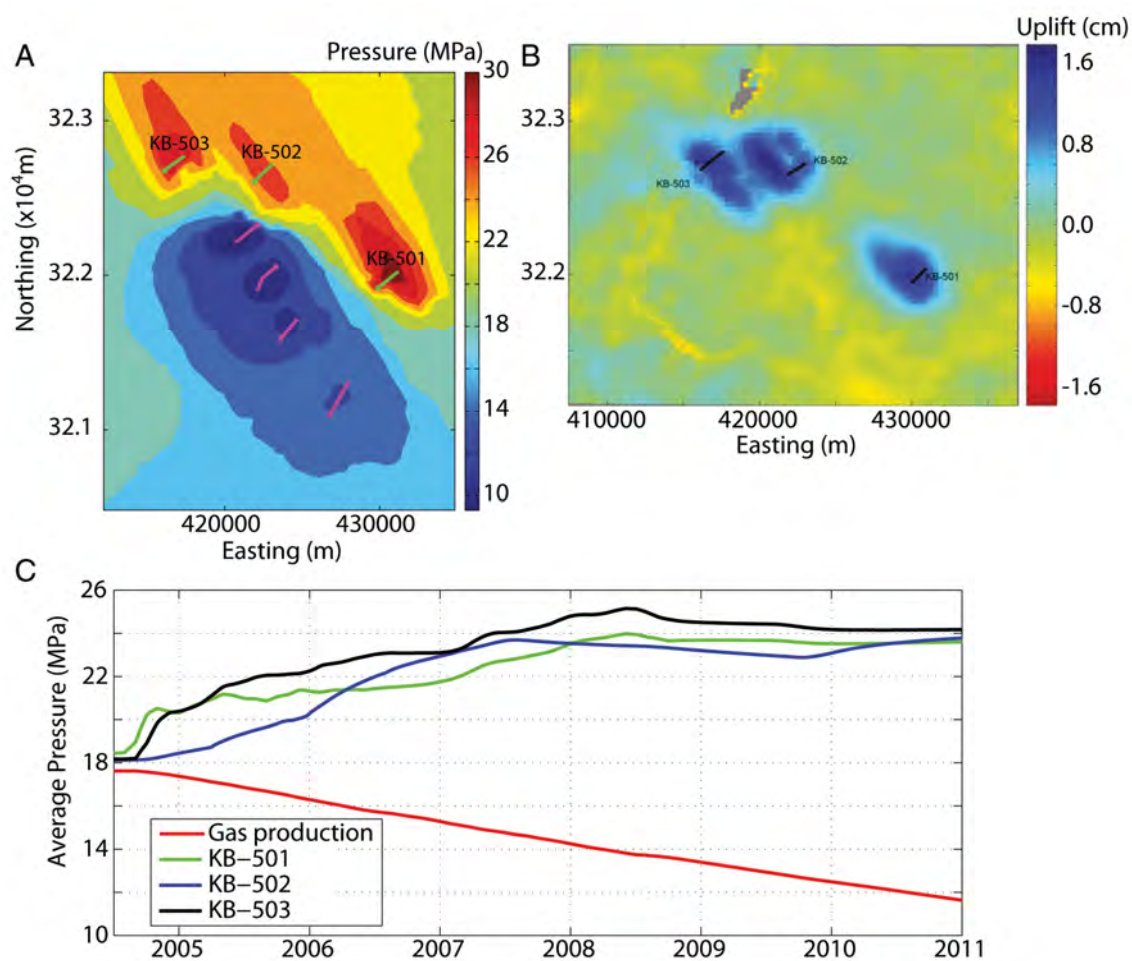
4275

4276
4277

4278 Figure 100: CO₂, water injection, and associated earthquakes at the Weyburn Oilfield,
 4279 Saskatchewan, Canada. Shaded periods: monitoring array was inoperative [from Verdon *et*
 4280 *al.*, 2013].

4281
4282

4283

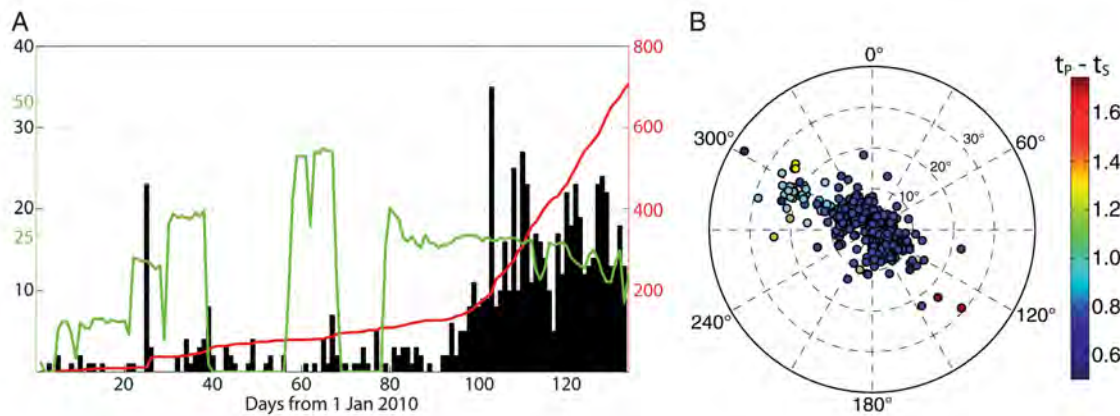
4284
4285

4286 Figure 101: Modelled pore pressure and geomechanical deformation at In Salah, Algeria. A:
 4287 Map of pore pressure after three years of injection. B: Surface uplift measured by InSAR. C:
 4288 Modelled pressure at the three injection wells and in the producing part of the reservoir [from
 4289 Verdon *et al.*, 2013].

4290

4291

4292



4293

4294

4295 Figure 102: Microseismicity at In Salah, Algeria. A: Black: daily seismicity rate; red:
 4296 cumulative number of events January-April 2010; green: CO₂ injection rate in millions of
 4297 standard cubic feet per day²⁴. B. Event arrival angles in polar projection, colored by
 4298 differential *S*- and *P*-wave arrival times [from Verdon *et al.*, 2013].

4299

4300

²⁴ 1 million standard cubic feet of gas per day at 15°C = 28,252.14 m³/day

4301

4302
4303

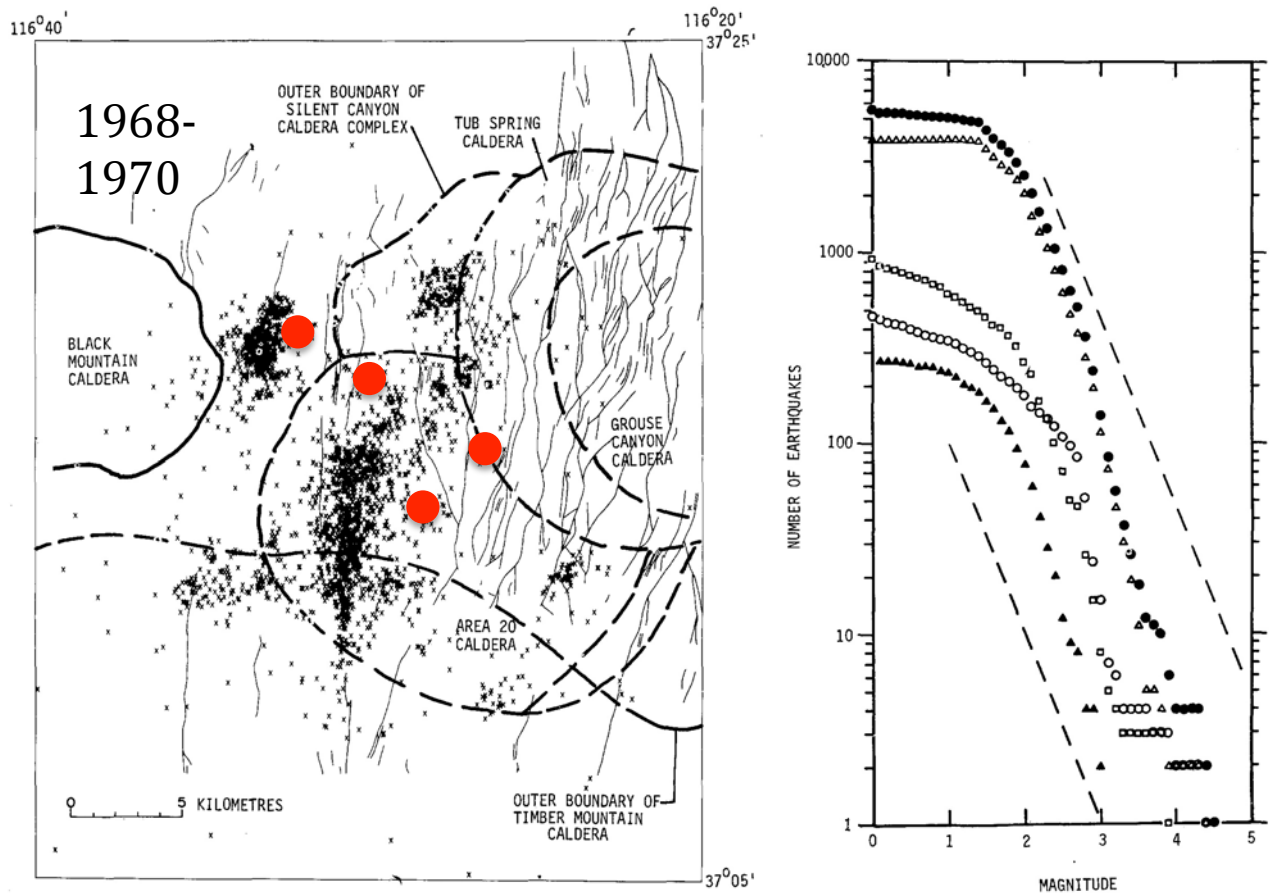
4304 Figure 103: Aerial photograph of the Nevada test site, USA. View of Yucca Flat looking
4305 south-southeast. Center of ring road is at $37^{\circ}\text{N } 9.57'$, $116^{\circ}\text{W } 4.63'$, elevation $4,400 \text{ m}^{25}$.

4306

4307

²⁵ https://en.wikipedia.org/wiki/Nevada_Test_Site

4308



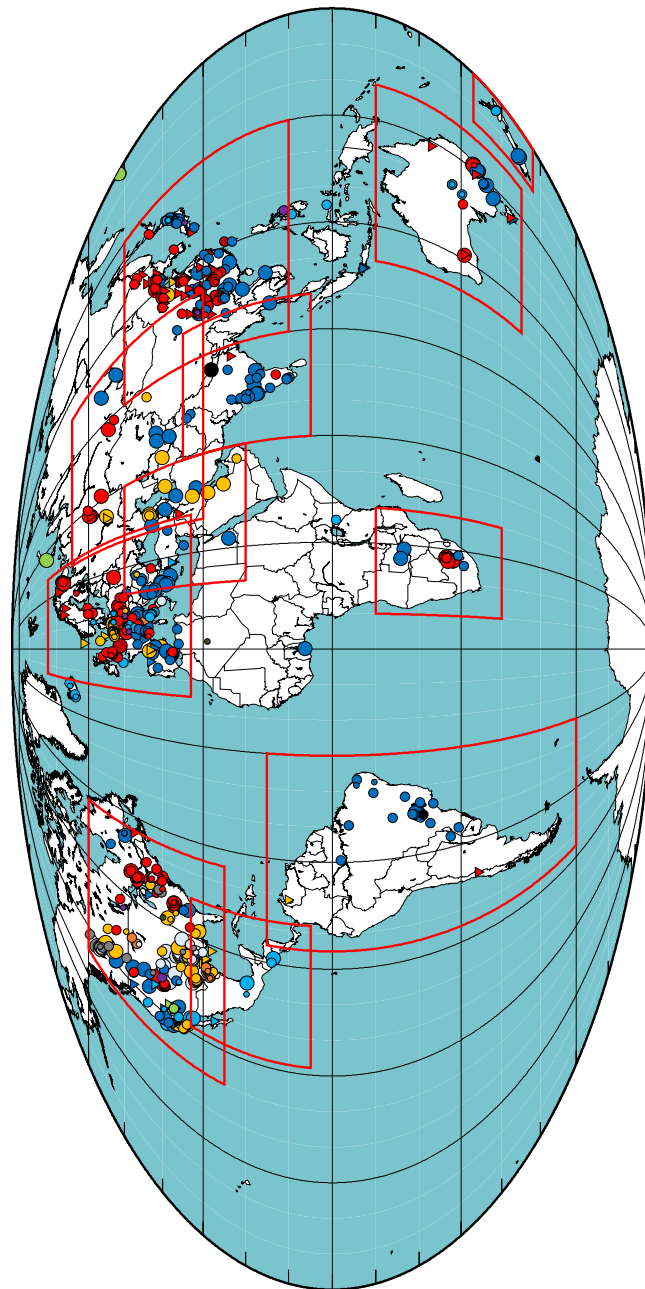
4309

4310

4311 Figure 104: Left: Epicenters of aftershocks of the Benham (1968), Jorum (1969), Purse
 4312 (1969), and Handley (1970) nuclear explosions at the Nevada Test Site. Heavy lines: caldera
 4313 boundaries; light lines: basin-range faults; red dots: locations of nuclear explosions. Right:
 4314 Frequency-magnitude distribution for aftershocks in Pahute Mesa [from Hamilton *et al.*,
 4315 1972]. Dots: entire recording period; open triangles: the period Benham to Purse; solid
 4316 triangles: Purse to Jorum; circles: Jorum to Handley; squares: Handley to the end. Dashed
 4317 lines have a slope of -1; the data above M 2 define “*b*-slopes” of about -1.4 [from McKeown,
 4318 1975].

4319

4320



4321
4322
4323
4324

4325 Figure 105: Cases of human-induced seismicity world-wide, in Mollweide projection,
4326 centered on the Greenwich meridian. Colors of symbols indicate different categories of
4327 seismogenic activity. Circle sizes indicate the magnitudes of the largest reported induced
4328 earthquakes in each category, and inverted triangles indicate cases for which this magnitude
4329 was not reported. Red boxes show the locations of the regional maps.

4330

4331

M_{MAX}				
?	< 2	2-4	> 4	
▼	•	●	●	Carbon Capture & Storage
▼	•	●	●	Construction
▼	•	●	●	Geothermal
▼	•	●	●	Groundwater Extraction
▼	•	●	●	Mining
▼	•	●	●	Nuclear Explosions
▼	•	●	●	Oil & Gas/Unspecified
▼	•	●	●	Oil & Gas/Wastewater Injection
▼	•	●	●	Oil & Gas/Conventional
▼	•	●	●	Oil & Gas/Hydrofracturing
▼	•	●	●	Research
▼	○	○	○	Waste Fluid Injection
▼	•	●	●	Water Reservoir Impoundment

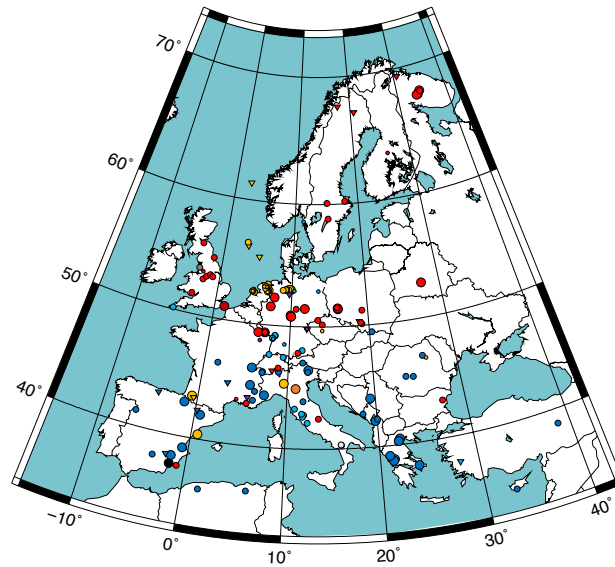
4332

4333

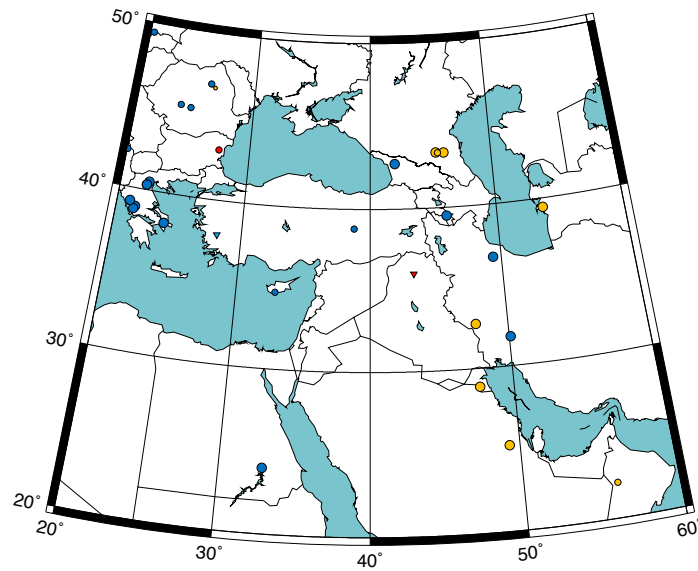
4334 (Legend for Figure 105.)

4335

4336



4337



4338

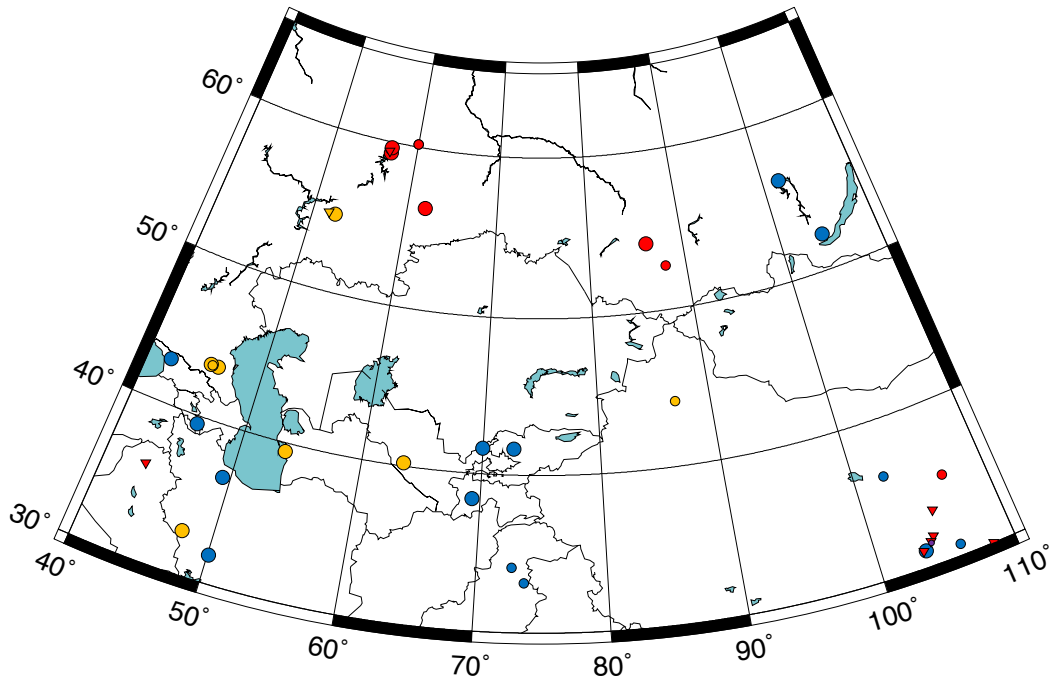
4339

4340 Figure 106: Same as Figure 105 except for (top) Europe, and (bottom) Middle East.

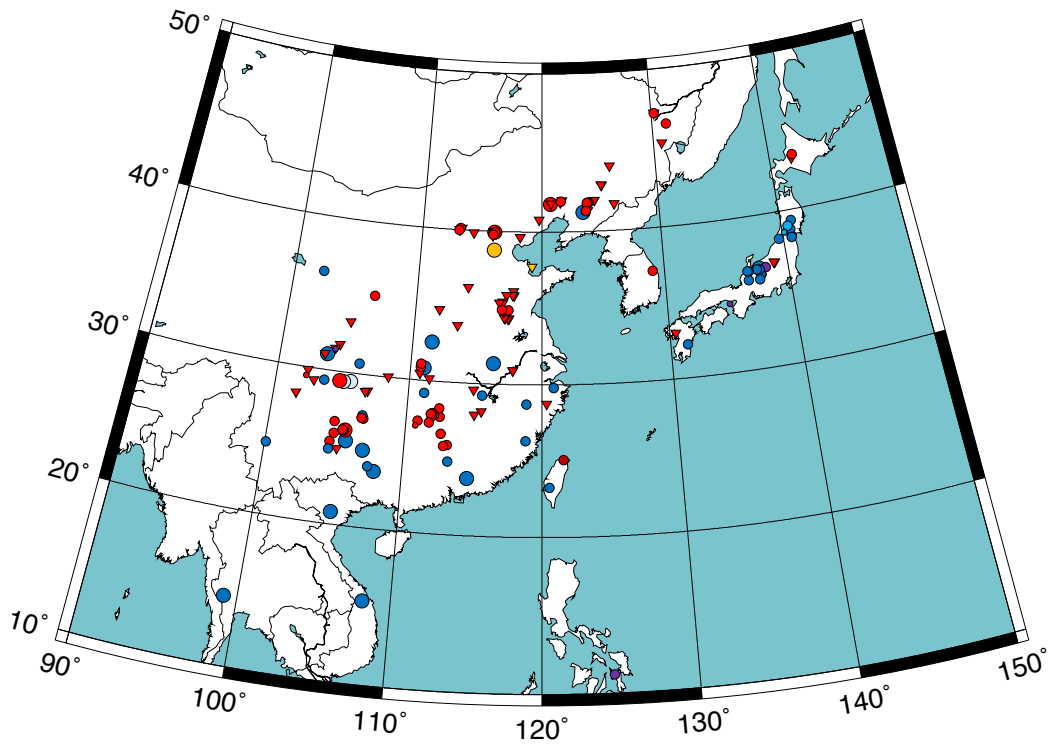
4341

4342

4343

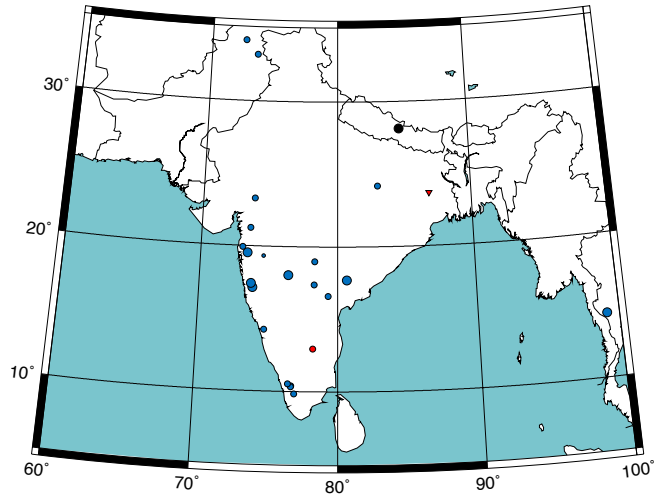


4344
4345
4346
4347

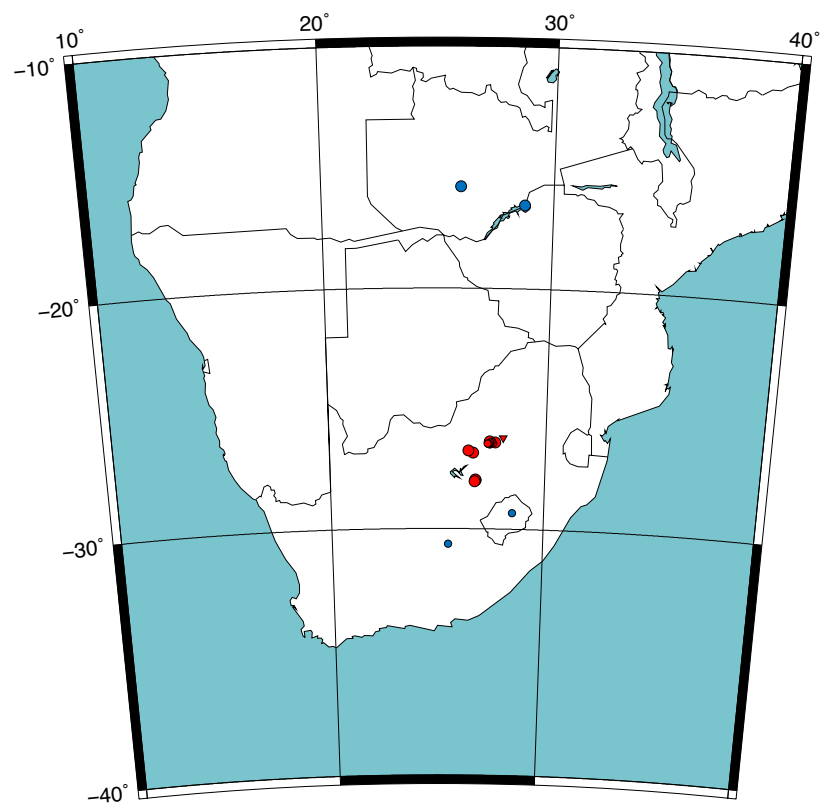


4348
4349
4350
4351
4352

Figure 107: Same as Figure 105 except for (top) central Asia, and (bottom) east Asia.



4353

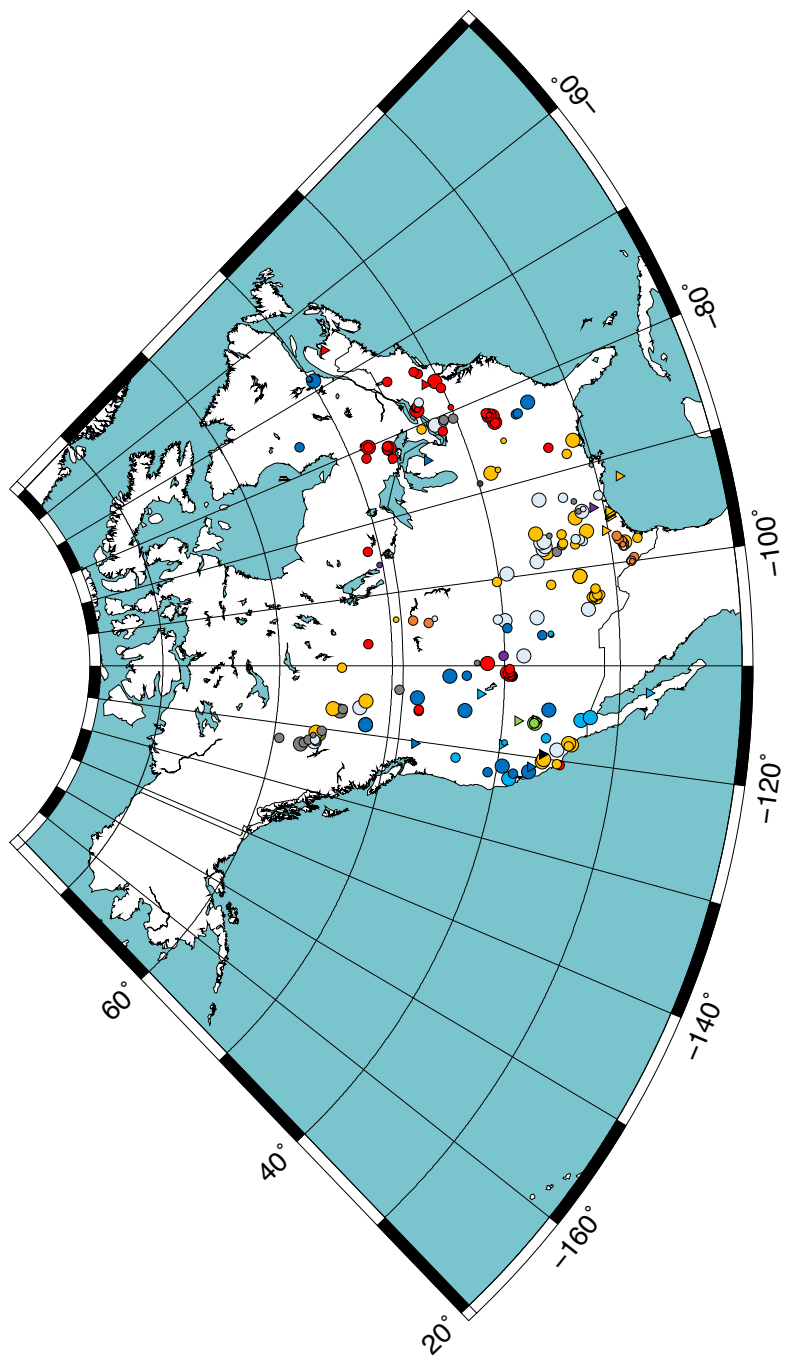


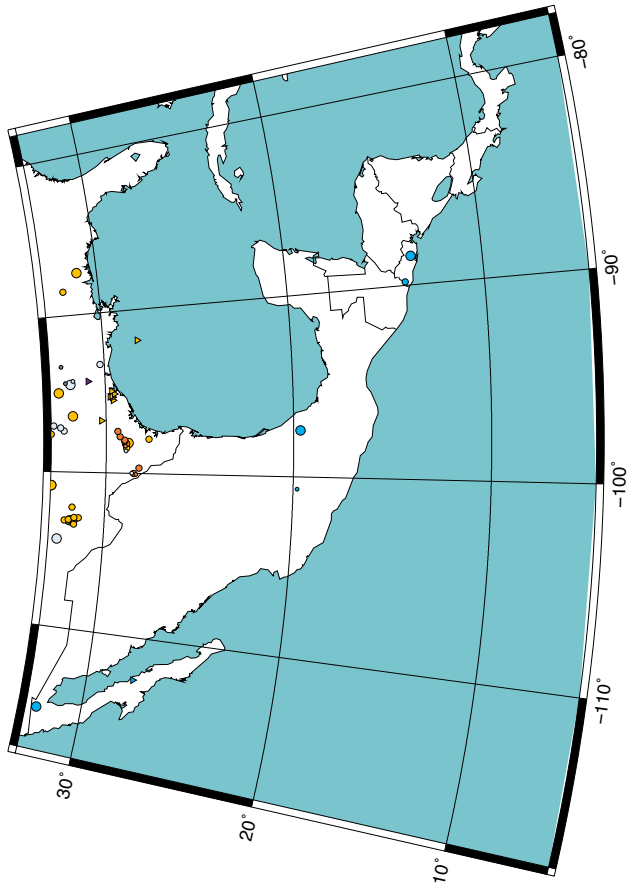
4354

4355

4356 Figure 108: Same as Figure 105 except for (top) India and vicinity, and (bottom) southern
 4357 Africa.

4358





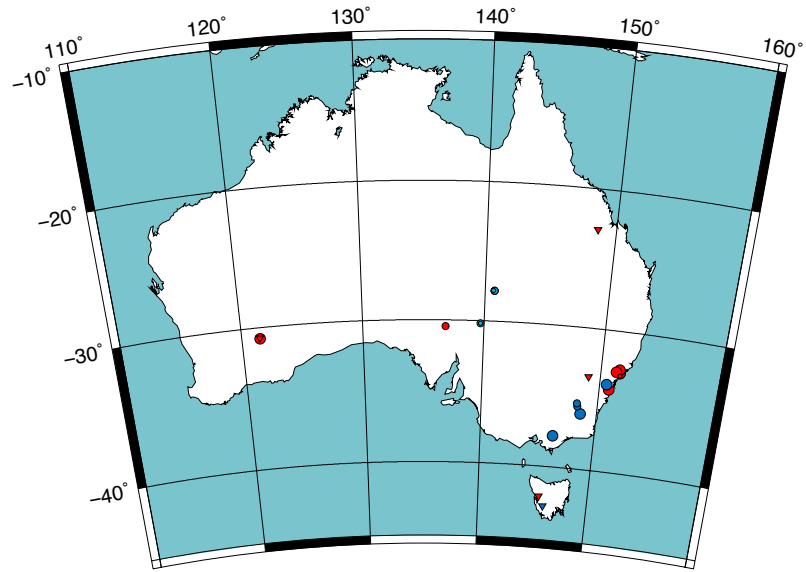
4360
4361

4362 Figure 109: Same as Figure 105 except for (top) North America, and (bottom) central
4363 America.

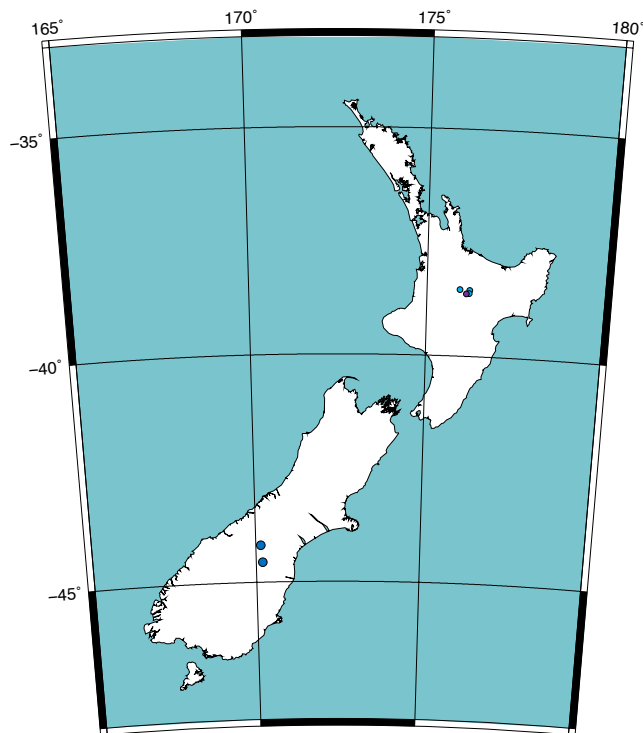


4364
4365

4366 Figure 110: Same as Figure 105 except for South America.



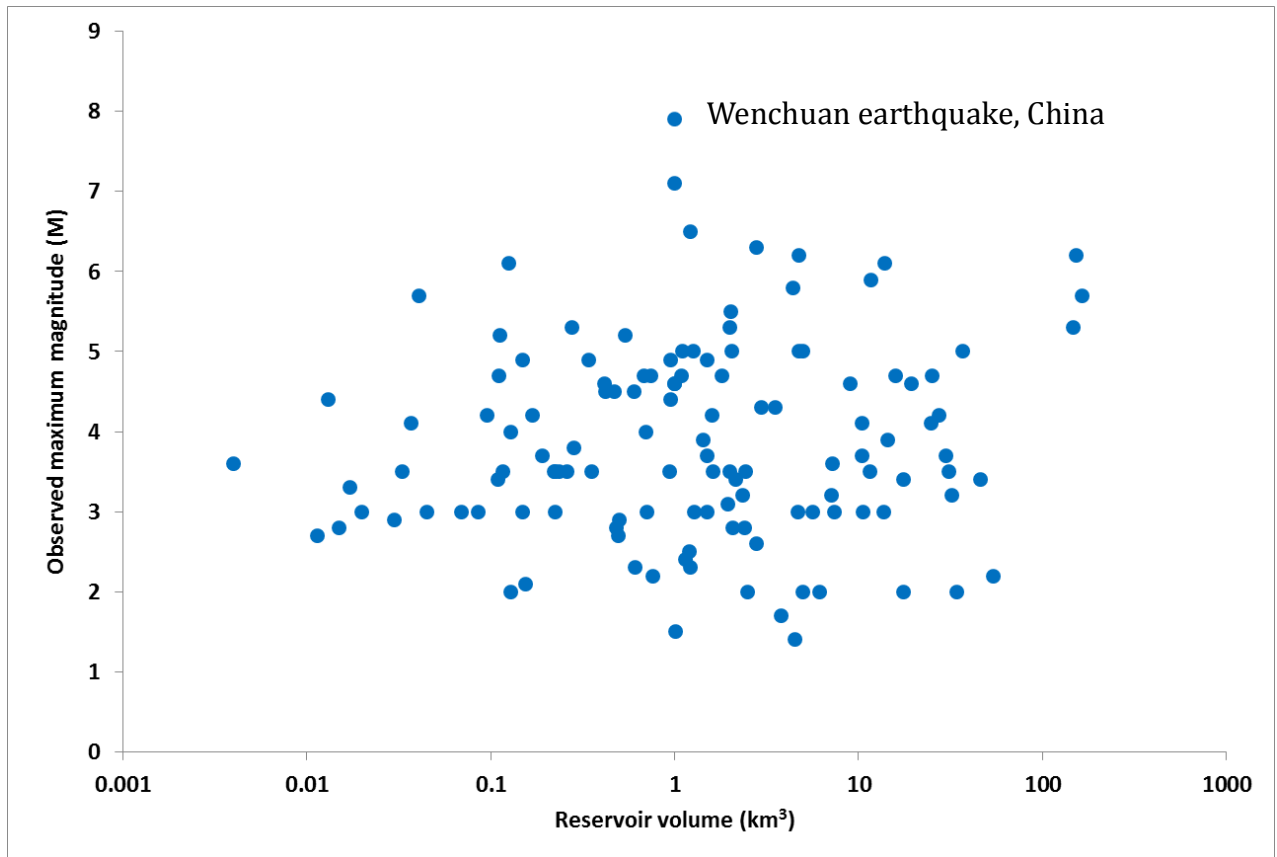
4367

4368
4369

4370

4371 Figure 111: Same as Figure 105 except for (top) Australia, and (bottom) New Zealand.

4372



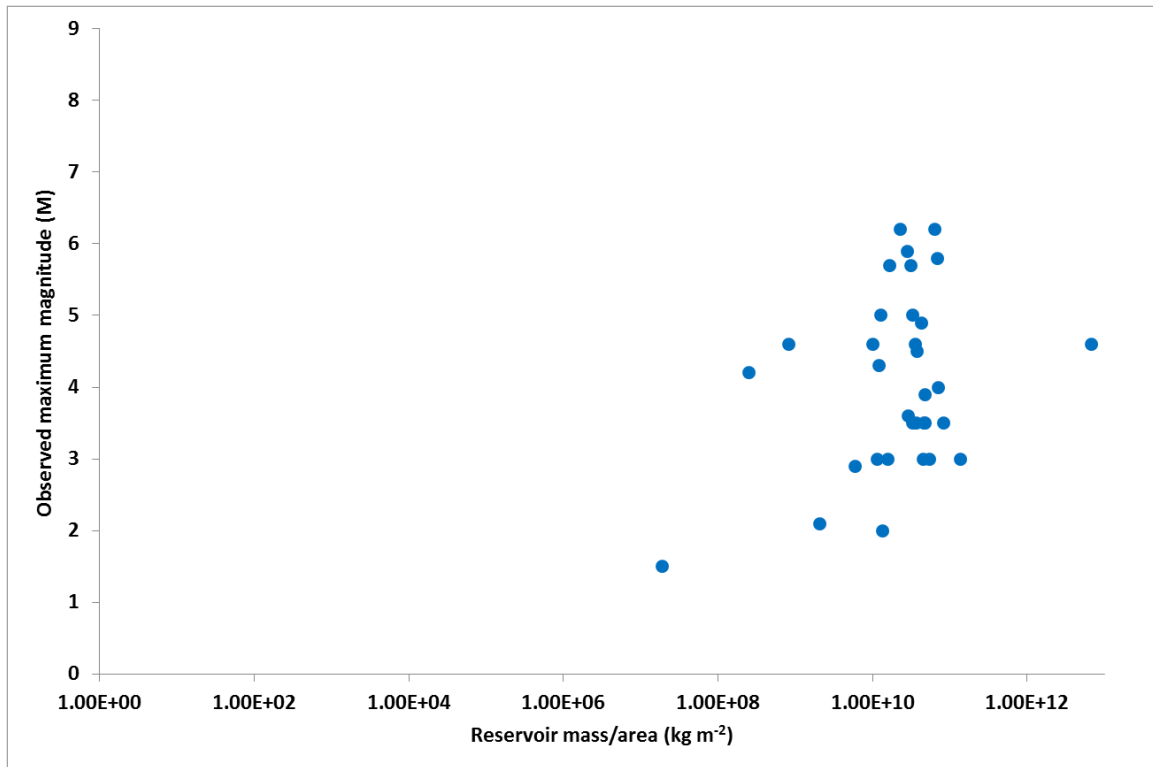
4373
4374

4375 Figure 112: Plot of M_{MAX} vs. water reservoir volume for the 126 cases for which data are
4376 available.

4377

4378

4379



4380

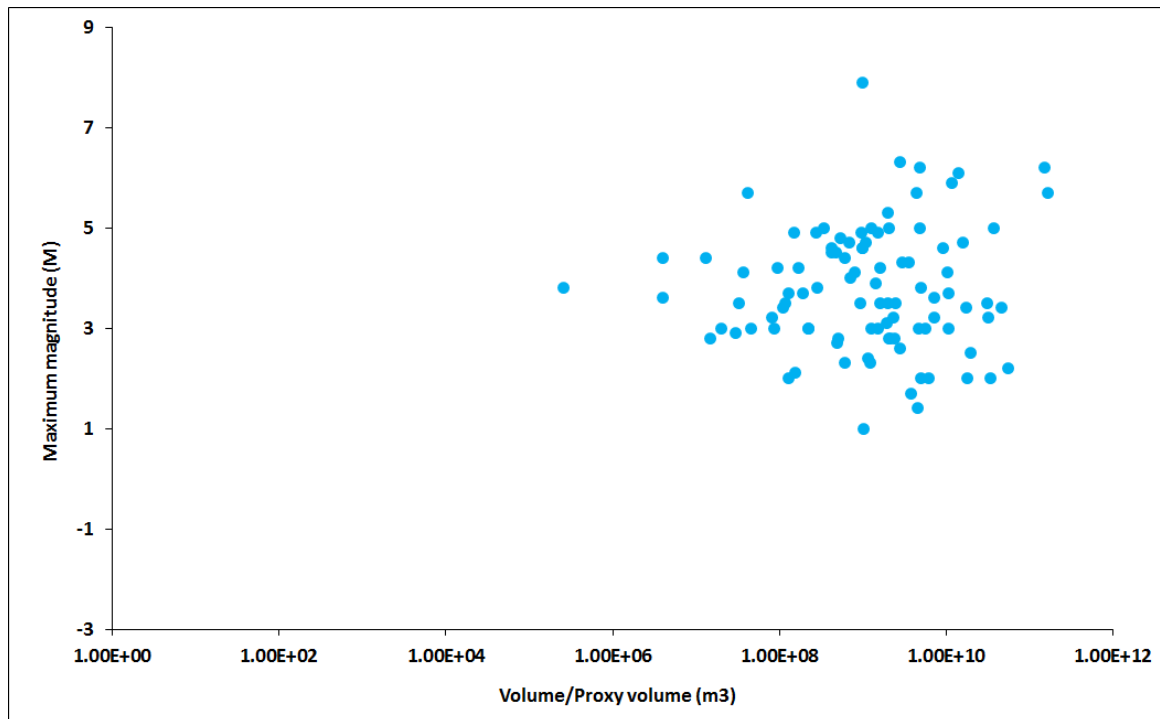
4381

4382 Figure 113: Plot of M_{MAX} vs. water reservoir mass per unit area for the 33 cases for which
4383 data are available.

4384

4385

4386



4387

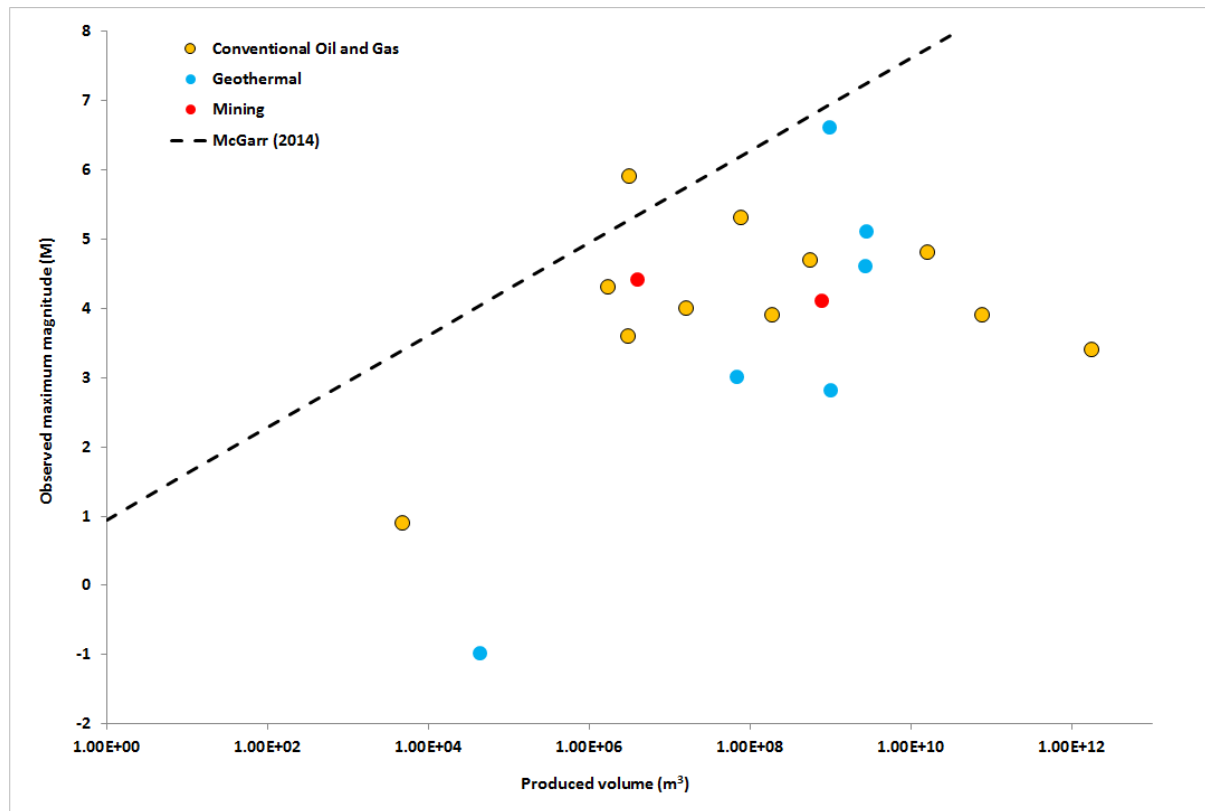
4388

4389 Figure 114: Plot of M_{MAX} vs. volume added or removed by surface operations.

4390

4391

4392



4393

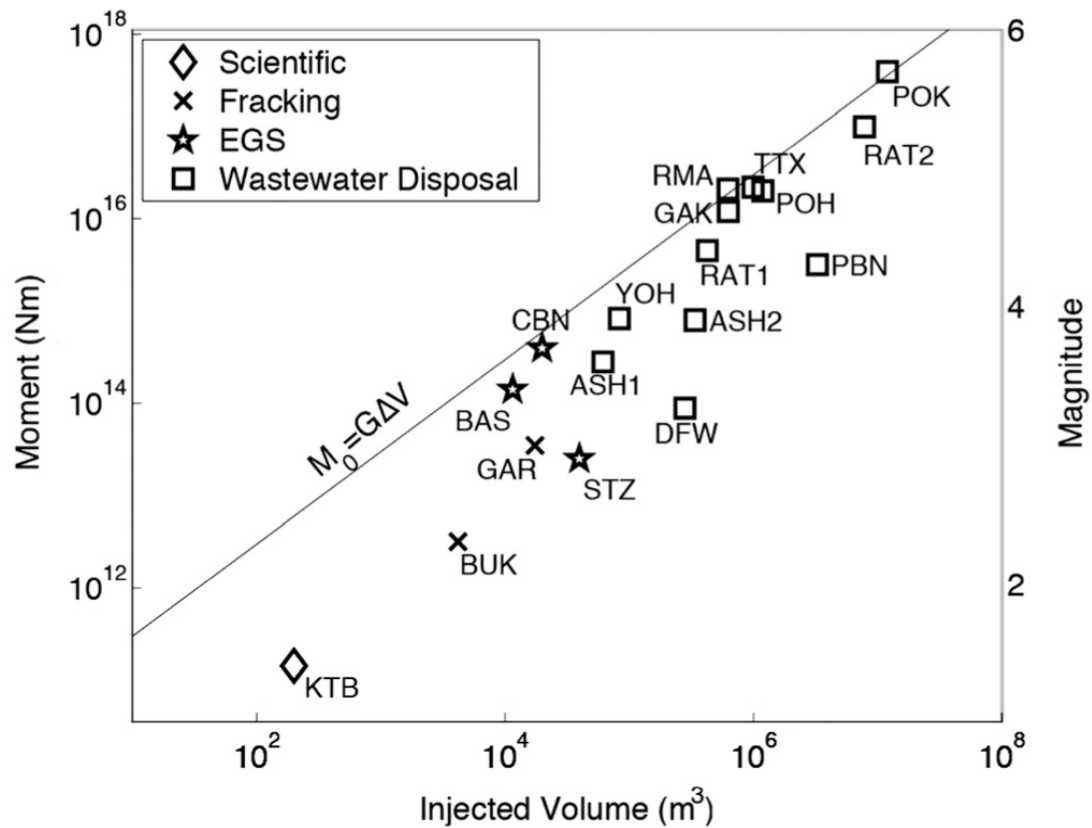
4394

4395 Figure 115: M_{MAX} vs. produced volume (m^3) for 23 projects that involved extraction of mass
 4396 from the subsurface. Some of these projects also involved injection, so their association with
 4397 projection is not certain. The upper limit to M_{MAX} proposed by McGarr [2014] on the basis of
 4398 theoretical considerations is also plotted.

4399

4400

4401



4402

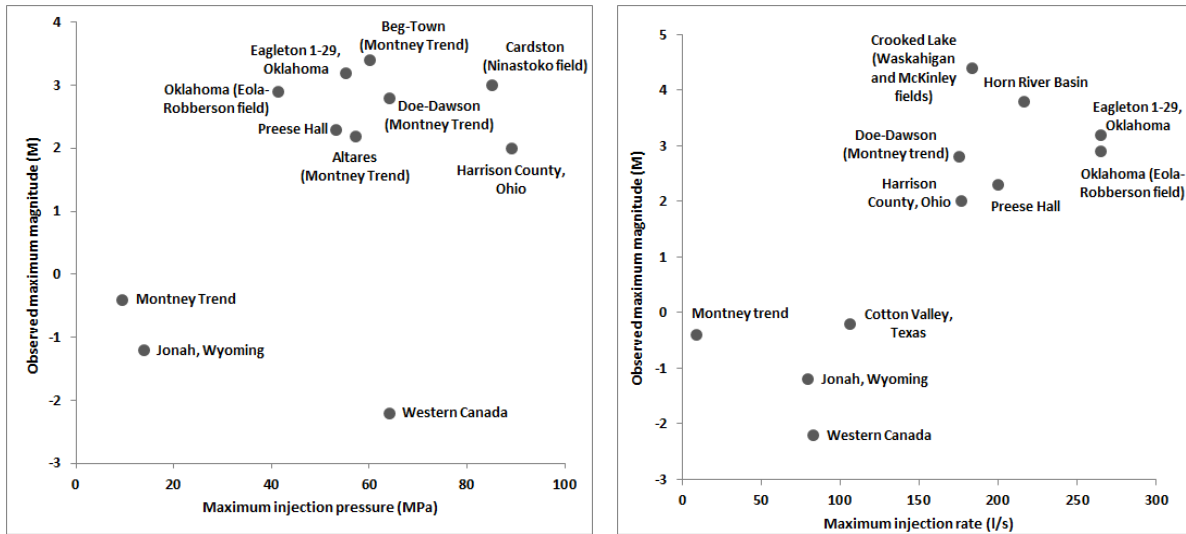
4403

4404 Figure 116: Maximum seismic moment and magnitude vs. total volume of injected fluid from
 4405 the start of injection until the time of the largest induced earthquake. The line relates the
 4406 theoretical upper bound seismic moment to the product of the modulus of rigidity and the
 4407 total volume of injected fluid, and fits the data well [from McGarr, 2014].

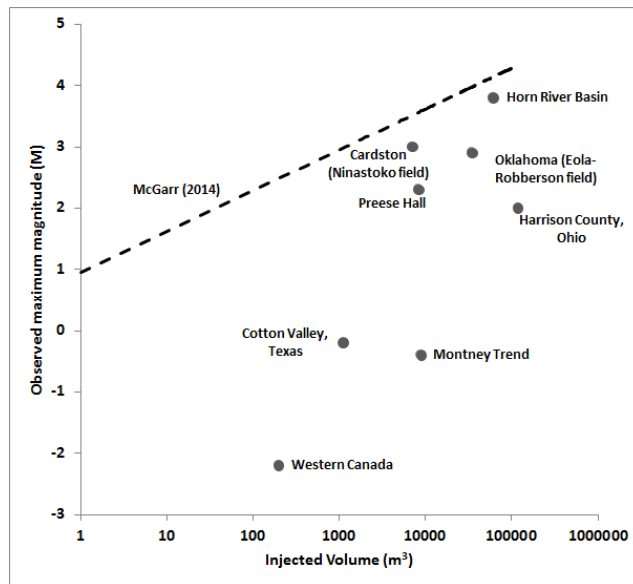
4408

4409

4410



4411



4412

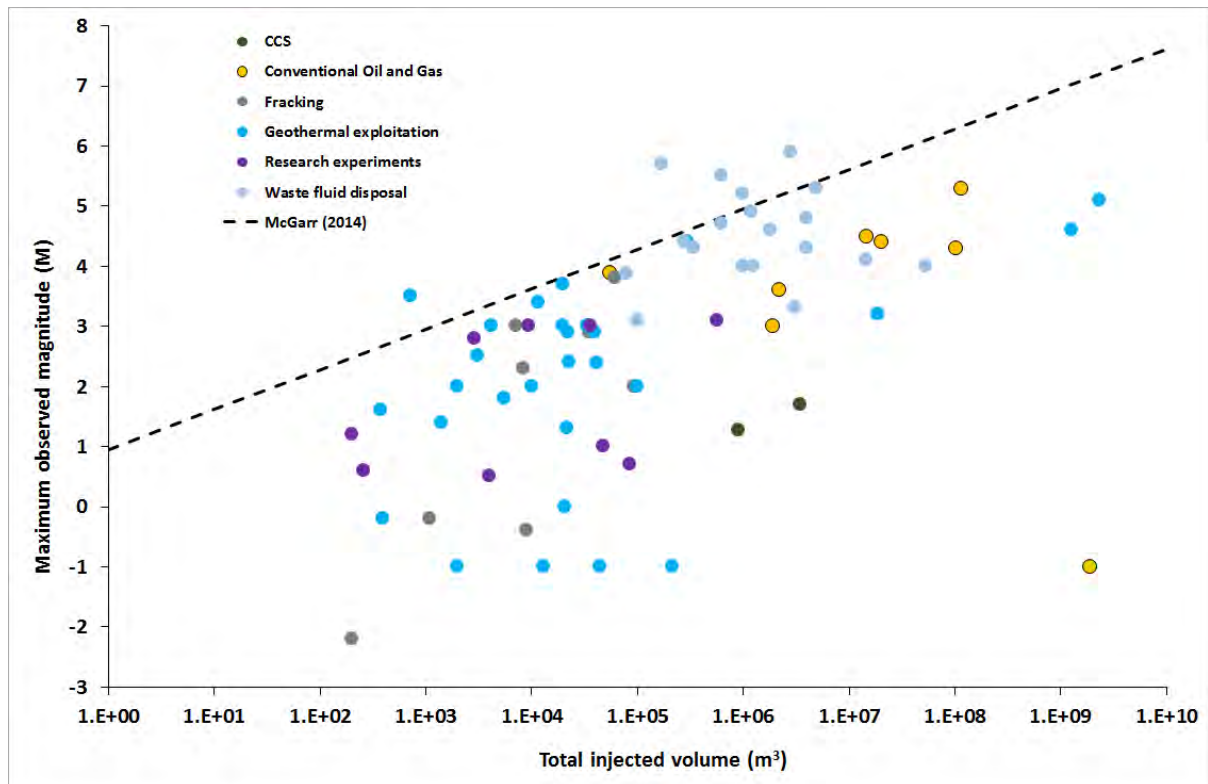
4413

4414 Figure 117: For all cases of shale-gas hydrofracturing-induced earthquakes in our database
 4415 where data are available, top left: M_{MAX} vs. maximum injection pressure, top right: M_{MAX} vs.
 4416 maximum injection rate, and bottom: M_{MAX} vs. injected volume.

4417

4418

4419



4420

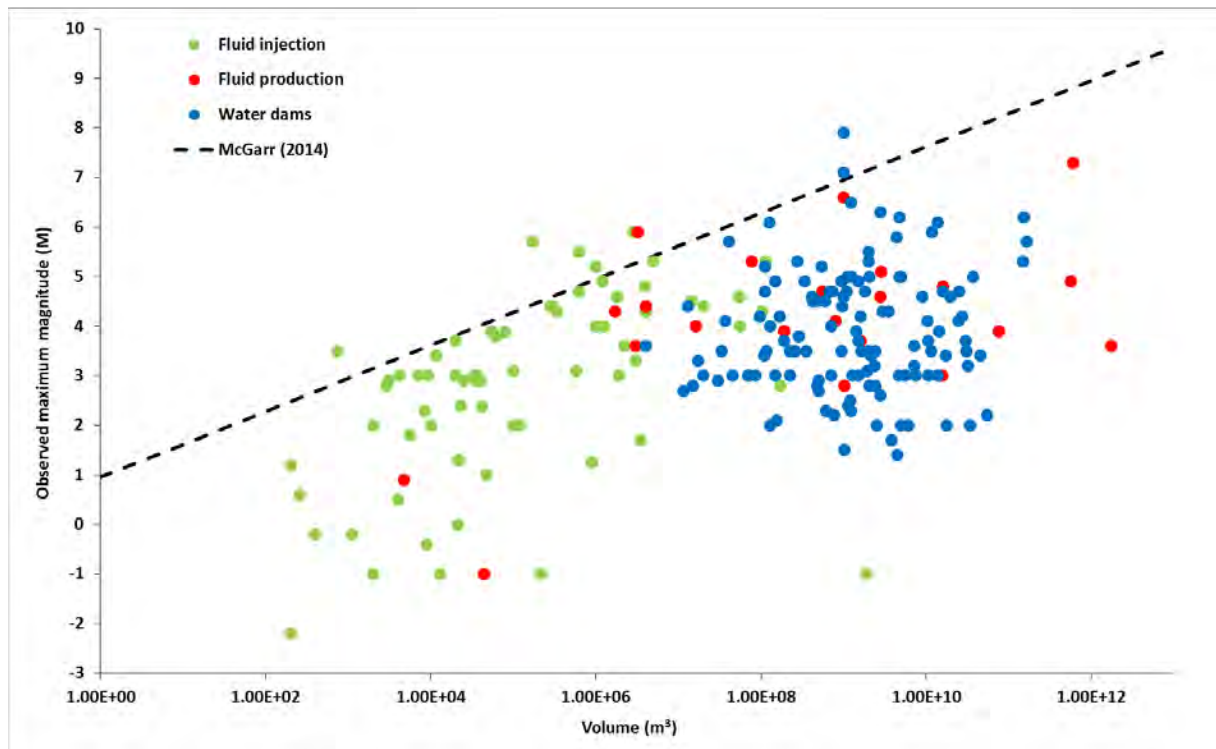
4421

4422 Figure 118: M_{MAX} vs. total injected volume for the 69 cases of induced seismicity for which
 4423 data are available. The upper-bound magnitude limit proposed by McGarr [2014] on the basis
 4424 of theoretical considerations is also plotted.

4425

4426

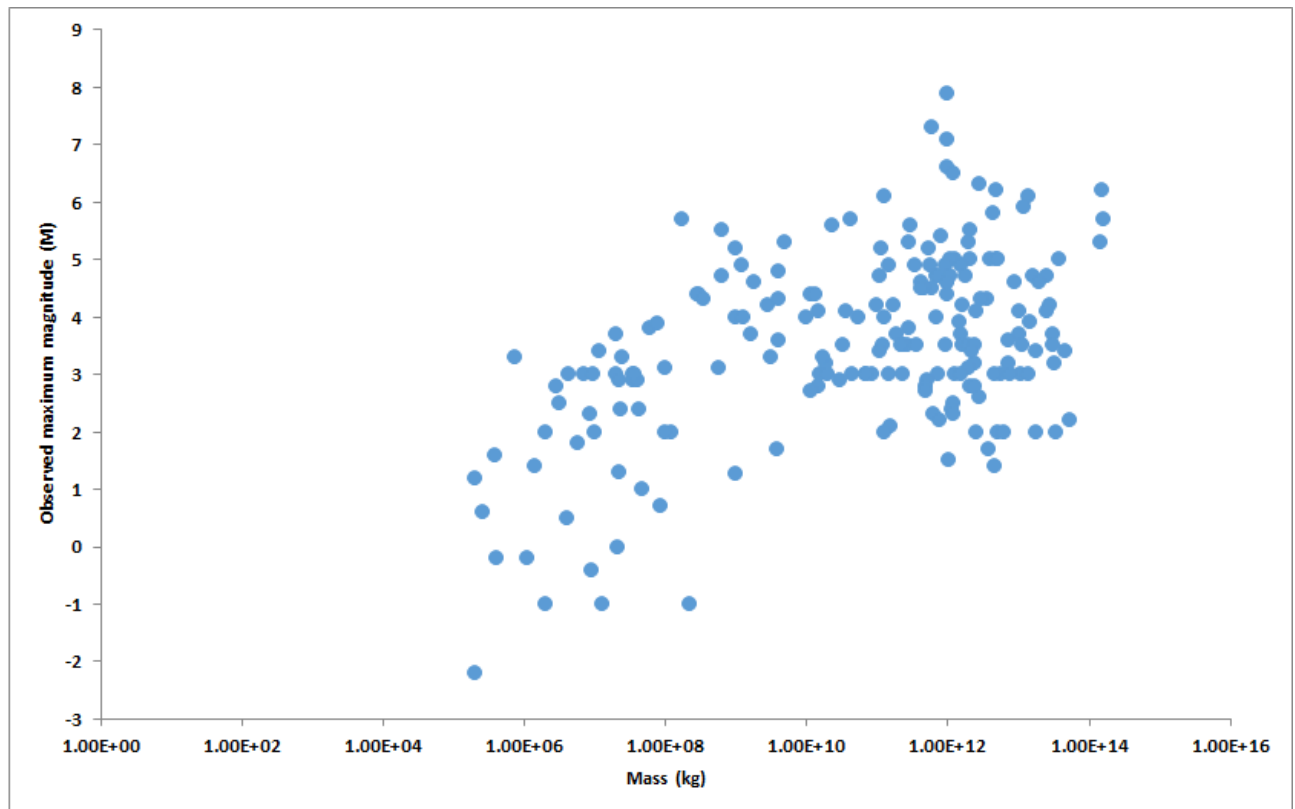
4427

4428
4429

4430 Figure 119: M_{MAX} vs volume or proxy volume of material removed or added for the 218
 4431 cases for which data are available, along with the relationship proposed by McGarr [2014] on
 4432 the basis of theoretical considerations. Volumes and proxy volumes were estimated as
 4433 follows: Water dams—the volume of the impounded reservoir; fluid injection or extraction—
 4434 fluid volume injected into or extracted from the subsurface; mining—mass of material
 4435 excavated, converted to volume using an appropriate density; construction—relevant mass
 4436 converted to volume using an appropriate density for the building materials; CCS—mass of
 4437 injected CO_2 converted to volume using a density of liquid CO_2 of 1100 kg/m^3 .

4438
4439

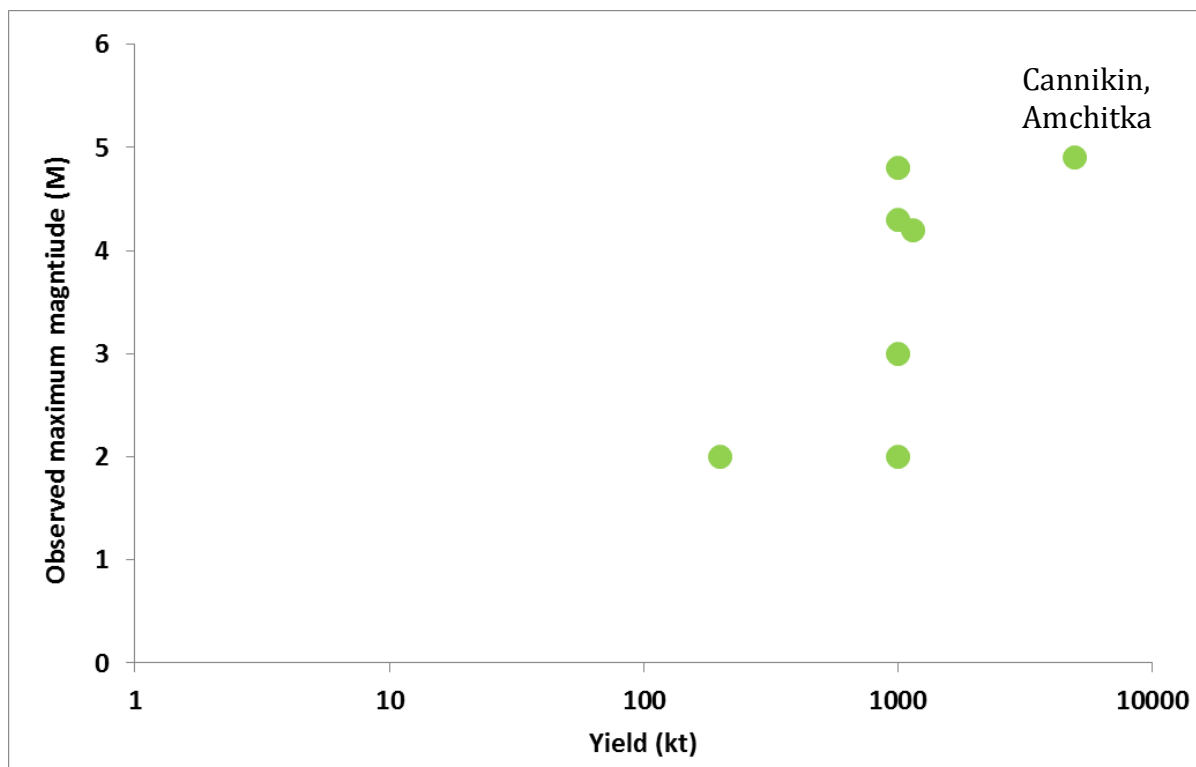
4440

4441
4442

4443 Figure 120: M_{MAX} vs. mass of material removed or added for the 203 cases where data are
4444 available. Water volumes were converted to mass using a density 1000 kg/m^3 . Oil and gas are
4445 not included in this plot except where quantity was reported in units of mass. Project types
4446 plotted include CCS, construction, conventional oil and gas, shale-gas hydrofracturing,
4447 geothermal, mining, research experiments, waste fluid injection and water reservoirs.

4448
4449

4450



4451

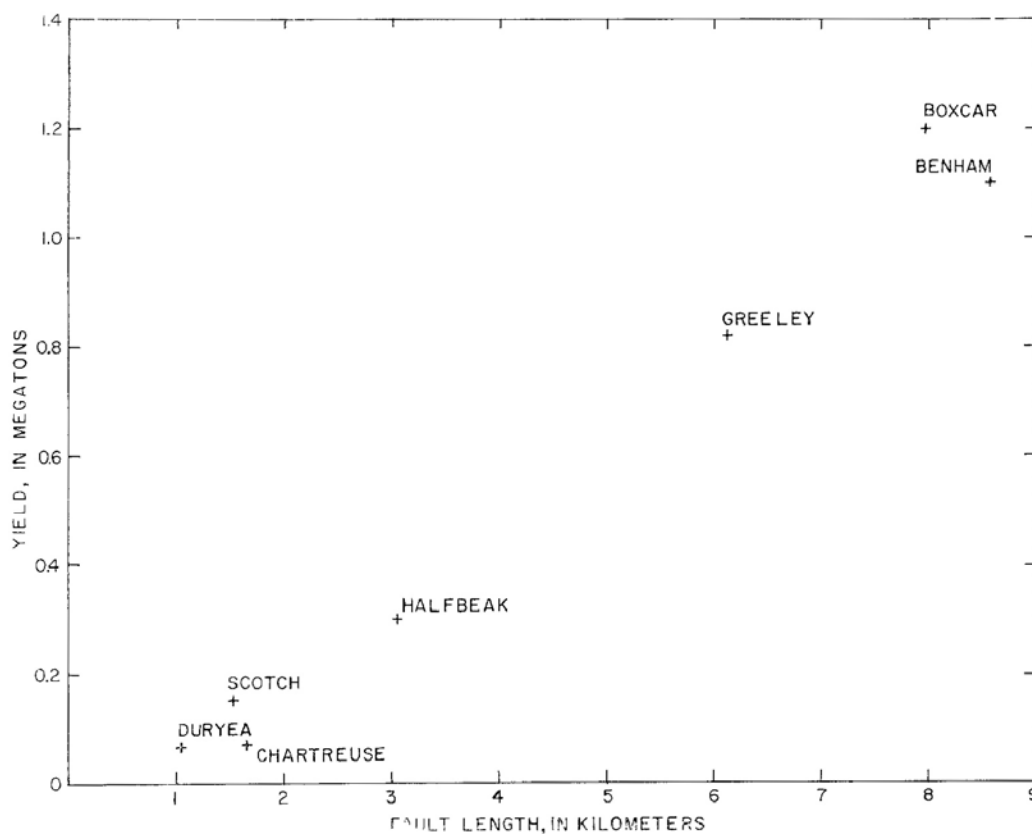
4452

4453 Figure 121: M_{MAX} vs. yield in kilotonnes for nuclear tests that activated faults for the seven
 4454 cases reported. Only one of these (Benham) is in common with the dataset of McKeown and
 4455 Dickey [1969] (Figure 122).

4456

4457

4458



4459

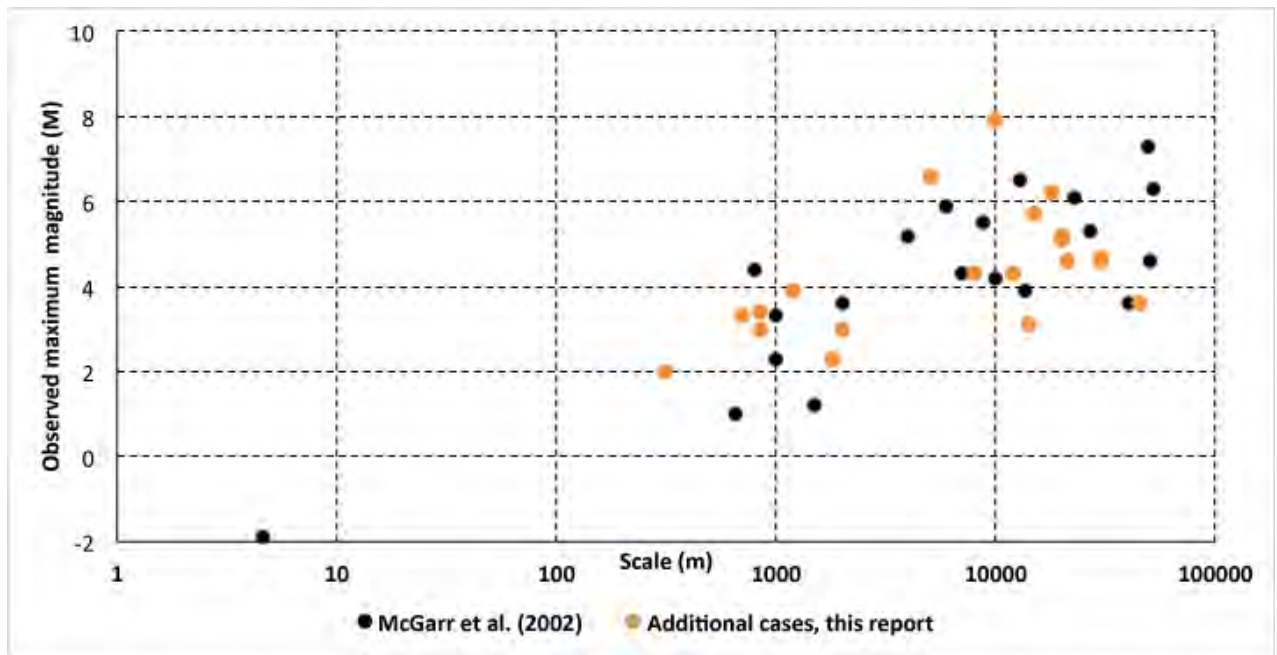
4460

4461 Figure 122: Fault length vs. yield for nuclear explosions that activated faults in Pahute Mesa,
4462 Nevada Test Site [from McKeown & Dickey, 1969].

4463

4464

4465



4466

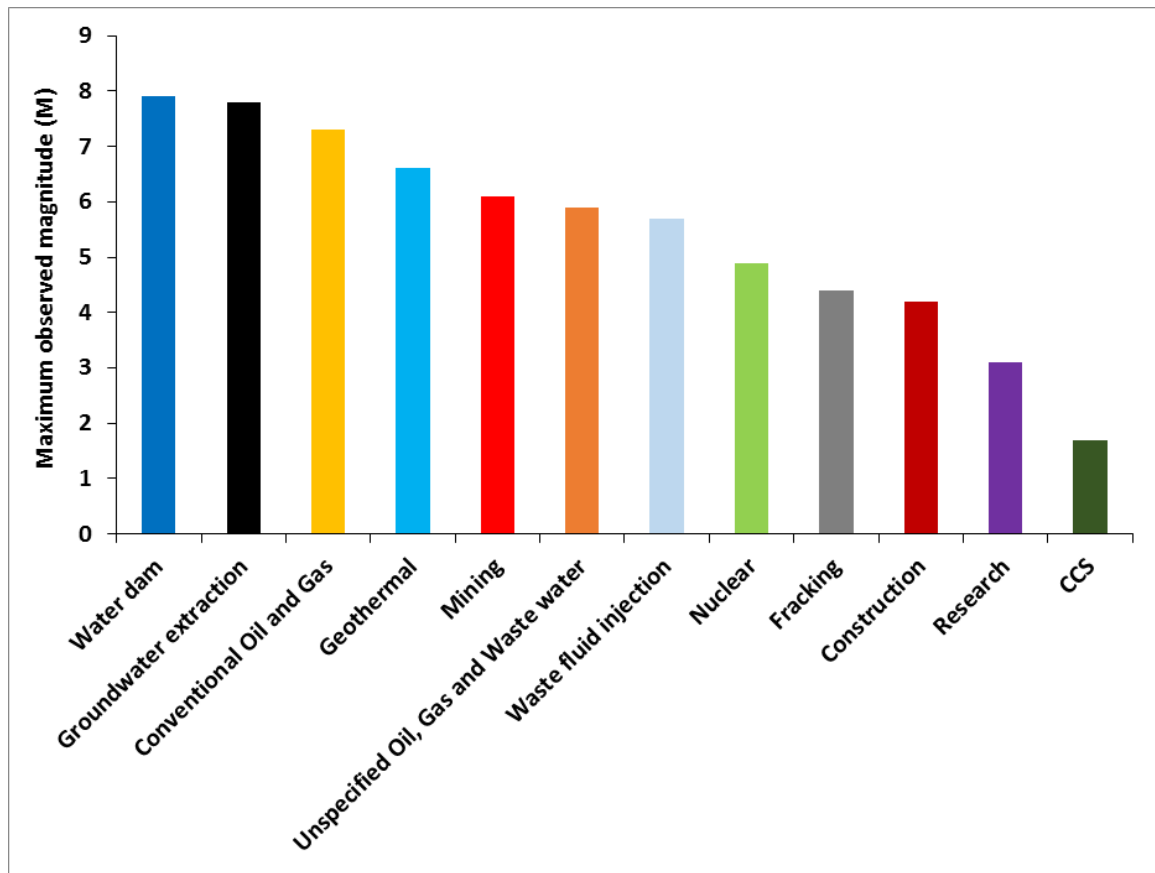
4467

4468 Figure 123: M_{MAX} vs. project scale in meters. Black dots: cases studied by McGarr *et al.*
 4469 [2002]; orange dots: 20 additional cases from our database. Project scale was estimated using
 4470 the longest dimension of the project, *e.g.*, the length of a water reservoir.

4471

4472

4473



4474

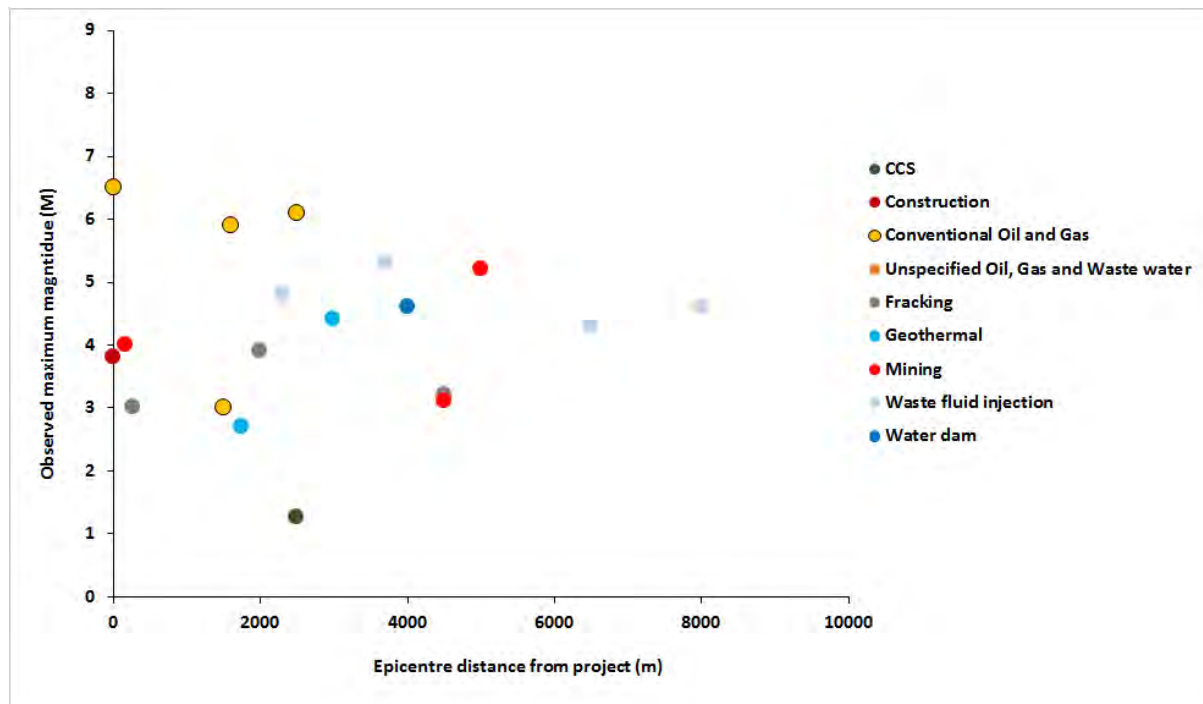
4475

4476 Figure 124: Histogram of M_{MAX} for different categories of project.

4477

4478

4479

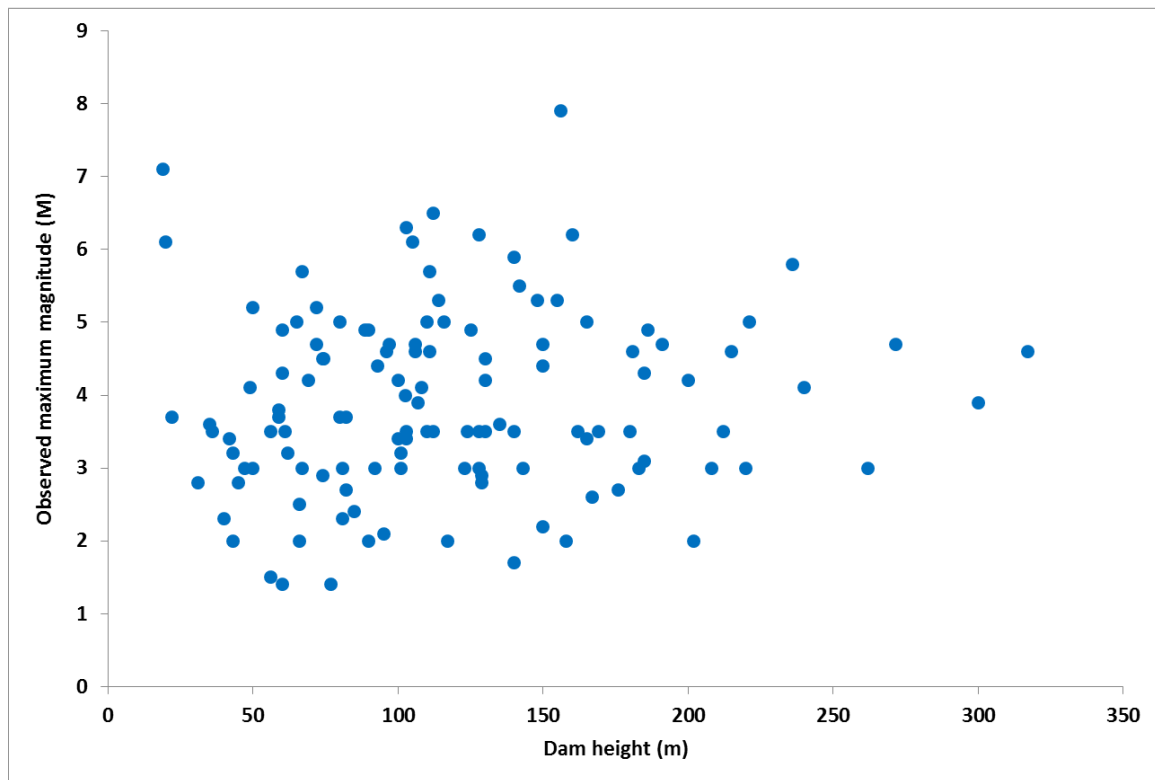
4480
4481

4482 Figure 125: M_{MAX} vs. distance from project for postulated induced earthquakes up to 10 km
 4483 away for the 19 cases where data are available.

4484

4485

4486



4487

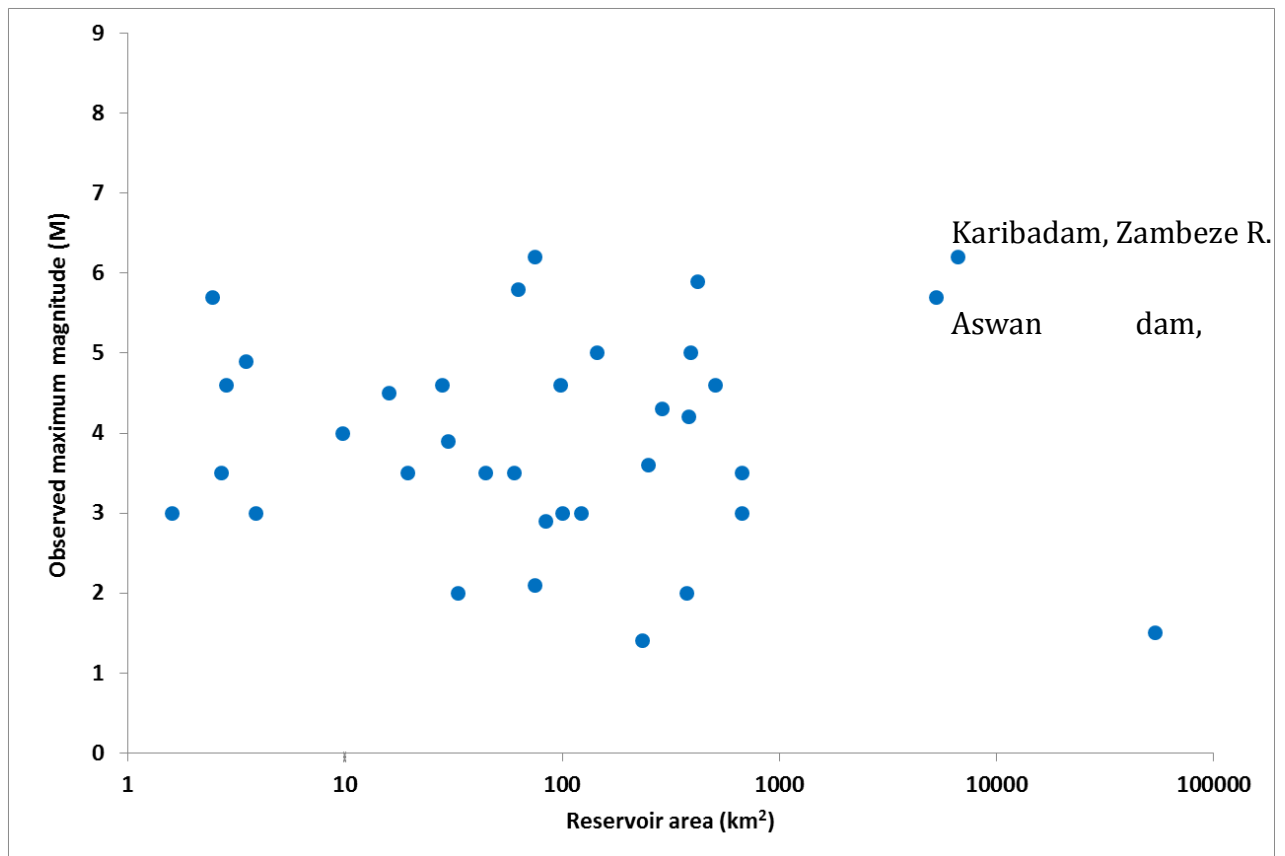
4488

4489 Figure 126: Plot of M_{MAX} vs. dam height for the 159 cases of seismogenic water reservoirs
4490 for which data are available.

4491

4492

4493



4494

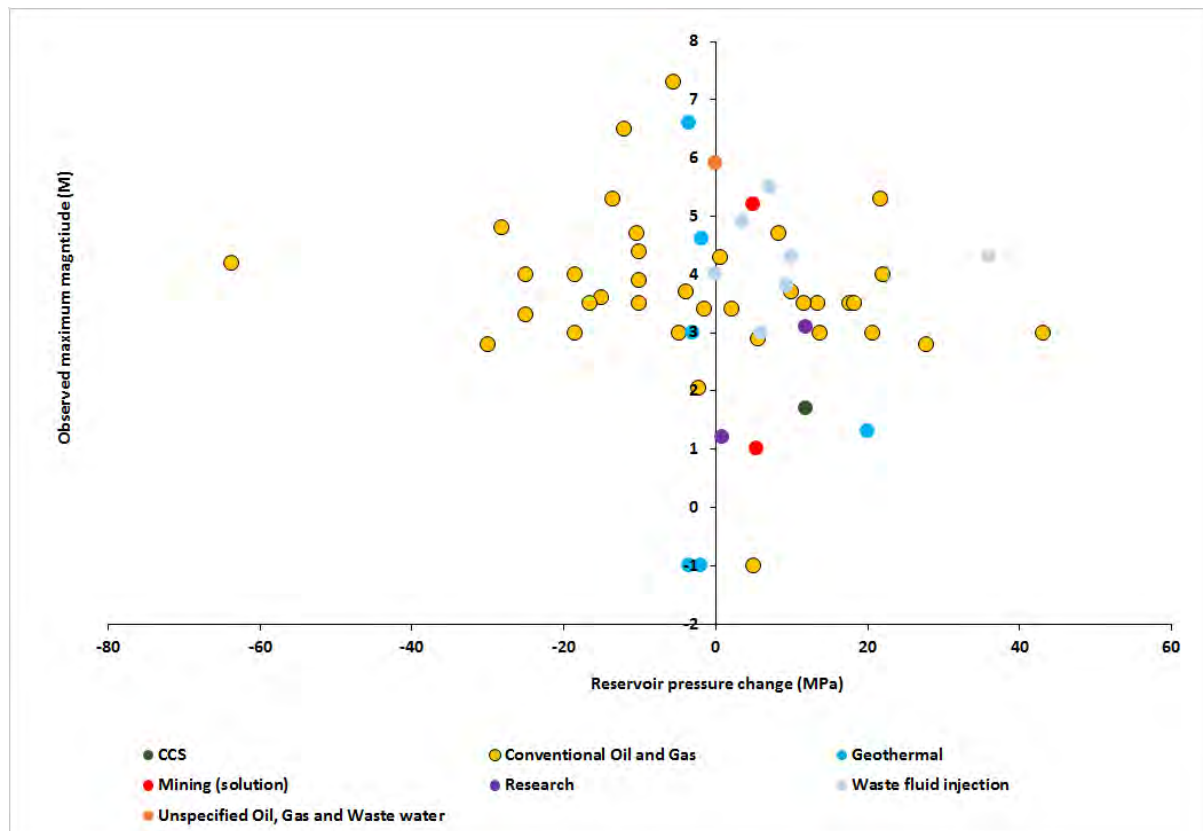
4495

4496 Figure 127: Plot of M_{MAX} vs. water reservoir area for the 35 cases for which data are
 4497 available.

4498

4499

4500



4501

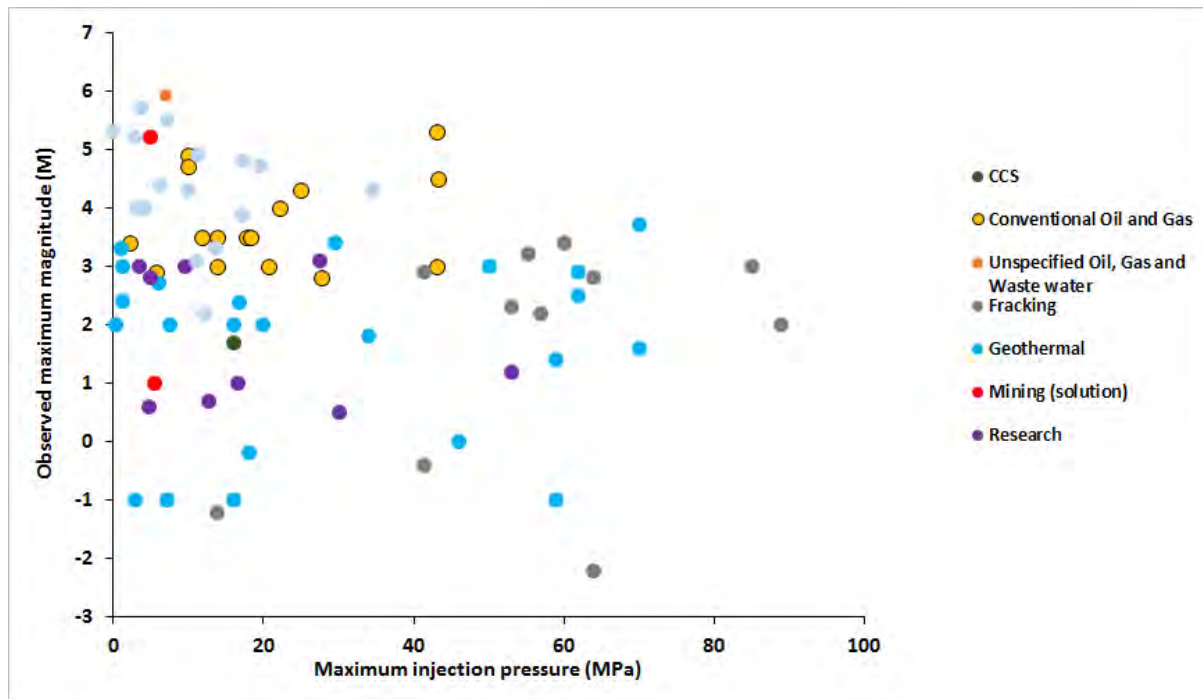
4502

4503 Figure 128: M_{MAX} vs. change in reservoir fluid pressure resulting from production/injection
 4504 for the 55 cases where data are available. We include 9 cases of conventional oil and gas
 4505 where the pressure change results from both injection and production.

4506

4507

4508



4509

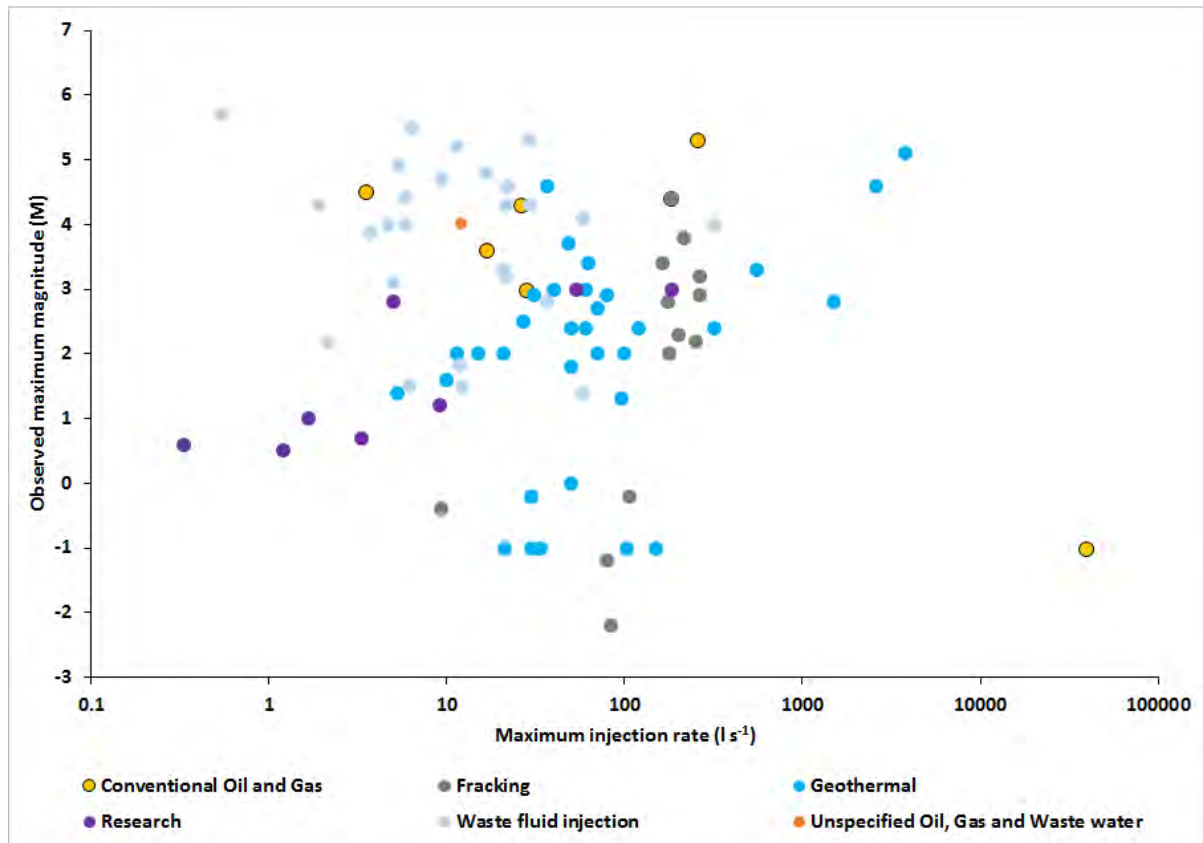
4510

4511 Figure 129: M_{MAX} vs. maximum wellhead injection pressure for the 79 cases where data are
4512 reported.

4513

4514

4515



4516

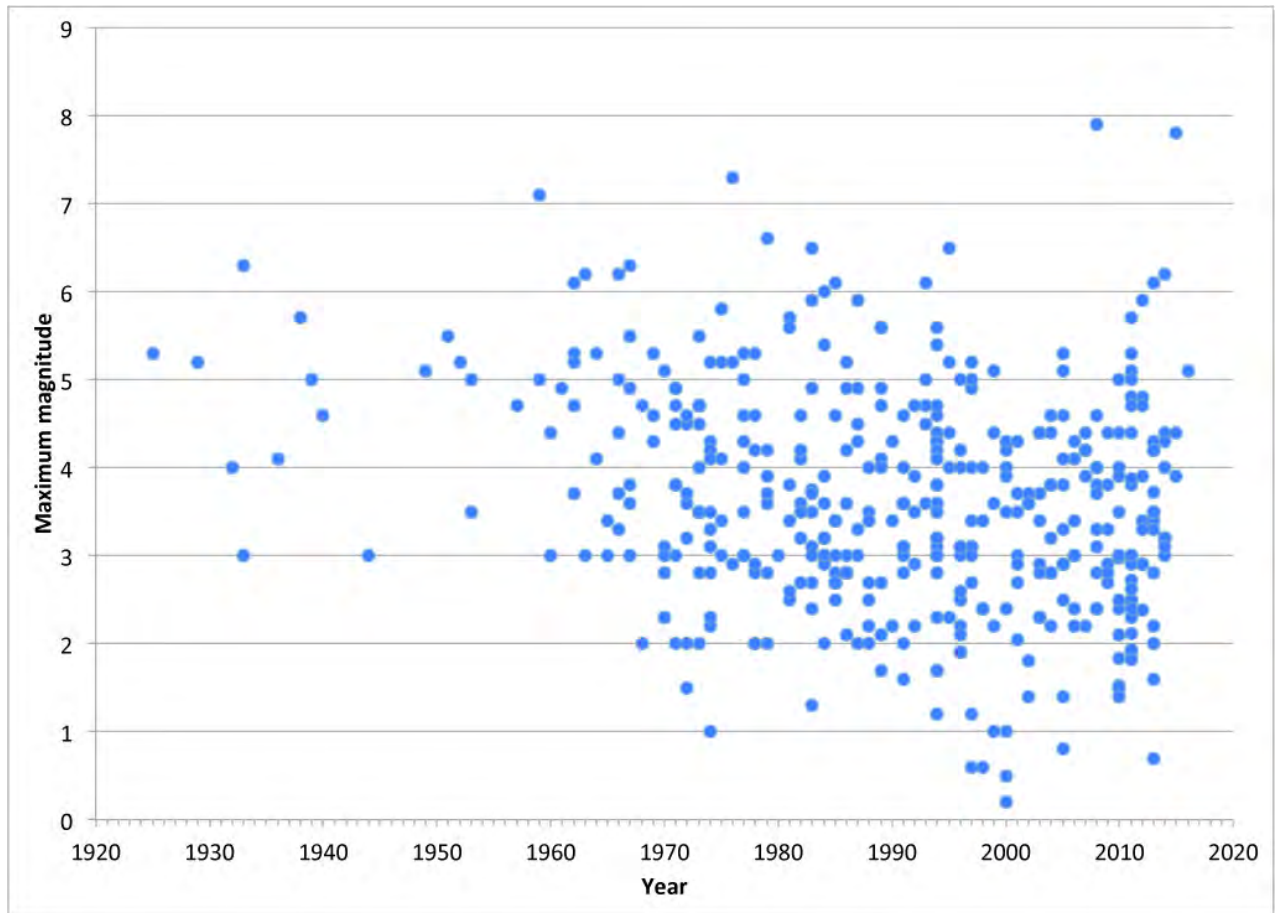
4517

4518 Figure 130: M_{MAX} vs. maximum injection rate for the 88 cases for which data are reported.
 4519 Rates of injection varied from 0.33 to $\sim 40,000$ l/s. At rates greater than ~ 1000 l s⁻¹, values
 4520 apply to entire fields rather than individual wells.

4521

4522

4523



4524

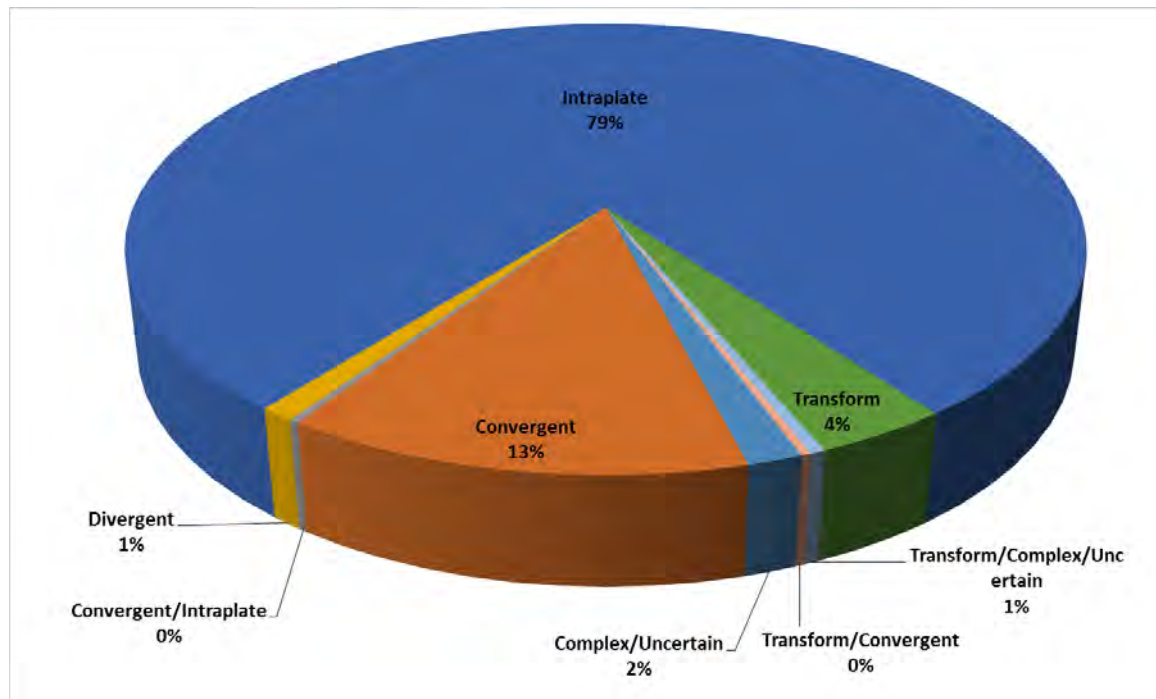
4525

4526 Figure 131: M_{MAX} vs. year for the 419 cases where data are available.

4527

4528

4529



4530

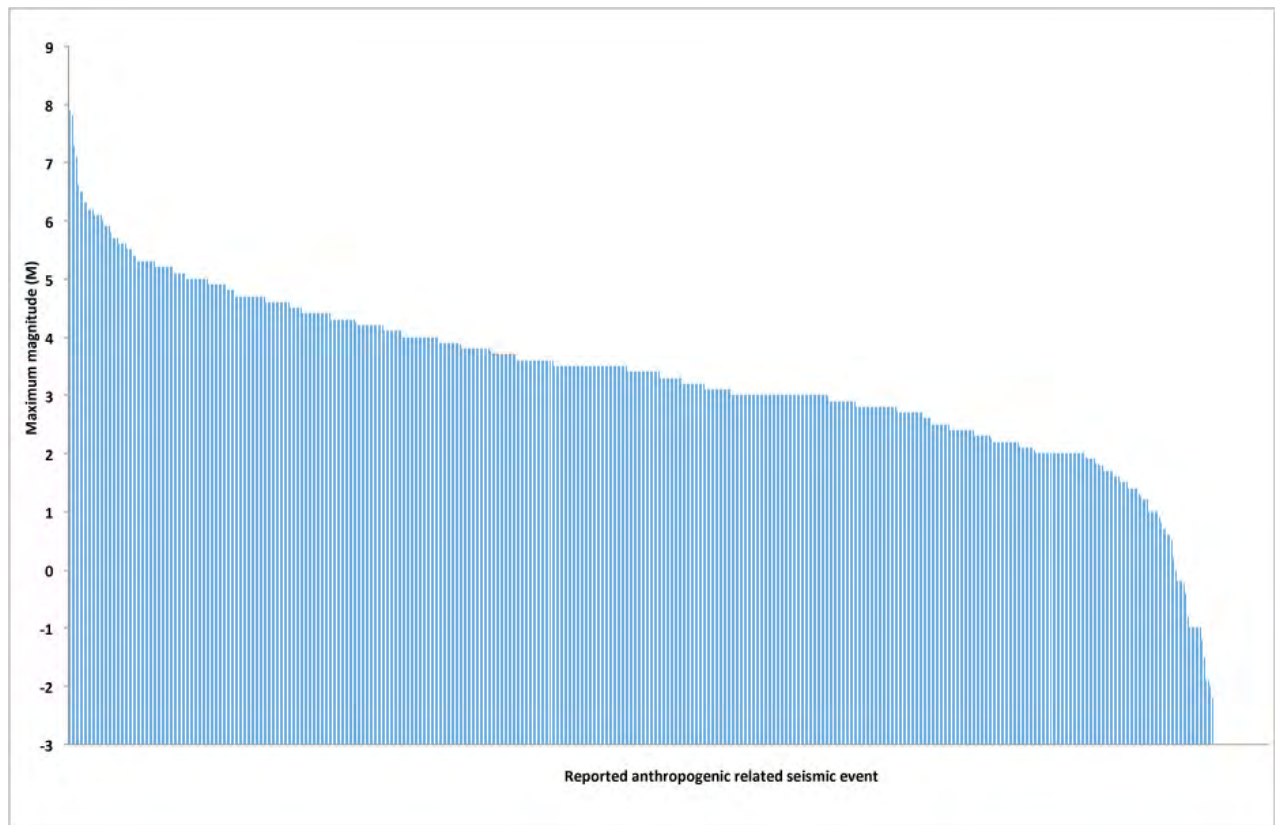
4531

4532 Figure 132: Tectonic settings of cases of human-induced earthquake activity.

4533

4534

4535



4536

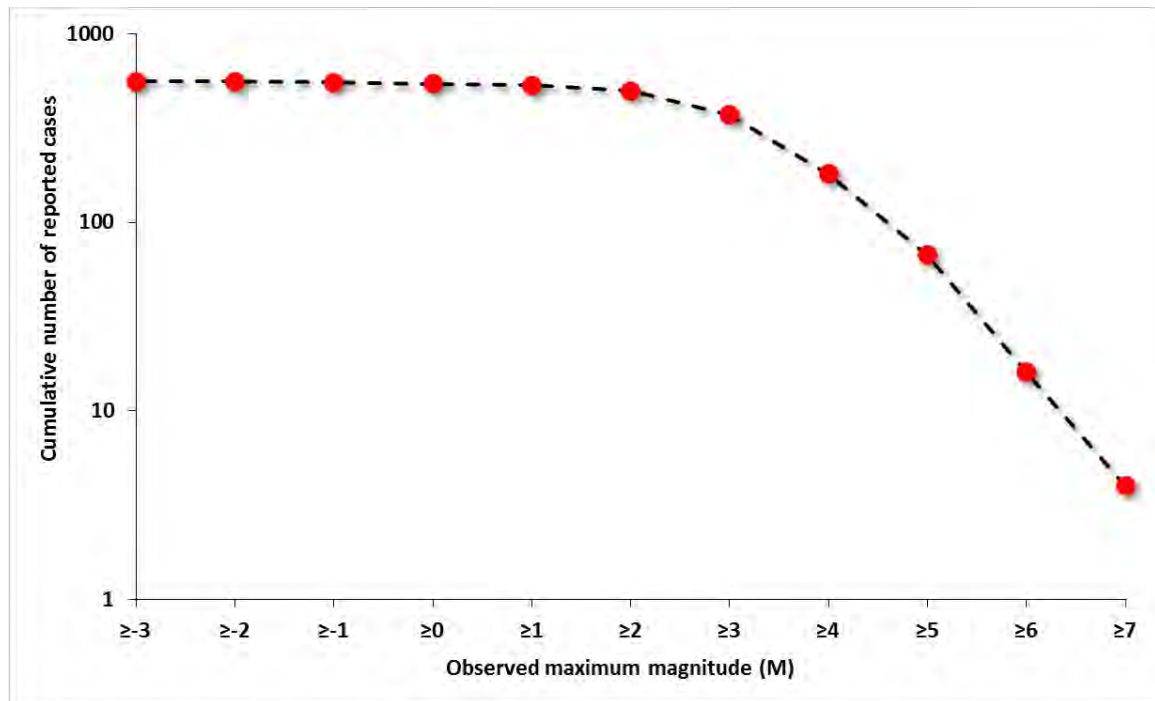
4537

4538 Figure 133: Histogram showing M_{MAX} for the 562 seismogenic projects where this parameter
4539 is recorded. No magnitudes are reported for 143 cases.

4540

4541

4542



4543

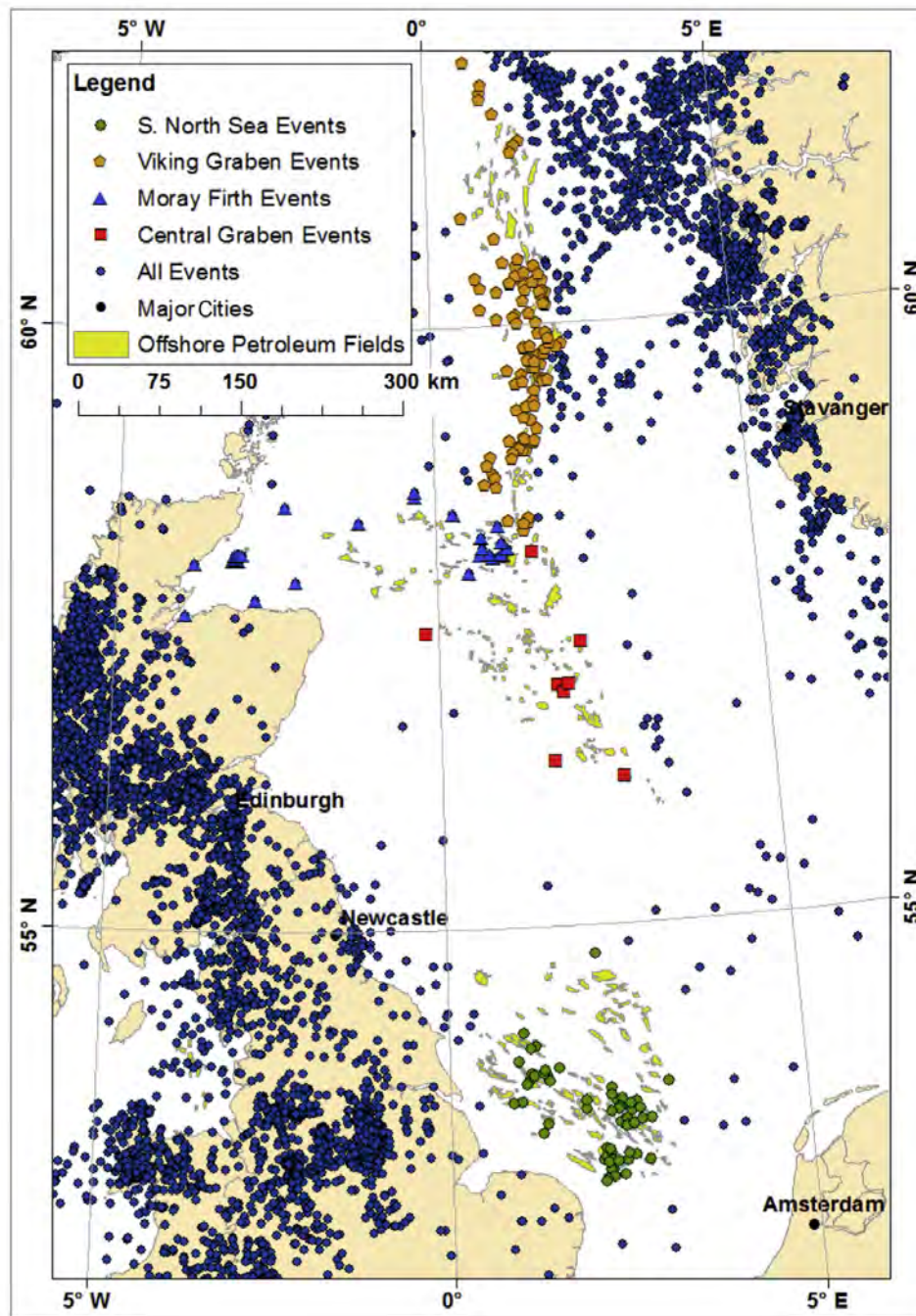
4544

4545 Figure 134: Cumulative number of reported cases of induced seismicity vs. M_{MAX} for the 562
4546 cases for which data are available.

4547

4548

4549



4550

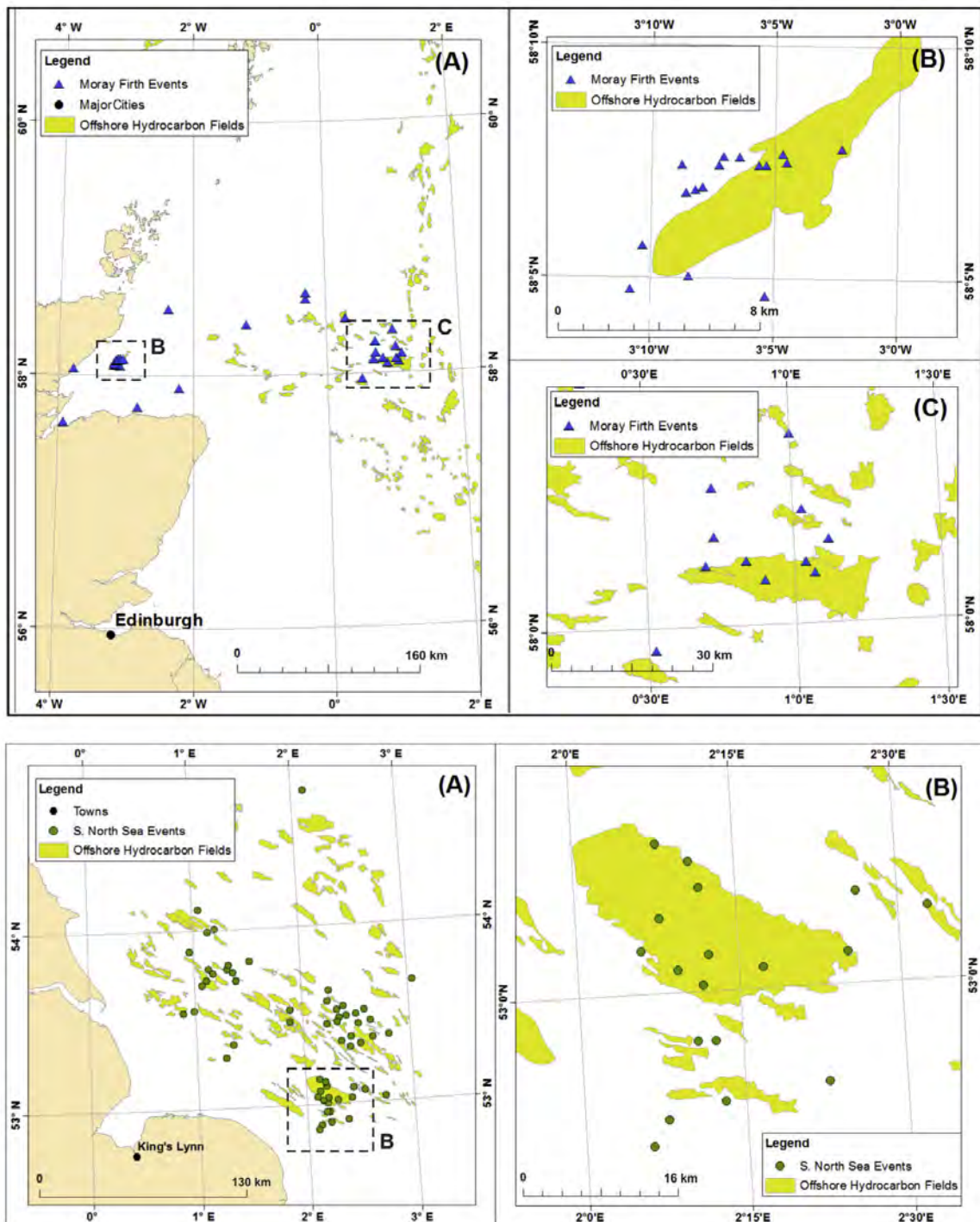
4551

4552 Figure 135: Epicenters from the UK earthquake catalog of the British Geological Survey.
 4553 Orange circles: Viking Graben events; blue triangles: Moray Firth events; red squares:
 4554 Central Graben events; green circles Southern North Sea Gas Province events; yellow
 4555 shading: offshore hydrocarbon fields [from Wilson *et al.*, 2015].

4556

4557

4558



4559

4560

4561 Figure 136: Expanded view of some parts of Figure 135. Top row: A—the Moray Firth.
 4562 Yellow: hydrocarbon fields; blue triangles: earthquakes. B—the Beatrice Oilfield. C—the
 4563 Britannia Gasfield. Bottom row: A—the Southern North Sea Gas Province. Green dots:
 4564 earthquakes. Bottom row: B—the Leman Gasfield [from Wilson *et al.*, 2015].

4565

4566
4567



4568

4569

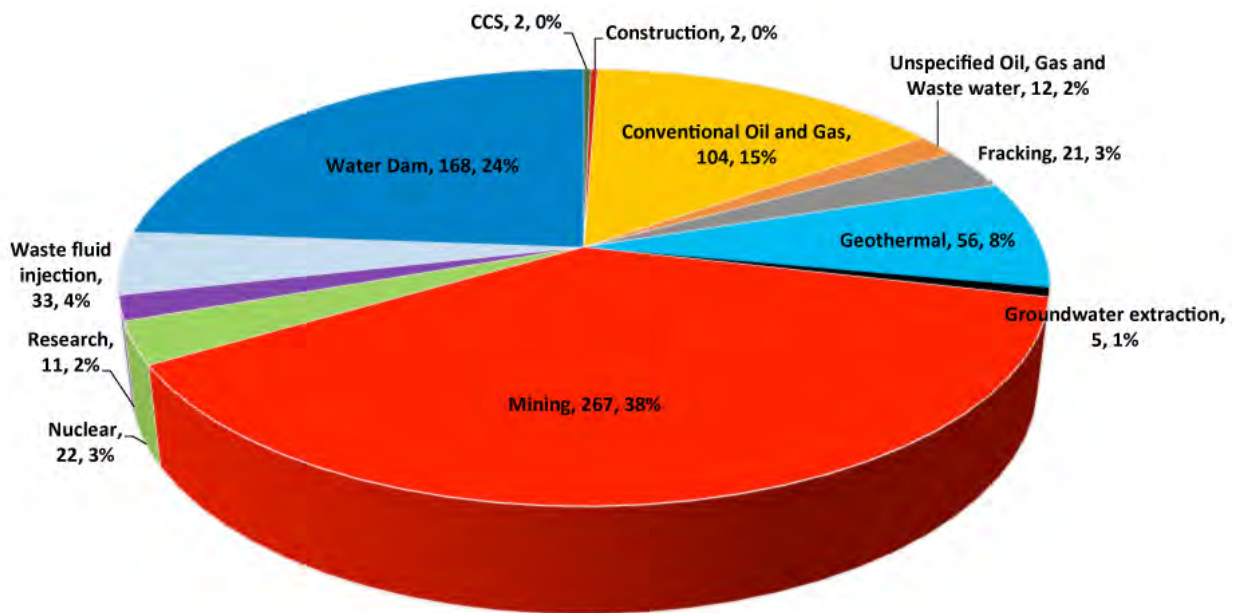
4570 Figure 137: Damage done to the cathedral in Canterbury, New Zealand, by the 2010 M 7.1
4571 earthquake²⁶.

4572

4573

²⁶ <http://www.npr.org/sections/parallels/2015/04/05/397093510/will-new-zealand-rebuild-the-cathedral-my-forefather-erected>

4574



4575

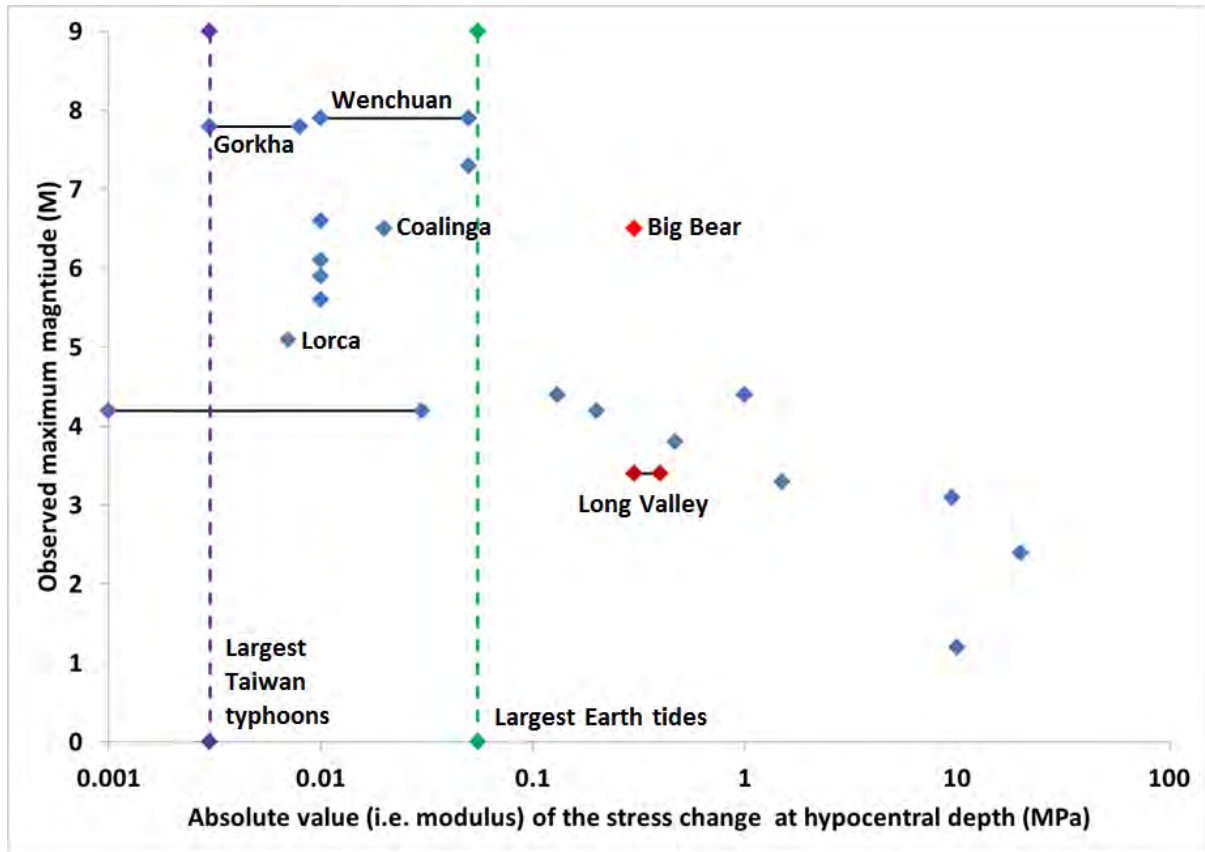
4576

4577 Figure 138: Percentage of total cases for each project category in the database.

4578

4579

4580



4581

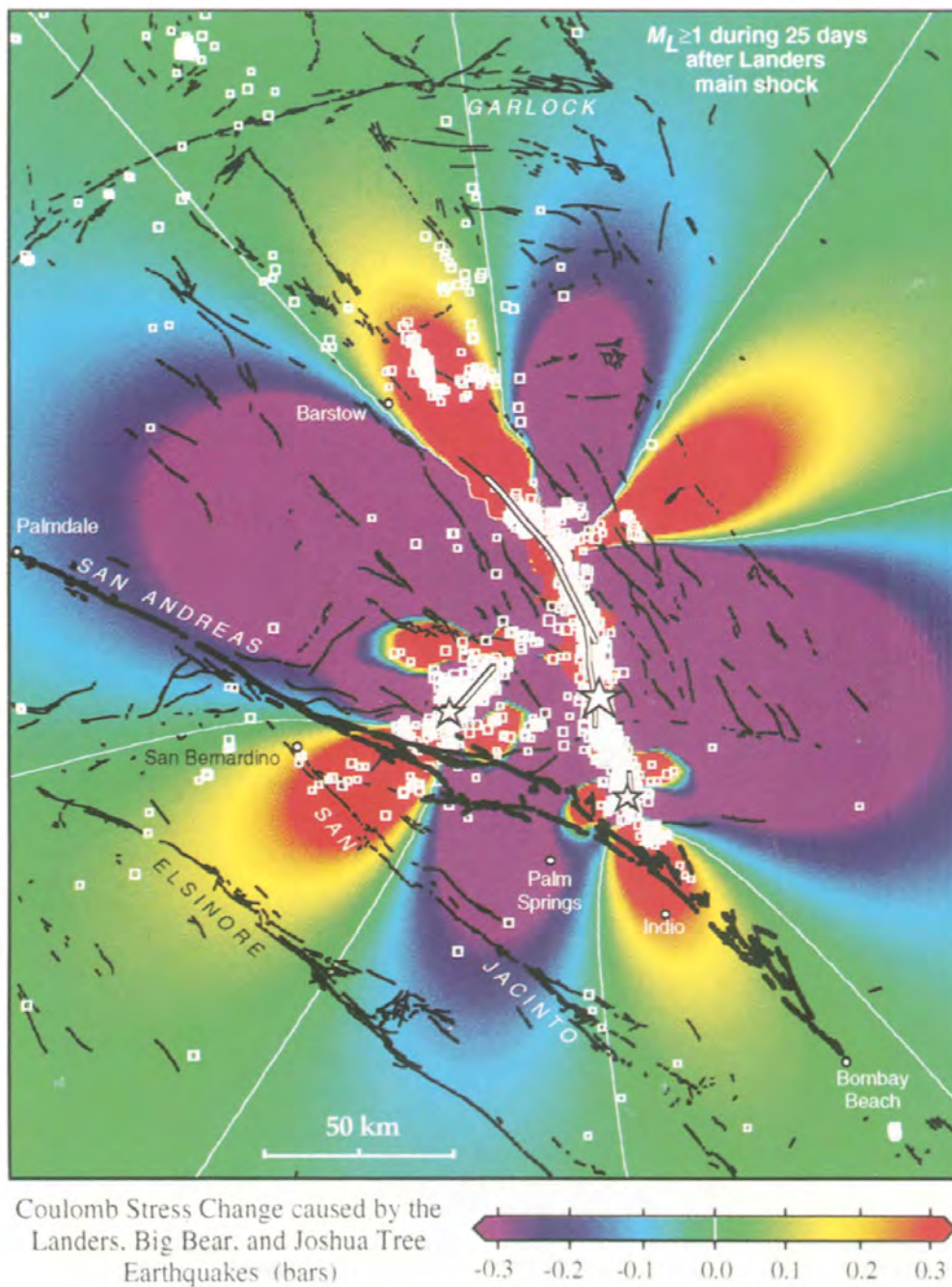
4582

4583 Figure 139: M_{MAX} vs. absolute value of stress changes calculated by various authors to have
 4584 occurred at the hypocentral depths of possibly induced earthquakes. Vertical dashed green
 4585 line: largest Earth tides; vertical dashed purple line: largest Taiwan typhoons. Blue diamonds:
 4586 earthquakes proposed to have been human-induced, diamonds connected by solid black lines:
 4587 ranges of stress changes calculated. Some example earthquakes are labeled. Red diamonds:
 4588 natural earthquakes that followed the 28th June 1992 M_w 7.3 Landers, California, earthquake
 4589 [data from Hill *et al.*, 1993]. The Big Bear earthquake is proposed to have been induced by
 4590 static stress changes, and the Long Valley earthquakes by remote triggering by the dynamic
 4591 stresses from surface waves.

4592

4593

4594



4595

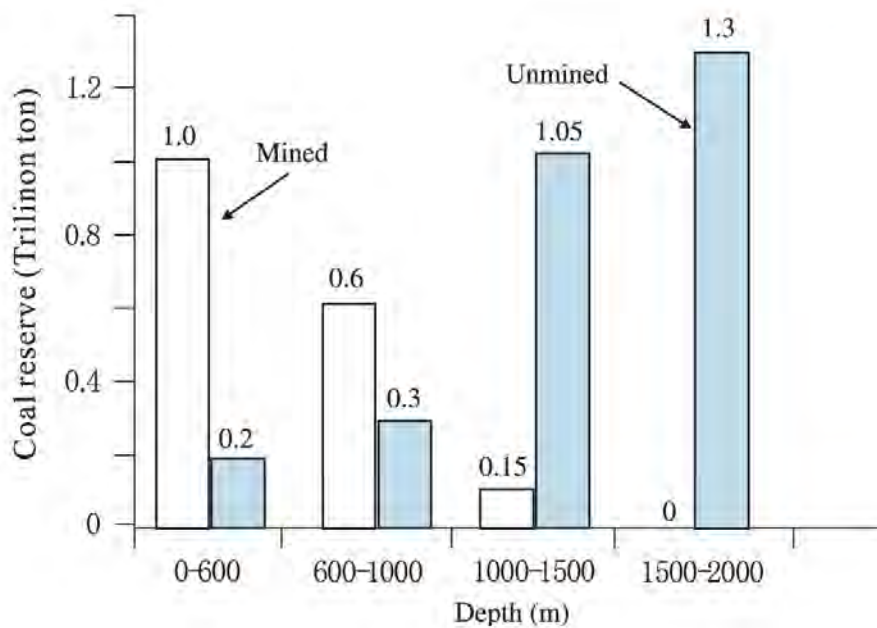
4596

4597 Figure 140: Coulomb stress changes at a depth of 6.25 km caused by the M_w 7.3 Lander,
 4598 California, earthquake and large aftershocks [from King *et al.*, 1994].

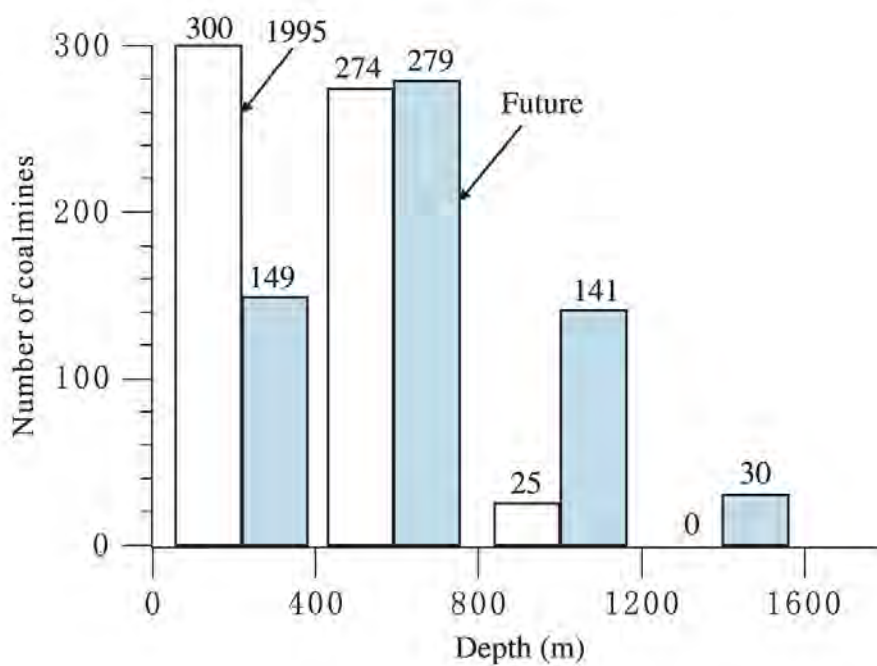
4599

4600

4601



4602



4603

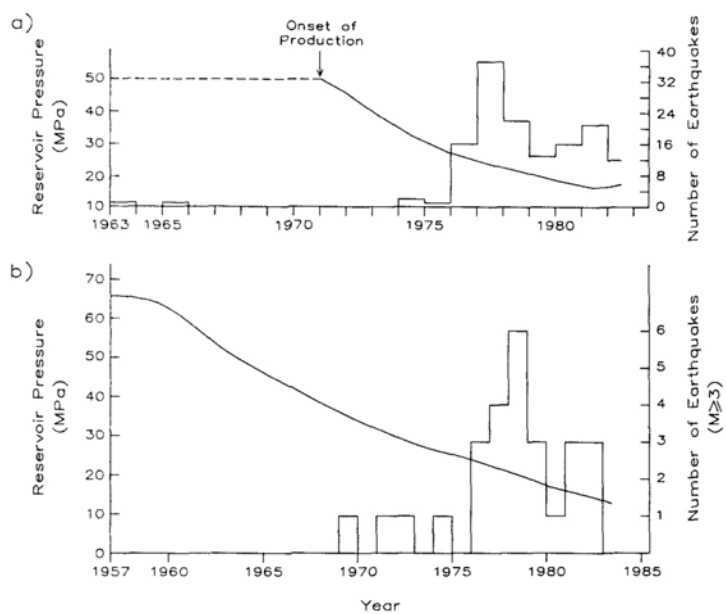
4604

4605 Figure 141: Top: Depth distribution of Chinese coal reserves (1995 statistics). Bottom: Depth
 4606 distribution of 599 state-owned Chinese coal mines [from Li *et al.*, 2007].

4607

4608

4609

4610
4611

4612 Figure 142: Number of earthquakes per year and decline in average reservoir pressure for a)
4613 the Strachan Field, Alberta, Canada, and b) the Pau basin, France [from Segall, 1989].

4614

4615

4616 Tables

4617

4618

4619 Table 1: Data recorded in the database

Column contents	Column contents
Country	Project name
Project type (subclass)	Longitude
Latitude	Project end date
Project start date	End date of seismicity or monitoring
Start date of seismicity or monitoring	Magnitude type
Delay time	Date of largest earthquake
Depth of largest earthquake	Distance of largest earthquake from induction activity
Year of largest earthquake	Lithology/resource
Distance of furthest earthquake from induction activity	Depth of induction activity
Typical depth of earthquakes	Previous seismicity
Tectonic setting	Injection/extraction rate
Dam height	Total volume or mass injected/extracted
Units of injection/extraction rate	Maximum wellhead pressure during injection
Units of total volume or mass injected/extracted	Stress change postulated to have induced earthquake
Change in reservoir pressure	Bottom-hole temperature
Area of project	References
Notes	References used by Davies <i>et al.</i> [2013]
Project type	

4620

4621

4622

4623

4624

4625

4626 Table 2: Classification categories of underground injection wells in The Code of Federal
 4627 Regulations of the USA (40 CFR 144.6-Classification of wells)²⁷.

4628

Class of well	Purpose
Class I	Industrial and Municipal Waste Disposal Wells
Class II	Oil and Gas Related Injection Wells
Class III	Injection Wells for Solution Mining
Class IV	Shallow Hazardous and Radioactive Injection Wells
Class V	Wells for Injection of Non-Hazardous Fluids into or Above Underground Sources of Drinking Water
Class VI	Wells Used for Geologic Sequestration of CO ₂

4629

4630

4631

²⁷ <https://www.epa.gov/uic/general-information-about-injection-wells#regulates>

4632

4633

4634

4635 Table 3: Induced seismicity statistics for the total numbers of projects of different types, the
 4636 number that are seismogenic, and related data.

Project type	# projects	# cases in the database	% projects that are seismogenic	Observed maximum magnitude (M_{MAX})	# seismogenic projects reported by Hitzman et al., (2013)	Source for # projects
CCS	75	2	2.67	1.7	-	Huaman and Jun (2014)
Construction	<i>unknown</i>	2	-	4.2	-	
Conventional oil and gas	67,000 fields	116	0.17	7.3	65	Li (2011)
Fracking	2,500,000 wells	21	0.00	4.4	2	King (2012)
Geothermal	<i>unknown</i>	56	-	6.6	26	Bertani (2010)
Groundwater extraction	<i>unknown</i>	5	-	7.8	-	
Mining	13,262 currently active mines	267	2.01	6.1	8 (“other”)	http://mrdata.usgs.gov/
Nuclear (Underground)	1,352 tests	22	1.63	4.9	-	Pavlovski (1998)
Research	<i>unknown</i>	13	-	3.1	-	
Waste fluid injection wells (Class II wells)	151,000 wells (USA only)	33	0.02	5.7	11	Hitzman <i>et al.</i> , (2013)
Water dam	6,862 reservoirs (>0.1 km ³)	168	2.45	7.9	44	Lehner <i>et al.</i> (2011)
Total		705			156	

4637

4638

4639

4640

4641

4642

4643 Table 4: Number of reported M_{MAX} values and number predicted from downward
 4644 extrapolation of the linear trend of earthquakes with M_{MAX} 5 - 7 shown in Figure 134.

M_{MAX}	# reported earthquakes	# predicted earthquakes
7	4	4
6	17	16
5	68	67
4	181	~250
3	371	~1000
2	497	~4000

4645

4646

4647

4648

4649

4650

4651 Table 5: Conversions for commonly used units of pressure

1 bar = 0.1 MPa, equivalent to ~ 4 m of rock overburden

1 atmosphere = 0.1 MPa

1 kg/cm² = 0.1 MPa

1 pound/inch² (psi) = 6.9 x 10⁻³ MPa

1 acre-foot/football field = 29 x 10⁻⁶ MPa (see footnote²⁸)

Hydrostatic gradient = 10 MPa/km

Lithostatic gradient = ~ 25 MPa/km

4652

4653

4654

4655

²⁸ American football, including end zones.

4656 Table 6: Stress changes associated with some natural processes postulated to induce
 4657 earthquakes.

Effect	Stress change (MPa)
Earth tides	0.05
Seismic static stress changes	0.03
Remote triggering	~0.5
Typhoons	0.003

4658

4659

4660

4661

4662 Table 7: Seven questions proposed by Davis and Frohlich [1993] to be diagnostic of
 4663 earthquakes induced by fluid injection [from Davis & Frohlich, 1993].

Question	Earthquakes Clearly Not Induced	Earthquakes Clearly Induced	I Denver, Colorado	II Painesville, Ohio
<i>Background Seismicity</i>				
1 Are these events the first known earthquakes of this character in the region?	NO	YES	YES	NO
<i>Temporal Correlation</i>				
2 Is there a clear correlation between injection and seismicity	NO	YES	YES	NO
<i>Spatial Correlation</i>				
3a Are epicenters near wells (within 5 km)?	NO	YES	YES	YES?
3b Do some earthquakes occur at or near injection depths?	NO	YES	YES	YES?
3c If not, are there known geologic structures that may channel flow to sites of earthquakes?	NO	YES	NO?	NO?
<i>Injection Practices</i>				
4a Are changes in fluid pressure at well bottoms sufficient to encourage seismicity?	NO	YES	YES	YES
4b Are changes in fluid pressure at hypocentral locations sufficient to encourage seismicity?	NO	YES	YES	NO?
TOTAL "YES" ANSWERS	0	7	6	3

4664

4665

4666

4667 Online material

4668 **A Method used to construct the database.**

4669

4670 In performing the literature review on which our database is founded, we proceeded as
4671 follows:

4672 1. A single-sheet Excel spreadsheet was constructed and the raw database of Davies *et*
4673 *al.* [2013] was imported. Additional columns were added for new types of data, *e.g.*,
4674 Earthquake Cause (main class) and Earthquake Cause (subclass);

4675 2. The entries were checked and updated where necessary. References were added
4676 where lacking;

4677 3. New cases were searched for using Google Scholar. Where possible (most cases)
4678 PDFs were downloaded, digitally filed, and entered into EndNote. Where a PDF of an
4679 entire paper or report was unobtainable, information from the abstract was used;

4680 4. Where data are not available, *e.g.*, maximum magnitude, the relevant spreadsheet cell
4681 is left blank;

4682 5. Entries in the database were double-checked;

4683 6. Where conflicting information is published, *e.g.*, different magnitudes, we report
4684 moment magnitude (M_W). If M_W is not available we report the largest magnitude from
4685 those available.

4686 **B Description of the database**

4687 We have assembled 705 cases of industrial projects postulated to have induced earthquakes.
4688 These cases include a wide range of project types. For a large majority of industrial projects
4689 in all categories, there are no reports of seismogenesis. However, it is clear that there is large-
4690 scale under-reporting.

4691 For the purpose of plotting figures, we divided the projects into the following categories:

4692 *Carbon Capture and Storage (CCS)*

4693 The implementation of CCS to combat climate change is still largely in the demonstration
4694 stage. To date there have been 75 CCS projects with eight of these on a commercial scale
4695 [Huaman & Jun, 2014]. Storage requires the injection of CO₂ into a subsurface formation.
4696 Two CCS projects are reported to have induced earthquakes—In Salah, Algeria and Decatur,
4697 Illinois, USA.

4698 *Construction*

4699 Projects where humans have built a structure or created artificial topography are classed as
4700 construction, with the exception of water dams which are categorized separately. Two such
4701 projects are reported to be linked to earthquakes, the erection of the Taipei 101, Taiwan,

4702 building and artificial accumulation of shingle deposits at Folkestone, UK. We searched for
 4703 reports of earthquakes associated with the construction of nearby Samphire Hoe. This is a
 4704 coastal park created using $\sim 10^{10}$ kg of chalk excavated on the English side of the Channel
 4705 Tunnel, an order of magnitude greater than accumulated at Folkestone. However, we found
 4706 none.

4707 *Conventional oil and gas (including unspecified oil, gas and waste-water projects)*

4708 There are approximately 67,000 oil- and gasfields globally. Our database contains 112
 4709 seismogenic projects in this category. The largest earthquake postulated to be related to such
 4710 projects is the 1976 M_S 7.3 earthquake near the Gazli Gasfield, Uzbekistan.

4711 *Shale-gas hydrofracturing*

4712 Hydraulic fracturing to increase oil and gas production has been practiced for several decades
 4713 but its recent use to extract gas from shale has attracted media attention. Every successful
 4714 hydrofracture job induces seismicity because the objective is to fracture rock. Despite the fact
 4715 that ~ 2.5 million such jobs have been completed, our database contains only 21 cases of
 4716 induced earthquakes. Of these cases, the largest earthquake reported was M_W 4.4 and
 4717 occurred in Canada in 2015.

4718 *Geothermal exploitation*

4719 There are 65 geothermal fields worldwide that produce >100 GW electric per year. Our
 4720 database contains 51 cases that have been linked to earthquakes. The largest earthquake
 4721 postulated to have been induced is the 1979 M_L 6.6 earthquake near the Cerro Prieto Field,
 4722 California.

4723 *Groundwater extraction*

4724 Our database contains five cases where earthquakes are postulated to be linked to large-scale
 4725 groundwater extraction. The largest of these case is the 2015 M_W 7.8 Gorkha, Nepal,
 4726 earthquake, which resulted in ~ 8000 deaths and $\sim \$10$ billion of economic loss, $\sim 50\%$ of the
 4727 Gross Domestic Product of Nepal.

4728 *Mining*

4729 Mining-related seismicity (gallery collapses, stope contractions, “rock bursts”, “coal bumps”,
 4730 faulting) accounts for 38% (267 cases) of the cases in our database, the largest category. The
 4731 U.S. Geological Survey estimates there are currently 13,262 active mines worldwide, in
 4732 addition to inactive and historic mines. There is likely under-reporting of mining seismicity.
 4733 The largest earthquake proposed to be induced by mining is the 2013 M_L 6.1 earthquake,
 4734 suggested to be linked to the Bachatsky open-cast coal mine, Russia. Other countries with M
 4735 ≥ 5 earthquakes postulated to be induced by mining include Australia, Canada, Germany,
 4736 Poland, South Africa and the US.

4737 *Underground nuclear explosions*

4738 We exclude the initial explosions from our database but recognize two types of related
 4739 induced seismicity:

4740 a) earthquakes associated with the collapse of the underground cavity created by the
4741 explosion, and

4742 b) earthquakes induced on local faults.

4743 The largest recorded seismic event of type a) was m_b 4.9 (the 5 Mt Cannikin test, Amchitka,
4744 Alaska, 1971). The largest reported event of type b) had m_b 4.8 (the 27th October 1973
4745 Novaya Zemlya test). Of 1,352 underground nuclear tests, 22 have been associated with
4746 earthquakes [Pavlovski, 1998].

4747 *Research*

4748 The database contains 13 projects classified as research. These involve injecting water into
4749 the subsurface or flooding abandoned mines. One of the earliest of these was that at the
4750 Rangely Oilfield, Colorado, where the largest induced earthquake in this category occurred,
4751 the 1970 M_L 3.1 event. Another notable project was the Kontinentales Tiefbohrprogramm der
4752 Bundesrepublik Deutschland (KTB), the German Continental Deep Drilling Program, in
4753 which small volumes of fluid were injected as deep as ~ 9 km, the deepest reported fluid
4754 injection to date.

4755 *Waste fluid injection*

4756 Seismicity induced by waste-fluid injection is increasing. Of the $> 151,000$ Class II waste-
4757 fluid injection wells in the USA, estimates for the rate of seismogenesis range from nine
4758 cases to $> 18,000$. Our database contains 33 cases in this category predominantly from the
4759 US and Canada. The largest earthquake postulated to be induced by this process is the 2011
4760 M_W 5.7 Prague, Oklahoma, earthquake.

4761 *Water dams*

4762 The database contains 168 cases of earthquakes possibly induced by impounding water
4763 behind dams. Approximately 2.5% of reservoirs with volumes > 0.1 km³ are reported to be
4764 seismogenic. The largest postulated reservoir-related earthquake is the great 2008 M_W ~ 8
4765 Wenchuan, earthquake, China (Zipingpu dam) which caused $\sim 90,000$ fatalities.

4766

4767

4768

4769 **C Explanations of database column headings.**

4770

Column Heading	Description
Country	Country where the project is/was geographically located
Eq cause (main class)	Overall project type, <i>e.g.</i> , geothermal, proposed to have caused the earthquake
Eq cause (subclass)	Type of project within the main class, <i>e.g.</i> , geothermal (injection), proposed to have caused the earthquake
Name	Project name
Latitude (°N)	Project latitude
Longitude (°W)	Project longitude
Start date of project	Start of project or main phase relevant to earthquakes
End date of project	End of project or main phase relevant to earthquakes
Start date of earthquakes or monitoring	Date of onset of seismicity (monitoring already in place) or the date monitoring commenced
End date of earthquakes or monitoring	Date seismicity ceased or the date monitoring equipment was removed
Delay time	Time between the start of the project and the onset of seismicity
No. eqs	Number of earthquakes recorded
Max magnitude (M_{MAX})	Observed maximum magnitude reported
Mag type	Type of magnitude reported for the maximum magnitude earthquake. Moment magnitude is reported if available. If moment magnitude was not reported, the largest magnitude of any type was recorded
Depth of largest eq (m)	Hypocentral depth of largest earthquake
Date of largest eq	Date of the largest earthquake
Year of largest eq	Year of the largest earthquake
Distance of M_{MAX} to project (m)	Horizontal distance of maximum magnitude

	earthquake from inducing project
Max distance to project (m)	Horizontal distance between the furthest observed earthquake (not necessarily the largest) and the inducing project
Lithology/resource	Reservoir lithology, <i>e.g.</i> , sandstone, or mining resource, <i>e.g.</i> , coal
Depth of most eq activity (m)	Depth at which most earthquake activity is observed
Depth of project (m)	Depth of the inducing activity, <i>e.g.</i> , the injection
Tectonic setting	Tectonic setting of project based on simple plate boundary model
Previous seismic activity	Notes on any seismicity prior to the start of the project
Dam height (m)	Height of the dam impounding the water reservoir
Injection/extraction rate (max unless stated, units in next column)	Rate of injection or extraction of material from the subsurface
Rate units	Units for rate of injection or extraction
Total volume or mass of material injected/extracted (units in next column)	Total volume or mass of material injected into or extracted from the subsurface. For dams: the volume of the water reservoir
Volume or mass units	Units for volume or mass of material
Pressure (MPa) (max unless stated)	Maximum (unless stated) well head injection pressure during the project
Change in reservoir pressure (MPa)	Change in pressure of fluid in the subsurface reservoir
Stress change (MPa)	Change in stress postulated to have induced the earthquake
Area ($\times 10^6$ m ²)	Area of the project, <i>e.g.</i> , surface area of water reservoir
BHT (°C)	Bottom-hole temperature of borehole
Notes	Additional information about project or data
Reference(s)	Source of information on project
Reference(s) from Davies <i>et al.</i> [2013]	Source(s) used by Davies <i>et al.</i> (2013) for project

4773

4774 **D List of the 705 entries in the database.**

4775

Country	Eq cause (main class)	Eq cause (subclass)	Name	Max mag (Mmax)	Mag type	Date of largest eq
Algeria	CCS	CO2 injection	In Salah	1.7	MW	
USA	CCS	CO2 injection	Decatur, Illinois, demonstration site	1.26	MW	
UK	Construction	Coastal engineering (geoengineering)	Folkestone	4.2	ML	2007/04/28
Taiwan	Construction	Construction	Taipei 101	3.8	ML	2004/10/23
Uzbekistan	Conventional Oil and Gas	Gas extraction and storage	Gazli	7.3	MS	1976/04/08
Canada	Conventional Oil and Gas	Secondary recovery (water injection)	Snipe Lake, Alberta	5.1	ML	1970/03/08
USA	Conventional Oil and Gas	Oil extraction	Long Beach (Wilmington and Huntington Beach oilfields), California	6.3	ML	1933
Iran	Conventional Oil and Gas	Oil extraction	Cheshmeh Khosh	6.2		2014/08/18
Canada	Conventional Oil and Gas	Oil extraction and Secondary recovery (water injection)	Eagle/Eagle West	4.3		1994/05/22
Canada	Conventional Oil and Gas	Secondary recovery	Gobles, Ontario	3.4		
Canada	Conventional Oil and Gas	Secondary recovery and Waste disposal	Cold Lake, Alberta	2	ML	
Italy	Conventional Oil and Gas	Gas extraction	Caviaga, Po Valley	5.5	ML	1951/05/15
Canada	Conventional Oil and Gas	EOR (CO2 injection/part CCS project)	Weyburn, Saskatchewan	-1		
USA	Conventional Oil and Gas	Gas extraction	El Reno, Oklahoma	5.2	ML	1952
USA	Conventional Oil and Gas	Oil extraction	Wilmington, California	5.1	ML	1949
China	Conventional Oil and Gas	Secondary recovery (water injection)	Renqiu	4.5	ML	1987/06/02
USA	Conventional Oil and Gas	Oil extraction	Richland County, Illinois	4.9	ML	1987
China	Conventional Oil and Gas	Secondary recovery (water injection)	Shengli, Shandong Province			
USA	Conventional Oil and Gas	Gas extraction	Fashing, Texas	4.8	MW	2011/10/20
Denmark	Conventional Oil and Gas	Oil and Gas extraction and Secondary recovery (water injection)	Dan			
Russia	Conventional Oil and Gas	Oil extraction	Starogroznenskoe	4.7	ML	1971/03/26
Kuwait	Conventional	Oil extraction and	Minagish/Umm	4.7		1993/06

	Oil and Gas	Burning	Gudair oil fields (for largest eq)			/02
USA	Conventional Oil and Gas	Gas extraction	Catoosa, Oklahoma	4.7	ML	
Norway	Conventional Oil and Gas	Secondary recovery (unintentional water injection into overburden)	Ekofisk	3	ML	2001/05 /07
Russia	Conventional Oil and Gas	Oil and gas extraction	Gudermes	4.5		
Germany	Conventional Oil and Gas	Gas extraction	Rotenberg /Neuenkirchen	4.4	MW	2004/10 /20
Norway	Conventional Oil and Gas		Vishund			
Romania	Conventional Oil and Gas	Secondary recovery (water injection)	Tazlau	-1.5	MW	
Spain	Conventional Oil and Gas	Gas storage	Castor	4.3	MW	2013/10 /01
Saudi Arabia	Conventional Oil and Gas	Oil and gas extraction	Ghawar	4.24	ML	
France	Conventional Oil and Gas	Gas extraction	Lacq (Arette)	4.2	ML	1978
USA	Conventional Oil and Gas	Oil extraction	Wortham-Mexia, Texas	4		1932/04 /09
Canada	Conventional Oil and Gas	Gas extraction	Strachan, Alberta	4	ML	
Russia	Conventional Oil and Gas	Oil extraction and Secondary recovery (water injection)	Romashkinskoye (Romashkino field), Volga-Ural	4	ML	1991/10 /28
Russia	Conventional Oil and Gas	Oil extraction and Secondary recovery?	Grozny, Chechen Republic	3.3	ML	
Germany	Conventional Oil and Gas	Gas extraction	Soltau	4	ML	1977/06 /02
Russia	Conventional Oil and Gas	Oil extraction and Secondary recovery (water injection)	Novo-Elkhovskoye, Volga-Ural			
USA	Conventional Oil and Gas	Oil and Gas extraction	Alice (Stratton field), Texas	3.9	mbLG	2010/04 /25
Germany	Conventional Oil and Gas	Gas extraction	Skye (Bassum, Niedersachsen)	3.8	ML	2005/07 /15
Turkmenistan	Conventional Oil and Gas	Oil extraction and Secondary recovery (water injection)	Barsa-Gelmes-Vishka	6		1984
USA	Conventional Oil and Gas	Oil extraction and Secondary recovery (water injection)	Coalinga, California	6.5	ML	1983
China	Conventional Oil and Gas	Gas extraction and storage	Hutubi, Southern Junggar Basin	3.6	ML	
USA	Conventional Oil and Gas	Oil extraction and Secondary recovery (water injection)	Kettleman North Dome, California	6.1	MW	1985
USA	Conventional Oil and Gas	Oil extraction and Secondary recovery (water injection)	Montebello (Whittier Narrows), California	5.9	ML	1987
Netherlands	Conventional Oil and Gas	Gas extraction	Bergermeer (Alkmaar)	3.5	MW	2001/09 /09
USA	Conventional Oil and Gas	Gas extraction	East Durant, Oklahoma	3.5	ML	

USA	Conventional Oil and Gas	Secondary recovery (water injection)	Cogdell Field, Texas	5.3	ML	1978/06/16
Netherlands	Conventional Oil and Gas	Gas extraction	Groningen	3.4	ML	2012/08/06
USA	Conventional Oil and Gas	Oil extraction and Secondary recovery (water injection)	Brewton (Big Escambia Creek, Little Rock, and Sizemore Creek fields), Alabama	4.9	MW	1997/10/24
USA	Conventional Oil and Gas	Oil extraction and Stimulation	Orcutt, California	3.5	ML	
USA	Conventional Oil and Gas	Oil extraction and Secondary recovery (water injection)	East Texas (Gladewater), Texas	4.7		1957/03/19
Netherlands	Conventional Oil and Gas	Gas extraction	Roswinkel	3.4	ML	1997/02/19
USA	Conventional Oil and Gas	EOR (CO2 injection)	Cogdell Field, Texas	4.4	MW	2011/09/11
USA	Conventional Oil and Gas	Secondary recovery	Kermit, Texas	4	ML	
USA	Conventional Oil and Gas	Oil and Gas extraction and Secondary recovery (water injection)	Imogene (Pleasanton), Texas	3.9	ML	1984/03/03
USA	Conventional Oil and Gas	Oil and gas extraction	War-Wink, Texas	3	ML	1975
USA	Conventional Oil and Gas	Production and Secondary recovery	Inglewood, California	3.7	ML	1962
USA	Conventional Oil and Gas	Oil extraction and Secondary recovery (water injection)	Falls City, Texas	3.6	mbLg	1991/07/20
USA	Conventional Oil and Gas	Gas/Brine extraction and Wastewater (injection)	Azle/Reno, Texas	3.6		
USA	Conventional Oil and Gas	Secondary recovery	Hunt, Alabama /Mississippi	3.6	ML	
Germany	Conventional Oil and Gas	Gas extraction	Visselhövede	2.9	ML	2012/02/13
Germany	Conventional Oil and Gas	Gas extraction	Völkersen	2.9	ML	2012/11/22
USA	Conventional Oil and Gas	Secondary recovery	Dollarhide, Texas/New Mexico	3.5	ML	
Germany	Conventional Oil and Gas	Gas extraction	Langwedel	2.8	ML	2008/04/03
Netherlands	Conventional Oil and Gas	Gas extraction	Eleveld	2.8	ML	1986/12/26
Netherlands	Conventional Oil and Gas	Gas extraction	Assen	2.8	ML	1986
USA	Conventional Oil and Gas	Secondary recovery	Keystone I&II, Texas	3.5	ML	
Netherlands	Conventional Oil and Gas	Gas extraction	Middelie	2.7	ML	1989/12/01
Netherlands	Conventional Oil and Gas	Gas extraction	Bergen	2.7	ML	2001/10/10
Germany	Conventional Oil and Gas	Gas extraction	Verden	2.5	ML	2011/05/02
Netherlands	Conventional Oil and Gas	Gas extraction	Annerveen	2.3	ML	1994/08/16

Netherlands	Conventional Oil and Gas	Gas extraction	Appelscha	2.3	ML	2003/06 /16
Netherlands	Conventional Oil and Gas	Gas extraction	Dalen	2.2	ML	1996/11 /17
Netherlands	Conventional Oil and Gas	Gas extraction	Roden	2.1	ML	1996/09 /02
France	Conventional Oil and Gas	Well collapse/Water injection	Lacq (Arette)	1.9	ML	1996/09 /18
Oman	Conventional Oil and Gas	Gas extraction	Shuiba reservoir	2.05	ML	2001/03 /04
Netherlands	Conventional Oil and Gas	Gas extraction	Emmen	2	ML	1991/02 /15
USA	Conventional Oil and Gas	Secondary recovery	Ward-Estes, Texas	3.5	ML	
USA	Conventional Oil and Gas	Secondary recovery	North Panhandle (Lambert), Texas	3.4	ML	
Netherlands	Conventional Oil and Gas	Gas extraction	VriesNoord	1.9		1996 (Dec.)
USA	Conventional Oil and Gas	Secondary recovery	Ward-South, Texas	3	ML	
Netherlands	Conventional Oil and Gas	Gas extraction	Emmen-Nieuw Amsterdam	1.7		1994 (Sep.)
Czech Republic	Conventional Oil and Gas	Gas storage	Příbram (Háje)	1.5	ML	
Netherlands	Conventional Oil and Gas	Gas extraction	Schoonebeek	1.4		2002 (Dec.)
Netherlands	Conventional Oil and Gas	Gas extraction	Coevorden	1.2		1997 (Feb.)
Netherlands	Conventional Oil and Gas	Gas extraction	Ureterp	1		1999 (Apr.)
Netherlands	Conventional Oil and Gas	Gas extraction	VriesCentraal	1		2000 (July)
USA	Conventional Oil and Gas	Oil extraction	Seventy Six oil field, Clinton County, Kentucky	0.9	MW	
Netherlands	Conventional Oil and Gas	Gas storage	Bergermeer	0.7		2013 (Oct.)
USA	Conventional Oil and Gas	Secondary recovery	Dora Roberts, Texas	3	ML	
USA	Conventional Oil and Gas	Secondary recovery	Monahans, Texas	3	ML	
Norway	Conventional Oil and Gas	Oil extraction	Valhall			
USA	Conventional Oil and Gas	Secondary recovery	Sleepy Hollow, Nebraska	2.9	ML	
USA	Conventional Oil and Gas	Secondary recovery and Stimulation	Love County, Oklahoma	2.8	ML	
USA	Conventional Oil and Gas	Oil and Gas extraction and Secondary recovery	Apollo-Hendrick, Texas	2	MD	
USA	Conventional Oil and Gas	Oil and gas extraction	South Houston, Texas			
USA	Conventional Oil and Gas	Oil and gas extraction	Clinton, Texas			
USA	Conventional Oil and Gas	Oil and gas extraction	MyKawa, Texas			
USA	Conventional Oil and Gas	Oil and gas	Blue Ridge, Texas			

	Oil and Gas	extraction				
USA	Conventional Oil and Gas	Oil and gas extraction	Webster, Texas			
USA	Conventional Oil and Gas	Oil and gas extraction	Goose Creek, Texas			
Venezuela	Conventional Oil and Gas	Oil and gas extraction	Costa Oriental, Lake Maracaibo			
USA	Conventional Oil and Gas	Oil extraction and Secondary recovery (water injection)	New Harmony, Indiana	1.8	MW	
USA	Conventional Oil and Gas	Secondary recovery (water injection)	South Eugene Island, Louisiana			
France	Conventional Oil and Gas	Gas extraction	Meillon			
Netherlands	Conventional Oil and Gas	Gas Storage	Norg			
Netherlands	Conventional Oil and Gas	Gas Storage	Grijpskerk			
USA	Conventional Oil and Gas	Stimulation	Austin Chalk, Giddings Field, Texas			
Canada	Fracking	Fracking (injection)	Northern Montney Earthquake, British Columbia	4.4	MW	2014/08/04
Canada	Fracking	Fracking (injection)	Crooked Lake (Fox Creek), Alberta (Waskahigan and McKinley fields)	4.4	ML	2015/01/23
Canada	Fracking	Fracking (injection)	Septimus (Montney Trend)	4.2	ML	2013/05/27
Canada	Fracking	Fracking (injection)	Fox Creek, Alberta	3.9	MW	2015/06/13
Canada	Fracking	Fracking (injection)	Horn River Basin	3.8	ML	2011/05/19
Canada	Fracking	Fracking (injection)	Beg-Town (Montney Trend)	3.4	ML	2013/08/21
Canada	Fracking	Fracking (injection)	Caribou (Montney Trend)	3.2	ML	2014/03/02
Canada	Fracking	Fracking (injection)	Cardston, Alberta (Ninastoko field)	3	ML	2011/12/04
Canada	Fracking	Fracking (injection)	Doe-Dawson (Montney Trend)	2.8	ML	2013/10/23
Canada	Fracking	Fracking (injection)	Altares (Montney Trend)	2.2	ML	2013/11/05
Canada	Fracking	Fracking (injection)	Montney Trend	-0.4	MW	
Canada	Fracking	Fracking (injection)	Western Canada	-2.2	MW	2006
UK	Fracking	Fracking (injection)	Preese Hall	2.3	ML	2011/04/01
USA	Fracking	Fracking (injection)	Eagleton 1-29, Oklahoma	3.2	ML	2014/07/07
USA	Fracking	Fracking (injection)	Poland Township, Ohio	3	ML	2014/03/10
USA	Fracking	Fracking (injection)	Oklahoma (Eola-Robberson field)	2.9	ML	2011/01/18
USA	Fracking	Fracking (injection)	Harrison County, Ohio	2	MW	2013/10/02

USA	Fracking	Fracking (injection+production ?)	Bienville Parish, Louisiana	1.9	ML	2011/10 /15
USA	Fracking	Fracking (injection)	Cotton Valley, Texas	-0.2	MW	1997/05 /14
USA	Fracking	Fracking (injection)	Jonah, Wyoming	-1.2		
USA	Fracking	Fracking (injection)	Hughes County, Oklahoma	-1.9		2007
Mexico	Geothermal	Geothermal (extraction)	Cerro Prieto (Imperial Valley)	6.6	ML	1979/10 /15
USA	Geothermal	EGS (circulation)	Salton Sea, California	5.1		2005
USA	Geothermal	EGS (circulation)	The Geysers	4.6		1982
Mexico	Geothermal	EGS (circulation)	Los Humeros	4.6	Md	1994/11 /25
El Salvador	Geothermal	EGS (injection)	Berlín	4.4	ML	2003/09 /16
Australia	Geothermal	EGS (injection)	Cooper Basin (Habanero 1)	3.7	MW	2003/11 /14
Italy	Geothermal	EGS (circulation)	Monte Amiata	3.5	ML	1983
Switzerland	Geothermal	EGS (injection)	Basel	3.4	ML	2006/12 /08
Switzerland	Geothermal	EGS (injection)	St. Gallen	3.3	MW	2013/07 /20
New Zealand	Geothermal	Geothermal (reinjection)	Rotokawa	3.3		2012 (Feb.)
Italy	Geothermal	EGS (circulation)	Larderello-Travale	3.2	ML	1982
New Zealand	Geothermal	Geothermal (reinjection)	Mokai	3.2		
Italy	Geothermal	EGS (injection)	Torre Alfina	3	ML	1977
El Salvador	Geothermal	EGS (injection)	Ahuachapan	3	ML	1991
Iceland	Geothermal	Geothermal (extraction)	Reykjanes	3	ML	2006
Australia	Geothermal	EGS (injection)	Cooper Basin (Habanero 4)	3	ML	
Italy	Geothermal	EGS (injection)	Latera	2.9	ML	1984/12 /09
France	Geothermal	EGS (injection)	Soultz (GPK-3)	2.9	ML	2003/06 /10
Australia	Geothermal	EGS (injection)	Cooper Basin (Habanero 1 restimulation)	2.9	ML	2005
USA	Geothermal	EGS (stimulation)	Coso	2.8		2004 (Aug.)
Germany	Geothermal	EGS (circulation)	Landau	2.7	ML	2009/08 /15
New Zealand	Geothermal	Geothermal (reinjection)	Ngatamariki	2.7		
Australia	Geothermal	EGS (injection)	Paralana 2	2.5	MW	2011/11 /13
Kenya	Geothermal	Geothermal (extraction)	Olkaria	2.5	Md	1996
Philippines	Geothermal	Geothermal (reinjection)	Puhagan	2.4	ML	1983 (Feb.)
France	Geothermal	EGS (injection)	Soultz (GPK-2)	2.4	MW	2000/07

						/16
Germany	Geothermal	EGS (circulation)	Unterhaching	2.4	ML	2008 (July)
Germany	Geothermal	EGS (injection)	Insheim	2.4	ML	2010 (Apr.)
Iceland	Geothermal	EGS (injection)	Hellisheidi	2.4	ML	
USA	Geothermal	EGS (injection)	Newberry	2.39	MW	2012/07 /12
Italy	Geothermal	EGS (injection)	Cesano	2	ML	1978
UK	Geothermal	EGS (circulation)	Rosemanowes	2	ML	1987/07 /12
Iceland	Geothermal	EGS (circulation)	Krafla	2	ML	
Japan	Geothermal	EGS (injection)	Ogachi (OGC-1)	2	MW	
Indonesia	Geothermal	EGS (circulation)	Lahendong	2		
Mexico	Geothermal	EGS (injection)	Los Azufres	1.9	Md	
Germany	Geothermal	EGS (injection)	Bad Urach	1.8	MW	2002
USA	Geothermal	EGS (injection)	Desert Peak, Nevada	1.7	ML	
France	Geothermal	EGS (injection)	Rittersshoffen, Alsace	1.6	Miv	2013/07 /02
Australia	Geothermal	EGS (injection)	Cooper Basin (Jolokia 1)	1.6	ML	
Australia	Geothermal	EGS (injection)	Paralana 2 DFIT	1.4	ML	
USA	Geothermal	EGS (injection)	Fenton Hill, New Mexico	1.3		1983
Germany	Geothermal	EGS (injection)	GeneSys, Hannover	0	ML	
Sweden	Geothermal	EGS (injection)	Fjällbacka	-0.2	ML	
Japan	Geothermal	EGS (injection)	Hijiori (SKG-2 injection/stimulation)	-1		1988
Germany	Geothermal	EGS (injection)	Groß-Schönebeck	-1	MW	2007
Iceland	Geothermal	EGS (circulation)	Laugaland	-1	ML	
Iceland	Geothermal	EGS (injection)	Svartsengi	-1	ML	
Japan	Geothermal	EGS (circulation)	Hijiori (SKG-2 circulation)	-1		
USA	Geothermal	EGS (injection)	Baca, New Mexico	-2		1982 (May)
Mexico	Geothermal	Drilling, Stimulation and Production tests	Tres Virgenes, LV-06			
Turkey	Geothermal	EGS (circulation)	Salavatli, Aydin			
USA	Geothermal	EGS (circulation)	Brady, Nevada			
Indonesia	Geothermal	EGS (injection)	Darajat			
Indonesia	Geothermal	EGS (injection)	Wayang Windu			
USA	Geothermal	EGS (circulation)	Raft River, Idaho			
Nepal		Groundwater (extraction)	Gorkha earthquake, Indo-Gangetic plains	7.8	MW	2015/04 /25
Spain		Groundwater (extraction)	Lorca	5.1	MW	2011/05 /11
Spain		Groundwater extraction/Water dam	Jaen (Giribaile reservoir)	3.72	MW	2013/05 /02
Brazil		Groundwater	Bebedouro, Paraná	2.9		2005

		(extraction)	Basin			(Mar.)
USA		Groundwater extraction	San Joaquin Valley			
Russia	Mining	Mining	Bachatsky, Kuzbass	6.1	ML	2013/06/18
Germany	Mining	Mining (collapse/fluid-induced rockburst)	Volkershausen (Ernst Thaelmann/Merker's mine)	5.6	ML	1989/03/13
Australia	Mining	Mining and Groundwater extraction	Newcastle	5.6	ML	1989/12/27
South Africa	Mining	Mining	President Brand Mine, Welkom	5.6	mb	1994/10/30
Australia	Mining	Mining	Ellalong	5.4	ML	1994/08/06
Australia	Mining	Mining	Maitland	5.3	ML	18/06/1868
Australia	Mining	Mining	Boolaroo	5.3	ML	1925/12/18
South Africa	Mining	Mining	Klerksdorp (DRDGold's North West Operations)	5.3	ML	2005/03/09
USA	Mining	Mining (solution)	Attica, New York	5.2	ML	1929/08/12
Germany	Mining	Mining	Sunna (Suenna)	5.2	ML	1975/06/23
South Africa	Mining	Mining	Welkom	5.2	ML	1976/12/08
USA	Mining	Mining (collapse)	Solvay mine, Wyoming	5.2	mb	1995/02/03
Russia	Mining	Mining (rock burst)	Umbozero Mine	5.1	ML	1999/08/17
Germany	Mining	Mining	Heringen	5	ML	
Poland	Mining	Mining	Lubin mine	5	ML	1977/03/24
South Africa	Mining	Mining	Hartebeesfontein	5	ML	1997/08/21
Australia	Mining	Mining	Kalgoorlie Super Pit	5	ML	2010/04/20
Canada	Mining	Mining (rockburst)	Wright-Hargreaves mine, Ontario	5		1905/05/17
South Africa	Mining	Mining	Free State Goldfield	4.7	ML	1989/01/25
South Africa	Mining	Mining	Carletonville	4.7	ML	1992/03/07
Russia	Mining	Mining (collapse)	Solikamsk, Upper Kama	4.7		1994/01/05
Germany	Mining	Mining (collapse)	Saale (Halle) (Teutschental mine)	4.6	MW	42/5/1940
China	Mining	Mining (solution)	Salt mine, Zigong, Sichuan	4.6	ML	1985/03/29
Germany	Mining	Mining	Ibbenbüren	4.6	ML	1991/05/16
USA	Mining	Mining	Moss No. 2, Virginia	4.5	ML	1972/05/20

USA	Mining	Mining (extraction and abandonment)	Cacoosing Valley (Sinking Springs), Pennsylvania	4.4	ML	1994/01/16
Russia	Mining	Mining (rock burst)	SKRU-2, Ural Mountains	4.4		1995/01/05
Australia	Mining	Mining	Appin, Tower and West Cliff Collieries	4.4		1999/03/17
Belarus	Mining	Mining	Soligorsk (Starobin deposit)	4.4		2003/12/18
South Africa	Mining	Mining	Savuka, Carletonville	4.4	ML	2007
China	Mining	Mining	Taiji mine, Beipiao, Liaoning	4.3	ML	1977/04/28
China	Mining	Mining	Chayuan mine, Shizhu, Sichuan	4.3	ML	1987/07/02
Russia	Mining	Mining (rock burst)	Kurgazakskaya Mine	4.3	ML	1990/05/28
China	Mining	Mining	Louguanshan #4 well, South Bureau, Sichuan	4.3	ML	1994/04/15
China	Mining	Mining	Weixi mine, Leshan, Sichuan	4.2	ML	1979/08/15
China	Mining	Mining	Mentougou mine, Beijing, Beijing	4.2	ML	1994/05/19
USA	Mining	Mining	Willow Creek, Utah	4.2	ML	2000/03/07
Poland	Mining	Mining	Rudna mine	4.2	ML	2013/03/19
Germany	Mining	Mining	Ruhr area	4.1	MW	1936/11/03
China	Mining	Mining	Huachu mine, Liuzhi, Guizhou	4.1	ML	1982/03/20
Russia	Mining	Mining (rock burst)	Kirovsky Mine, Khibiny Massif (Kola Peninsula)	4.1	ML	1989/04/16
Russia	Mining	Mining (rock burst)	Blinovo-Kamensky Mine	4.1	ML	1994/07/29
Canada	Mining	Mining	Creighton, Ontario	4.1	MN	2006/11/29
France	Mining	Mining	Lorraine	4	MW	1973/04/20
USA	Mining	Mining	Buchanan No. 1, Virginia	4	ML	1988/04/14
USA	Mining	Mining	Lynch mine, Kentucky	4		1995/03/11
South Africa	Mining	Mining	Western Deep Levels East	4	ML	1996/05/05
Germany	Mining	Mining	Saar (Primsmulde), Saarland	4	ML	2008/02/23
South Africa	Mining	Mining	Kloof	4	ML	
Italy	Mining	Mining (tunneling) and hydrologic changes	Gran Sasso	3.9		1992/08/25
South Africa	Mining	Mining	Deelkraal	3.9	ML	
South Africa	Mining	Mining	East Driefontain	3.9	ML	

Germany	Mining	Mining	Peissenberg	3.8	MW	1967/09 /16
China	Mining	Mining	Wacang/Shimacao/ Chenjiapo mines, Yichang, Hubei	3.8	ML	1971/06 /17
USA	Mining	Mining (collapse)	King #4, Utah	3.8	ML	1981/05 /14
USA	Mining	Mining	Lynch No. 37, Kentucky	3.8	ML	1994/08 /03
China	Mining	Mining	Wulong mine, Fuxin, Liaoning	3.8	ML	2004/06 /16
Canada	Mining	Mining	Copper Cliff North, Ontario	3.8	MN	2008/09 /11
Canada	Mining	Mining	Kidd Creek, Ontario	3.8	MN	2009/01 /06
South Africa	Mining	Mining	Elandsrand CSA Mine, Ostrava-Karvina Coal Basin	3.8	ML	1983/04 /27
Czech Republic	Mining	Mining	Nanshan mine, Hegang, Heilongjiang	3.75		
China	Mining	Mining	Laohutai mine, Fushun, Liaoning	3.7	ML	2001/02 /01
China	Mining	Mining	Saar/Lorraine	3.7	ML	2002/01 /26
Germany	Mining	Mining	Mponeng	3.7	MW	2008/02 /23
South Africa	Mining	Mining	Leeudoorn	3.7	ML	
South Africa	Mining	Mining	Huaibaoshi mine, Zigui, Yichang, Hubei	3.7	ML	
China	Mining	Mining	Belchatow	3.6	ML	1972/03 /13
Poland	Mining	Mining	Taozhuang mine, Zaozhuang, Shandong	3.6	ML	1979/08 /17
China	Mining	Mining	Jim Walter Resources, Inc., No. 4, Alabama	3.6	ML	1982/01 /07
USA	Mining	Mining (collapse and rockburst)	Liu zhi mine, Yingpan, Liuzhi, Guizhou	3.6	ML	1986/05 /07
China	Mining	Mining	Bingshuijing mine, Yingpan, Liuzhi, Guizhou	3.6	ML	1991/07 /09
China	Mining	Mining	Soldier Creek, Utah	3.6	ML	1991/07 /09
USA	Mining	Mining	Retsof, New York	3.6	ML	1993/01 /21
USA	Mining	Mining (collapse)	Genesee, New York	3.6		1994/03 /12
USA	Mining	Mining (collapse)	Tashtagol Mine	3.6		1994
Russia	Mining	Mining (rock burst)	Shunyuan mine, Zaozhuang, Shandong	3.6	ML	1999/10 /24
China	Mining	Mining (collapse)	Karnasurt Mine	3.6	ML	2002/05 /20
Russia	Mining	Mining (rock burst)		3.6	ML	2002/12

						/17
USA	Mining	Mining (collapse)	Cottonwood, Utah	3.5	ML	1992/07/05
Germany	Mining	Mining	Saar (Dilsburg Ost), Saarland	3.5	ML	2000 (Nov.)
Russia	Mining	Mining	Mine 15-15bis	3.5	ML	2010/02/13
Australia	Mining	Mining	Olympia Dam	3.5		2013/05/01
USA	Mining	Mining	Lucky Friday Mine, Idaho	3.5		
USA	Mining	Mining	Olga, West Virginia	3.4	ML	1965/04/26
UK	Mining	Mining (extraction and collapse)	North Staffordshire (Stoke on Trent)	3.4	mb	1975/07/15
USA	Mining	Mining (collapse)	Sunnyside #3, Utah	3.4	ML	1981/09/21
China	Mining	Mining	Xujiadong 711 mine, Chenzhou, Hunan	3.4	ML	1998/03/12
China	Mining	Mining	San he jian mine, Xuzhou, Jiangsu	3.4	ML	2003/05/08
China	Mining	Mining	Chengzi mine, Beijing, Beijing	3.4	ML	
USA	Mining	Mining	Wappingers Falls, New York	3.3	mbn	1974/06/07
USA	Mining	Mining	Trail Mountain, Utah	3.3	ML	1987/12/16
Germany	Mining	Mining (tunneling)	Saar (Primsmulde), Saarland (Roadway construction)	3.3	ML	2005 (May)
Canada	Mining	Mining	Garson, Ontario	3.3	MN	2008/12/05
China	Mining	Mining	Huating mine, Pingliang, Gansu	3.3	ML	
Canada	Mining	Mining (rockburst)	Campbell mine, Ontario	3.3	MN	
UK	Mining	Mining	Nottinghamshire	3.2	ML	1984/03/22
China	Mining	Mining	Niumasi mine, Shaoyang, Hunan	3.2	ML	1994/09/04
Russia	Mining	Mining (rock burst)	Mine 14-14bis	3.2	ML	2004/03/25
Sweden	Mining	Mining (rock burst)	Grängesberg ore mine	3.1	ML	1974/08/30
Germany	Mining	Mining	S-Harz	3.1	MW	1983/07/02
China	Mining	Mining	Xifeng Nan shan mine, Lindong, Guizhou	3.1	ML	1991/04/06
USA	Mining	Mining (collapse)	Star Point #2, Utah	3.1	ML	1991/02/06
Bulgaria	Mining	Mining (solution)	Provadia	3.1	MD	1994/06/20
China	Mining	Mining	Qixingjiezhen mine, Lianyuan, Hunan	3.1	ML	1996/03/28

China	Mining	Mining	Shanjiaocun mine, Panjiang, Guizhou	3.1	ML	1997/12 /05
China	Mining	Mining	Yueliangtian mine, Panjiang, Guizhou	3.1	ML	1997/12 /05
Canada	Mining	Mining	Macassa, Ontario	3.1	MN	2008/07 /12
India	Mining	Mining (abandonment)	Champion Reef, Kolar Gold field	3.09	ML	
Canada	Mining	Mining	Cory Mine, Saskatchewan	3	mb	1980/02 /29
USA	Mining	Mining (collapse)	Deer Creek, Utah	3	ML	1984/03 /21
USA	Mining	Mining (collapse)	Castle Gate #3, Utah	3	ML	1986/10 /30
USA	Mining	Mining	VP No. 3, Virginia	3	ML	1987/03 /04
China	Mining	Mining	Xindong mine, Shaoyang, Hunan	3	ML	1994/11 /20
USA	Mining	Mining	Skyline #3, Utah	3	ML	1996/06 /02
China	Mining	Mining	Fangshan mine, Beijing, Beijing	3	ML	1997/02 /18
USA	Mining	Mining (solution)	Cleveland, Ohio	3	ML	
USA	Mining	Mining (abandonment and flooding)	Mineville, New York	3	Mc	
USA	Mining	Mining	Galena mine, Idaho	3	ML	
Canada	Mining	Mining (rockburst)	Quirke mine, Ontario	3		
Poland	Mining	Mining	Polkowice mine	3	MW	
China	Mining	Mining	En kou mine, Lowde, Hunan	2.9	ML	1976/01 /08
USA	Mining	Mining	Dillsburg, Pennsylvania	2.9	ML	2009/04 /24
China	Mining	Mining	Huayazi mine, Zigui, Yichang, Hubei	2.8	ML	1973 (Mar.)
China	Mining	Mining	Sheng li mine, Fushun, Liaoning	2.8	ML	1978/09 /21
China	Mining	Mining	Da he bian mine, Shiucheng, Guizhou	2.8	ML	1985/07 /09
UK	Mining	Mining	Midlothian	2.8	ML	1986/10 /09
China	Mining	Mining	Mei tan ba mine, Xifenglun, Hunan	2.8	ML	1991/04 /23
China	Mining	Mining	Niwan mine, Xiangtan, Hunan	2.8	ML	2003/01 /17
China	Mining	Mining	Benxi Caitun mine, Shenyang, Liaoning	2.8	ML	2004/04 /13
China	Mining	Mining	Baidong mine, Datong, Shanxi	2.7	ML	1983 (Sep.)
China	Mining	Mining	Sijiaotian mine, Yingpan, Liuzhi, Guizhou	2.7	ML	1985/01 /21

China	Mining	Mining	Dizong mine, Yingpan, Liuzhi, Guizhou	2.7	ML	1985/01 /21
China	Mining	Mining	Dayong mine, Yingpan, Liuzhi, Guizhou	2.7	ML	1985/01 /21
Canada	Mining	Mining	Strathcona, Ontario	2.7	mN	1988/06 /19
China	Mining	Mining	Dahuatang mine, Shaoyang, Hunan	2.7	ML	1997/12 /04
China	Mining	Mining	Qingshan mine, Lianyuan, Hunan	2.6	ML	1996/07 /01
Sweden	Mining	Mining	Zingruvan	2.6	MW	
China	Mining	Mining	Longfeng mine, Fushun, Liaoning	2.5	ML	1981/02 /16
China	Mining	Mining	Doulishan mine, Lowde, Hunan	2.5	ML	1985/03 /04
China	Mining	Mining	Yan guan mine, Zigui, Yichang, Hubei	2.5	ML	1988/05 /14
France	Mining	Mining (abandonment and flooding)	Gardanne	2.5		2005 (Nov.)
Spain	Mining	Mining (collapse)	Lo Tacón (Torre Pacheco)	2.4	MW	1998/05 /02
Switzerland	Mining	Mining (tunneling)	MFS Faido (Gotthard basetunnel)	2.4	ML	2006/03 /25
Canada	Mining	Mining	Fraser, Ontario	2.4	MN	2008/10 /16
Korea	Mining	Mining	Dogye	2.4	ML	
USA	Mining	Mining	Lompoc diatomite mine, California	2.3	MD	1995/04 /05
USA	Mining	Mining	Florida, New York	2.3		2003
China	Mining	Mining	Gangdong mine, Shuangyashan, Heilongjiang	2.3	ML	
Sweden	Mining	Mining	Dannemora	2.27	MD	
China	Mining	Mining	Qiao tou he mine, Lowde, Hunan	2.2	ML	1974/05 /31
UK	Mining	Mining	Rotherham (Yorkshire)	2.2	ML	1988/10 /14
China	Mining	Mining	Kaiyang mine, Jinzhong, Kaiyang, Guizhou	2.2	ML	1990/10 /23
UK	Mining	Mining	Bargoed Mid Glamorgan (South Wales)	2.2	ML	1992/08 /17
South Africa	Mining	Mining	TauTona, Carletonville	2.2		2004/12 /12
Canada	Mining	Mining	Craig, Ontario	2.2	MN	2007/06 /22
Poland	Mining	Mining	Wujek mine	2.2	MW	
Poland	Mining	Mining	Ziemowit mine	2.2	MW	
Japan	Mining	Mining (hydraulic extraction rockburst)	Sunagawa mine	2.1	ML	1986/01 /29

UK	Mining	Mining	Buxton (Derbyshire)	2.1	ML	1989/09/04
China	Mining	Mining	Jinhuagong mine, Datong, Shanxi	2.1	ML	
UK	Mining	Mining	Sunderland (Durham and Northumberland)	2	ML	1988/05/05
China	Mining	Mining	Shuikoushan mine, Hengnan, Hunan	2	ML	
Czech Republic	Mining	Mining	Mayrau mine	2	ML	
UK	Mining	Mining	Bolton (Lancashire)	1.7	ML	1989/03/11
China	Mining	Mining	Shi xia jiang mine, Shaoyang, Hunan	1.6	ML	1991 (Dec.)
Finland	Mining	Mining	Pyhäsalmi	1.2	MW	
USA	Mining	Mining	Beatrice, Virginia	1	ML	1974/05/15
USA	Mining	Mining (solution)	Dale, New York	1	ML	
Australia	Mining	Mining (rock fracture)	Moonee Colliery Springfield Pike	0.6	MW	1998
USA	Mining	Mining (collapse)	Quarry, Pennsylvania	0.2	MW	2000/02/21
China	Mining	Mining	Dagandsham Hydropower Station	-0.2	MW	
France	Mining	Mining (solution)	Arkema-Vauvert	-0.24	MW	
Canada	Mining	Shaft excavation	Underground Research Laboratory, Manitoba	-1.9	MW	
South Africa	Mining	Mining (collapse)	Ophirton			1908
USA	Mining	Mining (collapse)	Wilkes-Barre, Pennsylvania			1954 (Feb.)
China	Mining	Mining (tunneling rock burst)	Dongguashan (Shizishan copper mine), Tongling, Hunan (Roadway construction)			1999 (Mar.)
China	Mining	Mining (tunneling rock burst)	Tianshengqiao II Hydropower Station (Head race tunnel construction)			1990/12/11
Chile	Mining	Mining	El Teniente			1992 (Mar.)
India	Mining	Mining	Chinakuri Colliery			
Russia	Mining	Mining	Gluboky Mine, Streltsovsk			
Australia	Mining	Mining	Mount Charlotte Mine			
Russia	Mining	Mining (collapse)	Berezniki-1 Mine			
Kazakhstan	Mining	Mining	Zhezkazgan Mine			
Australia	Mining	Mining	Southern Colliery, German Creek			
Japan	Mining	Mining	Horonai			
Norway	Mining	Mining (tunneling rock burst)	Road tunnel			

Sweden	Mining	Mining (tunneling rock burst)	Head race tunnel
Iraq	Mining	Mining (solution)	Mishraq
Sweden	Mining	Mining	Malmberget
Switzerland/Italy	Mining	Mining (tunneling rock burst)	Simplon Tunnel
Japan	Mining	Mining (tunneling rock burst)	Shimizu Tunnel
Japan	Mining	Mining (tunneling rock burst)	Kanetsu (Kan-Etsu) Tunnel
Sweden	Mining	Mining (tunneling rock burst)	Forsmark Nuclear Plant (Hydraulic tunnels construction)
Sweden	Mining	Mining (tunneling rock burst)	Ritsem Traffic Tunnel
China	Mining	Mining (tunneling rock burst)	Yuzixi I Hydropower Station (Head race tunnel construction)
China	Mining	Mining (tunneling rock burst)	Erlangshan Tunnel (Sichuan-Tibet Highway)
China	Mining	Mining (tunneling rock burst)	Qinling Railway Tunnel
China	Mining	Mining (tunneling rock burst)	Cangling Tunnel (Taizhou-Jiyun Highway)
China	Mining	Mining (tunneling rock burst)	Pubugou Hydropower Station
China	Mining	Mining (tunneling rock burst)	Jinping II Hydropower Station (Auxiliary tunnel)
China	Mining	Mining	Fuli mine, Hegang, Heilongjiang
China	Mining	Mining	Zhenxing mine, Hegang, Heilongjiang
China	Mining	Mining	Didao mine, Jixi, Heilongjiang
China	Mining	Mining	Yingcheng mine, Shulang, Jilin
China	Mining	Mining	Xian mine, Liaoyuan, Jilin
China	Mining	Mining	Tai xin mine, Liaoyuan, Jilin
China	Mining	Mining	Tiechang mine, Tonghua, Jilin
China	Mining	Mining	Hongtoushan mine, Fushun, Liaoning
China	Mining	Mining	Gaode mine, Fuxin, Liaoning
China	Mining	Mining	Dongliang mine, Fuxin, Liaoning
China	Mining	Mining	Guanshan mine, Beipiao, Liaoning
China	Mining	Mining	Benxi Niu xin tai mine, Shenyang, Liaoning

China	Mining	Mining	Binggou mine, Jianchang county, Liaoning
China	Mining	Mining	Chang/Zhang gou yu mine, Beijing, Beijing
China	Mining	Mining	Datai mine, Beijing, Beijing
China	Mining	Mining	Muchengjian mine, Beijing, Beijing
China	Mining	Mining	Tang shan mine, Kailuan, Hebei
China	Mining	Mining	Guan tai mine, Cixian, Hebei
China	Mining	Mining	Tongjialiang mine, Datong, Shanxi
China	Mining	Mining	Xin zhou yao mine, Datong, Shanxi
China	Mining	Mining	Meiyukou mine, Datong, Shanxi
China	Mining	Mining	Yongdingzhuang mine, Datong, Shanxi
China	Mining	Mining	Bayi mine, Zaozhuang, Shandong
China	Mining	Mining	Chaili mine, Zaozhuang, Shandong
China	Mining	Mining	Huafeng mine, Xinwen, Shandong
China	Mining	Mining	Sun cun mine, Xinwen, Shandong
China	Mining	Mining	Zhangzhuan mine, Xinwen, Shandong
China	Mining	Mining	Pan xi mine, Xinwen, Shandong
China	Mining	Mining	Dong tan mine, Yankuang, Shandong
China	Mining	Mining	Bao dian mine, Yankuang, Shandong
China	Mining	Mining	#2 mine, Weishanhu, Shandong
China	Mining	Mining	Qianqiu mine, Yima, Henan
China	Mining	Mining	Wumei mine, Hebi, Henan
China	Mining	Mining	Shier (Shi'er kuang?) mine, Pingdingshan, Henan
China	Mining	Mining	Quantai mine, Xuzhou, Jiangsu
China	Mining	Mining	Qishan mine, Xuzhou, Jiangsu
China	Mining	Mining	Zhangxiaolou mine, Xuzhou, Jiangsu

China	Mining	Mining	Zhangji mine, Xuzhou, Jiangsu
China	Mining	Mining	Yaoqiao mine, Datun, Jiangsu
China	Mining	Mining	Kong zhuang mine, Datun, Jiangsu
China	Mining	Mining	Leigu mine, Mianyang
China	Mining	Mining	Beichuan, Sichuan
China	Mining	Mining	Wuyi mine, Shanxi
China	Mining	Mining	Tianchi mine, Mianzhu, Sichuan
China	Mining	Mining	Yanshitai mine, Wansheng district, Nantong, Chongqing
China	Mining	Mining	Nantong mine, Nantong, Chongqing
China	Mining	Mining	Hua gu shan mine, Xinyu, Jiangxi
China	Mining	Mining	Bajing mine, Gaoan, Jiangxi
China	Mining	Mining	Tungsten ore mine, Jiangxi
China	Mining	Mining	Manganese mine, Zunyi, Guizhou
China	Mining	Mining	Dongguashan (Shizishan copper mine), Tongling, Hunan
China	Mining	Mining	South manganese mine, Huayuan, Hunan
China	Mining	Mining	Manganese mine, Taojiang, Hunan
China	Mining	Mining	Phosphorus mine, Yichang, Hubei
China	Mining	Mining	Fengdouyan, Jiupanshan, Qishuping and Beitou mines, Jiupanshan, Yichang, Hubei
China	Mining	Mining	Yangmuxi mine, Changyang, Yichang, Hubei
China	Mining	Mining	Songyi mine, Yichang, Hubei
China	Mining	Mining	Gaofeng mine, Dachangjingtian, Guangxi
China	Mining	Mining	Tongkeng mine, Dachangjingtian, Guangxi
China	Mining	Mining	Manganese mine, Dounan, Yunnan
China	Mining	Mining	Manganese mine, Heqing, Yunnan

China	Mining	Mining (tunneling rock burst)	Lujialiang Tunnel (Chongqing-Yichang Highway)		
Australia	Mining	Mining	Cadia		
Australia	Mining	Mining	Queenstown, Tasmania		
Canada	Mining	Mining (rockburst)	Brunswick No. 12 mine		
Canada	Mining	Mining (rockburst)	Denison mine, Ontario		
Poland	Mining	Mining	Pstrowski mine		
Japan	Mining	Mining (rock burst)	Miike mine		
USA	Nuclear	Seismicity/faulting following nuclear detonation	Cannikin	4.9	mb
Russia	Nuclear	Seismicity/faulting following nuclear detonation	Novaya Zemlya site	4.8	mb
USA	Nuclear	Seismicity/faulting following nuclear detonation	Milrow	4.3	mb
USA	Nuclear	Seismicity/faulting following nuclear detonation	Benham, Nevada	4.2	ML
USA	Nuclear	Seismicity/faulting following nuclear detonation	Jorum, Nevada	3	ML
USA	Nuclear	Seismicity/faulting following nuclear detonation	Purse, Nevada	2	ML
USA	Nuclear	Seismicity/faulting following nuclear detonation	Handley, Nevada	2	ML
USA	Nuclear	Seismicity/faulting following nuclear detonation	Faultless		
USA	Nuclear	Seismicity/faulting following nuclear detonation	Hard Hat, Nevada		
USA	Nuclear	Seismicity/faulting following nuclear detonation	Rex, Nevada		
USA	Nuclear	Seismicity/faulting following nuclear detonation	Halfbeak, Nevada		
USA	Nuclear	Seismicity/faulting following nuclear detonation	Greeley, Nevada		
USA	Nuclear	Seismicity/faulting following nuclear detonation	Bourbon, Nevada		
USA	Nuclear	Seismicity/faulting following nuclear detonation	Buff, Nevada		
USA	Nuclear	Seismicity/faulting following nuclear detonation	Charcoal, Nevada		
USA	Nuclear	Seismicity/faulting following nuclear	Chartreuse		

		detonation				
USA	Nuclear	Seismicity/faulting following nuclear detonation	Nash, Nevada			
USA	Nuclear	Seismicity/faulting following nuclear detonation	Dumont, Nevada			
USA	Nuclear	Seismicity/faulting following nuclear detonation	Tan, Nevada			
USA	Nuclear	Seismicity/faulting following nuclear detonation	Boxcar, Nevada			
USA	Nuclear	Seismicity/faulting following nuclear detonation	Duryea, Nevada			
USA	Nuclear	Seismicity/faulting following nuclear detonation	Scotch, Nevada			
USA	Oil and Gas	Oil and Water extraction	Fashing Region (D Cluster)	3		2010/12/21
USA	Oil and Gas	Oil and Water extraction	Dimmit County (K Cluster), Texas	2.98		2010/03/08
USA	Oil and Gas	Oil and Water extraction	Dimmit County (M Cluster), Texas	2.72		2011/06/26
USA	Oil and Gas	Oil and Water extraction	Fashing Region (H Cluster)	2.62		2011/05/22
USA	Oil and Gas	Oil and Water extraction	Fashing Region (G Cluster)	2.4		2011/04/09
USA	Oil and Gas	Oil and Water extraction	Fashing Region (C Cluster)	2.12		2011/07/05
USA	Oil and Gas	Oil and Water extraction	Fashing Region (Event B)	1.94		2011/01/15
USA	Oil and Gas	Oil and Water extraction	Dimmit County (L Cluster), Texas	1.83		2010/04/26
Italy	Oil and Gas/Waste fluid injection	Oil and Gas/Wastewater injection	Cavone and San Giacomo fields, Mirandola License (Emilia sequence)	5.9	ML	2012/05/20
USA	Oil and Gas/Waste fluid injection	Oil and Gas/Wastewater injection	Fashing Region (F Cluster), Texas	3		2010/03/08
USA	Oil and Gas/Waste fluid injection	Oil and Gas/Wastewater injection	Bakken, North Dakota	2.5		2010/03/21
USA	Oil and Gas/Waste fluid injection	Oil and Gas/Wastewater injection	Cedar Creek Anticline, Montana	2.1		2010/04/27
USA	Research	Research and Secondary recovery (water injection)	Rangely, Colorado	3.1	ML	1970/04/21
New Zealand	Research	Water injection	Wairakei	3		1984 (June)
Philippines	Research	Research (injection)	Tongonan Geothermal field	3	mc	
Japan	Research	Water injection	Matsushiro	2.8		1970/01/25
Germany	Research	Brine (KBr, KCl)	KTB	1.2	ML	1994

		injection				
China	Research	Research (injection)	WFSD-3P	1		
Germany	Research	Fluid injection	KTB	0.7	ML	
Japan	Research	Research (injection)	Nojima	0.6		1997
Germany	Research	Water injection	KTB	0.5	ML	2000
France	Research	Research (solution mining)	Cerville-Buissoncourt Laboratoire	-0.8	MW	
France	Research	Research (injection)	Souterrain à Bas Bruit			
Germany	Research	Mine flooding	Hope mine			
USA	Research	Waste disposal	Frio Formation, Beaumont, near Jasper County, Texas			
USA	Waste fluid injection	Wastewater (injection)	Prague, Oklahoma	5.7	MW	2011/11/06
USA	Waste fluid injection	Waste disposal	Rocky Mountain Arsenal (Denver), Colorado	5.5	ML	1967
USA	Waste fluid injection	Wastewater (injection)	Raton Basin, Colorado and New Mexico	5.3	MW	2011/08/23
China	Waste fluid injection	Wastewater (injection)	Rongchang gas field	5.2	ML	1997/08/13
USA	Waste fluid injection	Wastewater (injection)	Oklahoma	5.1		2016/02/13
USA	Waste fluid injection	Wastewater (injection)	Painesville (Perry), Ohio	4.9	MW	1986/01/31
USA	Waste fluid injection	Wastewater (injection)	Timpson, East Texas	4.8	MWrm t	2012/05/17
USA	Waste fluid injection	Wastewater (injection)	Arkansas	4.7		2011/02/27
USA	Waste fluid injection	Wastewater (injection)	Central Valley (WWF), California	4.6	MW	2005/09/22
China	Waste fluid injection	Wastewater (injection)	Huangjiachang gas field	4.4	ML	2009/02/16
USA	Waste fluid injection	Brine injection	Paradox Valley, Colorado	4.3		2000/05/27
USA	Waste fluid injection	Waste disposal	Ashtabula, Ohio	4.3	Mblg	2001/01/26
USA	Waste fluid injection	Wastewater injection	Cushing, Oklahoma	4.3	MW	2014 (Oct.)
USA	Waste fluid injection	Wastewater (injection)	Dagger Draw, New Mexico	4.1	MW	2005 (Dec.)
Canada	Waste fluid injection	Wastewater (injection)	Cordel (Brazeau Cluster)	4	ML	1997/03/31
Canada	Waste fluid injection	Wastewater (injection)	Graham (Montney Trend)	4	ML	2010
USA	Waste fluid injection	Wastewater injection	Marcotte oil field (Palco), Kansas	4		1989
USA	Waste fluid injection	Wastewater injection	Guthrie, Oklahoma	4		2014
USA	Waste fluid injection	Wastewater (injection)	Jones, Oklahoma	4		2008?
USA	Waste fluid	Wastewater	Youngstown, Ohio	3.88	MW	2011/12

	injection	(injection)				/31
USA	Waste fluid injection	Waste disposal	Lake Charles, Louisiana	3.8	ML	
USA	Waste fluid injection	Wastewater (injection)	Dallas-Fort Worth, Texas	3.3	mb	2009/05/16
USA	Waste fluid injection	Wastewater (injection)	Greeley, Colorado	3.2		2014/06/01
Canada	Waste fluid injection	Wastewater (injection)	Pintail (Montney Trend)	3.1	ML	2014
USA	Waste fluid injection	Waste disposal	El Dorado, Arkansas	3	ML	1983
USA	Waste fluid injection	Wastewater (injection)	Lillian (J-A cluster), Barnett Shale, Texas	3		2011/07/17
USA	Waste fluid injection	Deep fluid injection	Avoca, New York	2.9	Mblg	2001
USA	Waste fluid injection	Wastewater (injection)	Cleburne, Texas	2.8	MbLg	2009/06/09
Italy	Waste fluid injection	Wastewater injection	Val d'Agri oil field (CM2 well)	2.2	ML	2006
USA	Waste fluid injection	Wastewater injection	Fashing Region (A Cluster), Texas	1.82		2011/08/26
USA	Waste fluid injection	Wastewater injection	Dimmit County (Event J), Texas	1.52		2010/11/29
USA	Waste fluid injection	Wastewater injection	Center, Texas	1.5	ML	2010/12/01
USA	Waste fluid injection	Wastewater injection	Cedar Creek Anticline, North Dakota	1.4		2010/06/14
China	Water dam	Water dam	Zipingpu (Wenchuan earthquake)	7.9	MW	2008/05/12
USA	Water dam	Water dam	Lake Hebgen, Montana	7.1	MS	1959/08/17
Greece	Water dam	Water dam	Polyphyto	6.5	MS	1995/05/13
India	Water dam	Water dam	Koyna	6.3	MS	1967/12/10
Zambia–Zimbabwe	Water dam	Water dam	Kariba	6.2		1963/09/23
Greece	Water dam	Water dam	Kremasta	6.2		1966/02/05
China	Water dam	Water dam	Hsingfengkiang (Hsingfengchiang, Xinfengjiang)	6.1	MS	1962/03/18
India	Water dam	Water dam	Killari	6.1	MW	1993/09/30
Thailand	Water dam	Water dam	Srinagarind	5.9	ML	1983
USA	Water dam	Water dam	Oroville, California	5.8	ML	1975/08/01
Greece	Water dam	Water dam	Marathon	5.7		1938/07/20
Egypt	Water dam	Water dam	Aswan	5.7	ML	1981/11/14
Greece	Water dam	Water dam	Pournari	5.6	ML	1981/03/10

Australia	Water dam	Water dam	Warragamba (Varragamba)	5.5		1973/03 /09
Greece	Water dam	Water dam	Asomata	5.4	MS	1984/10 /25
France	Water dam	Water dam	Monteynard	5.3	ML	1962
Ghana	Water dam	Water dam	Akosombo	5.3		1964 (Nov.)
India	Water dam	Water dam	Kinnersani	5.3		1969/04 /13
Uzbekistan	Water dam	Water dam	Charvak	5.3	ML	1977/03 /15
USA	Water dam	Water dam	Coyote Valley (Leroy Anderson?), California	5.2		1962/06 /06
China	Water dam	Water dam	Shenwo/Shenwu	5.2	ML	1974/12 /02
Greece	Water dam	Water dam	Sfikia	5.2	MS	1986/02 /18
USA	Water dam	Water dam	Hoover (Lake Mead), Nevada/Arizona	5	ML	1939
Australia	Water dam	Water dam	Eucumbene	5		1959/05 /18
New Zealand	Water dam	Water dam	Benmore	5	ML	1966/07 /07
India	Water dam	Water dam	Warna (Warana)	5		1993
Australia	Water dam	Water dam	Thomson	5	ML	1996
Zambia	Water dam	Water dam	Itezhi-Tezhi	5		2011/07 /21
Japan	Water dam	Water dam	Kurobe	4.9	MS	1961/08 /19
Serbia	Water dam	Water dam	Bajina Basta	4.9	ML	1967/07 /03
USA	Water dam	Water dam	Kerr, Montana	4.9		1971/07 /28
India	Water dam	Water dam	Bhatsa	4.9	ML	1983/09 /15
Vietnam	Water dam	Water dam	Hoa Binh	4.9		1989
Russia	Water dam	Water dam	Lake Baikal	4.8		
Spain	Water dam	Water dam	Canelles	4.7		1962/06 /09
Iran	Water dam	Water dam	Sefia Rud	4.7		1968/08 /02
Canada	Water dam	Water dam	McNaughton (Mica)	4.7	ML	1973
China	Water dam	Water dam	Danjiangkou	4.7	ML	1973/11 /29
USA	Water dam	Water dam	Anderson, Idaho	4.7	ML	1973
Vietnam	Water dam	Water dam	Song Tranh 2	4.7		2012/11 /15
Georgia	Water dam	Water dam	Enguri (Inguri)	4.7		
Greece	Water dam	Water dam	Kastraki	4.6	ML	1969
Tadjikistan	Water dam	Water dam	Nurek	4.6	MS	1972/11 /27
Kyrgyzstan	Water dam	Water dam	Toktogul	4.6	ML	1977

New Zealand	Water dam	Water dam	Lake Pukaki	4.6	ML	1978/12 /17
Spain	Water dam	Water dam	Itoiz	4.6	mbLg	2004/09 /18
China	Water dam	Water dam	Three Gorges	4.6	ML	2008/11 /22
France	Water dam	Water dam	Vouglans	4.5	MW	1971/06 /21
China	Water dam	Water dam	Foziling	4.5		1973/08 /11
China	Water dam	Water dam	Dahua	4.5		1993
Italy	Water dam	Water dam	Pieve de Cadore	4.4		1960/01 /13
Italy	Water dam	Water dam	Piastra	4.4		1966/04 /07
China	Water dam	Water dam	Dongjing/Dongqing	4.4		2010/01 /17
USA	Water dam	Water dam	Clark Hill, South Carolina/Georgia	4.3	ML	1974/08 /02
Iran	Water dam	Water dam	Karun III	4.3	ML	2006/05 /12
Brazil	Water dam	Water dam	P. Colombia/Volta Grande	4.2		1974/02 /24
Armenia	Water dam	Water dam	Tolors	4.2		1982
Albania	Water dam	Water dam	Komani	4.2	ML	1986
Russia	Water dam	Water dam	Bratsk	4.2		1996
China	Water dam	Water dam	Longtan	4.2	ML	2007/07 /17
Spain	Water dam	Water dam	Camarillas	4.1		1964/04 /15
Canada	Water dam	Water dam	Mica	4.1		1974/01 /05
Canada	Water dam	Water dam	Manic-3, Quebec	4.1	mbLg	1975/10 /23
Brazil	Water dam	Water dam	Nova Ponte	4	mb	1998 (May)
Spain	Water dam	Water dam	Tous New	4	mb	2000/10 /08
USA	Water dam	Water dam	Jocassee, South Carolina	3.9	ML	1979/08 /25
Paraguay	Water dam	Water dam	Yacyreta	3.9	mR	2000/04 /28
Algeria	Water dam	Leakage from pumping between reservoirs (unintentional injection)	Beni Haroun dam/reservoir and the Oued Athmania reservoir	3.9	Md	2007/12 /18
China	Water dam	Water dam	Xiaowan	3.9	ML	2012/09 /16
USA	Water dam	Water dam	Keowee, South Carolina	3.8		1971/07 /13
India	Water dam	Water dam	Dhamni	3.8	ML	1994
USA	Water dam	Water dam	Palisades, Idaho	3.7		1966/06 /10

Brazil	Water dam	Water dam	Carmo do Cajuru	3.7		1972/01 /23
Brazil	Water dam	Water dam	Capivara	3.7		27/3/19 79, 07/01/1 989
Canada	Water dam	Water dam	LG 3, Quebec	3.7	ML	1983
Pakistan	Water dam	Water dam	Mangla	3.6	ML	1967/05 /28
China	Water dam	Water dam	Shengjiaxia (Shenjia Xiashuiku)	3.6		1984
Switzerland	Water dam	Water dam	Lac de Salanfe	3.5	MW	1953/10 /17
Australia	Water dam	Water dam	Blowering	3.5		1973/01 /06
Australia	Water dam	Water dam	Talbingo	3.5		1973/01 /06
Turkey	Water dam	Water dam	Keban	3.5		1973
Switzerland	Water dam	Water dam	Emosson	3.5	ML	1974
India	Water dam	Water dam	Idukki	3.5		1977/07 /02
India	Water dam	Water dam	Gandipet (Osman Sagar)	3.5	ML	1982
Italy	Water dam	Water dam	Ridracoli	3.5		1988
China	Water dam	Water dam	Yantan	3.5		1994
Poland	Water dam	Water dam	Czorsztyn Lake	3.5		2013/03 /01
France	Water dam	Water dam	Eguzon	3.5		
India	Water dam	Water dam	Nagarjuna Sagar	3.5		
Japan	Water dam	Water dam	Hitotsuse	3.5		
Japan	Water dam	Water dam	Arimine	3.5		
Japan	Water dam	Water dam	Kuzuryu	3.5		
Japan	Water dam	Water dam	Midono	3.5		
Japan	Water dam	Water dam	Makio	3.5		
Japan	Water dam	Water dam	Miomote	3.5		
Japan	Water dam	Water dam	Nagawado	3.5		
Japan	Water dam	Water dam	Narugo	3.5		
Japan	Water dam	Water dam	Ohkura	3.5		
Japan	Water dam	Water dam	Tohri (Tori)	3.5		
Japan	Water dam	Water dam	Uchikawa	3.5		
Japan	Water dam	Water dam	Yuda	3.5		
Brazil	Water dam	Water dam	Tucuruí	3.4		1985
China	Water dam	Water dam	Wujiangdu	3.4	ML	1985
China	Water dam	Water dam	Lubuge	3.4		1988
Brazil	Water dam	Water dam	Balbina	3.4	mb	1990/03 /25
France	Water dam	Water dam	Serre-Poncen	3.3		1966/08 /23
China	Water dam	Water dam	Zhelin	3.2	ML	1972/10 /14
India	Water dam	Water dam	Sriramsagar	3.2		1984/07

						/21
China	Water dam	Water dam	Shuikou	3.2		1994
Lesotho	Water dam	Water dam	Katse	3.1		1996
Algeria	Water dam	Water dam	Oued Fodda	3		1933 (May)
USA	Water dam	Water dam	Shasta, California	3		1944
Italy	Water dam	Water dam	Vajont	3	ML	1960
India	Water dam	Water dam	Mangalam	3		1963
Switzerland	Water dam	Water dam	Contra	3		1965 (Oct.)
Bosnia and Herzegovina	Water dam	Water dam	Grancarevo	3		1967
Japan	Water dam	Water dam	Kamafusa	3		1970
China	Water dam	Water dam	Qianjin	3		1971/10 /20
Brazil	Water dam	Water dam	Paraibuna– Paraitinga	3		1977
Brazil	Water dam	Water dam	Jaguari	3	mb	1985/12 /17
Cyprus	Water dam	Water dam	Kouris	3		1994- 1995
Brazil	Water dam	Water dam	Irapé	3	ML	2006/05 /14
India	Water dam	Water dam	Rihand	3		
India	Water dam	Water dam	Parambikulam	3		
India	Water dam	Water dam	Ukai	3		
Pakistan	Water dam	Water dam	Tarbela	3		
Thailand	Water dam	Water dam	Tsengwen (Zengwen)	3		
USA	Water dam	Water dam	Monticello (Fairfield), California	2.9		1978 (Oct.)
China	Water dam	Water dam	Tongjiezi	2.9		1992
China	Water dam	Water dam	Nanchong	2.8		1974/07 /25
China	Water dam	Water dam	Hunanzhen	2.8		1979
Brazil	Water dam	Water dam	Açu	2.8		1994
Romania	Water dam	Water dam	Vidra Lotru	2.8		
Romania	Water dam	Water dam	Vidraru-Arges	2.8		
Japan	Water dam	Water dam	Takase	2.7		1982
USA	Water dam	Water dam	Heron, New Mexico	2.7	ML	
Albania	Water dam	Water dam	Fierza	2.6		1981
India	Water dam	Water dam	Kadana	2.5		
Brazil	Water dam	Water dam	Miranda	2.4	mb	1998/04 /07
China	Water dam	Water dam	Nanshui	2.3		1970
China	Water dam	Water dam	Huangshi	2.3		1974/09 /21
Brazil	Water dam	Water dam	Serra da Mesa	2.2	mb	1999/06 /13
France	Water dam	Water dam	Sainte-Croix	2.2		

Italy	Water dam	Water dam	Pertusillio	2.1	ML	
USA	Water dam	Water dam	Cabin Creek, Colorado	2		1968
South Africa	Water dam	Water dam	Hendrik Verwoerd (Gariep)	2		1971
Spain	Water dam	Water dam	Almendra	2		1972 (Jan.)
Austria	Water dam	Water dam	Schlegeis	2		1973 (Apr.)
Brazil	Water dam	Water dam	Marimbondo	2	ML	1978/07 /25
Brazil	Water dam	Water dam	Sobradinho	2		1979
Brazil	Water dam	Water dam	Emborcacao	2		1984
India	Water dam	Water dam	Sholayar	2		
India	Water dam	Water dam	Sharavathi (Sharavati)	2		
Romania	Water dam	Water dam	Ivorul Muntelui- Bicaz	2		
Brazil	Water dam	Water dam	Xingó	1.7	mb	1994/07 /20
India	Water dam	Water dam	Mula	1.5		1972
Canada	Water dam	Water dam	Toulnostouc	1.4	mN	2005/02 /26
Brazil	Water dam	Water dam	Castanhão	1.4	mb	
Canada	Water dam	Hydroelectric tunnel	Toulnostouc	0.8	mN	2005/04 /09
France	Water dam	Water dam	Grandval			1963/08 /05
Spain	Water dam	Water dam	El Cenajo			1973
Australia	Water dam	Water dam	Gordon River Power Development Storage			
Indonesia	Water dam	Water dam	Saguling-Cirata			
Spain	Water dam	Water dam	El Grado			
Spain	Water dam	Water dam	La Cohilla			1975
USA	Water dam	Water dam	Rocky Reach, Washington			
USA	Water dam	Water dam	San Luis, California			
USA	Water dam	Water dam	Sanford, Michigan			

4776

4777

4778 **E Bibliography**

4779

4780 Adams, R. D. (1969), Seismic effects at Mangla Dam, Pakistan, *Nature*, 222, 1153-
4781 1155.

4782 Adushkin, V. V., V. Rodionov, N. S. Turuntaev, and A. E. Yudin (2000), Seismicity
4783 in the oil field.

- 4784 Adushkin, V. V., and A. Spivak (2015), Underground explosions, DTIC Document.
- 4785 Ake, J., K. Mahrer, D. O'Connell, and L. Block (2005), Deep-injection and closely
4786 monitored induced seismicity at Paradox Valley, Colorado, *Bulletin of the Seismological*
4787 *Society of America*, 95, 664-683.
- 4788 Albaric, J., V. Oye, N. Langet, M. Hasting, I. Lecomte, K. Iranpour, M. Messeiller,
4789 and P. Reid (2014), Monitoring of induced seismicity during the first geothermal
4790 reservoir stimulation at Paralana, Australia, *Geothermics*, 52, 120-131.
- 4791 Alcott, J. M., P. K. Kaiser, and B. P. Simser (1998), Use of microseismic source
4792 parameters for rockburst hazard assessment, in *Seismicity caused by mines, fluid*
4793 *injections, reservoirs, and oil extraction*, pp. 41-65, Springer.
- 4794 Al-Enezi, A., L. Petrat, R. Abdel-Fattah, and G. D. M. Technologie (2008), Induced
4795 seismicity and surface deformation within Kuwait's oil fields, paper presented at Proc.
4796 Int. Conf. Geol. Seismol.
- 4797 Allis, R. G., S. A. Currie, J. D. Leaver, and S. Sherburn (1985), Results of injection
4798 testing at Wairakei geothermal field, New Zealand, *Trans. GRC*, 289-294.
- 4799 Alvarez-Garcia, I. N., F. L. Ramos-Lopez, C. Gonzalez-Nicieza, M. I. Alvarez-
4800 Fernandez, and A. E. Alvarez-Vigil (2013), The mine collapse at Lo Tacón (Murcia,
4801 Spain), possible cause of the Torre Pacheco earthquake (2nd May 1998, se Spain),
4802 *Engineering Failure Analysis*, 28, 115-133.
- 4803 Amidzic, D., S. K. Murphy, and G. Van Aswegen (1999), Case study of a large
4804 seismic event at a South African gold mine, paper presented at 9th ISRM Congress,
4805 International Society for Rock Mechanics.
- 4806 Amos, C. B., P. Audet, W. C. Hammond, R. Bürgmann, I. A. Johanson, and G.
4807 Blewitt (2014), Uplift and seismicity driven by groundwater depletion in central
4808 California, *Nature*, 509, 483-486.
- 4809 Arabasz, W. J., J. Ake, M. K. McCarter, and A. McGarr (2002), Mining-induced
4810 seismicity near Joes Valley dam: Summary of ground-motion studies and assessment of
4811 probable maximum magnitude, Technical Report, University of Utah Seismograph
4812 Stations, Salt Lake City, Utah, 35 pp. Accessible online at www/seis.utah.edu/Reports/sitla2002b.
- 4814 Arabasz, W. J., S. J. Nava, M. K. McCarter, K. L. Pankow, J. C. Pechmann, J. Ake,
4815 and A. McGarr (2005), Coal-mining seismicity and ground-shaking hazard: A case study
4816 in the Trail Mountain area, Emery County, Utah, *Bulletin of the Seismological Society of*
4817 *America*, 95, 18-30.
- 4818 Arkhipova, E. V., A. D. Zhigalin, L. I. Morozova, and A. V. Nikolaev (2012), The
4819 Van earthquake on October 23, 2011: Natural and technogenic causes, paper presented at
4820 *Doklady Earth Sciences*, Springer.

- 4821 Armbruster, J. G., D. W. Steeples, and L. Seeber (1989), The 1989 earthquake
4822 sequence near Palco, Kansas: A possible example of induced seismicity (abstract),
4823 *Seismological Research Letters*, 60, 141.
- 4824 Asanuma, H., N. Soma, H. Kaieda, Y. Kumano, T. Izumi, K. Tezuka, H. Niitsuma,
4825 and D. Wyborn (2005), Microseismic monitoring of hydraulic stimulation at the
4826 Australian HDR project in Cooper Basin, paper presented at Proceedings World
4827 Geothermal Congress.
- 4828 Assumpção, M., V. Marza, L. Barros, C. Chimpliganond, J. E. Soares, J. Carvalho, D.
4829 Caixeta, A. Amorim, and E. Cabral (2002), Reservoir-induced seismicity in Brazil, in *The*
4830 *mechanism of induced seismicity*, pp. 597-617, Springer.
- 4831 Assumpção, M., T. H. Yamabe, J. R. Barbosa, V. Hamza, A. E. V. Lopes, L.
4832 Balancin, and M. B. Bianchi (2010), Seismic activity triggered by water wells in the
4833 Paraná Basin, Brazil, *Water Resources Research*, 46.
- 4834 Avouac, J.-P. (2012), Earthquakes: Human-induced shaking, *Nature Geoscience*, 5,
4835 763-764.
- 4836 Awad, M., and M. Mizoue (1995), Earthquake activity in the Aswan region, Egypt, in
4837 *Induced seismicity*, pp. 69-86, Springer.
- 4838 Baecher, G. B., and R. L. Keeney (1982), Statistical examination of reservoir-induced
4839 seismicity, *Bulletin of the Seismological Society of America*, 72, 553-569.
- 4840 Baisch, S., E. Rothert, H. Stang, R. Vörös, C. Koch, and A. McMahon (2015),
4841 Continued geothermal reservoir stimulation experiments in the Cooper Basin (Australia),
4842 *Bulletin of the Seismological Society of America*.
- 4843 Baisch, S., and R. Vörös (2011), Geomechanical study of Blackpool seismicity.
- 4844 Baisch, S., R. Vörös, R. Weidler, and D. Wyborn (2009), Investigation of fault
4845 mechanisms during geothermal reservoir stimulation experiments in the Cooper Basin,
4846 Australia, *Bulletin of the Seismological Society of America*, 99, 148-158.
- 4847 Baisch, S., R. Weidler, R. Vörös, D. Wyborn, and L. de Graaf (2006), Induced
4848 seismicity during the stimulation of a geothermal HFR reservoir in the Cooper Basin,
4849 Australia, *Bulletin of the Seismological Society of America*, 96, 2242-2256.
- 4850 Baker, K., D. Hollett, and A. Coy (2014, February), Geothermal technologies office
4851 2013 peer review report.
- 4852 Balassanian, S. Y. (2005), Earthquakes induced by deep penetrating bombing?, *Acta*
4853 *Seismologica Sinica*, 18, 741-745.
- 4854 Balfour, N., E. Borleis, C. Bugden, V. Dent, D. H. Glanville, D. Hardy, D. Love, M.
4855 Salmon, M. Sambridge, and A. Wallace (2014), Australian seismological report 2013.
- 4856 Bardainne, T., N. Dubos-Sallée, G. Sénéchal, P. Gaillot, and H. Perroud (2008),
4857 Analysis of the induced seismicity of the Lacq gas field (southwestern France) and model
4858 of deformation, *Geophysical Journal International*, 172, 1151-1162.

- 4859 Bardainne, T., P. Gaillot, N. Dubos-Sallée, J. Blanco, and G. Sénéchal (2006),
4860 Characterization of seismic waveforms and classification of seismic events using chirplet
4861 atomic decomposition. Example from the Lacq gas field (western Pyrenees, France),
4862 *Geophysical Journal International*, 166, 699-718.
- 4863 Basham, P. W. (1969), Canadian magnitudes of earthquakes and nuclear explosions in
4864 south-western North America, *Geophysical Journal International*, 17, 1-13.
- 4865 Bella, F., P. F. Biagi, M. Caputo, E. Cozzi, G. Della Monica, A. Ermini, W. Plastino,
4866 and V. Sgrigna (1998), Aquifer-induced seismicity in the central Apennines (Italy), *Pure*
4867 *and applied geophysics*, 153, 179-194.
- 4868 Bennett, T. J., M. E. Marshall, K. L. McLaughlin, B. W. Barker, and J. R. Murphy
4869 (1995), *Seismic characteristics and mechanisms of rockbursts*, DTIC Document.
- 4870 Bennett, T. J., K. L. McLaughlin, M. E. Marshall, B. W. Barker, and J. R. Murphy
4871 (1995), *Investigations of the seismic characteristics of rockbursts*, DTIC Document.
- 4872 Benz, H. M., N. D. McMahon, R. C. Aster, D. E. McNamara, and D. B. Harris
4873 (2015), Hundreds of earthquakes per day: The 2014 Guthrie, Oklahoma, earthquake
4874 sequence, *Seismological Research Letters*, 86, 1318-1325.
- 4875 Bertani, R. (2012), *Geothermal power generation in the world 2005–2010 update*
4876 *report*, *Geothermics*, 41, 1-29.
- 4877 Bertini, G., M. Casini, G. Gianelli, and E. Pandeli (2006), Geological structure of a
4878 long-living geothermal system, Larderello, Italy, *Terra Nova*, 18, 163-169.
- 4879 Białoń, W., E. Zarzycka, and S. Lasocki (2015), Seismicity of Czorsztyn Lake region:
4880 A case of reservoir triggered seismic process?, *Acta Geophysica*, 63, 1080-1089.
- 4881 Bischoff, M., A. Cete, R. Fritschen, and T. Meier (2010), Coal mining induced
4882 seismicity in the Ruhr area, Germany, *Pure and applied geophysics*, 167, 63-75.
- 4883 Bommer, J. J., S. Oates, J. M. Cepeda, C. Lindholm, J. Bird, R. Torres, G. Marroquín,
4884 and J. Rivas (2006), Control of hazard due to seismicity induced by a hot fractured rock
4885 geothermal project, *Engineering Geology*, 83, 287-306.
- 4886 Boucher, G., A. Ryall, and A. E. Jones (1969), Earthquakes associated with
4887 underground nuclear explosions, *Journal of Geophysical Research*, 74, 3808-3820.
- 4888 Bou-Rabee, F. (1994), Earthquake recurrence in Kuwait induced by oil and gas
4889 extraction, *Journal of Petroleum Geology*, 17, 473-480.
- 4890 Bou-Rabee, F., and A. Nur (2002), The 1993 M4.7 Kuwait earthquake: Induced by
4891 the burning of the oil fields, *Kuwait J. Sci. Eng.*, 29, 155-163.
- 4892 Bourne, S. J., and S. J. Oates (2014), An activity rate model of induced seismicity
4893 within the Groningen field.

- 4894 Bowers, D. (1997), The October 30, 1994, seismic disturbance in South Africa:
4895 Earthquake or large rock burst?, *Journal of Geophysical Research: Solid Earth*, 102,
4896 9843-9857.
- 4897 Breede, K., K. Dzebisashvili, X. Liu, and G. Falcone (2013), A systematic review of
4898 enhanced (or engineered) geothermal systems: Past, present and future, *Geothermal*
4899 *Energy*, 1, 1-27.
- 4900 British Columbia Oil and Gas Commission (BCOGC) (2012), Investigation of
4901 observed seismicity in the Horn River Basin.
- 4902 British Columbia Oil and Gas Commission (BCOGC) (2014), Investigation of
4903 observed seismicity in the Montney trend.
- 4904 Brodsky, E. E., and L. J. Lajoie (2013), Anthropogenic seismicity rates and
4905 operational parameters at the Salton Sea geothermal field, *Science*, 341, 543-546.
- 4906 Bromley, C. J., C. F. Pearson, and D. M. Rigor (1987), Microearthquakes at the
4907 Puhagan geothermal field, Philippines—a case of induced seismicity, *Journal of*
4908 *volcanology and geothermal research*, 31, 293-311.
- 4909 Brune, J. N., and P. W. Pomeroy (1963), Surface wave radiation patterns for
4910 underground nuclear explosions and small-magnitude earthquakes, *Journal of*
4911 *Geophysical Research*, 68, 5005-5028.
- 4912 Bukchin, B. G., A. Z. Mostinsky, A. A. Egorkin, A. L. Levshin, and M. H. Ritzwoller
4913 (2001), Isotropic and nonisotropic components of earthquakes and nuclear explosions on
4914 the Lop Nor test site, China, in *Monitoring the comprehensive nuclear-test-ban treaty:*
4915 *Surface waves*, pp. 1497-1515, Springer.
- 4916 Calò, M., C. Dorbath, and M. Frogneux (2014), Injection tests at the EGS reservoir of
4917 Soultz-Sous-Forêts. Seismic response of the GPK4 stimulations, *Geothermics*, 52, 50-58.
- 4918 Caloi, P., M. De Panfilis, D. Di Filippo, L. Marcelli, and M. C. Spadea (1956),
4919 *Terremoti della Val Padana del 15-16 Maggio 1951*, *Annals of Geophysics*, 9, 63-105.
- 4920 Carder, D. S. (1945), Seismic investigations in the Boulder dam area, 1940-1944, and
4921 the influence of reservoir loading on local earthquake activity, *Bulletin of the*
4922 *Seismological Society of America*, 35, 175-192.
- 4923 Carpenter, P. J., and I. W. El-Hussain, Reservoir induced seismicity near Heron and
4924 El Vado reservoirs, northern New Mexico, and implications for fluid injection within the
4925 San Juan Basin, paper presented at AAPG Annual Convention and Exhibition.
- 4926 Cesca, S., F. Grigoli, S. Heimann, Á. González, E. Buforn, S. Maghsoudi, E. Blanch,
4927 and T. Dahm (2014), The 2013 September–October seismic sequence offshore Spain: A
4928 case of seismicity triggered by gas injection?, *Geophysical Journal International*, 198,
4929 941-953.
- 4930 Chadha, R. K. (1995), Role of dykes in induced seismicity at Bhatsa reservoir,
4931 Maharashtra, India, in *Induced seismicity*, pp. 155-165, Springer.

- 4932 Chen, L., and P. Talwani (1998), Reservoir-induced seismicity in China, *Pure and*
4933 *applied geophysics*, 153, 133-149.
- 4934 Chouhan, R. K. S. (1986), Induced seismicity of Indian coal mines, *Physics of the*
4935 *earth and planetary interiors*, 44, 82-86.
- 4936 Chouhan, R. K. S. (1992), Combating the rockburst problem - a seismological
4937 approach, in *Induced seismicity*, edited by P. Knoll, Balkema, Rotterdam.
- 4938 Číž, R., and B. Růžek (1997), Periodicity of mining and induced seismicity in the
4939 Mayrau mine, Czech Republic, *Studia Geophysica et Geodaetica*, 41, 29-44.
- 4940 Cladouhos, T. T., S. Petty, Y. Nordin, M. Moore, K. Grasso, M. Uddenberg, M.
4941 Swyer, B. Julian, and G. Foulger (2013), Microseismic monitoring of Newberry volcano
4942 EGS demonstration, paper presented at Proceedings of the 38th Workshop on Geothermal
4943 Reservoir Engineering, Stanford, CA.
- 4944 Clark, D. (2009), Potential geologic sources of seismic hazard in the Sydney Basin,
4945 Proceedings volume of a one day workshop. *Geoscience Australia Record* 2009/11.
4946 115pp.
- 4947 Clarke, H., L. Eisner, P. Styles, and P. Turner (2014), Felt seismicity associated with
4948 shale gas hydraulic fracturing: The first documented example in Europe, *Geophysical*
4949 *Research Letters*, 41, 8308-8314.
- 4950 Dahm, T., S. Cesca, S. Hainzl, T. Braun, and F. Krüger (2015), Discrimination
4951 between induced, triggered, and natural earthquakes close to hydrocarbon reservoirs: A
4952 probabilistic approach based on the modeling of depletion-induced stress changes and
4953 seismological source parameters, *Journal of Geophysical Research: Solid Earth*, 120,
4954 2491-2509.
- 4955 Dahm, T., F. Krüger, K. Stammler, K. Klinge, R. Kind, K. Wylegalla, and J.-R.
4956 Grasso (2007), The 2004 Mw 4.4 Rotenburg, northern Germany, earthquake and its
4957 possible relationship with gas recovery, *Bulletin of the Seismological Society of America*,
4958 97, 691-704.
- 4959 Darold, A., A. A. Holland, C. Chen, and A. Youngblood (2014), Preliminary analysis
4960 of seismicity near Eagleton 1--29, Carter County, July 2014.
- 4961 Davies, R., G. Foulger, A. Bindley, and P. Styles (2013), Induced seismicity and
4962 hydraulic fracturing for the recovery of hydrocarbons, *Marine and Petroleum Geology*,
4963 45, 171-185.
- 4964 Davis, S. D., and C. Frohlich (1993), Did (or will) fluid injection cause earthquakes?-
4965 criteria for a rational assessment, *Seismological Research Letters*, 64, 207-224.
- 4966 Davis, S. D., P. A. Nyffenegger, and C. Frohlich (1995), The 9 April 1993 earthquake
4967 in south-central Texas: Was it induced by fluid withdrawal?, *Bulletin of the*
4968 *Seismological Society of America*, 85, 1888-1895.

- 4969 Davis, S. D., and W. D. Pennington (1989), Induced seismic deformation in the
4970 Cogdell oil field of west Texas, *Bulletin of the Seismological Society of America*, 79,
4971 1477-1495.
- 4972 De Pater, C. J., and S. Baisch (2011), Geomechanical study of Bowland Shale
4973 seismicity, Synthesis Report, 57.
- 4974 Deichmann, N., and J. Ernst (2009), Earthquake focal mechanisms of the induced
4975 seismicity in 2006 and 2007 below Basel (Switzerland), *Swiss Journal of Geosciences*,
4976 102, 457-466.
- 4977 Diaz, A. R., E. Kaya, and S. J. Zarrouk (2016), Reinjection in geothermal fields– a
4978 worldwide review update, *Renewable and Sustainable Energy Reviews*, 53, 105-162.
- 4979 Doblas, M., N. Youbi, J. De Las Doblas, and A. J. Galindo (2014), The 2012/2014
4980 swarmquakes of Jaen, Spain: A working hypothesis involving hydroseismicity associated
4981 with the hydrologic cycle and anthropogenic activity, *Natural hazards*, 74, 1223-1261.
- 4982 Doornenbal, H., and A. Stevenson (2010), Petroleum geological atlas of the southern
4983 Permian Basin area, EAGE.
- 4984 Doser, D. I., M. R. Baker, M. Luo, P. Marroquin, L. Ballesteros, J. Kingwell, H. L.
4985 Diaz, and G. Kaip (1992), The not so simple relationship between seismicity and oil
4986 production in the Permian Basin, west Texas, *Pure and applied geophysics*, 139, 481-506.
- 4987 Dost, B., and J. Spetzler (2015), Probabilistic seismic hazard analysis for induced
4988 earthquakes in Groningen; update 2015.
- 4989 Downing, J. A., Y. T. Prairie, J. J. Cole, C. M. Duarte, L. J. Tranvik, R. G. Striegl, W.
4990 H. McDowell, P. Kortelainen, N. F. Caraco, and J. M. Melack (2006), The global
4991 abundance and size distribution of lakes, ponds, and impoundments, *Limnology and
4992 Oceanography*, 51, 2388-2397.
- 4993 Dreger, D. S., S. R. Ford, and W. R. Walter (2008), Source analysis of the Crandall
4994 Canyon, Utah, mine collapse, *Science*, 321, 217-217.
- 4995 Durrheim, R. J. (2010), Mitigating the risk of rockbursts in the deep hard rock mines
4996 of South Africa: 100 years of research, in *Extracting the science: A century of mining
4997 research*, Brune, J. (eds), Society for Mining, Metallurgy, and Exploration, Inc, pp. 156-
4998 171.
- 4999 Durrheim, R. J., R. L. Anderson, A. Cichowicz, R. Ebrahim-Trollope, G. Hubert, A.
5000 Kijko, A. McGarr, W. Ortlepp, and N. van der Merwe (2006), The risks to miners, mines,
5001 and the public posed by large seismic events in the gold mining districts of South Africa,
5002 paper presented at Proceedings of the Third International Seminar on Deep and High
5003 Stress Mining, 2-4 October 2006, Quebec City, Canada.
- 5004 Durrheim, R. J., R. L. Anderson, A. Cichowicz, R. Ebrahim-Trollope, G. Hubert, A.
5005 Kijko, A. McGarr, W. D. Ortlepp, and N. van der Merwe (2006), Investigation into the
5006 risks to miners, mines, and the public associated with large seismic events in gold mining
5007 districts, Department of Minerals and Energy.

- 5008 Eagar, K. C., G. L. Pavlis, and M. W. Hamburger (2006), Evidence of possible
5009 induced seismicity in the Wabash Valley seismic zone from improved microearthquake
5010 locations, *Bulletin of the Seismological Society of America*, 96, 1718-1728.
- 5011 El-Hussain, I. W., and P. J. Carpenter (1990), Reservoir induced seismicity near
5012 Heron and El Vado reservoirs, northern New Mexico, *Bulletin of the Association of*
5013 *Engineering Geologists*, 27, 51-59.
- 5014 Ellsworth, W. L. (2013), Injection-induced earthquakes, *Science*, 341, 1225942.
- 5015 Emanov, A. F., A. A. Emanov, A. V. Fateev, E. V. Leskova, E. V. Shevkunova, and
5016 V. G. Podkorytova (2014), Mining-induced seismicity at open pit mines in Kuzbass
5017 (Bachatsky earthquake on June 18, 2013), *Journal of Mining Science*, 50, 224-228.
- 5018 Engdahl, E. R. (1972), Seismic effects of the Milrow and Cannikin nuclear
5019 explosions, *Bulletin of the Seismological Society of America*, 62, 1411-1423.
- 5020 Eremenko, V. A., A. A. Eremenko, S. V. Rasheva, and S. B. Turuntaev (2009),
5021 Blasting and the man-made seismicity in the Tashtagol mining area, *Journal of mining*
5022 *science*, 45, 468-474.
- 5023 Evans, K. F., A. Zappone, T. Kraft, N. Deichmann, and F. Moia (2012), A survey of
5024 the induced seismic responses to fluid injection in geothermal and CO₂ reservoirs in
5025 Europe, *Geothermics*, 41, 30-54.
- 5026 Fabriol, H., and A. Beauce (1997), Temporal and spatial distribution of local
5027 seismicity in the Chipilapa-Ahuachapán geothermal area, El Salvador, *Geothermics*, 26,
5028 681-699.
- 5029 Fajkiewicz, Z., and K. Jakiel (1989), Induced gravity anomalies and seismic energy as
5030 a basis for prediction of mining tremors, in *Seismicity in mines*, pp. 535-552, Springer.
- 5031 Farahbod, A. M., H. Kao, D. M. Walker, J. F. Cassidy, and A. Calvert (2015),
5032 Investigation of regional seismicity before and after hydraulic fracturing in the Horn
5033 River Basin, northeast British Columbia, *Canadian Journal of Earth Sciences*, 52, 112-
5034 122.
- 5035 Feng, Q., and J. M. Lees (1998), Microseismicity, stress, and fracture in the Coso
5036 geothermal field, California, *Tectonophysics*, 289, 221-238.
- 5037 Ferguson, G. (2015), Deep injection of waste water in the Western Canada
5038 Sedimentary Basin, *Groundwater*, 53, 187-194.
- 5039 Ferreira, J. M., G. S. França, C. S. Vilar, A. F. do Nascimento, F. H. R. Bezerra, and
5040 M. Assumpção (2008), Induced seismicity in the Castanhão reservoir, ne Brazil—
5041 preliminary results, *Tectonophysics*, 456, 103-110.
- 5042 Fletcher, J. B., and L. R. Sykes (1977), Earthquakes related to hydraulic mining and
5043 natural seismic activity in western New York state, *Journal of Geophysical Research*, 82,
5044 3767-3780.

- 5045 Folger, P. F., and M. Tiemann (2014), Human-induced earthquakes from deep-well
5046 injection: A brief overview, Congressional Research Service.
- 5047 Ford, S. R., D. S. Dreger, and W. R. Walter (2008), Source characterization of the 6
5048 August 2007 Crandall Canyon mine seismic event in central Utah, *Seismological*
5049 *Research Letters*, 79, 637-644.
- 5050 Friberg, P. A., G. M. Besana-Ostman, and I. Dricker (2014), Characterization of an
5051 earthquake sequence triggered by hydraulic fracturing in Harrison County, Ohio,
5052 *Seismological Research Letters*.
- 5053 Fritschen, R. (2010), Mining-induced seismicity in the Saarland, Germany, *Pure and*
5054 *applied geophysics*, 167, 77-89.
- 5055 Frohlich, C. (2012), Two-year survey comparing earthquake activity and injection-
5056 well locations in the Barnett Shale, Texas, *Proceedings of the National Academy of*
5057 *Sciences*, 109, 13934-13938.
- 5058 Frohlich, C., and M. Brunt (2013), Two-year survey of earthquakes and
5059 injection/production wells in the Eagle Ford Shale, Texas, prior to the Mw4.8 20 October
5060 2011 earthquake, *Earth and Planetary Science Letters*, 379, 56-63.
- 5061 Frohlich, C., and S. D. Davis (2002), *Texas earthquakes*, University of Texas Press.
- 5062 Frohlich, C., W. Ellsworth, W. A. Brown, M. Brunt, J. Luetgert, T. MacDonald, and
5063 S. Walter (2014), The 17 May 2012 M4.8 earthquake near Timpson, east Texas: An event
5064 possibly triggered by fluid injection, *Journal of Geophysical Research: Solid Earth*, 119,
5065 581-593.
- 5066 Frohlich, C., J. Glidewell, and M. Brunt (2012), Location and felt reports for the 25
5067 April 2010 mbLg 3.9 earthquake near Alice, Texas: Was it induced by petroleum
5068 production?, *Bulletin of the Seismological Society of America*, 102, 457-466.
- 5069 Frohlich, C., C. Hayward, B. Stump, and E. Potter (2011), The Dallas–Fort Worth
5070 earthquake sequence: October 2008 through May 2009, *Bulletin of the Seismological*
5071 *Society of America*, 101, 327-340.
- 5072 Frohlich, C., and E. Potter (2013), What further research could teach us about “close
5073 encounters of the third kind”: Intraplate earthquakes associated with fluid injection.
- 5074 Frohlich, C., J. I. Walter, and J. F. W. Gale (2015), Analysis of transportable array
5075 (USarray) data shows earthquakes are scarce near injection wells in the Williston Basin,
5076 2008–2011, *Seismological Research Letters*.
- 5077 Gahalaut, K., V. K. Gahalaut, and M. R. Pandey (2007), A new case of reservoir
5078 triggered seismicity: Govind Ballav Pant reservoir (Rihand dam), central India,
5079 *Tectonophysics*, 439, 171-178.
- 5080 Gaité, B., A. Ugalde, A. Villaseñor, and E. Blanch (2016), Improving the location of
5081 induced earthquakes associated with an underground gas storage in the Gulf of Valencia
5082 (Spain), *Physics of the Earth and Planetary Interiors*, 254, 46-59.

- 5083 Galybin, A. N., S. S. Grigoryan, and S. A. Mukhamediev (1998), Model of induced
5084 seismicity caused by water injection, paper presented at SPE/ISRM Rock Mechanics in
5085 Petroleum Engineering, Society of Petroleum Engineers.
- 5086 Gan, W., and C. Frohlich (2013), Gas injection may have triggered earthquakes in the
5087 Cogdell oil field, Texas, *Proceedings of the National Academy of Sciences*, 110, 18786-
5088 18791.
- 5089 Gasparini, P., P. Styles, S. Lasocki, P. Scandone, E. Huenges, F. Terlizzese, and S.
5090 Esposito (2015), The ICHESE report on the relationship between hydrocarbon
5091 exploration and the May 2012 earthquakes in the Emilia region (Italy) and their
5092 consequences.
- 5093 Gaucher, E., M. Schoenball, O. Heidbach, A. Zang, P. A. Fokker, J.-D. van Wees, and
5094 T. Kohl (2015), Induced seismicity in geothermal reservoirs: A review of forecasting
5095 approaches, *Renewable and Sustainable Energy Reviews*, 52, 1473-1490.
- 5096 Ge, S., M. Liu, N. Lu, J. W. Godt, and G. Luo (2009), Did the Zippingpu reservoir
5097 trigger the 2008 Wenchuan earthquake?, *Geophysical Research Letters*, 36.
- 5098 Gendzwil, D. J., R. B. Horner, and H. S. Hasegawa (1982), Induced earthquakes at a
5099 potash mine near Saskatoon, Canada, *Canadian Journal of Earth Sciences*, 19, 466-475.
- 5100 Genmo, Z., C. Huaran, M. Shuqin, and Z. Deyuan (1995), Research on earthquakes
5101 induced by water injection in China, in *Induced seismicity*, pp. 59-68, Springer.
- 5102 German, V. I. (2014), Rock failure prediction in mines by seismic monitoring data,
5103 *Journal of Mining Science*, 50, 288-297.
- 5104 Gestermann, N., T. Plenefisch, U. Schwaderer, and M. Joswig (2015), Induced
5105 seismicity at the natural gas fields in northern Germany, in *Schatzalp Induced Seismicity*
5106 *Workshop*, 10-13 March 2015, Davos, Switzerland.
- 5107 Gibowicz, S. J. (1998), Partial stress drop and frictional overshoot mechanism of
5108 seismic events induced by mining, in *Seismicity caused by mines, fluid injections,*
5109 *reservoirs, and oil extraction*, pp. 5-20, Springer.
- 5110 Gibowicz, S. J., A. Bober, A. Cichowicz, Z. Droste, Z. Dychtowicz, J. Hordejuk, M.
5111 Kazimierczyk, and A. Kijko (1979), Source study of the Lubin, Poland, tremor of 24
5112 March 1977, *Acta Geophys. Pol*, 27, 3-38.
- 5113 Gibowicz, S. J., Z. Droste, B. Guterch, and J. Hordejuk (1981), The Belchatow,
5114 Poland, earthquakes of 1979 and 1980 induced by surface mining, *Engineering Geology*,
5115 17, 257-271.
- 5116 Gibowicz, S. J., R. P. Young, S. Talebi, and D. J. Rawlence (1991), Source
5117 parameters of seismic events at the Underground Research Laboratory in Manitoba,
5118 Canada: Scaling relations for events with moment magnitude smaller than -2, *Bulletin of*
5119 *the Seismological Society of America*, 81, 1157-1182.
- 5120 Gibson, G., and M. Sandiford (2013), *Seismicity and induced earthquakes*, Office of
5121 the New South Wales Chief Scientist and Engineer.

- 5122 Gilyarov, V. L., E. E. Damaskinskaya, A. G. Kadomtsev, and I. Y. Rasskazov (2014),
5123 Analysis of statistic parameters of geoacoustic monitoring data for the Antey Uranium
5124 Deposit, *Journal of Mining Science*, 50, 443-447.
- 5125 Glowacka, E., and F. A. Nava (1996), Major earthquakes in Mexicali valley, Mexico,
5126 and fluid extraction at Cerro Prieto geothermal field, *Bulletin of the Seismological*
5127 *Society of America*, 86, 93-105.
- 5128 Göbel, T. (2015), A comparison of seismicity rates and fluid-injection operations in
5129 Oklahoma and California: Implications for crustal stresses, *The Leading Edge*, 34, 640-
5130 648.
- 5131 Godano, M., E. Gaucher, T. Bardainne, M. Regnier, A. Deschamps, and M. Valette
5132 (2010), Assessment of focal mechanisms of microseismic events computed from two
5133 three-component receivers: Application to the Arkema-Vauvert field (France),
5134 *Geophysical prospecting*, 58, 775-790.
- 5135 Goebel, T. H. W., S. M. Hosseini, F. Cappa, E. Hauksson, J. P. Ampuero, F.
5136 Aminzadeh, and J. B. Saleeby (2016), Wastewater disposal and earthquake swarm
5137 activity at the southern end of the Central Valley, California, *Geophysical Research*
5138 *Letters*.
- 5139 Goldbach, O. D. (2009), Flooding-induced seismicity in mines, paper presented at
5140 11th SAGA Biennial Technical Meeting and Exhibition.
- 5141 Gomberg, J., and L. Wolf (1999), Possible cause for an improbable earthquake: The
5142 1997 Mw 4.9 southern Alabama earthquake and hydrocarbon recovery, *Geology*, 27, 367-
5143 370.
- 5144 González, P. J., K. F. Tiampo, M. Palano, F. Cannavó, and J. Fernández (2012), The
5145 2011 Lorca earthquake slip distribution controlled by groundwater crustal unloading,
5146 *Nature Geoscience*, 5, 821-825.
- 5147 Gough, D. I., and W. I. Gough (1970), Load-induced earthquakes at Lake Kariba—II,
5148 *Geophysical Journal International*, 21, 79-101.
- 5149 Grasso, J.-R. (1992), Mechanics of seismic instabilities induced by the recovery of
5150 hydrocarbons, *Pure and applied geophysics*, 139, 507-534.
- 5151 Green, C. A., P. Styles, and B. J. Baptie (2012), Preese Hall shale gas fracturing
5152 review & recommendations for induced seismic mitigation: UK department of energy and
5153 climate change.
- 5154 Groos, J., J. Zeiß, M. Grund, and J. Ritter (2013), Microseismicity at two geothermal
5155 power plants at Landau and Insheim in the Upper Rhine Graben, Germany, paper
5156 presented at EGU General Assembly Conference Abstracts.
- 5157 Ground Water Research & Education Foundation (GWREF) (2013), White paper II
5158 summarizing a special session on induced seismicity.

- 5159 Grünthal, G. (2014), Induced seismicity related to geothermal projects versus natural
5160 tectonic earthquakes and other types of induced seismic events in central Europe,
5161 *Geothermics*, 52, 22-35.
- 5162 Guglielmi, Y., F. Cappa, J.-P. Avouac, P. Henry, and D. Elsworth (2015), Seismicity
5163 triggered by fluid injection—induced aseismic slip, *Science*, 348, 1224-1226.
- 5164 Guha, S. K., and D. N. Patil (1990), Large water-reservoir-related induced seismicity,
5165 *Gerlands Beitr Geophys*, 99, 265-288.
- 5166 Gupta, H. K. (2002), A review of recent studies of triggered earthquakes by artificial
5167 water reservoirs with special emphasis on earthquakes in Koyna, India, *Earth-Science*
5168 *Reviews*, 58, 279-310.
- 5169 Gupta, H. K. (2011), Artificial water reservoir triggered earthquakes, *Encyclopedia of*
5170 *Solid Earth Geophysics*, 15-24.
- 5171 Hamilton, R. M., B. E. Smith, F. G. Fischer, and P. J. Papanek (1972), Earthquakes
5172 caused by underground nuclear explosions on Pahute Mesa, Nevada test site, *Bulletin of*
5173 *the Seismological Society of America*, 62, 1319-1341.
- 5174 Haney, F., J. Kummerow, C. Langenbruch, C. Dinske, S. A. Shapiro, and F.
5175 Scherbaum (2011), Magnitude estimation for microseismicity induced during the KTB
5176 2004/2005 injection experiment, *Geophysics*, 76, WC47-WC53.
- 5177 Hasegawa, H. S., R. J. Wetmiller, and D. J. Gendzwill (1989), Induced seismicity in
5178 mines in Canada—an overview, *Pure and applied geophysics*, 129, 423-453.
- 5179 Hauksson, E., T. Göbel, J.-P. Ampuero, and E. Cochran (2015), A century of oil-field
5180 operations and earthquakes in the Greater Los Angeles Basin, southern California, *The*
5181 *Leading Edge*, 34, 650-656.
- 5182 Heck, N. H., and R. R. Bodle (1931), United States earthquakes 1929, US Coast and
5183 Geodetic Survey, Serial.
- 5184 Hedley, D. G. F., and J. E. Udd (1989), The Canada-Ontario-industry rockburst
5185 project, in *Seismicity in mines*, pp. 661-672, Springer.
- 5186 Heesakkers, V., S. K. Murphy, G. van Aswegen, R. Domoney, S. Addams, T.
5187 Dewers, M. Zechmeister, and Z. Reches (2005), The rupture zone of the M= 2.2
5188 earthquake that reactivated the ancient Pretorius fault in Tautona mine, South Africa,
5189 paper presented at AGU Fall Meeting Abstracts.
- 5190 Heick, C., and D. Flach (1989), Microseismicity in a flooded potash mine, the Hope
5191 mine, Federal Republic of Germany, in *Seismicity in mines*, pp. 475-496, Springer.
- 5192 Herrmann, R. B. (1978), A seismological study of two Attica, New York earthquakes,
5193 *Bulletin of the Seismological Society of America*, 68, 641-651.
- 5194 Hill, D. P., P. A. Reasenber, A. Michael, W. J. Arabaz, G. Beroza, D. Brumbaugh, J.
5195 N. Brune, R. Castro, S. Davis, and W. L. Ellsworth (1993), Seismicity remotely triggered
5196 by the magnitude 7.3 Landers, California, earthquake, *Science*, 260, 1617-1623.

- 5197 Holland, A. (2011), Examination of possibly induced seismicity from hydraulic
5198 fracturing in the Eola field, Garvin County, Oklahoma.
- 5199 Holland, A. A. (2013), Earthquakes triggered by hydraulic fracturing in south-central
5200 Oklahoma, *Bulletin of the Seismological Society of America*, 103, 1784-1792.
- 5201 Holmgren, J. (2015), Induced seismicity in the Dannemora mine, Sweden, Uppsala
5202 Universitet.
- 5203 Holschneider, M., G. Zöller, and S. Hainzl (2011), Estimation of the maximum
5204 possible magnitude in the framework of a doubly truncated Gutenberg–Richter model,
5205 *Bulletin of the Seismological Society of America*, 101, 1649-1659.
- 5206 Holub, K., J. Holečko, J. Rušajová, and A. Dombkova (2012), Long-term
5207 development of seismic monitoring networks in the Ostrava-Karviná coal mine district,
5208 *Acta Geodynamica et Geomaterialia*, 9, 115-132.
- 5209 Hong, T. K., C. E. Baag, H. Choi, and D. H. Sheen (2008), Regional seismic
5210 observations of the 9 October 2006 underground nuclear explosion in North Korea and
5211 the influence of crustal structure on regional phases, *Journal of Geophysical Research:*
5212 *Solid Earth*, 113.
- 5213 Hornbach, M. J., H. R. DeShon, W. L. Ellsworth, B. W. Stump, C. Hayward, C.
5214 Frohlich, H. R. Oldham, J. E. Olson, M. B. Magnani, and C. Brokaw (2015), Causal
5215 factors for seismicity near Azle, Texas, *Nature communications*, 6.
- 5216 Horner, R. B., J. E. Barclay, and J. M. MacRae (1994), Earthquakes and hydrocarbon
5217 production in the Fort St. John area of northeastern British Columbia, *Canadian Journal*
5218 *of Exploration Geophysics*, 30, 39-50.
- 5219 Horton, S. (2012), Disposal of hydrofracking waste fluid by injection into subsurface
5220 aquifers triggers earthquake swarm in central Arkansas with potential for damaging
5221 earthquake, *Seismological Research Letters*, 83, 250-260.
- 5222 Hough, S. E., and M. Page (2015), A century of induced earthquakes in Oklahoma?,
5223 *Bulletin of the Seismological Society of America*, 105, 2863-2870.
- 5224 Hsieh, P. A., and J. D. Bredehoeft (1981), A reservoir analysis of the Denver
5225 earthquakes: A case of induced seismicity, *Journal of Geophysical Research: Solid Earth*,
5226 86, 903-920.
- 5227 Hsiung, S. M., W. Blake, A. H. Chowdhury, and T. J. Williams (1992), Effects of
5228 mining-induced seismic events on a deep underground mine, *Pure and applied*
5229 *geophysics*, 139, 741-762.
- 5230 Hua, W., Z. Chen, S. Zheng, and C. Yan (2013), Reservoir-induced seismicity in the
5231 Longtan reservoir, southwestern China, *Journal of seismology*, 17, 667-681.
- 5232 Hua, W., H. Fu, Z. Chen, S. Zheng, and C. Yan (2015), Reservoir-induced seismicity
5233 in high seismicity region—a case study of the Xiaowan reservoir in Yunnan province,
5234 China, *Journal of Seismology*, 19, 567-584.

- 5235 Hua, W., S. Zheng, C. Yan, and Z. Chen (2013), Attenuation, site effects, and source
5236 parameters in the Three Gorges reservoir area, China, *Bulletin of the Seismological*
5237 *Society of America*, 103, 371-382.
- 5238 Huaman, R. N. E., and T. X. Jun (2014), Energy related CO₂ emissions and the
5239 progress on CCS projects: A review, *Renewable and Sustainable Energy Reviews*, 31,
5240 368-385.
- 5241 Husen, S., E. Kissling, and A. von Deschanden (2012), Induced seismicity during
5242 the construction of the Gotthard Base Tunnel, Switzerland: Hypocenter locations and
5243 source dimensions, *Journal of seismology*, 16, 195-213.
- 5244 Iannacchione, A. T., and J. C. Zelanko (1995), Occurrence and remediation of coal
5245 mine bumps: A historical review, Paper in Proceedings: Mechanics and Mitigation of
5246 Violent Failure in Coal and Hard-Rock Mines. US Bureau of Mines Spec. Publ, 01-95.
- 5247 Improta, L., L. Valoroso, D. Piccinini, C. Chiarabba, and M. Buttinelli (2015), A
5248 detailed analysis of initial seismicity induced by wastewater injection in the Val d'Agri
5249 oil field (Italy), in Schatzalp Induced Seismicity Workshop, 10-13 March 2015, Davos,
5250 Switzerland.
- 5251 Jaku, E. P., A. Z. Toper, and A. J. Jager (2001), Updating and maintaining the
5252 accident database, Safety in Mines Research Advisory Committee.
- 5253 Jiménez, A., K. F. Tiampo, A. M. Posadas, F. Luzón, and R. Donner (2009), Analysis
5254 of complex networks associated to seismic clusters near the Itoiz reservoir dam, *The*
5255 *European Physical Journal Special Topics*, 174, 181-195.
- 5256 Julià, J., A. A. Nyblade, R. Durrheim, L. Linzer, R. Gök, P. Dirks, and W. Walter
5257 (2009), Source mechanisms of mine-related seismicity, Savuka mine, South Africa,
5258 *Bulletin of the Seismological Society of America*, 99, 2801-2814.
- 5259 Julian, B. R., G. R. Foulger, and F. C. Monastero (2009), Seismic monitoring of EGS
5260 stimulation tests at the Coso geothermal field, California, using microearthquake
5261 locations and moment tensors, paper presented at Thirty-Fourth Workshop on Geothermal
5262 Reservoir Engineering, Stanford University, Stanford, California, February.
- 5263 Julian, B. R., A. Ross, G. R. Foulger, and J. R. Evans (1996), Three-dimensional
5264 seismic image of a geothermal reservoir: The Geysers, California, *Geophysical Research*
5265 *Letters*, 23, 685-688.
- 5266 Jupe, A. J., A. S. P. Green, and T. Wallroth (1992), Induced microseismicity and
5267 reservoir growth at the Fjällbacka hot dry rocks project, Sweden, *International journal of*
5268 *rock mechanics and mining sciences & geomechanics abstracts*, 29, 343-354.
- 5269 Justinic, A. H., B. Stump, C. Hayward, and C. Frohlich (2013), Analysis of the
5270 Cleburne, Texas, earthquake sequence from June 2009 to June 2010, *Bulletin of the*
5271 *Seismological Society of America*, 103, 3083-3093.
- 5272 Kaieda, H., H. Ito, K. Kiho, K. Suzuki, H. Suenaga, and K. Shin (2005), Review of
5273 the Ogachi HDR project in Japan, paper presented at World Geothermal Congress.

- 5274 Kaieda, H., S. Sasaki, and D. Wyborn (2010), Comparison of characteristics of micro-
5275 earthquakes observed during hydraulic stimulation operations in Ogachi, Hijiori and
5276 Cooper Basin HDR projects, paper presented at World Geothermal Congress.
- 5277 Kalkan, E. (2016), An automatic P-phase arrival-time picker, *Bulletin of the*
5278 *Seismological Society of America*.
- 5279 Kalkan, E., C. Gurbuz, and E. Zor (2014), The usage of correlation method for micro-
5280 earthquake analysis at Salavatli geothermal area, Aydin, Turkey, paper presented at AGU
5281 Fall Meeting Abstracts.
- 5282 Kaneko, K., K. Sugawara, and Y. Obara (1989), Microseismic monitoring for coal
5283 burst prediction in the Miike coal mine, *Gerlands Beitrage zur Geophysik*, 98, 447-460.
- 5284 Kangi, A., and N. Heidari (2008), Reservoir-induced seismicity in Karun III dam
5285 (southwestern Iran), *Journal of Seismology*, 12, 519-527.
- 5286 Kao, H., A. M. Farahbod, J. F. Cassidy, M. Lamontagne, D. Snyder, and D. Lavoie
5287 (2015), Natural resources Canada's induced seismicity research, in *Schatzalp Induced*
5288 *Seismicity Workshop*, 10-13 March 2015, Davos, Switzerland.
- 5289 Kaven, J. O., S. H. Hickman, A. F. McGarr, and W. L. Ellsworth (2015), Surface
5290 monitoring of microseismicity at the Decatur, Illinois, CO₂ sequestration demonstration
5291 site, *Seismological Research Letters*, 86, 1096-1101.
- 5292 Keck, R. G., and R. J. Withers (1994), A field demonstration of hydraulic fracturing
5293 for solids waste injection with real-time passive seismic monitoring, paper presented at
5294 SPE Annual Technical Conference and Exhibition, Society of Petroleum Engineers.
- 5295 Keiding, M., T. Árnadóttir, S. Jonsson, J. Decriem, and A. Hooper (2010), Plate
5296 boundary deformation and man-made subsidence around geothermal fields on the
5297 Reykjanes Peninsula, Iceland, *Journal of Volcanology and Geothermal Research*, 194,
5298 139-149.
- 5299 Keranen, K. M., C. Hogan, H. M. Savage, G. A. Abers, and N. van der Elst (2013),
5300 Variable seismic response to fluid injection in central Oklahoma, paper presented at AGU
5301 Fall Meeting Abstracts.
- 5302 Keranen, K. M., H. M. Savage, G. A. Abers, and E. S. Cochran (2013), Potentially
5303 induced earthquakes in Oklahoma, USA: Links between wastewater injection and the
5304 2011 Mw 5.7 earthquake sequence, *Geology*, 41, 699-702.
- 5305 Keranen, K. M., M. Weingarten, G. A. Abers, B. A. Bekins, and S. Ge (2014), Sharp
5306 increase in central Oklahoma seismicity since 2008 induced by massive wastewater
5307 injection, *Science*, 345, 448-451.
- 5308 Kerr, R. A. (2009), After the quake, in search of the science—or even a good
5309 prediction, *Science*, 324, 322-322.
- 5310 Kerr, R. A., and R. Stone (2009), A human trigger for the great quake of Sichuan?,
5311 *Science*, 323, 322-322.

- 5312 Kertapati, E. K. (1987), Saguling-Cirata water reservoirs along Citarum river west
5313 Java, Indonesia as reservoir induced seismicity, YY1-YY9.
- 5314 Kim, W. Y. (2013), Induced seismicity associated with fluid injection into a deep well
5315 in Youngstown, Ohio, *Journal of Geophysical Research: Solid Earth*, 118, 3506-3518.
- 5316 Kim, W.-Y., M. Gold, C. Schamberger, J. Jones, and H. Delano (2009), The 2008-
5317 2009 earthquake swarm near Dillsburg, Pennsylvania.
- 5318 King, G. C. P., R. S. Stein, and J. Lin (1994), Static stress changes and the triggering
5319 of earthquakes, *Bulletin of the Seismological Society of America*, 84, 935-953.
- 5320 King, G. E. (2012), Hydraulic fracturing 101: What every representative,
5321 environmentalist, regulator, reporter, investor, university researcher, neighbor and
5322 engineer should know about estimating frac risk and improving frac performance in
5323 unconventional gas and oil wells, paper presented at SPE Hydraulic Fracturing
5324 Technology Conference, Society of Petroleum Engineers.
- 5325 Kinscher, J., P. Bernard, I. Contrucci, A. Mangeney, J. P. Piguet, and P. Bigarre
5326 (2015), Location of microseismic swarms induced by salt solution mining, *Geophysical
5327 Journal International*, 200, 337-362.
- 5328 Király, E., V. Gischig, D. Karvounis, and S. Wiemer (2014), Validating models to
5329 forecasting induced seismicity related to deep geothermal energy projects, paper
5330 presented at Proceedings, 39th Workshop on Geothermal Reservoir Engineering.
- 5331 Kitano, K., Y. Hori, and H. Kaieda (2000), Outline of the Ogachi HDR project and
5332 character of the reservoirs, paper presented at World Geothermal Congress, Kyushu-
5333 Tohoku, Japan, May 28-June 10
- 5334 Klose, C. D. (2007), Coastal land loss and gain as potential earthquake trigger
5335 mechanism in SCRs, paper presented at AGU Fall Meeting Abstracts.
- 5336 Klose, C. D. (2007), Geomechanical modeling of the nucleation process of Australia's
5337 1989 M5.6 Newcastle earthquake, *Earth and Planetary Science Letters*, 256, 547-553.
- 5338 Klose, C. D. (2007), Mine water discharge and flooding: A cause of severe
5339 earthquakes, *Mine Water and the Environment*, 26, 172-180.
- 5340 Klose, C. D. (2010), Human-triggered earthquakes and their impacts on human
5341 security, *Achieving Environmental Security: Ecosystem Services and Human Welfare*,
5342 13-19.
- 5343 Klose, C. D. (2012), Evidence for anthropogenic surface loading as trigger
5344 mechanism of the 2008 Wenchuan earthquake, *Environmental Earth Sciences*, 66, 1439-
5345 1447.
- 5346 Klose, C. D. (2013), Mechanical and statistical evidence of the causality of human-
5347 made mass shifts on the Earth's upper crust and the occurrence of earthquakes, *Journal of
5348 Seismology*, 17, 109-135.

- 5349 Klose, C. D., and L. Seeber (2007), Shallow seismicity in stable continental regions,
5350 *Seismological Research Letters*, 78, 554-562.
- 5351 Knoll, P., G. Kowalle, K. Rother, B. Schreiber, and I. Paskaleva (1996), Analysis of
5352 microtremors within the Providia region near a salt leaching mine, in *Induced seismic
5353 events*, pp. 389-407, Springer.
- 5354 Kouznetsov, O., V. Sidorov, S. Katz, and G. Chilingarian (1995), Interrelationships
5355 among seismic and short-term tectonic activity, oil and gas production, and gas migration
5356 to the surface, *Journal of Petroleum Science and Engineering*, 13, 57-63.
- 5357 Kovach, R. L. (1974), Source mechanisms for Wilmington oil field, California,
5358 subsidence earthquakes, *Bulletin of the Seismological Society of America*, 64, 699-711.
- 5359 Kraaijpoel, D., D. Nieuwland, B. Wassing, and B. Dost (2012), Induced seismicity at
5360 an underground gas storage facility in the Netherlands, paper presented at EGU General
5361 Assembly Conference Abstracts.
- 5362 Kreitler, C. W. (1976), Faulting and land subsidence from ground-water and
5363 hydrocarbon production, Houston-Galveston, Texas, paper presented at Proceedings of
5364 the Anaheim Symposium.
- 5365 Kremenetskaya, E. O., and V. M. Trjapitsin (1995), Induced seismicity in the Khibiny
5366 Massif (Kola Peninsula), in *Induced seismicity*, pp. 29-37, Springer.
- 5367 Kundu, B., N. K. Vissa, and V. K. Gahalaut (2015), Influence of anthropogenic
5368 groundwater unloading in Indo-Gangetic Plains on the 25 April 2015 Mw 7.8 Gorkha,
5369 Nepal earthquake, *Geophysical Research Letters*, 42.
- 5370 Kwee, J. (2012), Micro-seismicity in the Bergermeer gas storage field, University of
5371 Utrecht, The Netherlands.
- 5372 Kwiatek, G., M. Bohnhoff, G. Dresen, A. Schulze, T. Schulte, G. Zimmermann, and
5373 E. Huenges (2010), Microseismicity induced during fluid-injection: A case study from the
5374 geothermal site at Groß Schönebeck, North German Basin, *Acta Geophysica*, 58, 995-
5375 1020.
- 5376 Lamontagne, M., Y. Hammamji, and V. Peci (2008), Reservoir-triggered seismicity at
5377 the Toulustouc hydroelectric project, Quebec north shore, Canada, *Bulletin of the
5378 Seismological Society of America*, 98, 2543-2552.
- 5379 Leblanc, G., and F. Anglin (1978), Induced seismicity at the Manic 3 reservoir,
5380 Quebec, *Bulletin of the Seismological Society of America*, 68, 1469-1485.
- 5381 Lee, M. F., P. Mikula, and E. Kinnarsly (2006), In situ rock stress measurements and
5382 stress change monitoring at Mt Charlotte gold mine, western Australia, paper presented at
5383 *In-Situ Rock Stress: International Symposium on In-Situ Rock Stress*, Trondheim,
5384 Norway, 19-21 June 2006, CRC Press.
- 5385 Lehner, B., C. R. Liermann, C. Revenga, C. Vörösmarty, B. Fekete, P. Crouzet, P.
5386 Döll, M. Endejan, K. Frenken, and J. Magome (2011), High-resolution mapping of the

- 5387 world's reservoirs and dams for sustainable river-flow management, *Frontiers in Ecology*
5388 *and the Environment*, 9, 494-502.
- 5389 Lei, X., S. Ma, W. Chen, C. Pang, J. Zeng, and B. Jiang (2013), A detailed view of
5390 the injection-induced seismicity in a natural gas reservoir in Zigong, southwestern
5391 Sichuan Basin, China, *Journal of Geophysical Research: Solid Earth*, 118, 4296-4311.
- 5392 Lei, X., G. Yu, S. Ma, X. Wen, and Q. Wang (2008), Earthquakes induced by water
5393 injection at ~3 km depth within the Rongchang gas field, Chongqing, China, *Journal of*
5394 *Geophysical Research: Solid Earth*, 113.
- 5395 Li, T., M. F. Cai, and M. Cai (2007), A review of mining-induced seismicity in China,
5396 *International Journal of Rock Mechanics and Mining Sciences*, 44, 1149-1171.
- 5397 Lin, C. H. (2005), Seismicity increase after the construction of the world's tallest
5398 building: An active blind fault beneath the Taipei 101, *Geophysical Research Letters*, 32.
- 5399 Lizurek, G., Ł. Rudziński, and B. Plesiewicz (2015), Mining induced seismic event on
5400 an inactive fault, *Acta Geophysica*, 63, 176-200.
- 5401 Llenos, A. L., and A. J. Michael (2013), Modeling earthquake rate changes in
5402 Oklahoma and Arkansas: Possible signatures of induced seismicity, *Bulletin of the*
5403 *Seismological Society of America*, 103, 2850-2861.
- 5404 Lockridge, J. S., M. J. Fouch, and J. R. Arrowsmith (2012), Seismicity within
5405 Arizona during the deployment of the Earthscope USarray transportable array, *Bulletin of*
5406 *the Seismological Society of America*, 102, 1850-1863.
- 5407 Long, L. T., and C. W. Copeland (1989), The Alabama, USA, seismic event and strata
5408 collapse of May 7, 1986, *Pure and applied geophysics*, 129, 415-421.
- 5409 Lorenz, J. C. (2001), The stimulation of hydrocarbon reservoirs with subsurface
5410 nuclear explosions, *Oil-Industry History*, 2, 56-63.
- 5411 Lovchikov, A. V. (2013), Review of the strongest rockbursts and mining-induced
5412 earthquakes in Russia, *Journal of Mining Science*, 49, 572-575.
- 5413 Ma, T. H., C. A. Tang, L. X. Tang, W. D. Zhang, and L. Wang (2015), Rockburst
5414 characteristics and microseismic monitoring of deep-buried tunnels for Jinping II
5415 hydropower station, *Tunnelling and Underground Space Technology*, 49, 345-368.
- 5416 Ma, W. (2012), Analysis on the disaster mechanism of rock collapse of M4.4
5417 reservoir-induced earthquake on January 17, 2010, at Dongjing reservoir in Guizhou
5418 Province, China, *Natural hazards*, 62, 141-148.
- 5419 Maggi, A., J. A. Jackson, D. Mckenzie, and K. Priestley (2000), Earthquake focal
5420 depths, effective elastic thickness, and the strength of the continental lithosphere,
5421 *Geology*, 28, 495-498.
- 5422 Mahdi, S. K. (1988), Tarbela reservoir a question of induced seismicity, in
5423 *International Conference on Case Histories in Geotechnical Engineering*.

- 5424 Majer, E. L. (2011), Workshop on induced seismicity due to fluid
5425 injection/production from energy-related applications, Lawrence Berkeley National
5426 Laboratory.
- 5427 Majer, E. L., R. Baria, M. Stark, S. Oates, J. Bommer, B. Smith, and H. Asanuma
5428 (2007), Induced seismicity associated with enhanced geothermal systems, *Geothermics*,
5429 36, 185-222.
- 5430 Majer, E. L., and J. E. Peterson (2008), The impact of injection on seismicity at The
5431 Geysers, California geothermal field, *International Journal of Rock Mechanics and*
5432 *Mining Sciences*, 44, 1079-1090.
- 5433 Malovichko, D., R. Dyagilev, D. Y. Shulakov, P. Butyrin, and S. V. Glebov (2009),
5434 Seismic monitoring of large-scale karst processes in a potash mine, *Controlling seismic*
5435 *hazard and sustainable development of deep mines*, 2, 989-1002.
- 5436 Matrullo, E., I. Contrucci, P. Dominique, M. Bennani, H. Aochi, J. Kinsher, P.
5437 Bernard, and P. Bigarré (2015), Analysis and interpretation of induced micro-seismicity
5438 by flooding of the Gardanne Coal Basin (Provence–southern France), paper presented at
5439 77th EAGE Conference and Exhibition-Workshops.
- 5440 Maurer, V., N. Cuenot, E. Gaucher, M. Grunberg, J. Vergne, H. Wodling, M.
5441 Lehujeur, and J. Schmittbuhl (2015), Seismic monitoring of the Rittershoffen EGS
5442 project (Alsace, France), paper presented at World Geothermal Congress.
- 5443 Maxwell, S. C., D. Cho, T. L. Pope, M. Jones, C. L. Cipolla, M. G. Mack, F. Henery,
5444 M. Norton, and J. A. Leonard (2011), Enhanced reservoir characterization using
5445 hydraulic fracture microseismicity, paper presented at SPE Hydraulic Fracturing
5446 Technology Conference, Society of Petroleum Engineers.
- 5447 Maxwell, S. C., and H. Fabriol (2004), Passive seismic imaging of CO₂ sequestration
5448 at Weyburn.
- 5449 Maxwell, S. C., U. Zimmer, R. W. Gusek, and D. J. Quirk (2009), Evidence of a
5450 horizontal hydraulic fracture from stress rotations across a thrust fault, *SPE Production &*
5451 *Operations*, 24, 312-319.
- 5452 Mazzoldi, A., A. Borgia, M. Ripepe, E. Marchetti, G. Ulivieri, M. della Schiava, and
5453 C. Allocca (2015), Faults strengthening and seismicity induced by geothermal
5454 exploitation on a spreading volcano, Mt. Amiata, Italia, *Journal of Volcanology and*
5455 *Geothermal Research*, 301, 159-168.
- 5456 McClure, M. W., and R. N. Horne (2014), Correlations between formation properties
5457 and induced seismicity during high pressure injection into granitic rock, *Engineering*
5458 *Geology*, 175, 74-80.
- 5459 McGarr, A. (1991), On a possible connection between three major earthquakes in
5460 California and oil production, *Bulletin of the Seismological Society of America*, 81, 948-
5461 970.

- 5462 McGarr, A. (2014), Maximum magnitude earthquakes induced by fluid injection,
5463 *Journal of Geophysical Research: Solid Earth*, 119, 1008-1019.
- 5464 McGarr, A., B. Bekins, N. Burkardt, J. Dewey, P. Earle, W. Ellsworth, S. Ge, S.
5465 Hickman, A. Holland, and E. Majer (2015), Coping with earthquakes induced by fluid
5466 injection, *Science*, 347, 830-831.
- 5467 McGarr, A., and D. Simpson (1997), A broad look at induced and triggered
5468 seismicity, *Rockbursts and Seismicity in Mines*, 385-396.
- 5469 McGarr, A., D. Simpson, and L. Seeber (2002), Case histories of induced and
5470 triggered seismicity, in *International geophysics series, international handbook of*
5471 *earthquake and engineering seismology*, pp. 647-664.
- 5472 McKavanagh, B., B. Boreham, K. McCue, G. Gibson, J. Hafner, and G. Klenowski
5473 (1995), The CQU regional seismic network and applications to underground mining in
5474 Central Queensland, Australia, *Pure and applied geophysics*, 145, 39-57.
- 5475 McKeown, F. A. (1975), Relation of geological structure to seismicity at Pahute
5476 Mesa, Nevada test site, *Bulletin of the Seismological Society of America*, 65, 747-764.
- 5477 McKeown, F. A., and D. D. Dickey (1969), Fault displacements and motion related to
5478 nuclear explosions, *Bulletin of the Seismological Society of America*, 59, 2253-2269.
- 5479 McNamara, D. E., H. M. Benz, R. B. Herrmann, E. A. Bergman, P. Earle, A. Holland,
5480 R. Baldwin, and A. Gassner (2015), Earthquake hypocenters and focal mechanisms in
5481 central Oklahoma reveal a complex system of reactivated subsurface strike-slip faulting,
5482 *Geophysical Research Letters*, 42, 2742-2749.
- 5483 McNamara, D. E., G. P. Hayes, H. M. Benz, R. A. Williams, N. D. McMahon, R. C.
5484 Aster, A. Holland, T. Sickbert, R. Herrmann, and R. Briggs (2015), Reactivated faulting
5485 near Cushing, Oklahoma: Increased potential for a triggered earthquake in an area of
5486 United States strategic infrastructure, *Geophysical Research Letters*, 42, 8328-8332.
- 5487 Mercerat, E. D., L. Driad-Lebeau, and P. Bernard (2010), Induced seismicity
5488 monitoring of an underground salt cavern prone to collapse, *Pure and applied geophysics*,
5489 167, 5-25.
- 5490 Mereu, R. F., J. Brunet, K. Morrissey, B. Price, and A. Yapp (1986), A study of the
5491 microearthquakes of the Gobles oil field area of southwestern Ontario, *Bulletin of the*
5492 *Seismological Society of America*, 76, 1215-1223.
- 5493 Milev, A. M., and S. M. Spottiswoode (2002), Effect of the rock properties on
5494 mining-induced seismicity around the Ventersdorp Contact Reef, Witwatersrand Basin,
5495 South Africa, in *The mechanism of induced seismicity*, pp. 165-177, Springer.
- 5496 Milne, W. G., and M. J. Berry (1976), Induced seismicity in Canada, *Engineering*
5497 *Geology*, 10, 219-226.

- 5498 Mirzoev, K. M., A. V. Nikolaev, A. A. Lukk, and S. L. Yunga (2009), Induced
5499 seismicity and the possibilities of controlled relaxation of tectonic stresses in the Earth's
5500 crust, *Izvestiya, Physics of the Solid Earth*, 45, 885-904.
- 5501 Moeck, I., T. Bloch, R. Graf, S. Heuberger, P. Kuhn, H. Naef, M. Sonderegger, S.
5502 Uhlig, and M. Wolfgramm (2015), The St. Gallen project: Development of fault
5503 controlled geothermal systems in urban areas, paper presented at World Geothermal
5504 Congress.
- 5505 Mogren, S., and M. Mukhopadhyay (2013), Study of seismogenic crust in the eastern
5506 province of Saudi Arabia and its relation to the seismicity of the Ghawar fields, paper
5507 presented at AGU Fall Meeting Abstracts.
- 5508 Morrison, D. M. (1989), Rockburst research at Falconbridge's Strathcona mine,
5509 Sudbury, Canada, *Pure and applied geophysics*, 129, 619-645.
- 5510 Mossop, A., and P. Segall (1999), Volume strain within The Geysers geothermal
5511 field, *Journal of Geophysical Research: Solid Earth*, 104, 29113-29131.
- 5512 Mulargia, F., and A. Bizzarri (2014), Anthropogenic triggering of large earthquakes,
5513 *Scientific Reports*, 4.
- 5514 Mulyadi (2010), Case study: Hydraulic fracturing experiment in the Wayang Windu
5515 geothermal field, paper presented at World Geothermal Congress, Bali, Indonesia, 25-29
5516 April 2010.
- 5517 National Research Council (NRC) (2013), Induced seismicity potential in energy
5518 technologies, National Academies Press, Committee on Induced Seismicity Potential in
5519 Energy Technologies.
- 5520 Neuhaus, C. W., and J. L. Miskimins (2012), Analysis of surface and downhole
5521 microseismic monitoring coupled with hydraulic fracture modeling in the Woodford
5522 Shale, paper presented at SPE Europec/EAGE Annual Conference, Society of Petroleum
5523 Engineers.
- 5524 Nicholson, C., E. Roeloffs, and R. L. Wesson (1988), The northeastern Ohio
5525 earthquake of 31 January 1986: Was it induced?, *Bulletin of the Seismological Society of
5526 America*, 78, 188-217.
- 5527 Nicholson, C., and R. L. Wesson (1992), Triggered earthquakes and deep well
5528 activities, *Pure and applied geophysics*, 139, 561-578.
- 5529 Nicholson, C. J. (1992), Earthquakes associated with deep well activities-comments
5530 and case histories, paper presented at The 33th US Symposium on Rock Mechanics
5531 (USRMS), American Rock Mechanics Association.
- 5532 Nicol, A., R. Carne, M. Gerstenberger, and A. Christophersen (2011), Induced
5533 seismicity and its implications for CO2 storage risk, *Energy Procedia*, 4, 3699-3706.
- 5534 Nuannin, P., O. Kulhanek, L. Persson, and T. Askemur (2005), Inverse correlation
5535 between induced seismicity and b-value, observed in the Zingruvan mine, Sweden, *Acta
5536 Geodynamica et Geomaterialia*, 2, 5.

- 5537 Ohtake, M. (1974), Seismic activity induced by water injection at Matsushiro, Japan,
5538 *Journal of Physics of the Earth*, 22, 163-176.
- 5539 Orlic, B., B. B. T. Wassing, and C. R. Geel (2013), Field scale geomechanical
5540 modeling for prediction of fault stability during underground gas storage operations in a
5541 depleted gas field in the Netherlands, paper presented at 47th US Rock
5542 Mechanics/Geomechanics Symposium, American Rock Mechanics Association.
- 5543 Orzol, J., R. Jung, R. Jatho, T. Tischner, and P. Kehrer (2005), The Genesys-Project:
5544 Extraction of geothermal heat from tight sediments, paper presented at World Geothermal
5545 Congress.
- 5546 Ottemöller, L., H. H. Nielsen, K. Atakan, J. Braunmiller, and J. Havskov (2005), The
5547 7 May 2001 induced seismic event in the Ekofisk oil field, North Sea, *Journal of*
5548 *Geophysical Research: Solid Earth*, 110.
- 5549 Oye, V., E. Aker, T. M. Daley, D. Kühn, B. Bohloli, and V. Korneev (2013),
5550 Microseismic monitoring and interpretation of injection data from the In Salah CO₂
5551 storage site (Krechba), Algeria, *Energy Procedia*, 37, 4191-4198.
- 5552 Oye, V., and M. Roth (2005), Source parameters of microearthquakes from the 1.5
5553 km deep Pyhäsalmi ore mine, Finland, paper presented at Proceedings, Thirtieth
5554 Workshop on Geothermal Reservoir Engineering, Stanford University, Stanford,
5555 California, January.
- 5556 Paskaleva, I., A. G. Aronov, R. R. Seroglazov, and T. I. Aronova (2006),
5557 Characteristic features of induced seismic processes in mining regions exemplified by the
5558 potassium salt deposits in Belarus and Bulgaria, *Acta Geodaetica et Geophysica*
5559 *Hungarica*, 41, 293-303.
- 5560 Pavlou, K., G. Drakatos, V. Kouskouna, K. Makropoulos, and H. Kranis (2016),
5561 Seismicity study in Pournari reservoir area (w. Greece) 1981–2010, *Journal of*
5562 *Seismology*, 20, 701-710.
- 5563 Pavlou, K., G. Kaviris, K. Chousianitis, G. Drakatos, V. Kouskouna, and K.
5564 Makropoulos (2013), Seismic hazard assessment in Polyphyto dam area (nw Greece) and
5565 its relation with the “unexpected” earthquake of 13 May 1995 (M_s= 6.5, nw Greece), *Nat.*
5566 *Hazards Earth Sys. Sci*, 13, 141-149.
- 5567 Pavlovski, O. A. (1998), Radiological consequences of nuclear testing for the
5568 population of the former USSR (input information, models, dose, and risk estimates), in
5569 *Atmospheric nuclear tests*, pp. 219-260, Springer.
- 5570 Pechmann, J. C., W. J. Arabasz, K. L. Pankow, R. Burlacu, and M. K. McCarter
5571 (2008), Seismological report on the 6 August 2007 Crandall Canyon mine collapse in
5572 Utah, *Seismological Research Letters*, 79, 620-636.
- 5573 Pennington, W. D., S. D. Davis, S. M. Carlson, J. DuPree, and T. E. Ewing (1986),
5574 The evolution of seismic barriers and asperities caused by the depressuring of fault planes
5575 in oil and gas fields of south Texas, *Bulletin of the Seismological Society of America*, 76,
5576 939-948.

- 5577 Petersen, M. D., C. S. Mueller, M. P. Moschetti, S. M. Hoover, A. L. Llenos, W. L.
5578 Ellsworth, A. J. Michael, J. L. Rubinstein, A. F. McGarr, and K. S. Rukstales (2016),
5579 One-year seismic hazard forecast for the central and eastern United States from induced
5580 and natural earthquakes, US Geological Survey.
- 5581 Petersen, M. D., C. S. Mueller, M. P. Moschetti, S. M. Hoover, J. L. Rubinstein, A. L.
5582 Llenos, A. J. Michael, W. L. Ellsworth, A. McGarr, and A. A. Holland (2015),
5583 Incorporating induced seismicity in the 2014 United States national seismic hazard
5584 model: Results of 2014 workshop and sensitivity studies, US Department of the Interior,
5585 US Geological Survey.
- 5586 Phillips, W. S., T. D. Fairbanks, J. T. Rutledge, and D. W. Anderson (1998), Induced
5587 microearthquake patterns and oil-producing fracture systems in the Austin Chalk,
5588 *Tectonophysics*, 289, 153-169.
- 5589 Phillips, W. S., J. T. Rutledge, L. S. House, and M. C. Fehler (2002), Induced
5590 microearthquake patterns in hydrocarbon and geothermal reservoirs: Six case studies, in
5591 *The mechanism of induced seismicity*, pp. 345-369, Springer.
- 5592 Piccinelli, F. G., M. Mucciarelli, P. Federici, and D. Albarello (1995), The
5593 microseismic network of the Ridracoli dam, north Italy: Data and interpretations, *Pure
5594 and applied geophysics*, 145, 97-108.
- 5595 Plotnikova, L. M., B. S. Nurtaev, J. R. Grasso, L. M. Matasova, and R. Bossu (1996),
5596 The character and extent of seismic deformation in the focal zone of Gazli earthquakes of
5597 1976 and 1984, $M > 7.0$, in *Induced seismic events*, pp. 377-387, Springer.
- 5598 Pomeroy, P. W., D. W. Simpson, and M. L. Sbar (1976), Earthquakes triggered by
5599 surface quarrying-the Wappingers falls, New York sequence of June, 1974, *Bulletin of
5600 the Seismological Society of America*, 66, 685-700.
- 5601 Pramono, B., and D. Colombo (2005), Microearthquake characteristics in Darajat
5602 geothermal field, Indonesia, paper presented at World Geothermal Congress 2005,
5603 Antalya, Turkey, 24-29 April, 2005.
- 5604 Prioul, R., F. H. Cornet, C. Dorbath, I. Dorbath, M. Ogena, and E. Ramos (2000), An
5605 induced seismicity experiment across a creeping segment of the Philippine fault, *Journal
5606 of geophysical research*, 105, 13,595-513,612.
- 5607 Rajendran, K. (1995), Sensitivity of a seismically active reservoir to low-amplitude
5608 fluctuations: Observations from Lake Jocassee, South Carolina, *Pure and applied
5609 geophysics*, 145, 87-95.
- 5610 Raleigh, C. B., J. H. Healy, and J. D. Bredehoeft (1976), An experiment in earthquake
5611 control at Rangely, Colorado, *Science*, 191, 1230-1237.
- 5612 Rastogi, B. K., C. V. R. K. Rao, R. K. Chadha, and H. K. Gupta (1986),
5613 Microearthquakes near Osmansagar reservoir, Hyderabad, India, *Physics of the earth and
5614 planetary interiors*, 44, 134-141.

- 5615 Redmayne, D. W. (1988), Mining induced seismicity in UK coalfields identified on
5616 the BGS national seismograph network, Geological Society, London, Engineering
5617 Geology Special Publications, 5, 405-413.
- 5618 Reyners, M. (1988), Reservoir-induced seismicity at Lake Pukaki, New Zealand,
5619 Geophysical Journal International, 93, 127-135.
- 5620 Ringdal, F., P. D. Marshall, and R. W. Alewine (1992), Seismic yield determination
5621 of Soviet underground nuclear explosions at the Shagan River test site, Geophysical
5622 Journal International, 109, 65-77.
- 5623 Rojas, E., P. Cavieres, R. Dunlop, and S. Gaete (2000), Control of induced seismicity
5624 at El Teniente mine Codelco-Chile, Proceeding, Massmin 2000, 777-781.
- 5625 Ross, A., G. R. Foulger, and B. R. Julian (1999), Source processes of industrially-
5626 induced earthquakes at The Geysers geothermal area, California, Geophysics, 64, 1877-
5627 1889.
- 5628 Rubinstein, J. L., W. L. Ellsworth, and A. McGarr (2012), The 2001-present triggered
5629 seismicity sequence in the Raton Basin of southern Colorado/northern New Mexico,
5630 paper presented at AGU Fall Meeting Abstracts.
- 5631 Rubinstein, J. L., W. L. Ellsworth, A. McGarr, and H. M. Benz (2014), The 2001-
5632 present induced earthquake sequence in the Raton Basin of northern New Mexico and
5633 southern Colorado, Bulletin of the Seismological Society of America.
- 5634 Rubinstein, J. L., and A. B. Mahani (2015), Myths and facts on wastewater injection,
5635 hydraulic fracturing, enhanced oil recovery, and induced seismicity, Seismological
5636 Research Letters, 86, 1060-1067.
- 5637 Rutledge, J. T., W. S. Phillips, and B. K. Schuessler (1998), Reservoir
5638 characterization using oil-production-induced microseismicity, Clinton County,
5639 Kentucky, Tectonophysics, 289, 129-152.
- 5640 Sanford, A. R., T. M. Mayeau, J. W. Schlue, R. C. Aster, and L. H. Jaksha (2006),
5641 Earthquake catalogs for New Mexico and bordering areas II: 1999-2004, New Mexico
5642 Geology, 28.
- 5643 Sargsyan, L. S. (2009), Reservoir-triggered seismicity in Armenian large dams,
5644 Journal of Seismology and Earthquake Engineering, 11, 153.
- 5645 Sasaki, S. (1998), Characteristics of microseismic events induced during hydraulic
5646 fracturing experiments at the Hijiori hot dry rock geothermal energy site, Yamagata,
5647 Japan, Tectonophysics, 289, 171-188.
- 5648 Sato, K., and Y. Fujii (1988), Induced seismicity associated with longwall coal
5649 mining, paper presented at International Journal of Rock Mechanics and Mining Sciences
5650 & Geomechanics Abstracts, Elsevier.
- 5651 Sato, K., and Y. Fujii (1989), Source mechanism of a large scale gas outburst at
5652 Sunagawa coal mine in Japan, Pure and applied geophysics, 129, 325-343.

- 5653 Sato, K., T. Isobe, N. Mori, and T. Goto (1986), 9. Microseismic activity associated
5654 with hydraulic mining, paper presented at International Journal of Rock Mechanics and
5655 Mining Sciences & Geomechanics Abstracts, Elsevier.
- 5656 Schlutz, R., V. Stern, and Y. J. Gu (2014), An investigation of seismicity clustered
5657 near the Cordel field, west central Alberta, and its relation to a nearby disposal well,
5658 Journal of Geophysical Research: Solid Earth, 119, 3410-3423,
5659 doi:10.1002/2013JB010836.
- 5660 Schultz, R., S. Mei, D. Pană, V. Stern, Y. J. Gu, A. Kim, and D. Eaton (2015), The
5661 Cardston earthquake swarm and hydraulic fracturing of the Exshaw Formation (Alberta
5662 Bakken Play), Bulletin of the Seismological Society of America.
- 5663 Schultz, R., V. Stern, M. Novakovic, G. Atkinson, and Y. J. Gu (2015), Hydraulic
5664 fracturing and the Crooked Lake sequences: Insights gleaned from regional seismic
5665 networks, Geophysical Research Letters, 42, 2750-2758.
- 5666 Seeber, L., J. G. Armbruster, and W.-Y. Kim (2004), A fluid-injection-triggered
5667 earthquake sequence in Ashtabula, Ohio: Implications for seismogenesis in stable
5668 continental regions, Bulletin of the Seismological Society of America, 94, 76-87.
- 5669 Seeber, L., J. G. Armbruster, W. Y. Kim, N. Barstow, and C. Scharnberger (1998),
5670 The 1994 Cacoosing Valley earthquakes near Reading, Pennsylvania: A shallow rupture
5671 triggered by quarry unloading, Journal of Geophysical Research: Solid Earth, 103, 24505-
5672 24521.
- 5673 Segall, P. (1985), Stress and subsidence resulting from subsurface fluid withdrawal in
5674 the epicentral region of the 1983 Coalinga earthquake, Journal of Geophysical Research:
5675 Solid Earth, 90, 6801-6816.
- 5676 Segall, P. (1989), Earthquakes triggered by fluid extraction, Geology, 17, 942-946.
- 5677 Semmane, F., I. Abacha, A. K. Yelles-Chaouche, A. Haned, H. Beldjoudi, and A.
5678 Amrani (2012), The earthquake swarm of December 2007 in the Mila region of
5679 northeastern Algeria, Natural hazards, 64, 1855-1871.
- 5680 Shapiro, S. A., C. Dinske, C. Langenbruch, and F. Wenzel (2010), Seismogenic index
5681 and magnitude probability of earthquakes induced during reservoir fluid stimulations, The
5682 Leading Edge, 29, 304-309.
- 5683 Shapiro, S. A., J. Kummerow, C. Dinske, G. Asch, E. Rothert, J. Erzinger, H. J.
5684 Kämpel, and R. Kind (2006), Fluid induced seismicity guided by a continental fault:
5685 Injection experiment of 2004/2005 at the German deep drilling site (KTB), Geophysical
5686 Research Letters, 33.
- 5687 Sherburn, S., S. Bourguignon, S. Bannister, S. Sewell, B. Cumming, C. Bardsley, J.
5688 Quinao, and I. Wallis (2013), Microseismicity at Rotokawa geothermal field, 2008 to
5689 2012, paper presented at Proceedings of the 35th New Zealand geothermal workshop.
5690 Rotorua, New Zealand.

- 5691 Sherburn, S., C. Bromley, S. Bannister, S. Sewell, and S. Bourguignon (2015), New
5692 Zealand geothermal induced seismicity: An overview.
- 5693 Shirley, J. E. (1980), Tasmanian seismicity—natural and reservoir-induced, *Bulletin*
5694 *of the Seismological Society of America*, 70, 2203-2220.
- 5695 Shivakumar, K., M. V. M. S. Rao, C. Srinivasan, and K. Kusunose (1996),
5696 Multifractal analysis of the spatial distribution of area rockbursts at Kolar gold mines,
5697 paper presented at International journal of rock mechanics and mining sciences &
5698 geomechanics abstracts, Elsevier.
- 5699 Silitonga, T. H., E. E. Siahaan, and Suroso (2005), A Poisson's ratio distribution from
5700 Wadati diagram as indicator of fracturing of Lahendong geothermal field, north Sulawesi,
5701 Indonesia, paper presented at World Geothermal Congress 2005, Antalya, Turkey, 24–29
5702 April, 2005.
- 5703 Simiyu, S. M., and G. R. Keller (2000), Seismic monitoring of the Olkaria geothermal
5704 area, Kenya Rift Valley, *Journal of volcanology and geothermal research*, 95, 197-208.
- 5705 Simpson, D. W., and W. Leith (1985), The 1976 and 1984 Gazli, USSR,
5706 earthquakes—were they induced?, *Bulletin of the Seismological Society of America*, 75,
5707 1465-1468.
- 5708 Simpson, D. W., and S. K. Negmatullaev (1981), Induced seismicity at Nurek
5709 reservoir, Tadjikistan, USSR, *Bulletin of the Seismological Society of America*, 71,
5710 1561-1586.
- 5711 Skoumal, R. J., M. R. Brudzinski, and B. S. Currie (2015), Earthquakes induced by
5712 hydraulic fracturing in Poland Township, Ohio, *Bulletin of the Seismological Society of*
5713 *America*, 105, 189-197.
- 5714 Son, M. (2015), Microevent detection based on waveform cross-correlation in the
5715 Dogye mining area, Korea, paper presented at 2015 AGU Fall Meeting.
- 5716 Stein, S., M. Liu, T. Camelbeeck, M. Merino, A. Landgraf, E. Hintersberger, and S.
5717 Kuebler (2015), Challenges in assessing seismic hazard in intraplate Europe, *Geological*
5718 *Society, London, Special Publications*, 432, SP432. 437.
- 5719 Stork, A. L., J. P. Verdon, and J.-M. Kendall (2015), The microseismic response at
5720 the In Salah carbon capture and storage (CCS) site, *International Journal of Greenhouse*
5721 *Gas Control*, 32, 159-171.
- 5722 Styles, P., P. Gasparini, E. Huenges, P. Scandone, S. Lasocki, and F. Terlizese
5723 (2014), Report on the hydrocarbon exploration and seismicity in Emilia region, 1-213.
- 5724 Suckale, J. (2009), Induced seismicity in hydrocarbon fields, *Advances in geophysics*,
5725 51, 55-106.
- 5726 Sumy, D. F., E. S. Cochran, K. M. Keranen, M. Wei, and G. A. Abers (2014),
5727 Observations of static coulomb stress triggering of the November 2011 M5.7 Oklahoma
5728 earthquake sequence, *Journal of Geophysical Research: Solid Earth*, 119, 1904-1923.

- 5729 Sun, X., and S. Hartzell (2014), Finite-fault slip model of the 2011 Mw 5.6 Prague,
5730 Oklahoma earthquake from regional waveforms, *Geophysical Research Letters*, 41, 4207-
5731 4213.
- 5732 Swanson, P. L. (1992), Mining-induced seismicity in faulted geologic structures: An
5733 analysis of seismicity-induced slip potential, *Pure and applied geophysics*, 139, 657-676.
- 5734 Sylvester, A. G., and J. Heinemann (1996), Preseismic tilt and triggered reverse
5735 faulting due to unloading in a diatomite quarry near Lompoc, California, *Seismological*
5736 *Research Letters*, 67, 11-18.
- 5737 Sze, E. K.-M. (2005), Induced seismicity analysis for reservoir characterization at a
5738 petroleum field in Oman, *Massachusetts Institute of Technology*.
- 5739 Tadokoro, K., M. Ando, and K. y. Nishigami (2000), Induced earthquakes
5740 accompanying the water injection experiment at the Nojima fault zone, Japan: Seismicity
5741 and its migration, *Journal of Geophysical Research: Solid Earth*, 105, 6089-6104.
- 5742 Talwani, P. (1995), Speculation on the causes of continuing seismicity near Koyna
5743 reservoir, India, *Pure and applied geophysics*, 145, 167-174.
- 5744 Tang, C., T. Ma, and X. Ding (2009), On stress-forecasting strategy of earthquakes
5745 from stress buildup, stress shadow and stress transfer (SSS) based on numerical approach,
5746 *Earthquake Science*, 22, 53-62.
- 5747 Tang, C. a., J. Wang, and J. Zhang (2010), Preliminary engineering application of
5748 microseismic monitoring technique to rockburst prediction in tunneling of Jinping II
5749 project, *Journal of Rock Mechanics and Geotechnical Engineering*, 2, 193-208.
- 5750 Taylor, O.-D. S., T. A. Lee III, and A. P. Lester (2015), Hazard and risk potential of
5751 unconventional hydrocarbon development-induced seismicity within the central United
5752 States, *Natural Hazards Review*, 16, 04015008.
- 5753 Taylor, O.-D. S., A. P. Lester, and T. A. Lee III (2015), Unconventional hydrocarbon
5754 development hazards within the central United States. Report 1: Overview and potential
5755 risk to infrastructure, DTIC Document.
- 5756 Telesca, L., T. Matcharasvili, T. Chelidze, and N. Zhukova (2012), Relationship
5757 between seismicity and water level in the Enguri high dam area (Georgia) using the
5758 singular spectrum analysis, *Natural Hazards and Earth System Science*, 12, 2479-2485.
- 5759 Terakawa, T., S. A. Miller, and N. Deichmann (2012), High fluid pressure and
5760 triggered earthquakes in the enhanced geothermal system in Basel, Switzerland, *Journal*
5761 *of Geophysical Research: Solid Earth*, 117.
- 5762 Terashima, T. (1981), Survey on induced seismicity at Mishraq area in Iraq, *Journal*
5763 *of Physics of the Earth*, 29, 371-375.
- 5764 Teyssoneyre, V., B. Feignier, J. Šilény, and O. Coutant (2002), Moment tensor
5765 inversion of regional phases: Application to a mine collapse, in *The mechanism of*
5766 *induced seismicity*, pp. 111-130, Springer.

- 5767 Tiira, T. (1996), Discrimination of nuclear explosions and earthquakes from
5768 teleseismic distances with a local network of short period seismic stations using artificial
5769 neural networks, *Physics of the Earth and Planetary Interiors*, 97, 247-268.
- 5770 TNO (2014), Literature review on injection-related induced seismicity and its
5771 relevance to nitrogen injection.
- 5772 Torcal, F., I. Serrano, J. Havskov, J. L. Utrillas, and J. Valero (2005), Induced
5773 seismicity around the Tous New dam (Spain), *Geophysical Journal International*, 160,
5774 144-160.
- 5775 Townend, J., and M. D. Zoback (2000), How faulting keeps the crust strong, *Geology*,
5776 28, 399-402.
- 5777 Trifu, C.-I., T. I. Urbancic, and R. P. Young (1995), Source parameters of mining-
5778 induced seismic events: An evaluation of homogeneous and inhomogeneous faulting
5779 models for assessing damage potential, *Pure and applied geophysics*, 145, 3-27.
- 5780 Trippi, M. H., H. E. Belkin, S. Dai, S. J. Tewalt, and C.-J. Chou (2014), USGS
5781 compilation of geographic information system (GIS) data representing coal mines and
5782 coal-bearing areas in China, US Geological Survey.
- 5783 Turbitt, T. (1988), *Bulletin of British earthquakes*. British Geological Survey
5784 technical report wl/88/11.
- 5785 Turuntaev, S. B. (1994), Temporal and spatial structures of triggered seismicity in
5786 Romashkinskoye oil-field, paper presented at Rock Mechanics in Petroleum Engineering,
5787 Society of Petroleum Engineers.
- 5788 Urban, E., and J. F. Lermo (2012), Relationship of local seismic activity, injection
5789 wells and active faults in the geothermal fields of Mexico, paper presented at Proceedings
5790 of Thirty-Seventh Workshop on Geothermal Reservoir Engineering, Stanford University,
5791 Stanford, CA, SGP-TR-194.
- 5792 Urban, E., and J. F. Lermo (2013), Local seismicity in the exploitation of Los
5793 Humeros geothermal field, Mexico, paper presented at Proceedings of the Thirty-Eighth
5794 Workshop on Geothermal Reservoir Engineering.
- 5795 Urbancic, T. I. J., V. J. Shumila, J. T. J. Rutledge, and R. J. J. Zinno (1999),
5796 Determining hydraulic fracture behavior using microseismicity, paper presented at Vail
5797 Rocks 1999, The 37th US Symposium on Rock Mechanics (USRMS), American Rock
5798 Mechanics Association.
- 5799 Vallejos, J. A., and S. D. McKinnon (2011), Correlations between mining and
5800 seismicity for re-entry protocol development, *International Journal of Rock Mechanics
5801 and Mining Sciences*, 48, 616-625.
- 5802 Valoroso, L., L. Improta, L. Chiaraluce, R. Di Stefano, L. Ferranti, A. Govoni, and C.
5803 Chiarabba (2009), Active faults and induced seismicity in the Val d'Agri area (southern
5804 Apennines, Italy), *Geophysical Journal International*, 178, 488-502.

- 5805 van der Elst, N. J., H. M. Savage, K. M. Keranen, and G. A. Abers (2013), Enhanced
5806 remote earthquake triggering at fluid-injection sites in the midwestern United States,
5807 *Science*, 341, 164-167.
- 5808 van der Voort, N., and F. Vanclay (2015), Social impacts of earthquakes caused by
5809 gas extraction in the province of Groningen, the Netherlands, *Environmental Impact*
5810 *Assessment Review*, 50, 1-15.
- 5811 Van Eck, T., F. Goutbeek, H. Haak, and B. Dost (2006), Seismic hazard due to small-
5812 magnitude, shallow-source, induced earthquakes in the Netherlands, *Engineering*
5813 *Geology*, 87, 105-121.
- 5814 Van Eijs, R. M. H. E., F. M. M. Mulders, M. Nepveu, C. J. Kenter, and B. C.
5815 Scheffers (2006), Correlation between hydrocarbon reservoir properties and induced
5816 seismicity in the Netherlands, *Engineering Geology*, 84, 99-111.
- 5817 Van Wees, J. D., L. Buijze, K. Van Thienen-Visser, M. Nepveu, B. B. T. Wassing, B.
5818 Orlic, and P. A. Fokker (2014), Geomechanics response and induced seismicity during
5819 gas field depletion in the Netherlands, *Geothermics*, 52, 206-219.
- 5820 Verdon, J. P. (2014), Significance for secure CO₂ storage of earthquakes induced by
5821 fluid injection, *Environmental Research Letters*, 9, 064022.
- 5822 Verdon, J. P., J.-M. Kendall, A. L. Stork, R. A. Chadwick, D. J. White, and R. C.
5823 Bissell (2013), Comparison of geomechanical deformation induced by megatonne-scale
5824 CO₂ storage at Sleipner, Weyburn, and In Salah, *Proceedings of the National Academy*
5825 *of Sciences*, 110, E2762-E2771.
- 5826 Walsh, F. R., and M. D. Zoback (2015), Oklahoma's recent earthquakes and saltwater
5827 disposal, *Science advances*, 1, e1500195.
- 5828 Walter, J. I., P. J. Dotray, C. Frohlich, and J. F. W. Gale (2016), Earthquakes in
5829 northwest Louisiana and the Texas–Louisiana border possibly induced by energy
5830 resource activities within the Haynesville Shale Play, *Seismological Research Letters*, 87,
5831 285-294.
- 5832 Wang, P., M. J. Small, W. Harbert, and M. Pozzi (2016), A Bayesian approach for
5833 assessing seismic transitions associated with wastewater injections, *Bulletin of the*
5834 *Seismological Society of America*.
- 5835 Wang, R., Y. J. Gu, R. Schultz, A. Kim, and G. Atkinson (2016), Source analysis of a
5836 potential hydraulic fracturing induced earthquake near Fox Creek, Alberta, *Geophysical*
5837 *Research Letters*.
- 5838 Wang, W., X. Meng, Z. Peng, Q. F. Chen, and N. Liu (2015), Increasing background
5839 seismicity and dynamic triggering behaviors with nearby mining activities around
5840 Fangshan pluton in Beijing, China, *Journal of Geophysical Research: Solid Earth*, 120,
5841 5624-5638.

- 5842 Wang, Z., C. N. Tang, T. H. Ma, L. C. Li, and Y. F. Yang (2012), Research on the
5843 surrounding rock damage of deep hard rock tunnels caused by bottom excavation, paper
5844 presented at Applied Mechanics and Materials, Trans Tech Publ.
- 5845 Weingarten, M., S. Ge, J. W. Godt, B. A. Bekins, and J. L. Rubinstein (2015), High-
5846 rate injection is associated with the increase in US mid-continent seismicity, *Science*,
5847 348, 1336-1340.
- 5848 Weiser, D. A. (2016), Maximum magnitude and probabilities of induced earthquakes
5849 in California geothermal fields: Applications for a science-based decision framework,
5850 University of California.
- 5851 Westbrook, G. K., N. J. Kuszniir, C. W. A. Browitt, and B. K. Holdsworth (1980),
5852 Seismicity induced by coal mining in Stoke-on-Trent (UK), *Engineering Geology*, 16,
5853 225-241.
- 5854 Wettainen, T., and J. Martinsson (2014), Estimation of future ground vibration levels
5855 in Malmberget town due to mining-induced seismic activity, *Journal of the Southern*
5856 *African Institute of Mining and Metallurgy*, 114, 835-843.
- 5857 Wheeler, R. L. (2009), Sizes of the largest possible earthquakes in the central and
5858 eastern United States-summary of a workshop, September 8-9, 2008, Golden, Colorado,
5859 US Geological Survey.
- 5860 Wilson, M. P., R. J. Davies, G. R. Foulger, B. R. Julian, P. Styles, J. G. Gluyas, and
5861 S. Almond (2015), Anthropogenic earthquakes in the UK: A national baseline prior to
5862 shale exploitation, *Marine and Petroleum Geology*, 30, e17.
- 5863 Windsor, C. R., P. Caviaras, E. Villaescusa, and J. Pereira (2006), Reconciliation of
5864 strain, structure and stress in the El Teniente mine region, Chile, paper presented at
5865 Proceedings of International Symposium on In Situ Rock Stress, Trondheim, Norway.
- 5866 Wiszniowski, J., N. Van Giang, B. Plesiewicz, G. Lizurek, D. Q. Van, L. Q. Khoi,
5867 and S. Lasocki (2015), Preliminary results of anthropogenic seismicity monitoring in the
5868 region of Song Tranh 2 reservoir, central Vietnam, *Acta Geophysica*, 63, 843-862.
- 5869 Wolhart, S. L., T. A. Harting, J. E. Dahlem, T. Young, M. J. Mayerhofer, and E. P.
5870 Lolon (2006), Hydraulic fracture diagnostics used to optimize development in the Jonah
5871 field, paper presented at SPE Annual Technical Conference and Exhibition, Society of
5872 Petroleum Engineers.
- 5873 Xie, L., K.-B. Min, and Y. Song (2015), Observations of hydraulic stimulations in
5874 seven enhanced geothermal system projects, *Renewable Energy*, 79, 56-65.
- 5875 Xiumin, M. A., L. I. Zhen, P. E. N. G. Hua, J. I. A. N. G. Jingjie, Z. H. A. O. Fang, H.
5876 A. N. Chaopu, Y. U. A. N. Pengxiang, L. U. Shengzhou, and P. E. N. G. Ligu (2015),
5877 Fluid-injection-induced seismicity experiment of the WFSD-3P borehole, *Acta Geologica*
5878 *Sinica (English Edition)*, 89, 1057-1058.

- 5879 Xu, N.-w., C.-a. Tang, H. Li, F. Dai, K. Ma, J.-d. Shao, and J.-c. Wu (2012),
5880 Excavation-induced microseismicity: Microseismic monitoring and numerical simulation,
5881 Journal of Zhejiang University SCIENCE A, 13, 445-460.
- 5882 Yeck, W. L., A. F. Sheehan, M. Weingarten, J. Nakai, and S. Ge (2014), The 2014
5883 Greeley, Colorado earthquakes: Science, industry, regulation, and media, paper presented
5884 at AGU Fall Meeting Abstracts.
- 5885 Younger, P. L., J. G. Gluyas, and W. E. Stephens (2012), Development of deep
5886 geothermal energy resources in the UK, Proceedings of the Institution of Civil Engineers-
5887 Energy, 165, 19-32.
- 5888 Yu, Q., C.-A. Tang, L. Li, G. Cheng, and L.-X. Tang (2015), Study on rockburst
5889 nucleation process of deep-buried tunnels based on microseismic monitoring, Shock and
5890 Vibration, 501, 685437.
- 5891 Zaliapin, I., and Y. Ben-Zion (2016), Discriminating characteristics of tectonic and
5892 human-induced seismicity, Bulletin of the Seismological Society of America.
- 5893 Zang, A., V. Oye, P. Jousset, N. Deichmann, R. Gritto, A. McGarr, E. Majer, and D.
5894 Bruhn (2014), Analysis of induced seismicity in geothermal reservoirs—an overview,
5895 Geothermics, 52, 6-21.
- 5896 Zedník, J., and J. Pazdírková (2014), Seismic activity in the Czech Republic in 2012,
5897 Studia Geophysica et Geodaetica, 58, 342.
- 5898 Zedník, J., J. Pospíšil, B. Růžek, J. Horálek, A. Boušková, P. Jedlička, Z. Skácelová,
5899 V. Nehybka, K. Holub, and J. Rušajová (2001), Earthquakes in the Czech Republic and
5900 surrounding regions in 1995–1999, Studia Geophysica et Geodaetica, 45, 267-282.
- 5901 Zhang, W.-d., and T.-h. Ma (2013), Research on characteristic of rockburst and rules
5902 of microseismic monitoring at headrace tunnels in Jinping II hydropower station, paper
5903 presented at Digital Manufacturing and Automation (ICDMA), 2013 Fourth International
5904 Conference on, IEEE.
- 5905 Zhang, Y., W. Feng, L. Xu, C. Zhou, and Y. Chen (2009), Spatio-temporal rupture
5906 process of the 2008 great Wenchuan earthquake, Science in China Series D: Earth
5907 Sciences, 52, 145-154.
- 5908 Zhang, Y., M. Person, J. Rupp, K. Ellett, M. A. Celia, C. W. Gable, B. Bowen, J.
5909 Evans, K. Bandilla, and P. Mozley (2013), Hydrogeologic controls on induced seismicity
5910 in crystalline basement rocks due to fluid injection into basal reservoirs, Groundwater, 51,
5911 525-538.
- 5912 Zoback, M. D., and S. M. Gorelick (2012), Earthquake triggering and large-scale
5913 geologic storage of carbon dioxide, Proceedings of the National Academy of Sciences,
5914 109, 10164-10168.
- 5915 Zoback, M. D., and H. P. Harjes (1997), Injection-induced earthquakes and crustal
5916 stress at 9 km depth at the KTB deep drilling site, Germany, Journal of Geophysical
5917 Research: Solid Earth, 102, 18477-18491.

5918 Zoback, M. D., and J. C. Zinke (2002), Production-induced normal faulting in the
5919 Valhall and Ekofisk oil fields, in *The mechanism of induced seismicity*, pp. 403-420,
5920 Springer.

5921